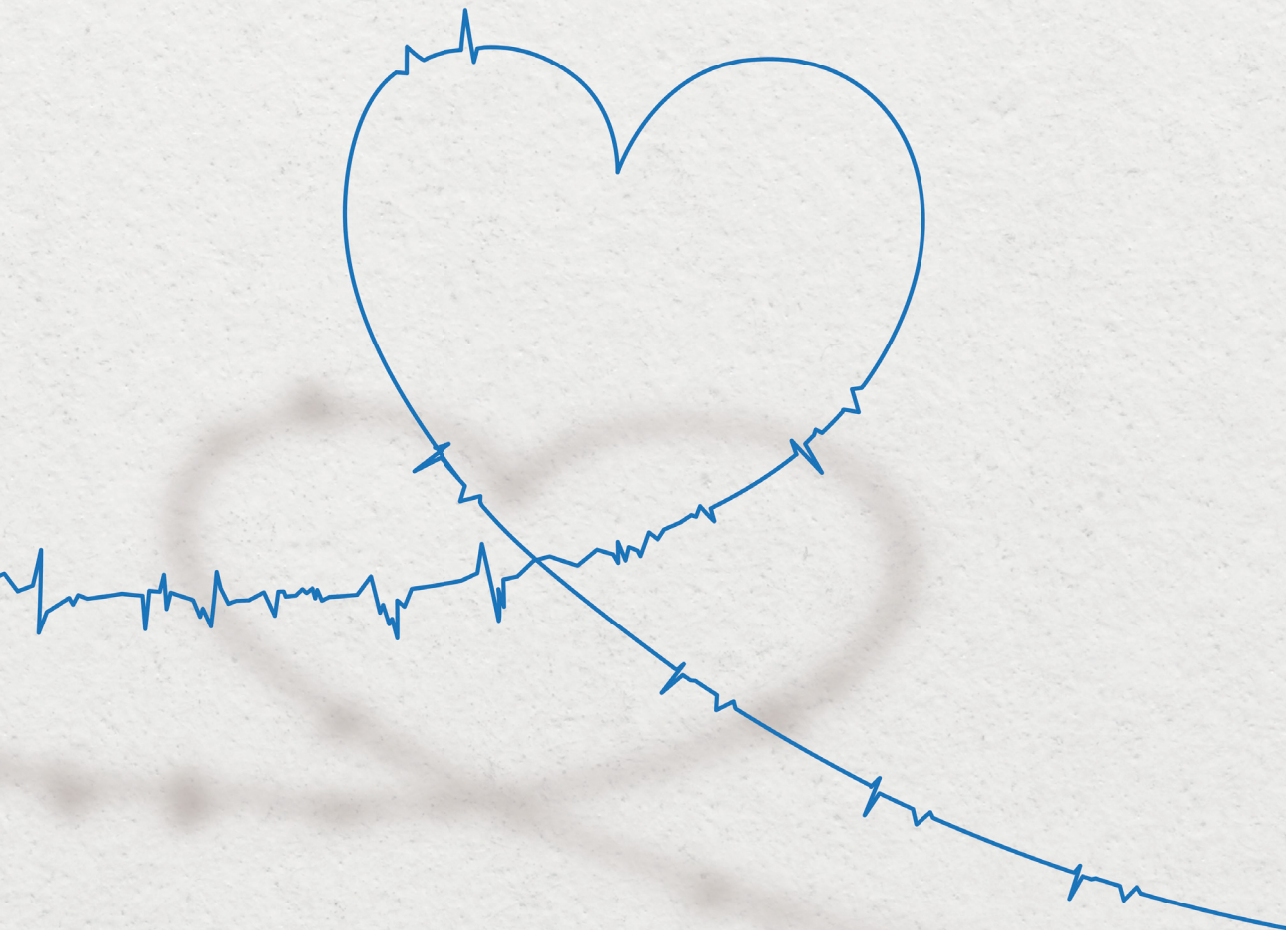


ATRIAL FIBRILLATION FROM A SINUS RHYTHM POINT OF VIEW



Eva Blankman - Lanthers

ATRIAL FIBRILLATION FROM A SINUS RHYTHM POINT OF VIEW

Eva A.H. Blankman – Lanthers

COLOFON

ISBN: 978-94-6416-579-1
Cover design & Lay-out: Publiiss | www.publiiss.nl
Print: Ridderprint | www.ridderprint.nl

© Copyright 2020: **Eva Blankman-Lanters, Woerden, The Netherlands**

All rights reserved. No part of this publication may be reproduced, stored in a retrieval system, or transmitted in any form or by any means, electronic, mechanical, by photocopying, recording, or otherwise, without the prior written permission of the author.

Atrial Fibrillation from a Sinus Rhythm Point of View

Atriumfibrilleren vanuit het oogpunt van sinusritme

PROEFSCHRIFT

ter verkrijging van de graad van doctor aan de
Erasmus Universiteit Rotterdam
op gezag van de
rector magnificus

Prof.dr. F.A. van der Duijn Schouten

en volgens besluit van het College voor Promoties.
De openbare verdediging zal plaatsvinden op

dinsdag 29 juni 2021 om 13:00 uur
door

Eva Anna Hendrika Blankman-Lanters
geboren te Breda

Erasmus University Rotterdam

The logo of Erasmus University Rotterdam, featuring a stylized, cursive script of the word "Erasmus" in black.

PROMOTIECOMMISSIE

Promotoren: Prof. dr. N.M.S. de Groot
Prof. B.J.J.M. Brundel

Overige leden: Prof. dr. F. Zijlstra
Prof. dr. A.J.J.C. Bogers
Prof. dr. D.R. Van Wagoner

Financial support by the Dutch Heart Foundation for the publication of this thesis is gratefully acknowledged.

The research described in this thesis was supported by a grant of the Dutch Heart Foundation
DHF grant nummer: 2013T144



Voor mijn Blankmannen

TABLE OF CONTENTS

1	General Introduction	11
	Lanterns EAH	
 PART I ELECTROPHYSIOLOGICAL MARKERS DURING SINUS RHYTHM		
2	Atrial Fibrillation: a never ending story?	31
	Lanterns EAH, Knops P, Kik C, de Groot NMS <i>Clinical Case Reports. 2019</i>	
3	Spatial distribution of conduction disorders during sinus rhythm	39
	Lanterns EAH, Yaksh A, Teuwen CP, van der Does LJME, Kik C, Knops P, van Marion DMS, Brundel BJJM, Bogers AJJC, Allesie MA, de Groot NMS <i>International Journal of Cardiology. 2017</i>	
4	The effects of valvular heart disease on atrial conduction during sinus rhythm	63
	van der Does LJME, Lanterns EAH, Teuwen CP, Mouws EMJP, Yaksh A, Knops P, Kik C, Bogers AJJC, de Groot NMS <i>Journal of Cardiovascular Translational Research. 2020</i>	
5	Impact of ischemic and valvular heart disease on atrial excitation: a high- resolution epicardial mapping study	79
	Mouws EMJP, Lanterns EAH, Teuwen CP, van der Does LJME, Kik C, Knops P, Yaksh A, Bekkers JA, Bogers AJJC, de Groot NMS <i>Journal of the American Heart Association. 2018</i>	
6	Epicardial breakthrough waves during sinus rhythm: depiction of the arrhythmogenic substrate?	101
	Mouws EMJP, Lanterns EAH, Teuwen CP, van der Does LJME, Kik C, Knops P, Bekkers JA, Bogers AJJC, de Groot NMS <i>Circulation: Arrhythmia and Electrophysiology. 2017</i>	
7	Relevance of conduction disorders in Bachmann's bundle during sinus rhythm in humans	125
	Teuwen CP, Yaksh A, Lanterns EAH, Kik C, van der Does LJME, Knops P, Taverne YJHJ, van de Woestijne PC, Oei FBS, Bekkers JA, Bogers AJJC, Allesie MA, de Groot NMS <i>Circulation: Arrhythmia and Electrophysiology. 2016</i>	
8	Distribution of conduction disorders in patients with congenital heart disease and right atrial volume overload	147
	Houck CA*, Lanterns EAH*, Heida A, Taverne YJHJ, van de Woestijne PC, Knops P, Roos-Serote MC, Roos-Hesselink JW, Bogers AJJC, de Groot NMS *Both authors contributed equally <i>Journal of the American College of Cardiology: Electrophysiology. 2020</i>	

PART II ELECTROPHYSIOLOGICAL MARKERS DURING ATRIAL FIBRILLATION

- 9 Dynamics of focal fibrillation waves during persistent atrial fibrillation** 167
Lanterns EAH, Allesie MA, de Groot NMS
Pacing and Clinical Electrophysiology. 2016
- 10 Direct proof of endo-epicardial asynchrony of the atrial wall during atrial fibrillation in humans** 173
de Groot NMS, van der Does LJME, Yaksh A, Lanterns EAH, Teuwen CP, Knops P. van de Woestijne CP, Bekkers JA, Kik C, Bogers AJJC, Allesie MA
Circulation: Arrhythmia and Electrophysiology. 2016

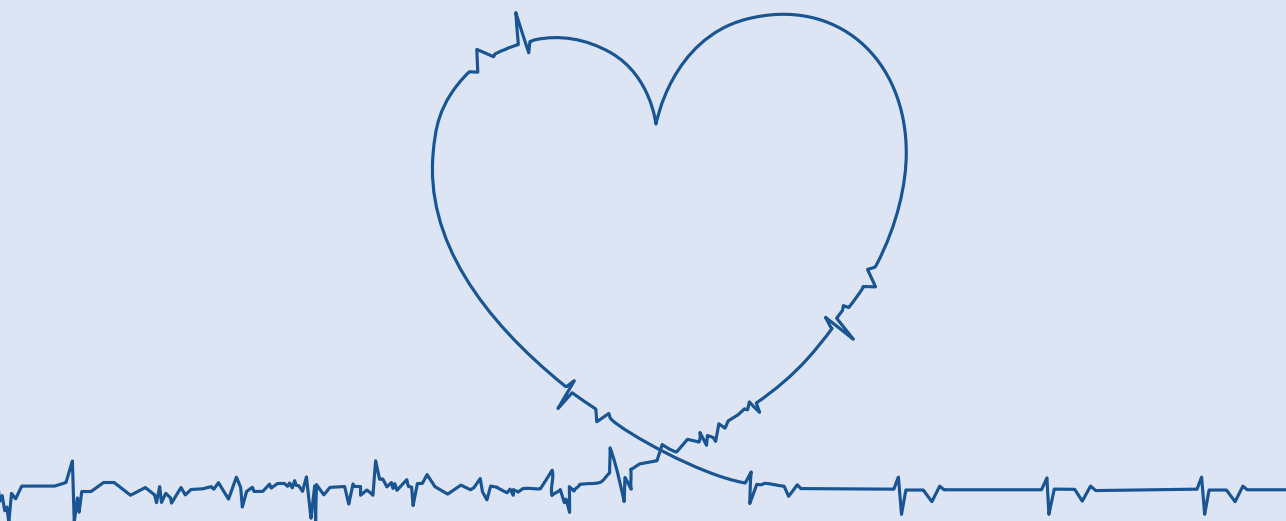
PART III CLINICAL MARKERS FOR PREDICTION OF ATRIAL FIBRILLATION

- 11 Intraoperative inducibility of atrial fibrillation does not predict early postoperative atrial fibrillation** 211
Lanterns EAH, Yaksh A, Teuwen CP, van der Does LJME, van Groningen NJ, Bogers AJJC, de Groot NMS
Journal of the American Heart Association. 2018
- 12 Early markers of atrial fibrillation recurrence after pulmonary vein isolation** 229
Lanterns EAH, Teuwen CP, Hokken T, Rohde S, Haitsma D, Zijlstra F, Jordaens LJM, de Groot NMS
Journal of Arrhythmia. 2020

PART IV BIOMARKERS FOR PREDICTION OF ATRIAL FIBRILLATION

- 13 Diagnosis and therapy of atrial fibrillation: the past, the present and the future** 245
van Marion DMS, Lanterns EAH, Wiersma M, Allesie MA, Brundel BJJM, de Groot NMS
Journal of Atrial Fibrillation. 2015
- 14 The future of atrial fibrillation therapy: intervention on heat shock proteins influencing electropathology is the next in line** 259
Lanterns EAH, van Marion DMS, Steen H de Groot NMS, Brundel BJJM
Netherlands Heart Journal. 2015

15	HALT&REVERSE: Hsf1 activators lower cardiomyocyt damage; towards a novel approach to reverse atrial fibrillation	283
	Lanters EAH, van Marion DMS, Kik X, Steen H, Bogers AJJC, Allessie MA, Brundel BJJM, de Groot NMS	
	<i>Journal of Translational Medicine. 2015</i>	
16	Evaluating serum heat shock protein levels as novel biomarkers for atrial fibrillation	297
	van Marion DMS*, Lanters EAH*, MD; Silva Ramos K, Li J, Marit Wiersma M, Baks-te Bulte L, Muskens A, de Groot NMS, Brundel BJJM	
	* Both authors contributed equally	
	<i>Cells. 2020</i>	
17	Biomarking the electropathological substrate: tissue and serum heat shock protein levels and their relation to atrial conduction properties	319
	Lanters EAH, van Marion DMS, Silva Ramos K, van der Does WFD, Brundel BJJM*, de Groot NMS*	
	* Both authors contributed equally	
18	General discussion and future perspectives	341
	Lanters EAH	
19	English Summary	349
	Lanters EAH	
20	Nederlandse samenvatting	355
	Lanters EAH	
21	Appendices	361
	PhD portfolio	362
	List of publications	367
	About the author	373
	Dankwoord	374





CHAPTER 1



GENERAL INTRODUCTION

Lanters EAH

INTRODUCTION

In 1906, Willem Einthoven was the first to document atrial fibrillation (AF) by means of an electrocardiogram (ECG). By then, the arrhythmia was already known for more than a century and was described in multiple manners, all referring to its irregular nature. During AF, the atria are activated in a rapid and highly irregular fashion which results in an irregular ventricular response. On surface ECG, the arrhythmia is characterized by the absence of distinct P-waves and irregular R-R intervals, as indicated in the lower panel of Figure 1.¹



Figure 1. Rhythm strips. Upper panel: rhythm strip showing sinus rhythm with characterizing positive P-wave preceding each QRS complex. The R-R intervals are regular. Lower panel: rhythm strip during atrial fibrillation. Notice the absence of P-waves and the fast and irregular R-R intervals.

Nowadays, AF is the most common supraventricular arrhythmia, with a prevalence varying from 0.1% up to 12% in the elderly.^{2, 3} The last years however, there is a growing number of young adults presenting with AF, especially (endurance) athletes.⁴ It is expected that the total number of patients diagnosed with AF will be doubled in 2050. Patients experience a wide variety of symptoms (if not asymptomatic), ranging from mild dyspnea to rapid palpitations and/or syncope. It is now known that AF is not just a benign arrhythmia. For example, the presence of AF subjects the patients to an increased risk of AF associated thrombo-embolic events and mortality. In addition, AF alone accounts for 30% of the total arrhythmia-related hospital admissions and healthcare costs.⁵ There is a variety of therapeutic modalities, ranging from anti-arrhythmic drugs to surgical ablation. Some therapies (for example pulmonary vein isolation (PVI) even aim to cure AF. Unfortunately, most patients experience AF recurrences. This is probably due to the inadequate understanding of the mechanisms and electropathological substrate underlying AF. It is therefore important to gain more insight into this topic. The mechanism and substrate can be investigated during sinus rhythm, atrial pacing and atrial fibrillation.

SINUS RHYTHM

In an attempt to find *the* mechanism underlying AF, the vast majority of research directly focuses on conduction properties during the arrhythmia or during atrial pacing. However, atrial

conduction properties during normal sinus rhythm (SR) have rarely been investigated and its importance is therefore unknown. In addition, it is necessary to understand variation in normal conduction properties, in order to define electropathology. At present, there is very little insight into atrial conduction properties during SR.

Electrical waves Exciting the atria generally originate from the sinus node area in the high right atrium. Boineau et al. performed epicardial mapping in 14 patients undergoing surgical ablation of an accessory pathway to investigate the location of the sinus node (area).⁶ They observed up to three different sites of SR impulse origin within one patient. Most the pacemaker sites was located along the sulcus terminalis and junction between the right atrium and the superior caval vein. However, sites of origin were also observed at the inferior caval vein or in the left atrium in case of escape beats. Epicardial and even transmural mapping of the general wavefront propagation during SR was also performed in a human heart Langendorff model (N=2) by Durrer et al.⁷ In this study, wavefronts during SR originated from a relatively large sinus node area, extending along the right atrial – caval junction. The impulse propagated from the sinus node region to the terminal crest, along the interatrial connections and finally to the left atrial appendage. Later, endocardial mapping studies showed that after activation of the right atrium, the left atrium is activated via the inter-atrial septum and Bachmann's Bundle.⁸ ⁹ Since Bachmann's Bundle cannot be reached via the endocardial mapping approach, proof was only obtained indirectly.

Propagation of electrical waves during SR can be impaired by lines of conduction block, as shown by Hansson et al.¹⁰ Epicardial mapping of the RA free wall revealed some degree of slowing of conduction in 3 out of 12 patients undergoing coronary surgery or surgical transection of an accessory pathway. Conduction disorders at the terminal crest region have also been described in patients with typical atrial flutter (endocardial mapping).¹¹ In addition, Federov et al. demonstrated an area of conduction block in the sinus node region using in vitro optical mapping¹². Left atrial epicardial mapping studies also described conduction block at the junction of the right superior pulmonary and the left atrium in 18 patients without AF.¹³

ATRIAL FIBRILLATION

With currently available diagnostic tools such as surface ECGs, Holter recordings and implantable loop recorders it is possible to detect AF and also to quantify the AF burden within a certain time window. However, it is not (yet) possible to determine the *mechanism* underlying AF in the individual patient. When AF is diagnosed, atrial remodeling is assumed to be already present in all patients, although in different stages. It is likely that patients with (longstanding) persistent AF have more advanced levels of atrial remodeling. Unfortunately, none of the diagnostic tools currently available in clinical practice allow identification or staging of this electrical *substrate*.

Once diagnosed, AF is classified according to its presenting pattern. If the episode is terminated within seven days (either self-terminating or cardioverted), it is considered paroxysmal AF. In case of persistent AF the episodes exceed the duration of seven days and becomes long-standing persistent if it is present for longer than a year (continuously). When AF is accepted and further rhythm control is no longer attempted, it is referred to as permanent AF.¹

Mechanisms of atrial fibrillation

Unfortunately, the mechanism(s) underlying AF are still under debate and consensus has not yet been reached. Initially, Moe et al hypothesized that AF was either due to true fibrillation (AF persists independently from the site of initiation) or to fibrillatory conduction.¹⁴ In the latter case, an ectopic focus discharges at a high frequency causing non-uniform excitation of the atria. Foci may either be fixed or shift throughout the atria. AF can also be caused by a combination of these proposed mechanisms. In his Multiple Wavelet Hypothesis, Moe explains that AF persistence depends on the number of fibrillation waves.¹⁴ An increasing number of waves would make AF termination less likely to occur. Whereas Moe experimented in isolated canine right atria, evaluation of this hypothesis was performed by Allesie et al in a Langendorff canine heart model.¹⁵ They showed that the critical number of waves needed for AF perpetuation was three to six.

In the following years, mechanisms underlying AF were studied in both experimental and clinical mapping studies. Overall, the investigators support the presence of either a focal (repetitive ectopic discharges) or reentry mechanism (e.g. mother-waves, rotors, multiple wavelets).¹⁶⁻²⁴ For example, ectopic beats originating from the sleeves of the pulmonary veins as triggers for AF initiation were firstly proposed by Haissaguerre in 1998, based on human endocardial mapping studies.²⁴ However, *non*-pulmonary vein foci located at e.g. the superior vena cava, posterior free wall of the left atrium, terminal crest and the interatrial septum also generate ectopic beats that may initiate AF episodes.^{25, 26}

Substrate underlying atrial fibrillation

From previous epicardial mapping studies during AF by Allesie and De Groot et al. we have learned that longitudinal dissociation in conduction and epicardial breakthrough waves (EBW) are key elements of the substrate underlying AF.^{27, 28} In paroxysmal AF most fibrillation waves are single, broad activation fronts. However, after progression to (long-standing) persistent AF a far more complex activation pattern including multiple (smaller) fibrillation waves and areas of conduction block exists.^{17, 27, 29} Compared to patients with electrically induced AF, the amount of conduction block was 4 times higher in patients with longstanding persistent AF.²⁷ In addition, the incidence of EBWs showed a 4-fold increase in the latter patient group.²⁸ The concept of EBWs during AF is further explained in Figure 2. The color-coded activation map in left panel shows synchronous activation of the endo- and the epicardium by a single fibrillation wave. In the right panel however, wavefront propagation in the epicardium is obstructed by an area of conduction block causing asynchronous conduction of the two layers. In this example, the wavefront traveling over the endocardium crosses over to the epicardial sites that has not yet been activated. Consequently, it “breaks through” and initiates an EBW at the epicardial layer.

Several potential mechanisms for EBWs have been proposed, including transmural conduction, transmural reentry, ectopic discharges and rotors. However, there are multiple observations that make focal activity as an underlying cause less likely.^{28, 30} First, electrogram morphology at the site of EBW origin showed R-waves (1) which suggests the presence of a depolarization wave propagating towards the epicardium from either the endocardium or from deeper transmural layers. Also, EBWs were not repetitive (2) and occurred throughout the

entire atria without a clear predilection site (3) as would be expected in case of focal activity. Finally, the coupling intervals were highly irregular, not as short as expected or could even be longer than the average cycle length (4). As repetivity was not observed, an intramural focus or transmural reentry is unlikely. If an intramural reentry underlies EBWs, than it would require a very low conduction velocity throughout the reentry circuit.

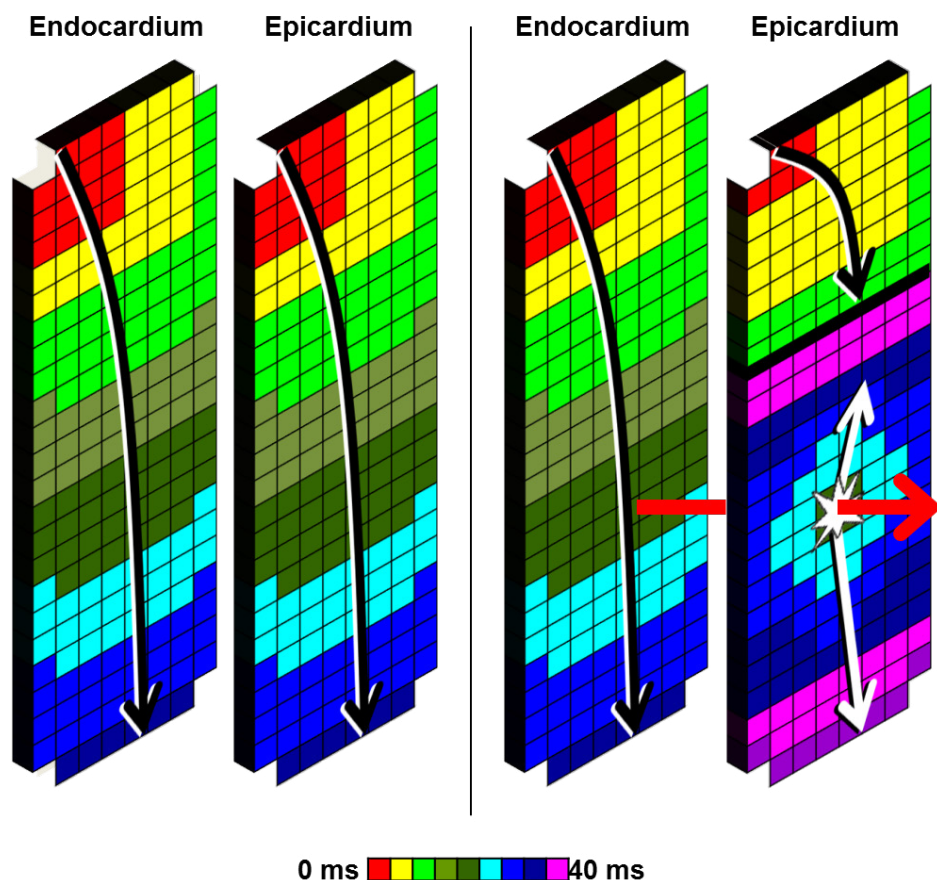


Figure 2. Epicardial breakthrough waves. Left panel: color-coded activation map showing synchronous activation of the endo- and epicardium by a single wavefront. Direction of propagation is indicated by the arrow and follows the color scheme provided below. Right panel: thick black line indicates an area of conduction block in the epicardial plane resulting in asynchronous wavefront propagation. The area behind the conduction block is not yet activated. The wavefront activating the endocardium can thus cross over to the endocardium and introduce an EBW. Black arrow: wavefront from a peripheral wave. Star: site of epicardial breakthrough. White arrow: wavefront from an EBW.

The latest proposed mechanism for AF originates from the EBWs as observed with epicardial mapping and is described in the Double Layer Hypothesis. This hypothesis adds a third dimension to the AF process. Whereas other hypotheses are all based on 2-dimensional conduction in either the endocardial or epicardial plane (dependent on the mapping approach), the Double Layer Hypothesis assumes transmural conduction between those planes.

Asynchronous electrical activation of these planes allows fibrillation waves to consequently cross from one layer to another. This results in EBWs constantly activating the opposite layer (Figure 2). EBWs are likely to further enhance the asynchrony and consequently the irregular patterns of activation during AF that eventually stabilize the process and may thus promote further AF persistence.

Within hours after first time AF onset, the process of electrical and structural remodeling and thus substrate formation commences. This principle (AF begets AF) has been explained extensively by *Wijffels et al* in a goat model.³¹ In the first six hours a significant decrease in fibrillation intervals was observed. If this interval passed the threshold of 120 ms, AF episode duration increased considerably. The atrial effective refractory period shortened with 35%, hereby making the atrial tissue more vulnerable for arrhythmia inducement after a premature beat. Table 1 summarizes alterations on structural, electrical and contractile levels.^{1, 31-35} The overall clinical result is that, due to AF persistence, patients are more prone to develop new AF episodes. In addition, these new episodes have increasing lengths. Hence, the ratio of sinus rhythm duration to AF duration decreases over time.

Table 1. Atrial remodeling as induced by atrial fibrillation

Structural remodeling	Electrical remodeling	Contractile remodeling
Extracellular matrix	Shortening of APD	Atrial hypocontractility
Fibrosis		
Inflammation		
Amyloid deposition		
Fat		
Myocyt	Shortening AFCL	
Apoptosis	Shortening AERP	
Necrosis		
Hypertrophy	Loss of rate adaptation	
Dedifferentiation		
Gap-junction remodeling		
Glycogen accumulation		
Increased diameter		
Microvascular changes		
Ion channel remodeling		
Calcium handling instability		

APD: action potential duration; AFCL: atrial fibrillation cycle length; AERP: atrial effective refractory period.

One of the proposed mechanisms underlying electrical remodeling (early and reversible) due to atrial fibrillation is based on alterations in calcium handling in AF.³⁵⁻³⁸ The increase in atrial rate during AF increases the Ca²⁺ load. Cardiac myocytes try to compensate the higher calcium levels by reducing the Ca²⁺ influx. This however, leads to a decrease in action potential duration and a shorter wavelength, which helps in maintaining AF episodes. The flowchart in Figure 3 illustrates that an increase of intracellular [Ca²⁺] leads to a higher likelihood of spontaneous Ca²⁺ release by the Sarcoplasmic reticulum. The intracellular calcium overload may provoke delayed afterdepolarizations, which in turn can produce triggered activity. Apart from the effect on electrical remodeling, the calcium overload also induces structural remodeling (late and irreversible) due to derailment of proteostasis (essential for e.g. protein synthesis and folding, Figure 3). Consequently, cardiomyocyte hypertrophy, fibroblast proliferation and

deposition of extracellular matrix lead to separation of adjacent bundles of cardiomyocytes and subsequently conduction block.³⁹ Redistribution of cell-cell connexins and downregulation of ion channels also cause impaired conduction.⁴⁰ Next to these conduction abnormalities, coupling of myofibroblast and cardiomyocytes also facilitates induction of spontaneous ectopic activity.⁴¹

Treatment of atrial fibrillation

According to current guidelines, therapeutic strategies should initially be aimed at rhythm control to avoid further electrical, structural and/or contractile remodeling.¹ Anti-arrhythmic drugs that widen the excitable period and thus decrease the number of fibrillation waves present in the atria include class I and class III drugs. Immediate conversion can be achieved in up to 75% and 97% of patients by respectively chemical or electrical cardioversion, however recurrences are very often observed afterwards.

Therapeutic modalities that are assumed to be curative include either trigger or substrate focused invasive procedures. By endovascular pulmonary vein isolation (PVI), ectopic triggers in the sleeves of the pulmonary veins are isolated, as illustrated in Figure 4. This can be achieved by either manual, Robotic or magnetic navigation. Cryoballoon or cryo- or radiofrequency energy, with or without the use of electroanatomical mapping systems are used at the physician's discretion. Despite the variety of techniques available, effect on patient outcome remains limited. One year after procedures, only 40-50% of patients remain free of AF.⁴²⁻⁴⁵ After multiple ablation procedure the success rate may increase to 79%.⁴⁶

Recurrences can be explained by incompleteness of the circular lesions around the pulmonary veins, however patients may also have developed a more substrate-dependent stage of AF. The strategy becomes more substrate focused when ablation of ganglionic plexi, complex fractionated atrial electrograms or rotors is included. The classic surgical PVI following the maze pattern also focusses on both trigger and substrate. Nonetheless, reported success rates vary from only 59% to 74% when performed in addition to the classical PVI.⁴⁷⁻⁴⁹ The fact that recurrence rates remain rather high despite all the technical possibilities indicates that at least part of the arrhythmogenic substrate underlying AF is still not fully understood. In order to increase the long-term AF free survival, it is thus necessary to gain insight into this arrhythmogenic substrate.

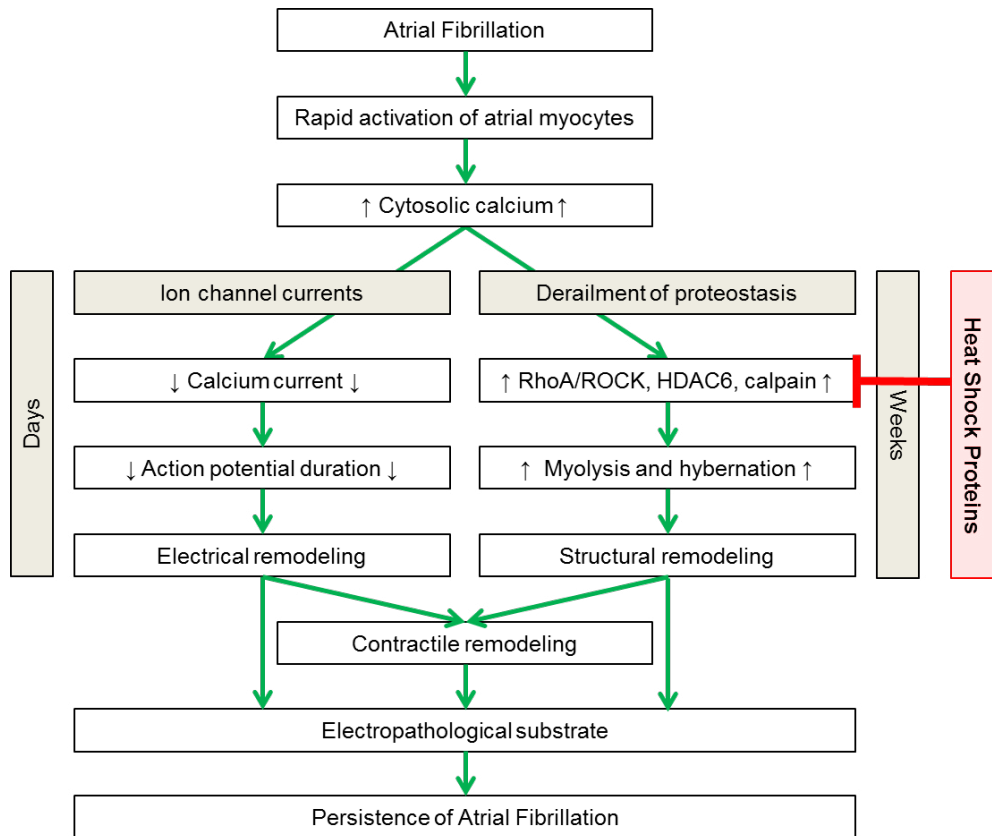


Figure 3. Atrial remodeling of the cardiomyocyte. Atrial fibrillation causes a calcium overload which leads to changes in ion channel currents and derailment of proteostasis. This in turn results in remodeling on electrical, structural and contractile levels that all contribute to the development of an electropathological substrate underlying AF persistence. Heat shock proteins inhibit the derailment of proteostasis by inhibition of RhoA/ROCK, HDAC6 and calpains.

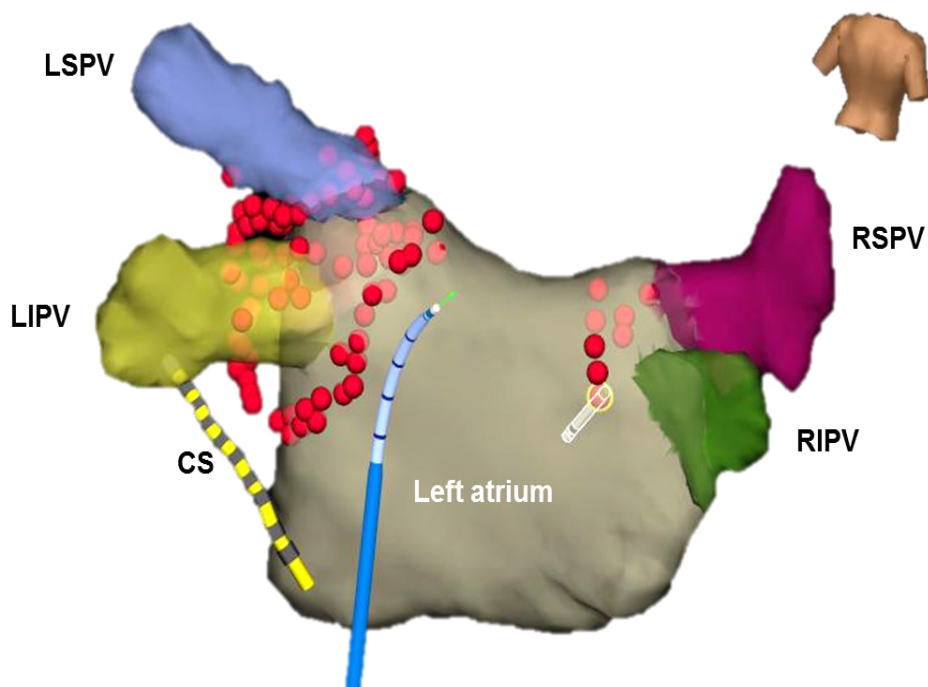


Figure 4. Pulmonary vein isolation. Posterior view of the left atrium with the ostia of the four pulmonary veins. The yellow catheter is positioned in the coronary sinus. The blue catheter represents the ablation catheter. Point-by-point encirclement (applications indicated by red dots) of the left pulmonary veins is completed. LSPV: left superior pulmonary vein; LIPV: left inferior pulmonary vein; RSPV: right superior pulmonary vein; RIPV: right inferior pulmonary vein; CS: coronary sinus.

BIOMARKERS FOR ATRIAL FIBRILLATION

Although mapping techniques offer a unique chance to evaluate the conductive properties on a personal and high-resolution scale, it remains invasive and is thus not suitable as a standard diagnostic test in daily clinical practice. To solve the problem of therapy-resistance of AF it is mandatory to assess the extensiveness of the electropathological substrate at time of diagnosis in each individual patient. Without knowledge on the severity of AF and the underlying mechanism, it is very hard (if not impossible) to individualize AF treatment. Besides the electrical markers that might be determined in a non-invasive manner, serum biomarkers are nowadays also an accessible tool for staging of a disease.

Multiple prospective, large cohort studies already investigated if for example CRP, BNP and (NT-pro)BNP were usable biomarkers.⁵⁰ However, they all used development of AF related adverse events as an endpoint, rather than development or progression of AF itself. Also, the biomarkers of interest were often non-specific and associated with multiple conditions predisposing for AF such as infection, heart failure or ischemia. As a result, associations between the proposed biomarkers and rhythm outcomes were absent.

As mentioned earlier, derailment of cardiomyocyte proteostasis promotes atrial remodeling. Proteostasis is assisted by various chaperones, including Heat Shock Proteins (HSPs). Due to myocyte stress (AF), HSPs are initially upregulated and help in protein refolding, prevent structural damage to contractile proteins and attenuate the breakdown of proteins.⁵¹⁻⁵⁴ They thus might prevent progression of atrial remodeling and consequently AF progression. However, HSP levels become exhausted over time, resulting in a derailment of proteostasis. The molecular pathways (also displayed in Figure 3) underlying derailed proteostasis include activation of calpains, RhoA/ROCK and HDAC6. Calpains are activated by an intracellular calcium overload in both *Drosophila* and human models. Activation initiates degradation of contractile and structural proteins, leading to myolysis of the cardiomyocyte.^{38, 55} RhoA-GTPases are also activated during AF and act as regulators of the actin cytoskeleton of cardiomyocytes. Activation of RhoA and subsequently ROCK results in impaired calcium homeostasis and induces conduction disorders, contractile dysfunction and alteration of the cardiomyocyte.^{51, 56} Upregulation of various members of the HSP family inhibits these three pathways that lead to atrial remodeling. In addition, antibody titers to e.g. HSP27, HSP60 and HSP70 were elevated in patients with myocardial infarction, metabolic syndrome or coronary artery disease.⁵⁷⁻⁶¹

BIOLOGICAL MARKERS FOR ATRIAL FIBRILLATION

AF is associated with various clinical parameters, including increasing age, hypertension, heart failure, coronary artery disease or valvular heart disease.^{62, 63} Furthermore, AF recurrences after PVI are associated with e.g. left atrial enlargement and low left atrial flow velocity.⁶⁴⁻⁶⁶ In contrast, more specific electrophysiological parameters associated with AF initiation or perpetuation are less clear.

One of the most well-accepted characteristics of AF is its highly irregular nature, marked by an irregular atrial fibrillation cycle length (AFCL). The AFCL is determined by action potential duration (refractory period) and an excitable period. Due to electrical remodeling, AF persistence causes a decrease of the refractory period, an increase in the number of fibrillatory waves and is consequently associated with shortening of the mean AFCL.³¹ It has been shown that (mean) AFCL is a predictor of termination of AF during ablation and is therefore suggested as a predictor for the arrhythmogenic substrate.^{67, 68} Also, mean AFCL is similar in both left and right atria of patients with longstanding persistent AF, suggesting more advanced stages of structural remodeling in these patients.^{69, 70}

AIM OF THE THESIS

In this thesis we aim to identify novel biological markers and biomarkers for AF initiation and/or progression. We hereto investigate atrial conduction properties during sinus rhythm and atrial fibrillation in patients with different underlying heart diseases. In addition, biomarkers including HSPs are determined in cardiac tissue and serum of the study subjects. Furthermore, clinical parameters such as AF inducibility and the incidence of atrial extrasystolic beats are tested as novel markers for AF development and/or recurrence.

OUTLINE OF THE THESIS

Although insights into the pathophysiology of atrial fibrillation have increased, the mechanism underlying AF is still not fully understood. **Chapter 2** illustrates this lacuna in our knowledge and how it affects therapy outcomes and thereby also outlines the importance of research in this field.

In **Chapter 3** we investigated not only the presence but also the spatial distribution of CB in the human epicardial surface. For this purpose, we performed high-resolution intra-operative epicardial mapping studies in patients undergoing coronary artery bypass grafting (CABG). By obtaining consecutive recordings at various predefined recording sites, the entire epicardial surface of the left and right atria and Bachmann's Bundle were explored. To investigate patients with other cardiovascular diseases, we performed similar mapping studies in patients with valvular heart disease (VHD). The result of this study are presented in **Chapter 4**. In **Chapter 5** we evaluate atrial activation patterns and the impact on total atrial activation times in patients with coronary artery disease and/or VHD using the same mapping approach.

Epicardial breakthrough waves (EBWs) have been identified as a cornerstone of the activation pattern during AF. In **Chapter 6** we examine the incidence and characteristics of EBWs during SR in a similar study population consisting of patients with coronary artery disease and/or VHD.

Since our mapping approach is one of the first to allow direct investigation of Bachmann's Bundle on a high-resolution scale, we present an in-depth analysis of this specific area of interest in **Chapter 7** including a further investigation on conduction disorders, patterns of activation and the presence of EBWs. Finally, characteristics of CB were also evaluated in an unique group of adult patients with uncorrected congenital heart defects (CHD), in whom structural (atrial) alterations and thus conduction disorders are assumed to be most pronounced. The results of this study are presented in **Chapter 8**.

In **Chapter 9** we present a typical patient with persistent AF. The presence and spatial distribution of EBWs during AF is evaluated by epicardial mapping. Thereafter, the first direct proof of endo-epicardial asynchrony in humans of this concept is thereafter provided in **Chapter 10**, using a simultaneous endo-epicardial mapping approach.

The next section of the thesis aims to identify novel clinical markers. In **Chapter 11** the predictive value of intra-operative AF inducibility for development of de novo early post-operative AF or AF recurrence is tested. Furthermore, we investigated the association between the number of atrial extrasystole prior to pulmonary vein isolation in AF patients and (timing of) post-procedural AF recurrences in **Chapter 12**.

The last part of the thesis focusses on chemical blood- and tissue based biomarkers. An overview of the development of diagnostic and therapeutic tools for AF as well as a more extensive background on HSPs is provided in **Chapter 13**. Furthermore, **Chapter 14** elaborates on the potentials of HSP as a druggable target in AF treatment. **Chapter 15** presents the outline of the HALT&REVERSE project. We present the first results of this project in the remaining two chapters. In **Chapter 16** we investigate various serum HSP levels in control patients and AF patients undergoing electrical cardioversion or pulmonary vein isolation. The relation

between serum HSP levels and presence of AF, type of AF and AF recurrence is evaluated. Finally, **Chapter 17** provides insight in both serum and tissue HSP levels in patients (with and without AF) undergoing cardiothoracic surgery. In addition, the serum and tissue HSP levels are correlated with electropathology as identified by epicardial mapping during SR.

REFERENCES

1. Kirchhof P, Benussi S, Kotecha D, Ahlsson A, Atar D, Casadei B, Castella M, Diener HC, Heidbuchel H, Hendriks J, Hindricks G, Manolis AS, Oldgren J, Popescu BA, Schotten U, Van Putte B, Vardas P and Group ESCSD. 2016 ESC Guidelines for the management of atrial fibrillation developed in collaboration with EACTS. *Eur Heart J*. 2016;37:2893-2962.
2. Miyasaka Y, Barnes ME, Gersh BJ, Cha SS, Bailey KR, Abhayaratna WP, Seward JB and Tsang TS. Secular trends in incidence of atrial fibrillation in Olmsted County, Minnesota, 1980 to 2000, and implications on the projections for future prevalence. *Circulation*. 2006;114:119-25.
3. Wilke T, Groth A, Mueller S, Pfannkuche M, Verheyen F, Linder R, Maywald U, Bauersachs R and Breithardt G. Incidence and prevalence of atrial fibrillation: an analysis based on 8.3 million patients. *Europace*. 2013;15:486-93.
4. Aizer A, Gaziano JM, Cook NR, Manson JE, Buring JE and Albert CM. Relation of vigorous exercise to risk of atrial fibrillation. *Am J Cardiol*. 2009;103:1572-7.
5. Patel NJ, Deshmukh A, Pant S, Singh V, Patel N, Arora S, Shah N, Chothani A, Savani GT, Mehta K, Parikh V, Rathod A, Badheka AO, Lafferty J, Kowalski M, Mehta JL, Mitrani RD, Viles-Gonzalez JF and Paydak H. Contemporary trends of hospitalization for atrial fibrillation in the United States, 2000 through 2010: implications for healthcare planning. *Circulation*. 2014;129:2371-9.
6. Boineau JP, Canavan TE, Schuessler RB, Cain ME, Corr PB and Cox JL. Demonstration of a widely distributed atrial pacemaker complex in the human heart. *Circulation*. 1988;77:1221-37.
7. Durrer D, van Dam RT, Freud GE, Janse MJ, Meijler FL and Arzbaecher RC. Total excitation of the isolated human heart. *Circulation*. 1970;41:899-912.
8. Lemery R, Birnie D, Tang AS, Green M, Gollob M, Hendry M and Lau E. Normal atrial activation and voltage during sinus rhythm in the human heart: an endocardial and epicardial mapping study in patients with a history of atrial fibrillation. *J Cardiovasc Electrophysiol*. 2007;18:402-8.
9. Tapanainen JM, Jurkko R, Holmqvist F, Husser D, Kongstad O, Makijarvi M, Toivonen L and Platonov PG. Interatrial right-to-left conduction in patients with paroxysmal atrial fibrillation. *J Interv Card Electrophysiol*. 2009;25:117-22.
10. Hansson A, Holm M, Blomstrom P, Johansson R, Luhrs C, Brandt J and Olsson SB. Right atrial free wall conduction velocity and degree of anisotropy in patients with stable sinus rhythm studied during open heart surgery. *Eur Heart J*. 1998;19:293-300.
11. Morton JB, Sanders P, Vohra JK, Sparks PB, Morgan JG, Spence SJ, Grigg LE and Kalman JM. Effect of chronic right atrial stretch on atrial electrical remodeling in patients with an atrial septal defect. *Circulation*. 2003;107:1775-1782.
12. Fedorov VV, Glukhov AV, Chang R, Kostecki G, Aferol H, Hucker WJ, Wuskell JP, Loew LM, Schuessler RB, Moazami N and Efimov IR. Optical mapping of the isolated coronary-perfused human sinus node. *J Am Coll Cardiol*. 2010;56:1386-94.
13. Lee G, Spence S, Teh A, Goldblatt J, Larobina M, Atkinson V, Brown R, Morton JB, Sanders P, Kistler PM and Kalman JM. High-density epicardial mapping of the pulmonary vein-left atrial junction in humans: insights into mechanisms of pulmonary vein arrhythmogenesis. *Heart Rhythm*. 2012;9:258-64.
14. Moe GK and Abildskov JA. Atrial fibrillation as a self-sustaining arrhythmia independent of focal discharge. *Am Heart J*. 1959;58:59-70.
15. Allesie M, Lammers WJEP, Bonke FIM and Hollen SJ. Experimental Evaluation of Moe's Multiple Wavelet Hypothesis of Atrial Fibrillation. *Cardiac Electrophysiology and Arrhythmias*. 1985:265-275.
16. Allesie MA, Bonke FI and Schopman FJ. Circus movement in rabbit atrial muscle as a mechanism of tachycardia. III. The "leading circle" concept: a new model of circus movement in cardiac tissue without the involvement of an anatomical obstacle. *Circ Res*. 1977;41:9-18.

17. Konings KT, Kirchhof CJ, Smeets JR, Wellens HJ, Penn OC and Allessie MA. High-density mapping of electrically induced atrial fibrillation in humans. *Circulation*. 1994;89:1665-80.
18. Mandapati R, Skanes A, Chen J, Berenfeld O and Jalife J. Stable microreentrant sources as a mechanism of atrial fibrillation in the isolated sheep heart. *Circulation*. 2000;101:194-9.
19. Jalife J, Berenfeld O and Mansour M. Mother rotors and fibrillatory conduction: a mechanism of atrial fibrillation. *Cardiovasc Res*. 2002;54:204-16.
20. Waldo AL. Mechanisms of atrial fibrillation. *J Cardiovasc Electrophysiol*. 2003;14:S267-74.
21. Moe GK, Rheinboldt WC and Abildskov JA. A Computer Model of Atrial Fibrillation. *Am Heart J*. 1964;67:200-20.
22. Narayan SM, Krummen DE, Shivkumar K, Clopton P, Rappel WJ and Miller JM. Treatment of atrial fibrillation by the ablation of localized sources: CONFIRM (Conventional Ablation for Atrial Fibrillation With or Without Focal Impulse and Rotor Modulation) trial. *J Am Coll Cardiol*. 2012;60:628-36.
23. Lewis T. Oliver-Sharpey Lectures ON THE NATURE OF FLUTTER AND FIBRILLATION OF THE AURICLE. *Br Med J*. 1921;1:551-5.
24. Haissaguerre M, Jais P, Shah DC, Takahashi A, Hocini M, Quiniou G, Garrigue S, Le Mouroux A, Le Metayer P and Clementy J. Spontaneous initiation of atrial fibrillation by ectopic beats originating in the pulmonary veins. *N Engl J Med*. 1998;339:659-66.
25. Inada K, Matsuo S, Tokutake K, Yokoyama K, Hioki M, Narui R, Ito K, Tanigawa S, Yamashita S, Tokuda M, Shibayama K, Miyayama S, Sugimoto K, Yoshimura M and Yamane T. Predictors of ectopic firing from the superior vena cava in patients with paroxysmal atrial fibrillation. *J Interv Card Electrophysiol*. 2015;42:27-32.
26. Lin WS, Tai CT, Hsieh MH, Tsai CF, Lin YK, Tsao HM, Huang JL, Yu WC, Yang SP, Ding YA, Chang MS and Chen SA. Catheter ablation of paroxysmal atrial fibrillation initiated by non-pulmonary vein ectopy. *Circulation*. 2003;107:3176-83.
27. Allessie MA, de Groot NM, Houben RP, Schotten U, Boersma E, Smeets JL and Crijns HJ. Electropathological substrate of long-standing persistent atrial fibrillation in patients with structural heart disease: longitudinal dissociation. *Circ Arrhythm Electrophysiol*. 2010;3:606-15.
28. de Groot NM, Houben RP, Smeets JL, Boersma E, Schotten U, Schalij MJ, Crijns H and Allessie MA. Electropathological substrate of longstanding persistent atrial fibrillation in patients with structural heart disease: epicardial breakthrough. *Circulation*. 2010;122:1674-82.
29. Yaksh A, Kik C, Knops P, Roos-Hesselink JW, Bogers AJ, Zijlstra F, Allessie M and de Groot NM. Atrial fibrillation: to map or not to map? *Neth Heart J*. 2014;22:259-66.
30. Lee G, Kumar S, Teh A, Madry A, Spence S, Larobina M, Goldblatt J, Brown R, Atkinson V, Moten S, Morton JB, Sanders P, Kistler PM and Kalman JM. Epicardial wave mapping in human long-lasting persistent atrial fibrillation: transient rotational circuits, complex wavefronts, and disorganized activity. *Eur Heart J*. 2014;35:86-97.
31. Wijffels MC, Kirchhof CJ, Dorland R and Allessie MA. Atrial fibrillation begets atrial fibrillation. A study in awake chronically instrumented goats. *Circulation*. 1995;92:1954-68.
32. Ausma J, Litjens N, Lenders MH, Duimel H, Mast F, Wouters L, Ramaekers F, Allessie M and Borgers M. Time course of atrial fibrillation-induced cellular structural remodeling in atria of the goat. *J Mol Cell Cardiol*. 2001;33:2083-94.
33. Ausma J, van der Velden HM, Lenders MH, van Ankeren EP, Jongsma HJ, Ramaekers FC, Borgers M and Allessie MA. Reverse structural and gap-junctional remodeling after prolonged atrial fibrillation in the goat. *Circulation*. 2003;107:2051-8.
34. Neuberger HR, Schotten U, Blaauw Y, Vollmann D, Eijssbouts S, van Hunnik A and Allessie M. Chronic atrial dilation, electrical remodeling, and atrial fibrillation in the goat. *J Am Coll Cardiol*. 2006;47:644-53.
35. Schotten U, Duytschaever M, Ausma J, Eijssbouts S, Neuberger HR and Allessie M.

Electrical and contractile remodeling during the first days of atrial fibrillation go hand in hand. *Circulation*. 2003;107:1433-9.

36. Nattel S, Burstein B and Dobrev D. Atrial remodeling and atrial fibrillation: mechanisms and implications. *Circ Arrhythm Electrophysiol*. 2008;1:62-73.

37. Greiser M, Lederer WJ and Schotten U. Alterations of atrial Ca(2+) handling as cause and consequence of atrial fibrillation. *Cardiovasc Res*. 2011;89:722-33.

38. Brundel BJ, Ausma J, van Gelder IC, Van der Want JJ, van Gilst WH, Crijns HJ and Henning RH. Activation of proteolysis by calpains and structural changes in human paroxysmal and persistent atrial fibrillation. *Cardiovasc Res*. 2002;54:380-9.

39. Ausma J, Wijffels M, Thone F, Wouters L, Allesie M and Borgers M. Structural changes of atrial myocardium due to sustained atrial fibrillation in the goat. *Circulation*. 1997;96:3157-63.

40. van der Velden HM, Ausma J, Rook MB, Hellemons AJ, van Veen TA, Allesie MA and Jongsma HJ. Gap junctional remodeling in relation to stabilization of atrial fibrillation in the goat. *Cardiovasc Res*. 2000;46:476-86.

41. Miragoli M, Salvarani N and Rohr S. Myofibroblasts induce ectopic activity in cardiac tissue. *Circ Res*. 2007;101:755-8.

42. Di Biase L, Fahmy TS, Patel D, Bai R, Civello K, Wazni OM, Kanj M, Elayi CS, Ching CK, Khan M, Popova L, Schweikert RA, Cummings JE, Burkhardt JD, Martin DO, Bhargava M, Dresing T, Saliba W, Arruda M and Natale A. Remote magnetic navigation: human experience in pulmonary vein ablation. *J Am Coll Cardiol*. 2007;50:868-74.

43. Luthje L, Vollmann D, Seegers J, Dorenkamp M, Sohns C, Hasenfuss G and Zabel M. Remote magnetic versus manual catheter navigation for circumferential pulmonary vein ablation in patients with atrial fibrillation. *Clin Res Cardiol*. 2011;100:1003-11.

44. Saliba W, Reddy VY, Wazni O, Cummings JE, Burkhardt JD, Haissaguerre M, Kautzner J, Peichl P, Neuzil P, Schibgilla V, Noelker G, Brachmann J, Di Biase L, Barrett C, Jais P and

Natale A. Atrial fibrillation ablation using a robotic catheter remote control system: initial human experience and long-term follow-up results. *J Am Coll Cardiol*. 2008;51:2407-11.

45. Bordignon S, Chun KR, Gunawardene M, Fuernkranz A, Urban V, Schulte-Hahn B, Nowak B and Schmidt B. Comparison of balloon catheter ablation technologies for pulmonary vein isolation: the laser versus cryo study. *J Cardiovasc Electrophysiol*. 2013;24:987-94.

46. Ganesan AN, Shipp NJ, Brooks AG, Kuklik P, Lau DH, Lim HS, Sullivan T, Roberts-Thomson KC and Sanders P. Long-term outcomes of catheter ablation of atrial fibrillation: a systematic review and meta-analysis. *J Am Heart Assoc*. 2013;2:e004549.

47. Wu SH, Jiang WF, Gu J, Zhao L, Wang YL, Liu YG, Zhou L, Gu JN, Xu K and Liu X. Benefits and risks of additional ablation of complex fractionated atrial electrograms for patients with atrial fibrillation: a systematic review and meta-analysis. *Int J Cardiol*. 2013;169:35-43.

48. Mikhaylov E, Kanidieva A, Sviridova N, Abramov M, Gureev S, Szili-Torok T and Lebedev D. Outcome of anatomic ganglionated plexi ablation to treat paroxysmal atrial fibrillation: a 3-year follow-up study. *Europace*. 2011;13:362-70.

49. Pokushalov E, Romanov A, Artyomenko S, Turov A, Shugayev P, Shirokova N and Katritsis DG. Ganglionated plexi ablation for longstanding persistent atrial fibrillation. *Europace*. 2010;12:342-6.

50. Kornej J, Apostolakis S, Bollmann A and Lip GY. The emerging role of biomarkers in atrial fibrillation. *Can J Cardiol*. 2013;29:1181-93.

51. Ke L, Meijering RA, Hoogstra-Berends F, Mackovicova K, Vos MJ, Van Gelder IC, Henning RH, Kampinga HH and Brundel BJ. HSPB1, HSPB6, HSPB7 and HSPB8 protect against RhoA GTPase-induced remodeling in tachypaced atrial myocytes. *PLoS One*. 2011;6:e20395.

52. Meijering RA, Henning RH and Brundel BJ. Reviving the protein quality control system: therapeutic target for cardiac disease in the elderly. *Trends Cardiovasc Med*. 2015;25:243-7.

53. Zhang D, Ke L, Mackovicova K, Van Der Want JJ, Sibon OC, Tanguay RM, Morrow G, Henning RH, Kampinga HH and Brundel BJ. Effects of different small HSPB members on contractile dysfunction and structural changes in a *Drosophila melanogaster* model for Atrial Fibrillation. *J Mol Cell Cardiol.* 2011;51:381-9.
54. Brundel BJ, Henning RH, Ke L, van Gelder IC, Crijns HJ and Kampinga HH. Heat shock protein upregulation protects against pacing-induced myolysis in HL-1 atrial myocytes and in human atrial fibrillation. *J Mol Cell Cardiol.* 2006;41:555-62.
55. Ke L, Qi XY, Dijkhuis AJ, Chartier D, Nattel S, Henning RH, Kampinga HH and Brundel BJ. Calpain mediates cardiac troponin degradation and contractile dysfunction in atrial fibrillation. *J Mol Cell Cardiol.* 2008;45:685-93.
56. Brown JH, Del Re DP and Sussman MA. The Rac and Rho hall of fame: a decade of hypertrophic signaling hits. *Circ Res.* 2006;98:730-42.
57. Novo G, Cappello F, Rizzo M, Fazio G, Zambuto S, Tortorici E, Marino Gammazza A, Corrao S, Zummo G, De Macario EC, Macario AJ, Assennato P, Novo S and Li Volti G. Hsp60 and heme oxygenase-1 (Hsp32) in acute myocardial infarction. *Transl Res.* 2011;157:285-92.
58. Giannessi D, Colotti C, Maltinti M, Del Ry S, Prontera C, Turchi S, Labbate A and Neglia D. Circulating heat shock proteins and inflammatory markers in patients with idiopathic left ventricular dysfunction: their relationships with myocardial and microvascular impairment. *Cell Stress Chaperones.* 2007;12:265-74.
59. Zhu J, Quyyumi AA, Rott D, Csako G, Wu H, Halcox J and Epstein SE. Antibodies to human heat-shock protein 60 are associated with the presence and severity of coronary artery disease: evidence for an autoimmune component of atherogenesis. *Circulation.* 2001;103:1071-5.
60. Birnie DH, Hood S, Holmes E and Hillis WS. Anti-heat shock protein 65 titres in acute myocardial infarction. *Lancet.* 1994;344:1443.
61. Pourghadamyari H, Moohebaty M, Parizadeh SM, Falsoleiman H, Dehghani M, Fazlinezhad A, Akhlaghi S, Tavallaie S, Sahebkar A, Paydar R, Ghayour-Mobarhan M and Ferns GA. Serum antibody titers against heat shock protein 27 are associated with the severity of coronary artery disease. *Cell Stress Chaperones.* 2011;16:309-16.
62. Zoni-Berisso M, Lercari F, Carazza T and Domenicucci S. Epidemiology of atrial fibrillation: European perspective. *Clin Epidemiol.* 2014;6:213-20.
63. Ball J, Carrington MJ, McMurray JJ and Stewart S. Atrial fibrillation: profile and burden of an evolving epidemic in the 21st century. *Int J Cardiol.* 2013;167:1807-24.
64. Combes S, Jacob S, Combes N, Karam N, Chaumeil A, Guy-Moyat B, Treguer F, Deplagne A, Boveda S, Marijon E and Albenque JP. Predicting favourable outcomes in the setting of radiofrequency catheter ablation of long-standing persistent atrial fibrillation: a pilot study assessing the value of left atrial appendage peak flow velocity. *Arch Cardiovasc Dis.* 2013;106:36-43.
65. Kanda T, Masuda M, Sunaga A, Fujita M, Iida O, Okamoto S, Ishihara T, Watanabe T, Takahara M, Sakata Y and Uematsu M. Low left atrial appendage flow velocity predicts recurrence of atrial fibrillation after catheter ablation of persistent atrial fibrillation. *J Cardiol.* 2015;66:377-81.
66. Neumann T, Wojcik M, Berkowitsch A, Erkapic D, Zaltsberg S, Greiss H, Pajitnev D, Lehinant S, Schmitt J, Hamm CW, Pitschner HF and Kuniss M. Cryoballoon ablation of paroxysmal atrial fibrillation: 5-year outcome after single procedure and predictors of success. *Europace.* 2013;15:1143-9.
67. Drewitz I, Willems S, Salukhe TV, Steven D, Hoffmann BA, Servatius H, Bock K, Aydin MA, Wegscheider K, Meinertz T and Rostock T. Atrial fibrillation cycle length is a sole independent predictor of a substrate for consecutive arrhythmias in patients with persistent atrial fibrillation. *Circ Arrhythm Electrophysiol.* 2010;3:351-60.
68. Ammar S, Hessling G, Paulik M, Reents T, Dillier R, Buiatti A, Semmler V, Kolb C, Haller B and Deisenhofer I. Impact of baseline atrial fibrillation cycle length on acute and long-term outcome of persistent atrial fibrillation ablation. *J Interv Card Electrophysiol.* 2014;41:253-9.

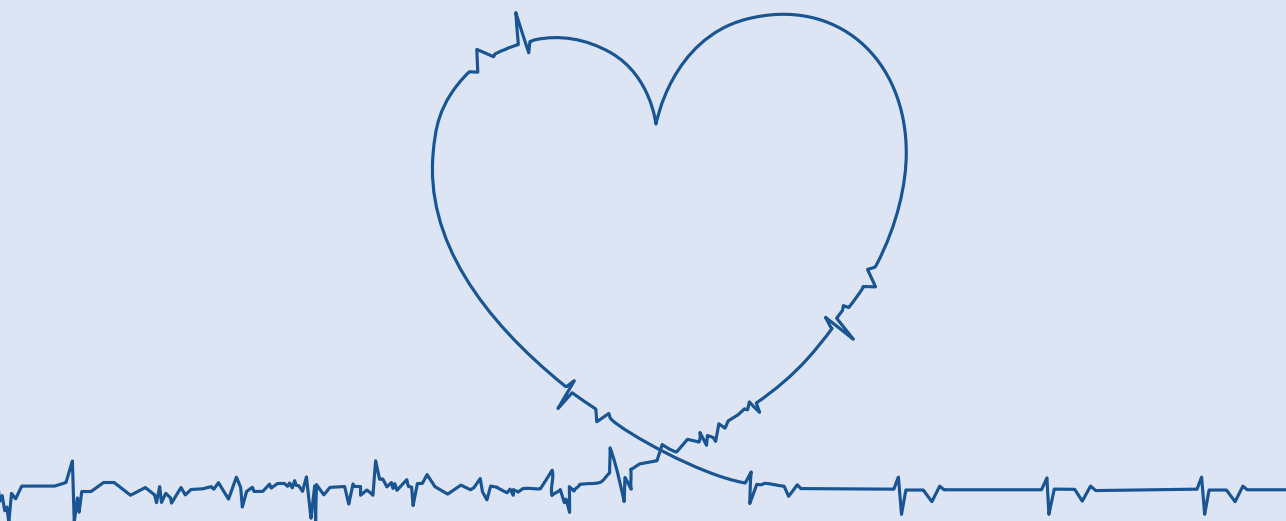
69. Akar JG, Everett THt, Kok LC, Moorman JR and Haines DE. Effect of electrical and structural remodeling on spatiotemporal organization in acute and persistent atrial fibrillation. *J Cardiovasc Electrophysiol*. 2002;13:1027-34.

70. Sahadevan J, Ryu K, Peltz L, Khrestian CM, Stewart RW, Markowitz AH and Waldo AL. Epicardial mapping of chronic atrial fibrillation in patients: preliminary observations. *Circulation*. 2004;110:3293-9.

PART I



ELECTROPHYSIOLOGICAL MARKERS DURING SINUS RHYTHM





CHAPTER 2

ATRIAL FIBRILLATION: A NEVER ENDING STORY?

Lanters EAH, Knops P, Kik C, de Groot NMS
Clinical Case Reports (2019)

ABSTRACT

Atrial fibrillation (AF) often recurs after ablative therapy. In our patient, intra-operative epicardial mapping during therapy resistant AF revealed highly dissociated atrial conduction patterns and that long lines of conduction block throughout the entire atria. Given the extensiveness of the substrate, it is not surprising that ablations were not successful.

INTRODUCTION

Atrial fibrillation (AF) recurrences after pulmonary vein isolation (PVI) may not only be caused by reconnection but also by the presence of an arrhythmogenic substrate elsewhere in the atria. In many patients (40-60%), AF tends to recur, also after multiple initially successful PVIs¹. Even additional substrate modification consisting of e.g. ablation of complex fractionated electrograms, does not cure AF in the vast majority of these patients².

Intra-operative high-resolution epicardial mapping provides insight into the severity of the arrhythmogenic substrate underlying persistence of AF. In the present case, we applied this technique to the entire atrial epicardial surface of a patient with a history of multiple failed ablations, to comprehend why currently available therapeutic strategies for AF were all prone to fail.

CASE REPORT

We present a male patient with longstanding persistent AF, who was diagnosed with paroxysmal AF at the age of 31. Failed anti-arrhythmic drug therapy included amiodarone, sotalol and metoprolol. For prevention of thrombo-embolic events, he used a vitamin K antagonist.

At age 49, transthoracic echocardiography showed left atrial dilatation (55x65 mm) with secondary mitral valve insufficiency and mild left ventricular dilatation (end-diastolic dimension 61 mm). Left ventricular function was normal and presence of coronary artery disease was ruled out by coronary angiography. The patient was referred to our hospital for mitral valve repair and concomitant surgical PVI (sPVI). A box lesion was created around the ostia of the pulmonary veins at the left atrial posterior wall using the Epicor Cardiac Ablation System (St Jude/Abbott, Illinois, USA). With this device, isolation of the pulmonary veins is achieved by the use of high intensity focused ultrasound. In addition, an mitral isthmus line was created extending from the caudal side of the box lesion to the mitral valve annulus (crossing the coronary sinus) and the left atrial appendage was amputated. Exit pacing was performed after surgical creation of the box lesion.

In the following years, he developed numerous AF recurrences in addition to a typical atrial flutter and multiple atrial tachyarrhythmia's (AT), all requiring electrical cardioversion. As a consequence, three endovascular right-sided ablation procedures were performed, including the creation of a linear lesion across the cavo-tricuspid isthmus and two unsuccessful ablations of different right-sided focal AT's. Immediate success after the consecutive endovascular ablation procedures (procedures 2nd-5th) was confirmed by the presence of a bi-directional block and/or non-inducibility of AT.

Seven years after the initial sPVI he was referred for redo sPVI (age 55). As the patient participated in a research project (QUASAR MEC2010-393), an intra-operative, high-resolution epicardial mapping procedure of the right and left atria and Bachmann's Bundle was performed during a persistent AF episode.

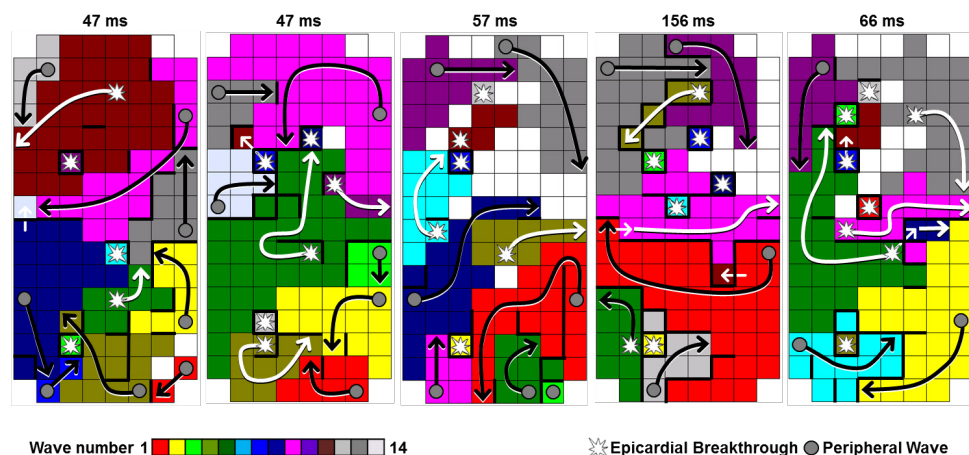


Figure 1 Patterns of activation. *Wavemaps illustrating the high complexity of patterns of atrial activation during atrial fibrillation. Different colors indicate the consecutive fibrillation waves. Arrows indicate the main trajectory of each fibrillation wave. Black arrow: peripheral fibrillation wave. White arrow: epicardial breakthrough ('focal') wave. Bold black lines indicate conduction block.*

A series of wavemaps, constructed during 790 milliseconds of AF, recorded at the right atrial free wall is shown in Figure 1. This site was selected as it was not targeted by any of the previous ablation procedures, and thus represents physiological atrial conduction in this patient, without the presence of potential iatrogenic conduction block, caused by earlier ablation. Activation of atrial tissue was highly dissociated due to multiple epicardial breakthrough waves and lines of conduction block, resulting in 66 fibrillation waves in only 790 ms. Conduction block was omnipresent. In 5 consecutive wavemaps, the total lengths of all lines of conduction block were 78mm (wavemap 1), 78mm (wavemap 2), 48mm (wavemap 3), 136mm (wavemap 4) and 90mm (wavemap 5). This corresponds with respectively 11.3%, 11.3%, 7.0%, 19.8% and 13.1% of the mapping area. At all other mapping sites in the remainder of the atria, patterns of activation were highly complex and varied from beat to beat. Epicardial breakthrough waves (EBW) were present in all wavemaps. The total amount was 31 and varied from 5 (wavemap 1) to 8 (wavemap 5) EBW per wavemap. This translates to 39 EBW per second at this specific mapping site.

After redo sPVI, electrical isolation was confirmed by the presence of an entrance block. One day after surgery, AF recurred. In addition, the patient developed bradycardia (day 3) for which a permanent DDD-pacemaker was implanted. Three years later, the patient still had ongoing AF episodes and a His bundle ablation was performed to control the ventricular heart rate.

DISCUSSION

The present case emphasizes the major importance of knowledge of the presence and extensiveness of the arrhythmogenic substrate underlying AF in the individual patient. In our patient, the highly complex atrial activation patterns and numerous EBW are indicative of substrate mediated AF. It is therefore to be expected that PVI will not be effective in eliminating AF.

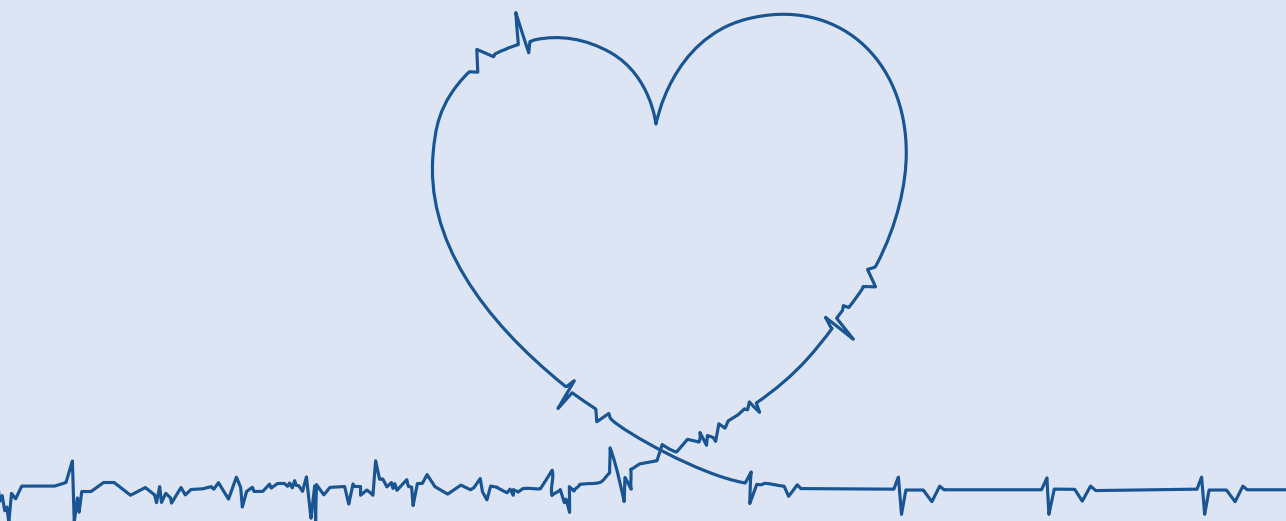
Prior studies showed that EBW are key elements of the arrhythmogenic substrate underlying AF³ and result most likely from endo-epicardial dissociation⁴. Substrate modification, such as ablation of complex fractionated electrograms or ganglionic plexi, or deployment of linear lesions for AF was not executed. However, these therapies are focusing on the substrate as more or less localized pathology, whereas in this case, electropathology is present diffusely throughout the entire left and right atria and Bachmann's bundle. Hence, even additional substrate modifying techniques would not have cured AF in this patient given the extensiveness of the arrhythmogenic substrate and the asynchronicity of activation patterns. Given the ever-growing population of patients with therapy resistant AF, further research into the arrhythmogenic substrate associated with AF persistence and ultimately development of new (patient tailored) therapeutic strategies are of utmost importance.

CONCLUSION

The current case illustrates that as long as the presence and extensiveness of the arrhythmogenic substrate underlying AF remains poorly understood and cannot be evaluated in the individual patient, none of the present available anti-arrhythmic treatment modalities will be effective.

REFERENCES

1. Ganesan AN, Shipp NJ, Brooks AG, Kuklik P, Lau DH, Lim HS, Sullivan T, Roberts-Thomson KC and Sanders P. Long-term outcomes of catheter ablation of atrial fibrillation: a systematic review and meta-analysis. *J Am Heart Assoc.* 2013;2:e004549.
2. Nademanee K, McKenzie J, Kosar E, Schwab M, Sunsaneewitayakul B, Vasavakul T, Khunnawat C and Ngarmukos T. A new approach for catheter ablation of atrial fibrillation: mapping of the electrophysiologic substrate. *J Am Coll Cardiol.* 2004;43:2044-53.
3. de Groot NM, Houben RP, Smeets JL, Boersma E, Schotten U, Schalij MJ, Crijns H and Allessie MA. Electropathological substrate of longstanding persistent atrial fibrillation in patients with structural heart disease: epicardial breakthrough. *Circulation.* 2010;122:1674-82.
4. de Groot N, van der Does L, Yaksh A, Lanfers E, Teuwen C, Knops P, van de Woestijne P, Bekkers J, Kik C, Bogers A and Allessie M. Direct Proof of Endo-Epicardial Asynchrony of the Atrial Wall During Atrial Fibrillation in Humans. *Circ Arrhythm Electrophysiol.* 2016;9.





CHAPTER 3

SPATIAL DISTRIBUTION OF CONDUCTION DISORDERS DURING SINUS RHYTHM

Lanters EAH, Yaksh A, Teuwen CP, van der Does LJME, Kik C, Knops P, van Marion DMS,
Brundel BJJM, Bogers AJCC, Allessie MA, de Groot NMS
International Journal of Cardiology (2017)

ABSTRACT

Background Length of lines of conduction block (CB) during sinus rhythm (SR) at Bachmann's bundle (BB) is associated with atrial fibrillation (AF). However, it is unknown whether extensiveness of CB at BB represents CB elsewhere in the atria. We aim to investigate during SR 1) the spatial distribution and extensiveness of CB 2) whether there is a predilection site for CB and 3) the association between CB and incidence of post-operative AF.

Methods During SR, epicardial mapping of the right atrium (RA), BB and left atrium was performed in 209 patients with coronary artery disease. The amount of conduction delay (CD, Δ local activation time ≥ 7 ms) and CB ($\Delta \geq 12$ ms) was quantified as % of the mapping area. Atrial regions were compared to identify potential predilection sites for CD/CB. Correlations between CD/CB and clinical characteristics were tested.

Results Areas with CD or CB were present in all patients, overall prevalence was respectively 1.4 (0.2-4.0)% and 1.3 (0.1-4.3)%. Extensiveness and spatial distribution of CD/CB varied considerably, however occurred mainly at the superior intercaval RA. Of all clinical characteristics, CD/CB only correlated weakly with age and diabetes ($P < 0.05$). A 1% increase in CD or CB caused a 1.1-1.5ms prolongation of the activation time ($P < 0.001$). There was no correlation between CD/CB and post-operative AF.

Conclusions CD/CB during SR in CABG patients with electrically non-remodeled atria show considerable intra-atrial, but also inter-individual variation. Despite these differences, a predilection site is present at the superior intercaval RA. Extensiveness of CB at the superior intercaval RA or BB does not reflect CB elsewhere in the atria and is not associated with post-operative AF.

INTRODUCTION

Conduction block (CB) is associated with genesis and perpetuation of cardiac arrhythmias¹. Previous studies have demonstrated that longitudinal dissociation in conduction is one of the key elements of the substrate underlying longstanding persistent atrial fibrillation (AF) in humans². Since atrial CB on a high resolution scale is mainly studied during AF, data on CB during sinus rhythm (SR) are scarce. If CB is already present during SR, it is most likely structural in nature. Some studies suggest an association between CB during SR and (development of) AF^{3,4}.

Zaman⁴ demonstrated the relevance of CB at the right atrium (RA) for intra-operative AF inducibility, although indirectly. Epicardial mapping was performed in 34 patients without a history of AF, undergoing coronary artery bypass grafting (CABG). The degree of fractionation of SR electrograms, most likely due to local CB, was higher in patients in whom AF was inducible than in non-inducible patients (96.2 vs. 74.9 Hz)⁴. During SR, the length of lines of CB at Bachmann's Bundle (BB) was associated with (development of) AF³. For this study, epicardial mapping studies of BB were performed in 185 patients with various underlying cardiac diseases. However, CB at the remainder of the right and left atria was not investigated and it is unknown whether CB at BB or RA is representative for CB elsewhere in the atria.

Hence, although the relevance of CB during SR for AF has been investigated at BB and RA, data on the physiological variation of CB at the entire atria are absent. We therefore aim to investigate 1) the spatial distribution and extensiveness of CB during SR and 2) whether there is a predilection site for CB during SR. This is evaluated by intra-operative, high-resolution epicardial mapping of the entire (electrically non-remodeled) atria in CABG patients without a history of AF. In addition, we examined if CB during SR is associated with development of early-post operative AF (PoAF).

METHODS

Study population

The study population consisted of patients without a history of AF undergoing elective CABG for coronary artery disease. This study is part of the QUASAR⁵ project and HALT&REVERSE⁶ project. Both studies are approved by the institutional Medical Ethical Committee (MEC-2010-054/MEC-2014-393) and all patients provided written informed consent. The study was carried out according to the principles of the Declaration of Helsinki. Patient characteristics were obtained from electronic patients files.

Mapping procedure

Epicardial mapping was performed prior to commencement to extra-corporal circulation⁷. A pacemaker wire attached to the terminal crest served as a temporal, bipolar reference electrode and a steel wire fixed to the subcutaneous tissue was used as an indifferent electrode. The mapping procedure was performed with electrode arrays consisting of 128 (diameter 0.65mm) or 192 unipolar electrodes (diameter 0.45mm). Inter-electrode distances of both devices are 2.0mm. Epicardial mapping during SR was conducted following a predefined

mapping scheme as demonstrated in the left upper panel in Figure 1, covering the entire epicardial surface of the RA, BB and left atrium (LA). The electrode array is shifted along imaginary lines with a fixed orientation at each position. We tried to avoid omission of areas at the expense of possible overlap between adjacent mapping sites. Mapping of the RA started at the cavo-tricuspid isthmus and continued perpendicular to the caval veins towards the right atrial appendage. BB is mapped from the tip of the left atrial appendage across the roof of the LA, behind the aorta towards the superior cavo-atrial junction. Mapping of the LA is performed from the lower border of the left inferior pulmonary vein (PV) along the left atrioventricular groove (LAVG) towards the left atrial appendage. The PV area (PVA) is mapped from the sinus transversus fold in between the right and left PV towards the LAVG³. Five seconds of SR were recorded from every mapping site, including unipolar epicardial electrograms, a bipolar reference electrogram, a surface ECG lead and a calibration signal of 2mV and 1000ms. Data was stored on hard disk after amplification (gain 1000), filtering (bandwidth 0.5-400 Hz), sampling (1 KHz) and analogue to digital conversion (16 bits).

Mapping data analysis

The center upper panel of Figure 1 shows a color-coded activation map of the RA free wall. Activation maps were constructed by annotating the steepest negative deflection of each extracellular potential, in case of a fractionated electrogram the steepest deflection is marked. Premature atrial complexes and aberrant beats were excluded. The averaged SR beat was used to quantify prevalence and amount of conduction delay (CD) and CB. For this purpose, differences in local activation times between neighboring electrodes were calculated. CD is defined as differences in local activation time of ≥ 7 ms and differences in local ≥ 12 ms as CB. In literature, the slowest conduction velocity during longitudinal propagation was measured around 20 cm/s.⁸ A somewhat lower value of <18 cm/s was chosen in order to be consistent with previous mapping studies in which we observed fractionated electrograms and activation from another direction at the other site of the line of CB.^{9, 10}

CD and CB are expressed as a percentage of the total available number of interelectrode connections. A more detailed description of the mapping data analysis is included in the supplemental materials.

To evaluate the spatial distribution of CD and CB, the atrial epicardial surface is subdivided in the following areas, which are also indicated in the right upper panel of Figure 1: 1) superior intercaval RA, 2) superolateral RA, 3) inferior intercaval RA, 4) inferolateral RA, 5) BB, 6) PVA and 7) LAVG. Within these areas, CD and CB were quantified per quadrants of 1cm². Quadrants were excluded for analysis when $\geq 50\%$ of the recorded electrograms had a slope threshold ≤ 80 mV/s and a signal-noise ratio <4 .

The lower panels of Figure 1 show an example of the reconstruction of CB maps. The left lower panel demonstrates isochronal maps; arrows indicate main trajectories of the SR wavefront. Combined CB and CD maps (center lower panel) were derived from the isochronal map and depict the spatial distribution of CD (blue lines) and CB (red lines). The median incidences (P50) of CD and CB in the entire atria were respectively 0.4% and 0.3%. The right lower panel indicates the amount of CB/cm² within the predefined atrial areas. Although rarely occurring in

this patient, areas of CD or CB were found at various sites within the superior intercaval RA, BB and PVA.

Intra-operative inducibility of atrial fibrillation

Intra-operative AF induction was attempted in every patient, see supplemental materials.

Early post-operative atrial fibrillation

Early PoAF was defined as the occurrence of an AF episode with a duration of at least 30 seconds during the first five days after surgery. PoAF was confirmed by electrocardiogram (ECG) or by continuous rhythm monitoring.

Statistical analysis

All data were tested for normality. Normally distributed data are expressed as mean±standard deviation, whereas skewed data are depicted as median(minimum-maximum). Although electrophysiological parameters are skewed, the mean is also provided for completeness and to enable comparison with other studies. Thus, electrophysiological parameters are expressed as mean, median(minimum-maximum). Spearman's test (ρ) was used to test correlations between clinical characteristics and non-normally distributed electrophysiological parameters. Categorical variables were compared using χ^2 -tests. Correction for multiple testing was not applied. A P-value <0.05 was considered statistically significant.

RESULTS

Study population

The study population consisted of 209 CABG patients (175 (83.7%) male, age 66±9.6 years). Baseline characteristics of the study population are summarized in Table S1; most patients had a normal left ventricular function (N = 152, 72.7%) without LA dilatation (N = 177, 84.7%).

Predilection sites for conduction delay

Four examples of the prevalence, extensiveness and spatial distribution of CD are illustrated by the CD maps in the upper panel of Figure 2. Reconstruction of the CD maps is clarified in Figure S1. The maps demonstrate not only intra-atrial variation but also show remarkable inter-individual differences. CD was present in all patients. The left upper panel of Figure 3 shows the median incidence of CD within the entire atria for each patient individually, ranging from 0.2 to 3.7% (median: 1.4%).

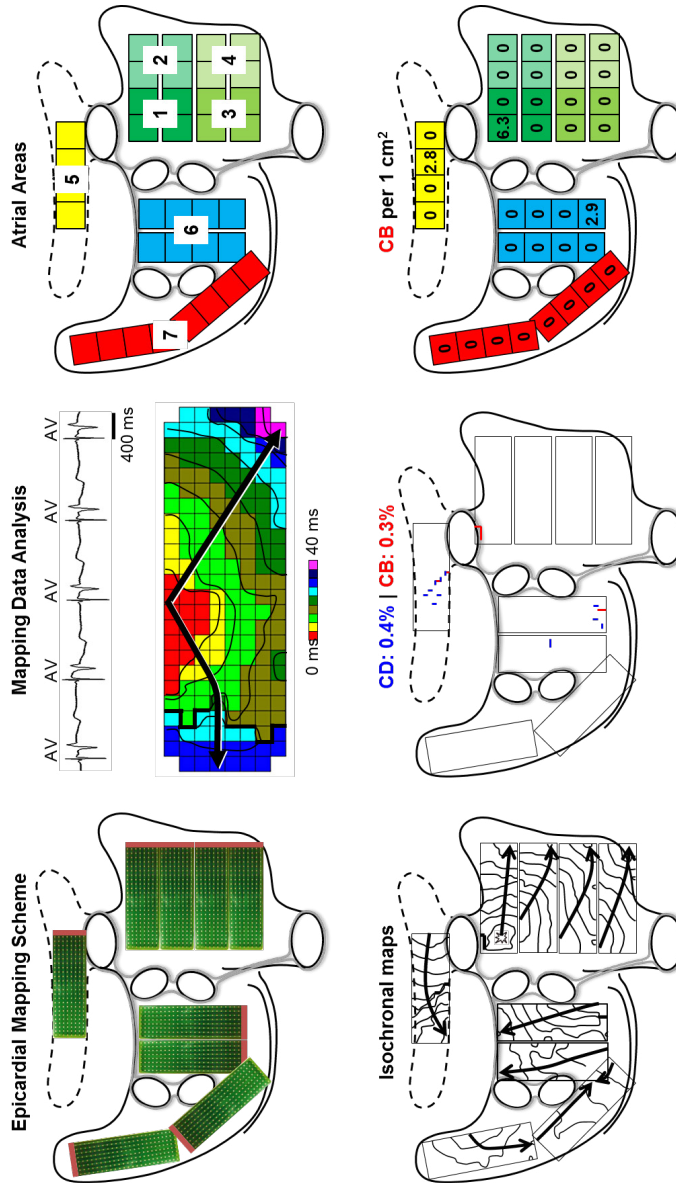


Figure 1. Epicardial mapping during sinus rhythm. Upper left panel: projection of the 192-unipolar electrode array on a schematic posterior view of the atria. Upper center panel: epicardial, unipolar sinus rhythm potentials recorded during 5 seconds of sinus rhythm (A: atrial potential; V: farfield ventricular signal) and corresponding color-coded activation map. Isochrones are drawn at 5ms intervals, arrow indicates the main trajectory of the wavefront, thick black lines represent areas of CB. Right upper panel: predefined atrial areas indicated by separate colors, see text for detailed explanation. 1) superior intercaval RA, 2) superolateral RA, 3) inferior intercaval RA, 4) inferolateral RA, 5) BB, 6) PVA and 7) LAVG. Lower left panel: local activation pattern with isochronal maps. Isochrones are drawn at 5ms. Lower center panel: combined CD map and CB map demonstrating the lengths, orientations and spatial distribution of CD (blue lines, median prevalence 0.4%) and CB (red lines, median prevalence 0.3%). Lower right panel: spatial distribution of CB per 1cm².

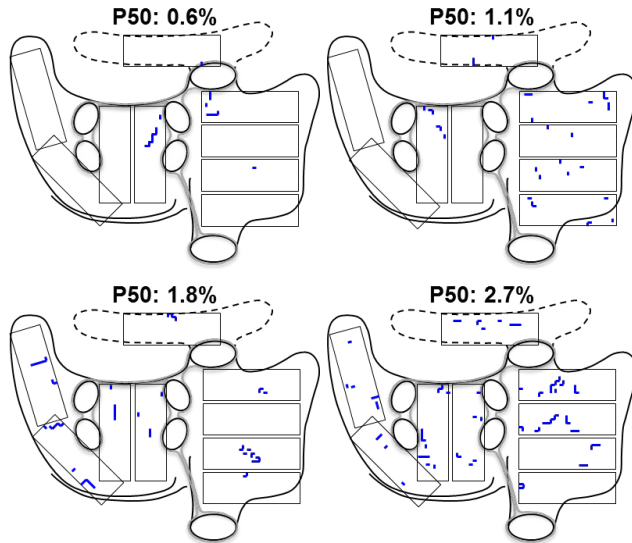
The prevalence and amount of CD within the predefined atrial areas are depicted in Table 1. The right upper panels of Figure 3 demonstrate the overall prevalence and amount of CD per atrial area. CD was most frequently observed at the superior intercaval RA (N=348 quadrants, 50%) and BB (N=273 quadrants, 45%), as depicted in the right upper panel of Figure 3. Not just the prevalence but also the amount of CD was highest at BB and RA, when compared with the remainder of the atria. Mean amount of CD at BB was 2.1%/cm² (median 0.0(0.0-19.4)%/cm²) and 2.5%/cm² (median 1.4(0.0-22.9)%/cm²) at the superior intercaval RA.

There were only mild correlations between the maximum amount of CD at BB or the superior intercaval RA and the total amount of CD in the entire atria: $\rho=0.346$, $P<0.001$ (BB) and $\rho=0.373$, $P<0.001$ (RA).

Predilection sites for conduction block

Areas with CB were observed in all patients. Amount of CB was correlated with the amount of CD ($\rho=0.506$, $P<0.001$). Median amount of CB of the entire atria ranged from 0.1% to 4.3% (median 1.3%), as shown in the left lower panel of Figure 3. Similar to CD, CB also showed remarkable intra-atrial and inter-individual differences, as shown in the lower panels of Figure 2 (see also Figure S1). In these patients with a low, median and high amount of lines of CB of variable lengths were observed at various sites at the RA, BB and LA. Despite these differences, a predilection site for CB was present at the superior intercaval RA (Table 1). In this area, both prevalence (52%) and amount (mean 4.6%/cm², 1.4(0-33.8)%/cm²) of CB were highest, as indicated in the lower right panels of Figure 3. A mild correlation existed between CB at BB and the total amount of CB in the entire atria: $\rho=0.380$, $P<0.001$ (BB). The correlation with CB/cm² at the superior intercaval RA was strongest: $\rho=0.601$, $P<0.001$.

Conduction Delay Maps



Conduction Block Maps

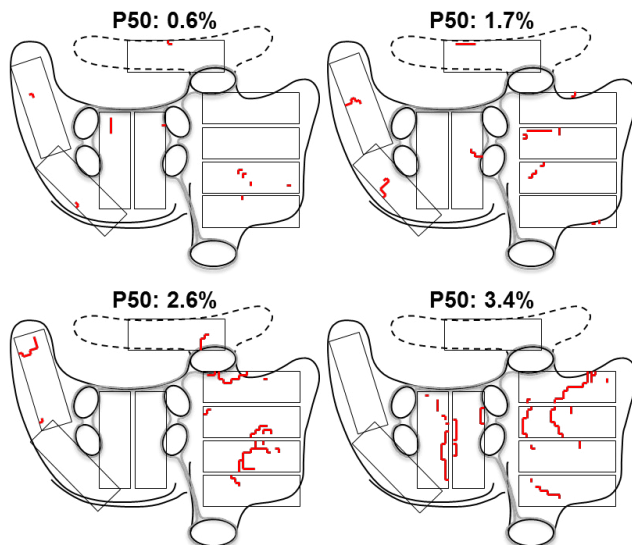


Figure 2. Intra-individual variation in conduction abnormalities. Upper panels: typical examples of CD maps. CD lines are indicated in blue. Lower panels: four examples of CB maps. Lines of CB are depicted in red. P50 indicates the amount of CD/CB on the total atrial epicardium. Maps were derived from isochronal maps, as explained in Figure S1.

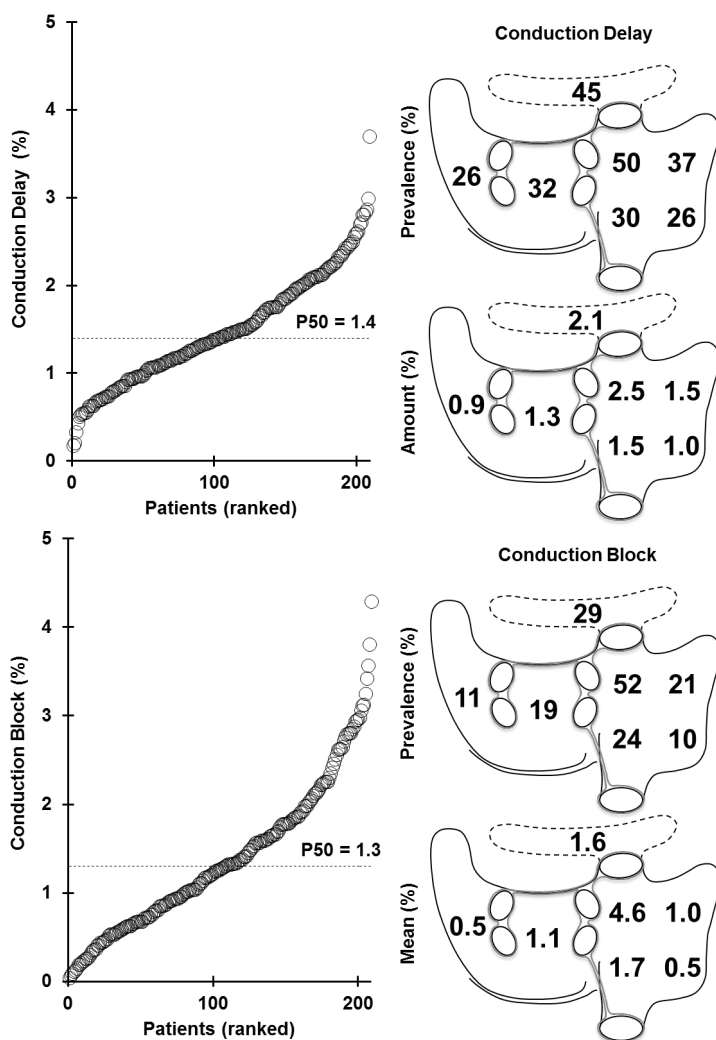


Figure 3. Quantification of conduction delay and conduction block. Left panels: mean amount of CD/CB at the entire atria. Patients are ranked according to an increment in atrial amount CD/CB. Right panels: prevalence of CD/CB per area and mean amount of CD/CB per 1cm² per area.

Correlation between conduction disorders and clinical profile

In general, amount of CD during SR was not, or only weakly correlated to clinical baseline characteristics. For example, the amount of CD at the entire atria was weakly correlated with age ($p=0.197$, $P=0.004$), gender ($p=0.166$, $P=0.016$), diabetes ($p=0.174$, $P=0.012$) and LA dilatation ($p=0.152$, $P=0.028$). Correlations between the quadrant with the highest amount of CD/cm² from any region were absent (all $P>0.05$). Exact correlation coefficients are provided in Table S2. The same was true for the amount of CB at the entire atria, which

(weakly) correlated to age ($p=0.205$, $P=0.003$), body surface area ($p=-0.176$, $P=0.011$) and diabetes ($p=0.203$, $P<0.05$). As depicted in Table S2, the strongest correlation was between the highest CB/cm² at the superior intercaval RA and age ($p=0.307$, $P<0.001$).

Finally, there was no correlation between CD/CB and intra-operative AF inducibility. Detailed results are included in the supplemental materials.

Correlation between conduction disorders and post-operative AF

The incidence of early PoAF was 30% (N=63). There was no correlation between development of PoAF and amount of CD ($p=0.032$, $P=0.650$) or CB ($p=0.017$, $P=0.813$) at the entire atria. Development of PoAF did not correlate with the highest amount of CD/cm² in any region ($p=0.03$, $P=0.608$) or CB/cm² ($p=0.185$, $P=0.007$). Incidence ($\chi^2=1.939$, $P=0.164$) or amount ($p=-0.022$, $P=0.753$) of CB at the superior intercaval RA did not correlate with PoAF.

Table 1. Quantification of conduction abnormalities per area

Prevalence CD		N (%)	
BB		273 (45%)	
Superior Intercaval RA		348 (50%)	
Inferior Intercaval RA		242 (30%)	
Superolateral RA		266 (37%)	
Inferolateral RA		207 (26%)	
PV		482 (32%)	
LAVG		324 (26%)	
Degree CD (%)	Mean	Median	Range
BB	2.1	0.0	0.0-19.4
Superior Intercaval RA	2.5	1.4	0.0-22.9
Inferior Intercaval RA	1.5	0.0	0.0-22.9
Superolateral RA	1.5	0.0	0.0-16.7
Inferolateral RA	1.0	0.0	0.0-19.4
PV	1.3	0.0	0.0-27.1
LAVG	0.9	0.0	0.0-20.3
Prevalence CB		N (%)	
BB		231 (29%)	
Superior Intercaval RA		362 (52%)	
Inferior Intercaval RA		190 (24%)	
Superolateral RA		152 (21%)	
Inferolateral RA		82 (10%)	
PV		288 (19%)	
LAVG		142 (11%)	

Prevalence CD Degree CB (%)	N (%)		
	Mean	Median	Range
BB	1.6	0.0	0.0-20.8
Superior Intercaval RA	4.6	1.4	0.0-33.8
Inferior Intercaval RA	1.7	0.0	0.0-28.2
Superolateral RA	1.0	0.0	0.0-20.8
Inferolateral RA	0.5	0.0	0.0-15.5
PV	1.1	0.0	0.0-20.6
LAVG	0.5	0.0	0.0-18.8

Mean, median and range (minimum-maximum) of prevalence and amount of CD and CB, per atrial area

DISCUSSION

Key findings

This study evaluated the prevalence, extensiveness and spatial distribution of CD and CB at the atrial epicardial surface during SR in patients with coronary artery disease and electrically non-remodeled atria. CD and CB were present in all patients, although in a low amount. The spatial distribution of CD/CB showed considerable inter-atrial and inter-individual variation. Despite these differences, a predilection site for both CD and CB was present at the superior intercaval RA. However, extensiveness of CD/CB at BB or RA was not representative for the degree of CD/CB elsewhere in the atria. The presence and extensiveness of conduction disorders were not, or only weakly correlated to development of early PoAF and clinical parameters including age, gender and cardiovascular risk factors.

Heterogeneity in conduction

Propagation of electrical waves through atrial myocardium is determined by membrane properties, tissue structure and wave front geometry¹¹. Conduction abnormalities play a crucial role in both genesis and perpetuation of atrial arrhythmias. It is generally assumed that the major cause of local conduction abnormalities is non-uniform tissue anisotropy due to interstitial fibrosis causing slowing of conduction and conduction block¹². We included patients with electrically non-remodeled atria, however, local conduction disorders caused by structural remodeling due to e.g. ageing, obesity, hypertension or (atrial) ischemia cannot be excluded¹³. In line with our study, Hansson et al.¹⁴ also found a small amount of conduction disorders during SR in 12 patients undergoing CABG or surgical transection of an accessory pathway. Epicardial mapping of the RA free wall using an 56 bipolar electrode array, revealed slowing of conduction (defined as propagation velocity 50% of the mean conduction velocity in that direction) in only 3 patients, at <13% of the total mapping area.

The amount of conduction disorders in our study population was low and mainly confined to the superior intercaval RA. Prior studies have also demonstrated conduction disorders primarily at the terminal crest region¹⁵. A functional conduction delay along the terminal crest, mainly in the transverse direction, was observed in patients with typical atrial flutter. This can be the result of a lower density of intercellular connections in the transverse direction of

the terminal crest¹⁶. Other explanations for preferential sites of conduction disorders at the superior intercaval RA include disruption of atrial myocardium by (branches of) the sinus node or sinus node artery¹⁷, pericardial folds near the superior caval vein or extensions of (resolved) sinus venosus myocardium¹⁸. In addition, Federov et al. demonstrated in an in vitro optical mapping study the presence of an area of conduction block in the sinus node region¹⁹.

In contrast to our observations, Lee et al.²⁰ found epicardial lines of conduction block at the junction of the right superior PV and the LA in 18 patients without AF. This discrepancy could be explained by different positions of the electrode arrays as their mapping device covered both the myocardial sleeves within the PVA and the posterior left atrial wall.

Development of post-operative atrial fibrillation

Sakamoto et al.²¹ performed intra-operative mapping during SR (60 unipolar electrodes, inter-electrode distances 3-5 mm) of the RA free wall in 52 patients with a variety of structural heart diseases. The presence of non-uniform activation patterns (defined as areas of conduction delay, conduction block or fusion of multiple wavefronts) was observed in 15 patients (29%) and was associated with PoAF²¹. However, in our study population, we could not establish a relation between PoAF and extensiveness of conduction disorders. It remains therefore unsure whether PoAF episodes are the result of the presence of a substrate, and in what extend triggers, such as sterile pericarditis, post-operative inflammation, changes in e.g. hemodynamics and fluid status provoked AF episodes²².

Clinical implications

Previous studies by Teuwen³ and Zaman⁴ demonstrated the relevance of CB at respectively BB and RA for (development of) AF. However, from their studies it remained unknown whether CB at these locations represented CB elsewhere in the atria. Based on the present study, we can conclude that, during SR, CD/CB at either one of these locations does not reflect the extensiveness of CD/CB in other atrial areas. A substantial intra- and inter-individual variation in CD/CB is present during SR in patients with ischemic heart disease. Areas of CD/CB in the present paper most likely represent the physiological variation in conduction during SR due to non-uniform anisotropic tissue in patients with electrically non-remodeled atria and coronary artery disease. Conduction disorders showed only weak, or no correlations with the clinical profile.

The effect of either CD/cm² or CB/cm² on the total activation time/1cm² was very limited and does not seem of clinical relevance. This is not surprising since the overall amount of conduction abnormalities was very low.

The mechanism and substrate underlying AF are still under debate and both endo- and epicardial mapping studies during SR and AF are performed to gain more insight. However, to conclude whether conduction is abnormal, optimal understanding of the physiological variation is of utmost importance. The present study thus provides a reference dataset that allows interpretation of conduction disorders observed during SR in patients with a history of AF and/or valvular disease. In addition, it is likely that conduction disorders associated with the arrhythmogenic substrate of AF may be more pronounced during pacing maneuvers, atrial extra systolic beats or AF. The present dataset facilitates further research into the substrate

and mechanisms underlying AF, by evaluating the relation between CD/CB during SR and AF, pacing or other arrhythmias. If, for example, the superior intercaval RA would be a predilection site for conduction abnormalities during AF, this could potentially serve as a novel therapeutic target.

Study limitations

Recordings of the interatrial septum could not be obtained with our closed beating heart mapping approach. The electrode array cannot be bent around the PVs and positioned in a stable and reproducible manner. The cutoff values for CD and CB are based on previous experiments, however, physiological, very slow conduction cannot be excluded. Due to our invasive mapping approach we were not able to include healthy control patients.

CONCLUSION

CD and CB during SR in CABG patients with electrically non-remodeled atria show considerable intra-atrial, but also inter-individual variation. Despite these differences, a predilection site for CB is present at the superior intercaval RA. However, extensiveness of CB at the superior intercaval RA or BB does not reflect CB elsewhere in the atria. There is no correlation between CD/CB during SR and development of early PoAF. Finally, this study creates a reference dataset for future mapping studies during either sinus rhythm, pacing or any arrhythmia.

REFERENCES

1. Kleber AG, Rudy Y. Basic mechanisms of cardiac impulse propagation and associated arrhythmias. *Physiol Rev* Apr 2004;84:431-488.
2. Allesie MA, de Groot NMS, Houben RPM, Schotten U, Boersma E, Smeets JL, Crijns HJ. Electropathological Substrate of Long-Standing Persistent Atrial Fibrillation in Patients With Structural Heart Disease. *Circ-Arrhythmia Elec* Dec 2010;3:606-615.
3. Teuwen CP, Yaksh A, Lanthers EA, et al. Relevance of Conduction Disorders in Bachmann's Bundle During Sinus Rhythm in Humans. *Circ Arrhythm Electrophysiol* May 2016;9:e003972.
4. Zaman JA, Harling L, Ashrafian H, Darzi A, Gooderham N, Athanasiou T, Peters NS. Post-operative atrial fibrillation is associated with a pre-existing structural and electrical substrate in human right atrial myocardium. *Int J Cardiol* Oct 1 2016;220:580-588.
5. van der Does LJ, Yaksh A, Kik C, Knops P, Lanthers EA, Teuwen CP, Oei FB, van de Woestijne PC, Bekkers JA, Bogers AJ, Allesie MA, de Groot NM. QUES for the Arrhythmogenic Substrate of Atrial fibrillation in Patients Undergoing Cardiac Surgery (QUASAR Study): Rationale and Design. *J Cardiovasc Transl Res* Jun 2016;9:194-201.
6. Lanthers EA, van Marion DM, Kik C, Steen H, Bogers AJ, Allesie MA, Brundel BJ, de Groot NM. HALT & REVERSE: Hsf1 activators lower cardiomyocyte damage; towards a novel approach to REVERSE atrial fibrillation. *J Transl Med* 2015;13:347.
7. Yaksh A, van der Does LJ, Kik C, Knops P, Oei FB, van de Woestijne PC, Bekkers JA, Bogers AJ, Allesie MA, de Groot NM. A novel intra-operative, high-resolution atrial mapping approach. *J Interv Card Electrophysiol* Dec 2015;44:221-225.
8. Spach MS, Dolber PC, Heidlage JF. Influence of the passive anisotropic properties on directional differences in propagation following modification of the sodium conductance in human atrial muscle. A model of reentry based on anisotropic discontinuous propagation. *Circ Res* Apr 1988;62:811-832.
9. Allesie MA, de Groot NM, Houben RP, Schotten U, Boersma E, Smeets JL, Crijns HJ. Electropathological substrate of long-standing persistent atrial fibrillation in patients with structural heart disease: longitudinal dissociation. *Circ Arrhythm Electrophysiol* Dec 2010;3:606-615.
10. Konings KT, Kirchhof CJ, Smeets JR, Wellens HJ, Penn OC, Allesie MA. High-density mapping of electrically induced atrial fibrillation in humans. *Circulation* Apr 1994;89:1665-1680.
11. Kleber AG, Rudy Y. Basic mechanisms of cardiac impulse propagation and associated arrhythmias. *Physiol Rev* Apr 2004;84:431-488.
12. Spach MS, Boineau JP. Microfibrosis produces electrical load variations due to loss of side-to-side cell connections: A major mechanism of structural heart disease arrhythmias. *Pace* Feb 1997;20:397-413.
13. Cochet H, Mouries A, Nivet H, et al. Age, Atrial Fibrillation, and Structural Heart Disease Are the Main Determinants of Left Atrial Fibrosis Detected by Delayed-Enhanced Magnetic Resonance Imaging in a General Cardiology Population. *J Cardiovasc Electr* May 2015;26:484-492.
14. Hansson A, Holm M, Blomstrom P, Johansson R, Luhrs C, Brandt J, Olsson SB. Right atrial free wall conduction velocity and degree of anisotropy in patients with stable sinus rhythm studied during open heart surgery. *Eur Heart J* Feb 1998;19:293-300.
15. Morton JB, Sanders P, Vohra JK, Sparks PB, Morgan JG, Spence SJ, Grigg LE, Kalman JM. Effect of chronic right atrial stretch on atrial electrical remodeling in patients with an atrial septal defect. *Circulation* Apr 8 2003;107:1775-1782.
16. Spach MS, Heidlage IF, Barr RC, Dolber PC. Cell size and communication: Role in structural and electrical development and remodeling of the heart. *Heart Rhythm* Oct 2004;1:500-515.
17. Sanchez-Quintana D, Cabrera JA, Farre J, Climent V, Anderson RH, Ho SY. Sinus node revisited in the era of electroanatomical mapping and catheter ablation. *Heart* Feb 2005;91:189-194.

18. Jongbloed MRM, Steijn RV, Hahurij ND, Kelder TP, Schalij MJ, Gittenberger-de Groot AC, Blom NA. Normal and abnormal development of the cardiac conduction system; implications for conduction and rhythm disorders in the child and adult. *Differentiation* Jul 2012;84.
19. Fedorov VV, Glukhov AV, Chang R, Kostecki G, Aferol H, Hucker WJ, Wuskell JP, Loew LM, Schuessler RB, Moazami N, Efimov IR. Optical mapping of the isolated coronary-perfused human sinus node. *J Am Coll Cardiol* Oct 19 2010;56:1386-1394.
20. Lee G, Spence S, Teh A, Goldblatt J, Larobina M, Atkinson V, Brown R, Morton JB, Sanders P, Kistler PM, Kalman JM. High-density epicardial mapping of the pulmonary vein-left atrial junction in humans: insights into mechanisms of pulmonary vein arrhythmogenesis. *Heart Rhythm* Feb 2012;9:258-264.
21. Sakamoto S, Yamauchi S, Yamashita H, Imura H, Maruyama Y, Ogasawara H, Hatori N, Shimizu K. Intraoperative mapping of the right atria[free wall during sinus rhythm: variety of activation patterns and incidence of postoperative atrial fibrillation. *Eur J Cardio-Thorac* Jul 2006;30:132-139.
22. Maesen B, Nijs J, Maessen J, Allesie M, Schotten U. Post-operative atrial fibrillation: a maze of mechanisms. *Europace* Feb 2012;14:159-174.
23. Spach MS, Dolber PC. Relating extracellular potentials and their derivatives to anisotropic propagation at a microscopic level in human cardiac muscle. Evidence for electrical uncoupling of side-to-side fiber connections with increasing age. *Circ Res* Mar 1986;58:356-371.
24. Spach MS, Kootsey JM. Relating the sodium current and conductance to the shape of transmembrane and extracellular potentials by simulation: effects of propagation boundaries. *IEEE Trans Biomed Eng* Oct 1985;32:743-755.

SUPPLEMENTAL MATERIALS

DETAILED METHODS

Intra-operative epicardial mapping procedure

The epicardial mapping procedure is performed during sinus rhythm, prior to commencement to extra-corporal circulation. A floppy electrode array, consisting of 128 or 192 unipolar electrodes, is attached to a flexible spatula. Electrode diameters are 0.65 mm and 0.45 mm respectively, inter-electrode distances are 2 mm. Corner electrodes do not record epicardial electrograms; hence 124 or 188 unipolar electrograms are recorded. The left upper panel of Figure 1 shows the 192 unipolar electrode array. A bipolar reference electrode is temporarily attached to the terminal crest. A steel wire, fixed to the subcutaneous tissue of the thoracic cavity serves as an indifferent electrode.

Recordings are obtained from the entire epicardial atrial surface, following a predefined mapping scheme. The left upper panel of Figure 1 illustrates the positioning of the electrode array on the epicardium in a schematic manner. The electrode array is shifted along anatomical structures with a fixed orientation at each position trying to avoid omission of areas at the expense of possible overlap between adjacent mapping sites. This approach covers the entire epicardial surface of the right atrium (RA), left atrium (LA), pulmonary vein (PV) area and Bachmann's Bundle (BB). Mapping of the RA started at the cavo-tricuspid isthmus and continued perpendicular to the caval veins towards the right atrial appendage. BB is mapped from the tip of the left atrial appendage across the roof of the LA, behind the aorta towards the superior cavo-atrial junction. Mapping of the LA is performed from the lower border of the left inferior pulmonary vein along the left atrioventricular groove towards the left atrial appendage. The PV area is mapped from the sinus transversus fold, in between the right and left PV, towards the atrioventricular groove.

Five seconds of SR were recorded from every mapping site, including 124 or 188 unipolar epicardial electrograms, a bipolar reference electrogram, surface ECG I and a calibration signal of 2mV and 1000ms. Data was stored on hard disk after amplification (gain 1000), filtering (bandwidth 0.5-400 Hz), sampling (1 KHz) and analogue to digital conversion (16 bits).

Determination of the local activation time

Figure S2 shows an example of electrograms recorded at the superior right atrium from one of the study subjects (raw data). As explained by Spach et al²³, the maximum negative slope of the extracellular potential coincides with the moment of the maximum change in transmembrane potential (V_{max} ; first time derivative, time difference < 50 μ s)²³. V_{max} corresponds with moment of maximum increase in sodium current and its conductance²⁴. The slope of each deflection is calculated per window of 2 ms. The maximum negative slope of the potential is marked as the local activation time of the corresponding electrode. Figure S3 shows the same selection of unedited electrograms as displayed in Figure S2. The steepest negative deflection of each negative atrial electrogram is marked, which in turn annotates the local activation time of the corresponding electrode. Premature atrial complexes and aberrant beats were excluded from this analysis.

Criteria for conduction delay and conduction block

To study the presence of conduction delay and block, local activation times were compared in areas of 2x2 electrodes. The upper panel of Figure S4 illustrates that each differences in local activation times were calculated between the index electrode and the adjacent electrodes on the right and immediately below in order to avoid double counting. With this approach, a total of N = 225 differences in local activation times (Δ LAT) were calculated for the 128 electrode array and N = 344 for the 192 electrode array.

The lower panel of Figure S4 shows examples of areas with conduction delay and/or conduction block. Conduction delay was defined as a difference in local activation time of ≥ 7 ms, indicated by a blue line. Differences of ≥ 12 ms were classified as conduction block, indicated by a red line. These cut-off values correspond with conduction velocities of ≤ 28 cm/s (delay) and ≤ 18 cm/s (block). In literature, the slowest conduction velocity during longitudinal propagation was measured around 20 cm/s.⁸ A somewhat lower value of <18 cm/s was chosen in order to be consistent with previous mapping studies in which we observed fractionated electrograms and activation from another direction at the other site of the line of conduction block.^{9, 10}

Figure S5 shows the reconstruction of a conduction block map. Magnification of a part of a color-coded activation map in the left panel shows the presence of an area of conduction block, based on differences in local activation times. Conduction block maps, as depicted in the right panel of Figure S5, are reconstructed with this approach. The percentage of conduction delay/block per area of interest is calculated as indicated by Formula Eq. S1:

$$\%CD = \frac{\text{Number of } \Delta\text{LAT} \geq 7 \text{ ms}}{\text{Total number of } \Delta\text{LAT}} \text{ and } \%CB = \frac{\text{Number of } \Delta\text{LAT} \geq 11 \text{ ms}}{\text{Total number of } \Delta\text{LAT}} \quad (\text{Formula Eq. S1})$$

Intra-operative inducibility of atrial fibrillation

AF induction was attempted in every patient. AF was induced by fixed rate atrial pacing, starting at a rate of 250 beats per minute with the use of a right atrial temporary pacemaker. If AF could not be induced, the pacing rate was gradually increased by 50 beats per minute up to 400 beats per minute. AF was defined as beat-to-beat changes in patterns of activation, AF cycle lengths and electrogram morphologies.

SUPPLEMENTAL RESULTS

Correlation between electrophysiological properties and AF inducibility

AF was inducible in 142 (71%) patients; in 29 patients (14%) only a regular atrial tachycardia was induced. Arrhythmias were not inducible in 30 patients (15%). In 8 of 209 patients without AF (4%) AF induction was not attempted due to patient related or technical considerations. Intra-operative inducibility of AF did not correlate with amount of CD ($p_s = 0.014$; $P = 0.837$) and amount of CB ($p_s = 0.121$; $P = 0.080$). Quadrants with the highest amount of CD/cm² ($p_s = 0.079$; $P = 0.257$) or CB/cm² ($p_s = 0.059$; $P = 0.396$) within each patient did not correlate with AF inducibility. The highest amount of CB/cm² ($p_s = 0.049$; $P = 0.488$), found at the superior

intercaval area of the RA, or presence of CB ($\chi^2 = 1.917$; $P = 0.590$) within this area did also not correlate with AF inducibility. In addition, development of PoAF was not associated with AF inducibility ($\chi^2 = 0.525$; $P = 0.913$).

Table S1. Baseline characteristics

Baseline Characteristics	
No. of patients (N)	209
Age, years	66 ± 9.6
Male gender (%)	175 (83.7)
BSA	1.99 ± 0.3
Hypertension (%)	131 (62.7)
Hypercholesterolemia (%)	91 (43.5)
Diabetes Mellitus (%)	72 (34.4)
Peripheral Vascular Disease (%)	29 (13.9)
Thyroid Disorder (%)	9 (4.3)
Echocardiography	
LVF (%)	
Normal function (%)	152 (72.7)
Mild dysfunction (%)	41 (19.6)
Moderate dysfunction (%)	7 (3.3)
Severe dysfunction (%)	1 (0.5)
LA Size (%)	
Dilated LA (>45mm) (%)	32 (15.3)

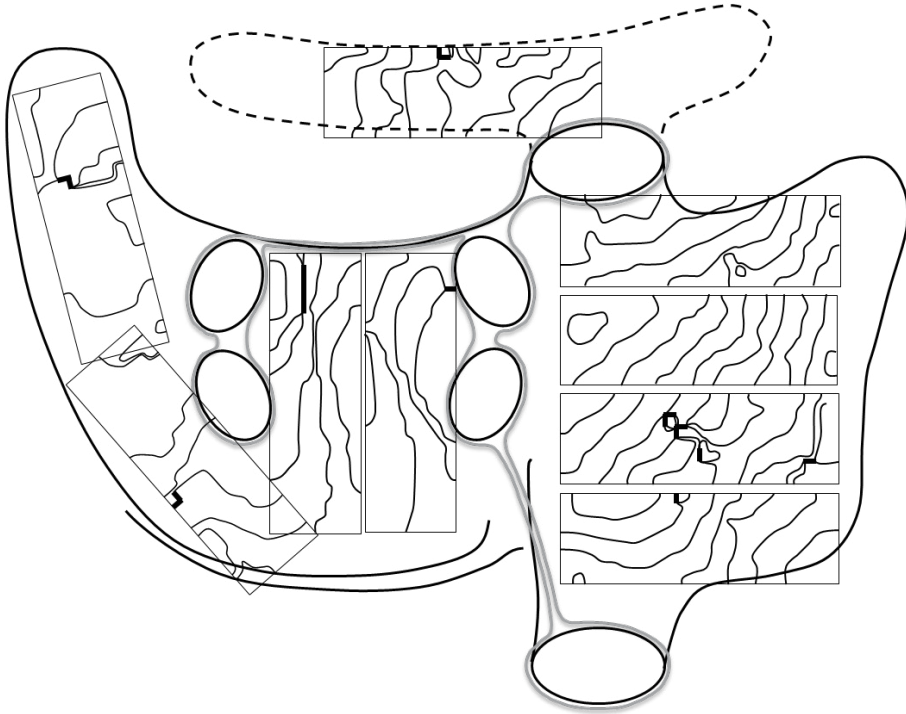
AF: atrial fibrillation; BSA: body surface area; LVF: left ventricular function; LA: left atrium.

Table S2. Correlation coefficient

		CD, entire atria	CD/cm ² max	CD/cm ² , max SI-RA	CD/cm ² max BB	CB, entire atria	CB/cm ² max	CB/cm ² , max SI-RA	CB/cm ² , max BB
Age	ρ	0.197	0.059	-0.050	0.113	0.205	0.307	0.112	0.229
	P	0.004	0.393	0.473	0.105	0.003	<0.001	0.110	0.001
Gender	ρ	0.166	0.069	0.025	0.084	0.129	0.087	0.108	0.078
	P	0.016	0.323	0.722	0.230	0.063	0.210	0.123	0.263
BSA	ρ	-0.90	-0.008	-0.008	-0.039	-0.176	-0.160	-0.169	-0.102
	P								
HT	ρ	0.179	0.906	0.906	0.578	0.011	0.021	0.015	0.144
	P	.042	-0.005	0.022	0.017	0.076	0.064	0.039	-0.006
	ρ	.548	0.946	0.749	0.809	0.276	0.354	0.579	0.937
DM	ρ	.174	0.196	0.001	0.057	0.203	0.160	0.147	0.035
	P	.012	0.005	0.989	0.413	0.003	0.021	0.035	0.618
HC	ρ	0.101	0.015	-0.030	0.037	0.057	-0.036	-0.015	-0.010
	P								
PVD	ρ	0.148	0.834	0.669	0.592	0.410	0.604	0.825	0.888
	P	0.094	0.067	-0.073	0.026	0.118	0.082	0.090	0.029
	ρ	0.177	0.337	0.294	0.709	0.088	0.240	0.199	0.676
TD	ρ	-0.028	-0.014	-0.017	0.024	0.068	-0.006	0.087	0.063
	P								
LA dill	ρ	0.686	0.840	0.813	0.730	0.327	0.933	0.210	0.363
	P	0.152	0.052	0.065	0.032	0.035	0.038	-0.021	0.005
LVF	ρ	0.028	0.451	0.353	0.642	0.610	0.581	0.765	0.938
	P	-0.003	-0.054	-0.111	0.032	-0.034	0.002	-0.095	0.025
	ρ	0.969	0.450	0.119	0.654	0.627	0.977	0.184	0.725
	P								

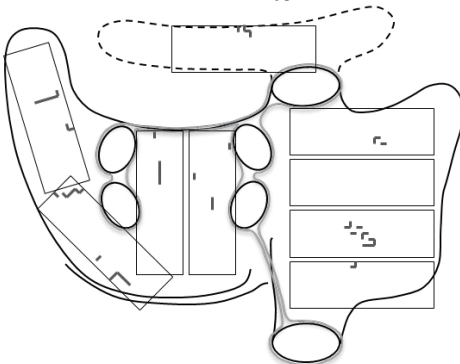
Max: maximum; CD: conduction delay; SI-RA: superior intercaval right atrium; BB: Bachmann's Bundle; BSA: body surface area; HT: hypertension; HC: hypercholesterolemia; PVD: peripheral vascular disease; TD: thyroid disease; LA dill: left atrial dilatation (>45mm); LVF: left ventricular function.

Isochronal Map



Conduction Delay Map

P50: 1.8%



Conduction Block Map

P50: 0.6%

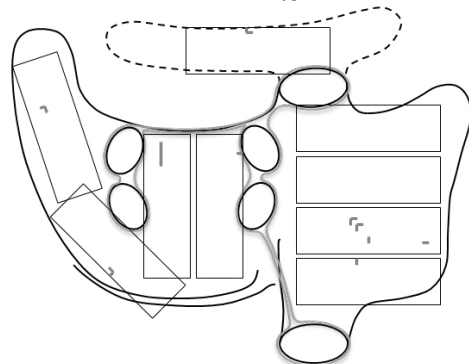


Figure S1. Reconstruction of conduction delay/block maps. Upper panel: isochronal maps from the consecutive mapping positions. Isochrones are drawn at 5 ms intervals. Left lower panel: conduction delay maps matching the isochronal maps in the upper panel. Lines of conduction delay are indicated in blue. Average amount of conduction delay at the mapped atrial surface: 1.8%. Right lower panel: conduction block maps corresponding with the isochronal map in the upper panel. Conduction block is depicted by red lines. Average amount of conduction block on the total atrial epicardium: 0.6%.

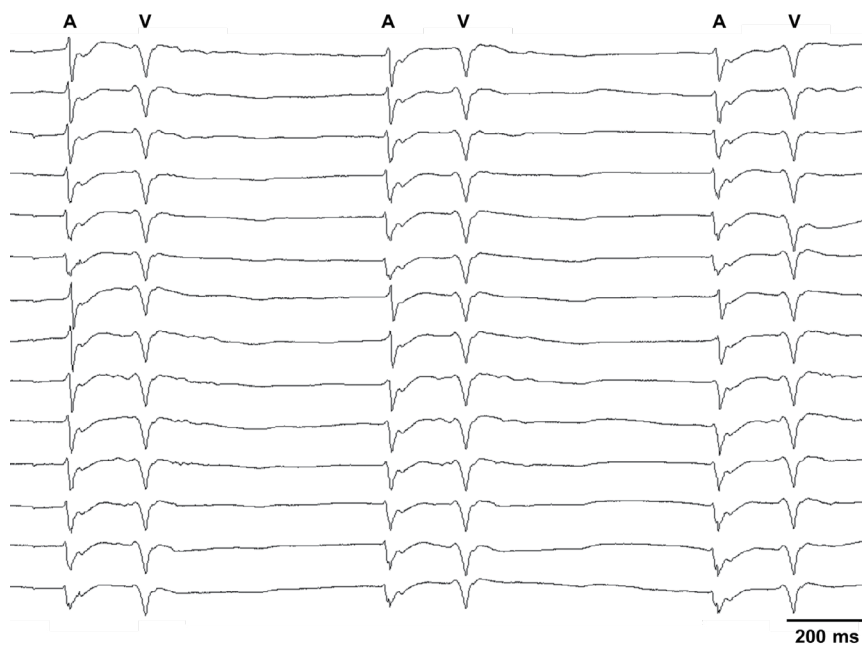


Figure S2. Raw epicardial electrograms. Typical example of a selection of epicardial electrograms, recorded from the superior right atrium. An atrial potential (A) and a farfield ventricular signal (V) can be distinguished.

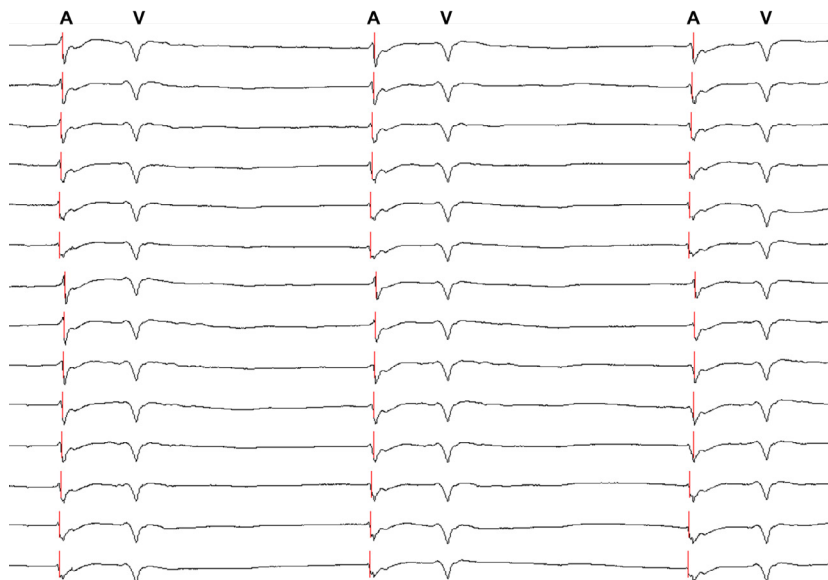


Figure S3. Marked epicardial electrograms. The same selection of epicardial electrograms as Figure S2. The steepest deflection of each atrial deflection is annotated.

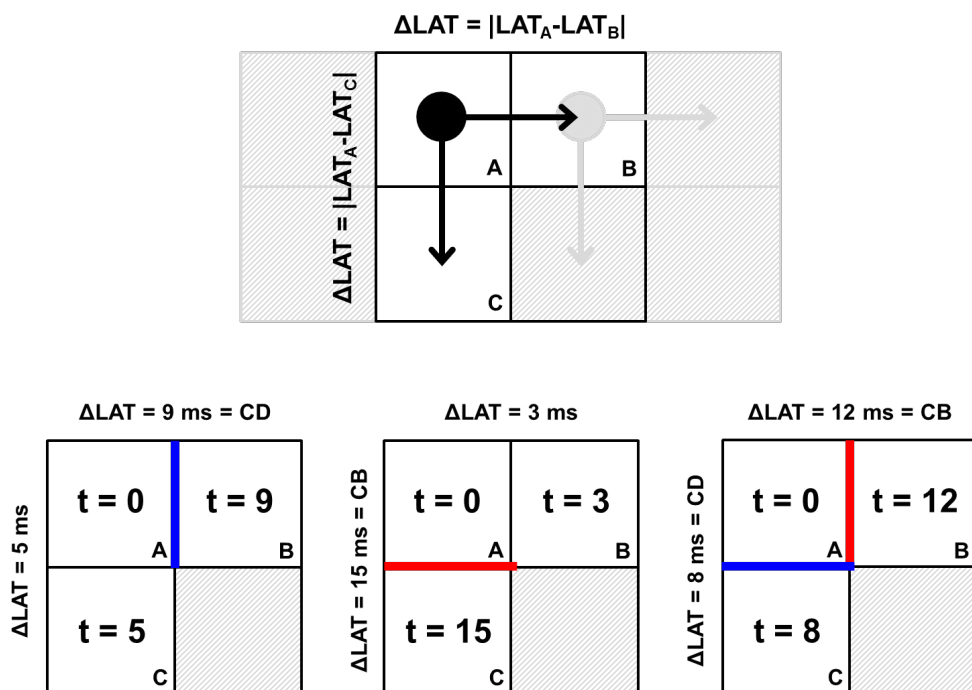


Figure S4. Identification of conduction delay/block. The presence of conduction disorders is evaluated in areas of 2x2 electrodes. The difference in local activation time is calculated between the right and inferior electrodes for each consecutive recording electrode. Conduction delay and conduction block are indicated with blue and red lines respectively. LAT: local activation time; CD: conduction delay; CB: conduction block.

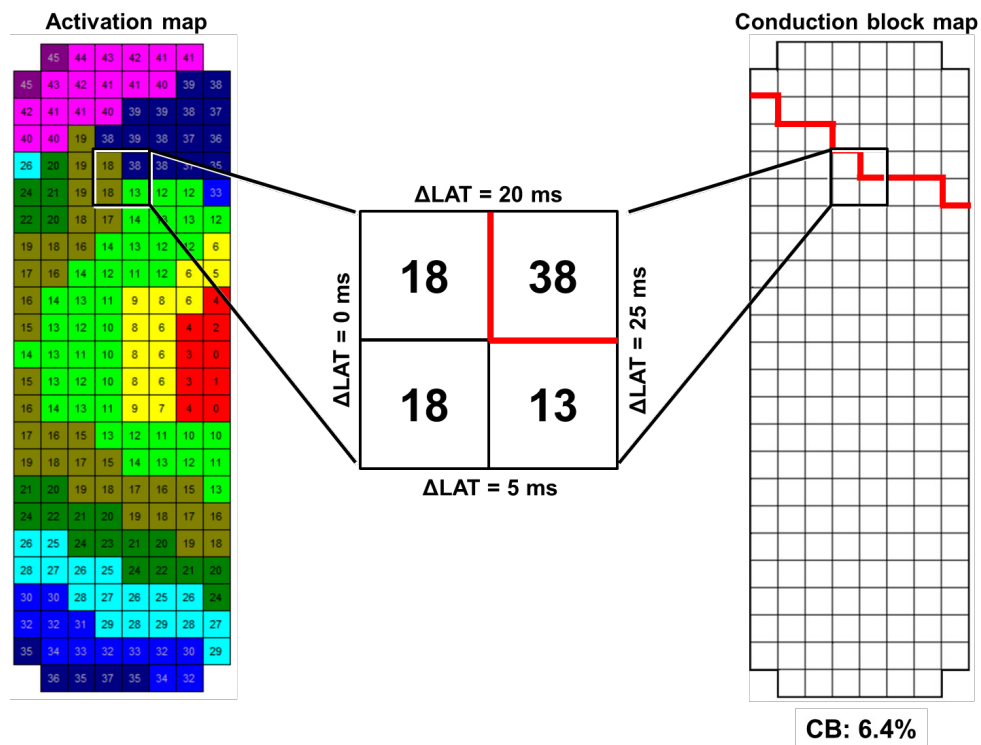
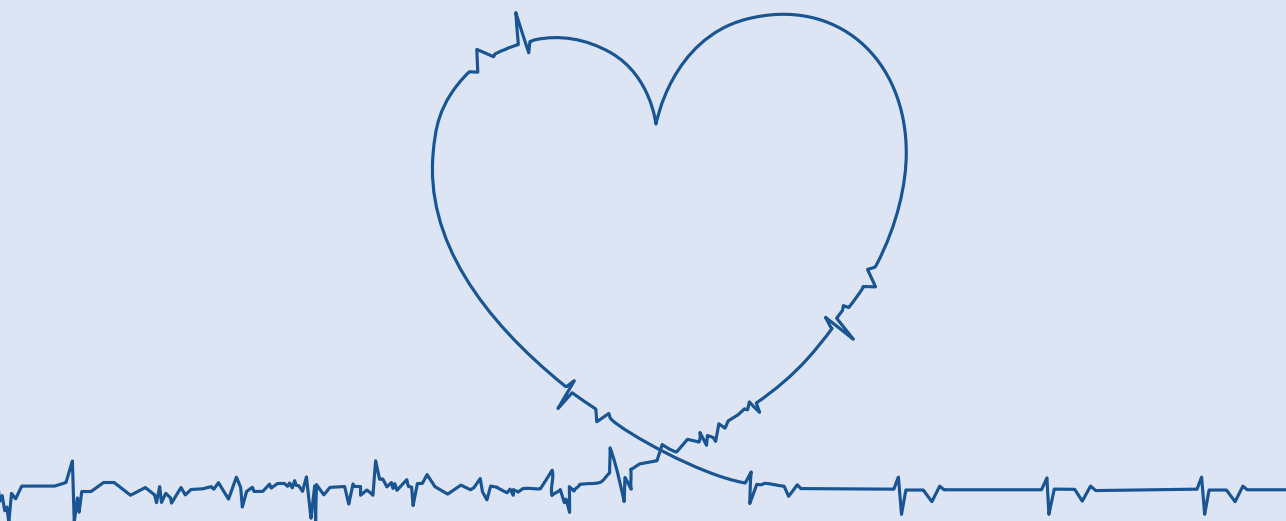


Figure S5. Construction of conduction block map. Left panel: color coded activation map, numbers indicate local activation time per electrode. Middle panel: magnification of a 2x2 area of the activation map with calculation of the difference in local activation time (ΔLAT) in order to identify conduction abnormalities. Right panel: conduction block map based on the activation map in the left panel. Amount of conduction block in this area is $12 / 188 = 6.4\%$. LAT: local activation time; CB: conduction block.





CHAPTER 4

THE EFFECTS OF VALVULAR HEART DISEASE ON ATRIAL CONDUCTION DURING SINUS RHYTHM

van der Does LJME, MD, Lanthers EAH, Teuwen CP, MD, Mouws EMJP, Yaksh A, Knops P,
Kik C, Bogers AJJC, de Groot NMS
Journal of Cardiovascular Translational Medicine (2020)

ABSTRACT

Background Different arrhythmogenic substrates for atrial fibrillation (AF) may underlie aortic valve (AV) and mitral valve (MV) disease.

Methods We located conduction disorders during sinus rhythm by high-resolution epicardial mapping in patients undergoing AV (n=85) or MV (n=54) surgery. Extent and distribution of conduction delay (CD) and block (CB) across the entire right and left atrial surface was determined from circa 1880 unipolar electrogram recordings per patient.

Results CD and CB was most pronounced at the superior intercaval area (2.5% of surface, maximal degree 6.6%/cm²). MV patients had a higher maximal degree of CD at the lateral left atrium than AV patients (4.2 vs 2.3%/cm², p=0.001). A history of AF was most strongly correlated to CD/CB at Bachmann's bundle and age.

Conclusions Although MV patients have more conduction disorders at the lateral left atrium, disturbed conduction at Bachmann's bundle during sinus rhythm indicates the presence of atrial remodeling which is related to AF episodes.

INTRODUCTION

Valvular heart disease predisposes to the occurrence of atrial tachyarrhythmias. Significant stenosis or regurgitation of heart valves has important hemodynamic effects on the atria that lead to structural atrial remodeling. In situations of pressure or volume overload the increased pressure on the atrial wall causes atrial dilation.¹ Chronic mechanical stretch initiates pathways that produce fibrosis and alter myocyte coupling and function.^{2,3} Consequently, electrical conduction in the atria becomes disrupted and can result in areas with slow and discontinuous conduction which may act as a substrate for tachyarrhythmias. The incidence of atrial fibrillation (AF) is higher in patients with mitral valve (MV) disease (26-54%) than in patients with aortic valve (AV) disease (10-13%), most likely due to higher left atrial loads in MV disease.^{4,5} Therefore, different types of atrial remodeling may take place in AV and MV disease.

It has been previously demonstrated that structural remodeling and not electrical remodeling is the major contributor to development of AF in models of chronic atrial stretch.³ The electrophysiological disturbances due to structural alterations in patients with valvular heart disease may also be identifiable during sinus rhythm. The purpose of this study is first to identify differences in the amount and distribution of high-resolution conduction disorders during sinus rhythm between patients with AV and MV disease. Secondly, we aim to determine if predilection sites of conduction disorders during sinus rhythm exist in patients with valvular heart disease who have developed clinical AF. A high-resolution epicardial mapping approach was performed to locate atrial areas with conduction abnormalities and identify the differences in conduction disorders between patients with AV and MV disease requiring surgical treatment.

METHODS

Study population

Patients of 18 years and older undergoing AV (mainly for aortic stenosis) or MV (for mitral regurgitation) surgery with or without coronary artery bypass grafting participated in this study. The study is part of the QUASAR study⁶ that was approved by the local ethics committee and all patients gave informed consent prior to surgery.

Study procedure

During surgery and prior to cardiopulmonary bypass, epicardial mapping was performed of the entire atrial surface with an electrode array containing 128 or 192 unipolar electrodes with an electrode diameter of 0.65 or 0.45mm and inter-electrode spacing of 2mm (GS Swiss PCB AG, Küssnacht, Switzerland). Five-second recordings of sinus rhythm were sequentially acquired from all epicardial accessible sites at the right atrium, left atrium and Bachmann's bundle. Patients that were in AF at the start of the procedure were electrically converted to sinus rhythm. A temporary pacemaker wire stitched to the terminal crest served as a reference signal during the recordings. The mapping procedure and mapping sites were previously described in detail.⁷ Mapping locations are also illustrated in the upper right panel of Figure 1. In case of the 128-electrode mapping array, each 192-array location consisted of two 128-array recordings. Unipolar electrograms were stored on hard disk after amplification, filtering (bandwidth 0.5-400Hz), sampling (1KHz) and analogue to digital conversion (16bits).

Mapping data analysis

Atrial deflections were detected automatically by marking of the steepest negative deflection with a minimal slope of 80 mV/s and signal to noise ratio >4 for each recorded electrogram in order to construct activation maps.⁶ The marked electrograms and activation maps were thereafter checked and manually corrected if necessary. Aberrant and premature atrial beats were excluded from analysis. Sinus rhythm activation maps were used to determine the incidence of conduction delay (CD) and conduction block (CB) on a high resolution scale (left panel, Figure 1). CD and CB were defined as a difference in activation time between adjacent electrodes of, respectively, 7-11ms and ≥ 12 ms (translating to an effective conduction velocity of 19–28 cm/sec and ≤ 18 cm/sec).⁸ The amount of CD and CB was calculated as a percentage per 1cm² quadrants. Figure 1 illustrates the subdivision of the entire mapping surface of each patient in 1cm² quadrants in which the percentages of CD and CB were determined.

Atrial distribution

The prevalence and degree of CD and CB in the patient groups were assessed separately for 7 atrial areas: 4 areas at the right atrium (the superior (1) and inferior (2) intercaval/ terminal crest area and the superior (3) and inferior (4) lateral right atrium), Bachmann's bundle (5), posterior left atrium between the pulmonary veins (6) and the lateral left atrium/ left atrial appendage (LAA) (7) (Figure 1, right lower panel). The prevalence of CD/CB per area is defined as the percentage of patients with presence of CD or CB in that area. For each area in every patient, the average degree of CD and CB was determined (average percentage CD/ CB of the 1cm² quadrants in that area) and also the maximal degree of CD and CB in 1cm² (CD/CB of the 1cm² quadrant with the highest amount of CD/CB).

Statistical analysis

Categorical clinical characteristics between the AV and MV group were compared with Chi-square or Fisher's exact tests. Continuous clinical data and electrophysiological data were not normally distributed and differences between the AV and MV group were evaluated with Mann-Whitney U tests. Electrophysiological mapping data are presented as median (minimum-maximum) values. To evaluate differences between areas, the area with the highest average and maximal degree of CD/CB was identified for each patient and the total incidences of highest amount of CD/CB were determined for each area. Differences in the incidence distributions between areas were first evaluated with the overall Cochran's Q test. Subsequently, McNemar tests were applied for a pair-wise comparison of each of the areas. We applied Bonferroni correction to adjust for inflation of type I error with repeated tests. A p-value $\leq 0.05/7$ was considered statistically significant for the comparison of patient groups (AV vs MV) within the 7 areas, whereas for the inter-areal comparisons a p-value threshold of $\leq 0.05/21$ was used. The rank-biserial correlation coefficient (skewed continuous/ ordinal data) and Phi coefficient (binary data) were determined to quantify the correlation between electrophysiological/clinical variables and a history of AF. Binary logistic regression analysis was performed to relate electrophysiological and clinical variables with incidence of postoperative AF. All analyses were performed with IBM SPSS Statistics version 21 (IBM corp., Armonk, NY).

67

Table 1. Clinical characteristics

	Total N(%)	AV N(%)	MV N(%)	P
No. of patients	139	85	54	
Age, years [IQR]	70 [12]	69 [13]	70 [14]	0.641
Male gender	89 (64)	59 (69)	30 (56)	0.097
Hypertension	67 (48)	48 (57)	19 (35)	0.014
Hypercholesterolemia	29 (21)	18 (21)	11 (20)	0.909
Diabetes mellitus	22 (16)	15 (18)	7 (13)	0.461
Coronary artery disease	66 (48)	43 (51)	23 (43)	0.358
Peripheral vascular disease	7 (5)	4 (5)	3 (6)	1.000
Atrial fibrillation	38 (27)	17 (20)	21 (39)	0.015
Valvular disease*				
- Aortic stenosis	81 (58)	74 (87)	7 (13)	
- Aortic regurgitation	26 (19)	18 (21)	8 (15)	
- Mitral stenosis	5 (4)	0	5 (9)	
- Mitral regurgitation	54 (39)	0	54 (100)	
- Tricuspid regurgitation	13 (9)	0	13 (24)	
Left ventricular function				0.019
- Normal	103 (74)	70 (82)	33 (61)	
- Mild dysfunction	25 (18)	11 (13)	14 (26)	
- Moderate dysfunction	11 (8)	4 (5)	7 (13)	
- Severe dysfunction	0	0	0	
Left atrial enlargement (>45 mm)	40 (29)	11 (13)	29 (54)	<0.001

* Valvular heart disease for which corrective surgery was performed. AV: aortic valve; MV: mitral valve; IQR: interquartile range

RESULTS

Clinical Characteristics

Epicardial high-resolution mapping during sinus rhythm was performed in 139 patients who underwent cardiac surgery for valvular heart disease. There were 89 (64%) male and 50 (36%) female patients with a median age of 70 (IQR=62-75) years. MV surgery was performed in 54 (39%) patients and 85 (61%) patients had valvular cardiac surgery for only AV disease. A total of 66 (47%) patients had significant coronary artery disease and 38 (27%) had a history of AF. All clinical characteristics are demonstrated in Table 1. Patients with MV disease presented more often with left atrial enlargement, left ventricular dysfunction and AF prior to surgery, hypertension was more often observed in AV disease.

Mapping Data

The median number of electrogram recordings of the entire atrial surface acquired by high-resolution mapping was 1880 (945-2356) per patient. Quadrants containing <50% electrogram recordings were excluded from analysis, which resulted in exclusion of 2.6% of the 4644 quadrants in total, and 32 (18-42) quadrants per patient were analyzed for presence of CD and CB. Median cycle length during mapping of sinus rhythm was not different between AV and MV patients (786ms (473-1735) and 784ms (533-1178), $p=0.28$). Cardioversion was performed before mapping of sinus rhythm in 16 patients (42%) with a history of AF. However, there were no differences in the amount of conduction disorders between patients with AF who received a cardioversion and those who were spontaneously in sinus rhythm.

Overall conduction delay and block in valvular heart disease

A certain amount of both CD and CB was present in (nearly) all of the patients during sinus rhythm and the prevalence ranged respectively between 0.17-3.4% (median 1.26%) and 0-3.58% (median 1.15%) of the atrial surface. Figure 2 demonstrates the degree of CD and CB of the entire atria in patients with AV and MV disease. There was no difference in the atrial amount of CD/CB between patients with AV or MV disease. Both maximal peak gradient of patients with only aortic valve stenosis ($n=64$, 78 ± 23 mmHg) and cycle length were not correlated to the total amount of CD and CB ($p=0.30$ and $p=0.93$).

Atrial distribution of conduction delay and block

Figure 3 demonstrates the average degree of CD and CB in each area for both groups. In Table 2 the maximal degrees of CD and CB for each area are shown. The largest difference in CD/CB between patients with AV and MV disease was seen at the lateral left atrial/LAA area. The maximal degree of CD at the lateral left atrium was higher in patients with MV disease and there was an overall trend towards more CD/CB at this site in the MV disease group. The average and maximal degree of CB was highest at the superior intercaval/terminal crest area of the right atrium (respectively 2.5% and 6.6%/cm², all $p\leq 0.001$). Long lines of CB are often seen towards the posterior area of the right atrium, also in two out of three of the youngest patients in our study group (21-24 years).

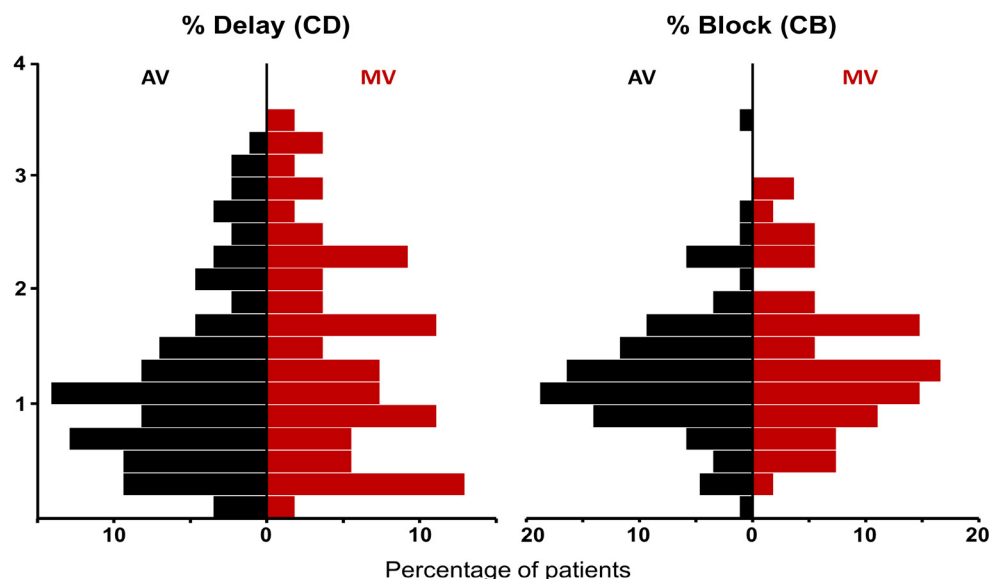


Figure 2. Overall conduction delay and block in valvular heart disease. Histograms of the amount of conduction delay and block (CD/CB) of the entire atrial surface in patients with aortic valve (AV) and mitral valve (MV) disease.

Relation of conduction disorders with pre- and postoperative AF

Table 3 illustrates the relation and differences in clinical and electrophysiological parameters between patients with and without preoperative AF. AF patients were older, had more left atrial enlargement (>45mm), total CD/CB and more CD/CB at Bachmann's bundle and the lateral left atrium. The strongest parameter correlated with preoperative AF was CD/CB at Bachmann's bundle ($r_{\text{b}}=0.40$, $p<0.001$) followed by age ($r_{\text{b}}=0.31$, $p=0.006$).

Postoperative continuous rhythm registrations of 121(87%) patients were available and analyzed for occurrence of early postoperative AF. Postoperative AF occurred in 52%. Presence of total amount of atrial CD and CB in the upper quartile, preoperative AF, left atrial enlargement, left ventricular dysfunction, hypertension, diabetes did not predict postoperative AF, only age was a limited risk factor for developing postoperative AF (OR 1.071, CI 1.023-1.122, $p = 0.004$). Neither univariate or multivariate logistic regression including CD and CB in the upper quartile per area separately showed associations between electrophysiological parameters and postoperative AF.

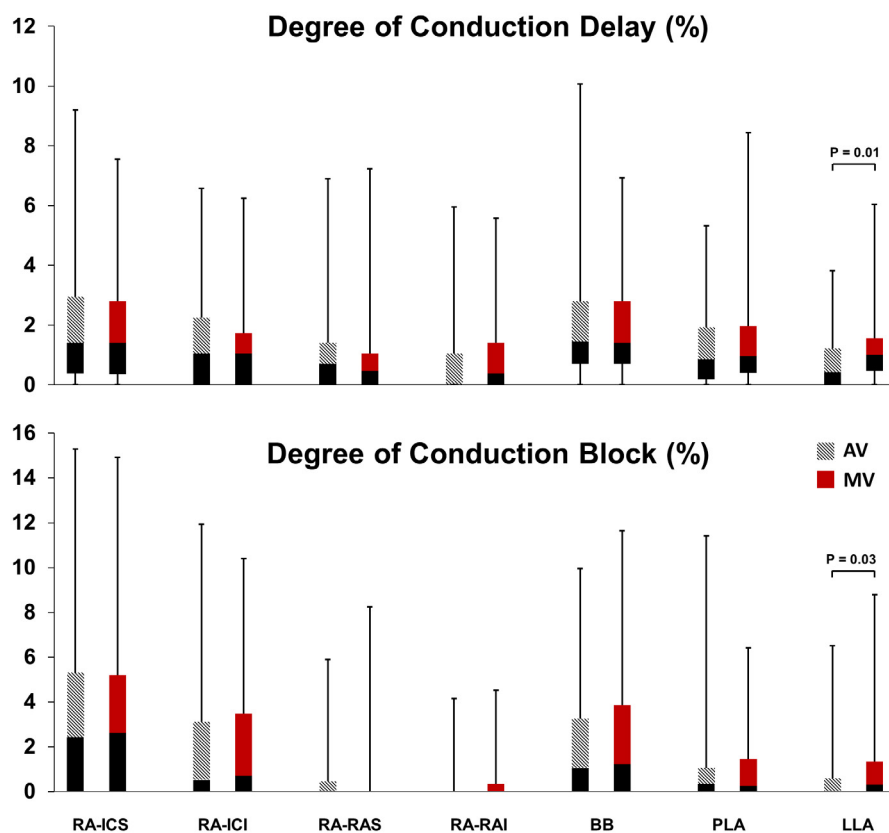


Figure 3. Conduction delay and block per atrial area. Boxplots of the average percentage of conduction delay and block (CD/CB) in each area in patients with AV and MV disease (error bars indicate minimum and maximum, box indicates Q1-median-Q3). The right atrial intercaval superior area (RA-ICS) has the highest amount of CB ($p < 0.001$, significant after Bonferroni correction). Patients with MV disease tend to have more CD/CB at the lateral left atrium (LLA). RA: right atrium; ICS/I: intercaval superior/ inferior; RAS/I: right appendage superior/ inferior; BB: Bachmann's bundle; PLA: posterior left atrium; LLA: lateral left atrium.

Table 2. Prevalence and maximal degree of CD and CB per area

Prevalence (% patients)		All			AV		MV	
		Max Degree (%/cm ²)	Prevalence (% patients)	Max Degree (%/cm ²)	Prevalence (% patients)	Max Degree (%/cm ²)	Max Degree (%/cm ²)	P-value*
RA-ICS	CD	78	4.1 (0-20.8)	79	4.2 (0-17.4)	77	4.0 (0-20.8)	0.391
	CB	73	6.6 (0-34.7)	74	6.3 (0-30.6)	72	6.9 (0-34.7)	0.635
RA-ICI	CD	70	2.8 (0-13.9)	72	2.8 (0-13.9)	66	2.9 (0-11.1)	0.578
	CB	55	2.1 (0-22.5)	53	2.1 (0-22.5)	59	2.8 (0-22.5)	0.696
RA-RAS	CD	63	1.4 (0-13.0)	65	1.4 (0-13.0)	59	1.4 (0-9.7)	0.489
	CB	32	0 (0-22.2)	38	0 (0-22.2)	24	0 (0-14.7)	0.138
RA-RAI	CD	53	1.4 (0-15.3)	47	0 (0-13.9)	62	1.5 (0-15.3)	0.118
	CB	20	0 (0-12.5)	15	0 (0-10.3)	26	0 (0-12.5)	0.086
BB	CD	84	4.2 (0-18.1)	82	4.2 (0-18.1)	87	4.2 (0-13.9)	0.847
	CB	70	3.5 (0-22.2)	71	2.8 (0-20.8)	67	4.2 (0-22.2)	0.630
PLA	CD	81	4.2 (0-18.8)	79	4.2 (0-18.8)	85	4.7 (0-18.1)	0.380
	CB	58	2.0 (0-23.6)	58	2.1 (0-23.6)	59	1.8 (0-19.6)	0.975
LLA	CD	75	2.8 (0-23.6)	69	2.8 (0-12.5)	85	4.2 (0-23.6)	0.001†
	CB	50	0 (0-20.8)	45	0 (0-20.8)	58	1.8 (0-17.4)	0.037

*P-value of maximal degree of CB/CD between AV and MV patients. †Significant after Bonferroni correction; CD: conduction delay; CB: conduction block; RA: right atrium; ICS/I: intercaval superior/inferior; RAS/I: right appendage superior/inferior; BB: Bachmann's bundle; PLA: posterior left atrium; LLA: lateral left atrium.

DISCUSSION

High-resolution mapping of the atria in patients with valvular heart disease demonstrated a high and heterogeneous occurrence of disturbances in electrical conduction during sinus rhythm. The highest prevalence was seen at the high right atrium. The overall degree of CD and CB did not differ between patients with AV and MV disease. However, the lateral left atrium demonstrated a higher maximal degree of CD per 1 cm² in patients with MV disease. Preoperative AF was most strongly correlated with conduction disorders at Bachmann's bundle and age.

Conduction block at the high right atrium

Both groups demonstrated a high prevalence and degree of CB at the high right atrium which is not specific for patients with left-sided valvular heart disease and is also observed in patients with coronary artery disease.⁸ The high right atrium is characterized by the sinoatrial node area and fractionated atrial electrograms are common at this site in patients with sinus node dysfunction.⁹ However, likely CB seen at this site is not caused by sinus node disease with advancing age, but anatomically determined. Even young patients in this study had long lines of CB lateral to the site of first activation. Previous studies have demonstrated that the sinus node is surrounded by arteries and connective tissue protecting the node from external electrical influences and that action potentials of the sinus node are conducted to atrial myocardium via specific exit pathways located superiorly and inferiorly. Lateral conduction towards the atrial septum, however, is blocked by the insulating tissue.^{10,11} Furthermore, the neighboring terminal crest is known for anisotropic conduction properties and slow conduction parallel to the crest which may also contribute to the observed CB at the high right atrium.¹²

Conduction disorders in AV versus MV disease

Both AV and MV disease have been associated with changes in the myocardial structure of the atria due to the altered hemodynamic effects.^{13,14} Structural remodeling can alter atrial electrophysiology and predispose to development of atrial tachyarrhythmias. The higher incidence of AF in MV disease suggests the presence of a higher degree of atrial remodeling in these patients. Roberts-Thomson et al. indeed demonstrated a larger amount of functional delay in conduction during pacing at the posterior left atrial wall in patients with MV disease compared to AV disease.¹⁵ However, these differences were not present during sinus rhythm. We have investigated the entire atrial surface and identified the lateral left atrium as a location with increased conduction delay in patients with MV disease.

Table 3. Correlation between a history of AF and clinical and electrophysiological characteristics

	No AF N=101	AF N=38	P-value	Correlation coefficient
Age, yr [IQR]	68 [12]	73 [11]	0.006	0.31
Hypertension (%)	58	45	0.161	
Diabetes mellitus (%)	14	21	0.301	
LA > 45 mm (%)	22	47	0.003	0.25†
LV function (N-R-M %)	72 - 19 - 9	79 - 16 - 5	0.401	
CD/CB (average % [IQR])				
Total	2.3 [2.0]	2.7 [2.3]	0.044	0.22
RA-ICS	4.7 [6.6]	4.5 [5.0]	0.277	
RA-ICI	2.5 [5.1]	1.1 [5.7]	0.183	
RA-RAS	0.5 [1.8]	0.8 [1.8]	0.718	
RA-RAI	0.4 [1.4]	0.4 [1.3]	0.456	
BB	2.3 [4.4]	5.9 [6.4]	0.000*	0.40
PV	1.6 [2.3]	1.8 [3.2]	0.125	
LA	1.0 [1.9]	1.8 [2.5]	0.009	0.29

* significant after Bonferroni correction; † Phi coefficient; AF: atrial fibrillation; IQR: interquartile range; LA: left atrium; LV: left ventricular; N-R-M: normal-reduced-moderate; CD: conduction delay; CB: conduction block; RA: right atrium; ICS/I: intercaval superior/ inferior; RAS/I: right appendage superior/ inferior; BB: Bachmann's bundle; PLA: posterior left atrium; LLA: lateral left atrium.

Atrial fibrillation and conduction disorders during sinus rhythm

In sinus rhythm, more CD was observed at the left posterior wall in MV patients with persistent AF than without AF.¹⁶ In our study, patients with MV disease had more conduction disorders at the lateral left atrium and a higher prevalence of AF. However, preoperative AF was most strongly correlated with conduction disturbances at Bachmann's bundle. Teuwen et al. has recently found that a high amount and long lines of CB at Bachmann's bundle during sinus rhythm predisposes for early postoperative AF in patients with coronary artery disease.¹⁷ The highly organized structure and anisotropic features could leave Bachmann's bundle more vulnerable to structural remodeling and disturbances in conduction that can even be identified during sinus rhythm. The myocardial strands crossing the right and left atrial roof are not enclosed by fibrous tissue and may perhaps be easily disrupted by stretch due to overload of either atrium.¹⁸ The histological study of Becker et al. demonstrated in fact that structural continuity of Bachmann's bundle is often compromised, especially in patients with AF.¹⁹ Conduction disorders at Bachmann's bundle have been proposed to be a measure of more general atrial electrical pathology.²⁰ However, we found that conduction disturbances in other areas during sinus rhythm are not related to AF.

Study limitations

The routine preoperative echocardiograms did not allow for a retrospective sampling of exact dimensions. This parameter was therefore limited to the used cut-off dimension. The atrial septum cannot be reached by epicardial mapping and is therefore not included in this study. The atrial areas are recorded in a sequential manner due to technical restrictions which may cause some overlap between recordings.

Clinical relevance

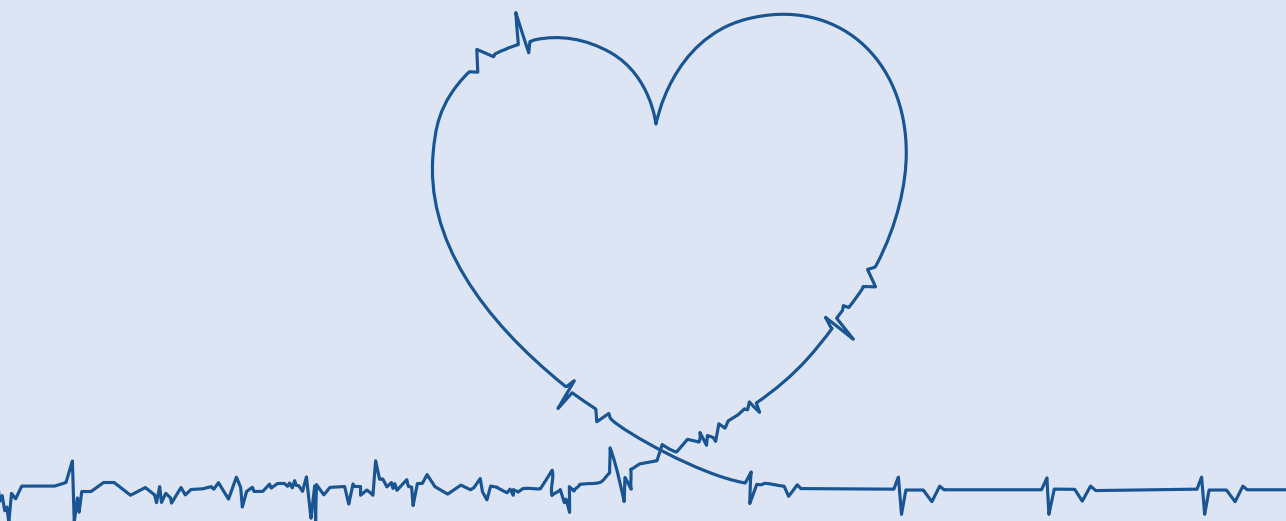
This study is the first to describe conduction disorders in high-resolution of the entire atrial surface during sinus rhythm in patients with valvular heart disease. It demonstrated that left atrial overload in MV disease also translates to more conduction disorders at the lateral left atrium during sinus rhythm and that Bachmann's bundle is most affected in MV and AV patients with AF. These findings help to further understand the structural damage caused by valvular heart disease that alters electrical conduction and most likely creates susceptibility for AF.

CONCLUSION

Excitation of the atria during sinus rhythm is heterogeneously disrupted in patients with AV and MV disease, however, in MV disease more conduction disorders present at the lateral left atrium. The occurrence of AF in presence of valvular heart disease is associated with increased conduction disturbances in sinus rhythm at Bachmann's bundle. Further research is necessary to determine the role of Bachmann's bundle and lateral left atrium in the occurrence of AF in patients with valvular heart disease.

REFERENCES

1. Darby A.E., Dimarco J.P. (2012). Management of atrial fibrillation in patients with structural heart disease. *Circulation*, 125, 945-957.
2. Verheule S., Wilson E., Everett T., Shanbhag S., Golden C. and Olgin J. (2003). Alterations in atrial electrophysiology and tissue structure in a canine model of chronic atrial dilatation due to mitral regurgitation. *Circulation*, 107, 2615-2622.
3. Kumar S., Teh A.W., Medi C., Kistler P.M., Morton J.B., Kalman J.M. (2012). Atrial remodeling in varying clinical substrates within beating human hearts: relevance to atrial fibrillation. *Prog Biophys Mol Biol*, 110, 278-294.
4. Iung B., Baron G., Tornos P., Gohlke-Barwolf C., Butchart E.G., Vahanian A. (2007). Valvular heart disease in the community: a European experience. *Curr Probl Cardiol*, 32, 609-661.
5. Sauter H.J., Dodge H.T., Johnston R.R., Graham T.P. (1964). The Relationship of Left Atrial Pressure and Volume in Patients with Heart Disease. *Am Heart J*, 67, 635-642.
6. van der Does L.J., Yaksh A., Kik C., et al. (2016). QUest for the Arrhythmogenic Substrate of Atrial fibrillation in Patients Undergoing Cardiac Surgery (QUASAR Study): Rationale and Design. *J Cardiovasc Transl Res*, 9, 194-201.
7. Yaksh A., van der Does L.J., Kik C., et al. (2015). A novel intra-operative, high-resolution atrial mapping approach. *J Interv Card Electrophysiol*, 4, 221-225.
8. Lanter E.A., Yaksh A., Teuwen C.P., et al. (2017). Spatial Distribution of Conduction Disorders during Sinus Rhythm. *Int J Cardiol*, 249, 220-225.
9. Centurion O.A., Fukatani M., Konoe A., et al. (1992). Different distribution of abnormal endocardial electrograms within the right atrium in patients with sick sinus syndrome. *Br Heart J*, 68, 596-600.
10. Fedorov V.V., Schuessler R.B., Hemphill M., et al. (2009). Structural and functional evidence for discrete exit pathways that connect the canine sinoatrial node and atria. *Circ Res*, 104, 915-923.
11. Fedorov V.V., Glukhov A.V., Chang R., et al. (2010). Optical mapping of the isolated coronary-perfused human sinus node. *J Am Coll Cardiol*, 56, 1386-1394.
12. Becker R., Bauer A., Metz S., et al. (2001). Intercaval block in normal canine hearts: role of the terminal crest. *Circulation*, 103, 2521-2526.
13. Anne W., Willems R., Roskams T., et al. (2005). Matrix metalloproteinases and atrial remodeling in patients with mitral valve disease and atrial fibrillation. *Cardiovasc Res*, 67, 655-666.
14. Kim S.J., Choisy S.C., Barman P., et al. (2011). Atrial remodeling and the substrate for atrial fibrillation in rat hearts with elevated afterload. *Circ Arrhythm Electrophysiol*, 4, 761-769.
15. Roberts-Thomson K.C., Stevenson I.H., Kistler P.M., et al. (2008). Anatomically determined functional conduction delay in the posterior left atrium relationship to structural heart disease. *J Am Coll Cardiol*, 51, 856-862.
16. Roberts-Thomson K.C., Stevenson I., Kistler P.M., et al. (2009). The role of chronic atrial stretch and atrial fibrillation on posterior left atrial wall conduction. *Heart Rhythm*, 6, 1109-1117.
17. Teuwen C.P., Yaksh A., Lanter E.A., et al. (2016). Relevance of Conduction Disorders in Bachmann's Bundle During Sinus Rhythm in Humans. *Circ Arrhythm Electrophysiol*, 9, e003972.
18. Ho S.Y., Anderson R.H., Sanchez-Quintana D. (2002). Gross structure of the atriums: more than an anatomic curiosity? *Pacing Clin Electrophysiol*, 25, 342-350.
19. Becker A.E. (2004). How structurally normal are human atria in patients with atrial fibrillation? *Heart Rhythm*, 1, 627-631.
20. van Campenhout M.J., Yaksh A., Kik C., et al. (2013). Bachmann's bundle: a key player in the development of atrial fibrillation? *Circ Arrhythm Electrophysiol*, 6, 1041-1046.





CHAPTER 5

IMPACT OF ISCHEMIC AND VALVULAR HEART DISEASE ON ATRIAL EXCITATION: A HIGH-RESOLUTION EPICARDIAL MAPPING STUDY

Mouws EMJP, Lanfers EAH, Teuwen CP, van der Does LJME, Kik C,
Knops P, Yaksh A, Bekkers JA, Bogers AJJC, de Groot NMS
Journal of the American Heart Association (2017)

ABSTRACT

Background The influence of underlying heart disease or presence of atrial fibrillation (AF) on atrial excitation during sinus rhythm (SR) is unknown. We investigated atrial activation patterns and total activation times of the entire atrial epicardial surface during SR in patients with ischemic and/or valvular heart disease (IHD, (i)VHD) with or without AF.

Methods Intra-operative epicardial mapping (N=128/192 electrodes, inter-electrode distances: 2mm) of the right atrium (RA), Bachmann's bundle (BB), left atrioventricular groove (LAVG) and pulmonary vein area (PVA) was performed during SR in 253 patients (186 male (74%), age 66±11years) with IHD (N=132, 52%) or (i)VHD (N=121, 48%).

Results As expected, SR origin was located in the RA superior intercaval region in 232 patients (92%). BB activation occurred via one wavefront from right-to-left (N=163, 64%), from the central part (N=18, 7%) or via multiple wavefronts (N=72, 28%). LAVG activation occurred via 1) BB: N=108, 43%, 2) PVA: N=9, 3% or 3) BB and PVA: N=136, 54%; depending on which route had the shortest interatrial conduction time ($p<0.001$). (i)VHD patients more often had central BB activation and LAVG activation via PVA compared to IHD patients (N=16 (13%) versus N=2 (2%); $p=0.009$ and N=86 (71%) versus N=59 (45%); $p<0.001$ respectively). Total activation times were longer in patients with AF (AF: 136±20 (92-186)ms; No AF: 114±17 (74-156)ms; $p<0.001$), due to prolongation of RA ($p=0.018$) and BB conduction times ($p<0.001$).

Conclusions Atrial excitation during SR is affected by underlying heart disease and AF, resulting in alternative routes for BB and LAVG activation and prolongation of total activation times. Knowledge on atrial excitation patterns during SR and its electro-pathological variations, as demonstrated in this study, is essential to further unravel the pathogenesis of AF.

INTRODUCTION

Excitation of the atria is determined by membrane properties, tissue structure and wavefront geometry.¹⁻³ Knowledge of atrial patterns of activation during sinus rhythm (SR) may enable detection of propagation abnormalities associated with development of atrial tachyarrhythmias such as atrial fibrillation (AF). Prior mapping studies demonstrated that electrical activity originating from the sinus node area, after having spread towards the superior vena cava (SVC) and the right atrial appendage (RAA), propagated from the right (RA) to the left atrium (LA) via Bachmann's Bundle (BB), the rim of the fossa ovalis region or the coronary sinus ostial connections.⁴⁻⁶ In these mapping studies, patterns of activation were reproducible and showed limited inter-individual variation. In vivo activation mapping of the entire RA and LA during SR has only been performed in a limited number of patients with a low spatial resolution. In addition, most mapping studies were performed on the endocardial surface and did therefore not include direct measurements of conduction along BB. At present, it is unknown whether atrial activation patterns, including interatrial conduction, are influenced by underlying heart disease or the presence of AF episodes. As patients with valvular heart disease are more susceptible to develop AF than patients with coronary artery disease, atrial activation patterns may also differ during SR.⁷

Aims of the present study are therefore to investigate in a large cohort of patients with ischemic and/or valvular heart disease whether atrial patterns of activation and total excitation time of the right and left atrium are influenced by patient characteristics and the presence of AF episodes.

METHODS

The data, analytic methods, and study materials will not be made available to other researchers for purposes of reproducing the results or replicating the procedure.

Study population

The study population consisted of 253 successive adult patients undergoing elective open heart coronary artery bypass grafting, aortic or mitral valve surgery or a combination of valvular and bypass grafting surgery in the Erasmus Medical Center Rotterdam. This study was approved by the institutional medical ethical committee (MEC2010-054/MEC2014-393)^{8,9}; written informed consent was obtained from all patients. Preoperative ECG and clinical data were extracted from electronic patient files. Preoperative surface ECGs were screened for the occurrence of interatrial block based on the Bayes criteria. Preoperative surface ECGs were screened for the occurrence of interatrial block based on the Bayes criteria.¹⁰

Mapping procedure

Epicardial high-resolution mapping was performed prior to commencement of extra-corporal circulation, as previously described in detail.¹¹⁻¹³ A 24-electrode array (2-mm inter-electrode distance) A temporary bipolar epicardial pacemaker wire was stitched to the RA free wall, serving as a temporal reference electrode. The indifferent electrode consisted of a steel wire fixed to subcutaneous tissue of the thoracic cavity. Epicardial mapping was performed

with a 128-electrode array, which was later replaced by a 192-electrode array to shorten the duration of the mapping procedure (electrode diameter respectively 0.65mm or 0.45mm, interelectrode distances 2 mm). Mapping was conducted by shifting the electrode array along predefined areas of the RA, BB and LA between anatomical borders in a systematic order, covering the entire atrial epicardial surface, in which omission of areas was avoided at the expense of possible small overlap between successive mapping sites, as illustrated in the upper left panel of Figure 1. The RA was mapped in 4 consecutive horizontal lines (RA1-4) from the cavotricuspid isthmus towards the RAA, perpendicular to the inferior and superior caval vein (ICV and SCV). Mapping of BB was performed from the border of the left atrial appendage (LAA) towards the superior cavo-atrial junction. The pulmonary vein area (PVA) was mapped from the sinus transversus along the borders of the right and left pulmonary veins (PVR and PVL) down towards the atrioventricular groove. The left atrioventricular groove (LAVG) was mapped from the lower border of the left inferior pulmonary vein (LA1) towards the LAA (LA2).

Five seconds of SR were recorded at every mapping site, including a surface ECG lead, a calibration signal of 2mV and 1000ms, a bipolar reference electrogram, and all unipolar epicardial electrograms.^{11a} 8 \u00d7 24-electrode array (2-mm inter-electrode distance) Recordings were sampled with a rate of 1kHz, amplified (gain 1000), filtered (bandwidth 0.5-400 Hz), analogue-to-digital converted (16-bits) and stored on a hard disk.^{11a} 8 \u00d7 24-electrode array (2-mm inter-electrode distance)

The upper left panel of Figure 1 shows all mapping locations, including RA1-4, BB, LA, PVR and PVL, on a schematic view of the atria. Examples of activation maps obtained from each of these sites are displayed in the upper right panel of Figure 1. Local activation maps during 5 seconds of SR were constructed by annotating the steepest negative slope of atrial potentials recorded at every electrode. Atrial extrasystolic beats were excluded from analysis.¹⁴⁻¹⁶ In order to reconstruct activation patterns of the entire epicardial surface, the time interval between the local activation time of the reference electrode (defined as zero point) and every electrode was calculated and depicted in color-code, as demonstrated in the total activation map in the lower right panel of Figure 1.

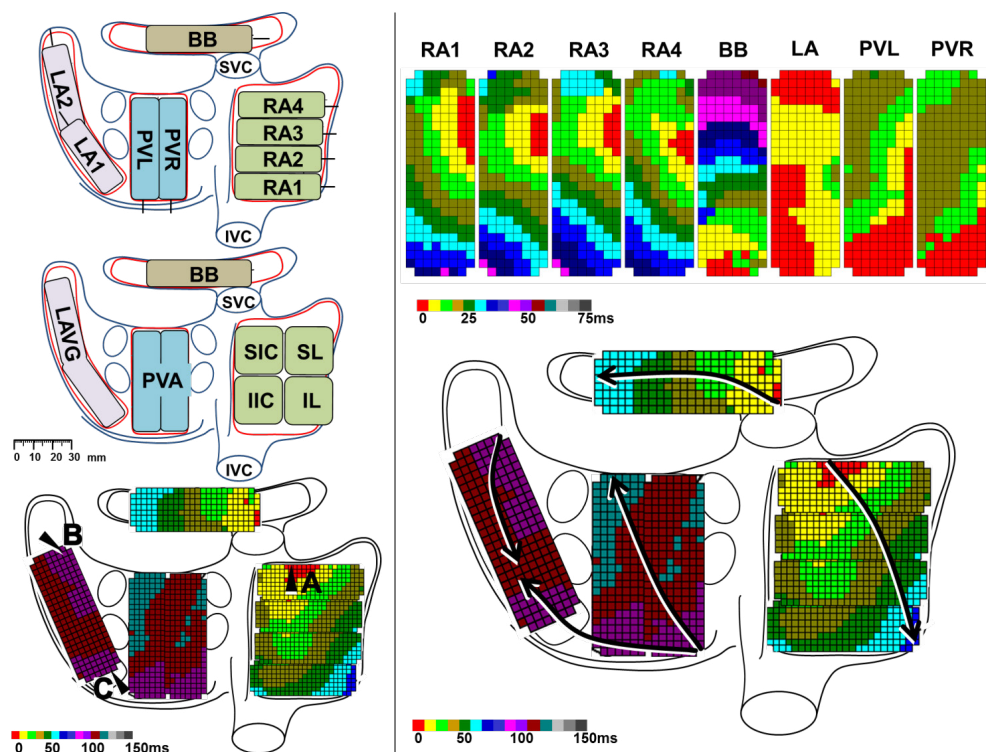


Figure 1. Activation mapping of the right and left atrium. Left panel: posterior view of the atria with epicardial mapping scheme (192 electrodes) (upper), classification of the anatomical regions (middle) and landmarks for calculation of duration of wavefront propagation from the origin of sinus rhythm (A) to the LAVG via BB (B) and via PVA (C). Upper Right panel: color-coded activation maps per mapping site; electrodes activated within the first 5 ms are colored red. Lower right panel: total activation map constructed relative to local activation times of the reference electrode which was defined as 0 ms. Arrows indicate main trajectories of SR waves at the different atrial regions. BB: Bachmann's Bundle; LA: left atrium; RA: right atrium; PVL: pulmonary veins left; PVR: pulmonary veins right; LAVG: left atrioventricular groove; PVA: pulmonary vein area; SIC: superior intercaval; SL: superolateral; IIC: inferior intercaval; IL: inferolateral; SVC: superior vena cava; IVC: inferior vena cava.

Activation mapping of the atrial epicardium

Supplemental Figure 1 provides a more extensive view of annotation of electrograms and construction of activation maps, enabling the display of the total activation map. In this example, the epicardial surface of RA is first excited by a broad wavefront originating from the superior intercaval (SIC) region. This wavefront then spreads across the RA and BB, towards the LA. In the LA, another wavefront emerges in coronary sinus region and propagates towards the left upper pulmonary vein. The LAVG is thus activated by 2 wavefronts, originating from both BB and PVA, merging in the middle of the LAVG.

Total activation times were calculated as the time interval (ms) between the earliest and latest activated electrode. As visualized in the lower left panel of Figure 1, the duration of propagation was calculated for wavefronts propagating from the origin of SR across BB towards the left

atrioventricular groove (LAVG) (Figure 1, point A to point B) and for wavefronts propagating from the SR origin through the limbus of the fossa ovalis or the coronary sinus ostium across the pulmonary vein area (PVA) towards the LAVG (Figure 1, point A to point C). The latter conduction route will be referred to as conduction via PVA.

Classification of patterns of activation

Patterns of activation and propagation direction were examined in all SR maps. The origin of RA activation was assigned to 1 of the 4 regions demonstrated in the lower left panel of Figure 1, including the superior intercaval (SIC), inferior intercaval (IIC), superolateral (SL) and inferolateral (IL) region.

Entry sites of SR wavefronts in BB were classified as right atrial, central, left atrial or multiple entry sites. A right atrial entry site was defined as a wavefront first entering the mapping array from the right side of BB, propagating towards the left side of BB, whereas in case of a left atrial entry site the initial activation was observed at the tip of the electrode positioned at the border of the left atrial appendage (LAA), spreading towards the right side of BB. A wavefront emerging in the middle of the mapping array propagating to either the right and/or left side was labeled as a central entry site. Excitation of the LAVG was described as activation via BB only, the PVA only, or a combination of both.

Statistical analysis

Normally distributed data are described by mean \pm SD (minimum-maximum) and analyzed with a student's T-test or a one way ANOVA. Skewed data are described by median (minimum-maximum) and analyzed with Kruskal-Wallis test or a Mann-Whitney U test. Categorical data are expressed as numbers and percentages and analyzed with χ^2 or Fisher exact test when appropriate. Multiple linear regression analysis was performed to identify independent predictors for prolonged total activation times. A p-value<0.05 was considered statistically significant. All statistical analyses were performed with IBM SPSS statistics for Windows, version 24 (IBM Corp., Armonk, N.Y., USA).

RESULTS

Study population

Characteristics of the study population (N=253, 186 male (74%), age 66 \pm 11 years) are summarized in Table 1. Patients had either ischemic heart disease (IHD) (N=132, 52%), valvular heart disease (VHD) (N=68, 27%) or a combination of valvular and ischemic heart disease (I/VHD) (N=53, 21%). VHD (N=121) was categorized by the predominant valvular lesion and consisted of aortic valve stenosis (N=68, 27%), aortic valve insufficiency (N=9, 4%) or mitral valve insufficiency (N=44, 17%). A minority of patients (N=43, 17%) had a history of AF, of whom 13 presented in AF and underwent SR mapping after electrocardioversion. AF was most prevalent in patients with mitral valve disease (N=16, 36%) compared to patients with aortic valve disease (N=14, 18%) or only ischemic heart disease (N=13, 10%) (p<0.001). Also, AF was more prevalent in patients with LA dilation (N=16, 30%) compared to patients without LA dilation (N=27, 14%) (p=0.004). Most patients had a normal left ventricular function

(LVF) (N=188, 74%) and the majority used class II (N=165, 65%) antiarrhythmic drugs. Patients were mapped with either a 128-polar (N=141, 56%) or a 192-polar electrode array (N=112, 44%). Mean cycle length (CL) was 857 ± 175 (473-1458)ms. Compared to IHD patients, (i) VHD patients more often had LA dilation ($p=0.007$) and AF ($p=0.001$), which was more often (longstanding) persistent ($p=0.007$). IHD patients more often used betablockers ($p<0.001$).

Table 1. Patient characteristics

	Total
Number of patients	253
Age	66 ± 11 (21–84)
Male	186(74)
BSA	2.0 ± 0.2 (1.5–2.8)
Underlying heart disease	N(%)
IHD	132(52)
VHD	68(27)
I/VHD	53(21)
Valvular Heart Disease	121(48)
Aortic Valve Stenosis	68(27)
Mild	2(1)
Moderate	14(5)
Severe	52(21)
Aortic Valve Insufficiency	9(4)
Mild	1(1)
Moderate	5(2)
Severe	3(1)
Mitral Valve Insufficiency	44(17)
Moderate	14(5)
Severe	30(12)
Left Atrial Dilation	53(21)
History of AF	43(17)
Paroxysmal	33(13)
Persistent	9(4)
Longstanding persistent	1(1)
Left ventricular function	
Normal	188(74)
Mild dysfunction	46(18)
Moderate dysfunction	17(7)
Severe dysfunction	2(1)
Antiarrhythmic drugs	175(69)
Class I	1(1)
Class II	165(65)
Class III	8(3)
Class IV	2(1)

AF: atrial fibrillation; BSA: body surface area; IHD: ischemic heart disease; VHD: valvular heart disease; I/VHD: ischemic and valvular heart disease.

Origin of atrial activation

Figure 2 shows 6 typical examples of different patterns of activation observed in our study population. The origin of atrial activation was located in the SIC region in 232 patients (92%; panels A-C). In the remaining patients, earliest activation was identified in the SL region (N=10, 4%; Panel D) or in the IIC region (N=11, 4%; Panel E, F). As expected, the location of the origin of atrial activation did not differ between patients with or without AF ($p=0.344$) and between patient with IHD or (i)VHD ($p=0.181$). In addition, CL did not differ between the various locations of the SR origin (SIC: 858 ± 178 (473-1458)ms; SL: 832 ± 162 (646-1081)ms; IIC: 861 ± 114 (666-1046)ms, $p=0.894$).

Excitation of Bachmann's bundle

Conduction along BB occurred mainly by a single wavefront, propagating from the right to the left side (N=163, 64%), as shown in panel A, D and E of Figure 2. Panel B demonstrates central activation of BB spreading towards both the right and left side; this pattern of activation occurred in 18 patients (7%). Activation of BB by multiple wavefronts originating from different entry sites was observed in 72 patients (29%). In 60 of these patients (83%), BB was activated by two separate wavefronts entering from the right side and from the central part of BB (Figure 2F). A combination of two wavefronts entering from the right and left side occurred in 2 patients (3%) (Figure 2C) and one patient (1%) showed activation of BB via the central part and the left side. In 9 patients (13%) BB was activated by three wavefronts entering from the right, left and central part of BB. BB activation patterns and the number of entry sites did not differ between patients without and with a history of AF ($p=0.570$ and $p=0.388$ respectively).

As illustrated in the upper panel of Figure 3, patterns of wavefront propagation along BB differed between IHD and (i)VHD ($p=0.009$). A wavefront entering in the central part of BB was observed most frequently in patients with (i)VHD (N=16, 13%) compared to IHD patients (N=2, 2%). BB activation patterns did not differ between patients with aortic or mitral VHD ($p=0.409$). The number of entry sites in BB was similar between IHD and (i)VHD ($p=0.557$).

Excitation of the left atrioventricular groove

Typical examples of activation patterns of the LAVG are shown in Figure 2. As illustrated in panels A, C, D and E, most patients (N=136, 54%) showed activation of the LAVG by two wavefronts originating from both BB and the PVA, indicating propagation of conduction through the fossa ovalis and the coronary sinus ostium. A single wavefront activating the LAVG via only BB (panel F) or PVA (panel B) occurred in 108 (42%) and 9 (4%) patients respectively. Location of the origin of SR did not influence the preferential use of either BB or PVA for interatrial propagation ($p=0.871$).

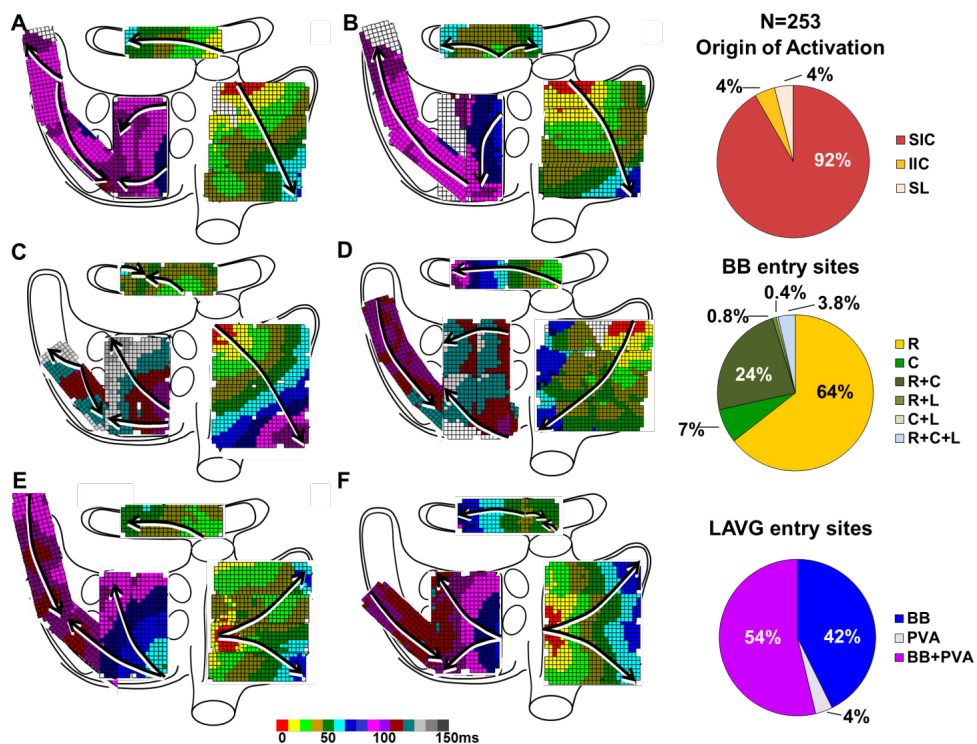


Figure 2. Atrial patterns of activation. Left panel: Examples of excitation of the atrial epicardial surface during SR. Arrows indicate main trajectories of SR waves at the different atrial regions; See text for detailed explanation. Right panel: Relative incidences of different locations of the origin of activation, entry sites at BB and the LAVG. BB: Bachmann's Bundle; C: central; L: left; LAVG: left atrioventricular groove; PVA: pulmonary vein area; R: right; SIC: superior intercaval; SL: superolateral; IIC: inferior intercaval.

Preferential interatrial routes for LAVG excitation were similar between patients without and with AF ($p=0.224$); LAVG activation via 1) a combination of BB and PVA (without AF: $N=109$, 52%; with AF: $N=27$, 63%), 2) BB only (without AF: $N=92$, 44%; with AF: $N=16$, 37%), or 3) PVA only (without AF: $N=9$, 4%; with AF: $N=0$). However, usage of interatrial routes differed between patients with IHD and (i)VHD ($P<0.001$). As displayed in the lower panel of Figure 3, activation via BB only was most frequently observed in IHD patients ($N=73$, 55%). In patients with (i)VHD, LAVG activation via BB only was observed in only 29% of patients ($N=35$), whereas propagation through the interatrial septum via the fossa ovalis or the coronary sinus across the PVA occurred in 86 patients (71%), of whom 6 patients (5%) showed LAVG activation via the PVA only. Type of VHD did not influence the use of different conduction routes ($p=0.760$). Examination of surface ECGs showed a mean p-wave duration of 98 ± 16 ms; p-wave duration was ≥ 120 ms in 58 patients (23%). However, complete interatrial conduction block according to the Bayes criteria in the inferior leads could not be confirmed in these patients. The incidence of partial interatrial block, defined by only a prolongation of P-wave duration ≥ 120 ms on the surface ECG, was similar for patients without and with AF ($N=51$ (24%) vs $N=7$ (16%)).

respectively, $p=0.255$), as well as for patients without and with LA dilation ($N=45$ (23%) vs $N=13$ (25%) respectively, $p=0.755$). Also, preferential routes of conduction towards the LAVG did not differ between those with a p-wave duration $<120\text{ms}$ and $\geq 120\text{ms}$.

Conduction time towards the left atrioventricular groove

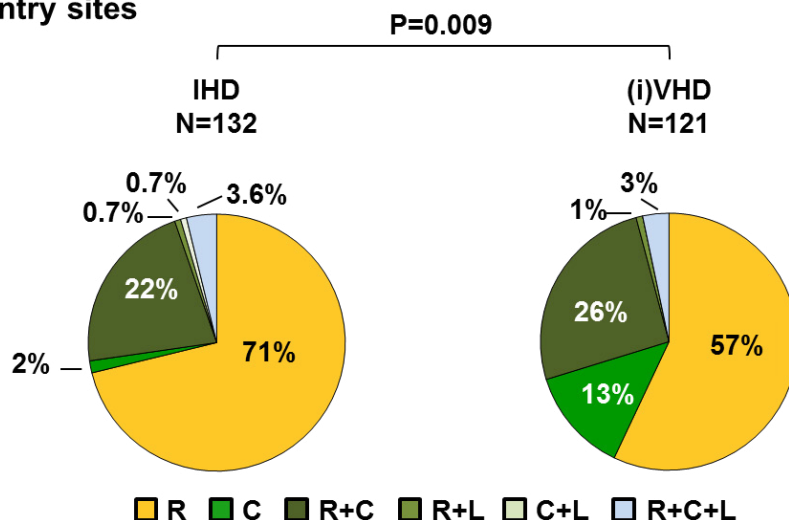
As depicted in Figure 1, conduction times towards the LAVG via BB or via PVA were assessed by calculation of the time interval between point A and B and between point A and C respectively. Time required for wavefronts to propagate from the SR origin to the LAVG via BB was 90 ± 18 (44-157)ms, while propagation to the LAVG via PVA was 101 ± 20 (43-160)ms ($p<0.001$). Figure 4 illustrates the differences in conduction times *towards* the LAVG, which were larger in those with one predominant route (BB or PVA), compared to those with a route via both BB and PVA ($p<0.001$). If LAVG was activated via both BB and PVA ($N=136$), total conduction time along BB was only 5 ± 13 (-47 to +30)ms shorter than via PVA. However, if LAVG was activated only via PVA ($N=9$), total conduction time via PVA was 20 ± 10 (+4 to +31) ms shorter than via BB (lower panels of Figure 4). Likewise, if LAVG was activated only via BB ($N=108$), total conduction time via BB was 21 ± 12 (-50 to +26)ms shorter than via PVA.

Duration of right and left atrial excitation

Total activation time of the entire atrial epicardial surface was 118 ± 19 (74-186)ms. The upper panel of Figure 5 shows differences in total activation times for patients without or with AF, various underlying heart diseases and without or with LA dilation. Similar data for the different atrial regions is depicted in Table 2. In patients with a history of AF, total activation times were longer than in patients without a history of AF; mean durations are respectively 136 ± 20 (92-186) and 114 ± 17 (74-156)ms ($p<0.001$). This difference was mainly due to a significant longer total activation time of the RA and BB in patients with AF (RA:

73 ± 13 (42-98)ms versus 67 ± 14 (32-142)ms, $p=0.018$; BB: 106 ± 20 (68-157)ms versus 87 ± 16 (44-151)ms, $p<0.001$), as demonstrated in the lower panel of Figure 5 and in Table 2. Total activation times of the LA were similar (without AF: 46 ± 15 (6-111)ms; with AF: 48 ± 17 (8-92)ms, $p=0.376$).

BB entry sites



LAVG entry sites

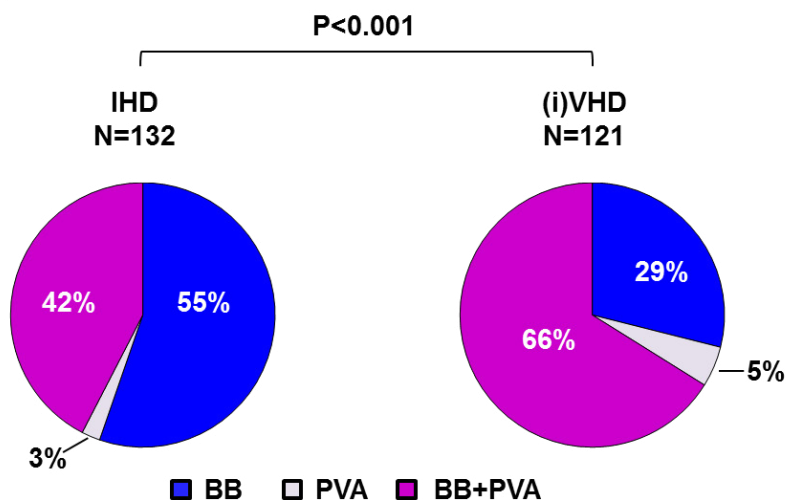


Figure 3. Activation of Bachmann's bundle and the left atrioventricular groove. Differences in incidences of entry sites of wavefronts at BB and LAVG between patients with IHD and (i)VHD. BB: Bachmann's Bundle; C: central; IHD: ischemic heart disease; (i)VHD: (ischemic and) valvular heart disease; L: left; LAVG: left atrioventricular groove; PVA: pulmonary vein area; R: right.

Patients with IHD or (i)VHD had similar total activation times with mean durations of respectively 117 ± 17 (74-156)ms and 119 ± 21 (77-186)ms ($p=0.318$). When analyzing the difference between IHD, AVD or MVD patients separately, similar total activation times were observed for AVD and IHD patients (total activation time: 116 ± 20 vs. 117 ± 17 ms respectively, $p=0.770$), whereas MVD patients had significantly longer total activation times than IHD

patients (125 ± 23 vs. 117 ± 17 ms respectively, $p=0.015$). Subsequently, dividing the entire cohort in patients without and with MVD showed longer total activation times in MVD patients compared to patients without MVD (125 ± 23 vs. 117 ± 18 ms respectively, $p=0.009$, Figure 5). Although no specific site of prolongation of conduction was found, BB showed a trend towards prolongation of conduction in these patients ($p=0.096$) (Table 2).

As depicted in Table 2, longer total activation times showed a strong association with LA dilation ($p<0.001$), yet remarkably, this was due only to prolongation of conduction on BB ($p<0.001$), rather than on LA ($p=0.717$). This is mainly the result of the fact that slow conduction on BB was largely compensated by LAVG activation via the PVA route so that LA activation times are not prolonged. As AF, MVD and LA dilation are closely intertwined, a multivariate analysis was performed in which also older age was taken into account. History of AF (B 18.58 (95%CI 12.8-24.4), $p<0.001$), LA dilation (B 8.27 (95%CI 2.8-13.7), $p=0.003$) and older age (B 0.28 (95%CI 0.08-0.48), $p=0.006$) were independent predictors for prolonged total activation times, whereas MVD (B 0.48 95%CI -5.4-6.4) $p=0.872$) was not.

DISCUSSION

Key findings

Intra-operative, high-resolution epicardial mapping of the entire atrial surface during SR demonstrated prolonged excitation of the atria in patients with a history of AF, which was mainly caused by longer total activation times of the RA and BB. Patients with MVD and with LA dilation had the highest prevalence of AF. Remarkably, LA dilation was associated with longer conduction times of BB and not of LA. In patients with (i)VHD, who most likely have the highest degree of structural remodeling, central BB excitation and interatrial conduction via both BB and PVA towards the LAVG was more prevalent. The predominance of different routes of interatrial conduction depended on conduction time towards the LAVG.

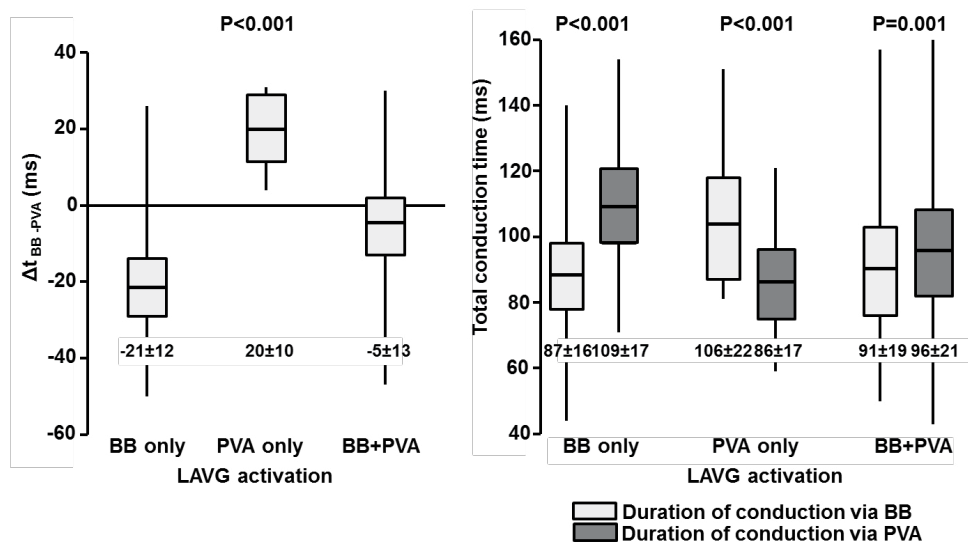


Figure 4. Conduction times towards the left atrioventricular groove. Time differences (left panel) and total conduction times (right panel) between BB and PVA conduction routes towards LAVG in patients with LAVG activation via BB only, PVA only or BB and PVA. BB: Bachmann's Bundle; LAVG: left atrioventricular groove; PVA: pulmonary vein area.

Location of the sinus node

In coherence with previous studies, we observed a certain variation in the location of the origin of activation along the intercaval line and the superior RA wall.^{6,17,18} However, we could not confirm a relation between mean SR CL and the various locations of SR origins. Previous studies demonstrated that there is a certain degree of inter-individual variety in the location of the sinus node area. Also within a patient, the leading pacemaker site within the sinus node can shift in position, depending on autonomic changes.^{17,18} Boineau et al. previously reported a correlation between the spatial position of the sinus origin and the SR cycle length.¹⁹ Faster heart rates were initiated from origins located more superiorly along the sulcus terminalis, whereas slower heart rates were initiated from origins located more inferiorly.¹⁹ Optical mapping studies by Fedorov et al. showed delayed sinus node activation followed by fast atrial activation via sinoatrial exit pathways.²⁰ They found a conduction delay of 82ms between earliest sinus node excitation and earliest excitation of the atrial myocardium.²⁰ Though the site of first sinus node excitation remained stable, earliest excitation of the atrial myocardium via the sinoatrial exit pathways could shift inferiorly when SR CL prolonged.²⁰

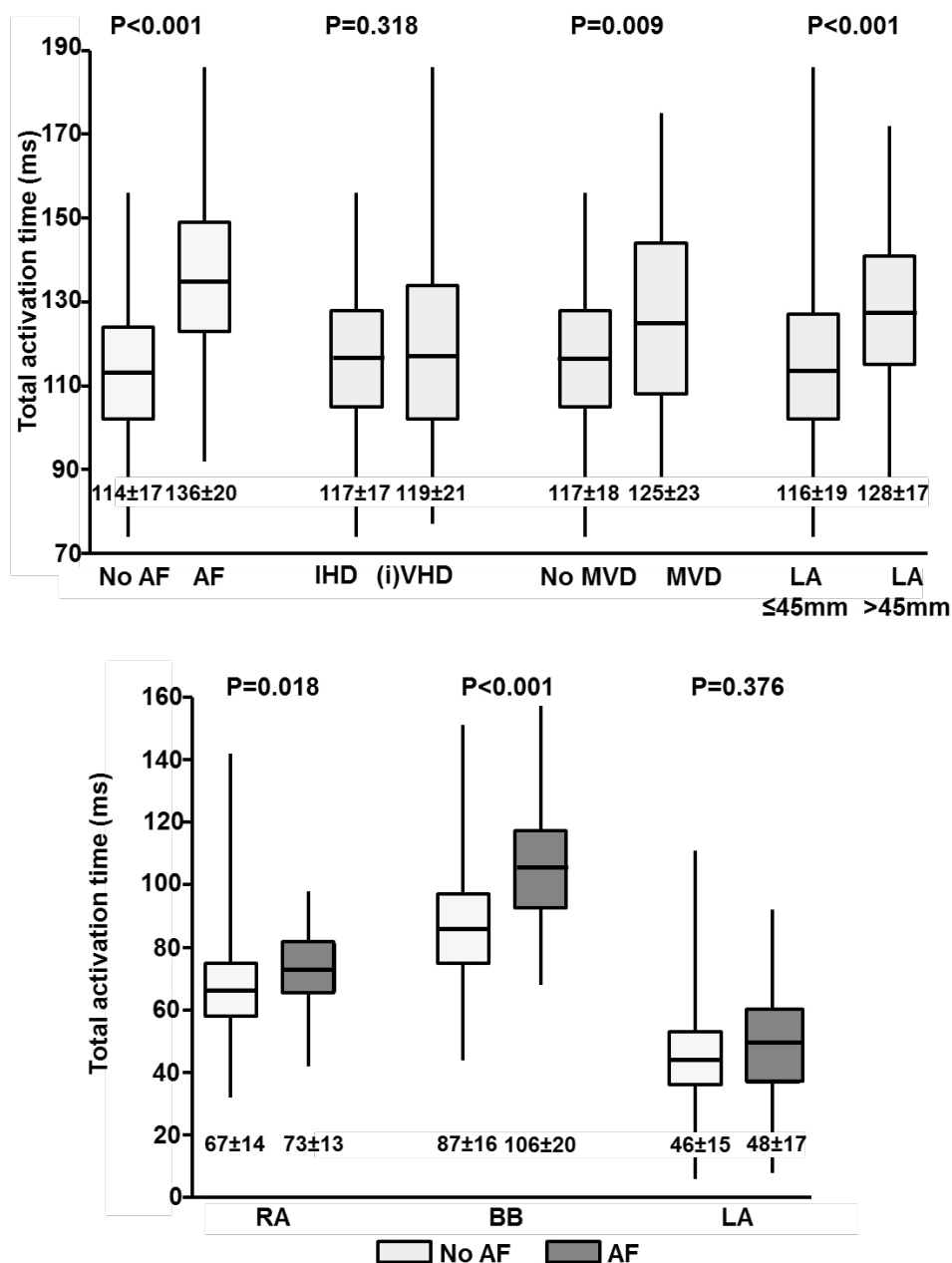


Figure 5. Differences in total activation times. Upper panel: Differences in total activation time of the entire atrial surface between patients without and with AF; various underlying heart diseases and without or with LA dilation. Lower panel: Differences in total activation time of RA, BB and LA separately between patients without and with AF. AF: atrial fibrillation; BB: Bachmann's bundle; IHD: ischemic heart disease; (i)VHD: (ischemic and) valvular heart disease; LA: left atrium; LAVG: left atrioventricular groove; MVD: mitral valve disease; PVA: pulmonary vein area; RA: right atrium.

Table 2. Activation times for various underlying heart diseases

Activation Times (ms)	No AF	AF	p-value
TAT	114±17	136±20	<0.001
BB	87±16	106±20	<0.001
RA	67±14	73±13	0.018
LA	46±15	48±17	0.376
	IHD	(i)VHD	
TAT	117±17	119±21	0.318
BB	88±17	91±19	0.181
RA	69±15	67±13	0.395
LA	47±15	46±15	0.391
	No MVD	MVD	
TAT	117±18	125±23	0.009
BB	89±17	94±22	0.096
RA	68±15	67±12	0.627
LA	46±15	47±17	0.790
	No LA dilation	LA dilation	
TAT	116±19	128±17	<0.001
BB	88±17	98±18	<0.001
RA	68±14	69±13	0.741
LA	47±15	46±15	0.717

AF: atrial fibrillation; BB: Bachmann's bundle; LA: left atrium; IHD: ischemic heart disease; (i)VHD: (ischemic and) valvular heart disease; MVD: mitral valve disease; RA: right atrium; TAT: total activation time.

Interatrial conduction

There was a large inter-individual variation in activation of BB in our study population. Prior studies have demonstrated muscular connections between BB and the interatrial septum, which can excite the center of BB.^{5,21–23} These muscular connections enable wavefronts to conduct via interatrial pathways such as the limbus of the fossa ovalis, the coronary sinus and interatrial bundles both superior and inferior along BB.^{5,23} SR wavefronts may propagate upwards in the interatrial septum and activate the central area of BB. Teuwen et al. indeed observed in 185 patients with IHD that lines of conduction block at BB may delay right-to-left excitation, thereby favoring conduction via other interatrial routes, such as the interatrial septum.²³ Conduction via one wavefront entering in the central part of BB was reported in 4% of their population and combinations of entry sites involving the central part of BB in 29% of IHD patients.²³ We found similar incidences in our cohort, although there were differences between underlying heart diseases with a far higher incidence of central entry sites in patients with (i)VHD. The overall preferential route of interatrial conduction in our study population was BB, with a right-to-left conduction pattern via a single wavefront in most patients. Also, interatrial conduction via PVA or a combination of BB and PVA was more likely to occur in patients with (i)VHD.

Activation of the LAVG via a wavefront originating at the anterosuperior side and propagating towards the posterior side of the LAVG is in coherence with the exit point of the outer left BB, whereas activation via the postero-septal wall can be interpreted as wavefronts propagating via the limbus of the fossa ovalis or the coronary sinus ostium.

The predominance of these alternative routes of conduction may be the result of damage to the thick and thin septa surrounding BB myocytes.²⁴ It has been suggested that increased atrial stretch delays conduction along BB.²⁴ We hypothesize that this layer is more likely to be damaged first by chronic atrial stretch which is more pronounced in VHD patients. Damage to this layer may thereby slow BB conduction and give rise to the predominance of activation patterns via alternative routes of interatrial conduction.

This hypothesis was further supported by the observation that in patients with conduction via only PVA, conduction via BB is considerably slower – up to 31 ms – than via PVA. Particularly patients with either AF, LA dilation or mitral valve disease showed longer total excitation times of the atria, which was all mostly influenced by conduction times along BB. Although MVD, LA dilation and AF are closely intertwined, our findings suggest that atrial activation times are particularly affected at BB and RA by remodeling due to the presence of AF, which might be secondarily enforced by atrial stretch as a result of MVD.

Interatrial block based on a biphasic p-wave morphology in the inferior leads in those with a p-wave duration ≥ 120 ms however could not be confirmed, nor did preferential routes of conduction towards the LAVG differ between those with a p-wave duration < 120 ms and ≥ 120 ms.

Study limitations

Most patients with AF in our study had paroxysmal AF instead of (longstanding) persistent AF. Electrical and structural remodeling in these patients is expected to be less, therefore differences between patients without and with AF in our study might be underestimated. Whether general anesthesia and intra-operative drugs influence conduction is yet to be investigated, however, a standard anesthetic protocol was used for all patients and SR was confirmed during all mapping procedures. Thus, possible effects of anesthesia would be equally dispersed among the patient population. In addition, high-resolution mapping of the interatrial septum was not performed with our closed beating heart approach.

CONCLUSION

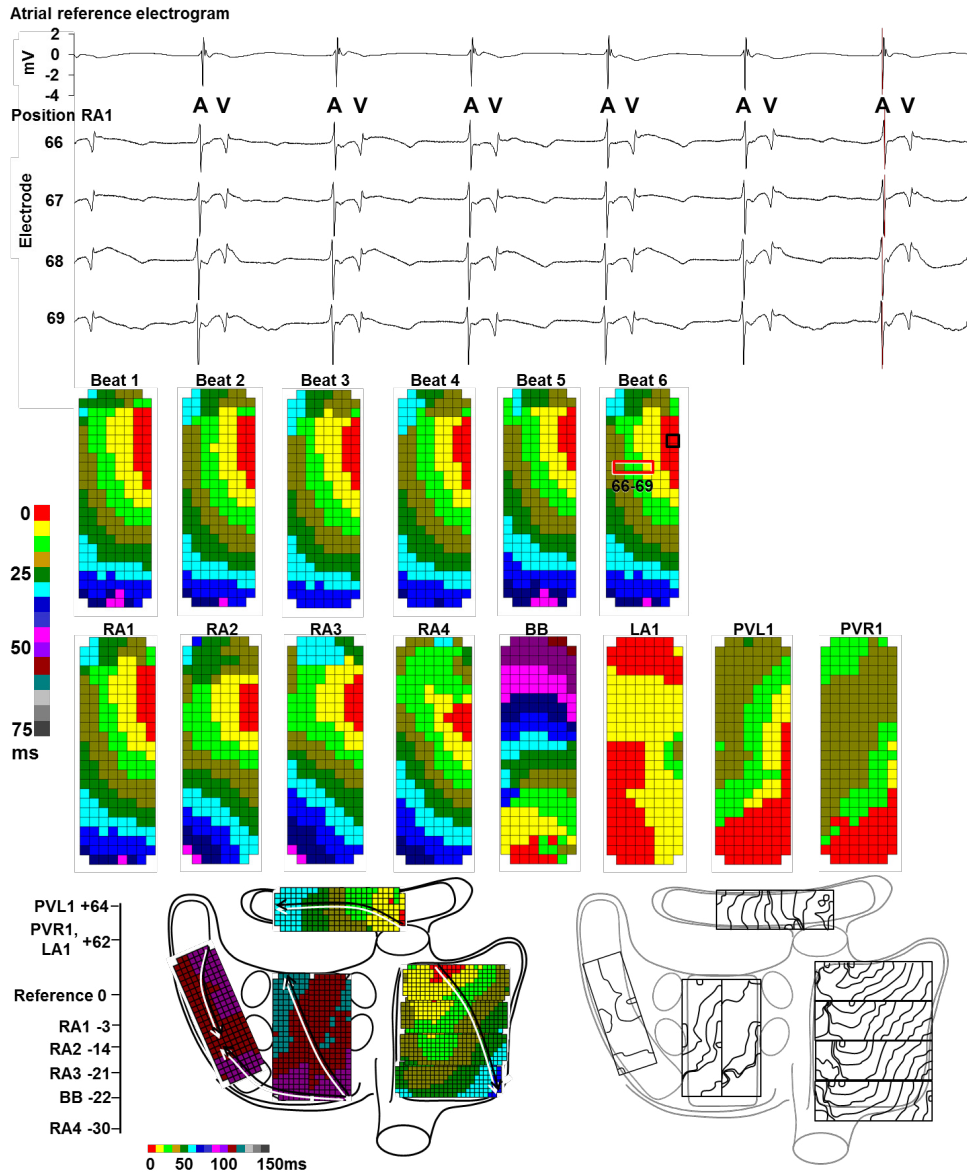
High-resolution mapping of the atrial epicardial surface during SR in a large cohort of IHD and/or VHD patients demonstrated a considerable inter-individual variation in excitation of the atria. RA and LA excitation are affected by underlying heart disease and presence of AF. BB appears most susceptible for damage due to MVD, LA dilation and AF, causing local conduction delay. Central BB excitation and interatrial conduction via both BB and PVA towards the LAVG was more prevalent in patients with (i)VHD, likely resulting from a severer degree of structural remodeling causing intra-atrial conduction delay. Knowledge on atrial excitation patterns during SR and its electro-pathological variations, as demonstrated in this study, is essential to further unravel the pathogenesis of AF.

REFERENCES

1. Fast VG, Kléber AG. Role of wavefront curvature in propagation of cardiac impulse. *Cardiovasc Res*. 1997;33:258–71.
2. Spach MS, Kootsey JM. The nature of electrical propagation in cardiac muscle. *Am J Physiol*. 1983;244:H3–22.
3. de Bakker JMT, van Rijen HM V. Continuous and discontinuous propagation in heart muscle. *J Cardiovasc Electrophysiol*. 2006;17:567–73.
4. Lemery R, Birnie D, Tang ASL, Green M, Gollob M, Hendry M, Lau E. Normal atrial activation and voltage during sinus rhythm in the human heart: an endocardial and epicardial mapping study in patients with a history of atrial fibrillation. *J Cardiovasc Electrophysiol*. 2007;18:402–8.
5. Tapanainen JM, Jurkko R, Holmqvist F, Husser D, Kongstad O, Mäkijärvi M, Toivonen L, Platonov PG. Interatrial right-to-left conduction in patients with paroxysmal atrial fibrillation. *J Interv Card Electrophysiol*. 2009;25:117–22.
6. Sakamoto S, Yamauchi S, Yamashita H, Imura H, Maruyama Y, Ogasawara H, Hatori N, Shimizu K. Intraoperative mapping of the right atrial free wall during sinus rhythm: variety of activation patterns and incidence of postoperative atrial fibrillation. *Eur J Cardiothorac Surg*. 2006;30:132–9.
7. Psaty BM, Manolio TA, Kuller LH, Kronmal RA, Cushman M, Fried LP, White R, Furberg CD, Rautaharju PM. Incidence of and Risk Factors for Atrial Fibrillation in Older Adults. *Circulation*. 1997;96:2455–2461.
8. van der Does LJME, Yaksh A, Kik C, Knops P, Lanthers EAH, Teuwen CP, Oei FBS, van de Woestijne PC, Bekkers JA, Bogers AJJC, Allesie MA, de Groot NMS. QUES for the Arrhythmogenic Substrate of Atrial fibrillation in Patients Undergoing Cardiac Surgery (QUASAR Study): Rationale and Design. *J Cardiovasc Transl Res*. 2016;9:194–201.
9. Lanthers EAH, van Marion DMS, Kik C, Steen H, Bogers AJJC, Allesie MA, Brundel BJJM, de Groot NMS. HALT & REVERSE: Hsf1 activators lower cardiomyocyte damage; towards a novel approach to REVERSE atrial fibrillation. *J Transl Med*. 2015;13:347.
10. Conde D, Seoane L, Gysel M, Mitrione S, Bayés De Luna A, Baranchuk A. Bayés' syndrome: The association between interatrial block and supraventricular arrhythmias. *Expert Rev Cardiovasc Ther*. 2015;13:541–550.
11. Yaksh A, van der Does LJ, Kik C, Knops P, Oei FB, van de Woestijne PC, Bekkers JA, Bogers AJ, Allesie MA, de Groot NM. A novel intra-operative, high-resolution atrial mapping approach. *J Interv Card Electrophysiol*. 2015;44:221–225.
12. Kik C, Mouws EMJP, Bogers AJJC, de Groot NM. Intra-operative mapping of the atria: the first step towards individualization of atrial fibrillation therapy? *Expert Rev Cardiovasc Ther*. 2017;15:537–545.
13. Mouws EMJP, Lanthers EAH, Teuwen CP, van der Does LJME, Kik C, Knops P, Bekkers JA, Bogers AJJC, de Groot NMS. Epicardial Breakthrough Waves During Sinus Rhythm. *Circ Arrhythmia Electrophysiol*. 2017;10:e005145.
14. de Groot N, van der Does L, Yaksh A, Lanthers E, Teuwen C, Knops P, van de Woestijne P, Bekkers J, Kik C, Bogers A, Allesie M. Direct Proof of Endo-Epicardial Asynchrony of the Atrial Wall During Atrial Fibrillation in Humans. *Circ Arrhythmia Electrophysiol*. 2016;9:e003648.
15. de Groot N, Houben R, Smeets J, Boersma E, Schotten U, Schalij M, Crijns H, Allesie M. Electropathological Substrate of Longstanding Persistent Atrial Fibrillation in Patients With Structural Heart Disease: Epicardial Breakthrough. *Circulation*. 2010;122:1674–1683.
16. Allesie MA, De Groot NMS, Houben RPM, Schotten U, Boersma E, Smeets JL, Crijns HJ. Electropathological substrate of long-standing persistent atrial fibrillation in patients with structural heart disease: longitudinal dissociation. *Circ Arrhythm Electrophysiol*. 2010;3:606–15.
17. Boineau JP, Canavan TE, Schuessler RB, Cain ME, Corr PB, Cox JL. Demonstration of a widely distributed atrial pacemaker complex in the human heart. *Circulation*. 1988;77:1221–1237.

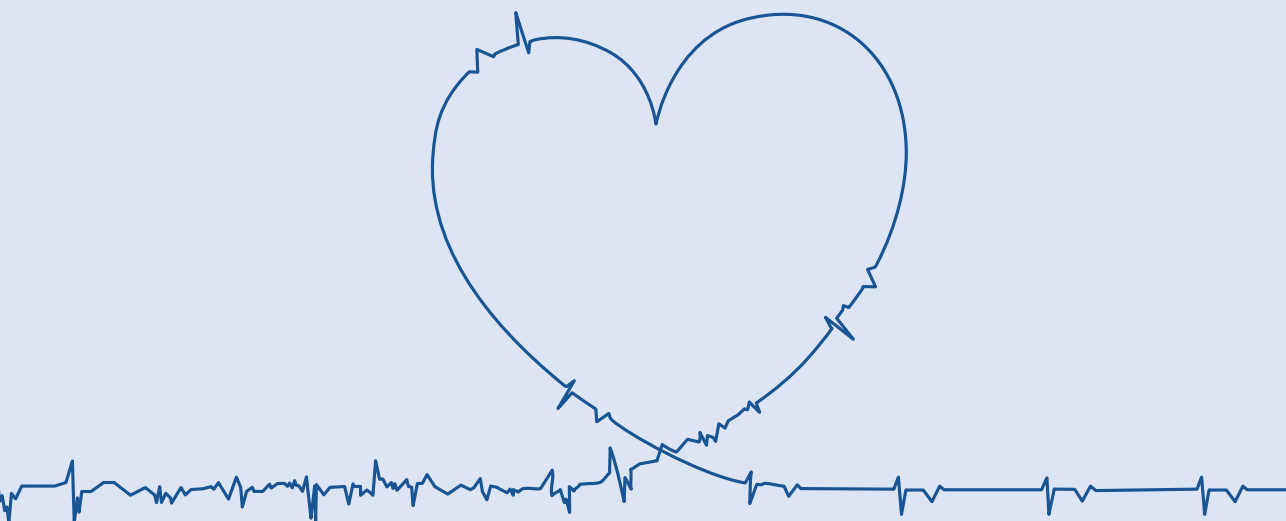
18. Stiles MK, Brooks AG, Roberts-Thomson KC, Kuklik P, John B, Young GD, Kalman JM, Sanders P. High-density mapping of the sinus node in humans: Role of preferential pathways and the effect of remodeling. *J Cardiovasc Electrophysiol*. 2010;21:532–539.
19. Boineau J, Schuessler R, Roeske W, Autry L, Miller C, Wylds A. Quantative relation between sites of atrial impulse origin and cycle length. *Am J Physiol*. 1983;245:H781-9.
20. Fedorov V V, Glukhov A V, Chang R, Kostecki G, Aferol H, Hucker WJ, Wuskell JP, Loew LM, Schuessler RB, Moazami N, Efimov IR. Optical mapping of the isolated coronary-perfused human sinus node. *J Am Coll Cardiol*. 2010;56:1386–94.
21. Ho SY, Sanchez-Quintana D, Cabrera JA, Anderson RH. Anatomy of the left atrium: implications for radiofrequency ablation of atrial fibrillation. *J Cardiovasc Electrophysiol*. 1999;10:1525–33.
22. Platonov PG, Mitrofanova L, Ivanov V, Ho SY. Substrates for intra-atrial and interatrial conduction in the atrial septum: anatomical study on 84 human hearts. *Heart Rhythm*. 2008;5:1189–95.
23. Teuwen CP, Yaksh A, Lanthers EAH, Kik C, van der Does LJME, Knops P, Taverne YJHJ, van de Woestijne PC, Oei FBS, Bekkers JA, Bogers AJJC, Allessie MA, de Groot NMS. Relevance of Conduction Disorders in Bachmann's Bundle During Sinus Rhythm in Humans. *Circ Arrhythm Electrophysiol*. 2016;9:e003972.
24. van Campenhout MJH, Yaksh A, Kik C, de Jaegere PP, Ho SY, Allessie M a, de Groot NMS. Bachmann's bundle: a key player in the development of atrial fibrillation? *Circ Arrhythm Electrophysiol*. 2013;6:1041–6.

SUPPLEMENTAL MATERIAL



Supplemental Figure 1. Construction of total SR map. In the upper panel, the reference electrogram as well as the electrograms recorded at mapping position RA1 at electrode 66, 67, 68, and 69 are shown. In each electrogram, an atrial potential (A) and a farfield ventricular potential (V) can be distinguished. At position RA1, 6 successive SR beats were recorded. Activation maps were constructed by marking the steepest negative slope of the unipolar electrograms. In the last beat (no. 6), the steepest negative slope of all unipolar electrograms is annotated by a red line. Activation maps of all beats recorded at RA1 are displayed. In beat number 6, electrodes 66-69 are marked by a red square. For each activation map, the earliest activated electrode, as annotated in the electrograms, is marked as $t=0$. In the example of beat 6, the electrode marked by the black square is the earliest activated electrode, local activation times of electrodes 66, 67,

68 and 69 are respectively 15, 13, 11 and 8ms after the earliest activated electrode. Similar to the construction of each activation map, the reference electrogram allows time alignment of the various recorded mapping positions, by correcting for the time intervals between activation maps. In this way, the total activation map, a view in which maps are thus time aligned, can be displayed. For further clarification of details of patterns of activation the corresponding isochronal maps are displayed next to the total SR map, in which isochrones are drawn at every 5ms. A: atrial; BB: Bachmann's bundle; LA: left atrium; RA: right atrium; PVL: pulmonary veins left; PVR: pulmonary veins right; V: ventricular



CHAPTER 6



EPICARDIAL BREAKTHROUGH WAVES DURING SINUS RHYTHM: DEPICTION OF THE ARRHYTHMOGENIC SUBSTRATE?

Mouws EMJP, Lanthers EAH, Teuwen CP, van der Does LJME, Kik C,
Knops P, Bekkers JA, Bogers AJJC, de Groot NMS
Journal of the American Heart Association (2018)

ABSTRACT

Background Epicardial breakthrough waves (EBW) during atrial fibrillation (AF) are important elements of the arrhythmogenic substrate and result from endo-epicardial asynchrony (EEA), which also occurs to some degree during SR. We examined the incidence and characteristics of EBW during SR and its possible value in the detection of the arrhythmogenic substrate associated with AF.

Methods Intraoperative epicardial mapping (interelectrode distances 2mm) of the right atrium (RA), Bachmann's bundle (BB), the left atrioventricular groove (LAVG) and the pulmonary vein area (PVA) was performed during SR in 381 patients (289 male, 67±10years) with ischemic and/or valvular heart disease (IHD,(i)VHD). EBW were referred to as sinus node breakthrough waves (SNBW) if they were the earliest right atrial activated site.

Results A total of 218 EBW and 57 SNBW were observed in 168 patients (44%). EBW mostly occurred at RA (N=105, 48%) and LAVG (N=67, 31%), followed by BB (N=27, 12%) and PVA (N=19, 9%)($p<0.001$). EBW occurred most often in IHD patients (N=114, 49%) compared to (i) VHD patients (N=26, 17%)($p<0.001$). EBW-electrograms most often consisted of double and fractionated potentials (N=137, 63%). In case of single potentials, an R-wave was observed in 88% (N=71) of EBW, as opposed to 21% of SNBW (N=5)($p<0.001$). Fractionated EBW-potentials were more often observed at RA and BB ($p<0.001$).

Conclusions During SR, EBW are present in over a third of patients, particularly in thicker parts of the atrial wall. Features of SR EBW indicate that muscular connections between endo and epicardium underlie EBW and that a slight degree of EEA required for EBW to occur is already present in some areas during SR. Hence, an anatomical substrate is present, which may enhance the occurrence of EBW during AF, thereby promoting AF persistence.

INTRODUCTION

Epicardial breakthrough waves (EBW) during atrial fibrillation (AF) result from endo-epicardial asynchrony (EEA) and are important elements of the arrhythmogenic substrate.^{1,2} In patients with persistent AF, a 4-fold higher incidence of EBW was observed compared to patients with induced AF.² During AF, EBW appear frequently, are non-repetitive and have a widespread distribution over the right and left atrium.³ In addition, clearly identifiable R-waves were observed in EBW fibrillation potentials recorded at the breakthrough origin, distinguishing EBW from ectopic focal activity giving rise to potentials consisting of only an S-deflection.² Based on these observations, EBW are presumed to be the result of transmural conduction through muscular bundles connecting the endo- with the epicardial layer, as has been demonstrated in several experimental studies.^{4,5}

Schuessler et al. performed simultaneous endo- and epicardial activation mapping during sinus rhythm (SR), pacing and AF in isolated canine atria and observed EBW.⁴ During AF, it was assumed that these EBW were the result of transmural reentry using muscle bundles allowing conduction between the endo- and epicardial layers.⁴ Transmural reentry as the underlying mechanism of EBW was indeed confirmed by Gray et al. using transillumination recordings in the Langendorff perfused sheep heart.⁵

For transmural conduction to occur, a certain degree of EEA is mandatory.² Recent simultaneous endo- and epicardial mapping studies in humans have demonstrated a high degree of EEA in patients with AF up to 56% of the recorded atrial sites.^{6,7} EEA does not only exist during AF, but also during SR, particularly in areas with a thicker atrial wall.⁴ Local activation times measured at opposite endo- and epicardial recording sites showed differences up to 13 ms.⁴ The oblique transmural angle of wavefronts propagating through the atrial wall and the presence of areas of conduction disorders, for example caused by deposition of fibrotic tissue, enhance EEA.⁸⁻¹² We hypothesized that EEA during SR, resulting in the presence of EBW, is more pronounced in patients with electrical or structural remodeled atria due to e.g. underlying heart disease or episodes of AF. We therefore conducted a high resolution epicardial mapping study in order to examine the incidence and characteristics of EBW during SR in a large cohort of patients with ischemic, valvular or combined heart disease (IHD, VHD, (i)VHD), with or without a history of AF.

METHODS

Study population

The study population consisted of 381 successive patients undergoing elective open heart surgery in the Erasmus Medical Center Rotterdam with a minimum age of 18 years. Patients underwent either coronary artery bypass grafting, aortic or mitral valve surgery or a combination of valvular and bypass grafting surgery. This study was approved by the institutional medical ethical committee (MEC2010-054/MEC2014-393)^{13,14} this single-center study aims to identify the arrhythmogenic areas underlying AF by intra-operative, high-resolution, multi-site epicardial mapping in 600 patients with different heart diseases. Participants are divided into 12 groups according to the underlying heart diseases and presence of prior AF episodes. Mapping is performed with a 192-electrode array for 5-10\u00a0s during sinus rhythm and (induced and written informed consent was obtained from all patients.

Postoperative rhythm monitoring by ECG and holter recordings, derived from the moment of arrival on the intensive care unit until the fifth postoperative day or until hospital discharge, were used for detection of early postoperative AF. Clinical data was extracted from electronic patient files.

Mapping procedure

Epicardial high-resolution mapping was performed prior to commencement to extra-corporal circulation, as previously described in detail.¹⁵ A bipolar epicardial pacemaker wire, serving as a temporal reference electrode, was stitched to the RA free wall. A steel wire fixed to subcutaneous tissue of the thoracic cavity served as indifferent electrode. Epicardial mapping was performed using a 128- unipolar electrode array, which was later replaced by a 192- unipolar electrode array (electrode diameter respectively 0.65mm or 0.45mm, interelectrode distances 2 mm). Mapping was conducted by shifting the electrode array along predefined areas of the RA and LA between anatomical borders in a systematic order, covering the entire atrial epicardial surface, as illustrated in the upper left panel of Figure 1.

The RA was mapped in 4 consecutive horizontal lines (RA1-4) from the cavotricuspid isthmus towards the RAA, perpendicular to the inferior and superior caval vein (ICV and SCV). Mapping of BB was performed from the tip of the left atrial appendage (LAA) towards the superior cavo-atrial junction. The pulmonary vein (PVA) area was mapped from the sinus transversus along the borders of the right and left pulmonary veins (PVR and PVL) down towards the atrioventricular groove. The left atrioventricular groove (LAVG) was mapped from the lower border of the left inferior pulmonary vein (LA1) towards the LAA (LA2).

At every mapping site, 5 seconds of SR were recorded, including a surface ECG lead, a calibration signal of 2mV and 1000ms, a bipolar reference electrogram, and all unipolar epicardial electrograms.¹⁵

Activation mapping of the atrial epicardium

The upper left panel of Figure 1 shows all mapping locations, including RA1-4, BB, LA1-2, PVR and PVL, on a schematic posterior view of the atrial surface.

The steepest negative slope of atrial potentials recorded at every electrode was annotated in order to construct a local activation map during 5 seconds of SR; atrial extrasystolic beats were excluded from analysis.^{2,6,16} When the time difference between 2 adjacent electrodes was <12ms (17ms for oblique distances), the electrode site was added to the territory of the surrounding wave. This cut-off value was based on previous studies reporting an effective atrial conduction velocity for continuous waves of 17cm/s.¹⁶ Time differences of respectively ≥ 7 and ≥ 12 ms between adjacent electrodes are marked as areas of conduction delay (CD) and block (CB).

Epicardial breakthrough waves

EBW were defined as new wavefronts arising in the middle of the mapping area which could not be explained by propagation of a wavefront in the epicardial plane. Similar to EBW during AF, EBW during SR had to meet the following criteria, which have previously been described in detail:^{2,3,6,16} epicardial mapping (244 electrodes) 1) the breakthrough site must be located at least 2 electrodes away from the border of the mapping array. In case of electrograms of poor quality recorded from the edge of the mapping array, at least 1 reliable activation time should be available between the breakthrough site and the border of the mapping area; 2) the breakthrough site had to be activated earlier than all surrounding electrodes, unless the breakthrough site was the earliest activated site of a new wavefront arising after a line of conduction block, as shown in the example in the lower panel of Figure 1. If electrodes adjacent to the origin were activated simultaneously, all electrodes surrounding this area should also be activated later; 3) the breakthrough site had to be present in every successive SR beat; 4) electrograms in the breakthrough region should not be distorted by e.g. artefacts or QRS complexes; 5) slope, amplitude and duration of potentials at the breakthrough origin had to be respectively ≥ 0.05 V/sec, ≥ 0.2 mV and ≤ 35 ms, as previously described.⁶

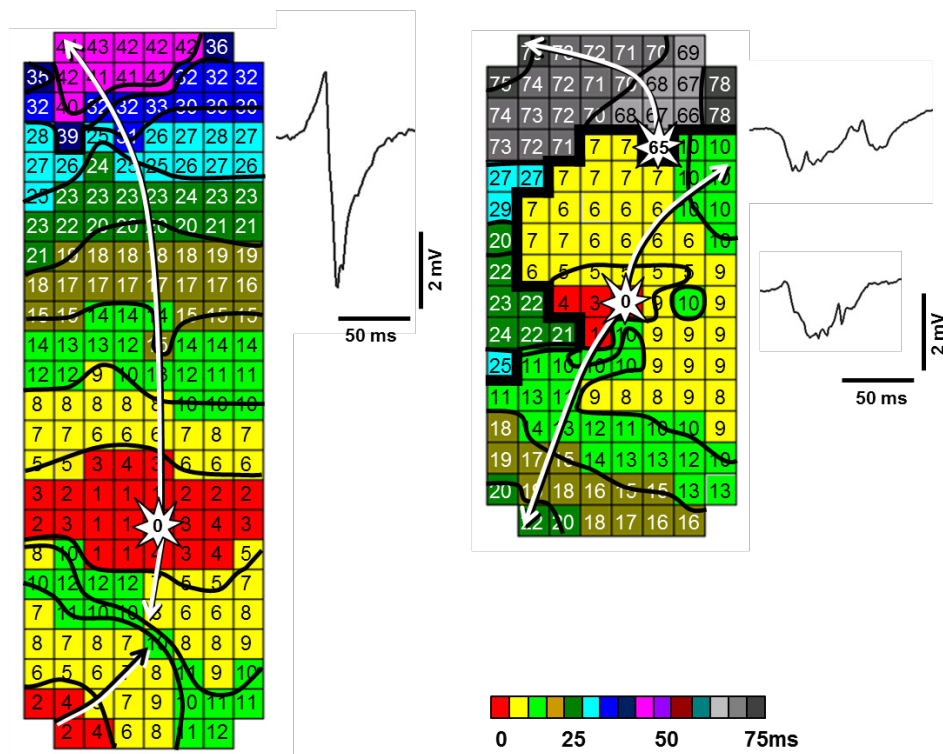
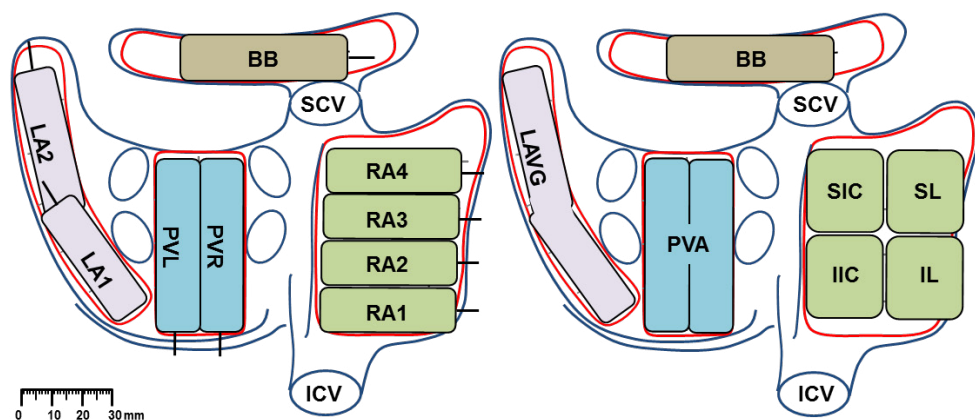


Figure 1. Methods. Upper panel: epicardial mapping scheme and classification of the atrial surface in atrial regions. Lower panel: examples of activation maps with EBW; isochrones are drawn at 5ms intervals; thick black lines indicate lines of conduction block; origin of EBW is demonstrated by asterisks; arrows display the main wave trajectories. Note that the EBW emerging in the left activation map and the lower EBW emerging in the right activation map are both activated earlier than all surrounding electrodes, as opposed to the upper EBW in the right activation map. This latter EBW emerges as the origin of the new wavefront behind a line of conduction block and therefore is not activated earlier

than all surrounding electrodes. BB: Bachmann's bundle; ICV: inferior caval vein; IIC: inferior intercaval; IL: inferolateral; LA: left atrium; LAVG: left atrioventricular groove; PVA: pulmonary vein area; PVL: pulmonary veins left; PVR: pulmonary veins right; RA: right atrium; SCV: superior caval vein; SIC: superior intercaval; SL: superolateral.

EBW of which the origin was also the earliest activated site of the RA were assumed to be the result of sinus node activity and will be referred to as sinus node breakthrough waves (SNBW). These SNBW will be described separately. Spatial distribution of EBW was examined by assigning them to atrial regions, as displayed in the upper right panel of Figure 1, including the superior intercaval, inferior intercaval, superolateral and inferolateral (SIC, IIC, SL, IL) region of the RA; BB; LAVG and PVA.

Prematurity indices of SNBW and EBW were calculated by dividing the averaged SNBW and EBW cycle length (CL) by the average SR CL based on 5 seconds of recorded SR and presented as a percentage.

Statistical analysis

Normally distributed data are described by mean \pm SD(minimum-maximum) and analysed with a student's T-test or a one way ANOVA. Our patient population is of sufficient size to also perform t-tests or ANOVA on data following a skewed distribution, since the distribution of their means in multiple sample tests will follow normality. However, representation of these skewed data by means and standard deviations may give a misleading view. Therefore, we chose to describe skewed data by median(minimum-maximum) and analysed these data with non-parametric tests, i.e. Kruskal-Wallis test or Mann-Whitney U test. Categorical data are expressed as numbers and percentages and analysed with χ^2 or Fisher exact test when appropriate. A p-value <0.05 was considered statistically significant.

RESULTS

Study population

Characteristics of the study population (N=381, 289 male (76%), age 67 ± 10 years) are summarized in Table 1. Patients either had only IHD (N=231, 61%), only VHD (N=85, 22%) or I/VHD (N=65, 17%). VHD (N=150, 39%) was categorized by the predominant valvular lesion and consisted of aortic valve stenosis (N=82, 22%), mitral valve insufficiency (N=58, 15%), aortic valve insufficiency (N=9, 2%) or mitral valve stenosis (N=1, 0.3%). A minority of patients (N=59, 16%) had a history of AF, which was more prevalent in patients with mitral valve disease (N=23, 39%) compared to patients with aortic valve disease (N=19, 21%) or only IHD (N=17, 7%) ($p<0.001$). Most patients had a normal left ventricular function (LVF) (N=289, 76%) and the majority used class II (N=259, 68%) or III (N=16, 4%) antiarrhythmic drugs. Patients were mapped with either a 128-polar (N=219, 57%) or a 192-polar electrode array (N=162, 43%).

Table 1. Patient characteristics

Number of patients	381
Age	67±10(21–84)
Male	289(76)
Body surface area	2.0±0.2(1.5–2.8)
Underlying heart disease	N(%)
IHD	231(61)
VHD	85(22)
I/VHD	65(17)
Valvular Heart Disease	150 (39)
Aortic Valve Stenosis	82(22)
Mild	2(1)
Moderate	19(5)
Severe	61(16)
Aortic Valve Insufficiency	9(4)
Mild	1(1)
Moderate	5(2)
Severe	3(1)
Mitral Valve Stenosis	1(1)
Severe	1(1)
Mitral Valve Insufficiency	58(12)
Moderate	16(4)
Severe	42(12)
Left Atrial dilatation >45mm	77(20)
History of AF	59(16)
Paroxysmal	43(11)
Persistent	15(4)
Longstanding persistent	1(1)
Left ventricular function	
Normal	289(76)
Mild dysfunction	68(18)
Moderate dysfunction	22(6)
Severe dysfunction	2(1)
Antiarrhythmic drugs	283(74)
Class I	2(1)
Class II	259(68)
Class III	16(4)
Class IV	4(1)

AF: atrial fibrillation; IHD: ischemic heart disease; VHD: valvular heart disease; I/VHD: ischemic and valvular heart disease.

Mean SR cycle length (CL) was 858±176(473-1458)ms. For all performed analyses as described in the results section there were no differences between patients with VHD or I/VHD, therefore these two patient groups were combined and referred to as (i)VHD.

Incidence of epicardial breakthrough waves

Figure 2 shows 6 examples of color-coded activation maps in which the origin of the SNBW or EBW is indicated by a white asterisk; arrows display main trajectories of breakthrough waves. These EBW activate a relative large area before merging with the SR wavefront propagating in the epicardial plane. The upper middle panel of Figure 2 shows an EBW located at BB, in which the peripheral wavefront enters the mapping array from the lower left side. An EBW emerges just below the center of the mapping array, which merges with the peripheral wavefront at 11ms and activates the remaining surface towards the upper part of the mapping array. Similar patterns of activation and merging of wavefronts can be seen in the other panels of Figure 2. Unipolar potentials recorded at the origin of the breakthrough sites and the 8 surrounding electrodes are shown next to the activation maps and will be discussed in the next paragraph.

EBW may also occur after a line of conduction block, as exemplified in the lower right activation map shown in Figure 1. Here, an EBW first emerges in the center of the mapping array and activates the surrounding atrial surface. In the upper right part of the mapping area, the area behind the long line of conduction block (thick black line) is 58ms later activated by another EBW.

A total of 275 EBW were observed in 168 patients (44%), of which 57 (21%) occurring at the RA were SNBW, as their origin was the earliest activated site during SR. The remaining 218 EBW were observed in 140 patients (37%), including 105 EBW (48%) at the RA, 27 (12%) at BB and 86 (40%) at the LA. A minority of 28 EBW (13%) occurred after a line of conduction block.

When distinguishing aortic valve disease (AVD) from mitral valve disease (MVD) and IHD, there was a gradual increase in the incidence of EBW from 13% (N=12) in AVD patients to 24% (N=14) in MVD patients and 49% (N=114) in IHD patients ($p < 0.001$).

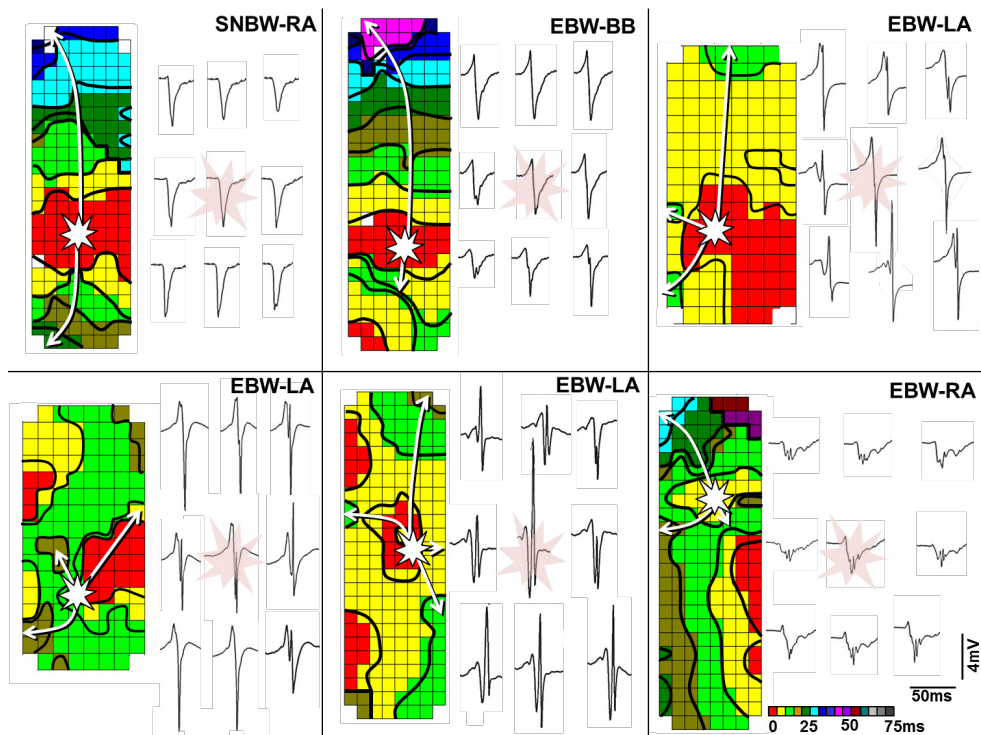


Figure 2. Examples SNBW and EBW. Examples of color-coded activation maps with SNBW and EBW at RA, LA and BB: the origin of the EBW is indicated with an asterisk. Arrows display the main wave trajectory of the breakthrough. Unipolar electrograms acquired from the breakthrough site (asterisk) and its 8 surrounding electrodes are displayed next to the corresponding activation maps. Black lines indicate areas with conduction block. Panels represent activation patterns of areas at the RA, BB and LA. The mapping area is activated by wavefronts traveling in the epicardial plane as well as by new focal wavefronts arising in the middle of the mapping area (asterisk). The upper left panel displays an SNBW with S morphology, the remaining panels display EBW with electrograms consisting of single, double and fractionated potentials. BB: Bachmann's bundle; EBW: epicardial breakthrough wave; LA: left atrium; RA: right atrium; SNBW: sinus node breakthrough wave.

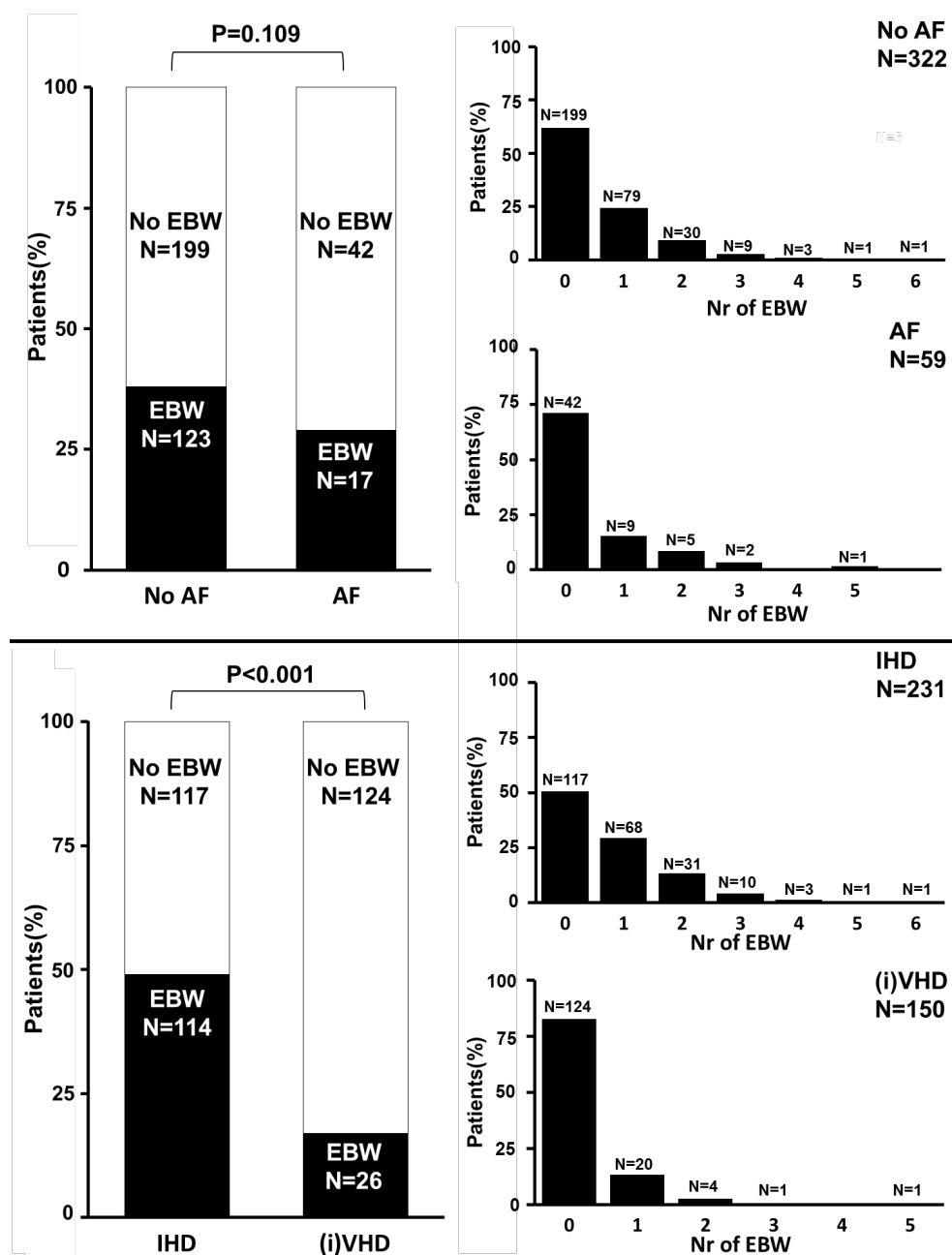


Figure 3. Incidence of EBW. Upper panels: incidences and frequency histograms of EBs in patients without and with AF separately. Lower panels: incidences and frequency histograms of EBs in patients with IHD and (i)VHD separately. AF: atrial fibrillation; EBW: epicardial breakthrough wave; IHD: ischemic heart disease; (i)VHD: (ischemic and) valvular heart disease.

Table 2 displays the amount of CD and CB as a percentage of the entire mapped atrial surface. Patients with EBW showed higher amounts of CD (No EBW: 1.23(0.17-4.00); EBW: 1.59(0.21-4.00), $p<0.001$) and CB (No EBW: 1.10(0.00-6.59); EBW: 1.50(0.07-5.10), $p<0.001$). Also, the amount of CD was higher in IHD patients (1.42(0.18-4.00)) than in (i)VHD patients (1.27 (0.17-4.00) $p=0.028$). However, when comparing the amount of conduction delay and block between AVD, MVD and IHD patients separately, no difference was observed (AVD: 1.25 (0.17-4.00); MVD: 1.33 (0.30-2.93); IHD: 1.42 (0.18-4.00), $p=0.077$). Amount of conduction block was similar for the various disease states, as shown in Table 2.

Table 2. Conduction delay and block

Condition	%CD(min-max)	%CB(min-max)
No EBW	1.23(0.17-4.00)	1.10(0.00-6.59)
EBW	1.59(0.21-4.00)	1.50(0.07-5.10)
p-value	<0.001	<0.001
No AF	1.33(0.17-3.82)	1.23(0.04-6.59)
AF	1.56(0.30-4.00)	1.32(0.00-4.70)
p-value	0.065	0.183
IHD	1.42(0.18-4.00)	1.26(0.04-4.48)
(i)VHD	1.27(0.17-4.00)	1.20(0.00-6.59)
p-value	0.028	0.923
AVD	1.25(0.17-4.00)	1.14(0.10-6.07)
MVD	1.33(0.30-2.93)	1.36(0.00-6.59)
IHD	1.42(0.18-4.00)	1.26(0.04-4.48)
p-value	0.077	0.418

AF: atrial fibrillation; AVD: aortic valve disease; CB: conduction block; CD: conduction delay; EBW: epicardial breakthrough wave; MVD: mitral valve disease; IHD: ischemic heart disease; (i)VHD: (ischemic and) valvular heart disease.

Electrogram morphology of epicardial breakthrough waves

Examples of EBW and their unipolar electrograms recorded at the origin of the breakthrough sites and the 8 surrounding electrodes are shown in Figure 2. A large variation in the amplitude and morphology of unipolar electrograms recorded at EBW origins was observed, including single potentials with only an S-wave (upper left panel), single potentials with an rS or RS morphology (upper middle and right panel), double potentials (lower left and middle panel) and fractionated potentials (lower right panel).

Incidences of electrogram morphologies recorded at the origin of SNBW and EBW are shown in Figure 4. Electrograms at the origin of 57 SNBW consisted of single (N=24, 42%), double (N=16, 28%) or fractionated potentials (N=17, 30%). In case of a single potential, the majority showed only an S-wave (N=19, 79%), whereas 21% (N=5) showed an rS-wave morphology, as displayed in the middle left panel of Figure 4.

Electrograms at the origin of 218 EBW consisted of single (N=81, 37%) or fragmented potentials (N=137, 63%), which were either double (N=89, 41%) or fractionated (N=48, 22%) (upper left panel Figure 4). Single potentials were either without (N=10, 12%) or with an R-wave (N=71, 88%). Those with an R-wave showed an RS (N=21, 30%) or rS (N=50, 70%) morphology, as shown in the middle left panel of Figure 4.

Electrogram morphology differed significantly between EBW occurring behind a line of conduction block and EBW that did not occur behind a line of block ($p<0.001$), as shown in the upper right panel of Figure 4. More than half of the unipolar electrograms recorded at the origin of EBW presenting after conduction block consisted of fractionated potentials (N=15, 54%), whereas this was only 17% (N=33) of EBW occurring in areas without conduction block. The incidence of double potentials was similar between EBW in areas without conduction block and those occurring behind conduction block (N=78, 41% and N=11, 39% respectively). Single potentials were far more often observed in EBW not arising after a line of conduction block (N=79, 42%) compared to EBW after block lines (N=2, 7%). In addition, electrograms of EBW origins recorded at the RA and BB more often showed double and fractionated potentials than electrograms recorded at the LA ($p<0.001$), as shown in the middle right and lower left panel of Figure 4.

No difference in electrogram morphology was observed between patients without and with AF ($p=0.882$), nor between patients with IHD and with (i)VHD ($p=0.207$) (lower right panel of Figure 4).

Spatial distribution of epicardial breakthrough waves

As summarized in Table 3, EBW were most prevalent at the RA (N=105), followed by the LA (N=86) and BB (N=27). Most EBW at RA occurred in the SIC region (N=56, 53%), followed by the SL (N=23, 22%) and IIC region (N=21, 20%). Only a minority of EBW at RA occurred at the IL region (N=5, 5%). Of the EBW observed at LA (N=86), most were located

Table 3. Incidence of EBW per mapping site

	Total	No AF	AF	P-value	IHD	(i)VHD	P-value
No of pts	381	322	59		231	150	
Pts with EBW	140(37)	123(38)	17(29)	0.109	114(49)	26(17)	<0.001
No of EBW	218	188	30		182	36	
RA regions	105(48)	92(49)	13(43)	0.568	87(48)	18(50)	0.809
SIC	56(26)	49(26)	7(23)	0.751	44(24)	12(33)	0.251
IIC	21(10)	18(10)	3(10)	0.942	17(9)	4(11)	0.742
SL	23(11)	20(11)	3(10)	0.916	22(12)	1(3)	0.097
IL	5(2)	5(2)	0(0)	0.366	4(2)	1(3)	0.832
BB	27(12)	22(12)	5(17)	0.443	25(14)	2(6)	0.173
LA regions	86(40)	74(39)	12(40)	0.947	70(38)	16(44)	0.502
PVA	19(9)	16(9)	3(10)	0.788	17(9)	2(6)	0.462
LAVG	67(31)	58(31)	9(30)	0.925	53(29)	14(39)	0.246

AF: atrial fibrillation; EBW: epicardial breakthrough waves; (i)VHD: (ischemic and) valvular heart disease; RA: right atrium; SIC: superior intercaval; IIC: inferior intercaval; SL: superolateral; IL: inferolateral; BB: Bachmann's bundle; LA: left atrium; PVA: pulmonary vein area; LAVG: left atrioventricular groove.

at the LAVG (N=67, 78%) in comparison to the PVA (N=19, 22%). Most patients had EBW at a single atrial site (N=88, 63%), whereas in 52 patients (37%), EBW were observed at multiple atrial sites (range 2-6). As shown in Table 4, a combination of multiple EBW occurred most frequently at the SIC region (N=13, 25), followed by a combination of multiple EBW at the LAVG (N=8, 15%) and a combination of the LAVG and BB (N=7, 13%). As indicated in Table 3, the spatial distribution of EBW over RA, LA and BB was similar between patients with and without AF and between patients with IHD and (i)VHD.

Prematurity of epicardial breakthrough waves

The left panel of Figure 5 displays CL recorded at the origins of SR, SNBW and EBW. Median SR CL was 862ms and, as expected, did not differ from median SNBW CL (869ms) and EBW CL (854 ms) ($p=0.606$). SNBW and EBW CL were highly correlated with SR CL (Pearson rho 0.986; $p<0.001$ and Pearson rho 0.904 $p<0.001$ respectively). Median prematurity indices of SNBW and EBW were respectively 100% and 100%, as visualized in the right panels of Figure 5.

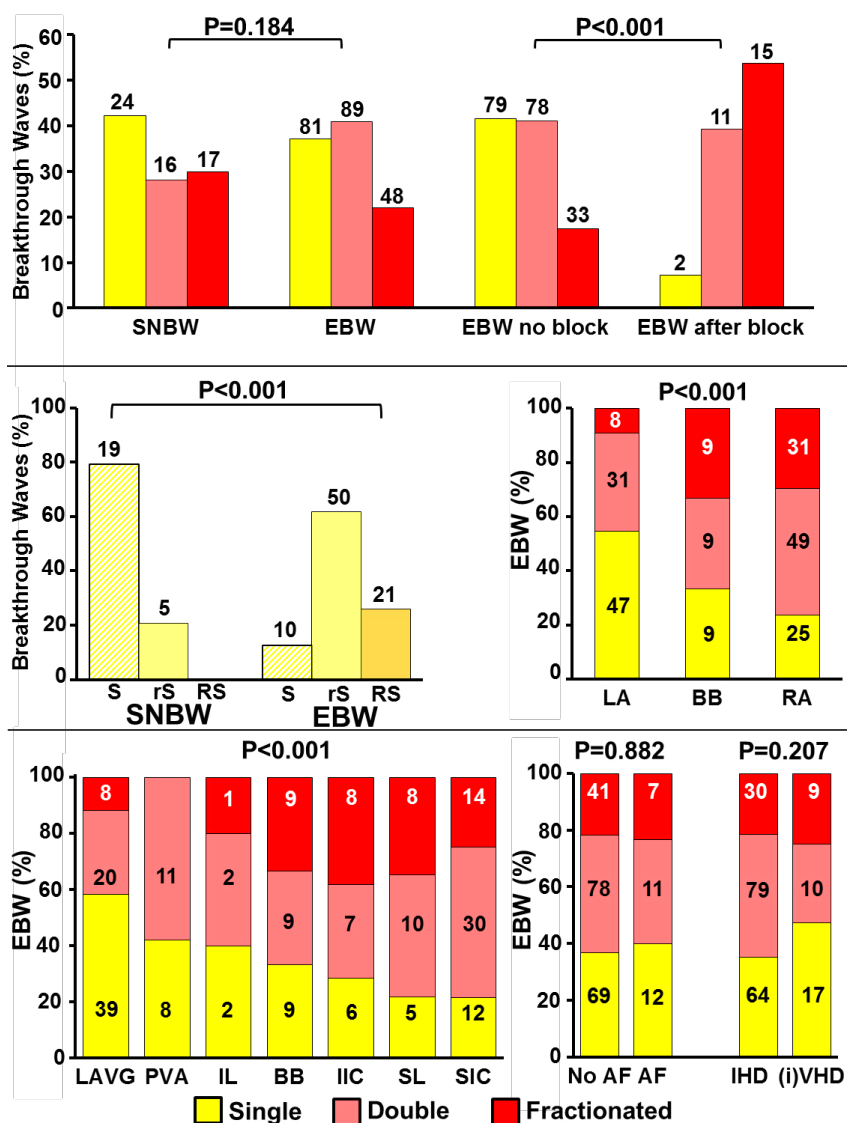


Figure 4. Electrogram Morphology of SNBW and EBW. Upper left panel: Incidence of single, double and fractionated potentials in SNBW, EBW(all), EBW without conduction block and EBW after conduction block separately. Upper right panel: distribution of electrogram morphologies recorded at SNBW and EBW origins. Lower left panel: relative incidences of EBW with single, double and fractionated potentials for each atrial region separately. Lower right panel: relative incidences of EBW with single, double and fractionated potentials in patients without and with AF and in patients with IHD and (i) VHD. AF: atrial fibrillation; BB: Bachmann's bundle; EBW: epicardial breakthrough wave; IHD: ischemic heart disease; (i) VHD: (ischemic and) valvular heart disease; IIC: inferior intercaval; IL: inferolateral; LAVG: left atrioventricular groove; PVA: pulmonary vein area; SNBW: sinus node breakthrough wave; SIC: superior intercaval; SL: superolateral.

Early postoperative AF

Postoperative ECG holter recordings were available for 350 patients (92%). For the remaining 31 patients (8%), ECG's were available for detection of AF. A total of 140 patients (37%) developed early postoperative AF, of whom in 109 patients (78%) AF was de novo. The presence of EBW during SR did not predispose for the development of early postoperative AF ($p=0.732$). Also, neither the number of EBW nor the type of EBW, i.e. EBW occurring after conduction block, was associated with development of postoperative AF ($p=0.968$ and $p=0.605$ respectively).

Table 4. Incidence of combinations of EBW predilection sites in 52 patients with multiple EBW

Mapping site	SIC	IIC	SL	IL	BB	PVA	LAVG
SIC	13(25)						
IIC	5(10)	0(0)					
SL	1(2)	0(0)	3(6)				
IL	1(2)	2(4)	0(0)	0(0)			
BB	3(6)	4(8)	3(6)	0(0)	3(6)		
PVA	3(6)	2(4)	2(4)	1(2)	4(8)	0(0)	
LAVG	6(12)	4(8)	3(6)	2(4)	7(13)	4(8)	8(15)

EBW: epicardial breakthrough wave; SIC: superior intercaval; IIC: inferior intercaval; SL: superolateral; IL: inferolateral; BB: Bachmann's bundle; PVA: pulmonary vein area; LAVG: left atrioventricular groove.

DISCUSSION

Key findings

EBW occur frequently during SR and were observed in over one third of the patients. They particularly emerged in thicker regions of the atria, such as the RA and the LAVG near the LAA. The majority of unipolar SR-electrograms recorded at EBW origins consisted of either double or fractionated potentials, indicating local asynchronous activation. Additionally, the vast majority of single potentials of EBW had a clearly identifiable R-peak, indicating propagation of a wavefront from deeper layers within the atrial wall towards the epicardium. These observations suggest that muscular connections between endo- and epicardium underlie EBW and that a slight degree of EEA, necessary for the occurrence of EBW, is already present during SR.

Features of EBW during sinus rhythm

EBW during SR were observed in a large number of patients. Of the EBW observed at RA, a considerable number represented the earliest activated site during SR (i.e. SNBW). Although some electrograms recorded at the SNBW origin contained potentials with a small R-wave, the vast majority consisted of potentials with an S-wave morphology. This finding supports the hypothesis that these SNBW most likely resulted from automatic cellular discharge, hence sinus node activity. In contrast, the vast majority of electrograms recorded at the origin of EBW that were not the result of sinus node activity showed clearly identifiable R-waves, indicating the presence of depolarization waves approaching the epicardial surface. This feature

suggests that these EBW originated from deeper layers of the atrial wall. We observed a high incidence of double and fractionated potentials at EBW origins, indicating asynchronous activation of adjacent cardiomyocytes.¹⁷ but rather transmembrane potentials recorded in the vicinity of the bipolar electrodes were normal. Despite the normal transmembrane potentials, activation time in regions where fractionated electrograms occurred was prolonged. However, prolonged activation time by itself did not cause fractionation, since fractionated electrograms were not recorded from normal preparations in which conduction was markedly slowed by a superfusate containing 16 mM potassium and epinephrine. Unipolar electrograms recorded with glass microelectrodes (tip size 1 to 5 microns Durrer et al. reported that epicardial excitation patterns reflect the movement of endocardial and intramural fronts, as the activation front does not actually spread over the epicardial surface, but excitation spreads from endocardium to epicardium.¹⁸ Therefore, he assumed that epicardial activation patterns generally reflect endocardial excitation, in which slight variations in wall thickness, for instance due to presence of muscle bundles or due to pathological processes such as fibrotic depositions, may account for asynchronous activation of closely adjacent epicardial areas.¹⁸

The higher incidence of EBW in IHD patients may be explained by extensive areas of myocardial ischemia and fibrotic depositions at the atrial myocardium associated with the presence of coronary artery disease, -leading to areas of slowing of conduction, conduction block and enhanced local dispersion of refractoriness.^{19,20}

Our observations support the hypotheses that EBW are indeed the result of structural remodeling due to underlying cardiac diseases. If areas of conduction block occur in the 2-dimensional epicardial plane, it is likely they are also present in 3-dimensional endo-epicardial plane. The resulting EEA then enables transmural conduction to occur. EBW are presumed to result from EEA and are an important element of the arrhythmogenic substrate underlying AF. Previous studies reported that the incidence of EBW during AF is considerably higher in patients with longstanding persistent AF in comparison to electrically induced AF^{2,16} and that during AF, EBW appear throughout the entire atrium in a non-repetitive manner without evident predilection sites.^{3,7}

The fact that EBW during AF were mostly non-repetitive events is likely a direct result of the beat to beat variation in atrial activation patterns during AF. Consequently, EBW appear on various sites, depending on excitability of the epicardial layer at the specific moment that wavefronts propagate through the asynchronously activated endo-epicardial layer.

The key feature of SR is that every beat results in more or less the same activation pattern. Thus, the SR wavefront of every beat will reach electrically dissociated sites from the same direction. In the presence of a muscular connection between the endo- and epicardial layer, the wavefront appears at the same epicardial site during each consecutive SR beat, as we observed in our mapping data.

One could argue that EBW occurring during each consecutive SR beat are in fact the result of ectopic transmural foci, which also create unipolar potentials with small R-waves. However, our study showed that CL of EBW and CL of SNBW did not differ from CL of consecutive beats recorded at the origin of SR and that prematurity indices of EBW and SNBW were 100%. When

EBW would be the result of focal discharge, competition with the sinus node would be expected; CL would then likely be shorter and a certain degree of prematurity would be present.

Spatial distribution of EBW during sinus rhythm

Most EBW occurred at the RA, which corresponds with the more chaotic architecture of RA compared to LA. Wall thickness of RA is much less uniform than of LA, due to the terminal crest and its pectinate muscles which constitute a considerable proportion of RA.²¹ RA wall thickness varies from 5-8mm at the terminal groove to about 2mm at the anterior and posterior side of the vestibulum of the tricuspid valve.²¹ This chaotic architecture caused by alternating thick and thin areas facilitates EEA and thus transmural conduction from the endo- to the epicardial layer and vice versa, as demonstrated previously in sheep atria.⁵ In support of our hypothesis, double and fractionated potentials were more frequently observed at RA and BB as opposed to the LA.

EBW: depiction of the arrhythmogenic substrate?

Features of EBW electrogram morphology in combination with the repetitive occurrence of EBW during SR, their higher prevalence in patients with IHD and the fact that they occur mostly on thicker atrial regions such as the RA, all indicate the presence of an anatomical substrate. This anatomical substrate can be physiological, such as the mere fact that the presence of myocardial bundles cause certain areas of the atrial wall to be slightly thicker and therefore result in EEA, enabling EBW to occur. To a certain extent, the presence of a limited number of EBW merely as a result of EEA due to physiological differences in wall thickness in otherwise electrically and structurally normal atria are assumed to have limited

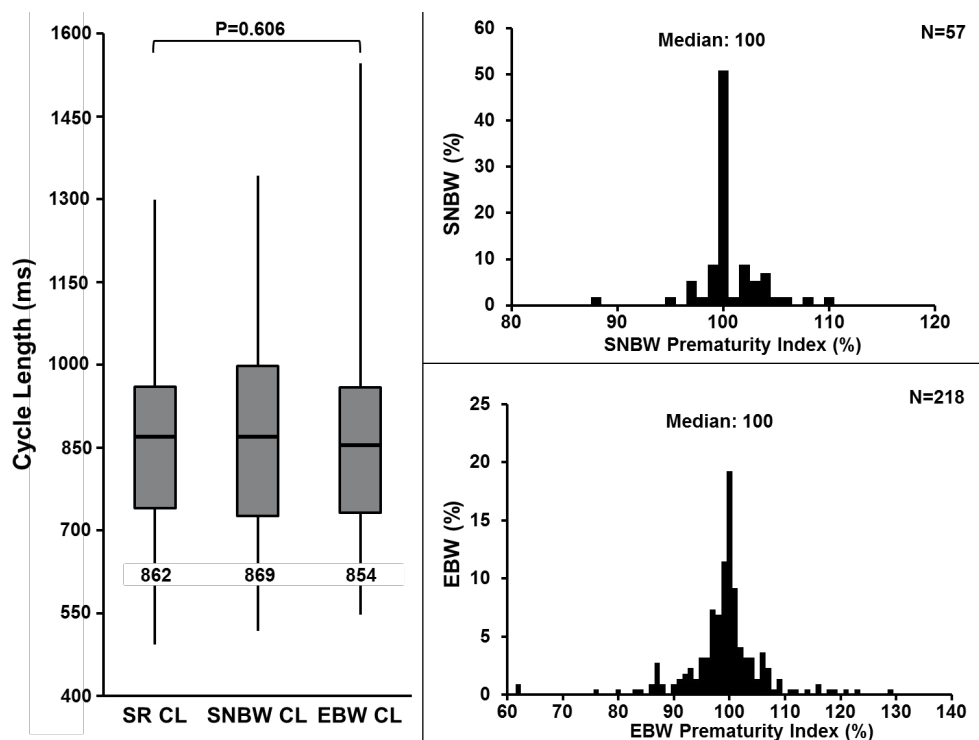


Figure 5. EBW and SNBW prematurity. Left panel: CL of SR-, SNBW- and EBW- origins (minimum- interquartile range-maximum). Right panels: frequency histogram of prematurity indices of SNBW and EBW. CL: cycle length; EBW: epicardial breakthrough wave; SNBW: sinus node breakthrough wave; SR: sinus rhythm.

impact on the SR activation pattern as the EBW will be integrated in the large broad SR wavefront. However, this physiological substrate can be enforced by pathophysiological processes, such as fibrosis, enhancing EEA. During AF, the presence of multiple wavelets increases EEA, promoting EBW to occur. In addition, AF induced structural remodeling further enhances the degree of EEA, and thus the appearance of EBW. This vicious cycle of EEA stimulating EBW and vice versa may promote AF persistence.

When observing multiple EBW spread over the atria, this may be an indicator of an extensive arrhythmogenic substrate and might be a future parameter in predicting outcome of AF therapy. When the arrhythmogenic substrate is more extensive throughout the atria, therapies addressing focal sources are likely to fail.

Study limitations

In the present study, incidences of EBW were similar between patients with and without a history of AF. This might be due to the limited number of patients with (longstanding) persistent AF in this study, as most patients had a history of paroxysmal AF in whom less electrical and structural remodeling is expected. A small amount of EBW occurred after conduction block, defined as a difference of ≥ 12 ms in local activation time between two adjacent

electrodes. Theoretically, these EBW could be the result of very slow conduction and thus be a discontinuous conduction wave.¹⁶ Also, we could only perform epicardial mapping and thereby we cannot correlate presence of EBW to endocardial breakthroughs.

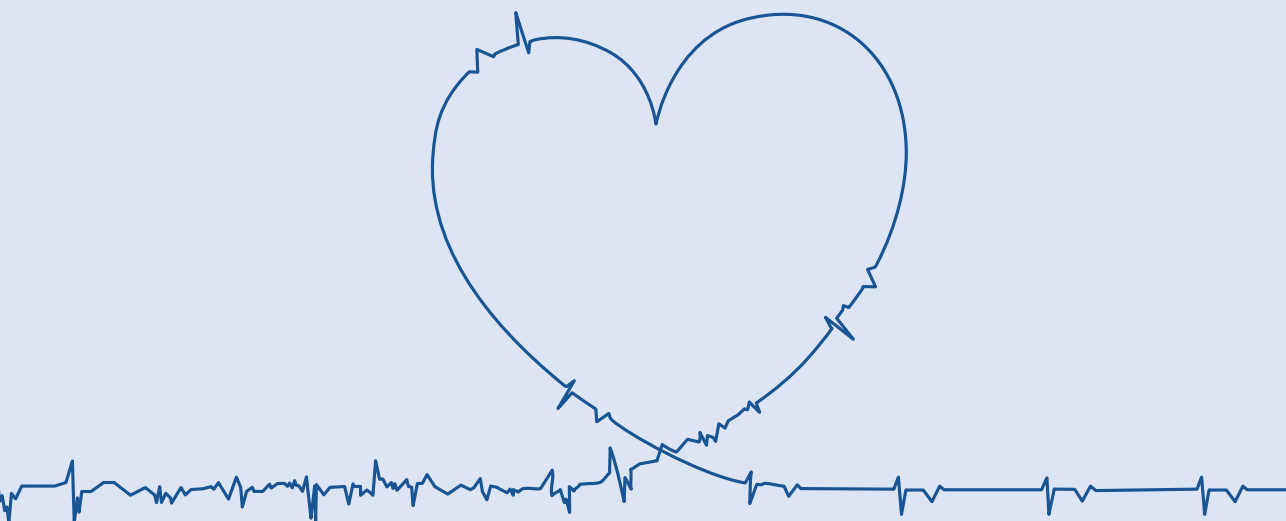
CONCLUSION

EBW not only occur during AF, but also during SR. Features of EBW, as demonstrated in the present study, provide further evidence of transmural conduction as the underlying mechanism. EBW are the result of a certain degree of EEA and the presence of an anatomical substrate, which may be particularly enforced by ischemic heart disease. Although a direct association with AF episodes could not be determined, it is likely that further aggravation of structural remodeling enhances local conduction disorders and thus EEA. This will, in the presence of muscular connections between the endo-epicardial layer, facilitate transmural propagation of wavefronts, resulting in EBW and hence, development of AF.

REFERENCES

1. Eckstein J, Zeemering S, Linz D, Maesen B, Verheule S, van Hunnik A, Crijns H, Allesie MA, Schotten U, Eckstein J, Zeemering S, Linz D, Maesen B, Verheule S, Hunnik A van, Crijns H, Allesie MA, Schotten U. Transmural conduction is the predominant mechanism of breakthrough during atrial fibrillation: evidence from simultaneous endo-epicardial high-density activation mapping. *Circ Arrhythm Electrophysiol*. 2013;6:334–41.
2. de Groot N, Houben R, Smeets J, Boersma E, Schotten U, Schalij M, Crijns H, Allesie M. Electropathological Substrate of Longstanding Persistent Atrial Fibrillation in Patients With Structural Heart Disease: Epicardial Breakthrough. *Circulation*. 2010;122:1674–1683.
3. Lanthers EAH, Allesie MA, de Groot NMS. Dynamics of Focal Fibrillation Waves during Persistent Atrial Fibrillation. *Pacing Clin Electrophysiol*. 2015;39:403–4.
4. Schuessler RB, Kawamoto T, Hand DE, Mitsuno M, Bromberg BI, Cox JL, Boineau JP. Simultaneous epicardial and endocardial activation sequence mapping in the isolated canine right atrium. *Circulation*. 1993;88:250–63.
5. Gray RA, Pertsov AM, Jalife J. Incomplete Reentry and Epicardial Breakthrough Patterns During Atrial Fibrillation in the Sheep Heart. *Circulation*. 1996;94:2649–2661.
6. de Groot N, van der Does L, Yaksh A, Lanthers E, Teuwen C, Knops P, van de Woestijne P, Bekkers J, Kik C, Bogers A, Allesie M. Direct Proof of Endo-Epicardial Asynchrony of the Atrial Wall During Atrial Fibrillation in Humans. *Circ Arrhythmia Electrophysiol*. 2016;9:e003648.
7. van der Does LJME, Kik C, Bogers AJJC, Allesie MA, de Groot NMS. Dynamics of Endo- and Epicardial Focal Fibrillation Waves at the Right Atrium in a Patient With Advanced Atrial Remodelling. *Can J Cardiol*. 2016;32:1260.e19–1260.e21.
8. Houben RPM, de Groot NMS, Smeets JLRM, Becker AE, Lindemans FW, Allesie MA. S-wave predominance of epicardial electrograms during atrial fibrillation in humans: indirect evidence for a role of the thin subepicardial layer. *Heart Rhythm*. 2004;1:639–47.
9. Goudis CA, Kallergis EM, Vardas PE. Extracellular matrix alterations in the atria: insights into the mechanisms and perpetuation of atrial fibrillation. *Europace*. 2012;14:623–30.
10. Kumar S, Teh AW, Medi C, Kistler PM, Morton JB, Kalman JM. Atrial remodeling in varying clinical substrates within beating human hearts: Relevance to atrial fibrillation. *Prog Biophys Mol Biol*. 2012;110:278–294.
11. Verheule S, Wilson E, Everett T, Shanbhag S, Golden C, Olgin J. Alterations in atrial electrophysiology and tissue structure in a canine model of chronic atrial dilatation due to mitral regurgitation. *Circulation*. 2003;107:2615–22.
12. Burstein B, Nattel S. Atrial fibrosis: mechanisms and clinical relevance in atrial fibrillation. *J Am Coll Cardiol*. 2008;51:802–9.
13. van der Does LJME, Yaksh A, Kik C, Knops P, Lanthers EAH, Teuwen CP, Oei FBS, van de Woestijne PC, Bekkers JA, Bogers AJJC, Allesie MA, de Groot NMS. QUES for the Arrhythmogenic Substrate of Atrial fibrillation in Patients Undergoing Cardiac Surgery (QUASAR Study): Rationale and Design. *J Cardiovasc Transl Res*. 2016;9:194–201.
14. Lanthers EAH, van Marion DMS, Kik C, Steen H, Bogers AJJC, Allesie MA, Brundel BJJM, de Groot NMS. HALT & REVERSE: Hsf1 activators lower cardiomyocyte damage; towards a novel approach to REVERSE atrial fibrillation. *J Transl Med*. 2015;13:347.
15. Yaksh A, van der Does LJ, Kik C, Knops P, Oei FB, van de Woestijne PC, Bekkers J a, Bogers AJ, Allesie M a, de Groot NM. A novel intra-operative, high-resolution atrial mapping approach. *J Interv Card Electrophysiol*. 2015;44:221–5.
16. Allesie MA, de Groot NMS, Houben RPM, Schotten U, Boersma E, Smeets JL, Crijns HJ. Electropathological substrate of long-standing persistent atrial fibrillation in patients with structural heart disease: longitudinal dissociation. *Circ Arrhythm Electrophysiol*. 2010;3:606–15.

17. Gardner PI, Ursell PC, Fenoglio JJ, Wit AL. Electrophysiologic and anatomic basis for fractionated electrograms recorded from healed myocardial infarcts. *Circulation*. 1985;72:596–611.
18. Durrer D, Van Dam R, Freud G, Janse MJ, Meijler FL, Arzbaecher RC. Total Excitation of the Isolated Human Heart. *Circulation*. 1970;41:899–912.
19. Nguyen TP, Qu Z, Weiss JN. Cardiac fibrosis and arrhythmogenesis: the road to repair is paved with perils. *J Mol Cell Cardiol*. 2014;70:83–91.
20. Heusch G, Libby P, Gersh B, Yellon D, Böhm M, Lopaschuk G, Opie L. Cardiovascular remodelling in coronary artery disease and heart failure. *Lancet (London, England)*. 2014;383:1933–43.
21. Wang K, Ho SY, Gibson DG, Anderson RH. Architecture of atrial musculature in humans. *Br Heart J*. 1995;73:559–65.





CHAPTER 7

RELEVANCE OF CONDUCTION DISORDERS IN BACHMANN'S BUNDLE DURING SINUS RHYTHM IN HUMANS

Teuwen CP, Yaksh A, Lanthers EAH, Kik C, van der Does LJME, Knops P,
Taverne YJHJ, van de Woestijne PC, Oei FBS, Bekkers JA,
Bogers AJJC, Allessie MA, de Groot NMS
Circulation: Arrhythmia and Electrophysiology (2016)

ABSTRACT

Background Bachmann's bundle (BB) is considered to be the main route of interatrial conduction and to play a role in development of atrial fibrillation (AF). The goals of this study are to characterize the presence of conduction disorders in BB during sinus rhythm and to study their relation with AF.

Methods High-resolution epicardial mapping (192 unipolar electrodes, inter-electrode distance: 2mm) of sinus rhythm was performed in 185 patients during coronary artery bypass surgery of whom 13 had a history of paroxysmal AF (PAF). Continuous rhythm monitoring was used to detect post-operative AF (PoAF) during the first 5 post-operative days.

Results In 67% of the patients BB was activated from right to left; in the remaining patients from right and middle (21%), right, central and left (8%) or central (4%) site. Mean effective conduction velocity was 89cm/s. Conduction block was present in most patients (75%; median 1.1%, range 0–12.8) and was higher in patients with PAF compared to patients without a history of AF (3.2% vs 0.9%, $p=0.03$). A high amount of conduction block ($>4\%$) was associated with de-novo PoAF ($p=0.02$). Longitudinal lines of conduction block $>10\text{mm}$ were also associated with PoAF ($p=0.04$).

Conclusions BB may be activated through multiple directions, but the predominant route of conduction is from right-to-left. Conduction velocity across BB is around 90cm/s. Conduction is blocked in both longitudinal and transverse direction in the majority of patients. Conduction disorders, particularly long lines of longitudinal conduction block, are more pronounced in patients with AF episodes.

INTRODUCTION

About a century ago, Jean George Bachmann examined conduction across a muscular band of parallel, longitudinal orientated muscle fibers running from the right auricle at the superior cavo-atrial junction over the roof of the left atrium (LA) towards the left atrial appendage (LAA). This bundle, which came to be called Bachmann's bundle (BB),¹ is considered to be the preferential route of interatrial conduction. Whether this is because of the presence of specialized conduction tissue or the parallel-aligned orientation of the muscle bundles remains controversial.²⁻⁸ In vivo measurements of interatrial conduction velocity in canine hearts demonstrated that the effective conduction velocity across BB is considerable higher compared to other atrial sites.^{5, 6, 9} Creation of a surgical lesion across BB resulted in interatrial conduction block and caused biphasic P waves on the surface electrocardiogram.¹⁰ Clinical studies have demonstrated that biphasic P waves predispose to development of atrial fibrillation (AF).¹¹⁻¹³ It was therefore assumed that conduction disorders within BB play a major role in the pathophysiology of AF, although the exact mechanism is not understood.^{11, 14, 15} So far, conduction properties of BB in humans have never been investigated in detail. In this study, we therefore performed direct high-resolution mapping of BB during sinus rhythm (SR) in patients undergoing coronary artery bypass surgery (CABG) in order to examine 1) whether conduction disorders are present at BB, 2) the extensiveness of conduction disorders and their impact on LA excitation and 3) differences in characteristics of conduction disorders between patients with and without AF episodes.

METHODS

This study is part of a prospective observational project, entitled "QEst for Arrhythmogenic Substrate of Atrial fibRillation" (QUASAR), which was approved by the Medical Ethical Committee in the Erasmus Medical Center (MEC 2010-054). The QUASAR project adheres to the declaration of Helsinki principles and written informed consent was obtained from all patients prior to the surgical procedure.

Study population

Epicardial mapping was performed in 185 patients undergoing elective CABG. Patients with paced atrial rhythm, Wolff-Parkinson-White syndrome, renal failure, previous open chest cardiac surgery, prior ablative therapy, presence of assist devices and prior radiation for chest malignancies were excluded. Patient characteristics are summarized in Table 1. Thirteen patients (age 70±5years, 62% male) had paroxysmal AF (PAF) since 2 years (range 4 months – 23 years); the remaining 172 patients (age 65±9years, 155 (85%) male) had no history of AF. None of the patients had a typical biphasic p-wave in the inferior leads of the surface ECG. Mapping was performed in patients with a mean heart rate of 71±13 beats per minute.

Epicardial high-resolution mapping

Epicardial high-resolution mapping was performed after sternotomy during normothermia and prior to extra-corporal circulation. A bipolar pacemaker-wire serving as a temporal reference electrode was placed at the right atrial free wall and a steal wire was attached to subcutaneous tissue in the thorax as an indifferent electrode. BB was mapped with electrode

arrays containing either 128 or 192 unipolar electrodes (inter-electrode distances: 2.0mm) with lengths of respectively 32 and 48mm; the width of both arrays was 16mm.

Mapping of BB was performed by positioning the mapping array within the sinus transversus, behind the aorta with its tip against the LAA, as demonstrated in Figure 1. In case of the 128-electrode mapping array, the device was pulled backwards over the roof of the LA towards the superior cavo-atrial junction.

Five seconds of SR were recorded at every mapping site. The recordings included surface ECG lead I, the right atrial bipolar reference electrogram, a calibration signal with an amplitude of 1mV and a duration of 1000ms. Recordings were made with a custom-made mapping system with an amplifier (gain 1000), filter (bandwidth 0.5-400 Hz) and an analogue-to-digital data converter (16 bits). All data were sampled at 1 KHz and stored on hard disk.

Analysis of the mapping data

Signals were analyzed with custom-made software, as previously described in detail.¹⁶⁻¹⁹ Color-coded activation maps of every SR beat were automatically created by marking the steepest negative deflection of extracellular potentials. An averaged SR activation map was then constructed by time-alignment of all individual beats recorded during 5 seconds of SR, thereby excluding aberrant and atrial premature beats. These averaged activation maps were used for analysis of voltages, conduction velocities, conduction blocks and patterns of activation. Voltage maps were constructed by measuring peak-to-peak amplitudes of unipolar SR potentials.

As demonstrated in the lower panel of Figure 1, the mapping array was divided in 3 equally sized quadrants (16x16mm) to examine differences in conduction velocity over the right, and left part of BB. Conduction velocity across BB was measured by automatically constructing isochrones at every 5ms. The main trajectories of propagation were created perpendicular to the isochrones.^{18, 20} For the first part, the main trajectory was constructed from the initial isochrone at 5ms back to the onset of the wave front. If the onset of the wave front consisted of multiple electrodes, the electrode which resulted in the most perpendicular trajectory in relation to the isochrone was chosen as start of the wave front. From the first isochrone, the trajectory was constructed between consecutive isochrones choosing the most perpendicular segment to the next isochrone until the last activated electrode was reached. When the last activated site covers more than one electrode, again the electrode resulting in the most perpendicular line was chosen. Conduction velocity was subsequently calculated by summing the lengths of all segments between the isochrones and dividing it by the time difference of the earliest and latest activated electrode.

Table 1. Patient Characteristics

	No AF	Paroxysmal AF	P-value
No. of patients (N)	172	13	
Age, years \pm SD	65 \pm 9	70 \pm 5	0.05
Male gender(%)	147 (85)	8 (62)	0.04
BMI, kg/m² \pm SD	28 \pm 5	28 \pm 4	1.0
Hypertension(%)	104 (60)	10 (77)	0.38
Hypercholesterolemia(%)	74 (43)	5 (38)	1.0
Diabetes Mellitus(%)	60 (35)	5 (38)	0.77
Peripheral Vascular Disease(%)	22 (13)	1 (8)	1.0
Thyroid Disorder(%)	6 (3)	0	1.0
Echocardiography			
LVF (%)	167 (97)	13 (100)	0.06
Normal function(%)	130 (78)	8 (62)	
Mild dysfunction(%)	30 (18)	4 (31)	
Moderate dysfunction(%)	6 (4)	1 (8)	
Severe dysfunction(%)	1 (1)	0 (0)	
LA Size(%)			
Dilated LA (>45mm) (%)	23 (14)	3 (23)	0.38

BMI: Body Mass Index; LA: Left atrium; LVF: Left ventricular function.

Differences in activation time ('local conduction delay') between neighboring electrodes were calculated in areas of 2x2 electrodes. The maximum local conduction delay between two adjacent electrodes was calculated to determine the incidence of slowing of conduction and conduction block. Slowing of conduction was defined as a local conduction delay of ≥ 7 ms corresponding to a conduction velocity < 28 cm/s and conduction block as a local conduction delay of ≥ 12 ms corresponding to a conduction velocity < 18 cm/s, as previously described.^{17, 18} Lengths of all lines of conduction block were measured and they were subdivided into longitudinal or transversal lines of conduction block. Longitudinal conduction block was determined as lines of conduction block that interrupt wave fronts emerging in longitudinal direction and transverse block vice versa.

In order to study variation in patterns of activation of BB during SR, entry sites of SR wave fronts into BB were labeled as right atrial, central, left atrial or combined entry sites. A right atrial entry site was defined as a wave front first entering the mapping array from the right side and propagating towards the left side of BB whereas in case of a left atrial entry site activation started from the tip of the electrode positioned at the border of the LAA and spreads towards the right side of BB. A wave front emerging in the middle of the mapping array propagating to either the right and/or left side was labeled as a central entry site. Simultaneously activated areas (conduction velocities > 200 cm/s) within BB were also labeled as central entry sites.

Post-operative atrial fibrillation

Early post-operative AF (PoAF) was defined as sustained AF episodes lasting longer than 30 seconds. The incidence of PoAF was determined using continuous rhythm monitoring up to the first 5 days after cardiac surgery. The occurrence of PoAF was correlated with the amount of conduction block and the length of lines of the conduction block.

Statistical analysis

Normally distributed continuous variables are presented as mean \pm SD and skewed data as median (minimum – maximum). Categorical data are expressed as numbers and percentages. Data were compared using either Student *t*-Test, Mann-Whitney *U* test, χ^2 or Fisher exact test when appropriate. Correlation between voltage or conduction velocity and patient characteristics were made by using linear Pearson regression model. Adjustments were made for gender, age, body mass index, hypertension, diabetes, hyperlipidemia, peripheral vascular disease, left ventricular function and LA dilatation. Multivariate logistic regression models were used to test the relation between slow conduction or conduction block and the same patient characteristics. As a result of the small groups with a high amount of slow conduction and conduction block, univariate analyses were done to select the determinant of interest. Age, gender, a history of AF, hypertension, diabetes, left ventricular function and/or left atrial dilatation were chosen. In addition, the association between conduction block and PoAF was also investigated with logistic regression models. Due to the limited number of patients with PoAF, univariate analyses were performed to select properties of interest for multivariate analysis for the prediction of PoAF with conduction block. Type of conduction block, age, gender, hypertension and LA dilatation were included in the multivariate analysis for PoAF. A *p*-value <0.05 was considered as statistically significant.

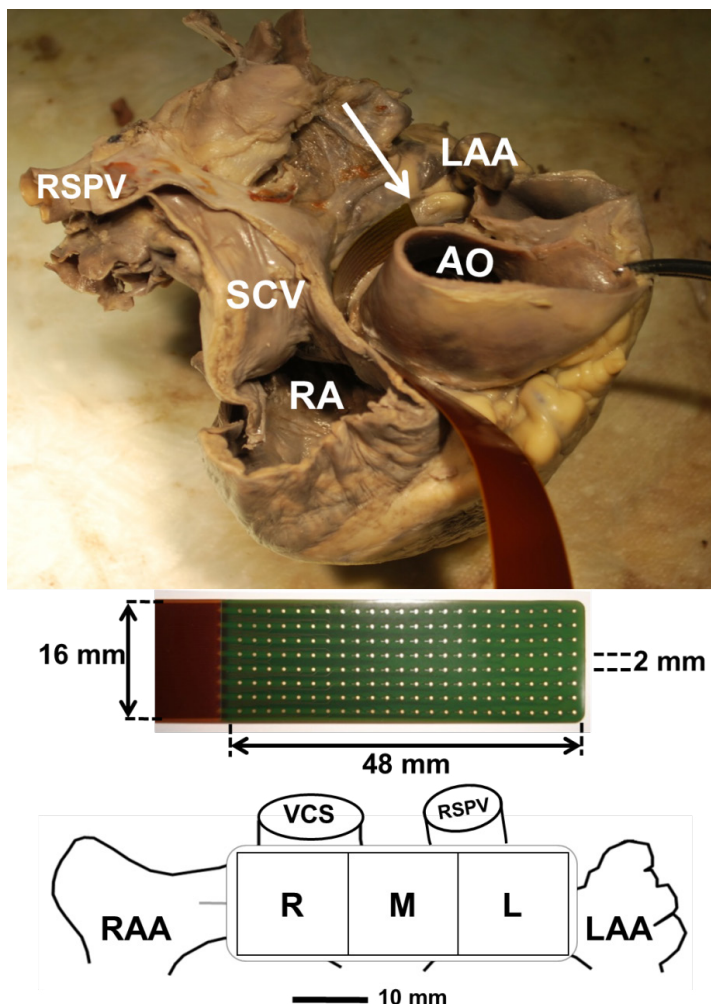


Figure 1. Mapping of Bachmann's bundle. Upper panel: post-mortem human heart from a right lateral superior view. Epicardial mapping of Bachmann's bundle is performed by introducing the mapping array behind the aorta and positioning its tip against the border of the left atrial appendage (white arrow). Middle panel: 192 unipolar electrode mapping array (interelectrodes distances of 2mm) covering an area of 48X16mm. Lower panel: schematic view of the position of the mapping array on BB. The mapping area was subdivided in 3 different quadrants of 16X16mm and labeled as right, central and left side. AO: aorta; LAA: left atrial appendage; RA: right atrium; RAA: right atrial appendage; RSPV: right superior pulmonary vein; SVC: superior caval vein.

RESULTS

Patterns of activation

Figure 2 shows color-coded SR activation maps of BB demonstrating the different types of patterns of activation observed in our study population. Arrows indicate main direction of

propagation. In the majority of the patients (N=124, 67%), BB was activated by a single wave front propagating from the right to the left side of BB as demonstrated in the upper left map of Figure 2. However, in 53 patients (29%), BB was activated by multiple wave fronts entering BB from different sites. In case of multiple different entry sites, wave fronts either collided or were separated by areas of conduction block. The upper right map of Figure 2 shows wave fronts entering on the right side and central part of BB, which was observed in 21% of the patients. Activation of BB from the right, left side and central part of BB occurred in 8% of the patients. A typical example is given in the lower left map; wave fronts not only enter BB from the right and the left side, but a large wave front also emerges in the central part of BB (dashed asterisk) and activates a large area more or less simultaneously. In the remaining 8 patients (4%), a wave front entered in the central part of BB and spread subsequently to both the right and left side of BB (lower right map). There was no difference in incidences of the various patterns of activation between patients without a history of AF and with PAF ($p=0.72$).

Peak-to-peak amplitude of sinus rhythm potentials

Mean voltages of all unipolar SR potentials ($N=218\pm29$ /patient) were 3.0 ± 1.4 mV and ranged from 0.3 to 7.2mV. Lower averaged voltages were associated with ageing ($p<0.001$) and female gender ($p=0.046$); there were no correlations with a history of PAF, increased body mass index, hypertension, diabetes, hyperlipidemia, peripheral vascular disease, left ventricular dysfunction or LA dilatation ($P>0.05$). Intra-individual variation in voltages across BB was 7.4 ± 3.2 mV (minimum: 0.5 ± 0.3 mV; maximum: 8.0 ± 3.3 mV).

Conduction velocity

The frequency distribution of the different effective conduction velocities of wave fronts propagating from the right to the left side of BB is shown in Figure 3 for the right side (left panel), central part (middle panel) and left side (right panel). In all patients, the effective conduction velocity did not differ between the right side (90 ± 24 cm/s), central part (88 ± 16 cm/s) or left side (89 ± 15 cm/s) of BB ($p>0.05$); mean effective conduction velocity over the entire length of BB was 89 ± 13 cm/s (range 57 – 128 cm/s). Lower conduction velocity was associated with lower voltages ($p=0.002$). Mean effective conduction velocity was not dependent on age ($p=0.35$) and was comparable between patients with PAF (97 ± 15 cm/s) and patients without a history of AF (89 ± 13 cm/s; $p=0.09$). Areas of slow conduction were observed in the majority of the patients ($N=172$; 93%); the median amount of slow conduction in all patients was 1.8% (0 – 9.2) and showed a trend towards a higher amount of slow conduction in patients with PAF compared to patients without a history of AF (2.6% (0.9 – 6.5) versus 1.7% (0 – 9.2), $p=0.07$). Furthermore, a high amount of slow conduction (>2% or >4% slow conduction) was not associated with a higher age ($p=0.16$ and $p=0.33$).

Characteristics of conduction block

A frequency histogram of the amount of conduction block at BB is illustrated in the upper panel of Figure 4. In all patients, the median prevalence of conduction block was 1.1% and the mean prevalence was 1.9%. Areas of conduction block were present in the majority of the patients ($N=138$, 75%); in the remaining 47 patients (25%) conduction block did not occur. In patients with conduction block, the amount of conduction block varied from 0.2% to 12.8%

(median prevalence: 1.8%). Conduction block was higher in patients with PAF compared to patients without a history of AF (3.2% (range 0 – 11.6) vs. 0.9% (range 0 – 12.8), $p=0.03$). Representative examples of the spatial distribution of areas of conduction block in patients with a variable amount of conduction block are depicted in the color-coded activation maps and corresponding conduction block maps in the middle panel of Figure 4. As can be seen in these maps, lines of conduction block occurred not only in the longitudinal direction, but also in the transverse direction of propagation. Electrograms around lines of conduction block showed both double potentials and fractionated potentials (lower panel Figure 4).

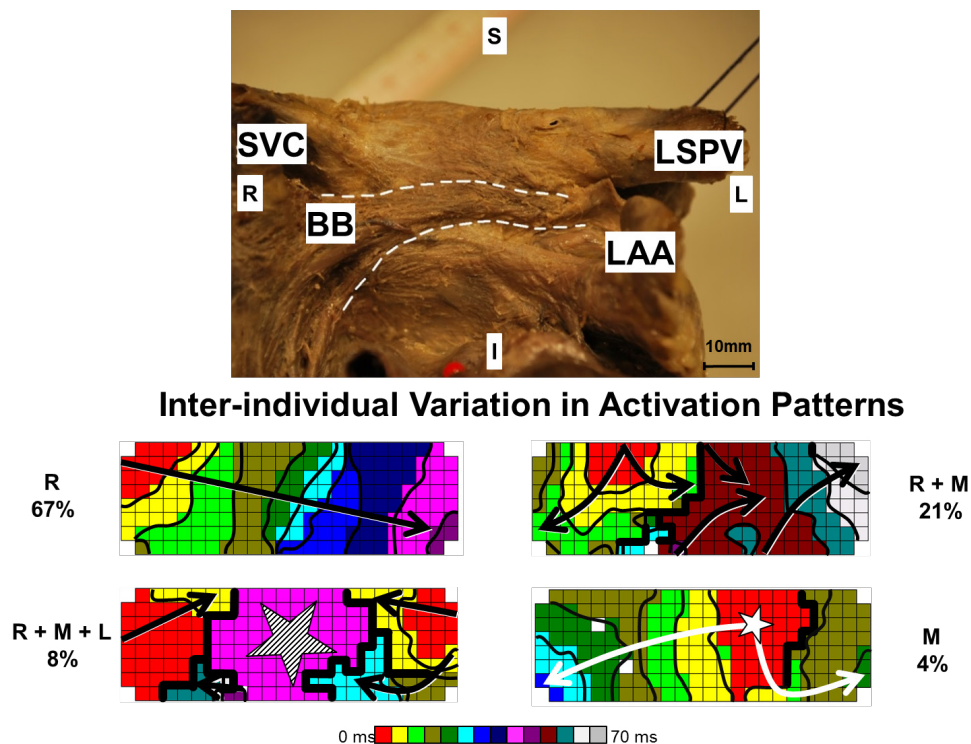


Figure 2. Activation patterns at Bachmann's bundle. Upper panel: a post-mortem human heart with a superior view at Bachmann's bundle. Lower panel: color-coded activation maps illustrating the 4 different patterns of activation observed at Bachmann's bundle. Propagation started either at the right (upper left map; $N=124$), right and central upper right map; $N=39$), right, central and left (lower left map; $N=14$) or solely from the central part (lower right map; $N=8$). Isochrones are drawn at 5 ms intervals and arrows indicate the main direction of propagation. See text for detailed explanation. BB: Bachmann's Bundle; I: inferior; L: left; LAA: left atrial appendage; LSPV: left superior pulmonary vein; R: right; S: superior; SVC: superior caval vein.

In the entire study population, the prevalence of longitudinal and transverse lines of conduction block ranged from respectively 0 to 12.8% (median: 1.3%) and 0 to 12.8% (median: 1.0%, $p<0.01$). Patients with PAF had a higher amount of conduction block in both longitudinal (1.1% (0 – 12.8) vs. 4.0% (0 – 11.7), $p=0.03$) and transverse direction (1.0% (0 – 12.8) vs. 1.9% (0 – 12.3), $p=0.03$).

As lines of longitudinal conduction block affect the right-to-left propagation across BB, the maximum lengths of all lines of longitudinal conduction block across BB were measured. Figure 5 shows the relative frequency of the maximal lengths of all longitudinal lines of conduction block observed in patients without a history of AF (left panel) or with PAF (right panel). Patients with PAF had longer lines of longitudinal conduction block than patients without a history of AF (median 8mm vs 2 mm, $p=0.03$).

In most patients without a history of AF (51%), there were no or only small areas (2mm) of longitudinal conduction block. Long lines of longitudinal conduction block (≥ 12 mm) were measured in only 12% of the patients ($N=20$). Although there were only 13 patients with PAF, solely 3 patients had no or small areas of conduction block. Five patients in this group (38%) had long lines of conduction block (≥ 12 mm). The maximum length of transverse lines of conduction block was also longer in patients with PAF than without AF (median 6mm (range 0 – 20mm) vs 2mm (range 0 – 20mm), $p=0.03$).

Impact of longitudinal conduction block on right-to-left propagation

The effects of longitudinal lines of conduction block on total activation time of BB and thus arrival time in the LA were determined for all patients mapped with the 192 unipolar mapping array with a single wave front propagating from the right to left side of BB ($N=52$). The initial arrival times of these wave fronts at the LAA in relation to initial activation of BB for every patient individually are plotted in the upper panel of Figure 6. As can be seen, there is no effect of the length of the lines of longitudinal conduction block on the time required for right-to-left activation of BB.

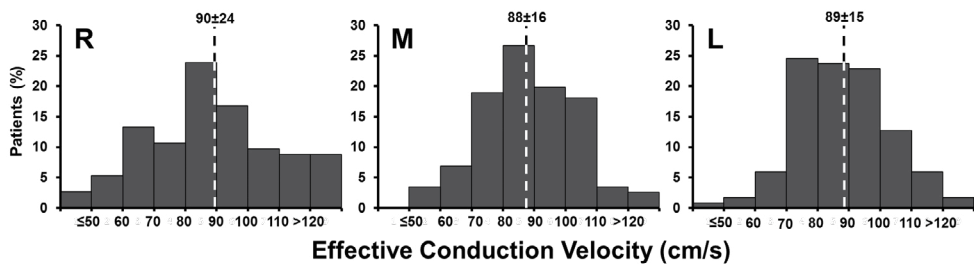


Figure 3. Effective conduction velocity across Bachmann's bundle. Relative frequency histograms in patients ($N=124$) with wave fronts propagating from right-to-left demonstrating the effective conduction velocity across Bachmann's bundle in the right side (left panel), central part (mid panel) and left side (right panel).

Explanations for this observation are given in the lower panels of Figure 6. The left activation map shows a line of conduction block with a length of 12mm with no effect on the right-to-left conduction. The wave front propagated around the line of conduction block without any conduction delay and arrived at the LAA side 44ms after the first activation of BB. The middle and right activation maps demonstrate that even a complete line of conduction block (16mm) across BB did not affect the arrival time at the LAA as in these patients areas behind the lines of conduction block were activated by wave front emerging from other sites, including the left and central part of BB. As a result, the activation of the LAA site in these patients occurred only 33ms and 22ms after the first moment of activation of BB.

Early post-operative atrial fibrillation

During the first 5 post-operative days, AF was observed in 56 patients (30%) including 7 patients (13%) who already had pre-operative PAF. The incidence of de novo PoAF is plotted for each patient individually without a history of AF in Figure 7 and ranked according to the intraoperatively determined prevalence of longitudinal conduction block (x-axis). There was a large variation in the length of areas of longitudinal conduction block in patients who developed PoAF. Although 10 patients (50%) with long lines of longitudinal conduction block developed PoAF, patients without or only small areas (2mm) of conduction block in longitudinal direction also frequently developed PoAF (N=20; 23%).

The lower panel in Figure 7 shows the results of univariate and multivariate analyses. A higher age was not related with the occurrence of PoAF in patients without a history of AF (OR 1.0, 95% CI 1.0 – 1.1, $p=0.31$). Although an equal amount of conduction block was found in patients with PoAF compared to patients without PoAF ($p=0.09$, not shown in Figure 7), >4% conduction block was associated with development of PoAF (OR 3.1, 95% CI 1.2 – 8.1, $p=0.02$). When analyzing the amount of conduction block for the different orientations separately, there was no difference between the amount of transverse ($p=0.06$) or longitudinal conduction block ($p=0.14$) and development of PoAF. Also, a higher risk of development of PoAF was not associated with >4% conduction block in either longitudinal ($p=0.28$) or transverse direction ($p=0.26$).

In patients without a history of AF, the length of lines of longitudinal conduction block did not differ between patients with and without PoAF (median 4mm vs 2mm, $p=0.07$). However, patients with PoAF had more often long lines (≥ 12 mm) of longitudinal conduction block (N=11) compared to patients without PoAF (N=9, $p<0.01$). Patients with long lines of longitudinal conduction block had a 3 times higher risk (OR 2.9; 95% CI 1.1 – 8.2; $p=0.04$) of developing PoAF, whereas patients with lines of conduction block of 12mm or longer in transverse direction had the same risk of developing PoAF (OR 2.2; 95% CI 0.51 – 9.9; $p=0.28$).

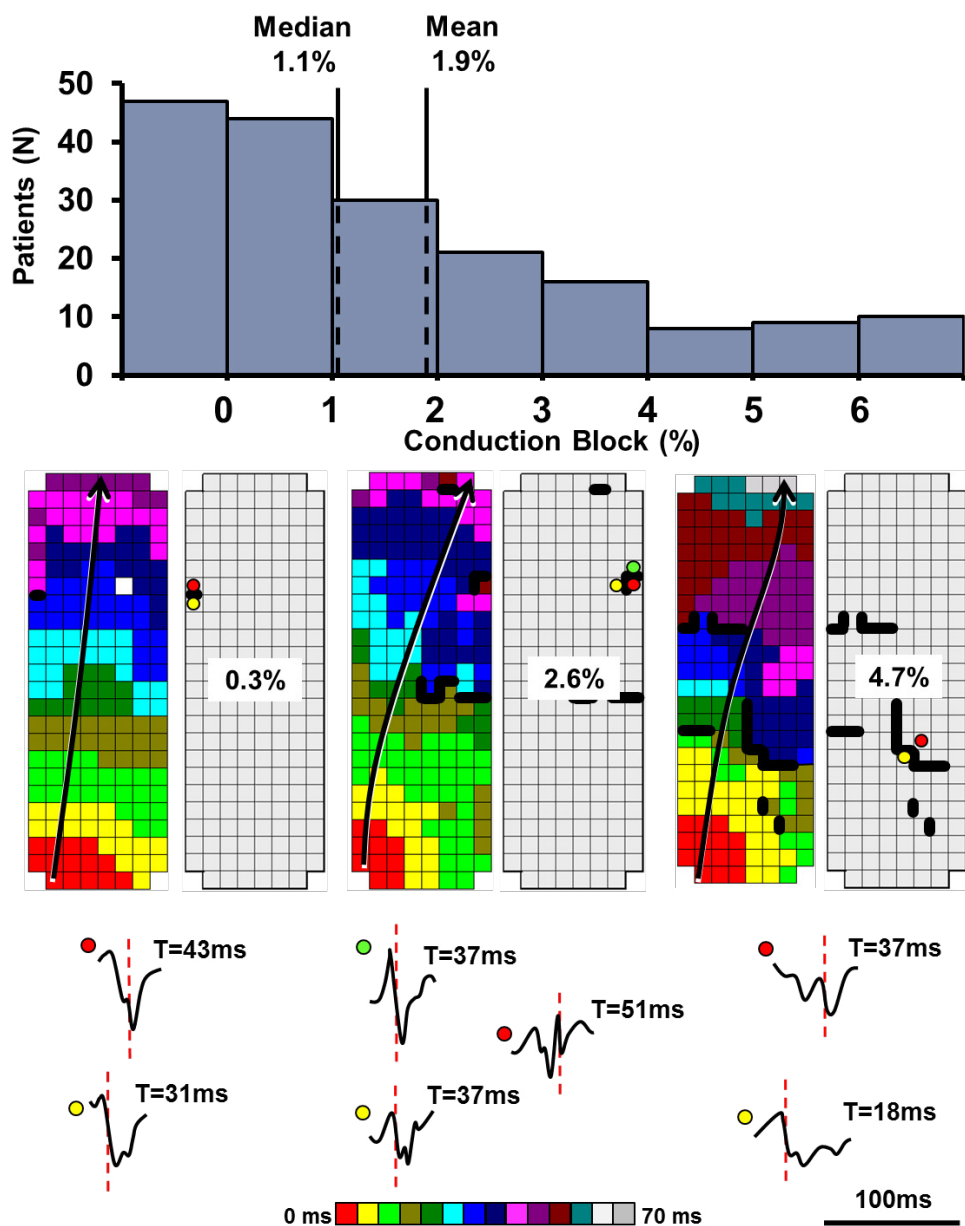


Figure 4. Conduction block. Upper panel: frequency histogram demonstrating the incidence of conduction block across Bachmann's bundle. Lower panel: color-coded activation maps and conduction block maps with a varying amount of conduction block ranging from 0.3% up to 4.7%. Examples of epicardial unipolar potentials recorded from areas of conduction block are shown outside the map. The color-coded circles in front of the electrogram correspond to the areas of block indicated in the conduction block maps.

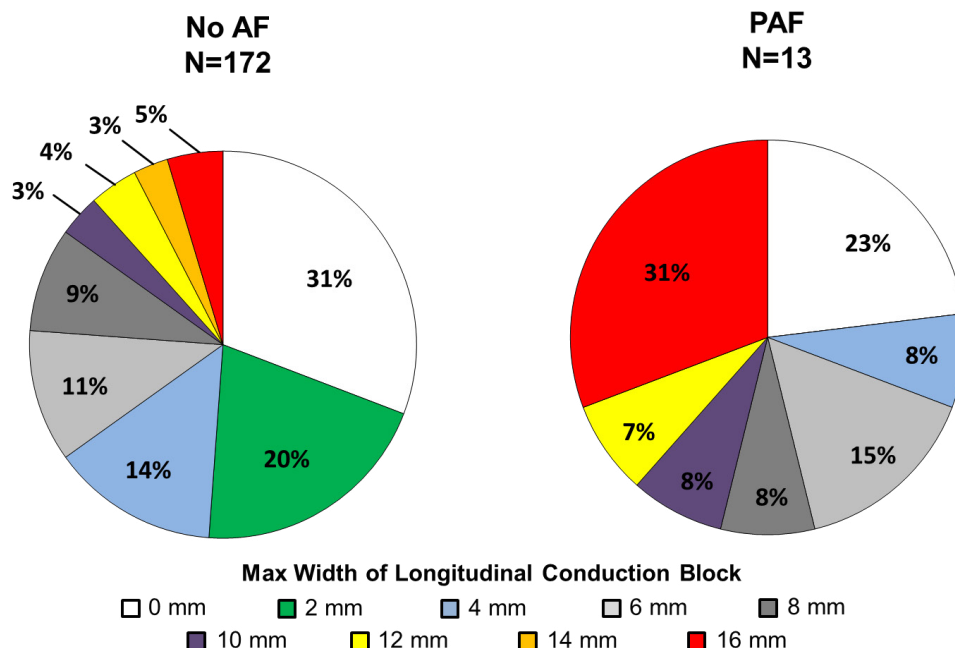


Figure 5. Longitudinal conduction block in Bachmann's bundle. Two pies illustrating relative incidence of the maximum lengths of lines of conduction block across Bachmann's bundle in patients without a history of AF (left panel) and with paroxysmal AF (PAF) (right panel).

DISCUSSION

High-resolution epicardial mapping of BB during SR in patients with coronary artery disease showed that BB was activated by multiple wave fronts, entering BB not only from the right side, but also from the left side and central part in a considerable number of patients. The average effective conduction velocity across BB was approximately 89 cm/s and did not differ between patients with or without AF. Lines of conduction block were found in the majority of the patients (74%) and occurred both in longitudinal and transverse direction. The effect of these lines of conduction block on excitation of the LA was limited. However, a high amount of conduction block and long lines of longitudinal conduction block were associated with the presence of PoAF.

Preferential, but not the only interatrial route

Experimental studies demonstrated that crushing of BB led to significant delay in excitation of the LA.¹ However, in our study population, the presence of long lines of longitudinal conduction block did not result in delayed LAA activation as areas behind the lines of conduction block were activated by wave fronts emerging from either the left side and/or central part of BB.

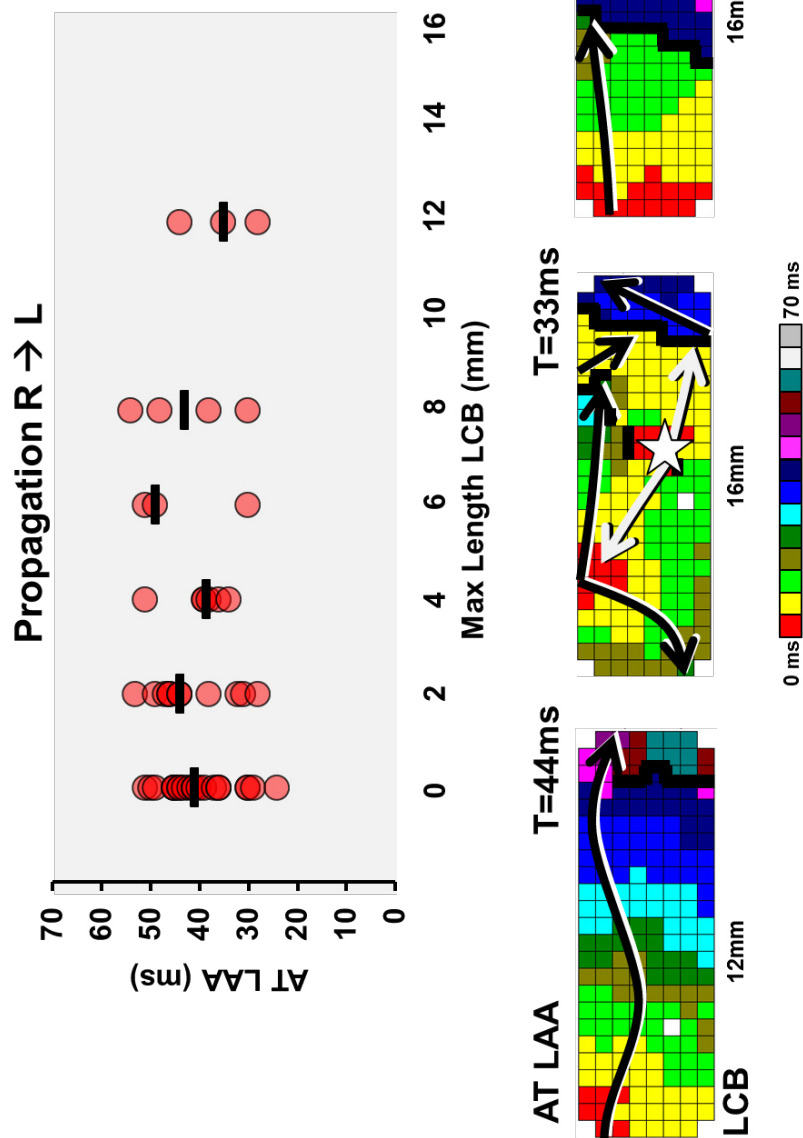
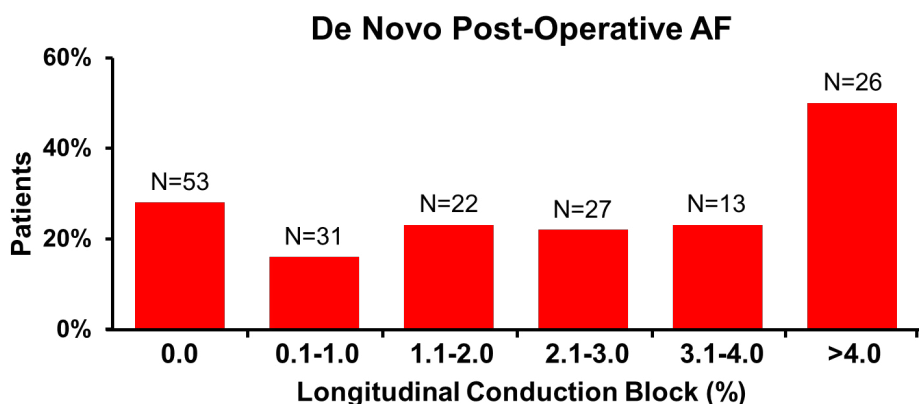


Figure 6. Impact of longitudinal lines of conduction block. Upper panel: the effect of the maximum length of line of conduction block in longitudinal direction and the first activation of the left atrial appendage is plotted for all patients (N=124) with a single right-to-left wave front across Bachmann's bundle. Lower panel: examples of the effect on the left atrial appendage activation time by different maximum lengths of lines of longitudinal conduction block. The left map illustrates a broad wave front curving around the line of conduction block. The middle and right map demonstrate a right-to-left wave front with a complete line of longitudinal conduction block co-existing with wave fronts entering BB from the central part (white or dashed asterisk) and/or left side.



Determinant	Univariate Analysis OR (95% CI)	p-value	Multivariate Analysis OR (95% CI)	p-value
Age	1.0 (0.99 – 1.1)	0.12	1.0 (0.98 – 1.1)	0.31
Male gender	2.2 (0.72 – 6.9)	0.16	2.5 (0.77 – 8.0)	0.13
Hypertension	1.3 (0.64 – 2.5)	0.49	1.3 (0.62 – 2.8)	0.47
LA dilatation	1.9 (0.75 – 4.7)	0.18	1.6 (0.61 – 4.2)	0.34
>4% CB	3.1 (1.2 – 7.6)	0.02	3.1 (1.2 – 8.1)	0.02

Figure 7. Relation between the amount of longitudinal conduction block and development of early post-operative AF. Upper panel: The effect of the amount of longitudinal conduction block on development of early post-operative AF in patients without a history of AF (N=172). Lower panel: Results of univariate and multivariate logistic regression between clinical determinants and development of early post-operative AF. LA: left atrium; AF: atrial fibrillation; CB: conduction block.

As demonstrated in previous studies, our observations confirm that BB is not the exclusive route of inter-atrial conduction and that propagation of electrical waves from the right to the LA occurs along other interatrial pathways when conduction across BB is impaired. These other interatrial pathways include the limbus of the fossa ovalis, the coronary sinus and interatrial bundles both superior and inferior along BB.²¹⁻²⁴

Conduction across BB has so far only indirectly been examined by using endocardial and epicardial mapping techniques.²⁵⁻²⁷ In patients who underwent catheter ablation of AF, three-dimensional electro-anatomical (non-)contact mapping techniques were used to examine the first LA activation site during SR. The earliest LA activation was frequently observed at the antero-superior LA, which was assumed to be the end of BB. Activation at this site was either solitary or simultaneously with other interatrial sites, which often included the postero-septal wall or the limbus of the fossa ovalis.^{26, 27} Similar to these findings, we also observed that in the majority of our patients, a single wave front propagated across BB from the right to the LA, which may initially activate the LA.

In 30% of our patients, BB was activated by wave fronts emerging in the central part of the mapping area. Although some studies observed that BB is isolated from the interatrial

septum, others suggested that muscular connections between BB and the interatrial septum are present.^{8, 24, 28} It is therefore likely that when right-to-left conduction along BB is delayed, BB can also be excited by wave fronts conducting faster in other interatrial pathways, (e.g. limbus of fossa ovalis or coronary sinus) propagating upwards in the interatrial septum and activating the central area of BB.

Interestingly, wave fronts not only entered BB on the right side and propagated leftwards, but also entered on the left side and propagated rightwards. These left sided wave fronts emerged both early and late in relation to the onset of activation of the right side of BB. This can be explained by the presence of the aforementioned additional bundles parallel to BB, crossing the roof of the LA.²⁴ When wave fronts propagate faster across these parallel bands than BB, they can enter BB relatively early on the left side and collide with the right to leftwards propagating wave fronts. When conduction across BB is delayed, interatrial conduction occurs in other interatrial pathways resulting in late excitation at the left side of BB, depending on the length and degree of conduction delay of the pathway taken. Besides that, a wave front emerging from the left side in BB in the presence of a long line of conduction block could also be explained by turning of a wave front around the end of the line of conduction block outside the mapping array. However, as the mapping array covers the entire width of BB, this is unlikely.

Bachmann's bundle, the superconductor?

Propagation of wave fronts occurs faster in longitudinal than transverse direction. It is therefore assumed that longitudinal parallel orientation of the fibers in BB results in higher conduction velocity, thereby making BB a preferential route of interatrial conduction. In addition, some studies suggest that the fibers of BB have specific characteristics similar to components of the specialized Purkinje fibers, such as a higher resting membrane potential, rapid velocity upstroke of the action potential, distinct overshoot and a broader phase 2 plateau.^{5, 6} However, in contrast to the Purkinje cells, action potentials in BB abbreviated after application of acetylcholine, which suggests BB cardiomyocytes differ from the Purkinje cells of the cardiac conduction system.⁵ Altogether, these studies showed that cardiomyocytes of BB have cell characteristics similar to both the specialized conduction system and atrial cardiomyocytes.

The effective conduction velocity across BB measured in animal studies was often faster at BB than other atrial sites.^{4, 5, 9} Goodman et al. performed mapping in a Langendorff-perfused canine heart with a 5-point electrode array.⁹ They observed a maximum conduction velocity of 300 cm/s in BB, which is comparable with conduction velocity in specialized Purkinje fibers. However, in our study population, we measured an effective conduction velocity of 'only' 89cm/s in BB which is comparable with conduction velocities at other sites in the atria.²⁹ Previous studies found higher effective conduction velocities across BB by measuring velocity between only a few points. Conduction velocity in BB could have been overestimated as wave fronts propagating from the right to the LA might fuse with wave fronts entering the central part of BB. This results in a large simultaneously activated areas, which could mimic fast propagation of a single wave front between the first and last activated site. In our study population, the effective conduction velocity might also have been overestimated due to late merging of wave fronts arising from deeper layers. Only single wavefronts propagating from

the right to left site of BB were chosen in order to minimize the risk of overestimation. Yet, despite the presence of only one single wave front, a different angle of the wave front entering BB, which is highly anisotropic in nature, can influence conduction velocity. On the other hand, areas of simultaneous activation ($>200\text{cm/s}$) were interpreted as central entry sites of wave fronts propagating partially through deeper layers. They were sometimes observed after a line of conduction block whereas they also collided with a right-to-left propagating wave front without being separated by lines of conduction block. In the latter case, the conduction velocity could have been overestimated.

The role of Bachmann's bundle in the pathophysiology of AF

Waldo et al. made surgical lesions in BB of dogs and observed significant changes in the P-wave morphology and duration.¹⁰ Delay in BB led to partial interatrial conduction block whereas complete block of BB caused advanced interatrial conduction block which was characterized by biphasic p-waves, particularly in the inferior leads on the surface ECG. Clinical studies have shown that advanced interatrial conduction block increases the risk of developing atrial tachyarrhythmias including AF.^{12, 13}

The role of BB in initiation and perpetuation of AF has been investigated in animal studies.^{14, 30, 31} In the goat model of Allesie, initiation of AF episodes were preceded by atrial extrasystolic beats that were blocked at the middle of BB.¹⁴ Subsequently, re-excitation at the same side of the line of conduction block suggested re-entry in BB. Mapping during AF of both atria and the interatrial septum in a sterile pericarditis canine model revealed multiple unstable re-entry circuits involving the interatrial septum.^{30, 31} As BB was the most commonly used interatrial pathway for these reentry circuits, the investigators suggested that BB is essential for perpetuation of AF.³⁰ In this same canine model, complete transection of BB with radiofrequency ablation resulted in termination and non-inducibility of AF.³¹

We observed multiple entry-sites of BB during SR in patients with and without lines of conduction block. A line of conduction block across the entire width of BB did not result in delayed left atrial activation and the specific p-wave alterations associated with development of AF. These findings differ from the earlier observations of p-wave alterations after surgical transection of BB. In case of complete surgical transection of BB, other muscular connections, e.g. interatrial septal pathways to BB, may also be disrupted.

According to these earlier studies, BB may play an important role in development of AF, although the exact mechanism remains unclear. Although over 20% of the patients without or with only a small area of conduction block developed PoAF, a high amount of conduction block and long lines of longitudinal conduction block were associated with de novo PoAF. These results indicate that the length of lines of conduction block facilitate reentry and hence development of AF. Yet, patients without (long) lines of conduction block developed both PAF and PoAF as well, suggesting that not only areas of conduction block in BB are involved in development of AF. The amount of conduction block at BB may merely reflect electrical disease which is also present elsewhere in the atria. Other atrial sites may contain more extensive areas of conduction block and thus play a larger role in the pathophysiology of AF. Becker microscopically examined BB, terminal crest and pulmonary vein areas in 20 post-

mortem mainly known with coronary artery disease; 10 patients had a history of PAF.³² In all patients, fibro-fatty tissue and fibrotic patches were found which may cause conduction disorders as a result of disruption of cell-to-cell connections.^{29, 30} These histological changes were more common in patients with PAF which may explain the higher amount of conduction block in patients with PAF in our study population. As all examined areas – pulmonary veins, terminal crest and BB – were more affected in patients with PAF, delayed intra-atrial conduction predisposing to development of AF is probably the result of extensive conduction block throughout the atria and interatrial connections rather than conduction block across BB only. In addition, conduction disorder may be further impaired by e.g. atrial extrasystolic beats which in turn initiate AF episodes.

Study limitations

Mapping of BB is solely performed at the epicardial surface and does not provide any information of wave fronts propagating partially in deeper layers or emerging from other atrial sites. Hence, only the effective conduction velocity can be assessed. Also, the definition of slow conduction and conduction block remains arbitrary and very slow conduction cannot definitely be excluded. In the individual patient, the exact proportions of BB are unknown and the mapping array might not always have covered the entire BB. However, previous studies demonstrated that the size of BB equals approximately the size of the mapping array. Also, our study did not provide any information on conduction properties at other atrial sites. Due to the small group of patients with a history of AF, comparison between patients with and without a history of AF was limited. In line with that, a lack of power might explain the absence of a significant relation between slowing of conduction velocity, a higher age and development of PoAF.

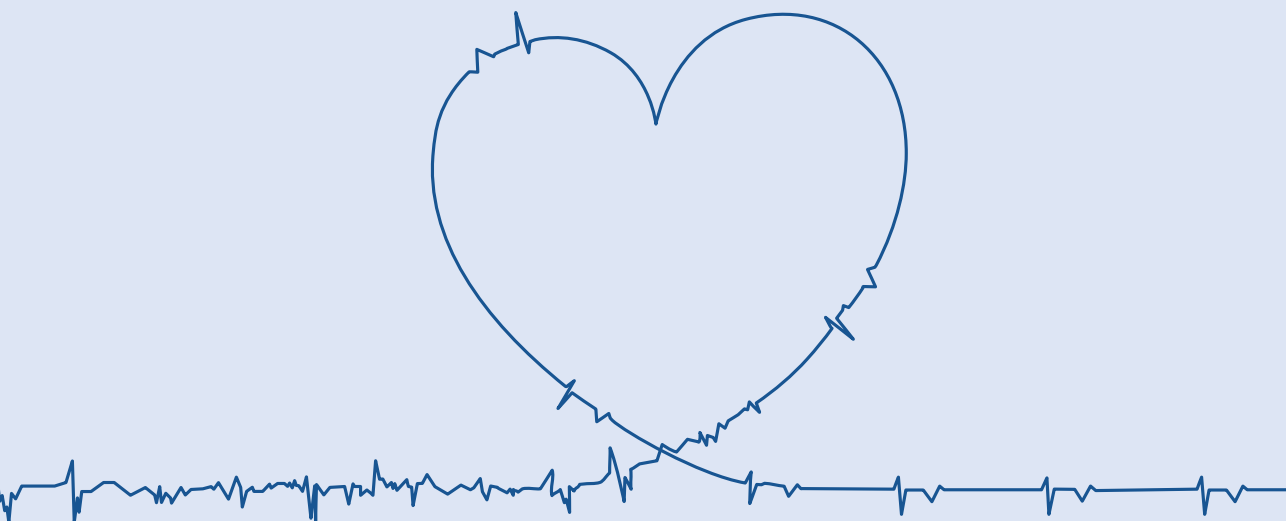
CONCLUSION

High-resolution mapping of BB in humans with coronary artery disease during SR demonstrated that BB may be the preferential route of interatrial conduction, but can be activated from other directions as well. As a consequence, conduction disorders exclusively in BB have limited impact on LA excitation. Despite the longitudinal orientation of BB fibers, BB is not the 'superconductor' as previously suggested. Conduction is blocked in both longitudinal and transverse direction in the majority of the patients. Conduction disorders, particularly long lines of longitudinal conduction block, are more pronounced in patients with AF episodes.

REFERENCES:

1. Bachmann G. The inter-auricular time interval. *Am J Physiol.* 1916;41:309-320.
2. James TN. The Connecting Pathways between the Sinus Node and a-V Node and between the Right and the Left Atrium in the Human Heart. *Am Heart J.* 1963;66:498-508.
3. Lemery R, Guiraudon G, Veinot JP. Anatomic description of Bachmann's bundle and its relation to the atrial septum. *Am J Cardiol.* 2003;91:1482-1485, A1488.
4. Dolber PC, Spach MS. Structure of canine Bachmann's bundle related to propagation of excitation. *Am J Physiol.* 1989;257:H1446-1457.
5. Wagner ML, Lazzara R, Weiss RM, Hoffman BF. Specialized conducting fibers in the interatrial band. *Circ Res.* 1966;18:502-518.
6. Childers RW, Merideth J, Moe GK. Supernormality in Bachmann's bundle. An in vitro and in vivo study in the dog. *Circ Res.* 1968;22:363-370.
7. Ho SY, Anderson RH, Sanchez-Quintana D. Atrial structure and fibres: morphologic bases of atrial conduction. *Cardiovasc Res.* 2002;54:325-336.
8. Platonov PG, Mitrofanova L, Ivanov V, Ho SY. Substrates for intra-atrial and interatrial conduction in the atrial septum: anatomical study on 84 human hearts. *Heart Rhythm.* 2008;5:1189-1195.
9. Goodman D, van der Steen AB, van Dam RT. Endocardial and epicardial activation pathways of the canine right atrium. *Am J Physiol.* 1971;220:1-11.
10. Waldo AL, Bush HL, Jr., Gelband H, Zorn GL, Jr., Vitikainen KJ, Hoffman BF. Effects on the canine P wave of discrete lesions in the specialized atrial tracts. *Circ Res.* 1971;29:452-467.
11. Agarwal YK, Aronow WS, Levy JA, Spodick DH. Association of interatrial block with development of atrial fibrillation. *Am J Cardiol.* 2003;91:882.
12. Ariyaratnam V, Fernandes J, Kranis M, Apiyasawat S, Mercado K, Spodick DH. Prospective evaluation of atrial tachyarrhythmias in patients with interatrial block. *Int J Cardiol.* 2007;118:332-337.
13. Bayes de Luna A, Cladellas M, Oter R, Torner P, Guindo J, Marti V, Rivera I, Iturralde P. Interatrial conduction block and retrograde activation of the left atrium and paroxysmal supraventricular tachyarrhythmia. *Eur Heart J.* 1988;9:1112-1118.
14. Duytschaever M, Danse P, Eysbouts S, Alessie M. Is there an optimal pacing site to prevent atrial fibrillation?: an experimental study in the chronically instrumented goat. *J Cardiovasc Electrophysiol.* 2002;13:1264-1271.
15. van Campenhout MJ, Yaksh A, Kik C, de Jaegere PP, Ho SY, Alessie MA, de Groot NM. Bachmann's bundle: a key player in the development of atrial fibrillation? *Circ Arrhythm Electrophysiol.* 2013;6:1041-1046.
16. Yaksh A, Kik C, Knops P, Roos-Hesselink JW, Bogers AJ, Zijlstra F, Alessie M, de Groot NM. Atrial fibrillation: to map or not to map? *Neth Heart J.* 2014;22:259-266.
17. de Groot NM, Houben RP, Smeets JL, Boersma E, Schotten U, Schalij MJ, Crijns H, Alessie MA. Electropathological substrate of longstanding persistent atrial fibrillation in patients with structural heart disease: epicardial breakthrough. *Circulation.* 2010;122:1674-1682.
18. Alessie MA, de Groot NM, Houben RP, Schotten U, Boersma E, Smeets JL, Crijns HJ. Electropathological substrate of long-standing persistent atrial fibrillation in patients with structural heart disease: longitudinal dissociation. *Circ Arrhythm Electrophysiol.* 2010;3:606-615.
19. Rogers JM, Usui M, KenKnight BH, Ideker RE, Smith WM. Recurrent wavefront morphologies: a method for quantifying the complexity of epicardial activation patterns. *Ann Biomed Eng.* 1997;25:761-768.
20. Kay MW, Gray RA. Measuring curvature and velocity vector fields for waves of cardiac excitation in 2-D media. *IEEE Trans Biomed Eng.* 2005;52:50-63.
21. Sanchez-Quintana D, Davies DW, Ho SY, Osizlok P, Anderson RH. Architecture of the atrial

- musculature in and around the triangle of Koch: its potential relevance to atrioventricular nodal reentry. *J Cardiovasc Electrophysiol.* 1997;8:1396-1407.
22. Mitrofanova L, Ivanov V, Platonov PG. Anatomy of the inferior interatrial route in humans. *Europace.* 2005;7 Suppl 2:49-55.
23. Chauvin M, Shah DC, Haissaguerre M, Marcellin L, Brechenmacher C. The anatomic basis of connections between the coronary sinus musculature and the left atrium in humans. *Circulation.* 2000;101:647-652.
24. Ho SY, Sanchez-Quintana D, Cabrera JA, Anderson RH. Anatomy of the left atrium: implications for radiofrequency ablation of atrial fibrillation. *J Cardiovasc Electrophysiol.* 1999;10:1525-1533.
25. Markides V, Schilling RJ, Ho SY, Chow AW, Davies DW, Peters NS. Characterization of left atrial activation in the intact human heart. *Circulation.* 2003;107:733-739.
26. Tapanainen JM, Jurkko R, Holmqvist F, Husser D, Kongstad O, Makijarvi M, Toivonen L, Platonov PG. Interatrial right-to-left conduction in patients with paroxysmal atrial fibrillation. *J Interv Card Electrophysiol.* 2009;25:117-122.
27. Lemery R, Birnie D, Tang AS, Green M, Gollob M, Hendry M, Lau E. Normal atrial activation and voltage during sinus rhythm in the human heart: an endocardial and epicardial mapping study in patients with a history of atrial fibrillation. *J Cardiovasc Electrophysiol.* 2007;18:402-408.
28. Papez JW. Heart musculature of the atria. *Am J Anat.* 1920-21;27:255-277.
29. Hansson A, Holm M, Blomstrom P, Johansson R, Luhrs C, Brandt J, Olsson SB. Right atrial free wall conduction velocity and degree of anisotropy in patients with stable sinus rhythm studied during open heart surgery. *Eur Heart J.* 1998;19:293-300.
30. Kumagai K, Khrestian C, Waldo AL. Simultaneous multisite mapping studies during induced atrial fibrillation in the sterile pericarditis model - Insights into the mechanism of its maintenance. *Circulation.* 1997;95:511-521.
31. Kumagai K, Uno K, Khrestian C, Waldo AL. Single site radiofrequency catheter ablation of atrial fibrillation: studies guided by simultaneous multisite mapping in the canine sterile pericarditis model. *J Am Coll Cardiol.* 2000;36:917-923.
32. Becker AE. How structurally normal are human atria in patients with atrial fibrillation? *Heart Rhythm.* 2004;1:627-631.





CHAPTER 8

DISTRIBUTION OF CONDUCTION DISORDERS IN PATIENTS WITH CONGENITAL HEART DISEASE AND RIGHT ATRIAL VOLUME OVERLOAD

Houck CA*, Lanthers EAH*, Heida A, Taverne YJHJ, van de Woestijne PC, Knops P,
Roos-Serote MC, Roos-Hesselink JW, Bogers AJJC, de Groot NMS

**Both authors contributed equally*

Journal of the American College of Cardiology: Clinical Electrophysiology (2020)

ABSTRACT

Background Patients with an interatrial shunt are prone to developing atrial fibrillation (AF), which may be related to conduction disorders occurring due to atrial stretch. The aim of this study was to quantify characteristics of atrial conduction disorders in patients with right atrial (RA) volume overload.

Methods Thirty-one patients undergoing surgery for an interatrial shunt (49 ± 14 years) underwent epicardial sinus rhythm mapping of the RA, Bachmann's bundle (BB) and left atrium (LA). Conduction delay (CD) was defined as inter-electrode conduction time (CT) of 7-11ms and conduction block (CB) as $CT \geq 12$ ms. Prevalence of CD/CB (percentage of mapped region), length of lines, and severity of CB (75th percentile of CTs ≥ 12 ms) were analyzed.

Results All patients had some degree of CD and CB. Prevalence of CD and CB was higher in the RA and BB than in the LA ($p < 0.0083$ after Bonferroni correction). The longest CB line within each patient was found in the RA in most patients (52%). Inter-individual variation in prevalence and lengths of lines was considerable. CB was more severe in the RA than in the LA ($p < 0.0083$). Within the RA, conduction disorders were more prevalent and more severe in the intercaval region than in the RA free wall ($p < 0.05$).

Conclusions In patients with an interatrial shunt, conduction disorders during sinus rhythm are most pronounced in the RA – particularly the intercaval region – and BB. Knowledge of the conduction during sinus rhythm is essential to determine the relevance of conduction disorders for initiation and perpetuation of AF.

INTRODUCTION

Atrial septal defect (ASD) is one of the more common congenital heart defects which often remains undiagnosed until adulthood. The interatrial left-to-right shunt causes volume overload, dilatation and stretch of the right atrium (RA). A long-term consequence of ASD is the development of atrial fibrillation (AF), which is associated with substantial morbidity.¹ AF prevalence is considerably higher in ASD patients than in the general population^{1,2}, which suggests the substrate underlying AF in these patients is either different or more severe.

A key factor determining risk of AF is age at ASD repair, as this will determine the duration of right atrial volume overload and stretch.¹ The consequences of atrial stretch have been described extensively in humans with atrial volume overload.³⁻⁶ A prime consequence is the presence of atrial conduction abnormalities, which may be aggravated by a longer stretch duration. It is assumed that atrial conduction abnormalities are crucially involved in initiation and perpetuation of AF.⁷

In ASD patients, conduction abnormalities have been found in both the right and left atrium. Morton et al. reported that conduction delay at the crista terminalis was significantly more pronounced in ASD patients than in control subjects.³ Roberts-Thomson et al. also compared ASD patients with control subjects and demonstrated the presence of conduction abnormalities in the LA, as well as low voltage regions, increased inducibility of AF and echocardiographic LA dilatation in ASD patients.⁴

However, the spatial distribution of conduction disorders across both atria, including Bachmann's bundle (BB), in patients with longstanding RA volume overload has so far not been studied. In order to be able to interpret the relevance of conduction disorders for initiation and perpetuation of AF in this specific patient population, it is essential to understand their characteristics and spatial distribution within the atria during sinus rhythm.

The aim of this study was therefore to quantify the characteristics of atrial conduction disorders during sinus rhythm in adult patients with an interatrial left-to-right shunt, and to establish whether predilection sites exist. To this end, we performed intra-operative, high-resolution epicardial mapping of the RA, BB and LA in patients undergoing surgical correction of the defect.

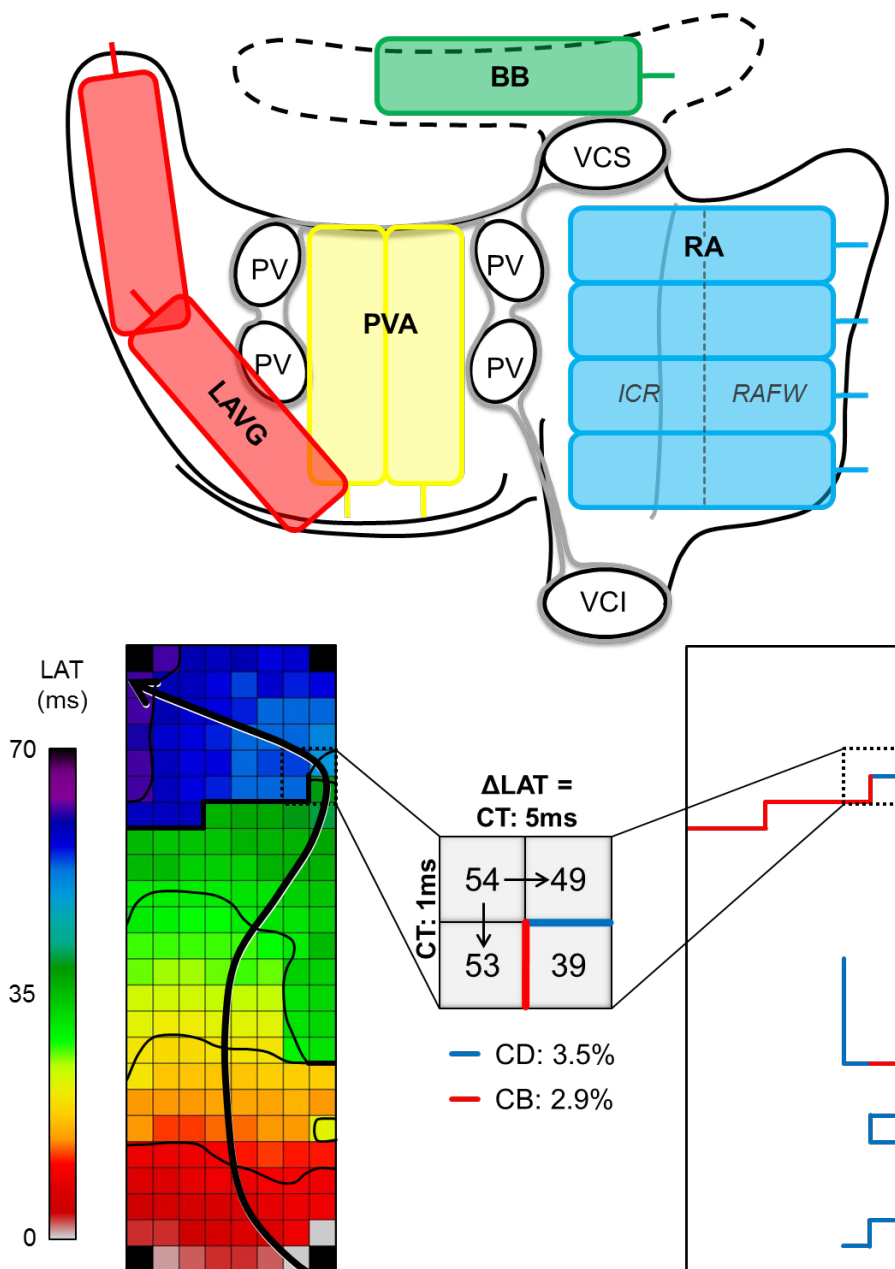


Figure 1. High-resolution epicardial mapping. Upper panel: mapping sites on a schematic posterior view of the atria. Lower panel: color-coded activation map recorded on BB with isochrones drawn at 10ms (left) and conduction delay/block map (right).

BB: Bachmann's bundle, CB: conduction block, CD: conduction delay, CT: conduction time, ICR: intercaval region, LAVG: left atrioventricular groove, LAT: local activation time, PVA: pulmonary vein area, PV: pulmonary vein, RA: right atrium, RAFW: right atrial free wall, VCI: vena cava inferior, VCS: vena cava superior.

METHODS

Study population

The study population consisted of 31 adult patients with a congenital interatrial left-to-right shunt, scheduled for the first surgical correction of the defect. This study was approved by the institutional medical ethical committee (MEC-2010-054, MEC-2014-393). All patients provided written informed consent. Patient characteristics were obtained from electronic files. LA and RA dimensions were assessed on 2D echocardiography and dilatation was defined according to the guidelines.⁸

Epicardial mapping

Epicardial mapping during sinus rhythm was performed prior to commencement of extracorporeal circulation. A detailed description of the methods is provided in the Supplemental Material. The electrode array (128/192 unipolar electrodes, inter-electrode distance 2mm) was placed on each consecutive mapping site (upper panel Figure 1), including the RA (from cavo-tricuspid isthmus towards the RA appendage, perpendicular to the caval veins), BB (between the border of the LA appendage and the superior cavo-atrial junction), left atrioventricular groove (LAVG; from the lower border of the left inferior pulmonary vein towards the LA appendage), and the pulmonary vein area (PVA; from the sinus transversus along the borders of the pulmonary veins towards the atrioventricular groove).

Local activation maps were constructed by annotating the steepest negative deflection of atrial potentials on every electrode. Difference in local activation time was calculated between each electrode and the adjacent right and lower electrode, resulting in two inter-electrode conduction times (lower panel Figure 1). Consistent with prior mapping studies, conduction delay (CD) and conduction block (CB) were defined as conduction times of respectively 7-11ms and ≥ 12 ms between two adjacent electrodes, corresponding to effective conduction velocities of respectively 18 to 29 cm/s and < 18 cm/s.^{9,10} Prevalence of CD/CB was defined as the number of inter-electrode conduction times satisfying the definitions for CD/CB as a percentage of the total number of inter-electrode conduction times measured in a sampled region. Prevalence of CD/CB was calculated for all mapping regions combined as well as for each region separately (RA, BB, LAVG, PVA). Lines of CD, CB and continuous CDCB were defined as uninterrupted series of inter-electrode CD, CB or a combination of CD and CB and length was measured on a 2mm resolution scale. Severity of CB was defined as the 75th percentile of CTs ≥ 12 ms. To further analyze the spatial distribution of conduction disorders within the RA, the RA surface was subdivided into 2 areas: the intercaval region and the RA free wall (upper panel Figure 1).

Table 1. Patient characteristics

	Total N = 31	No history of AF N = 26	History of AF N = 5
Age (years)	49±14 (18-70)	47±14 (18-70)	55±13 (37-69)
Female	18(58)	16(62)	2(40)
Type of congenital heart defect			
Secundum ASD	18(58)	14(54)	4(80)
SVD with PAPVR	11(36)	10(39)	1(20)
PAPVR	2(7)	2(8)	0
BMI	27.6±4.6	28±4.7	25.5±3.6
RA volume (ml/m ²)	49(20-99)	50(20-76)	41(38-99)
RA dilatation	26(84)	23(89)	3(60)
LA dimension (cm/m ²)	2.2±0.4	2.2±0.4	2.3±0.4
LA dilatation	10(32)	8(31)	2(40)
Left ventricular function			
Normal	26(84)	21(81)	5(100)
Mild dysfunction	4(13)	4(15)	0
Moderate dysfunction	1(3)	1(4)	0
Right ventricular function*			
Normal	25(81)	20(83)	5(100)
Mild dysfunction	2(7)	2(8)	0
Moderate dysfunction	2(7)	2(8)	0
Antiarrhythmic drugs			
Class II	10(32)	7(27)	3(60)
Class III	2(6)	0	2(40)

Values are expressed as N(%), median (minimum-maximum), or mean ± SD (minimum-maximum). * Not available in 2 patients. There were no statistically significant differences between patients with and without a history of AF. AF: atrial fibrillation, ASD: atrial septal defect, BMI: body mass index, PAPVR: partial abnormal pulmonary venous return, SVD: sinus venosus defect.

Statistical analysis

Normally distributed continuous variables were expressed as mean ± standard deviation (minimum-maximum) and skewed variables as median (minimum-maximum). A paired samples t-test or Wilcoxon signed-rank test was used to compare continuous parameters between the four atrial regions and between the intercaval region and RA free wall. Bonferroni correction was applied for comparison of the four regions; a p-value of <0.0083 (0.05/6) was considered statistically significant. Categorical data was presented as numbers and percentages and compared with the chi-squared test. Univariate linear regression was performed with dependent variables including prevalence, median length of lines and length of the longest line of CB and continuous CDCB and independent variables including age, indexed RA volume (ml/m²) and indexed LA diameter (cm/m²). If the model did not conform to the assumptions of linear regression, log-transformation of the dependent variable was

performed and subsequently, if necessary, of the independent variable or of both variables. A p-value <0.05 was considered statistically significant, except if Bonferroni correction was applied.

RESULTS

Patient characteristics

Clinical characteristics of the study population are summarized in Table 1. Most patients had a secundum ASD (n=18, 58%), followed by a sinus venosus defect with partial abnormal pulmonary venous return in 11 patients (36%) and isolated partial abnormal pulmonary venous return in 2(7%). The RA was dilated in 26 patients (84%) and LA dilatation was present in 10 patients (32%). Five patients had a history of paroxysmal AF; clinical characteristics did not differ significantly between patients with and without a history of AF. One patient had a history of atrial flutter. Median (minimum-maximum) cycle length during sinus rhythm was 833ms (638-1326) and did not differ between the atrial regions ($p>0.0083$).

Regional differences in heterogeneity in conduction

The upper panel of Figure 2 illustrates examples of distribution of CD and CB within the atria of 3 patients, showing considerable intra-atrial and inter-individual variation. All patients had some degree of CD in each atrial region; median prevalence of CD within all regions combined was 2.9% (1.7-5.4). The lower left panel of Figure 2 demonstrates prevalence of CD for each atrial region. The highest prevalence of CD was measured in BB (3.9% (0.7-8.1)), followed by RA (3.2%, 0.4-7.6). CD was less prevalent in the PVA (2.5%, 0.2-6.5, BB vs. PVA: $p=0.001$) and LAVG (2.2%, 0.2-5, RA vs. LAVG: $p=0.003$, BB vs. LAVG: $p<0.001$).

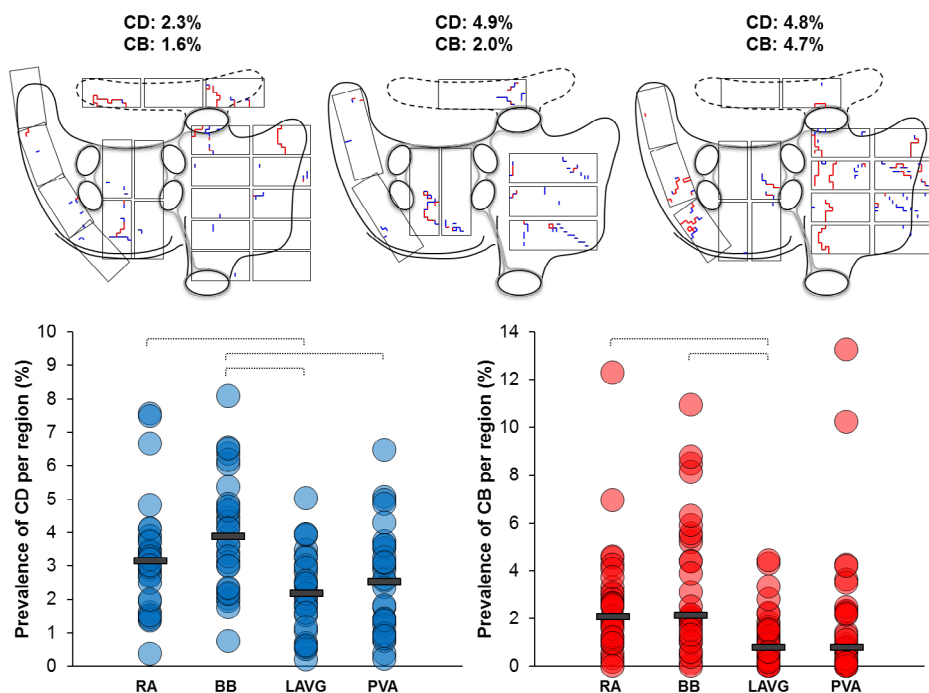


Figure 2. Prevalence of CD and CB. Upper panel: spatial distribution of CD and CB in 3 patients. Lower left panel: prevalence of CD. Lower right panel: prevalence of CB. Bars indicate median. Dashed lines indicate $p < 0.0083$. BB: Bachmann's bundle, CB: conduction block, CD: conduction delay, LAVG: left atrioventricular groove, PVA: pulmonary vein area, RA: right atrium.

Compared to CD, median prevalence of CB within all regions combined was lower (1.9%, 0.6-7). All patients had some degree of CB in at least 2 atrial regions, including the RA (n=30, 97%), BB (n=30, 97%), LAVG (n=26, 87%) or PVA (n=26, 87%). Prevalence of CB for every atrial region is displayed in the lower right panel of Figure 2; inter-individual variation was high, particularly in BB. Median prevalence of CB was lower in the LAVG (0.8%, 0-4.4) than in BB (2.1%, 0-10.9, $p=0.001$) and RA (2.1%, 0-12.3, $p=0.004$). The upper left panel of Figure 3 demonstrates that in most patients, the highest prevalence of CB within each patient was found in BB (n=15, 48%), followed by the RA (n=9, 29%). The lower left panel of Figure 3 visualizes for each patient the prevalence of CB in every atrial region; patients are ranked according to prevalence of CB in BB. Again, this graph illustrates the inter-individual variation in CB. There was no relation between the prevalence of CB in the various atrial regions.

Characteristics of areas of conduction disorders

Examples in the upper panel of Figure 4 show that areas of CD and CB formed either long, continuous CDCB lines (left panel) or shorter, diffusely scattered lines (right panel). As demonstrated in the lower left panel of Figure 4, CD lines were short and varied only between 2 and 8mm across all regions; they were the shortest in the RA ($p < 0.0083$). Median lengths of CB and continuous CDCB lines did not differ between the various atrial regions.

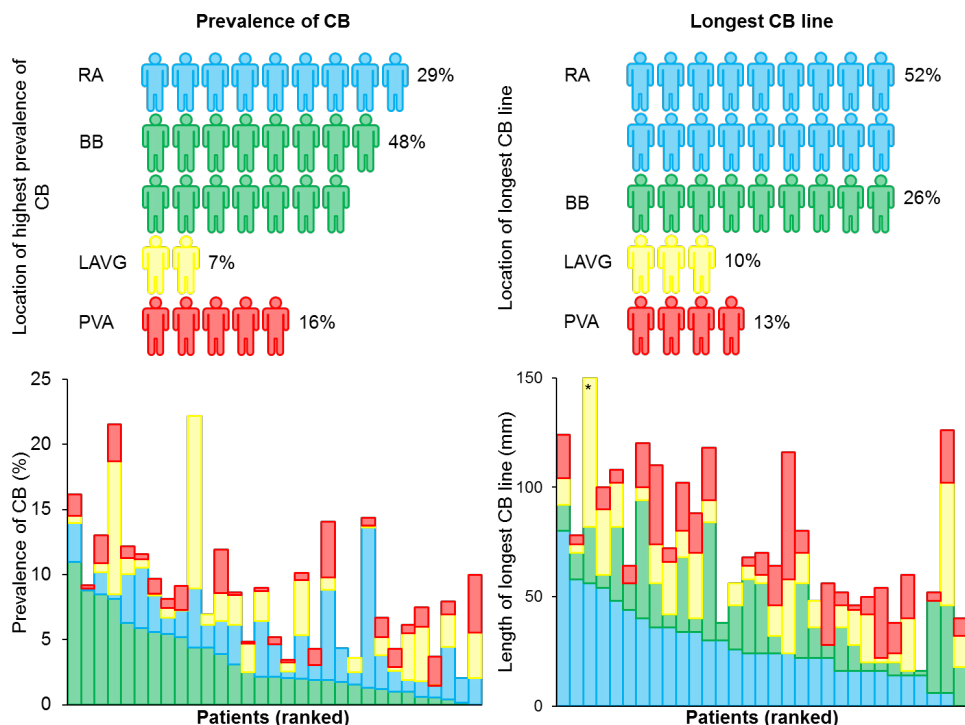


Figure 3. Intra-atrial and inter-individual variation in distribution of CB. Upper left panel: location of the highest prevalence of CB within every patient. Lower left panel: prevalence of CB in the atrial regions; patients are ranked according to prevalence of CB in BB. Upper right panel: location of the longest CB line within every patient. Lower right panel: lengths of the longest CB lines in the atrial regions; patients are ranked according to length of lines in the RA. * length of this line was 172mm. BB: Bachmann's bundle, CB: conduction block, LAVG: left atrioventricular groove, PVA: pulmonary vein area, RA: right atrium.

Length of the longest line of CD in all patients was 14mm (4-50), of CB 18mm (2-172) and of continuous CDCB 29mm (4-190). These CB lines were longer in the RA than LAVG (24mm, 16-38 vs. 12mm, 6-24, $p=0.008$) (lower right panel Figure 4).

The longest CB line within each patient was most often located in the RA ($n=16$, 52%), followed by BB ($n=8$, 26%; upper right panel Figure 3). Similar to the prevalence of CB, both length and distribution of the longest CB lines also varied considerably between individuals, as demonstrated in the lower right panel of Figure 3. There was no relation between lengths of CB lines measured in the various atrial regions.

When comparing patients with a secundum ASD ($N=18$) and sinus venosus defect ($N=11$), patients with a secundum ASD had more CB in BB (mean \pm standard deviation (minimum-maximum): $4.6 \pm 3.2\%$ (0-10.9) vs. $1.5 \pm 0.8\%$ (0.4-3.1), $p=0.001$) and longer CB lines in BB (longest line: $26.6 \pm 12.2\text{mm}$ (2-54) vs. $8.9 \pm 4.8\text{mm}$ (4-20), $p<0.001$); similar findings were observed for continuous CDCB. There were no differences in the other atrial regions. Older age

was associated with higher prevalence of CB and continuous CDCB in the RA (respectively $b=0.006 \log(\%)/\text{year}$, $p=0.042$ and $b=0.008 \log(\%)/\text{year}$, $p=0.016$) and with length of the longest continuous CDCB line in the RA ($b=0.711 \text{ mm/year}$, $p=0.018$). LA dimension was associated with both prevalence of continuous CDCB in BB ($b=2.743 \text{ } \%/(\text{cm}/\text{m}^2)$, $p=0.046$) and length of the longest continuous CDCB line in BB ($b=17.637 \text{ mm}/(\text{cm}/\text{m}^2)$, $p=0.021$).

Severity of conduction disorders

The upper panel of Figure 5 shows an example of the relative distribution of all CTs measured within the atria in one patient. The middle right panel demonstrates corresponding distribution of CD and CB lines. Most CTs were short (73% $\leq 2\text{ms}$), indicating absence of conduction disorders. Similarly, in the entire study population, most CTs were $\leq 2\text{ms}$ (median: 78%, 67-83). Though the 90th percentiles of all CTs were short, they were longer in both RA and BB than LAVG and PVA (RA: 5ms, 3-16, BB: 5ms, 3-13, LAVG: 3ms, 2-6, PVA: 4ms, 2-27, $p<0.0083$). Histograms in the lower left panel of Figure 5 illustrate relative distribution of CTs $\geq 12\text{ms}$ (i.e. CB) for each atrial region in this same patient. CB appeared to be most severe in the RA and, to a lesser extent, the LAVG. In the entire study population, however, CB was more severe in the RA than the LAVG and PVA ($p<0.0083$; lower right panel Figure 5).

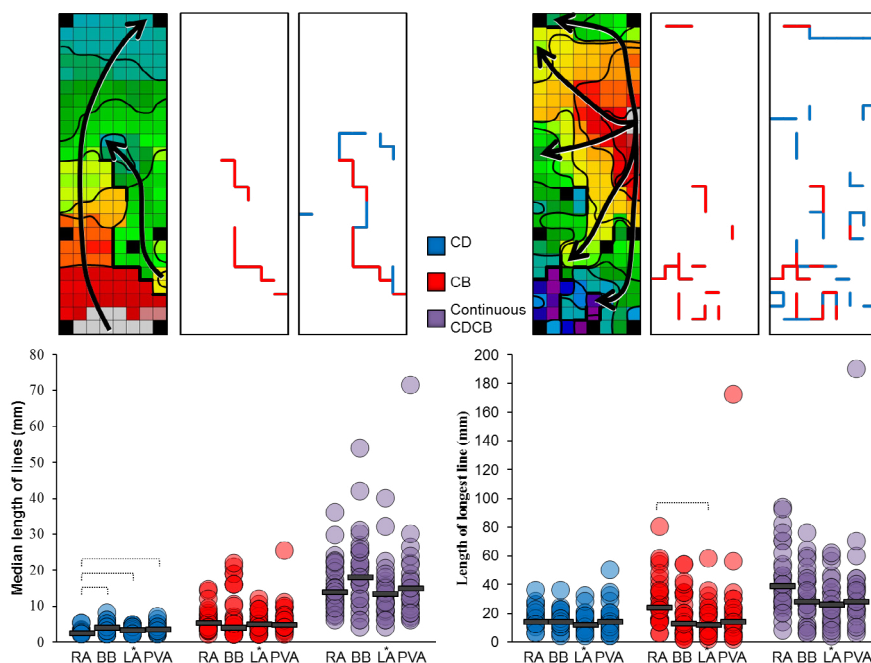


Figure 4. Characteristics of areas of conduction disorders. Upper panels: examples of interconnected CD and CB lines creating long, continuous CDCB lines (left panel; recorded on the PVA) or shorter, diffusely scattered lines (right panel; recorded on the RA). Isochrones are drawn at 5ms. Arrows indicate main trajectories of activation. Lower left panel: median length of lines. Lower right panel: length of the longest lines. Bars indicate median. Dashed lines indicate $p<0.0083$. BB: Bachmann's bundle, CB: conduction block, CD: conduction delay, LA*: left atrioventricular groove, PVA: pulmonary vein area, RA: right atrium.

Heterogeneity in right intra-atrial conduction

The upper left panel of Figure 6 shows a typical example of the distribution of areas of CD, CB and continuous CDCB within the RA. As demonstrated in the upper right panel, prevalence of both CD and CB was higher in the intercaval region than in the RA free wall. In addition, lines of CB and continuous CDCB in the intercaval region were not only longer than in the RA free wall, but they were also more severe (lower panels Figure 6).

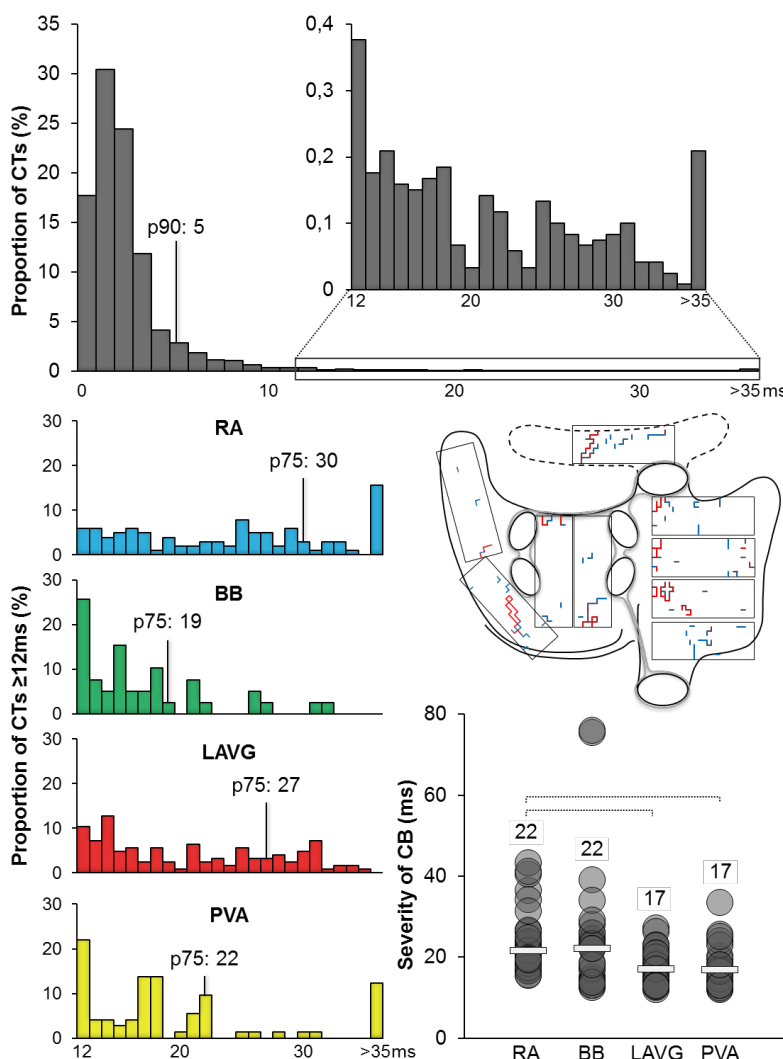


Figure 5. Severity of conduction disorders. Upper panel: relative distribution of CTs within the atria in one patient. Distribution of CD and CB lines (middle right panel) and relative distribution of CTs ≥ 12 ms for each atrial region (lower left panel) in the same patient. Lower right panel: severity of CB. Bars and numbers indicate median. Horizontal dashed lines indicate $p < 0.0083$. BB: Bachmann's bundle, CD: conduction delay, CB: conduction block, CT: conduction time, LAVG: left atrioventricular groove, PVA: pulmonary vein area, RA: right atrium.

History of atrial fibrillation

When comparing patients with and without a history of AF, prevalence and characteristics of conduction disorders only differed in BB, yet only 5 patients (16%) had a history of AF. Patients with AF had a higher prevalence of CB (6.3%, 1.3-8.5 vs. 2.0%, 0-10.9, $p=0.047$) and longer lines of CB (longest line: 34mm, 12-40 vs. 12mm, 2-54, $p=0.041$), although severity of CB was similar. Prevalence and lines of continuous CDCB did not differ.

DISCUSSION

This high-resolution, epicardial mapping study is the first to report the prevalence, spatial distribution and severity of conduction disorders in the RA, BB and LA in patients with RA volume overload resulting from an interatrial shunt. Although these patients have longstanding volume overload and stretch of the RA, conduction disorders were not exclusively located in the RA, but also in BB and – to a lesser extent – the LA. Overall, conduction disorders were most prevalent in the RA and BB and most severe in the RA, although considerable inter-individual variation was observed. Further analysis of the RA revealed a predilection site for conduction disorders in the intercaval region.

Consequences of chronic right atrial stretch

The concept of electrical remodeling in response to atrial stretch has been studied extensively in humans with cardiovascular disease causing atrial stretch, including congestive heart failure, mitral regurgitation, and ASD.³⁻⁶ Acute atrial dilatation increases spatial heterogeneity in conduction, which can result in a reduction in conduction velocity and the formation of lines of intra-atrial conduction block.¹¹ These conduction abnormalities may become aggravated during chronic atrial stretch, as is the case in adult patients with unrepaired ASD. The presence of lines of CB makes it more likely for reentrant circuits to develop, which, when combined with atrial enlargement, may increase the likelihood of AF development.⁷

Atrial stretch has also been associated with structural myocardial remodeling.^{12,13} These structural changes are thought to contribute to increased heterogeneity in atrial conduction. Macchiarelli et al. analyzed RA tissue samples from four children aged 1, 4, 6 and 6 years undergoing surgery for ASD and found atrial fibrosis and other significant myocardial degenerative changes in the two older children.¹² Another study that examined RA tissue samples from 65 adult patients with RA overload due to unrepaired CHD showed that, compared with similar samples from healthy age-matched controls, these samples had more structural remodeling including fibrosis.¹³ The age of these patients – which determines the duration of overload and stretch – was associated with various histological markers of structural RA remodeling. In line with this observation was our finding that with increasing age, conduction disorders in the RA became more prevalent and created longer lines of CB. Electrical and structural remodeling in ASD patients have also occur in the LA. Roberts-Thomson et al. have shown that ASD patients have significant LA enlargement as well as LA electrophysiological abnormalities that include conduction disorders, low voltage regions and increased inducibility of AF.⁴ Comparative measurements in the RA have not been reported. Although we found conduction disorders to be present in the LAVG and the PVA, the extent and severity of these conduction disorders were considerably lower than those in the RA.

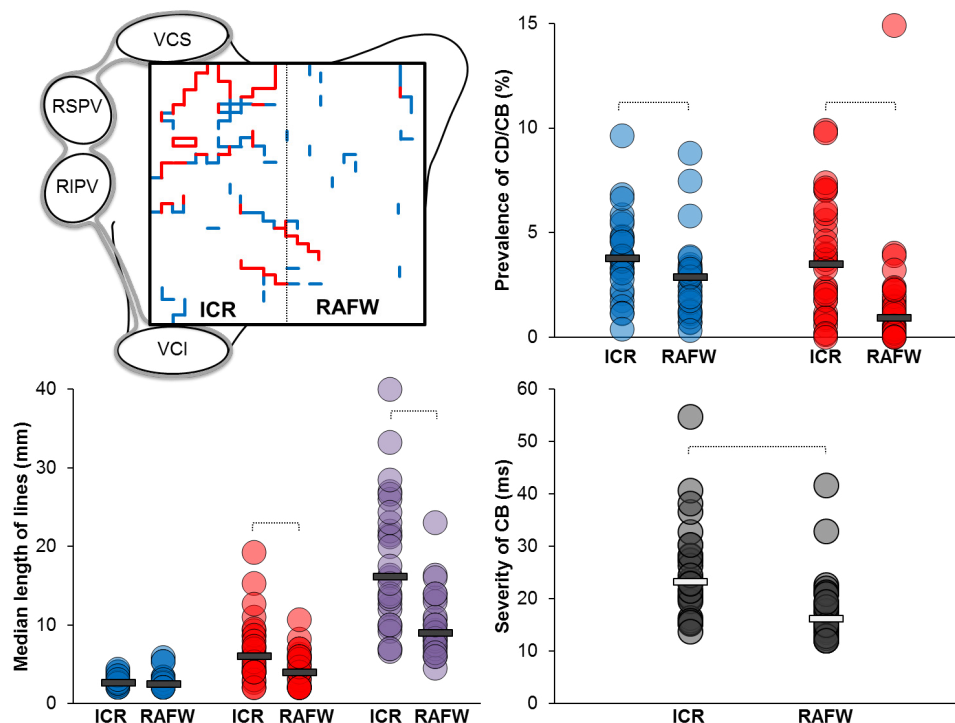


Figure 6. Heterogeneity in right intra-atrial conduction. Upper left panel: example of distribution of CD (blue) and CB (red) lines in the intercaval region and RA free wall. Upper right panel: prevalence of CD and CB. Lower left panel: median length of CD, CB and continuous CDCB (purple) lines. Lower right panel: severity of CB. Bars indicate median. Dashed lines indicate $p < 0.05$. CB: conduction block, CD: conduction delay, ICR: intercaval region, RAFW: right atrial free wall, RIPV: right inferior pulmonary vein, RSPV: right superior pulmonary vein, VCI: vena cava inferior, VCS: vena cava superior.

Bachmann's bundle

Our study is the first to demonstrate a high prevalence of conduction disorders in BB in patients with RA volume overload. The presence of conduction disorders in BB was associated with LA dimension rather than RA dimension or age. A possible explanation for this association lies in the embryonic development of the atria. BB is a muscular bundle on the atrial septal roof connecting the RA and LA. Jongbloed et al. demonstrated in mouse embryos that on the right side, BB is connected to the septum spurium, which is continuous with the left and right venous valves guarding the sinus venosus. On the left side, BB is connected to the left atrioventricular ring bundle, which continues into the dorsal wall of the LA and pulmonary veins.¹⁴ This suggests that, anatomically, BB may be connected more to LA tissue rather than RA tissue. An enlarged LA may therefore confer more stretch and thus stress on BB than an enlarged RA, thereby giving rise to conduction disorders in BB.

Previous studies have suggested a potential role for BB in the pathophysiology of AF. Indeed, despite the small number of patients in our study who had a history of AF, these patients

were more likely to have more extensive CB in BB than patients without a history of AF. The mechanism by which conduction disorders in BB may contribute to the initiation and perpetuation of AF is still under investigation. One theory proposes an association between interatrial conduction block and the development of AF.¹⁵ However, Teuwen et al. performed epicardial mapping in patients with ischemic heart disease and showed that long lines of conduction block in BB did not result in delayed LA activation, because wavefronts emerging from the central or left part of BB activated the areas behind lines of conduction block.¹⁶ This implies that conduction abnormalities in BB do not necessarily cause interatrial conduction block. The most likely theory is that conduction abnormalities in BB facilitate the formation of reentrant circuits and hence development of AF.^{16,17}

Conduction disorders in the right atrium

Studies in patients with chronic atrial volume overload^{3,6} and in patients without structural heart disease causing atrial volume overload¹⁸ have demonstrated the presence of functional conduction delay in the region of the crista terminalis. Conduction disorders in this region are involved in the development of both typical and atypical atrial flutter and AF.^{18,19} The crista terminalis is a relatively thick muscle band, from which the pectinate muscles arise anterolaterally towards the RA appendage. The areas containing pectinate muscles act as RA volume reserve during increased preloading conditions. This anatomical and functional distinction might explain the predisposition for conduction disorders in the intercaval region – which roughly corresponds to the region of the crista terminalis – in the presence of RA volume overload, as also observed in our study and that of Morton et al.³ However, the presence of conduction abnormalities in this region may also be related to anatomical barriers rather than a specific disease process.¹⁸ Due to the invasive nature of our mapping approach, it was not possible to study healthy control subjects. Lanfers et al. performed epicardial sinus rhythm mapping in 209 patients without a history of AF undergoing coronary artery bypass grafting, and found a predilection site for conduction disorders in the superior intercaval region.²⁰ Although these patients do not qualify as a suitable control group due to the potential effects of ischemia on atrial conduction, these findings do suggest that conduction abnormalities in this region may not be specific to patients with RA volume overload.

The crista terminalis is a highly anisotropic region due to directional differences in gap junction distribution which result in impaired transverse conduction as opposed to preserved longitudinal conduction.^{18,21} The sinus rhythm wave generally originates from the superior intercaval region, traveling along the crista terminalis in a more longitudinal rather than transverse direction. It is therefore possible that mapping during sinus rhythm has left additional conduction disorders caused by tissue anisotropy in this region undetected. Given that our study found extensive conduction disorders in the intercaval region – with marked differences within the RA and between the RA and LA – we propose that mapping during pacing maneuvers will uncover even more conduction disorders in this region.

Conduction disorders in the RA may be involved in the development of both AF and atrial flutter. In 7 dogs with sterile pericarditis, Ortiz et al. demonstrated by epicardial mapping of the RA free wall that a certain length of a line of CB was required for either stable (atrial flutter) or unstable reentry (AF) to occur. Atrial flutter required a long line of CB together with areas

of slow conduction, whereas AF occurred when areas of slow conduction disappeared, the cycle length decreased and lines of CB shortened. On the one hand, our findings of prominent conduction disorders in the RA may relate to the development of postoperative atrial flutter by serving as areas of slow conduction supporting a stable reentrant circuit around the atriotomy scar. On the other hand, these conduction disorders may also result in unstable reentrant circuits mitigating across the atrial wall, giving rise to AF.

Reverse electrical and structural remodeling

It remains unknown whether electrical and structural changes resulting from RA volume overload can be reversed after repair of the defect. While ASD repair during childhood is known to reduce the chances of AF during long-term follow-up, in adults the age at repair does not seem to lower the risk for AF.¹ It is therefore likely that in adults, the damage has already been done and the resultant RA remodeling is – at least in part – irreversible.³ In their study in adults undergoing ASD closure, Morton et al. showed incomplete normalization of RA and LA size and persistence of conduction disorders at the crista terminalis after percutaneous ASD closure, although late electrophysiological evaluation was only performed in 4 of 12 patients.³ However, another study in 21 adult patients with severe mitral stenosis undergoing mitral commissurotomy demonstrated both immediate and late reversal of structural and conduction abnormalities, although the late measurements were only performed in the RA.²²

Study Limitations

Only a limited number of patients with a history of AF were included in this study, partly due to the relative rarity of these patients and partly because sinus rhythm could not always be obtained in patients with AF. Therefore, our comparison of patients with and without a history of AF should be interpreted with caution. This study was primarily designed to quantify the distribution of conduction disorders within the atria in patients with RA volume overload, rather than to find abnormalities specifically associated with AF. Mapping of the interatrial septum was not possible due to our closed-heart mapping approach.

CONCLUSION

In order to improve treatment strategies aimed at eliminating AF, it is essential to understand the underlying substrate, which may be different or more severe in patients with RA volume overload than in the general population. Conduction disorders during sinus rhythm in these patients are most prevalent in the RA and BB and most severe in the RA. A predilection site for conduction disorders within the RA is present in the intercaval region, which is likely related to the conduction properties of the crista terminalis and the pectinate muscles. The next step will be to determine the relevance of these conduction disorders for initiation and perpetuation of AF. The considerable inter-individual variation observed in this study emphasizes the need for a patient-tailored approach to further unravel the substrate of AF in these patients

REFERENCES

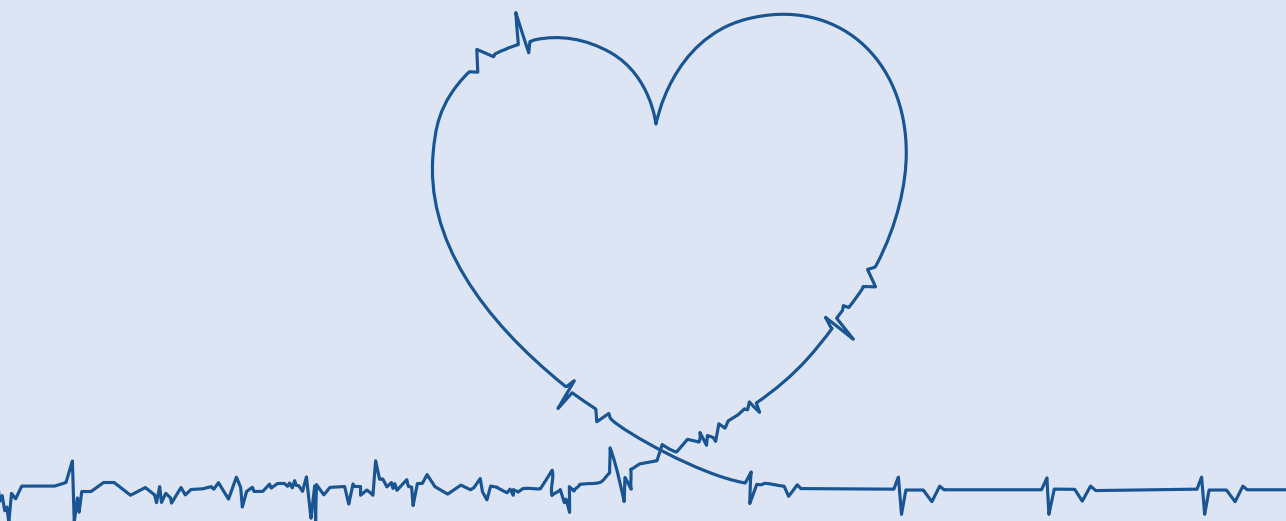
1. Murphy JG, Gersh BJ, McGoon MD et al. Long-term outcome after surgical repair of isolated atrial septal defect. Follow-up at 27 to 32 years. *N Engl J Med* 1990;323:1645-50.
2. Heeringa J, van der Kuip DA, Hofman A et al. Prevalence, incidence and lifetime risk of atrial fibrillation: the Rotterdam study. *Eur Heart J* 2006;27:949-53.
3. Morton JB, Sanders P, Vohra JK et al. Effect of chronic right atrial stretch on atrial electrical remodeling in patients with an atrial septal defect. *Circulation* 2003;107:1775-82.
4. Roberts-Thomson KC, John B, Worthley SG et al. Left atrial remodeling in patients with atrial septal defects. *Heart Rhythm* 2009;6:1000-6.
5. Roberts-Thomson KC, Stevenson I, Kistler PM et al. The role of chronic atrial stretch and atrial fibrillation on posterior left atrial wall conduction. *Heart Rhythm* 2009;6:1109-17.
6. Sanders P, Morton JB, Davidson NC et al. Electrical remodeling of the atria in congestive heart failure: electrophysiological and electroanatomic mapping in humans. *Circulation* 2003;108:1461-8.
7. Ortiz J, Niwano S, Abe H, Rudy Y, Johnson NJ, Waldo AL. Mapping the conversion of atrial flutter to atrial fibrillation and atrial fibrillation to atrial flutter. Insights into mechanisms. *Circ Res* 1994;74:882-94.
8. Lang RM, Badano LP, Mor-Avi V et al. Recommendations for cardiac chamber quantification by echocardiography in adults: an update from the American Society of Echocardiography and the European Association of Cardiovascular Imaging. *Eur Heart J Cardiovasc Imaging* 2015;16:233-70.
9. Allessie MA, de Groot NM, Houben RP et al. Electropathological substrate of long-standing persistent atrial fibrillation in patients with structural heart disease: longitudinal dissociation. *Circ Arrhythm Electrophysiol* 2010;3:606-15.
10. de Groot NM, Houben RP, Smeets JL et al. Electropathological substrate of longstanding persistent atrial fibrillation in patients with structural heart disease: epicardial breakthrough. *Circulation* 2010;122:1674-82.
11. Eijsbouts SC, Majidi M, van Zandvoort M, Allessie MA. Effects of acute atrial dilation on heterogeneity in conduction in the isolated rabbit heart. *J Cardiovasc Electrophysiol* 2003;14:269-78.
12. Macchiarelli G, Nigri G, Martinotti A, DiDio LJ. Subcellular structure of the atrial myocardium of children in cases of atrial septal defect. *J Submicrosc Cytol Pathol* 1992;24:395-400.
13. Ueda A, Adachi I, McCarthy KP, Li W, Ho SY, Uemura H. Substrates of atrial arrhythmias: histological insights from patients with congenital heart disease. *Int J Cardiol* 2013;168:2481-6.
14. Jongbloed MR, Schalij MJ, Poelmann RE et al. Embryonic conduction tissue: a spatial correlation with adult arrhythmogenic areas. *J Cardiovasc Electrophysiol* 2004;15:349-55.
15. Bayes de Luna A, Cladellas M, Oter R et al. Interatrial conduction block and retrograde activation of the left atrium and paroxysmal supraventricular tachyarrhythmia. *Eur Heart J* 1988;9:1112-8.
16. Teuwen CP, Yaksh A, Lanter EA et al. Relevance of Conduction Disorders in Bachmann's Bundle During Sinus Rhythm in Humans. *Circ Arrhythm Electrophysiol* 2016;9:e003972.
17. Kumagai K, Khrestian C, Waldo AL. Simultaneous multisite mapping studies during induced atrial fibrillation in the sterile pericarditis model. Insights into the mechanism of its maintenance. *Circulation* 1997;95:511-21.
18. Olgin JE, Kalman JM, Fitzpatrick AP, Lesh MD. Role of right atrial endocardial structures as barriers to conduction during human type I atrial flutter. Activation and entrainment mapping guided by intracardiac echocardiography. *Circulation* 1995;92:1839-48.
19. Cox JL, Canavan TE, Schuessler RB et al. The surgical treatment of atrial fibrillation. II. Intraoperative electrophysiologic mapping and description of the electrophysiologic basis of atrial flutter and atrial fibrillation. *J Thorac Cardiovasc Surg* 1991;101:406-26.

20. Lanthers EAH, Yaksh A, Teuwen CP et al. Spatial distribution of conduction disorders during sinus rhythm. *Int J Cardiol* 2017;249:220-225.
21. Saffitz JE, Kanter HL, Green KG, Tolley TK, Beyer EC. Tissue-specific determinants of anisotropic conduction velocity in canine atrial and ventricular myocardium. *Circ Res* 1994;74:1065-70.
22. John B, Stiles MK, Kuklik P et al. Reverse remodeling of the atria after treatment of chronic stretch in humans: implications for the atrial fibrillation substrate. *J Am Coll Cardiol* 2010;55:1217-26.

PART II



ELECTROPHYSIOLOGICAL MARKERS DURING ATRIAL FIBRILLATION





CHAPTER 9

DYNAMICS OF FOCAL FIBRILLATION WAVES DURING PERSISTENT ATRIAL FIBRILLATION

Lanters EAH, Allesie MA, de Groot NMS
Pacing and Clinical Electrophysiology (2015)

ABSTRACT

The incidence and appearance of focal fibrillation waves on the right and left atrial epicardial surface were visualized during 10 seconds of persistent atrial fibrillation in a 71-year-old female patient with valvular heart disease. The frequent, non-repetitive, widespread and capricious distribution of focal waves suggest that transmural conduction of fibrillation waves is most likely the mechanism underlying focal fibrillation waves.

CASE REPORT

The incidence and appearance of focal fibrillation waves on the right and left atrial epicardial surface were visualized during 10 seconds of persistent atrial fibrillation (AF) in a 71-year-old female patient undergoing cardiothoracic surgery for tricuspid valve insufficiency, and symptomatic rheumatic mitral valve stenosis and insufficiency. She had persistent AF for approximately six months. The atria were dilated and left ventricular function was preserved. Intra-operative epicardial mapping of the right atrial free wall and left posterior wall was performed before cardiopulmonary bypass using a 192 (inter-electrode distance 2mm) unipolar electrode array. Electrograms were recorded with a 256-channel mapping system (bandwidth, 0.5 to 400 Hz; sampling rate 1 kHz; resolution, 16 bits). Focal waves were detected with custom-made mapping software^{1,2}. The movie and figure 1 show breakthrough sites of all consecutive focal waves occurring during 10 seconds of AF. The appearance of a red asterisk indicates the site at which a breakthrough wave emerged. Sometimes, multiple focal waves appear more or less simultaneously. The sizes of the asterisks are proportional to the number of fibrillation waves occurring at that site during the 10 seconds. Focal waves are widely distributed over the entire epicardial surface, but occur within some regions more frequently than at others. Though focal waves may arise at the same site within the recording period, they were never repetitive. Previous mapping studies have reported that 'focal' fibrillation waves occur frequently during AF, particularly in the left atrium. Ectopic discharges, transmural conduction and (intra-mural) reentry have all been suggested as underlying mechanisms³. Figure 1 shows examples of unipolar electrograms recorded at the origin of various focal waves, in which distinct R waves with varying magnitudes can be identified. Although waves emerged at the same location at the epicardium (indicated by brackets), the unipolar R wave amplitude and extent of fractionation varied. It is therefore not likely that the focal waves are the result of a rapidly firing ectopic focus or a rotor. However, in case of a QS morphology, ectopic activity cannot be ruled out. The frequent, non-repetitive, widespread and capricious distribution of focal waves suggest that transmural conduction of fibrillation waves is most likely the mechanism underlying focal fibrillation waves. This implicates that the different layers of the atrial myocardium are activated in an asynchronous manner. The layers constantly excite each other as fibrillation waves travel from the endo- to the epicardium, or vice versa, thus providing a potential substrate for stabilization of AF. Hence, dissociation of endo- and epicardium facilitates three-dimensional propagation of fibrillation waves, contributing to perpetuation of AF.

The phenomenon of endo-epicardial dissociation causing focal waves throughout the entire atria could explain why current ablative strategies are not successful in all patients. Pulmonary vein isolation can be a curative treatment in patients with (trigger-dependent) paroxysmal AF. However, procedural success rates decrease in patients with more advanced (substrate mediated) stages of AF. Even when more extensive ablations are performed, recurrences are frequently observed. However, present ablative strategies aim to isolate a trigger, or focus on specific sites with fractionated electrograms or presumed rotors, whereas the process of endo-epicardial dissociation affects the entire left and right atrium.

In conclusion, we described the occurrence of frequent, non-repetitive and widespread focal waves at the atrial epicardial surface, as obtained by high-resolution epicardial mapping in a patient with valvular, persistent AF. Focal waves are most likely the result of transmural conduction.

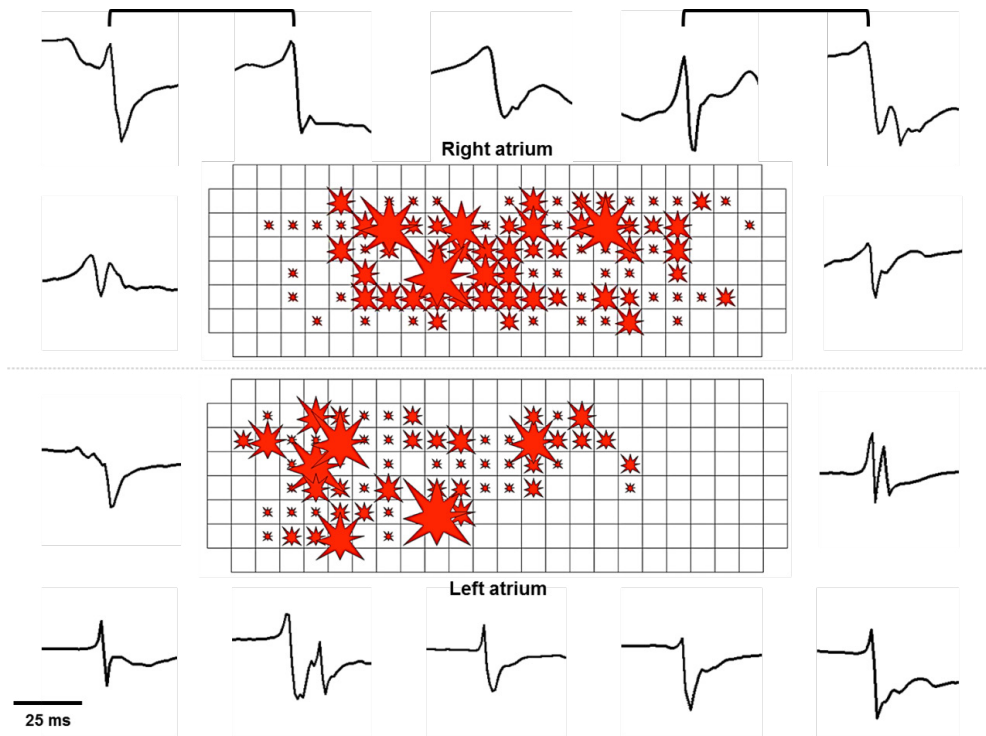
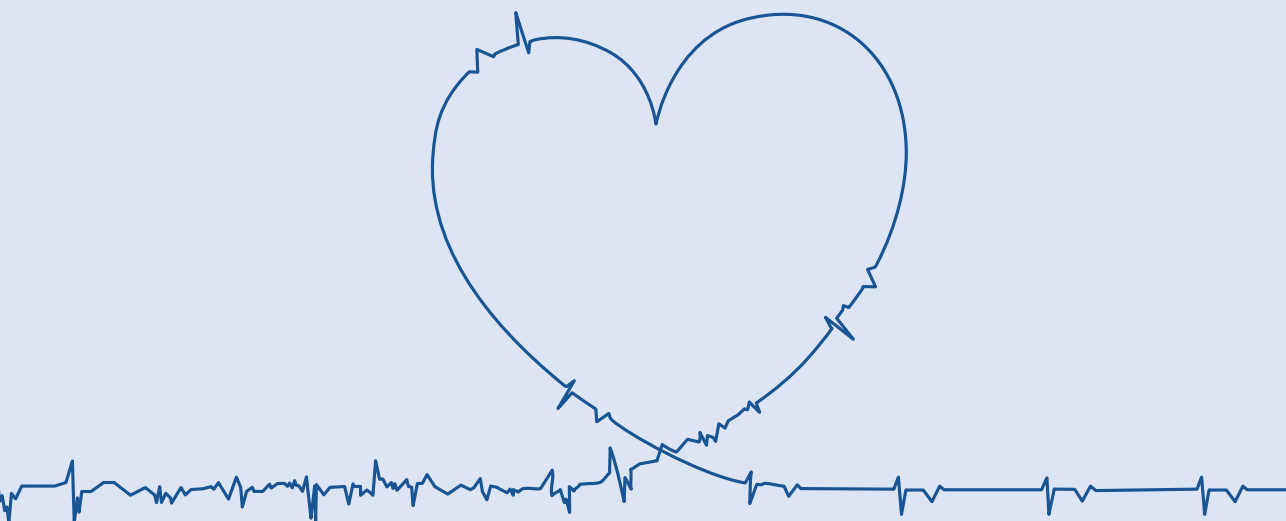


Figure 1. Distribution of breakthrough sites. Summary of all focal fibrillation waves emerging at the right (upper panel) and left (lower panel) atrial epicardium within 10 sec of AF. The sizes of the asterisks are proportional to the total number of focal waves arising at that specific site within the recording period. Examples of unipolar electrograms recorded at the origin of focal waves at the right and left atrium are provided. Brackets indicate electrograms obtained from “repetitive focal waves” sites.

REFERENCES

1. de Groot NMS, Houben RPM, Smeets JL, Boersma E, Schotten U, Schalij MJ, Crijns H, et al. Electropathological Substrate of Longstanding Persistent Atrial Fibrillation in Patients With Structural Heart Disease Epicardial Breakthrough. *Circulation* 2010; 122, 1674-1682.
2. Allessie MA, de Groot NMS, Houben RPM, Schotten U, Boersma E, Smeets JL, Crijns HJ. Electropathological Substrate of Long-Standing Persistent Atrial Fibrillation in Patients With Structural Heart Disease. *Circ-Arrhythmia Elec.* 2010; 3, 606-615.
3. Yaksh A, Kik C, Knops P, Roos-Hesselink JW, Bogers AJJC, Zijlstra F, Allessie M, et al. Atrial fibrillation: to map or not to map? *Netherlands Heart Journal* 2014; 22, 259-266.



CHAPTER 10



DIRECT PROOF OF ENDO-EPICARDIAL ASYNCHRONY OF THE ATRIAL WALL DURING ATRIAL FIBRILLATION IN HUMANS

de Groot NMS, van der Does LJME, Yaksh A, Lanthers EAH, Teuwen CP, Knops P, van de
Woestijne PC, Bekkers JA, Kik C, Bogers AJJC, Allessie MA
Circulation: Arrhythmia and Electrophysiology (2016)

ABSTRACT

Background The presence of focal fibrillation waves during atrial fibrillation (AF) can, beside ectopic activity, also be explained by asynchronous activation of the atrial endo- and epicardial layer and transmurally propagating fibrillation waves. In order to provide direct proof of endo-epicardial asynchrony, we performed simultaneous high-resolution mapping of the right atrial endo-and epicardial wall during AF in humans.

Method Intra-operative mapping of the endo- and epicardial right atrial wall was performed during (induced) AF in 10 patients with AF (paroxysmal: N=3, persistent: N=4, longstanding persistent: N=3) and 4 patients without a history of AF. A clamp made of two rectangular 8x16 electrode arrays (inter-electrode distance 2mm) was inserted into the incision in the right atrial appendage. Recordings of 10 seconds of AF were analysed to determine the incidence of asynchronous endo-epicardial activation times (≥ 15 ms) of opposite electrodes.

Results Asynchronous endo-epicardial activation ranged between 0.9-55.9% without preference for either side. Focal waves appeared equally frequent at endocardium and epicardium (11% vs 13%, $p=0.18$). Using strict criteria for breakthrough (presence of an opposite wave within 4mm and ≤ 14 ms before the origin of the focal wave), the majority (65%) of all focal fibrillation waves could be attributed to endo-epicardial excitation.

Conclusions We provided the first evidence for asynchronous activation of the endo-epicardial wall during AF in humans. Endo-epicardial asynchrony may play a major role in the pathophysiology of AF and may offer an explanation why in some patients therapy fails.

INTRODUCTION

Epicardial high density mapping in patients with AF and valvular heart disease has demonstrated that a considerable portion of fibrillation waves showed a focal spread of activation.¹ These focal waves were rarely repetitive and mainly appeared as solitary events. They could occur virtually everywhere in the atria and their coupling interval was often longer than the dominant AF cycle length. In addition, unipolar electrograms recorded at the origin of focal waves, exhibited small R-waves. Based on this indirect evidence, it was postulated that fibrillation waves with a focal pattern of activation could result from endo-epicardial breakthrough (EEB).¹ Since EEBs can only occur in the presence of electrical asynchrony between the endo- and epicardial layer, we hypothesized that the substrate of AF consists of layers of dissociated fibrillation waves that constantly 'feed' each other.¹ In order to demonstrate that endo-epicardial asynchrony (EEA) exists during AF, we performed simultaneous high-resolution, mapping of the endo- and epicardial wall of the right atrium in patients with or without a history of AF undergoing cardiac surgery for coronary artery disease and/or valvular heart disease.

METHODS

Study population

The study sample consisted of 14 patients (10 male, 67±8.3 years) without a history of AF (N=4) and with a history of AF (N=10). Surgical procedures that were performed included cardiac coronary bypass surgery (N=9), mitral valve surgery (N=7), aortic valve replacement (N=2) and tricuspid valve surgery (N=4). Three patients had paroxysmal AF, 4 persistent AF and 3 had persistent AF lasting longer than a year (LSPAF). Atrial enlargement was present in 5 patients. Clinical characteristics of the study population are provided in Table 1.

The mapping protocol was approved by the institutional ethical committee (MEC2010-054) and written informed consent was obtained from all patients prior to the surgical procedure. This study adhered to the declaration of Helsinki principles.

Intra-operative mapping procedure

The mapping study was performed immediately after sternotomy. Following heparinization and arterial cannulation, a temporary bipolar epicardial pacemaker wire was stitched to the right atrial free wall and served as a temporal reference electrode. The indifferent electrode consisted of a steal wire fixed to subcutaneous tissue of the thoracic cavity.

Table 1. Clinical characteristics

ID no.	Age (y)	Gender	History of AF	Cardiac surgery	LVF	Atrial dimension
1	65	M	No AF	CABG	good	normal
2	56	M	Persistent	MVP+TVP	good	normal
3	82	M	No AF	CABG	good	normal
4	53	M	Persistent	CABG	poor	RA enlargement
5	66	M	Persistent	MVP+AVR	moderate	LA+RA enlargement
6	80	M	Paroxysmal	CABG+MVP	good	normal
7	63	F	No AF	CABG	good	normal
8	67	M	No AF	CABG	good	normal
9	75	F	LSPAF	MVP+TVP	good	LA+RA enlargement
10	59	M	Persistent	CABG	moderate	normal
11	64	F	LSPAF	MVP+TVP	good	LA enlargement
12	64	M	Paroxysmal	CABG+AVR	good	normal
13	70	F	LSPAF	MVP+TVP	good	LA+RA enlargement
14	71	M	Paroxysmal	CABG+MVP	moderate	normal

M: male; F: female; AF: atrial fibrillation; LSPAF: longstanding persistent atrial fibrillation; CABG: coronary artery bypass grafting; MVP/R: mitral valve plasty/ replacement; TVP: tricuspid valve plasty; AVR: aortic valve replacement; LVF: left ventricular function; RA: right atrium; LA: left atrium.

If patients were in sinus rhythm at the onset of the mapping procedure, AF was induced by fixed rate pacing at the right atrial free wall using an additional temporary bipolar pacing wire. The induction protocol started at a rate of 200 beats per minute (bpm). If induction was not successful after 3 burst attempts, the rate was increased by 50bpm, up to maximal 400bpm until AF occurred or atrial refractoriness was reached.

Prior to commencement to extra-corporal circulation, a high-resolution endo-epicardial mapping clamp was introduced through the right atrial incision for the venous cannula and closed with a purse-string suture. The mapping device was positioned towards the crista terminalis and consisted of two identical rectangular electrode arrays of 8x16 electrodes (interelectrode distance 2mm) positioned opposite to each other (Figure 1). The electrode arrays (GS Swiss PCB AG, Küssnacht, Switzerland) consist of an electroless nickel immersion gold (ENIG) plated electrode array, mounted on a thin, flexible DuPont™ Pyralux® copper-clad (25µm thickness) polyimide laminate, and coverlay composite (25µm) film (0.18mm). As the space constant of the atrial myocardium is ≈ 2 mm, the effective spatial resolution of 2.0 mm makes it unlikely that narrow fibrillation wavefronts will not be detected.²

All recordings were amplified (gain 1000), filtered (bandwidth 0.5-400Hz), sampled (1KHz) and analogue to digital converted (12bits). A calibration signal of 2mV amplitude and 1000ms pulse width was stored simultaneously with atrial electrograms on hard disk using a computerized mapping system. After completion of the mapping procedure, AF was terminated by electrical cardioversion or sustained until cardioplegia was conducted, depending on the operators' preference. Ten seconds of AF were recorded from every patient.

Mapping data

Series of endo- and epicardial wavemaps of 10 seconds AF were reconstructed from the two sets of 128 unipolar fibrillation electrograms, using custom-made software which has been previously described in detail.^{1,3} For every electrode, local activation times were determined by marking the steepest negative deflection of the unipolar fibrillation electrograms. In case of a fractionated potential, the steepest negative deflection was chosen. At every electrode at either the endo- or epicardial layer, differences in endo-epicardial activation times were determined by measuring the smallest time delay within the opposite square base of 3x3 electrodes (Figure 2).

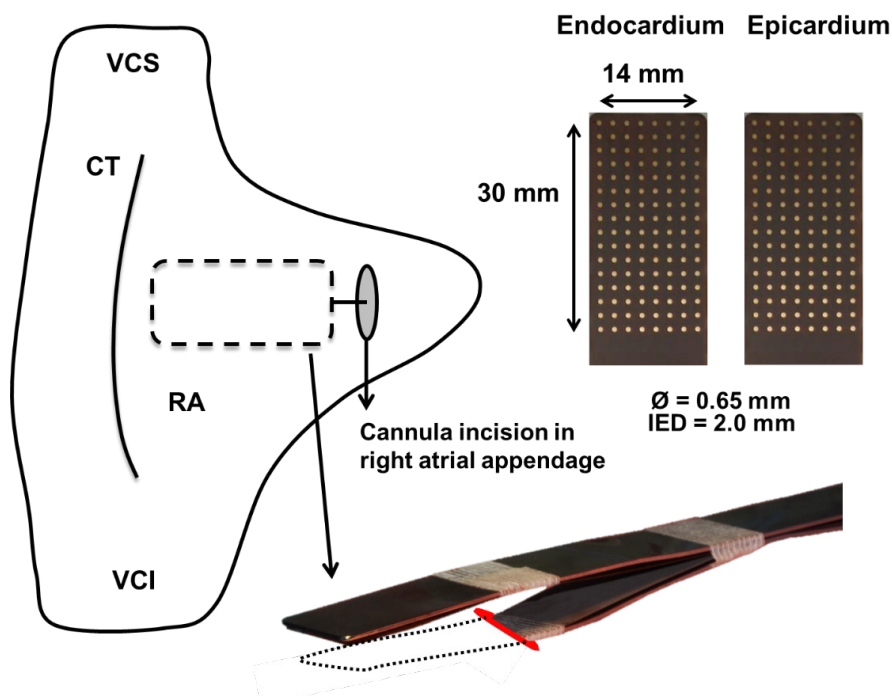


Figure 1. Endo-epicardial mapping device and technique. The mapping device consists of two rectangular 8x16 electrode arrays with an interelectrode distance (IED) of 2mm fixed to spatulas and positioned precisely opposite to each other. During epi-endocardial mapping the endocardial leg is inserted in the right atrium (RA) through the incision of the venous cannula and closed with a purse-string suture. The array is positioned towards the crista terminalis (CT). VCS/VCI: vena cava superior/ inferior.

The total amount of EEA during the entire recording period was expressed as the percentage of transmural differences of ≥ 15 ms for all endo- and epicardial recording sites. The combined asynchrony map (lower right panel of Figure 2) shows the longest time delay for every endo-epicardial electrode couple. Wavemapping was used to identify the individual fibrillation waves. The starting point of the first fibrillation waves was the earliest activated site within the mapping area. Next, the entire mapping area was scanned in steps of 1ms. For all electrodes activated during every step, the shortest time difference with the 8 neighboring electrodes was calculated. When the time difference was ≤ 12 ms (17ms for oblique distances), the electrode

site was added to the territory of the surrounding wave. In case of a time difference >12 ms, the electrode was annotated as the starting point of a new wave. In the wavemap, fibrillation waves are color-coded according to their moment of entrance in the mapping area and the colors demarcate the area activated by that specific fibrillation wave.⁴

Wavemaps also identify focal waves at either the endo- or epicardial surface. Focal fibrillation waves had to meet previously defined criteria. The breakthrough site of the focal fibrillation wave had to be located at least 2 electrodes away from the border of the mapping array and at least 1 reliable activation time should be available between the breakthrough site and the border of the mapping area. The morphology of the electrograms in the breakthrough region should not be distorted by large QRS complexes or artifacts. If this is the case, the wave is excluded from analysis. The focal wave should at least cover 4 electrodes. The origin of a focal wave had to be activated earlier than all surrounding electrodes. If electrodes adjacent to the origin were activated simultaneously, all electrodes surrounding this area should also be activated later. Shift of the local activation time to a maximum of 3ms earlier or later at the earliest activated electrode(s) should not result in disappearance of the focal wave. If a breakthrough site emerged along the border of another fibrillation wave, the time delay between that wave and the origin of the breakthrough had to be at least 40 ms.¹ All these criteria were checked manually by 2 independent investigators. A more detailed description of the mapping criteria with examples is provided in the online supplemental material.

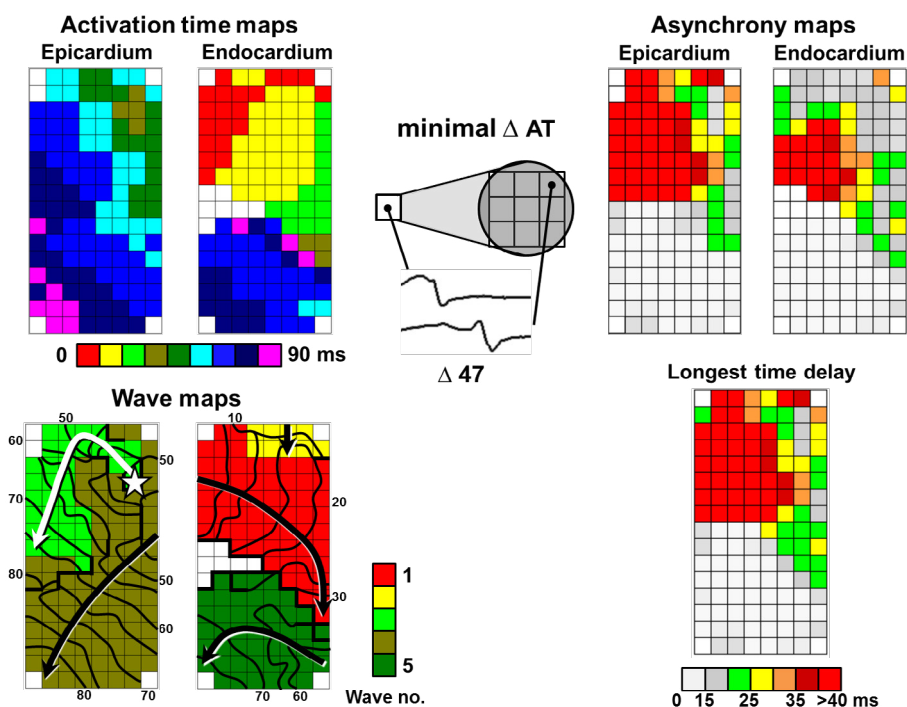


Figure 2. Construction of activation, wave and asynchrony maps. Activation times determined at each individual electrode of endocardial and epicardial arrays are depicted in color-coded activation maps starting at the time of first

activation. Wavemaps are automatically constructed which demonstrate the number and sequence of appearance of different waves activating the mapping area and also illustrate the origin of focal waves beginning within the mapping area (white asterisk). Isochrones are set with intervals of 5 ms and indicate the main trajectory of each wave (black/white arrows). Thick black lines indicate conduction block ($\Delta > 12\text{ms}$). The asynchrony map of either the endo- or epicardial layer consists of the endo-epicardial activation times defined by the smallest interval of the opposite nine activation times; the total asynchrony map shows the longest time delay assessed at every coupled recording site.

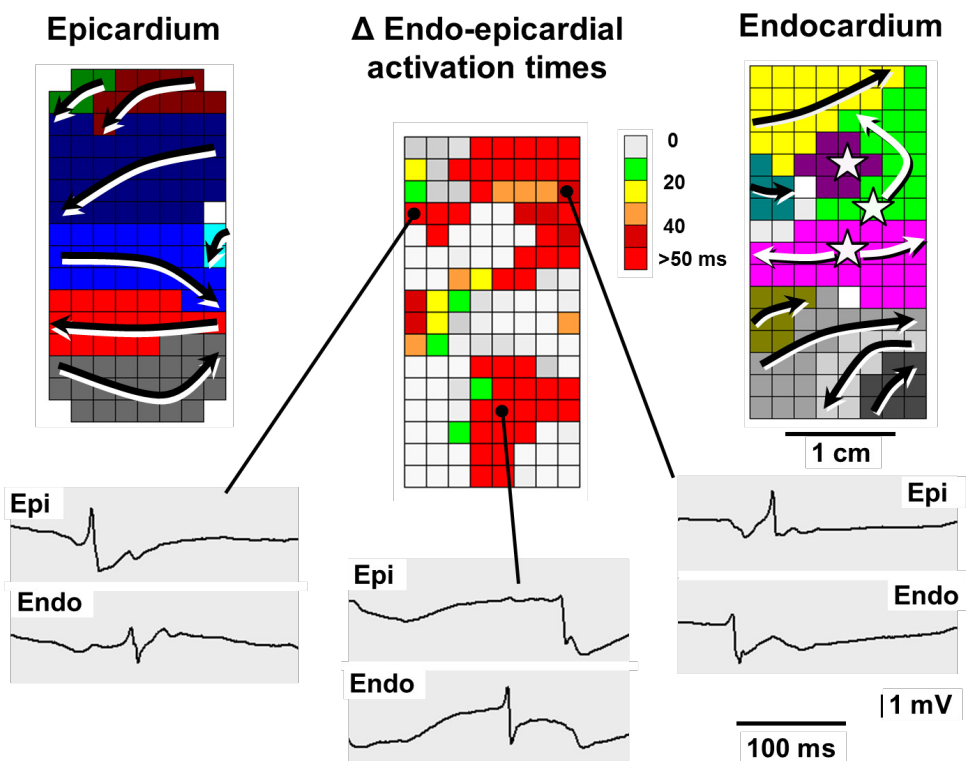


Figure 3. Endo-epicardial asynchrony in a patient with longstanding persistent AF. The maps represent a single AF-cycle of 190ms. The left and right panels show simultaneous wavemaps of the sub-epicardium and sub-endocardium of a part of the free wall of the right atrium (3.0 x 1.4cm). The colors indicate the sequence of appearance of the different fibrillation waves (rainbow scheme followed by a grayscale). The arrows indicate the main trajectories of the waves. The sub-epicardium of the right atrium was activated by 7 narrow fibrillation waves, entering the mapping area from various directions. The endocardium was activated by 9 waves, 3 of them arising as focal waves in the middle of the mapping area (white asterisks). The local endo-epicardial time-differences are plotted in the central map. As a result of the different activation patterns at the endo- and epicardial surface, major differences in endo-epicardial activation times existed (up to $>50\text{ms}$). There was considerable spatial dispersion in EEA, with differences in endo- and epicardial activation times ranging from 0 to $>50\text{ms}$. The 3 electrogram-pairs at the bottom, clearly show the marked differences in endo- and epicardial activation times. Sometimes the epicardium was activated earlier (left panel), sometimes the endocardium (middle and right panels).

To assess whether focal fibrillation waves could originate from endo-epicardial breakthrough, in each case the opposite layer was examined for the presence of a fibrillation wave that could have served as a source for the focal wave. The presence of an opposite wavefront, within 4mm distance and less than 15ms before the origin of the focal wave, was considered to reflect transmural conduction based on normal atrial conduction properties. In this case, the focal wave could from a theoretically point of view be attributed to endo-epicardial breakthrough.

Statistical analysis

The Wilcoxon signed rank test was performed to assess the occurrence of EEA and focal waves between the epi- and endocardium.

RESULTS

Endo-epicardial asynchrony

In the entire study population, the average percentage of missing data due to poor contact of the mapping array was $7.8 \pm 4.9\%$. The amount of conduction block was similar in the epicardial and endocardial plane with incidences of respectively $10.8 \pm 5.1\%$ and $10.8 \pm 4.6\%$. Simultaneous epi- and endocardial wavemaps of a single AF-cycle recorded in a patient with longstanding persistent AF demonstrating EEA are shown in Figure 3. In this example, marked differences in activation patterns of the endo- and epicardial wall existed; almost all fibrillation waves at the endo- and epicardial surface appeared at different times and/or propagated in different directions.

In this same patient, the spatio-temporal variation in EEA during 10 seconds of AF is demonstrated in Figure 4. The degree of EEA varied considerably at different locations and at different times. No clear predominance of either the endocardial or the epicardial layer was observed. Examples of unipolar electrogram-pairs around the plots illustrate the high spatio-temporal variation in EEA.

As demonstrated in Figure 5, the total degree of EEA in our study population varied widely between 0.9 and 55.9% and there was no clear difference between endo-epicardial and epi-endocardial asynchrony (respectively $7.8 \pm 7.7\%$ and $7.2 \pm 7.2\%$).

Focal fibrillation waves

In total 1199 focal fibrillation waves were observed, 579 arising at the sub-endocardium and 620 at the sub-epicardium. The equal distribution of focal fibrillation waves between both sides is shown in panel C of Figure 5. Applying the previously stated strict criteria for endo-epicardial breakthrough, 784 of all 1199 focal waves (65%) could be attributed to result from endo-epicardial excitation presuming that normal conduction occurs between endo-epicardium (66% of the endocardial and 65% of the epicardial focal waves) (Table 2). Examples of pairs of endo-epicardial wavemaps showing focal fibrillation waves originating from EEB of fibrillation waves from the opposite layer are given in Figure 6.

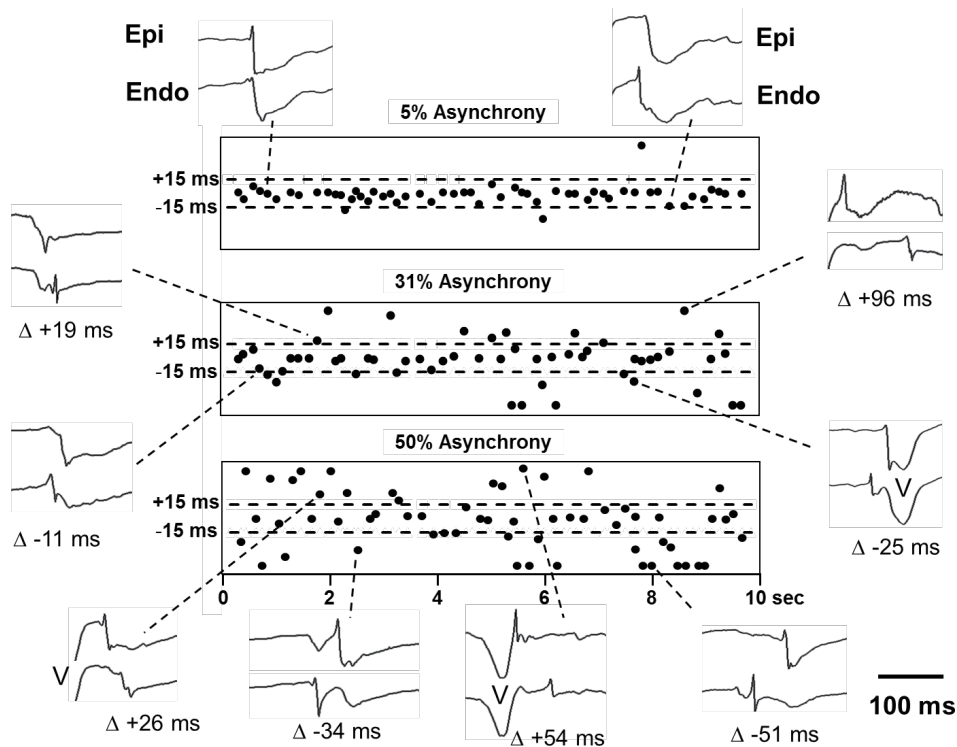


Figure 4. Spatial and temporal variation in endo-epicardial asynchrony during longstanding persistent AF. Endo-epicardial asynchrony plots of 10 seconds of AF, recorded at 3 different locations of the right atrial free wall in a patient with AF. The dashed horizontal lines demarcate the band of endo-epicardial synchrony; data points $> \pm 50$ ms are clipped. At different sites, the degree of EEA (delay ≥ 15 ms) varied from 5% (top panel), 31% (middle) and 50% (bottom). In addition to spatial dispersion, EEA also showed a strong temporal variation. As can be seen from the middle and lower plots, differences in endo-epicardial activation time seemed to occur randomly, without a clear predominance of either the sub-endocardial or sub-epicardial layer. Examples of pairs of unipolar endo- and epicardial electrograms demonstrating the spatial temporal variation are given around the plots.

Table 2. Endo-epicardial asynchrony and focal waves

ID no.	AFCL (ms)	Endo-epicardial asynchrony (%)	Endocardium earlier (%)	Epicardium earlier (%)	Endo-epicardial activation SD (ms)	Endocardial fibrillation waves			Epicardial fibrillation waves		
						No. waves	Focal waves	Breakthroughs (% of focal)	No. waves	Focal waves	Breakthroughs (% of focal)
1	206±28	0.9	0.4	0.5	4.2	115	4	75	112	2	100
2	181±28	1.1	0.5	0.6	4.4	140	8	87	140	12	92
3	175±32	2.6	1.7	0.9	7.7	192	10	60	224	10	80
4	246±28	3.1	1.6	1.5	5.5	186	32	56	187	42	81
5	150±28	5.0	3.1	1.9	8.5	277	21	90	294	34	94
6	182±40	5.4	2.5	2.9	9.4	347	54	81	257	39	92
7	141±24	6.8	3.4	3.4	12.7	239	5	40	251	11	73
8	140±27	10.6	4.5	6.1	12.3	445	59	83	337	37	73
9	147±40	21.3	10.8	10.5	18.2	553	116	66	657	137	55
10	189±40	22.0	14.1	8.0	19.6	494	89	54	470	94	55
11	224±46	23.8	13.6	10.2	23.7	343	61	69	345	54	57
12	189±40	25.3	11.4	13.8	25.4	321	83	55	329	83	59
13	151±35	26.0	12.7	13.3	20.4	480	21	86	372	25	80
14	183±37	55.9	28.7	27.2	37.2	188	16	25	257	40	30
Total/ mean	-	15.0	7.8	7.2	-	4320	579	66	4232	620	65

AFCL = atrial fibrillation cycle length; SD = standard deviation

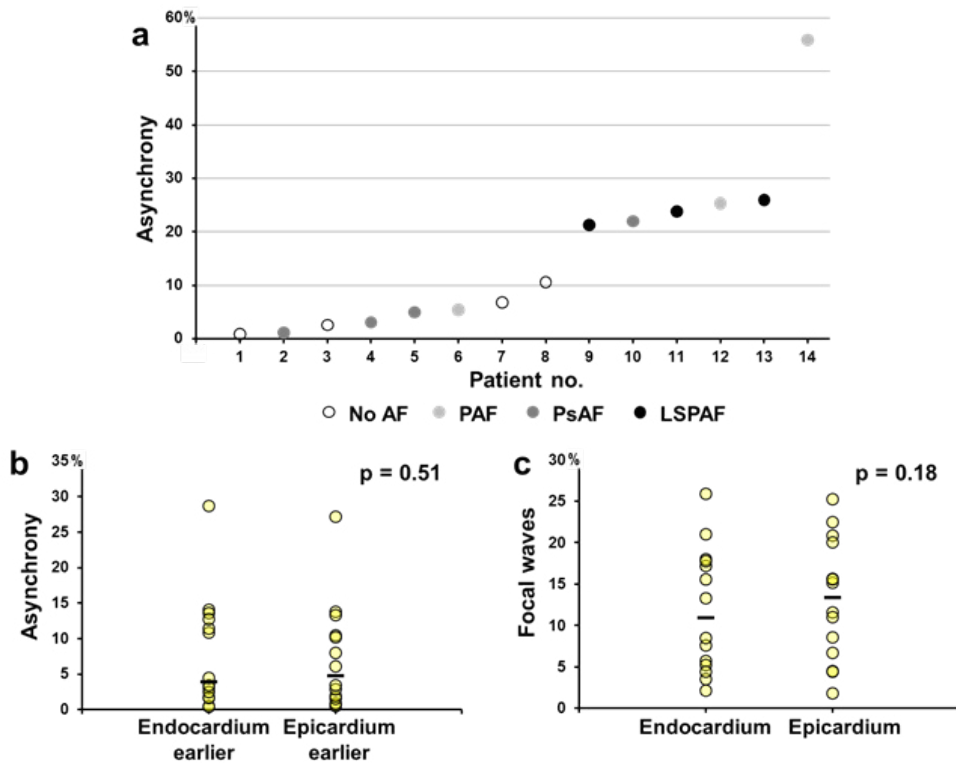


Figure 5. Endo-epicardial asynchrony levels and focal waves. (a) graph demonstrating the total amount of EEA plotted for every patient separately; patients are ranked according to the degree of EEA. Type of AF (none, paroxysmal, persistent, longstanding persistent) is illustrated by the different grayscale tones. (b,c) Dot plots and medians of (b) the incidence of asynchrony where endocardium versus epicardium is activated earlier in respect to the other and (c) the percentage of focal waves (of total number of waves) recorded at the endocardium and epicardium. For both parameters, there was no difference between the endocardial and epicardial layer ($p=0.51$ and $p=0.18$).

DISCUSSION

Despite the relatively small number of patients, our data clearly show that a significant degree of EEA is present in the right atrium in patients with AF. Simultaneous endo-

epicardial mapping of isolated canine atria, both during sinus rhythm and atrial pacing, only showed small differences in activation times ($<1\text{ms}$). However, during atrial tachyarrhythmias, activation of the endo- and epicardial layers has been shown to become more asynchronous (up to 25ms), particularly in the thicker parts of the atria.^{5,6} In isolated fibrillating sheep atria, breakthrough sites appeared to be related to sub-endocardial muscle structures, the three-dimensional structure of the atria determining the appearance of focal waves during AF.⁷ The concept that endo-epicardial dissociation might play an important role in the maintenance of AF, stems from experimental studies in the goat model of persistent AF.⁸⁻¹⁰ These studies showed that the endo- and epicardial layers of the atrial wall became progressively dissociated

during the first 6 months of AF. After that time, fibrillation waves in the endo- and epicardial layers often propagated at different speed and in different directions, and endo-epicardial breakthroughs became more abundant.^{8,9}

In this study, the incidence of endo-epicardial asynchrony tended to be higher in patients with AF, though we did not observe a clear relation between duration of AF and degree of EEA. This can be explained by the fact that we did not map the left atrium and that if EEA of the left atrial wall also exists, it may play a more important role in the pathophysiology of AF. Also, our study population contained a small number of patients with a variety of cardiac diseases. We provided additional data that most focal fibrillation waves could be explained by endo-epicardial excitation. Lee et al. also frequently observed focal fibrillation waves without any sustained focal activity in 18 patients with persistent AF.¹¹ In contrast, low-density mapping studies using a 64-pole basket catheter, have suggested that AF is maintained by a limited number of rapid stable sources (rotors and/or ectopic foci).^{12,13} Body surface mapping during AF elucidated the presence of non-sustained reentries and focal breakthroughs in certain domains of the atria.¹⁴ Recently, we have discussed the discrepancies in the interpretation of high- and low resolution mapping of AF in detail in a crosstalk paper.^{15,16}

The present study supports the concept that during AF, the endo- and epicardial layers of the atrial wall can be asynchronously activated.^{1,16} The presence of dissociated layers of fibrillation waves, will highly stabilize the fibrillatory process because, as soon as fibrillation waves die out, they can be replaced by breakthroughs from the opposite side.

In such a substrate, each layer will serve as a multi-site generator for the other layer. During 10 seconds of AF, more than 20-30 focal waves appeared at each side of the atrial wall, in an area of only 2.6cm.¹ Extrapolating this number to the entire atrial surface, the total number of focal breakthrough waves can be estimated to exceed 10.000 per minute. However, we like to emphasize that the presence of EEA, off course does not disprove that also reentry and focal activity may contribute to the maintenance of AF. In different stages of the development of a substrate of AF, the contribution of different mechanisms for perpetuation of AF may vary. We fully acknowledge the large body of evidence that reentrant and focal mechanisms are operative during atrial fibrillation.¹⁷⁻²⁰ In fact, not all focal fibrillation waves in our patients could be attributed to endo-epicardial breakthrough, and sometimes two focal waves appeared simultaneously at the endo- and epicardial surface. Equally, our data do not rule out the possibility that some of the endo-epicardial breakthroughs formed part of a transmural reentrant circuit. However, we venture to suggest that progressive, AF induced, structural atrial remodeling gradually transforms the atrial wall into multiple layers of narrow dissociated wavelets. With time, more and more focal breakthroughs will be generated, which progressively stabilizes the fibrillatory process. At the end, the main source of fibrillation waves is formed by an abundant number of focal breakthroughs, occurring virtually everywhere in the atria. This is in agreement with the recent finding of Haissaguerre et al., that the number of driver regions increased with the duration of AF, until after 6 months almost the entire atrial wall acted as a driver (6 of all 7 regions).¹⁴ It also explains why the termination rate of AF by driver ablation sharply declined after 6 months of AF.¹⁴

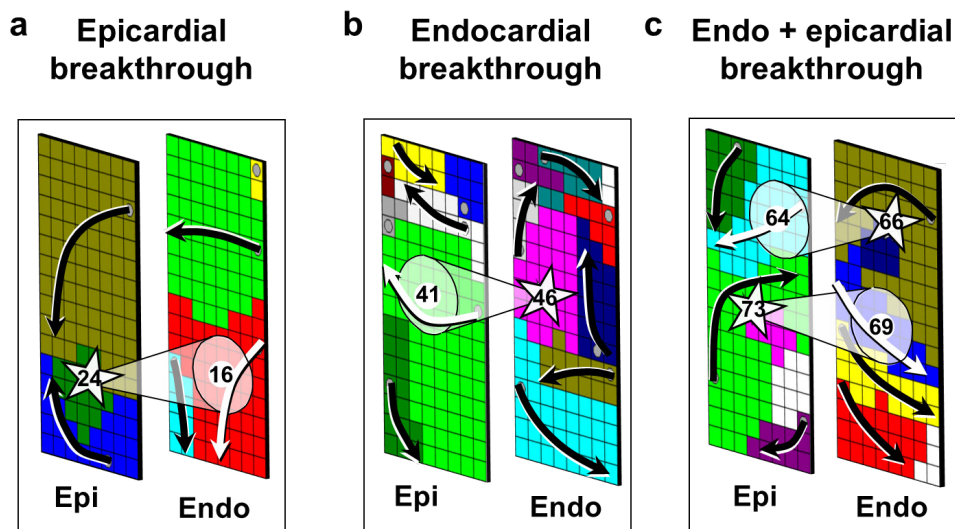


Figure 6. Three examples of endo-epicardial breakthroughs in a patient with longstanding persistent AF. (a) A focal wave appeared at the epicardial surface at $t=24$ (white asterisk). As can be seen from the associated endocardial wavemap, just a couple of milliseconds before an endocardial fibrillation wave (red) had passed that site at $t=16$ ms. A transmural conduction time of only 8ms was taken as supportive evidence that the focal wave could be due to endo-epicardial breakthrough. (b) An example of a focal wave arising at the endocardium at $t=46$. Again a fibrillation wave in the opposed layer (green) had passed that site just 5ms before (at $t=41$). (c) Two breakthroughs occurred at about the same time, one at the endocardium at $t=66$ and one at the epicardium at $t=73$ ms. In both cases, in the opposite layer a fibrillation wave passing the site of origin of the focal waves a few ms earlier at respectively $t=64$ and $t=69$, indicating that the focal waves could result from endo-epicardial breakthrough.

Study limitations

Our study population is presently limited to 14 patients and a larger number of patients is obviously required for a meaningful statistical analysis and to study the relation between persistence of AF and the degree of electrical asynchrony. Expanding the study population will also allow for statements about a possible correlation between EEA and breakthroughs. Moreover, the effective spatial resolution of the recordings is dependent on the number of electrodes with good tissue contact. Another limitation is, that so far, only a limited part of the atria has been accessible for endo-epicardial mapping (4.2cm² of the right atrium). In order to get a full understanding of the role of EEA in the development of the substrate of AF, endo-epicardial mapping of the left atrium is needed as well. However, the left atrium is not standardly opened during cardiac surgery, only during selected procedures. In addition, opening the left atrium before cardiopulmonary bypass is associated with a considerable increase in the risk for air embolism which may cause brain injury. Therefore, we decided it was not ethically responsible to perform endo-epicardial mapping of the left atrium for this pilot study.

Clinical implications

Knowledge of the substrate and various mechanisms of perpetuation of human AF is of great importance to understand the natural history of AF. At different stages, the substrate of AF may require different treatment modalities. At an early stage pulmonary vein isolation alone might be sufficient, whereas in a later stage also compartmentalization of the atria will be necessary to restore sinus rhythm. Furthermore, when the endo-and epicardial layers of the atria have become electrically dissociated, even extensive ablative therapies may be ineffective and palliative therapy would be a better option. Knowledge of the vulnerable parameter(s) for perpetuation of AF, and the ability to diagnose the stage of development of the substrate of AF, are essential for an individualized and staged therapy of atrial fibrillation.

REFERENCES

1. de Groot NMS, Houben RP, Smeets JL, Boersma E, Schotten U, Schalij MJ, Crijns H, Allessie MA. The electropathological substrate of longstanding persistent atrial fibrillation in patients with structural heart disease: epicardial breakthrough. *Circulation*. 2010;122:1674-1682.
2. Sakamoto Y, Goto M. A study of the membrane constant in the dog myocardium. *Jap J Physiol*. 1970;20:30-41.
3. Allessie MA, de Groot NM, Houben RP, Schotten U, Boersma E, Smeets JL, Crijns HJ. The electropathological substrate of longstanding persistent atrial fibrillation in patients with structural heart disease: longitudinal dissociation. *Circ Arrhythm Electrophysiol*. 2010;3:606-615.
4. Rogers JM, Usui M, KenKnight BH, Ideker RE, Smith WM. Recurrent wavefront morphologies: a method for quantifying the complexity of epicardial activation patterns. *Ann Biomed Eng*. 1997;25:761-768.
5. Schuessler RB, Kawamoto T, Hand DE, Mitsuno M, Bromberg BI, Cox JL, Boineau JP. Simultaneous epicardial and endocardial activation sequence mapping in the isolated canine right atrium. *Circulation*. 1993;88:250-263.
6. Derakhchan K, Li D, Courtemanche M, Smith B, Brouillette J, Pagé PL, Nattel S. Method for simultaneous epicardial and endocardial mapping of in vivo canine heart: application to atrial conduction properties and arrhythmia mechanisms. *J Cardiovasc Electrophysiol*. 2001;12:548-555.
7. Gray RA, Pertsov AM, Jalife J. Incomplete reentry and epicardial breakthrough patterns during atrial fibrillation in the sheep heart. *Circulation*. 1996;94:2649-2661.
8. Eckstein J, Maesen B, Linz D, Zeemering S, van Hunnik A, Verheule S, Allessie M, Schotten U. Time course and mechanisms of endo-epicardial electrical dissociation during atrial fibrillation in the goat. *Cardiovasc Res*. 2011;4:816-824.
9. Eckstein J, Zeemering S, Linz D, Maesen B, Verheule S, van Hunnik A, Crijns H, Allessie MA, Schotten U. Transmural conduction is the predominant mechanism of breakthrough during atrial fibrillation: evidence from simultaneous endo-epicardial high-density activation mapping. *Circ Arrhythm Electrophysiol*. 2012;6:334-341.
10. Verheule S, Eckstein J, Linz D, Maesen B, Bidar E, Gharaviri A, Schotten U. Role of endo-epicardial dissociation of electrical activity and transmural conduction in the development of persistent atrial fibrillation. *Progress in Biophysics and Molecular Biology*. 2014;115:173-185.
11. Lee G, Kumar S, Teh A, Madry A, Spence S, Larobina M, Goldblatt J, Brown R, Atkinson V, Moten S, Morton JB, Sanders P, Kistler PM, Kalman JM. Epicardial wave mapping in human long-lasting persistent AF: transient rotational circuits, complex wave fronts and disorganized activity. *Eur Heart J*. 2014;35:86-97.
12. Narayan SM, Krummen DE, Shivkumar K, Clopton P, Rappel WJ, Miller JM. Treatment of atrial fibrillation by the ablation of localized sources: CONFIRM (CONventional ablation for atrial fibrillation with or without Focal Impulse and Rotor Modulation) trial. *J Am Coll Cardiol*. 2012;60:628-636.
13. Narayan SM, Shivkumar K, Krummen DE, Miller JM, Rappel WJ. Panoramic electrophysiological mapping but not electrogram morphology identifies stable sources for human atrial fibrillation: stable atrial fibrillation rotors and focal sources relate poorly to fractionated electrograms. *Circ Arrhythm Electrophysiol*. 2013;6:58-67.
14. Haissaguerre M, Hocini M, Denis A, Shah AJ, Komatsu Y, Yamashita S, Daly M, Amraoui S, Zellerhoff S, Picat MQ, Quotb A, Jesel L, Lim H, Ploux S, Bordachar P, Attuel G, Meillet V, Ritter P, Derval N, Sacher F, Bernus O, Cochet H, Jais P, Dubois R. Driver domains in persistent atrial fibrillation. *Circulation*. 2014;130:530-538.
15. Narayan SM, Jalife J. CrossTalk proposal: Rotors have been demonstrated to drive human atrial fibrillation. *J Physiol*. 2014;592:3163-3166.
16. Allessie MA and de Groot NM. CrossTalk opposing view: Rotors have not been demonstrated to be the drivers of atrial fibrillation. *J Physiol*. 2014;592:3167-3170.

17. Andrade J, Khairy P, Dobrev D, Nattel S. The clinical profile and pathophysiology of atrial fibrillation: relationships among clinical features, epidemiology, and mechanisms. *Circ Res*. 2014;114:1453-1468.
18. Nattel S, Shiroshita-Takeshita A, Brundel BJ, Rivard L. Mechanisms of atrial fibrillation: lessons from animal models. *Prog Cardiovasc Dis*. 2005;48:9-28.
19. Schotten U, Verheule S, Kirchhof P, Goette A. Pathophysiological mechanisms of atrial fibrillation: a translational appraisal. *Physiol Rev*. 2011;91:265–325.
20. Heijman J, Voigt N, Nattel S, Dobrev D. Cellular and molecular electrophysiology of atrial fibrillation initiation, maintenance, and progression. *Circ Res*. 2014;114:1483-1499

SUPPLEMENTAL MATERIALS

Mapping Criteria

Step I. Subtraction of ventricular complexes

Before determination of the local activation time, ventricular complexes were eliminated from the unipolar electrograms using a subtracting technique as previously described in detail by Hoekstra et al.¹ In short, for each fibrillation electrogram an individual template of the ventricular far field was obtained by averaging all time windows of ± 70 ms around the R-waves detected from surface ECG lead I. Subtraction of these individual QRS templates from the fibrillation electrograms reduces the ventricular far field potentials and results in a more or less 'clean' unipolar atrial fibrillation electrograms.

Step II. Determination of the local activation time

Examples of electrograms recorded from both the endo- and epicardium and endo-epicardial (a)synchrony are demonstrated in Figures 1 and 2.

Local activation times were determined by detecting the maximum downslope of the unipolar fibrillation potential, as this coincides with the moment of maximum rate of rise of the transmembrane potential (time differences less than 50 μ s).² In turn, the maximum rate of rise of the transmembrane potential corresponds with the maximum increase in sodium current and its conductance.³ The height of the negative slope is measured during a 2 ms period. From the moment of the maximum downslope, time windows both backward and forward in time are scanned to detect the moment of respectively the positive and negative peak of the fibrillation potential. The duration of a non-fractionated potential is then defined as the time difference between the moment of its negative and positive peak. In case of a fractionated potential, the deflection with the steepest down slope was chosen; its duration is defined as the time between the preceding positive and following negative deflection.⁴ The duration of a fibrillation potential had to be ≤ 35 ms. The negative slope and amplitude of the unipolar fibrillation potentials depend on numerous variables.^{5,6} Hence, cut-off values applied also vary, depending on the signal-to-noise ratios of the recordings and lower limits were set at 0.05 V/sec and 0.2 mV.^{5,6,7,8} All fibrillation potentials with slopes < 0.05 V/sec, amplitudes < 0.2 mV and durations > 35 ms are thus regarded as either far field or poor contact potentials.

After detection of the local activation time, a blanking period of 40 ms was applied in both directions. Though we do not know exactly what the refractory period during AF is, it is estimated to be approximately 50 ± 13 ms.⁹ Hence, comparable to previous studies, by choosing a blanking period of 40ms we avoid overestimation of the number of fibrillation waves by marking fibrillation potentials, which are most likely double potentials with interspike intervals between > 0 and ≤ 40 ms caused by areas of conduction block.^{10,11}

Step III. WaveMapping

A wavemapping approach was used to identify individual fibrillation waves. This wavemapping technique has also been described in prior studies.^{2,3,12,13} The starting point of the first fibrillation waves was the earliest activated site within the mapping area. Next, the entire mapping area was scanned in steps of 1ms. For all electrodes activated during every step, the shortest time difference with the 8 neighboring electrodes was calculated. When the time difference

was ≤ 12 ms (17 ms for oblique distances), the electrode site was added to the territory of the surrounding wave. In case of a time difference > 12 ms, the electrode was annotated as the starting point of a new wave. In the wavemap, fibrillation waves are color-coded according to their moment of entrance in the mapping area and the colors demarcate the area activated by that specific fibrillation wave. The cut-off value of > 12 ms used for separating individual fibrillation waves corresponds for 2 mm inter-electrode distances with an effective conduction velocity of 17 cm/s, which is equivalent to the continuous conduction velocities reported for atrial myocardium of intact hearts.¹⁴ For separation of the fibrillation waves the requirement of a lower limit CV must be fulfilled along the whole boundary of the wave which of course does not exclude the possibility of slow conduction within parts of the fibrillation waves. Choosing a different cut-off value will lead to a lower or higher number of fibrillation waves. However, this change is very gradual and has no major effects on the measured differences in the number of focal waves. Only at extreme cut-off values our analysis will become useless because it either no longer separates the different fibrillation waves, or results in a very high degree of spatial fractionation, resembling a mosaic-like pattern of numerous small waves that only propagate over very short distances. Based on the origin of the fibrillation wave, three different types of fibrillation waves were distinguished 1) peripheral waves, entering the mapping area from outside the electrode array, 2) epicardial breakthrough, appearing at the epicardial surface inside the mapping area, and 3) discontinuous conduction waves; defined as fibrillation waves starting with a delay of 13 to 40 ms from the boundary of another wave.¹²⁻¹³ If a fibrillation wave originates along the border of another fibrillation wave it could theoretically be the result of very slow conduction. In order to avoid overestimation of the number of focal waves, we classified these waves as discontinuous fibrillation waves. Applications of this wavemapping technology have been described previously.¹²⁻¹³

Focal fibrillation waves had to meet several criteria. The breakthrough site of the focal fibrillation wave had to be located at least 2 electrodes away from the border of the mapping array and at least 1 reliable activation time should be available between the breakthrough site and the border of the mapping area in order to exclude propagation from the border of the mapping array. An example is given in Figure 3. The relation between the percentage of endocardial or epicardial focal fibrillation waves and the distance from the origin of the focal wave to the border of the mapping array is shown in Table 1. Next, it is manually checked whether the morphology of fibrillation potentials in the breakthrough region is distorted by large QRS complexes or artifacts due to e.g. movements of the electrodes in order to avoid false positive focal waves; examples are shown in Figure 4.

In case of a fractionated electrogram, marking of one of the other deflections should not result in disappearance of the focal fibrillation wave (Figure 5). In order to include only focal waves which have a more or less considerable impact on endo-epicardial asynchrony, we choose cut-off value of 4 electrodes. Table 2 shows how many focal waves will disappear when a cut-off value of 5 or 6 electrodes would have been chosen. The origin of a focal wave had to be activated earlier than all surrounding electrodes. If electrodes adjacent to the origin were activated simultaneously, all electrodes surrounding this area should also be activated later. Shift of the local activation time to a maximum of 3 ms earlier or later at the earliest activated electrode(s) should not result in disappearance of the focal wave. Typical examples of focal waves resulting from these criteria are provided in Figure 6.

Table 1. Location of the origin of focal fibrillation waves

Row distance to border	Endocardial focal waves	Epicardial focal waves
2	25%	25%
3	37%	36%
4	38%	39%

Table 2. Size of the focal waves

	Endocardial focal waves	Epicardial focal waves
4 electrodes	5.0%	5.6%
5 electrodes	4.5%	5.2%
6 electrodes	3.8%	4.6%

Epicardium

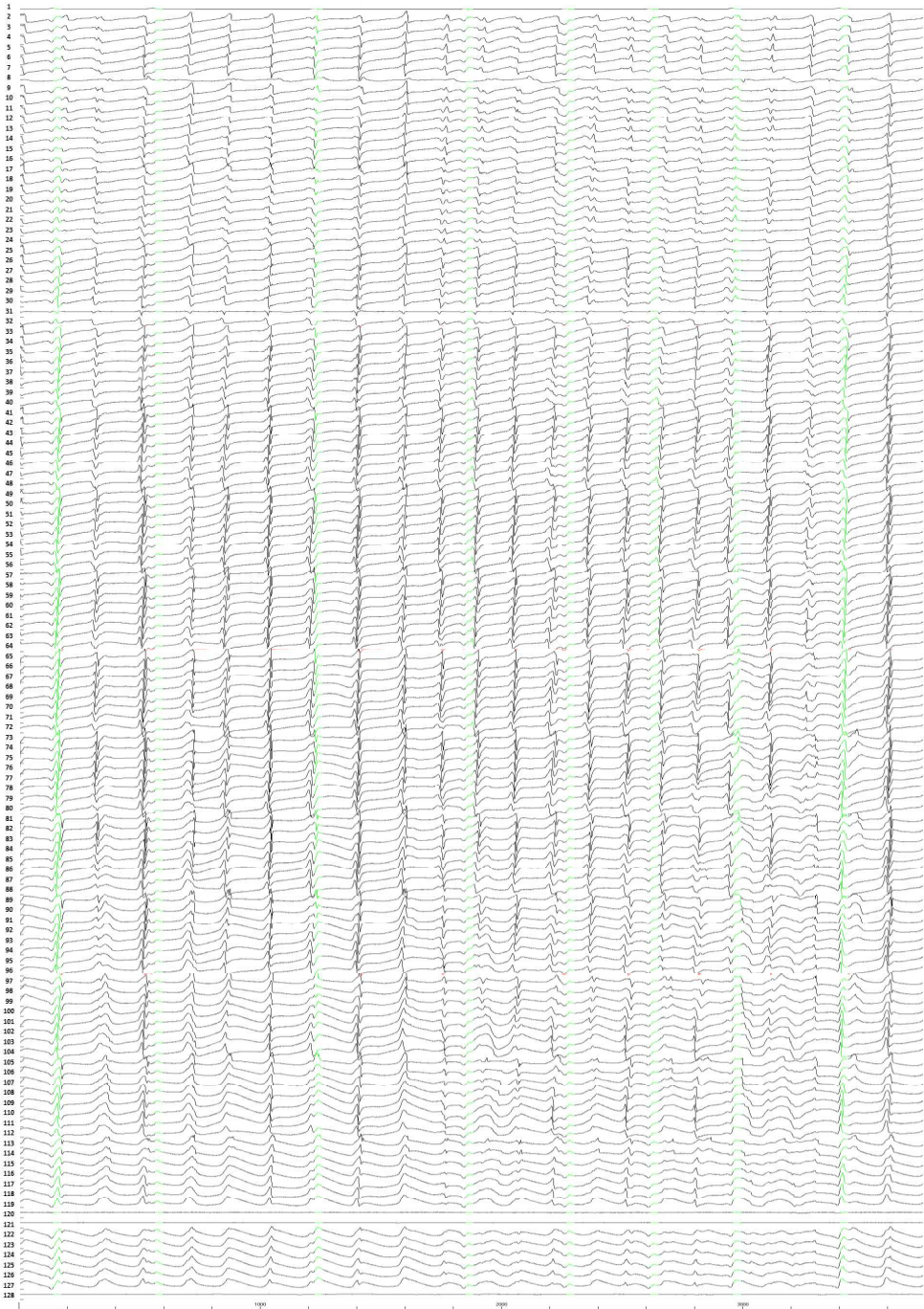
1	2	3	4	5	6	7	8
9	10	11	12	13	14	15	16
17	18	19	20	21	22	23	24
25	26	27	28	29	30	31	32
33	34	35	36	37	38	39	40
41	42	43	44	45	46	47	48
49	50	51	52	53	54	55	56
57	58	59	60	61	62	63	64
65	66	67	68	69	70	71	72
73	74	75	76	77	78	79	80
81	82	83	84	85	86	87	88
89	90	91	92	93	94	95	96
97	98	99	100	101	102	103	104
105	106	107	108	109	110	111	112
113	114	115	116	117	118	119	120
121	122	123	124	125	126	127	128

Endocardium

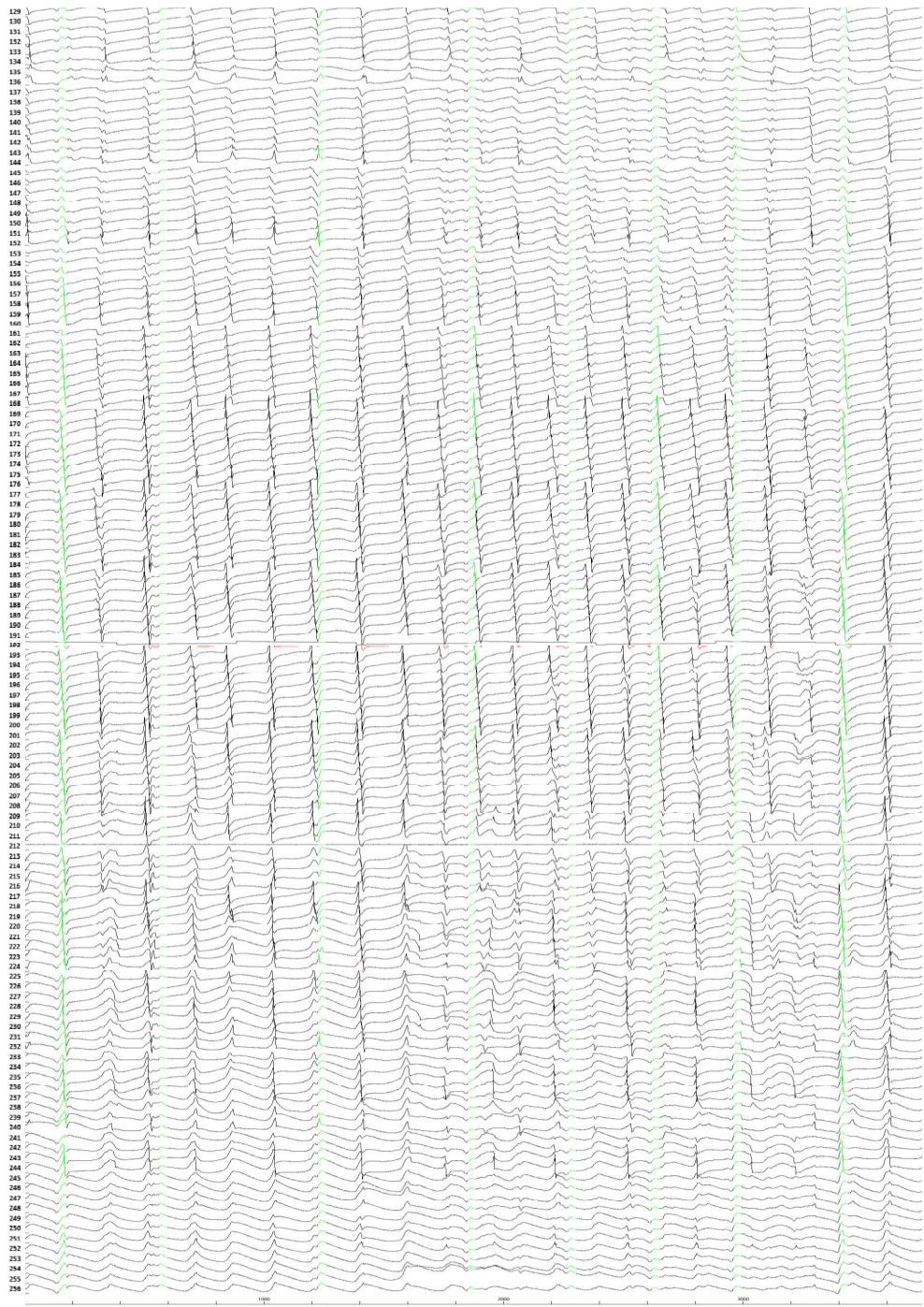
136	135	134	133	132	131	130	129
144	143	142	141	140	139	138	137
152	151	150	149	148	147	146	145
160	159	158	157	156	155	154	153
168	167	166	165	164	163	162	161
176	175	174	173	172	171	170	169
184	183	182	181	180	179	178	177
192	191	190	189	188	187	186	185
200	199	198	197	196	195	194	193
208	207	206	205	204	203	202	201
216	215	214	213	212	211	210	209
224	223	222	221	220	219	218	217
232	231	230	229	228	227	226	225
240	239	238	237	236	235	234	233
248	247	246	245	244	243	242	241
256	255	254	253	252	251	250	249

Figure 1. The total set of endo- and epicardial electrograms of two patients. The position of the electrode numbers in the arrays is illustrated below. The green colored segments in the electrogram tracings indicate the ventricular far field complexes. The superimposed black traces are the signals after application of the ventricular far field subtracting technique as described above. The yellow bands in the marked electrogram figures depict the time window in which the electrodes are activated in that AF beat.

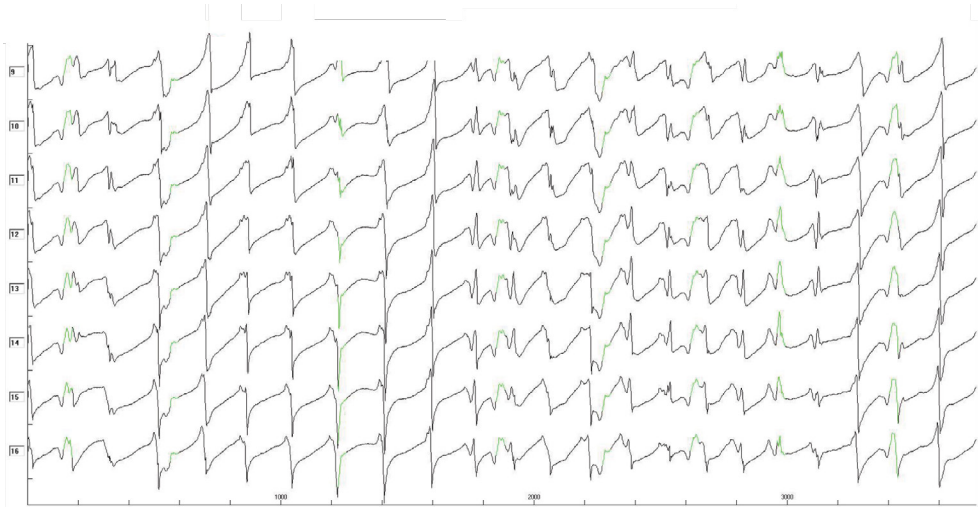
Patient 5 – Epicardial Electrograms



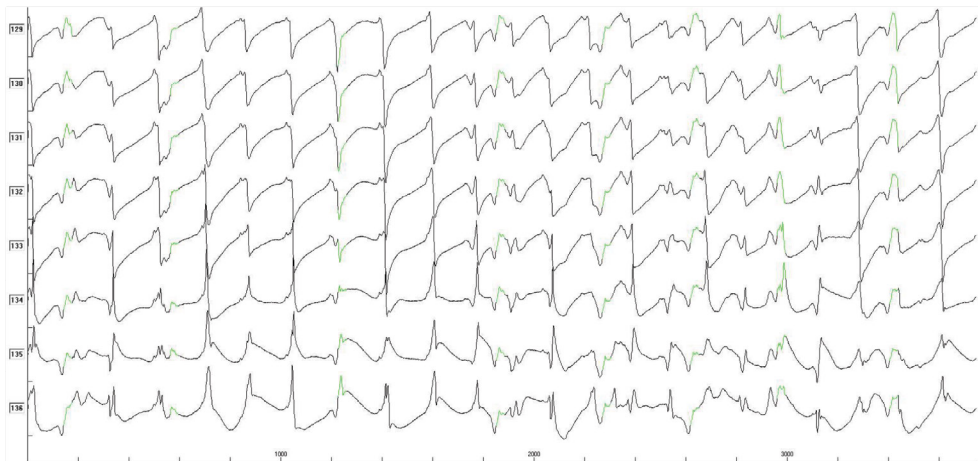
Patient 5 – Endocardial Electrograms



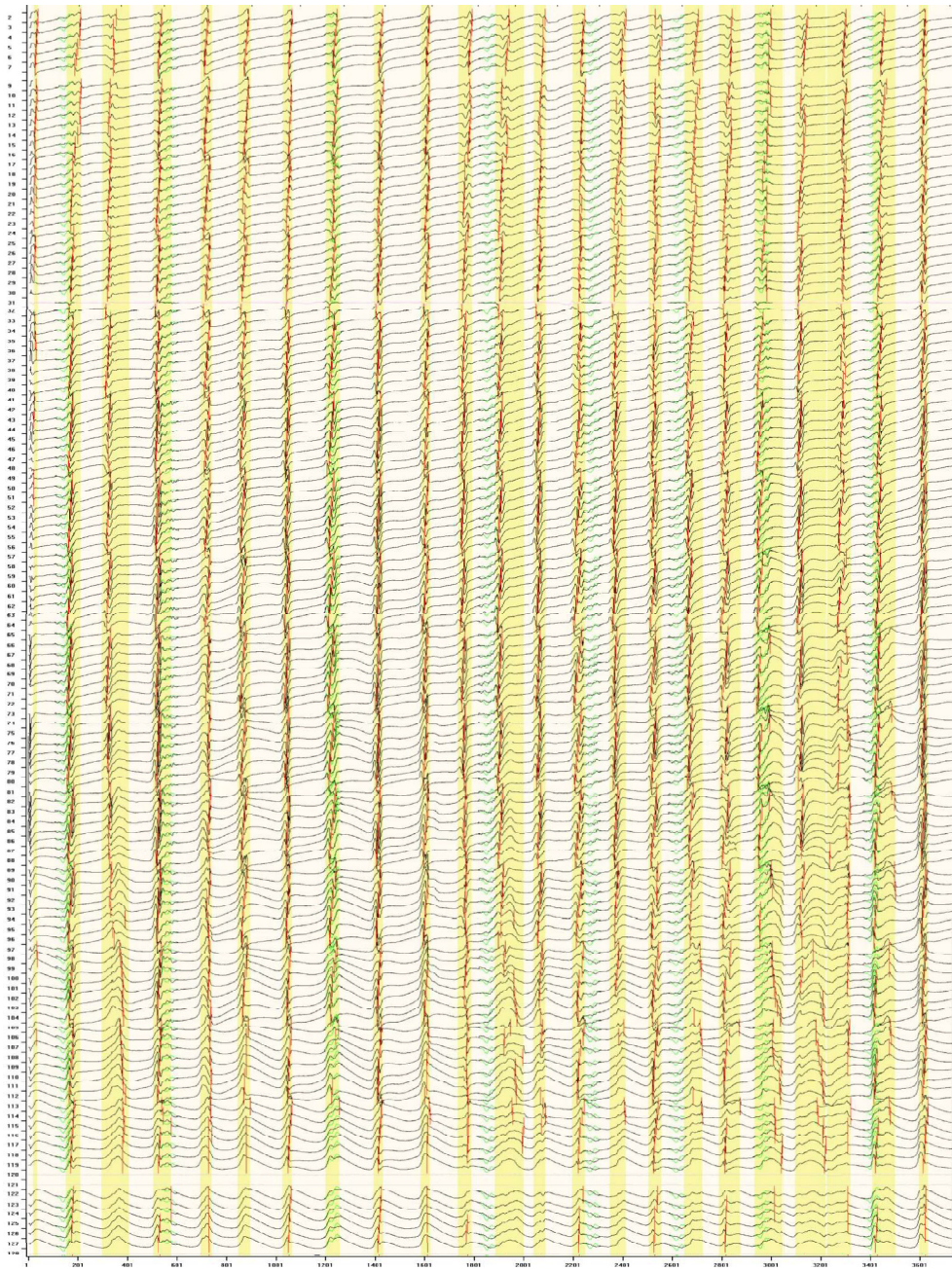
Magnified Epicardial Electrograms



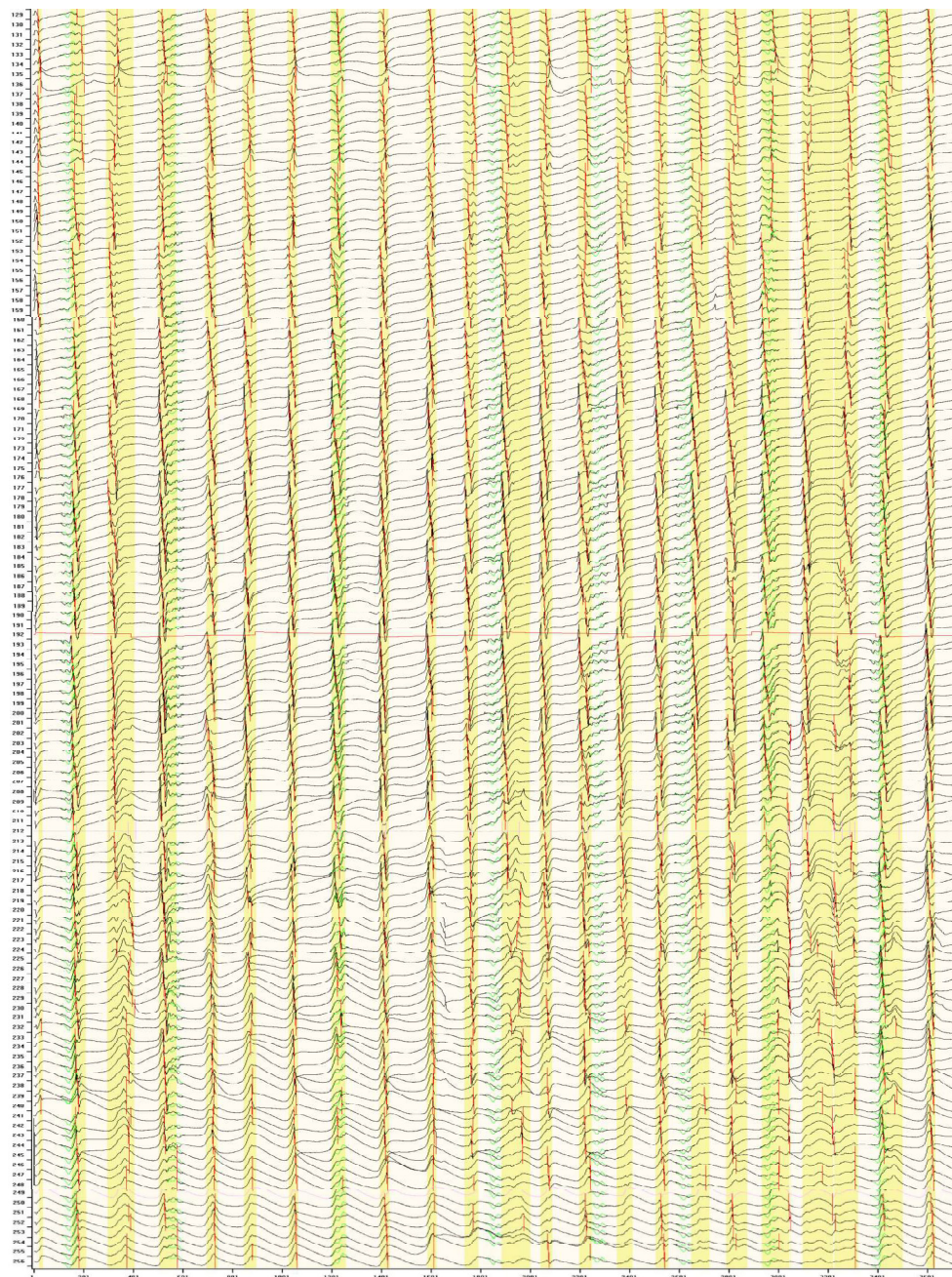
Magnified Endocardial Electrograms



Patient 5 – Marked Epicardial Electrograms

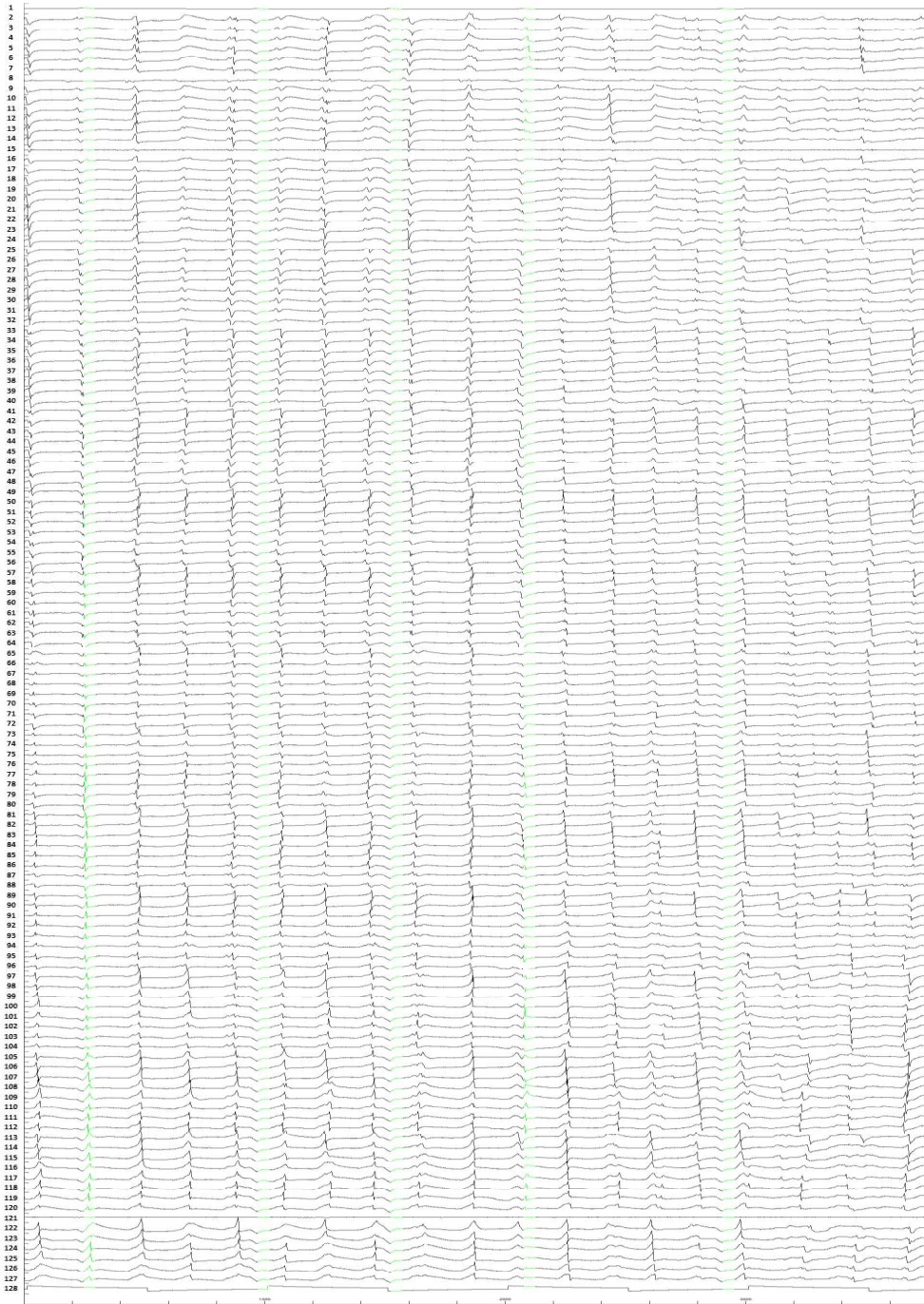


Patient 5 – Marked Endocardial Electrograms

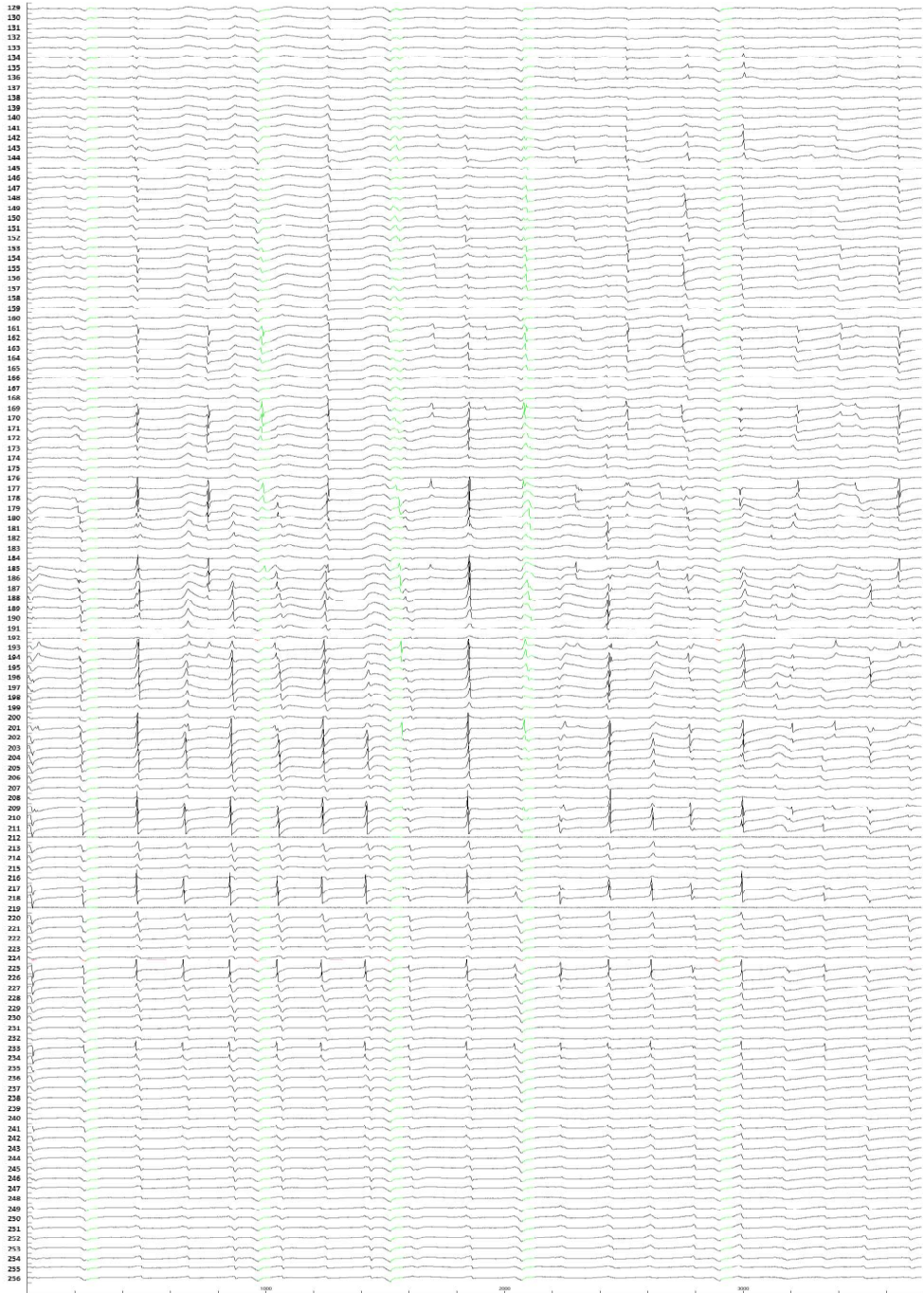


10

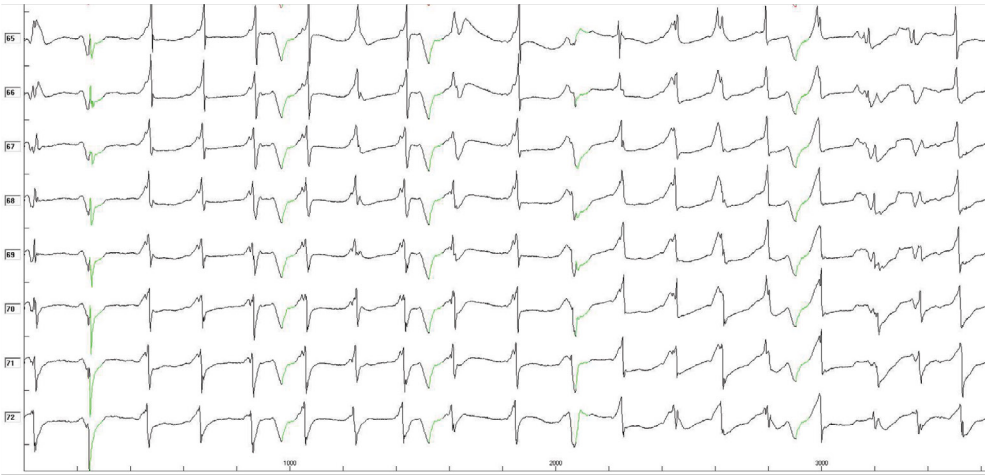
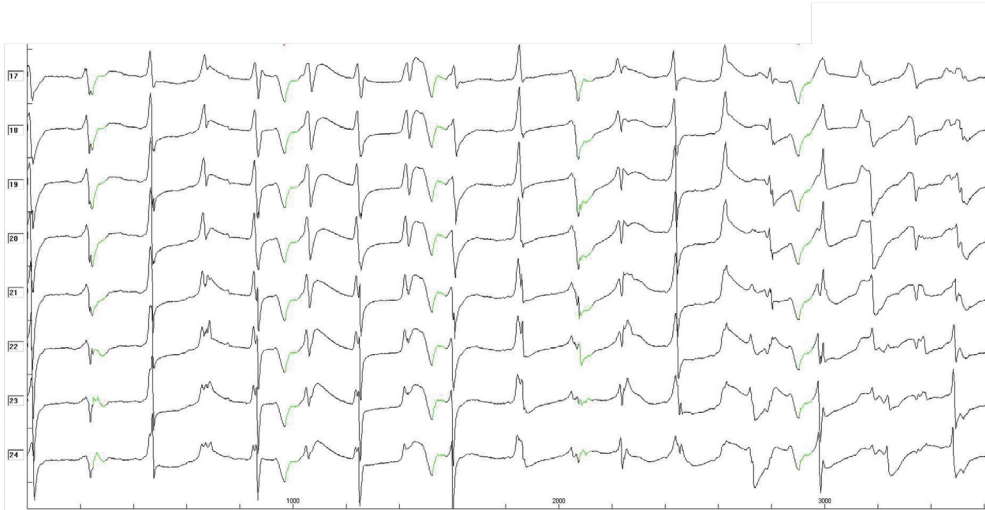
Patient 14 – Epicardial Electrograms



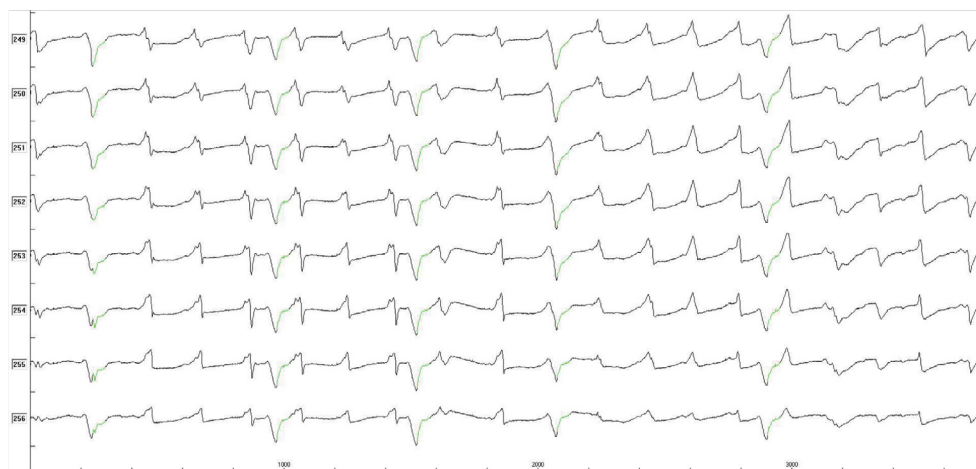
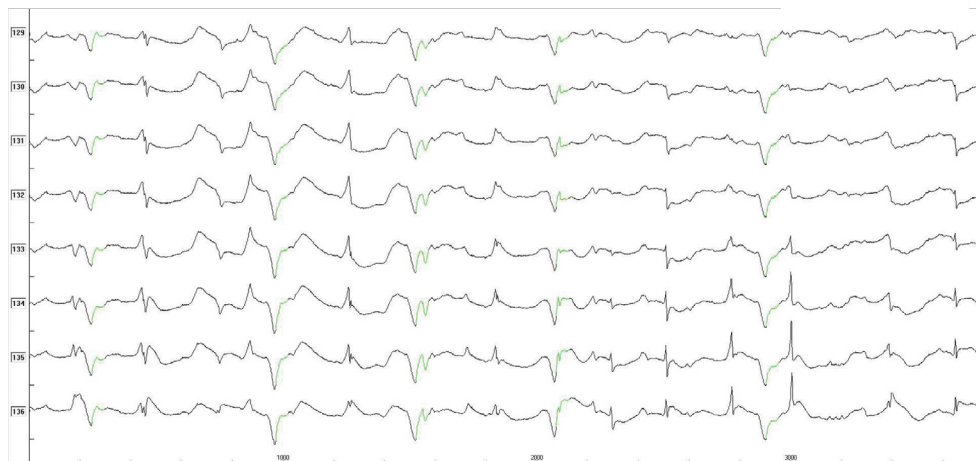
Patient 14 – Endocardial Electrograms



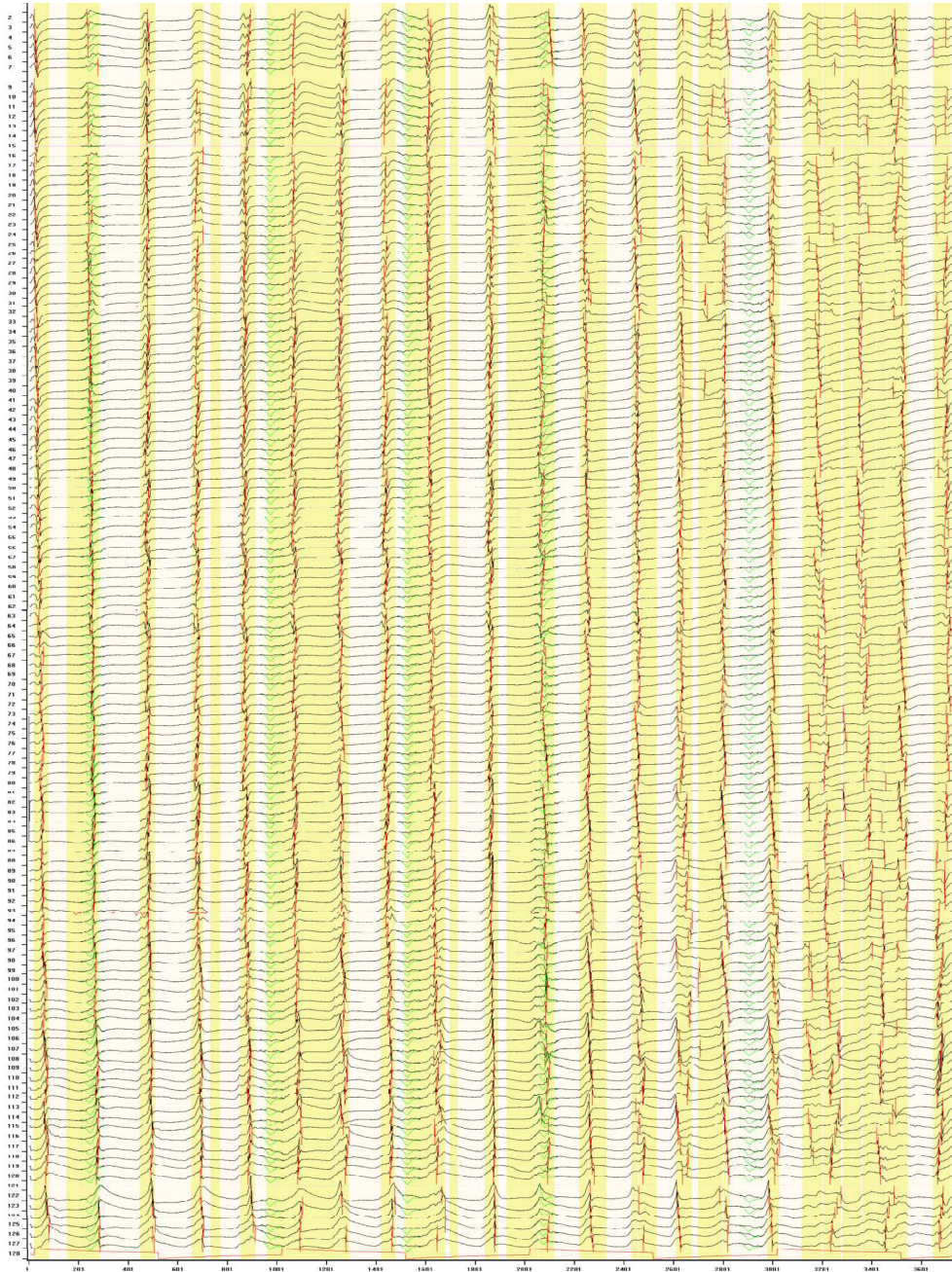
Patient 14 – Magnified Epicardial Electrograms



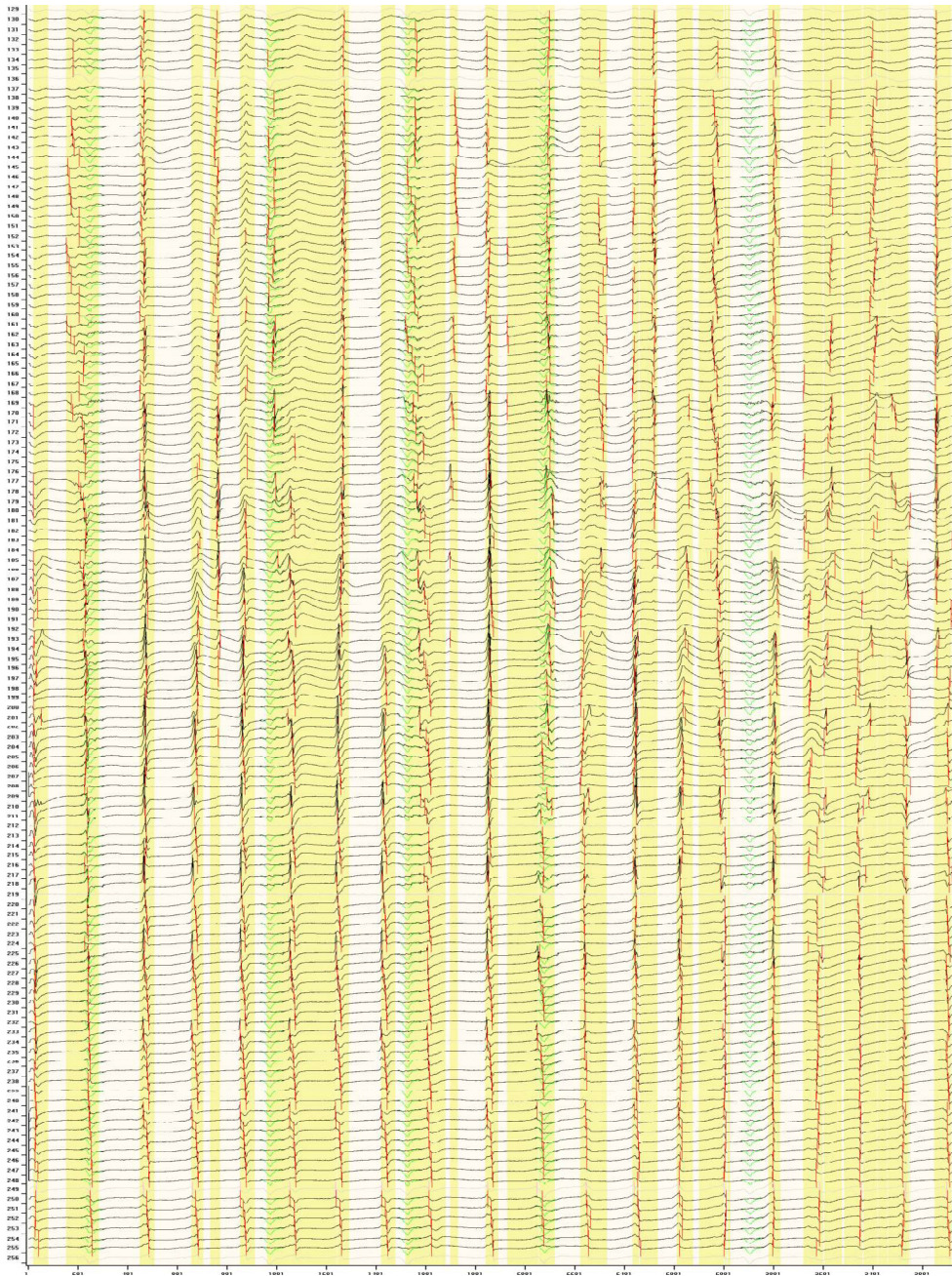
Patient 14 – Magnified Endocardial Electrograms



Patient 14 – Marked Epicardial Electrograms



Patient 14 – Marked Endocardial Electrograms



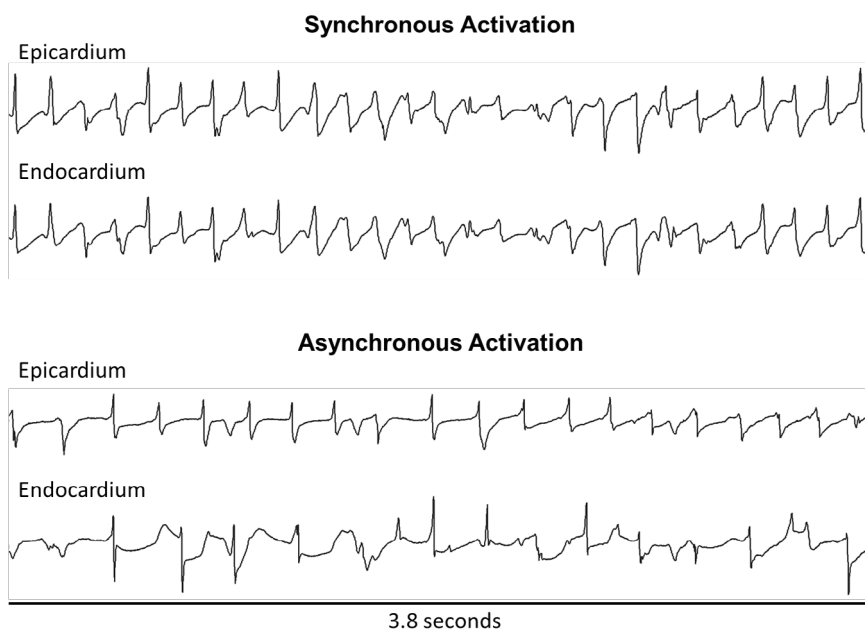


Figure 2. Examples of two opposite electrogram recordings showing synchronous and asynchronous activation.

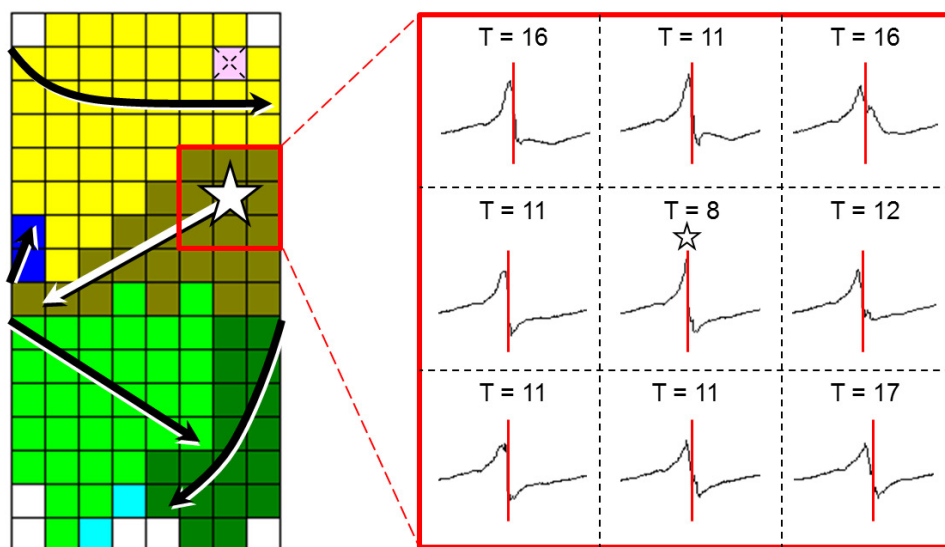


Figure 3. Focal wave originating near the border of the mapping array.

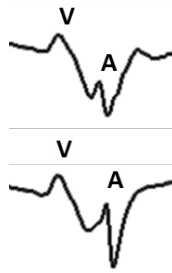
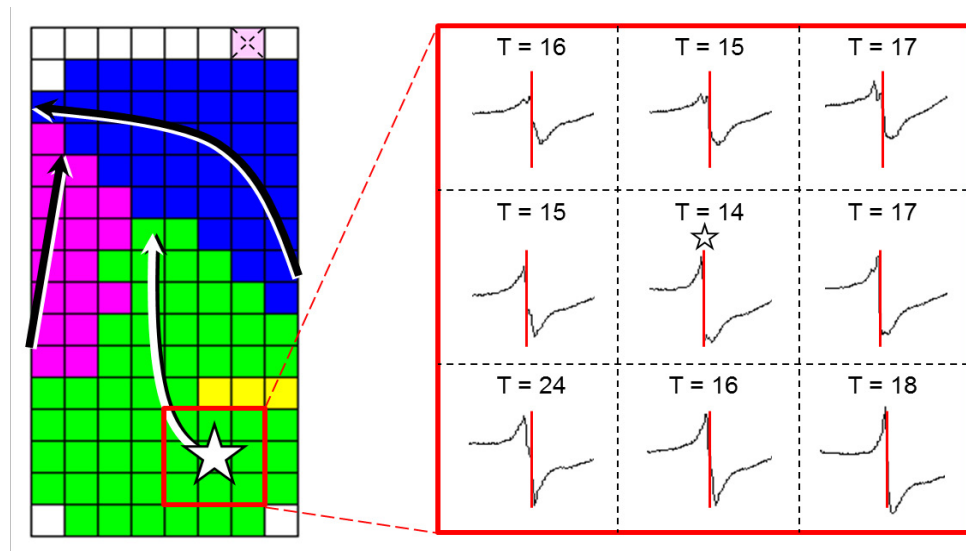


Figure 4. Distortion of the morphology of an atrial fibrillation potential by a far field QRS complex.



T=5 vs T=17

Figure 5. Fractionated potential next to the origin of a 'focal' wave.



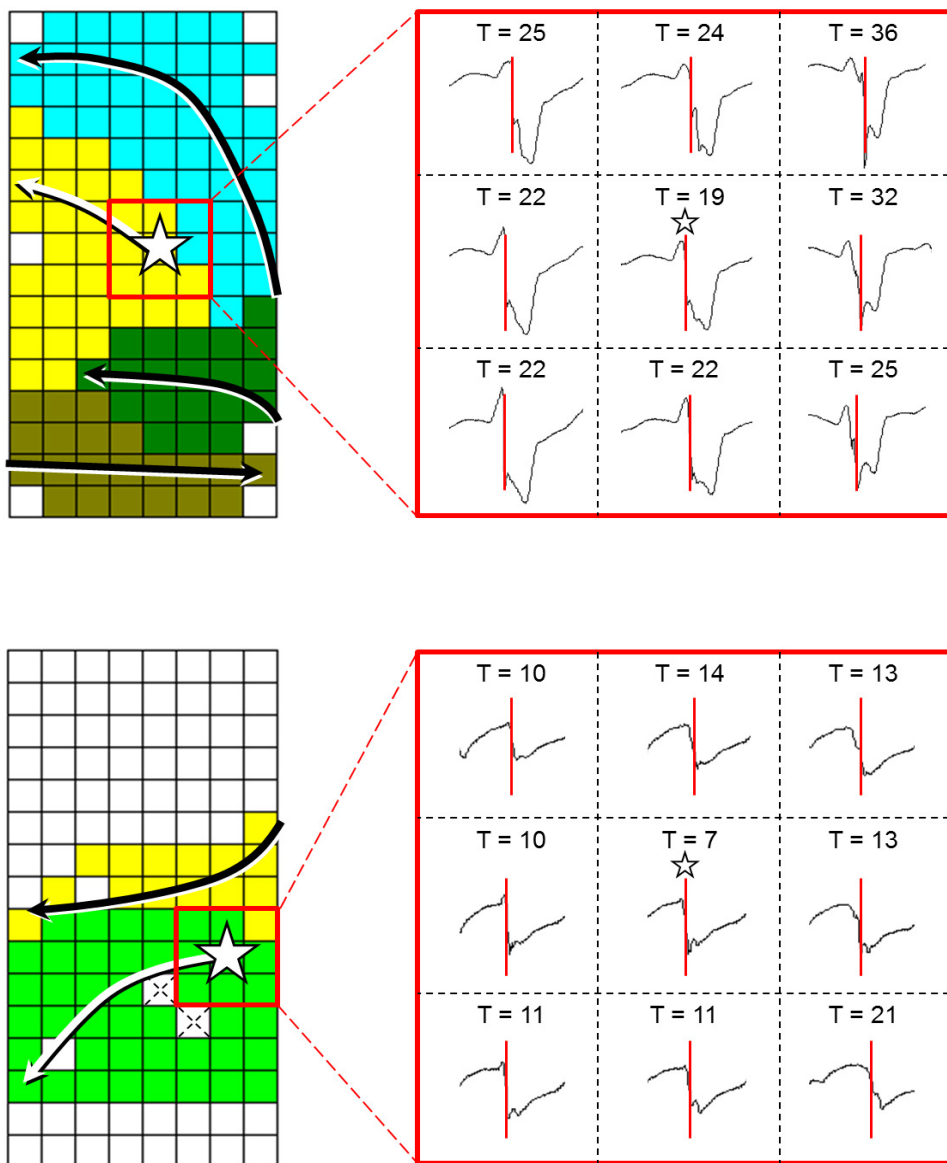


Figure 6. Wavemaps demonstrating typical examples of focal fibrillation waves.

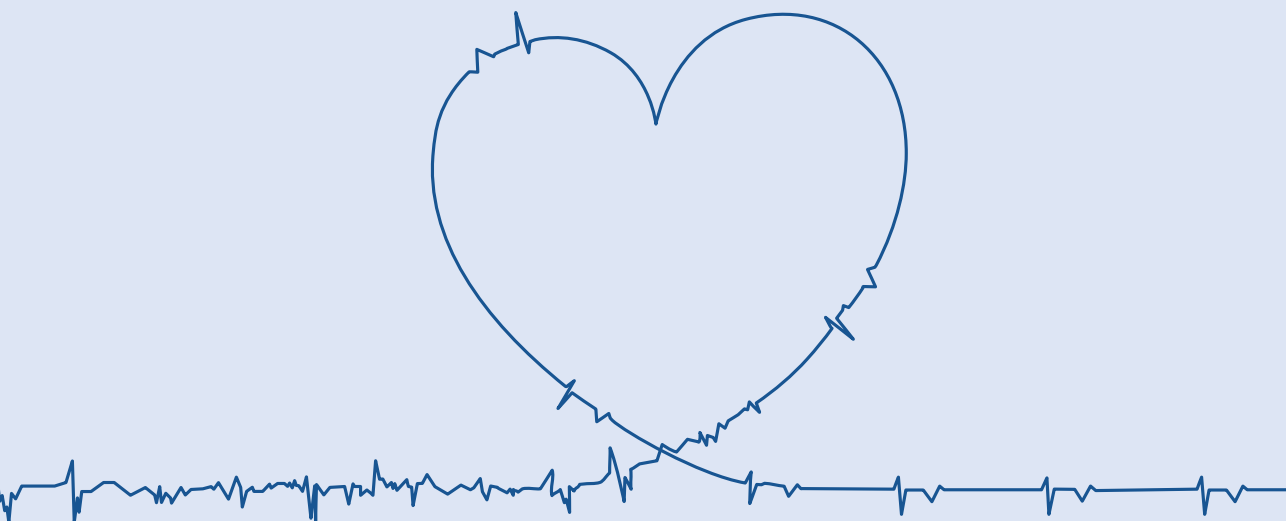
REFERENCES

1. Hoekstra BP, Diks CG, Allesie MA, DeGoede J. Spatial correlation analysis of atrial activation patterns during sustained atrial fibrillation in conscious goats. *Arch Physiol Biochem.* 2000;108:313-331.
2. Spach MS, Dolber PC. Relating extracellular potentials and their derivatives to anisotropic propagation at a microscopic level in human cardiac muscle. Evidence for electrical uncoupling of side-to-side fiber connections with increasing age. *Circ Res.* 1986;58:356-371.
3. Spach MS, Kootsey JM. Relating the sodium current and conductance to the shape of transmembrane and extracellular potentials by simulation: effects of propagation boundaries. *IEEE Trans Biomed Eng.* 1985;32:743-755.
4. Rogers JM, Usui M, KenKnight BH, Ideker RE, Smith WM. Recurrent wavefront morphologies: a method for quantifying the complexity of epicardial activation patterns. *Ann Biomed Eng.* 1997;25:761-768.
5. Kleber AEG, Rudy Y. Basic Mechanisms of Cardiac Impulse Propagation and Associated Arrhythmias. *Physiol Rev.* 2004;84:431-488.
6. de Groot NMS, Schalij MJ, Zeppenfeld K, Blom NA, van der Velde ET, van der Wall EE, Schalij MJ. Voltage and activation mapping: how the recording technique affects the outcome of catheter ablation procedures in patients with congenital heart disease. *Circulation.* 2003;108:2099-2106.
7. Biermann M, Shenasa M, Borggrefe M, Hindricks G, Haverkamp W, Breithardt G. Chapter 2. The interpretation of cardiac electrograms, 15-39. From Cardiac Mapping, 2nd edition. From Cardiac Mapping. Shenasa M, Borggrefe M, Breithardt G.
8. Biermann M, Borggrefe M, Johna R, Haverkamp W, Shenasa M, Breithardt G. Precision and reproducibility of cardiac mapping. Chapter 8. Precision and reproducibility of cardiac mapping. Chapter 8. 157-186. From Cardiac Mapping, 2nd edition. From Cardiac Mapping. Shenasa M, Borggrefe M, Breithardt G.
9. Hertevig EJ, Yuan S, Carlson J, Kongstad-Rasmussen O, Olsson SB. Evidence for electrical remodelling of the atrial myocardium in patients with atrial fibrillation. A study using the monophasic action potential recording technique. *Clin Physiol Funct Imaging.* 2002;22:8-12
10. Konings KT, Kirchhof CJ, Smeets JR, Wellens HJ, Penn OC, Allesie MA. High-density mapping of electrically induced atrial fibrillation in humans. *Circulation.* 1994;89:1665-1680.
11. Konings KT, Smeets JL, Penn OC, Wellens HJ, Allesie MA. Configuration of unipolar atrial electrograms during electrically induced atrial fibrillation in humans. *Circulation.* 1997;95:1231-1241.
12. Allesie MA, de Groot NM, Houben RP, Schotten U, Boersma E, Smeets JL, Crijns HJ. The electropathological substrate of longstanding persistent atrial fibrillation in patients with structural heart disease: longitudinal dissociation. *Circ Arrhythm Electrophysiol.* 2010;3:606-615.
13. de Groot NMS, Houben RP, Smeets JL, Boersma E, Schotten U, Schalij MJ, Crijns H, Allesie MA. The electropathological substrate of longstanding persistent atrial fibrillation in patients with structural heart disease: epicardial breakthrough. *Circulation.* 2010;122:1674-1682.
14. Spach MS, Dolber PC, Heidlage JF. Influence of the passive anisotropic properties on directional differences in propagation following modification of the sodium conductance in human atrial muscle. A model of reentry based on anisotropic discontinuous propagation. *Circ Res.* 1988;62:811-832.

PART III



CLINICAL MARKERS FOR PREDICTION OF ATRIAL FIBRILLATION



CHAPTER 11

11



INTRAOPERATIVE INDUCIBILITY OF ATRIAL FIBRILLATION DOES NOT PREDICT EARLY POSTOPERATIVE ATRIAL FIBRILLATION

Lanters EAH, Teuwen CP, Yaksh A, Kik C, van der Does LJME, Mouws EMJP, Knops P, van
Groningen NJ, Hokken T, Bogers AJJC, de Groot NMS
Journal of the American Heart Association (2018)

ABSTRACT

Background Early postoperative atrial fibrillation (EPoAF) is associated with thrombo-embolic events, prolonged hospitalization and development of late PoAF (LPoAF). It is however unknown if EPoAF can be predicted by intra-operative AF inducibility. The aims of this study are therefore to explore 1)the value of intraoperative inducibility of AF for development of both EPoAF and LPoAF and 2)the predictive value of *de novo* EPoAF for recurrence of LPoAF.

Methods Patients (N=496, 75% male), undergoing cardiothoracic surgery for coronary and/or valvular heart disease were included. AF induction was attempted by atrial pacing, prior to extracorporeal circulation. All patients were on continuous rhythm monitoring until discharge to detect EPoAF. During a follow-up period of 2 years, LPoAF was detected by ECG's and Holter recordings.

Results Sustained AF was inducible in 56% of patients. There was no difference in patients with or without AF prior to surgery ($P=0.159$), or between different types of surgery ($P=0.687$). In patients without a history of AF, incidence of EPoAF and LPoAF was 37% and 2%. EPoAF recurred in 58% patients with pre-operative AF, 53% developed LPoAF. There were no correlations between intraoperative inducibility and EPoAF or LPoAF ($P>0.05$). EPoAF was not correlated with LPoAF in patients without a history of AF ($P=0.116$), in contrast to patients with AF prior to surgery($P<0.001$).

Conclusions Intraoperative AF inducibility does not predict development of either EPoAF or LPoAF. In patients with AF prior to surgery, EPoAF is correlated with LPoAF recurrences. This correlation is absent in patients without AF prior to surgery.

INTRODUCTION

Over the past decades, cardiac surgery has become an established treatment modality for various cardiovascular diseases. However, despite improved surgical techniques and healthcare over the years, atrial fibrillation (AF) is still frequently observed in the early post-operative period. Reported incidences of early postoperative AF (EPoAF) range from 10% to 65%¹⁻⁴. EPoAF is associated with thrombo-embolic complications and prolonged hospitalization^{3, 5, 6}. A previous study demonstrated, although in a small population (N=50) with coronary artery disease, that intraoperative inducibility of AF could be a predictor for development of EPoAF⁷. However, this was never validated in a larger population with a variety of cardiovascular diseases.

In addition, EPoAF is known to increase the risk of late postoperative AF (LPoAF)^{6, 8, 9}, yet the predictive value of intraoperative inducibility was never investigated. The latest European guidelines advise to consider long-term oral anticoagulants in case of EPoAF as prevention for thrombo-embolic complications (Class IIa)¹⁰. However, they also concluded that additional research is mandatory to investigate the predictive value of short-lasting (<24 hours) EPoAF episodes for development of LPoAF. Hence, there is a need to identify patients at risk for EPoAF, and subsequently to determine whether these patients are also at risk for LPoAF.

The aims of this study are therefore to explore 1) the value of intraoperative inducibility of AF for development of both EPoAF and LPoAF and 2) the predictive value of *de novo* EPoAF episodes of any duration >30 seconds for recurrence of LPoAF.

METHODS

The data, analytic methods, and study materials will not be made available to other researchers for purposes of reproducing the results or replicating the procedure.

Study population

The study population consisted of 496 adult patients, scheduled for elective cardiac surgery, including isolated coronary artery bypass grafting (CABG), isolated valvular heart surgery (VHS), a combination of VHS and CABG (VHS+CABG) or correction of a congenital heart defect (CHD, Figure 1). Patients with an atrial pacing device, previous ablation of atrial arrhythmias, severe renal failure or patients requiring mechanical or inotropic support prior to the surgical procedure were not eligible for inclusion. Surgical pulmonary vein isolation (sPVI) was performed in a selection of patients with a history of AF. Classification of AF was performed according to the latest guidelines¹⁰.

Patients were included in either the QUASAR¹¹ (QEst for the Arrhythmogenic Substrate of Atrial fibrillation) or HALT&REVERSE¹² (HSF1 activators lower cardiomyocyte damage; towards a novel approach to reverse AF) project, which were both approved by the institutional medical ethical committee (MEC2010-054 and MEC2014-393). All patients provided written informed consent prior to inclusion. Clinical characteristics were obtained from electronic patient files.

Intraoperative induction of AF by electrical stimulation

QUASAR and HALT&REVERSE are high-resolution epicardial mapping studies, designed to investigate the arrhythmogenic substrate underlying AF. For this purpose, mapping is performed during either spontaneous or electrically induced AF. AF induction is attempted in every patient prior to commencement of extra-corporal circulation by fixed rate pacing at the right atrial appendage, delivered by a temporary pacemaker wire (pulse width: 2ms, output 10mA). Pacing started at a rate of 200 bpm and if AF was not induced after 2 attempts, the rate was gradually increased by steps of 50 bpm. If AF was not induced at a pacing rate of 400 bpm or loss of capture occurred, attempts were terminated and AF was considered non-inducible¹³. Attempts for inducibility of AF were categorized as 1) non-inducibility, 2) non-sustained AF (nsAF; self-terminating during mapping procedure), 3) non-sustained atrial flutter (nsAFL), 4) sustained AF (sAF, not self-terminating during mapping procedure, approximately 4 minutes) and 5) sustained AFL (sAFL).

Early postoperative atrial fibrillation

Postoperative cardiac rhythms were continuously recorded during the first 4 – 5 days. Telemetry recordings, electrocardiograms (ECGs) and patient records were all manually evaluated for the presence of AF episodes. EPoAF was defined as irregular RR intervals in the absence of distinct P-waves, with a duration of at least 30 seconds occurring within 14 days after the surgery.

Late postoperative atrial fibrillation

For this sub-analysis, we only included those patients that completed a 2 year follow-up period by March 2017, or developed AF within this period. LPoAF was detected on either ECGs or 24-hour Holter recordings. If applicable, additional rhythm registrations obtained during the follow-up period were requested from the referring hospital.

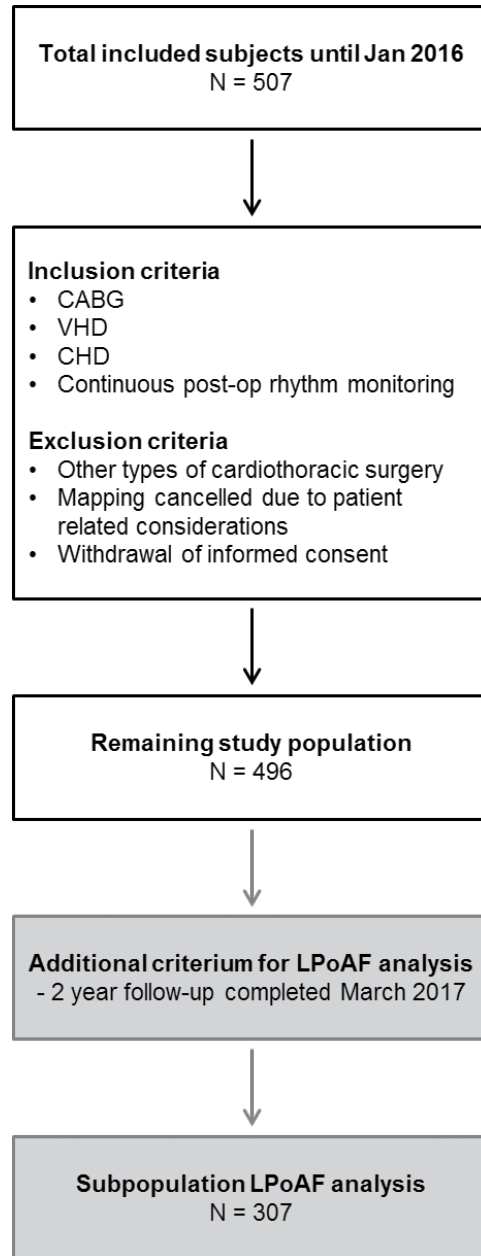


Figure 1. Flowchart patient inclusion. CABG: coronary artery bypass grafting; VHD: valvular heart disease; CHD: congenital heart disease; LPoAF: late postoperative atrial fibrillation.

Statistical analysis

All data were tested for normality. Continuous, normally distributed data are expressed as mean±SD and skewed data as median (P25-P75). Student's T-tests were used to compare normally distributed continuous clinical parameters. Non-normally distributed clinical parameters were compared by non-parametric tests including Mann-Whitney-U-test. Fisher Exact or χ^2 tests were applied for categorical variables. The correlation between EPoAF, LPoAF, AF induction and clinical characteristics was examined using Pearson or Spearman's tests where applicable. A P-value of <0.05 was considered statistically relevant. Statistical analyses were performed using IBM SPSS Statistics 24 (IBM Corporation, Armonk, NY, USA).

RESULTS

Study population

The study population consisted of 496 patients (age 67±11 years, 373 (75%) male). Baseline characteristics are summarized in Table 1. The majority of patients (N=273, 55%) underwent CABG surgery, whereas VHS, or VHS+CABG was performed in respectively 122 (25%) and 82 (16%) patients. The remaining 19 (4%) patients underwent first time surgical correction of a CHD including mainly patients with either atrial or ventricular septal defects.

A history of AF was present in 125 (25%) patients and was either paroxysmal (N=54, 43.2%), persistent (N=47, 37.6%), long-standing persistent (N=22, 17.6%) or permanent (N=2, 1.6%). Eighty (64%) of these patients underwent concomitant sPVI.

Intraoperative inducibility of AF

At the start of the mapping procedure, spontaneous AF was present in 77 (15.5%) patients with a history of AF. In addition, 7 (1.4%) patients without a history of AF converted spontaneously to AF during surgery, prior to mapping. Pacing was not performed due to patient related or technical issues in another 11 (2.2%) patients.

AF induction was attempted in all 401 remaining patients. As depicted in Panel A of Figure 2, sAF was successfully induced in 56% of these patients, whereas in 10% AF was non-sustained. Either sAFL or nsAFL was induced in respectively 6% and 7%. In 21% of patients, arrhythmias were not inducible despite adequate pacing attempts.

Panel B shows AF inducibility for patients without (N=357) and with preoperative (N=44) AF separately. Induction of sAF was equally successful in patients with preoperative AF (73%) and patients without (54%, P=0.159). Intraoperative inducibility per type of surgery is indicated in Panel C of Figure 2. There was no difference in AF inducibility between the various groups, P=0.687.

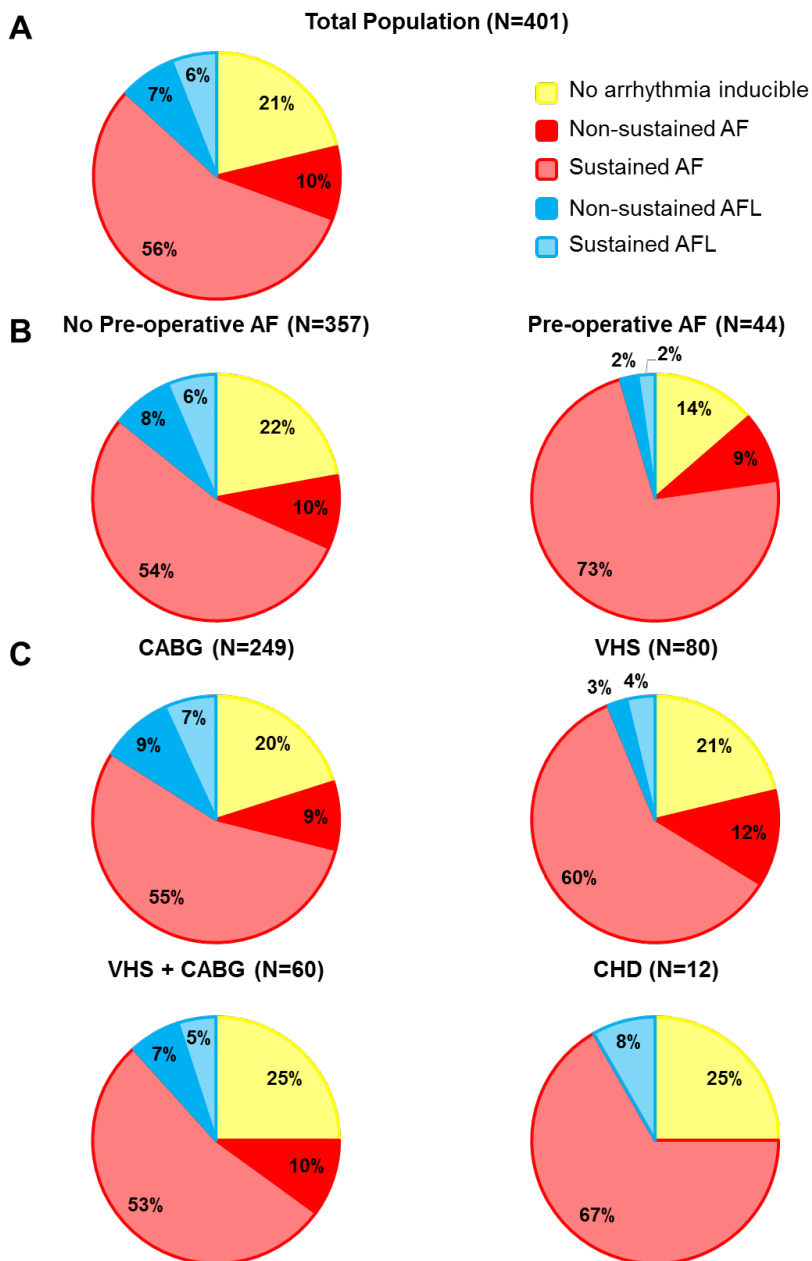


Figure 2. Intraoperative inducibility. Results of intraoperative inducibility of various atrial tachyarrhythmias for the total study population (panel A), for patients without or with AF prior to surgery (panel B) and per type of cardiac surgery (panel C). AF: atrial fibrillation; AFL: atrial flutter.

Table 1. Baseline characteristics

	Total	No AF	AF	P-value[‡]
Population, N (%)	496 (100)	371 (75)	125 (25)	
Group, N (%)				
CABG	273 (55)	246 (66)	27 (22)	<0.001
VHS	122 (25)	58 (16)	64 (51)	
VHS/CABG	82 (16)	56 (15)	26 (21)	
CHD	19 (4)	11 (3)	8 (6)	
Age (years), mean±SD	67±11	65±11	71±9	<0.001
Male gender, N (%)	373 (75)	289 (78)	84 (67)	0.017
Hypertension, N (%)	276 (56)	206 (56)	70 (56)	0.926
Diabetes, N (%)	129 (26)	102 (27)	27 (22)	0.194
Hyperlipidemia, N (%)	162 (33)	136 (37)	26 (21)	0.001
BMI (kg/m ²), mean±SD	27.7±4.3	27.8±4.2	27.7±4.5	0.935
Anti-arrhythmic drugs*, N (%)	367 (75)	271 (73)	96 (77)	0.408
Class I	2 (0.4)	2 (1)	0 (0)	0.399
Class II	367 (66)	254 (68)	75 (60)	<0.001
Class III	27 (5)	5 (1)	22 (18)	<0.001
Class IV	17 (3)	13 (4)	4 (3)	0.801
Left Ventricular Function, N (%)				0.059
Normal	364 (73)	282 (76)	82 (66)	0.023
Mild impairment	96 (19)	68 (18)	28 (22)	0.319
Moderate impairment	34 (7)	20 (5)	14 (11)	0.026
Severe impairment	2 (1)	1 (1)	1 (1)	0.418
Left atrial dilatation†, N (%)	132 (27)	66 (18)	66 (53)	<0.001
AF type prior to CS, N (%)			54 (43.2)	
Paroxysmal AF			47 (37.6)	
Persistent AF			22 (17.6)	
Long-standing Persistent AF			2 (1.6)	
Permanent AF				
Surgical ablation			80 (64)	

AF: atrial fibrillation; BMI: Body Mass Index; CABG: coronary artery bypass grafting; CHD: congenital heart disease; CS: cardiac surgery; VHS: heart valve surgery; *patients could use more than one type of AAD, therefore the sum of all classes is not 100%, †dimension >45mm, ‡comparing No AF and AF.

Early postoperative atrial fibrillation

Overall, EPoAF developed in 211 (43%) patients, including 138 (37%) patients without and 73 (58%) patients with preoperative AF (P<0.001). Clinical characteristics of patients with and without EPoAF are depicted in Table 2. Most initial EPoAF episodes occurred at day 3 (N=76, 36%) and day 4 (N=53, 25%), as opposed to day 1 (N=17, 8%), day 2 (N=23, 11%), day 5 (N=25, 12%), day 6 (N=9, 4%), day 7 (N=5, 2%), day 8 (N=2, 1%) and day 11 (N=1, 1%). Figure 3 shows the cumulative onset of EPoAF per post-operative day, for patients with (red bars) and without (green bars) pre-operative AF separately. EPoAF developed earlier (P<0.001). in patients with AF prior to surgery (day 3±2) prior to surgery, than in patients without (day 4±1).

In the subpopulation of 80 patients in whom sPVI was performed, EPoAF developed in 44% (N=35), compared to the recurrence of EPoAF in 84% (N=38) of the patients in whom ablation was not performed ($P<0.001$).

EPoAF terminated spontaneously in only 6 patients. Patients received class II (N=113), class III (N=68) and/or digoxin (N=45) as treatment for EPoAF. In 33 patients, EPoAF was treated by a combination of electrical cardioversion and anti-arrhythmic drugs.

At discharge to the center of referral after 5(5-7)days, AF was present in 55 (11%) patients, including 14 (4%) patients without pre-operative AF and 41 (34%) patients with pre-operative AF, despite failed attempts to restore sinus rhythm in 75% (N=42).

Relation with intraoperative inducibility

The upper panel of Figure 4 indicates the proportion of patients (N=357) that developed de novo EPoAF, for each type of induced arrhythmia separately. There was no correlation between the type of intraoperatively induced arrhythmia and development of EPoAF ($P>0.05$). Similar results were obtained for patients with pre-operative AF (N=44) that developed EPoAF recurrences, as indicated in the lower panel of Figure 4 ($P>0.05$).

Late postoperative atrial fibrillation

A total of 307 (62%) patients completed the 2 year follow-up period, and/or reached the study end-point (LPoAF). Forty-four patients (14%) developed LPoAF during follow-up, including only 4 (2%) patients without pre-operative AF. AF recurred in 40 (53%) patients with pre-operative AF ($P<0.001$). As expected, the incidence of LPoAF recurrences was lower in patients who underwent ablation than in patients in whom ablation was not performed: 25% versus 44%, $P=0.021$. Table 3 shows additional clinical characteristics of patients with and without LPoAF.

Overall time to LPoAF diagnosis was 6 (3-6) months and was similar in patients with (N=40, 6 (3-6)) and patients without (N=4, 8 (3-21)) pre-operative AF ($P=0.708$).

Table 2. Clinical characteristics of patients with and without EPoAF

	No AF			AF		
	No EPoAF (N=233)	EPoAF (N=138)	P-value	No EPoAF (N=52)	EPoAF (N=73)	P-value
Group, N (%)			0.006			0.951
CABG	160 (69)	86 (62)		10 (19)	17 (23)	
VHS	38 (16)	20 (15)		27 (52)	37 (51)	
VHS/CABG	25 (11)	31 (22)		12 (23)	14 (19)	
CHD	10 (4)	1 (<1)		3 (6)	5 (7)	
Age (years), mean±SD	63±12	69±8	<0.001	68±10	72±7	0.014
Gender (male, %)	182 (78)	107 (78)	0.897	33 (63)	47 (64)	0.427
Hypertension, N (%)	128 (55)	78 (57)	0.766	28 (54)	42 (58)	0.682
Diabetes, N (%)	65 (28)	37 (27)	0.821	7 (13)	20 (28)	0.062
Hyperlipidemia, N (%)	87 (37)	49 (36)	0.723	11 (21)	15 (21)	0.934
BMI (kg/m ²), mean±SD	28±4	27±4	0.554	27±4	28±5	0.107
Anti-arrhythmic drugs, N (%)			0.081			0.978
Class I	1 (<1)	1 (<1)		0	0	
Class II	153 (66)	101 (73)		30 (58)	45 (62)	
Class III	4 (2)	1 (<1)		11 (21)	11 (15)	
Class IV	8 (3)	5 (4)		2 (4)	2 (3)	
Left Ventricular Function, N (%)			0.180			0.148
Normal	185 (79)	97 (70)		38 (73)	44 (60)	
Mild impairment	36 (15)	32 (23)		7 (13)	21 (29)	
Moderate impairment	11 (5)	9 (7)		6 (12)	8 (11)	
Severe impairment	1 (<1)	0		1 (2)	0	
Left atrial dilatation, N (%)	40 (17)	26 (19)	0.684	21 (40)	45 (62)	0.019
AF type prior to CS, N (%)						0.116
Paroxysmal AF				26 (50)	28 (38)	
Persistent AF				15 (29)	32 (44)	
Long-standing Persistent AF				11 (21)	10 (14)	
Permanent AF				0	3 (4)	
Surgical ablation, N (%)				45 (87)	35 (48)	<0.001

AF: atrial fibrillation; EPoAF: early post-operative atrial fibrillation; CABG: coronary artery bypass grafting; VHS: valvular heart surgery; CHD: congenital heart disease; CS: cardiac surgery.

Relation late postoperative AF and intraoperative inducibility

In 3 (75%) patients with de novo LPoAF, intraoperative induction resulted in sAF, the fourth patient had sAFL. In patients with AF prior to surgery, 2 patients with LPoAF were non-inducible during surgery, 2 patients had nsAF, 8 patients had sAF and 1 had sAFL. However, in the majority of patients (N=27, 35%) AF was spontaneously present at the start of the procedure. As a consequence, there was no correlation between type of arrhythmia induced and development of LPoAF for either patients without ($P=0.163$) or with ($P=0.211$) AF prior to surgery.

Relation early post-operative and late post-operative atrial fibrillation

Four patients without AF prior to surgery developed LPoAF, including 1 patient without and 3 patients with EPoAF. Consequently, there was no correlation between EPoAF and LPoAF in this subgroup ($P=0.116$). LPoAF recurrences in the subgroup with AF prior to surgery was observed in 6 patients without and 34 patients with EPoAF episodes, resulting in a significant correlation between EPoAF and LPoAF: $\rho=0.370$ and $P<0.001$. Day of EPoAF onset did not correlate with LPoAF development ($P=0.390$).

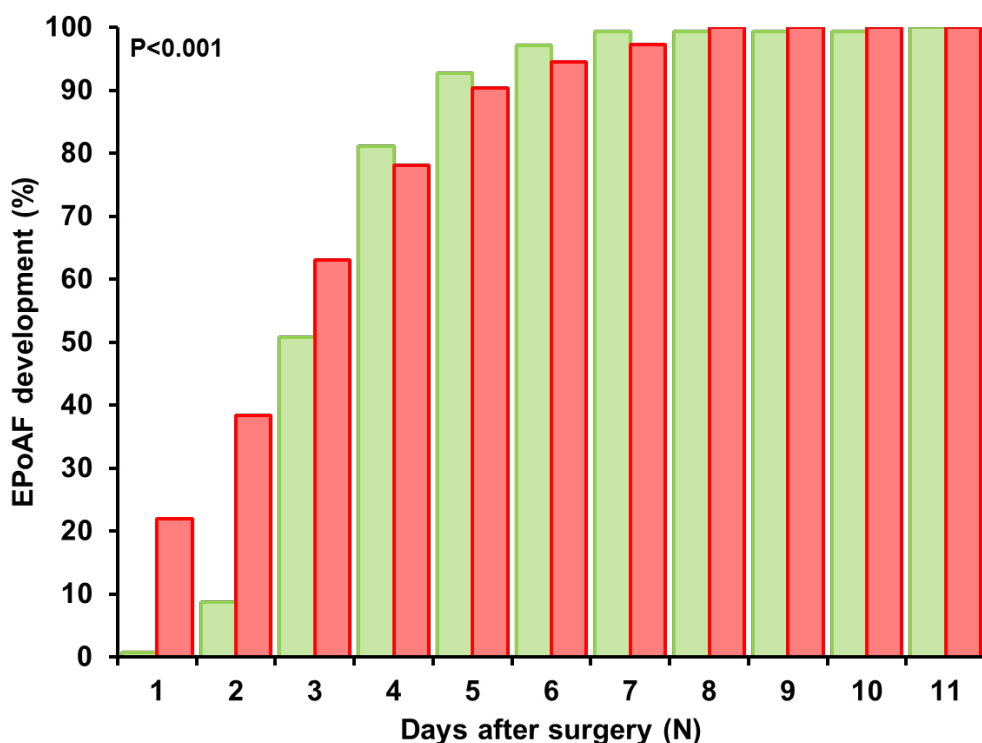


Figure 3. Early post-operative AF. Cumulative proportion of EPoAF onset per post-operative day for patients without (green bars) or with (red bars) AF prior to surgery.

DISCUSSION

Key findings

Intraoperative AF is inducible in the vast majority of patients. However, it is not correlated with development of EPoAF or LPoAF. In patients without AF prior to surgery, the incidence of LPoAF is very low and not related to the presence of EPoAF. Clinical patient characteristics did not influence intraoperative AF inducibility or development of either EPoAF or LPoAF.

AF: atrial fibrillation; LPoAF: late post-operative atrial fibrillation; CABG: coronary artery bypass grafting; VHS: valvular heart surgery; CHD: congenital heart disease; CS: cardiac surgery

Table 3. Clinical characteristics of patients with and without LPoAF

	No AF			AF		
	No LPoAF (N=367)	LPoAF (N=4)	P-value	No LPoAF (N=85)	LPoAF (N=40)	P-value
Group, N (%)			0.010			0.498
CABG	245 (67)	1 (25)		19 (22)	8 (20)	
VHS	58 (16)	0		42 (49)	22 (55)	
VHS/CABG	53 (14)	3 (75)		20 (24)	6 (15)	
CHD	11 (3)	0		4 (5)	4 (10)	
Age (years), mean±SD	65±11	69±9	0.486	70±9	71±8	0.613
Gender (male, %)	285 (78)	4 (100)	0.284	54 (64)	30 (75)	0.203
Hypertension, N (%)	205 (56)	1 (25)	0.217	51 (60)	19 (48)	0.189
Diabetes, N (%)	101 (28)	1 (25)	0.911	18 (21)	9 (23)	0.867
Hyperlipidemia, N (%)	153 (42)	1 (25)	0.627	19 (22)	7 (18)	0.533
BMI (kg/m ²), mean±SD	28±4	27±3	0.798	27±4	29±5	0.163
Anti-arrhythmic drugs, N(%)			0.929			0.032
Class I	2 (1)	0		0	0	
Class II	251 (68)	3 (75)		54 (64)	21 (53)	
Class III	5 (1)	0		17 (55)	5 (13)	
Class IV	13 (4)	0		4 (5)	0	
Left Ventricular Function, N (%)			0.303			0.604
Normal	279 (76)	3 (75)		58 (68)	24 (60)	
Mild impairment	68 (19)	0		18 (21)	10 (25)	
Moderate impairment	19 (5)	1 (25)		8 (9)	6 (15)	
Severe impairment	1 (<1)	0		1 (1)	0	
Left atrial dilatation, N (%)	64 (17)	2 (50)	0.090	37 (44)	28 (70)	0.002
AF type prior to CS, N (%)						0.260
Paroxysmal AF				34 (40)	20 (50)	
Persistent AF				33 (39)	13 (33)	
Long-standing Persistent AF				17 (20)	4 (10)	
Permanent AF				1 (1)	2 (5)	
<i>Surgical ablation, N (%)</i>				<i>60 (71)</i>	<i>20 (50)</i>	<i>0.025</i>

Relation between inducibility and early post-operative atrial fibrillation

The predictive value of AF inducibility for development of EPoAF after cardiothoracic surgery has so far solely been investigated by Lowe et al.⁷. AF was induced in 72% of 50 patients without a history of AF undergoing CABG, slightly more than in our population. They reported a sensitivity and specificity of AF inducibility for predicting EPoAF of respectively 94% and 41%.

In the present study, AF was inducible in the majority of patients and the incidence of *de novo* EPoAF was 37% (overall EPoAF: 43%) which is comparable to incidences reported by other investigators^{2, 6, 8}. However, a correlation between inducibility of AF and development of EPoAF was absent. Not only did we include a larger study population, we also tested our hypothesis in patients with various underlying heart diseases. Within all these subgroups, these correlations were lacking. In the study by Lowe et al., all anti-arrhythmic drugs were discontinued peri- and post-operatively, whereas in our study all pre-operatively prescribed drugs were continued. As a result, AF inducibility is less likely to occur in our cohort.

Although the exact mechanisms of EPoAF are not fully understood, it is generally accepted that it is highly multifactorial in nature¹⁴. Factors promoting development of EPoAF following cardiothoracic surgery include for example inflammatory response, sympathetic activation and oxidative stress. In addition, EPoAF is not solely initiated by the presence of these triggers, but also depends on the presence and extensiveness of an arrhythmogenic substrate^{13, 15}. Atrial alterations on structural, electrical and contractile levels cause a higher vulnerability for development of AF¹⁶. Previous studies showed that, in patients in sinus rhythm, the extent of this arrhythmogenic substrate is highly variable in patients with similar clinical profiles¹⁷⁻¹⁹. Hence, all these factors might contribute to the lacking correlation between AF inducibility alone and development of EPoAF.

Late post-operative AF

The incidence of LPoAF in patients without AF prior to surgery in our study was only 2%. Subsequently, correlations between either AF inducibility or EPoAF and development of LPoAF were absent. This is in contrast to other reports, where incidence of LPoAF was both higher and correlated to EPoAF⁹. In a matched cohort of 488 patients without AF undergoing off-pump CABG, development of LPoAF was evaluated during a 41±23 month follow-up period. LPoAF developed in 1.4% of patients without EPoAF, compared to 10.2% of patients with EPoAF ($P < 0.001$). The difference in LPoAF prevalence is most likely due to the longer follow-up period (up to 87 months) in the latter study group.

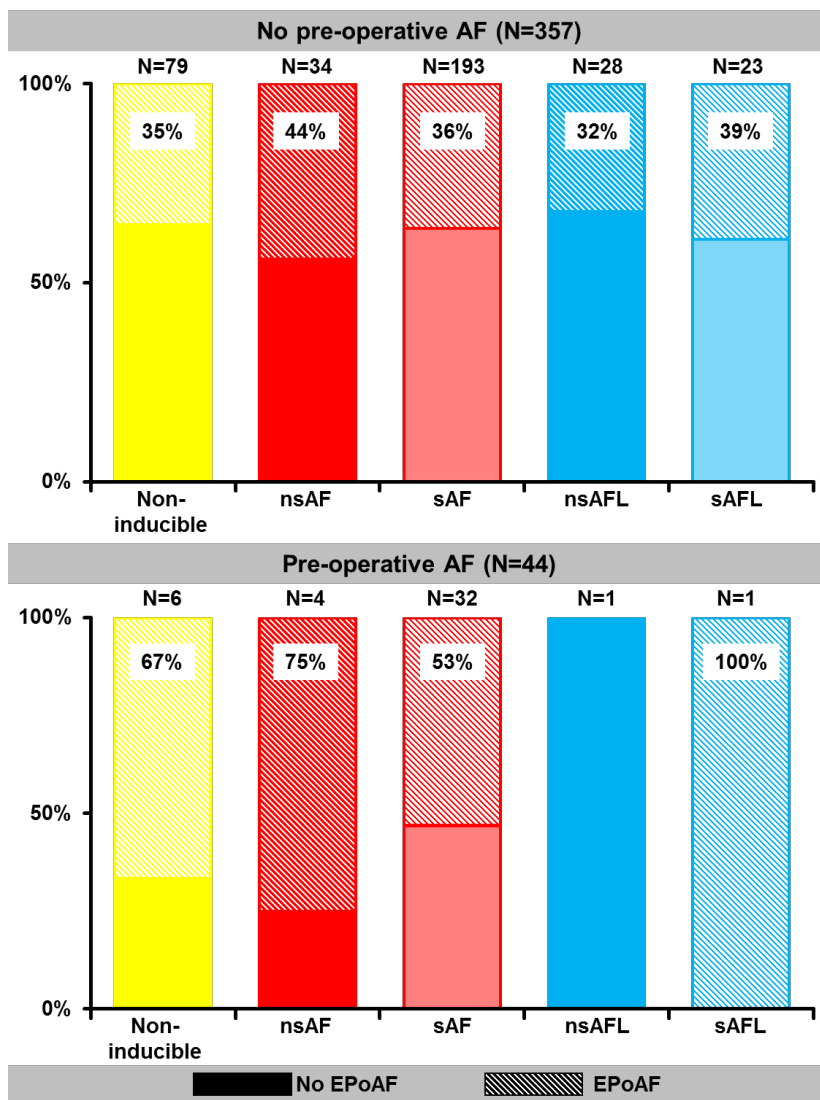


Figure 4. Relation between intraoperative inducibility and early post-operative AF. Proportion of patients that develop EPoAF (dashed) per type of arrhythmia induced, for patients without (upper panel) and with (lower panel) AF prior to surgery.

In another cohort, consisting of 571 CABG patients, EPoAF developed in 29%. Patients with EPoAF had an 8-fold increase in the risk of LPoAF development during a 3 year follow-up period⁶. Ambrosetti⁸ followed 710 patients after CABG and/or VHS. The overall LPoAF prevalence was 11% as was associated with development of EPoAF. It is however unknown whether patients had AF or other arrhythmias prior to surgery. In the present study, the overall LPoAF incidence was 14% and is thus comparable to the results provided by Ambrosetti.

Given the variances in prevalence of LPoAF and the low prevalence in our cohort, the causative relation between cardiothoracic surgery and LPoAF might be questionable. Although one can advocate for the presence of such a relation if LPoAF develops shortly after surgery, this becomes uncertain when LPoAF develops more than several months after surgery. By that time, surgery associated triggers including e.g. sterile inflammatory responses and oxidative stress are no longer present. However, general risk factors for AF such as decompensated heart failure and infections are more likely to be responsible for triggering of LPoAF episodes. Development of LPoAF recurrences after surgical ablation in the present study was 25%. This is somewhat similar to previous studies, reporting 66-69% success rates 1 year after concomitant surgical ablation^{20, 21}.

Clinical implications

EPoAF episodes in the current population are usually transient and not predictive for LPoAF. Based on our findings, one could argue whether long-term oral anticoagulants are indeed mandatory, although included as a class IIa indication in the AF guidelines¹⁰. A more conservative approach in this subpopulation may be justified with the present dataset.

In patients with AF prior to surgery in whom surgical ablation for AF was performed, recurrence rates remain relatively high. As a consequence, these patients should be monitored closely for LPoAF recurrences, before discontinuation of oral anti-coagulants can even be considered.

Study limitations

During long-term follow-up, LPoAF had to be documented on ECGs or Holter recordings. Consequently, asymptomatic short-lasting AF episodes could have been missed. For the subanalysis regarding late post-operative AF we choose to only include patients who completed the 2 year follow-up, or developed LPoAF within this period. Since a selection of patients did not yet reach the 2 year end-point, they were not included for the subanalysis.

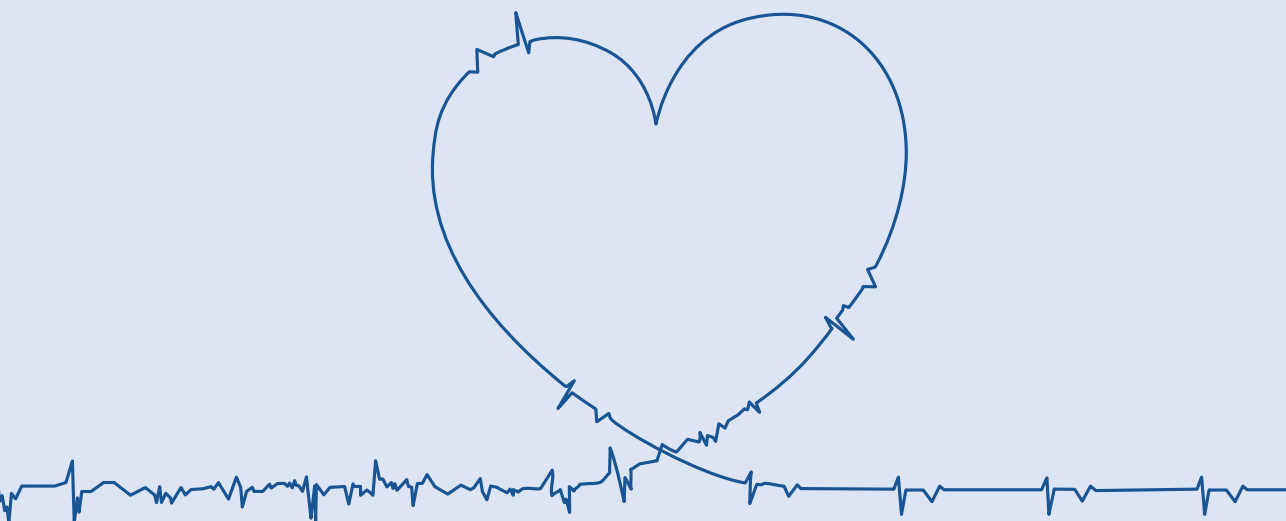
CONCLUSION

Intraoperative AF inducibility does not predict development of either EPoAF or LPoAF. In patients with AF prior to surgery, EPoAF is correlated with LPoAF recurrences. This correlation is absent in patients without AF prior to surgery in whom the incidence of LPoAF is very low.

REFERENCES

- Echahidi N, Pibarot P, O'Hara G, Mathieu P. Mechanisms, prevention, and treatment of atrial fibrillation after cardiac surgery. *J Am Coll Cardiol*. 2008;51:793-801
- Creswell LL, Schuessler RB, Rosenbloom M, Cox JL. Hazards of postoperative atrial arrhythmias. *Ann Thorac Surg*. 1993;56:539-549
- Mathew JP, Fontes ML, Tudor IC, Ramsay J, Duke P, Mazer CD, Barash PG, Hsu PH, Mangano DT, Investigators of the Ischemia R, Education F, Multicenter Study of Perioperative Ischemia Research G. A multicenter risk index for atrial fibrillation after cardiac surgery. *JAMA*. 2004;291:1720-1729
- Ahlsson A, Bodin L, Fengsrud E, Englund A. Patients with postoperative atrial fibrillation have a doubled cardiovascular mortality. *Scand Cardiovasc J*. 2009;43:330-336
- El-Chami MF, Kilgo P, Thourani V, Lattouf OM, Delurgio DB, Guyton RA, Leon AR, Puskas JD. New-onset atrial fibrillation predicts long-term mortality after coronary artery bypass graft. *J Am Coll Cardiol*. 2010;55:1370-1376
- Ahlsson A, Fengsrud E, Bodin L, Englund A. Postoperative atrial fibrillation in patients undergoing aortocoronary bypass surgery carries an eightfold risk of future atrial fibrillation and a doubled cardiovascular mortality. *Eur J Cardiothorac Surg*. 2010;37:1353-1359
- Lowe JE, Hendry PJ, Hendrickson SC, Wells R. Intraoperative identification of cardiac patients at risk to develop postoperative atrial-fibrillation. *Annals of Surgery*. 1991;213:388-392
- Ambrosetti M, Tamarin R, Griffo R, De Feo S, Fattiroli F, Vestri A, Riccio C, Temporelli PL, Ital III. Late postoperative atrial fibrillation after cardiac surgery: A national survey within the cardiac rehabilitation setting. *J Cardiovasc Med*. 2011;12:390-395
- Lee SH, Kang DR, Uhm JS, Shim J, Sung JH, Kim JY, Pak HN, Lee MH, Joung B. New-onset atrial fibrillation predicts long-term newly developed atrial fibrillation after coronary artery bypass graft. *Am Heart J*. 2014;167:593-600 e591
- Kirchhof P, Benussi S, Kotecha D, Ahlsson A, Atar D, Casadei B, Castella M, Diener HC, Heidbuchel H, Hendriks J, Hindricks G, Manolis AS, Oldgren J, Popescu BA, Schotten U, Van Putte B, Vardas P, Agewall S, Camm J, Baron Esquivias G, Budts W, Carerj S, Casselman F, Coca A, De Caterina R, Devereux S, Dobrev D, Ferro JM, Filippatos G, Fitzsimons D, Gorennek B, Guenoun M, Hohnloser SH, Kolh P, Lip GY, Manolis A, McMurray J, Ponikowski P, Rosenhek R, Ruschitzka F, Savelieva I, Sharma S, Suwalaki P, Tamargo JL, Taylor CJ, Van Gelder IC, Voors AA, Windecker S, Zamorano JL, Zeppenfeld K. 2016 esc guidelines for the management of atrial fibrillation developed in collaboration with eacts. *Eur Heart J*. 2016;37:2893-2962
- van der Does LJ, Yaksh A, Kik C, Knops P, Lanter EA, Teuwen CP, Oei FB, van de Woestijne PC, Bekkers JA, Bogers AJ, Allesie MA, de Groot NM. Quest for the arrhythmogenic substrate of atrial fibrillation in patients undergoing cardiac surgery (quasar study): Rationale and design. *J Cardiovasc Transl Res*. 2016
- Lanter EA, van Marion DM, Kik C, Steen H, Bogers AJ, Allesie MA, Brundel BJ, de Groot NM. Halt & reverse: Hsf1 activators lower cardiomyocyte damage; towards a novel approach to reverse atrial fibrillation. *J Transl Med*. 2015;13:347
- Yaksh A, van der Does LJ, Kik C, Knops P, Oei FB, van de Woestijne PC, Bekkers JA, Bogers AJ, Allesie MA, de Groot NM. A novel intra-operative, high-resolution atrial mapping approach. *J Interv Card Electrophysiol*. 2015;44:221-225
- Maesen B, Nijs J, Maessen J, Allesie M, Schotten U. Post-operative atrial fibrillation: A maze of mechanisms. *Europace*. 2012;14:159-174
- Zaman JA, Harling L, Ashrafian H, Darzi A, Gooderham N, Athanasiou T, Peters NS. Post-operative atrial fibrillation is associated with a pre-existing structural and electrical substrate in human right atrial myocardium. *Int J Cardiol*. 2016;220:580-588
- Wijffels MC, Kirchhof CJ, Dorland R, Allesie MA. Atrial fibrillation begets atrial fibrillation. A study in awake chronically instrumented goats. *Circulation*. 1995;92:1954-1968

17. Mouws E, Lanthers EAH, Teuwen CP, van der Does L, Kik C, Knops P, Bekkers JA, Bogers A, de Groot NMS. Epicardial breakthrough waves during sinus rhythm: Depiction of the arrhythmogenic substrate? *Circ Arrhythm Electrophysiol.* 2017;10
18. Lanthers EAH, Yaksh A, Teuwen CP, van der Does L, Kik C, Knops P, van Marion DMS, Brundel B, Bogers A, Allessie MA, de Groot NMS. Spatial distribution of conduction disorders during sinus rhythm. *Int J Cardiol.* 2017;249:220-225
19. Teuwen CP, Yaksh A, Lanthers EA, Kik C, van der Does LJ, Knops P, Taverne YJ, van de Woestijne PC, Oei FB, Bekkers JA, Bogers AJ, Allessie MA, de Groot NM. Relevance of conduction disorders in bachmann's bundle during sinus rhythm in humans. *Circ Arrhythm Electrophysiol.* 2016;9:e003972
20. Beukema WP, Sie HT, Misier AR, Delnoy PP, Wellens HJ, Elvan A. Intermediate to long-term results of radiofrequency modified maze procedure as an adjunct to open-heart surgery. *Ann Thorac Surg.* 2008;86:1409-1414
21. Damiano RJ, Jr., Badhwar V, Acker MA, Veeragandham RS, Kress DC, Robertson JO, Sundt TM. The cure-af trial: A prospective, multicenter trial of irrigated radiofrequency ablation for the treatment of persistent atrial fibrillation during concomitant cardiac surgery. *Heart Rhythm.* 2014;11:39-45



CHAPTER 12



EARLY MARKERS OF ATRIAL FIBRILLATION RECURRENCE AFTER PULMONARY VEIN ISOLATION

Lanters EAH, Teuwen CP, Hokken T, Rohde S, Haitisma DB,
Zijlstra F, Jordaens LJLM, de Groot NMS
Journal of Arrhythmia (2019)

ABSTRACT

Background Post procedural atrial extrasystole (AES) frequency predicts atrial fibrillation (AF) recurrence after pulmonary vein isolation (PVI) in patients with paroxysmal AF. However, the predictive value of pre-procedural AES frequency is unknown. We investigate whether pre-procedural AES frequency is a feasible marker to predict (timing of) AF recurrence after PVI.

Methods Patients (N=684) with paroxysmal or persistent AF undergoing first-time PVI were evaluated for 1) the frequency of AES/day on Holter recordings without AF prior to PVI, 2) AF episodes during the 90-day blanking period and 3) AF recurrences afterwards. The correlation between AES/day and both development and timing of AF recurrences was tested.

Results Pre-procedural AES/day was similar in patients with paroxysmal (66(20-295) AES/day) and persistent AF (115(12-248)AES/day, $P=0.915$). During the blanking period, 302(44.2%) patients showed AF episodes. AF recurred in 379(55.4%) patients at 203(105-400) days after PVI. AF recurred more frequently in patients with persistent (N=104(69.3%)) than in patients with paroxysmal AF (N=275(51.5%), $P<0.001$). Frequency of AES prior to PVI was not correlated with development ($P=0.203$) or timing ($P=0.478$) of AF recurrences. AF recurrences occurred both more frequently ($P<0.001$) and earlier ($P<0.000$) in patients with AF during the blanking period.

Conclusions AES/day prior to PVI is not correlated with (timing of) AF during the blanking period or AF recurrences, and is therefore not a feasible marker for AF recurrences in patients with PAF. AF during the blanking period is correlated with AF recurrence.

INTRODUCTION

Atrial fibrillation (AF) is often triggered by atrial extrasystoles (AES), originating from the pulmonary vein (PV) area¹. Isolation of these triggers, by means of creating circular lesions around the PVs, is a potential curative treatment modality for AF. Reported 1-year AF free survival rates after PV isolation (PVI) vary from 50 to 81%². AF recurs more frequently in patients with persistent AF (PeAF) than in patients with paroxysmal AF (PAF)³. It is generally assumed that in the former group, AF is mediated by an arrhythmogenic substrate, rather than by triggers. Identification of individual patients at risk for AF recurrences remains challenging. Clinical markers associated with AF recurrence include atrial dilatation, valvular heart disease and type of AF⁴.

The value of daily AES frequency *after* PVI for AF recurrences has been investigated previously in patients with PAF^{5, 6}. However, it is unknown whether AES frequency *prior to* PVI is a feasible marker to predict AF recurrence after PVI. Advanced atrial remodeling, due to e.g. AF, might result in increased AES frequency⁷. If AES prior to PVI were to result from non-PV foci, this could relate to AF recurrence after PVI. Since remodeled patients are also more prone to develop recurrences³, AES frequency prior to PVI could be a non-invasive, clinical marker that allows identification of subjects with a high risk for non-successful PVI outcome. Hence, AES frequency prior to PVI potentially allow early recognition of patients at risk for AF recurrence. Subsequently, this marker might be used to tailor treatment of AF to the individual patient. The aim of the current study is therefore to investigate whether AES frequency prior to PVI is associated with (timing of) development of AF in the blanking period and (timing of) AF recurrence during long-term follow-up, not only in patients with PAF but also PeAF.

METHODS

This retrospective, observational study is part of the “Arrhythmias predicted by ExtraSystoles” (A.E.S.) study. The study was approved by the institutional medical ethical committee (MEC-2016-062) and complies to the Declaration of Helsinki. Written informed consent was not obliged.

Patients undergoing first-time radiofrequency or cryoballoon PVI for drug-resistant PAF or PeAF in the Erasmus MC between 2004 and August 2015, with ≥ 1 Holter recording prior to or after ablation were evaluated. Exclusion criteria included longstanding PeAF or the absence of Holter registrations. The follow-up period extended until the end of July 2016. Clinical data were obtained from the electronic patient files.

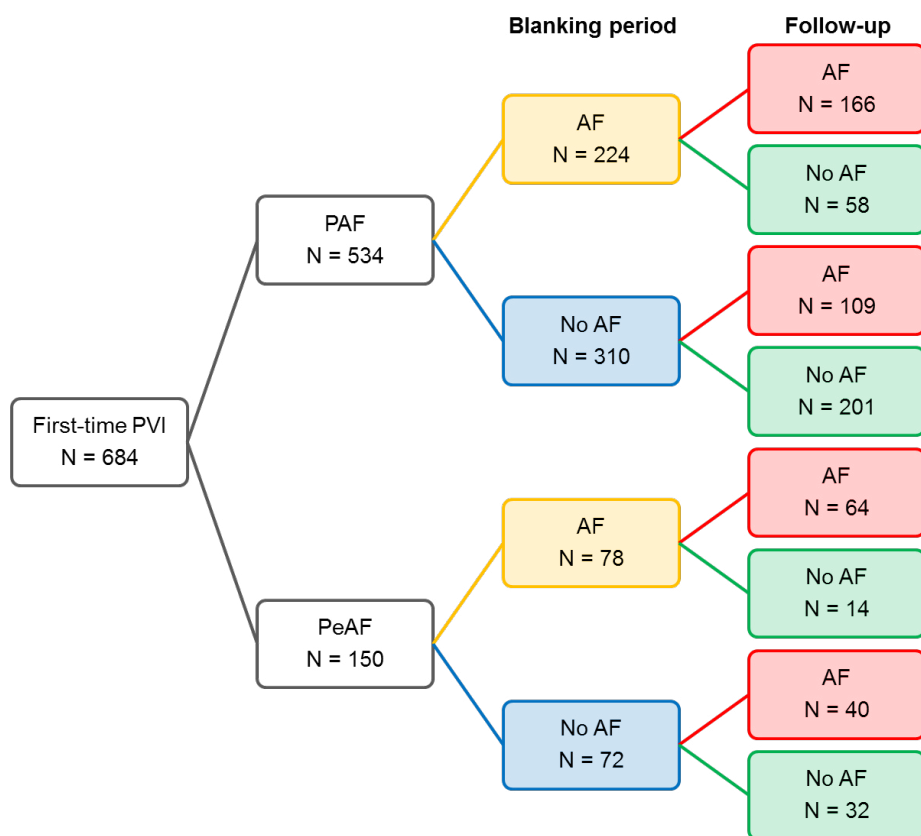


Figure 1. AF recurrence after first-time PVI. Flowchart illustrating the amount of patients with AF recurrences per type of AF prior to PVI and for patients with and without AF during the 90-day blanking period. PVI=pulmonary vein isolation; PAF=paroxysmal atrial fibrillation; PeAF=persistent atrial fibrillation; AF=atrial fibrillation.

Bêta-blockers or other anti-arrhythmic agents were not with-held prior to PVI. Drugs were continued during the first three months and thereafter discontinued to discretion of the electrophysiologist.

Patients underwent an endovascular PVI by means of radiofrequency or cryoballoon ablation. Catheter manipulation was either manual or remotely controlled. In case of radiofrequency ablation, catheter navigation was supported by electro-anatomical mapping. Immediate procedural success was defined as the presence of an exit block.

All post-procedural rhythms from various rhythm recording devices such as 12 lead surface ECG, continuous Holter registration, and implantable loop recorders were evaluated for the presence of AF^{8, 9}. The amount of AES on Holter recordings was standardized per 24 hours (AES/day). Since AES do not occur during AF episodes, Holter recordings with AF (either paroxysms or continuous) were not included for these calculations. A total AES count could

not be retrieved in 13 patients. We defined AF recurrences according to the latest guidelines, hence any documented AF episode after the blanking period^{8,9}. Consequently, AF episodes within the 90-day blanking period were not considered AF recurrences. The study endpoint was AF recurrence.

All data were tested for normality. Normally distributed, continuous data are expressed as mean±standard deviation, whereas dichotomous variables are depicted as number (percentage). Comparison of these data was performed using respectively Students *t*-test and χ^2 test. Non-parametric tests (including Kruskal-Wallis and Mann-Whitney U Tests) were applied for comparison of continuous, skewed data, which is presented as median (interquartile range). Wilcoxon signed ranks test was performed to compare two related samples of continuous, skewed variables. Spearman's rank (ρ) was applied to test the correlation between non-normally distributed continuous variables and/or categorical parameters. Due to non-normally distributed data in the amount of AES/day calculated from baseline Holter recordings, patients were categorized into quartiles of AES/day, to evaluate its effect on AF recurrences. AF free survival after PVI in various patient categories was studied with Kaplan Meier curves and log-rank testing. A P-value of 0.05 was considered statistically significant.

RESULTS

The total study population consisted of 684 patients (486 (71.1%) males). Clinical baseline characteristics of all patients are depicted in Table 1. The majority of patients underwent cryoballoon ablation (N=396, 57.9%). In 288 patients (42.1%), ablation was performed with radiofrequency energy, either manually (N=211) or with magnetic (N=47) or robotic (N=30) navigation systems. AF was paroxysmal in 534 patients (78.1%), the remaining 150 patients (21.9%) had PeAF. Prior to PVI, ≥ 1 anti-arrhythmic drugs were used by 368 (93.3%) patients, as shown in Table 1. Successful isolation of the PVs (criteria according to the recent AF guidelines)^{8,9} was achieved in all patients.

Electrophysiological parameters of all Holter recordings are summarized in Table 2. Holter recordings were performed 118(65-193) days prior to PVI. In 261(43.6%) patients, the Holter recordings showed either paroxysms or continuous AF: 140(53.6%) and 121(46.4%) recordings respectively. In 326 Holter recordings without AF episodes, a median frequency of 66(20-295) AES/day was observed on Holter recordings prior to PVI of patients with PAF

Table 1. Baseline characteristics

	Overall (N=684)
Age (yrs)	57.8±9.7
Gender (male, N (%))	486(71.1)
Type AF (N, (%))	
Paroxysmal	534 (78.1)
Persistent	150 (21.9)
Time since diagnosis (years)	3.0(1.0-6.5)
Type PVI	
Cryoballoon	396 (57.9)
Radiofrequency	288 (42.1)
<i>Echocardiography</i>	
Left atrial volume index (ml/m ²)	40.8±13.3
Left Ventricular Function (N, (%))	
Normal ¹	570 (83.3)
Mild impairment ²	92 (13.5)
Moderate impairment ³	20 (2.9)
Severe impairment ⁴	2 (0.3)
<i>Anti-arrhythmic drug usage</i>	
Class I	259 (37.9)
Class II	288 (42.1)
Class III	312 (45.6)
Class IV	50 (7.3)
<i>Cardiovascular Risk Factors</i>	
Hypertension (N, (%))	260 (38.0)
Hyperlipidemia (N, (%))	96 (14.0)
Diabetes Mellitus (N, (%))	48 (7.0)
Thyroid Disease (N, (%))	55 (8.0)
Body Mass Index (kg/m ²)	27.2±4.1

AF: atrial fibrillation; PVI: pulmonary vein isolation; BSA: body surface area; ¹ ejection fraction >50%; ² ejection fraction 40-50%; ³ ejection fraction 30-40%; ⁴ ejection fraction <30%

(N=288), whereas patients with PeAF (N=38) had 115(12-248) AES/day (P=0.915). The AES/day frequency was not correlated with anti-arrhythmic drug usage (all classes and digoxine P>0.05).

The amount of AES/day weakly correlated with age ($p=0.266$, $P<0.001$), gender ($p=-0.137$, $P=0.014$), LA volume ($p=0.212$, $P=0.006$) and diabetes ($p=0.132$, $P=0.017$). There was no correlation between AES/day and time since AF diagnosis, type of AF prior to PVI or left ventricular function or anti-arrhythmic drug usage (all $P>0.05$). In addition, none of the other known (cardiac) risk factors including BMI, hypertension, hyperlipidemia and thyroid disease correlated with AES/day (all $P>0.5$).

AF during the blanking period occurred in 302 patients (44.2%), which is depicted in the flowchart in Figure 1. Clinical variables including gender, age, body mass index, hypertension,

diabetes mellitus, hyperlipidemia, anti-arrhythmic drug usage and left ventricular function were not correlated with AF during the blanking period. However, thyroid disease ($p = 0.105$; $P = 0.006$) and type of AF ($p = 0.084$; $P = 0.028$) correlated (weakly) with AF during the blanking period. First AF episodes were documented 7.0(2.0-20.0) days after the procedure. Incidence was higher in patients with PeAF (N=78, 52.0%) than PAF (N=224, 41.9%) prior to PVI ($P=0.028$). There was no difference in the moment of the first

Table 2. Holter registrations

	Prior to PVI (N=599)
Average Heart Rate (bpm)	69 (61-80)
AF on Holter (N,%)	261 (43.6)
• Paroxysmal AF	172 (32.2)
• Paroxysms	126 (23.6)
• Continuous	46 (8.6)
• Persistent AF	89 (59.3)
• Paroxysms	14 (9.3)
• Continuous	75 (50.0)
AES/day (N)	68 (18-289)
• Paroxysmal AF	N=288
	66 (20-295)
• Persistent AF	N=38
	115 (12-248)

PVI: pulmonary vein isolation; bpm: beats per minute; AF: atrial fibrillation; AES: atrial extrasystole

AF episode between patients with PAF or PeAF: 8(2-22) versus 5(2-15) days after procedure ($P=0.092$). The incidence of AES/day prior to PVI was not associated with presence of AF episodes in the blanking period for both patients with PAF ($P=0.374$) or PeAF ($P=0.053$). Also, AES/day prior to PVI did not correlate with *timing* of AF episodes during the blanking period, in patients with PAF ($P=0.274$) and patients with PeAF ($P=0.422$).

Median follow-up time after PVI was 604(177-1822) days. Overall, AF recurred after the blanking period in 55.4% of the population (N=379) at 203(105-400) days after the procedure. The flowchart in Figure 1 shows the number of patients with AF episodes during the blanking period and AF recurrences for patients with paroxysmal or persistent AF separately. Furthermore, Figure 2 shows the fluctuations in the rhythm outcome per year of procedure for the overall study population ($P=0.003$).

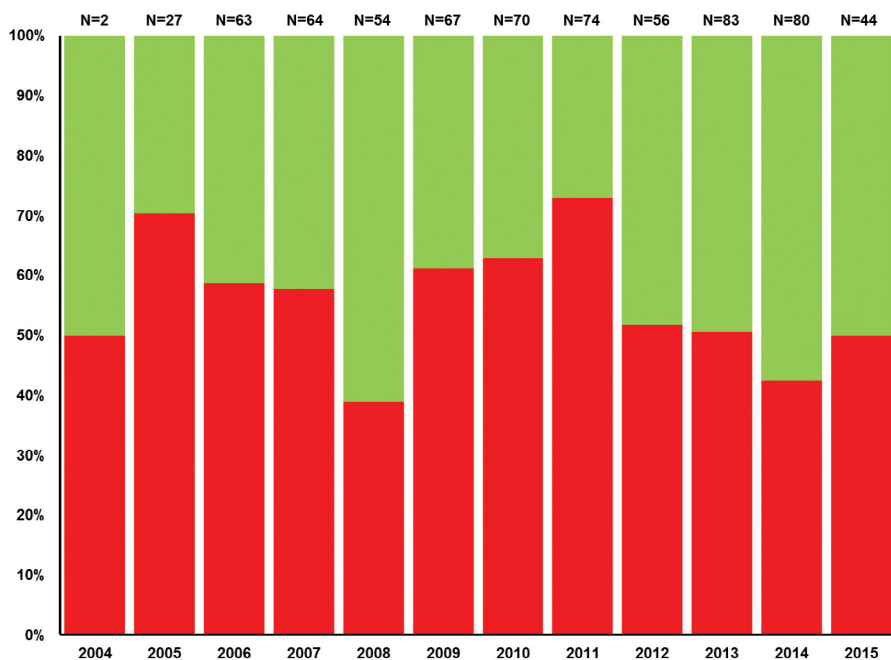


Figure 2. AF recurrence per year. Proportion of patients with AF recurrences (red) or without AF recurrences (green) after first-time pulmonary vein isolation, for each year separately.

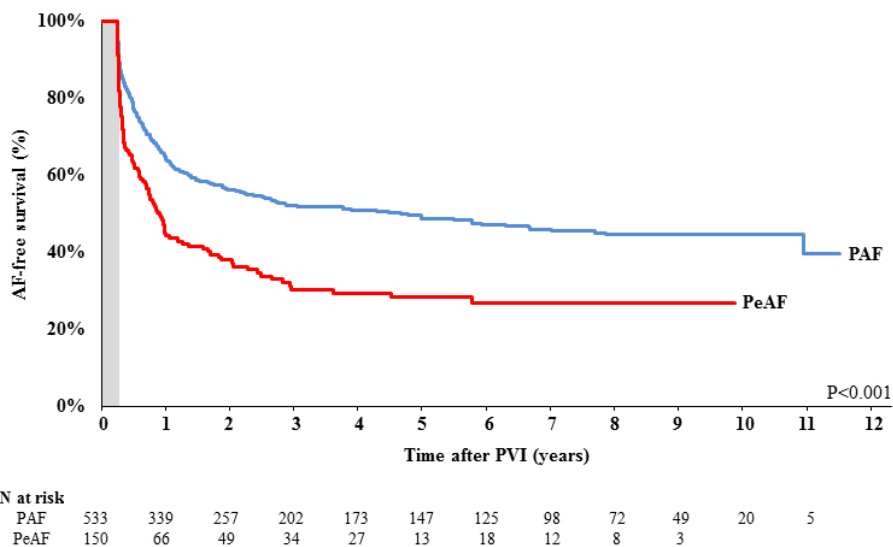


Figure 3. AF-free survival per type AF. Freedom from AF recurrences for patients with PAF (blue line) and PeAF (red line) during long-term follow-up. 90-day blanking period is indicated in grey. AF: atrial fibrillation; PAF: paroxysmal AF; PeAF: persistent AF; PVI: pulmonary vein isolation.

As illustrated in Figure 3, AF recurred more frequently in patients with PeAF (N=104 (69.3%)) than in patients with PAF (N=275 (51.5%), $P<0.001$). The majority of recurrences was observed in the first year after PVI and timing of first AF recurrence was similar in both patient groups: 168 (102-355) versus 213 (107-419) days ($P=0.112$). In 218(31.8%) patients, at least one re-do PVI was performed. Reconduction of 543 PVs was observed in 196 (92.9%) patients undergoing redo ablation and occurred equally frequent in patients with PAF or PeAF ($P=0.886$) and equally frequent after cryoballoon or radiofrequency ablation ($P=0.877$). AF recurrence was not correlated to anti-arrhythmic drug usage at baseline.

Kaplan Meier curves in Figure 4 show the AF-free survival for patients with PAF or PeAF prior to PVI with (solid lines) and without (dashed lines) AF during the blanking period separately. AF recurred more frequently in patients with (N=230, 76.2%), than in patients without AF during the blanking period (N=149, 39.0%; $P<0.001$). The curves also show that AF recurrences occurred *earlier* in both patients with PAF en PeAF with AF during the blanking period ($P<0.001$).

Overall, AES/day prior to PVI was not correlated with AF recurrence and time to first recurrence: $\rho=0.071$, $P=0.203$ and $\rho=-0.055$, $P=0.478$. The left panel of Figure 5 shows that AF recurrences in patients with paroxysmal AF prior to PVI occur equally in all four quartiles of AES/day. The right panel depicts AF-free survival for patients with persistent AF. In both patient groups, AES/day prior to PVI did not correlate with either AF recurrence or time to recurrence (Table 3).

Table 3. AES frequency and AF recurrence

	AES/day prior to PVI	Quartile AES prior to PVI
Paroxysmal AF		
AF during blanking period	$\rho=0.053$; $P=0.374$	$\rho=0.045$; $P=0.448$
Time to AF during blanking period	$\rho=0.107$; $P=0.274$	$\rho=0.058$; $P=0.552$
AF recurrence	$\rho=0.073$; $P=0.215$	$\rho=0.062$; $P=0.293$
Time to AF recurrence	$\rho=-0.047$; $P=0.574$	$\tau=-0.032$; $P=0.702$
Persistent AF		
AF during blanking period	$\rho=0.316$; $P=0.053$	$\rho=0.282$; $P=0.086$
Time to AF during blanking period	$\rho=0.244$; $P=0.422$	$\rho=0.285$; $P=0.345$
AF recurrence	$\rho=0.058$; $P=0.729$	$\rho=0.078$; $P=0.640$
Time to AF recurrence	$\rho=-0.182$; $P=0.385$	$\rho=-0.145$; $P=0.490$

DISCUSSION

The present study demonstrates that AES/day prior to PVI is not correlated with (timing of) AF in the blanking period or with (timing of) AF recurrence in PAF. As expected, AF recurrences are more frequent in patients with PeAF than with PAF. As an incidental finding, we showed that development of AF in the blanking period was correlated with AF recurrence afterwards. The predictive value of AES for development of new-onset AF has been widely studied¹⁰⁻¹². In a

large cohort of 1,357 patients with various underlying diseases, Acharya et al.¹² demonstrated that patients with ≥ 100 AES/day have a higher risk for development of new-onset AF (HR 2.97). Recently, this was also confirmed for patients with congenital heart disease¹¹. The predictive value of AES for development of AF recurrences was mainly examined *after* PVI in patients with PAF^{5, 6}, whereas the present study evaluates the value of AES *prior* to PVI in both PAF and PeAF patients. Gang et al.⁵ showed in a prospective study in 220 patients with PAF that ≥ 142 AES/day on the 6 month Holter recording was associated with a higher risk of AF recurrences after PVI (HR 2.84). However, the relation between AES prior to PVI and the long-term AF free survival after PVI was not yet described. In this era of patient tailored medicine, a more accurate estimation of the expected procedural outcome is desired for selecting the optimal strategy for each individual patient. Therefore, we examined whether a higher incidence of AES prior to PVI is associated with AF recurrences. Since this was not the case, it is most likely not a feasible marker in clinical practice. Although it is generally assumed that AES in patients with AF mainly originate from the PV area, other origins, for example the superior vena cava have also been described^{1, 13, 14}. After PVI, AES can either result from non-PV foci or from e.g. reconnection of the initially isolated PVs. In case these AES initiate AF episodes, additional ablation of these non-PVI foci could potentially cure AF in these patients. The group of Lin et al.¹⁴ showed that acute success rates of ablation of these foci were highly variable and depending on the origin of ectopy: e.g. superior vena cava (96%, N=27), posterior free wall of the left atrium (63%, N=5), crista terminalis (100%, N=10) and interatrial septum (0%, N=1). During long-term follow-up, AF recurred in 36.8% (N= 25) patients¹⁴. At present, additional ablation of non-PV foci (if reproducible) is included as a Class IIa recommendation in clinical guidelines on management of patients with AF. In the present study, AF also recurred in the absence of PV reconnection. This suggests that AES initiating AF are most likely generated by non-PV foci. Besides the above mentioned non-PV foci, AES might also be generated by other atrial areas. It is generally accepted that AF episodes induce structural and electrical remodeling of the atria^{15, 16}. As a result, cardiomyocyte hypertrophy, fibroblast proliferation and deposition of extracellular matrix lead to separation of adjacent bundles of cardiomyocytes and subsequently conduction block¹⁷. Redistribution of cell-cell connexins and downregulation of ion channels also cause impaired conduction¹⁸. Next to these conduction abnormalities, coupling of myofibroblast and cardiomyocytes also facilitates induction of spontaneous ectopic activity⁷. An intracellular calcium overload, due to atrial stress, may provoke delayed afterdepolarizations, which in turn can produce triggered activity. Altogether, this suggests that (micro)reentry and/or ectopic activity are more likely to occur in remodeled atria, which in turn may lead to an increased number of AES.

A 90-day blanking period after PVI is recommended in both European and American guidelines^{8, 9}. AF episodes within this window may result from post-procedural inflammation, edema or recovery phase. Arrhythmias in the blanking period would therefore be nonspecific and not directly related to treatment failure. Nonetheless, episodes of AF or other arrhythmias during this blanking period are frequently reported¹⁹.

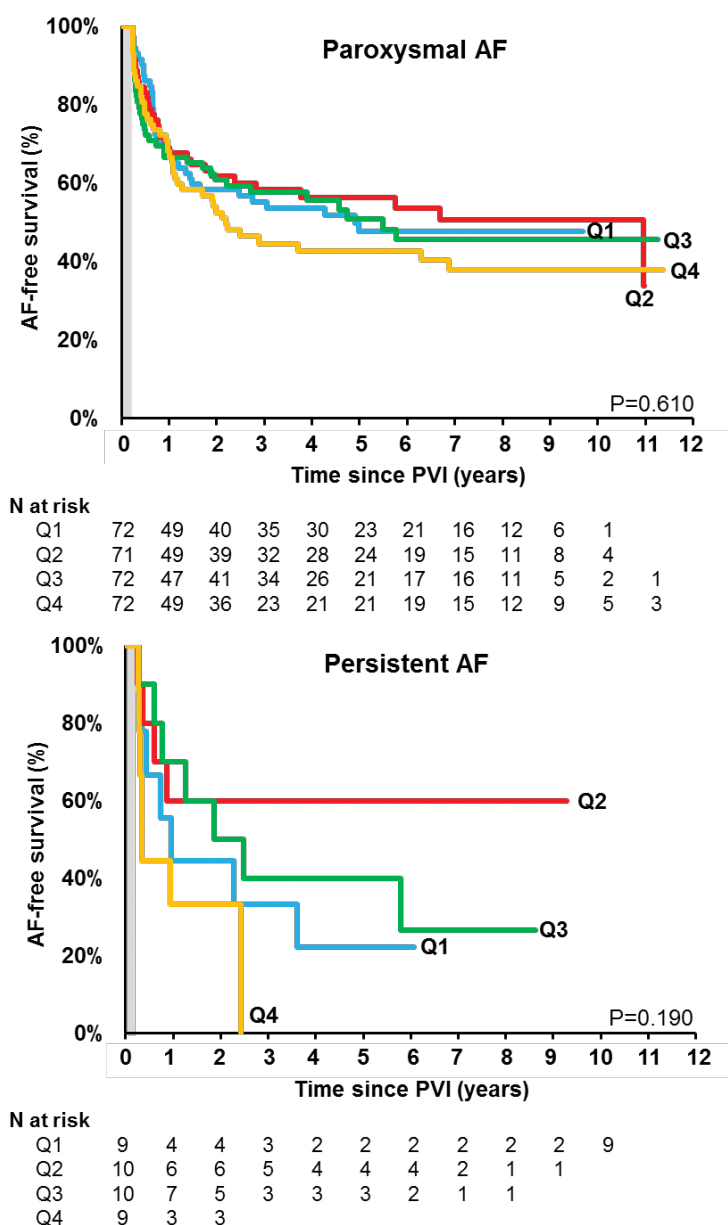


Figure 5. AF-free survival per quartile AES prior to PVI. Left panel: freedom from AF recurrences after PVI for paroxysmal AF, patients are categorized according to the number of AES/day at Holter recordings prior to PVI. Blue line: Q1 = <20ES/day. Red line: Q2 = 20-66AES/day. Green line: Q3 = 66-295AES/day. Yellow line: Q4 = >295AES/day. Right panel: freedom from AF recurrences after PVI for persistent AF, patients are categorized according to the number of AES/day prior to PVI. Blue line: Q1 = <12AES/day. Red line: Q2 = 12-115AES/day. Green line: Q3 = 115-248AES/day. Yellow line: Q4 = >248AES/day. 90-day blanking period is indicated in grey. AF: atrial fibrillation; AES: atrial extrasystole.

In a recent study, Willems et al.²⁰, examined the value of the 90-day blanking period in 401 patients undergoing first-time PVI for PAF. They show that one-year freedom from any AT decreased significantly to 28.7% if AF occurred during the blanking period, which was the case in 49.1% of the population. Also, timing of latest symptomatic AT was correlated with time to AF recurrence²⁰. The present study confirms the decrease in AF free survival in patients with not only PAF but also PeAF who have AF during the blanking period. Other AT were not included. In addition, a similar pattern is observed in patients with PeAF.

Due to the retrospective study design, not all Holter recordings prior to and after PVI were available. Most patients used anti-arrhythmic drugs, this might have influenced AES/day, although there was no difference in amount of AES in patients with or without anti-arrhythmic drugs and correlations between AES/day and drug usage were lacking. Asymptomatic and/or short lasting AF paroxysms might be missed if the patient was not connected to rhythm monitoring devices. AES frequency can vary from day to day and are influenced by for example autonomic tone and physical activity. Prolonged recordings might give a more accurate reflection of the AES frequency. For optimal comparison of AES/day between the different types of AF, a larger number of Holter recordings from PeAF patients is most likely required. Origin of AES could not be determined using three lead Holter registrations.

CONCLUSION

The amount of AES/day prior to PVI is not correlated to (timing of) AF episodes in the blanking period, or with (timing of) AF recurrences and is therefore not suitable as a biomarker to identify PAF patients at risk for AF recurrences. However, patients with AF episodes during the blanking period develop AF recurrences earlier than patients without early AF episodes.

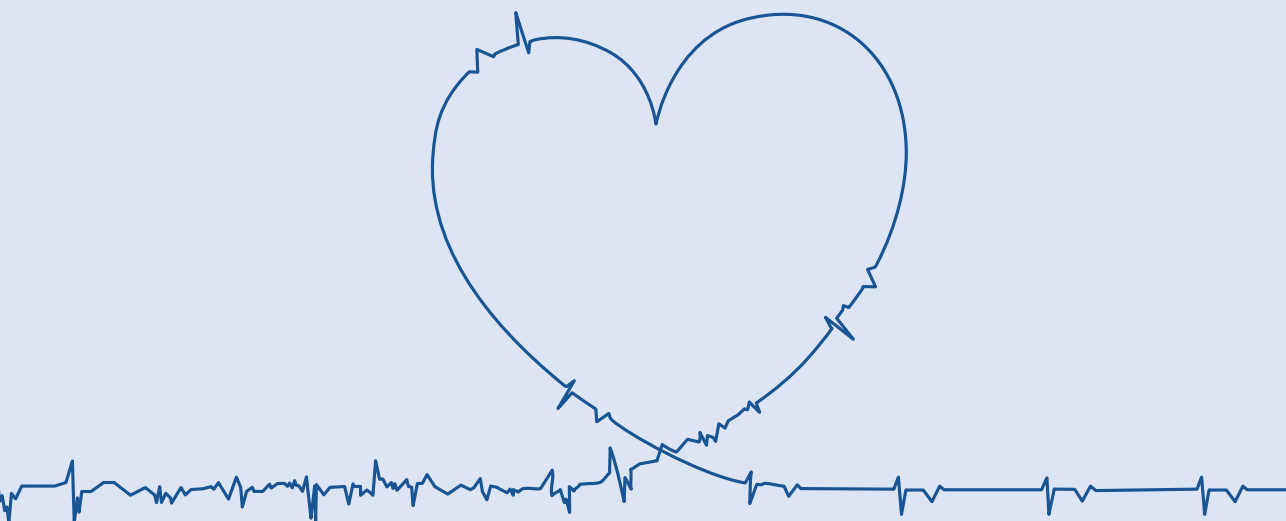
REFERENCES

1. Haissaguerre M, Jais P, Shah DC, et al. Spontaneous initiation of atrial fibrillation by ectopic beats originating in the pulmonary veins. *N Engl J Med*. 1998;339(10):659-66.
2. Ang R, Domenichini G, Finlay MC, Schilling RJ, Hunter RJ. The Hot and the Cold: Radiofrequency Versus Cryoballoon Ablation for Atrial Fibrillation. *Curr Cardiol Rep*. 2015;17(9):631.
3. Oral H, Knight BP, Tada H, et al. Pulmonary vein isolation for paroxysmal and persistent atrial fibrillation. *Circulation*. 2002;105(9):1077-81.
4. D'Ascenzo F, Corleto A, Biondi-Zoccai G, et al. Which are the most reliable predictors of recurrence of atrial fibrillation after transcatheter ablation?: a meta-analysis. *Int J Cardiol*. 2013;167(5):1984-9.
5. Gang UJ, Nalliah CJ, Lim TW, et al. Atrial ectopy predicts late recurrence of atrial fibrillation after pulmonary vein isolation. *Circ Arrhythm Electrophysiol*. 2015;8(3):569-74.
6. Yamane T, Date T, Kanzaki Y, et al. Behavior of atrial ectopic beats before and after pulmonary vein isolation in patients with atrial fibrillation: a reduction in the number and arrhythmogenicity of ectopic firings. *Heart Rhythm*. 2006;3(12):1421-7.
7. Miragoli M, Salvarani N, Rohr S. Myofibroblasts induce ectopic activity in cardiac tissue. *Circ Res*. 2007;101(8):755-8.
8. January CT, Wann LS, Alpert JS, et al. 2014 AHA/ACC/HRS guideline for the management of patients with atrial fibrillation: a report of the American College of Cardiology/American Heart Association Task Force on Practice Guidelines and the Heart Rhythm Society. *J Am Coll Cardiol*. 2014;64(21):e1-76.
9. Kirchhof P, Benussi S, Kotecha D, et al. 2016 ESC Guidelines for the management of atrial fibrillation developed in collaboration with EACTS. *Eur Heart J*. 2016;37(38):2893-962.
10. Chong BH, Pong V, Lam KF, et al. Frequent premature atrial complexes predict new occurrence of atrial fibrillation and adverse cardiovascular events. *Europace*. 2012;14(7):942-7.
11. Teuwen CP, Korevaar TI, Coolen RL, et al. Frequent atrial extrasystolic beats predict atrial fibrillation in patients with congenital heart defects. *Europace*. 2016.
12. Acharya T, Tringali S, Bhullar M, et al. Frequent Atrial Premature Complexes and Their Association With Risk of Atrial Fibrillation. *Am J Cardiol*. 2015;116(12):1852-7.
13. Inada K, Matsuo S, Tokutake K, et al. Predictors of ectopic firing from the superior vena cava in patients with paroxysmal atrial fibrillation. *J Interv Card Electrophysiol*. 2015;42(1):27-32.
14. Lin WS, Tai CT, Hsieh MH, et al. Catheter ablation of paroxysmal atrial fibrillation initiated by non-pulmonary vein ectopy. *Circulation*. 2003;107(25):3176-83.
15. Wijffels MC, Kirchhof CJ, Dorland R, Allesie MA. Atrial fibrillation begets atrial fibrillation. A study in awake chronically instrumented goats. *Circulation*. 1995;92(7):1954-68.
16. Brundel BJ, Ausma J, van Gelder IC, et al. Activation of proteolysis by calpains and structural changes in human paroxysmal and persistent atrial fibrillation. *Cardiovasc Res*. 2002;54(2):380-9.
17. Ausma J, Wijffels M, Thone F, Wouters L, Allesie M, Borgers M. Structural changes of atrial myocardium due to sustained atrial fibrillation in the goat. *Circulation*. 1997;96(9):3157-63.
18. van der Velden HM, Ausma J, Rook MB, et al. Gap junctional remodeling in relation to stabilization of atrial fibrillation in the goat. *Cardiovasc Res*. 2000;46(3):476-86.
19. Mugnai G, de Asmundis C, Hunuk B, et al. Second-generation cryoballoon ablation for paroxysmal atrial fibrillation: Predictive role of atrial arrhythmias occurring in the blanking period on the incidence of late recurrences. *Heart Rhythm*. 2016;13(4):845-51.
20. Willems S, Khairy P, Andrade JG, et al. Redefining the Blanking Period After Catheter Ablation for Paroxysmal Atrial Fibrillation: Insights From the ADVANCE (Adenosine Following Pulmonary Vein Isolation to Target Dormant Conduction Elimination) Trial. *Circ Arrhythm Electrophysiol*. 2016;9(8).

PART IV



BIOMARKERS FOR PREDICTION OF ATRIAL FIBRILLATION



CHAPTER 13



THE FUTURE OF ATRIAL FIBRILLATION THERAPY: INTERVENTION ON HEAT SHOCK PROTEINS INFLUENCING ELECTROPATHOLOGY IS THE NEXT IN LINE

Lanters EAH, van Marion DMS, Steen H, de Groot NMS, Brundel BJJM
Netherlands Heart Journal (2015)

ABSTRACT

Atrial fibrillation (AF) is the most common age-related cardiac arrhythmia accounting for one-third of hospitalizations. Treatment of AF is difficult, which is rooted in the progressive nature of electrical and structural remodelling, called electropathology, which makes the atria more vulnerable for AF. Importantly, structural damage of the myocardium is already present when AF is diagnosed for the first time. Currently, no effective therapy resolving this damage is known.

Previously, we observed that exhaustion of cardio-protective heat shock proteins (HSPs) contributes to structural damage in AF patients. Also, boosting of HSPs, by the heat shock factor-1 (HSF-1) activator geranylgeranylacetone (GGA), halted AF initiation and progression in experimental cardiomyocyte and dog models for AF. However, it is still unclear whether induction of HSPs also prolongs the arrhythmia free interval after, for example, cardioversion of AF.

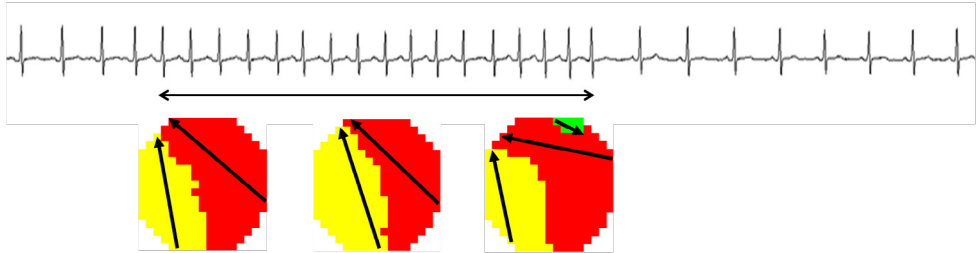
In this review, we discuss the role of HSPs in the pathophysiology of AF and give an outline of the HALT&REVERSE project, initiated by the HALT&REVERSE Consortium and the AF Innovation Platform. This project will elucidate whether HSPs 1) reverse cardiomyocyte electropathology and thereby halt AF initiation and progression and 2) represent novel biomarkers which predict the outcome of AF conversion and/or occurrence of post-surgery AF.

INTRODUCTION

Atrial fibrillation (AF) represents the arrhythmia with the highest prevalence, accounting for one third of hospitalizations related to cardiac rhythm disturbances.¹ The main risk factors to develop AF include age, cardiac surgery, valvular heart disease, congestive heart disease, ischemic cardiomyopathy, obesity, hypertension and diabetes mellitus. These risk factors cause atrial stretch and dilation and condition the heart for AF.¹ Patients with AF are frequently encountered in daily clinical practice. The goal of therapy in AF is, ideally, to abolish AF episodes and to restore sinus rhythm. This in turn re-establishes atrioventricular synchrony and improves atrial function. Despite extensive research, treatment of AF remains difficult, which is rooted in the persistent and progressive nature of this arrhythmia. An initiator, trigger and substrate are mandatory for development of AF. In this manuscript we will focus on the substrate underlying AF.

AF persistence is caused by progressive changes in the electrophysiology and structure of atrial cardiomyocytes, as demonstrated in a goat model for AF.² In this model AF resulted in shortening of the atrial effective refractory period and reversion of the physiological rate adaptation (shortening of the atrial refractory period at slower heart rates), facilitating induction and stability of AF. Similar findings have been reported in humans. The goat model of AF also revealed that longstanding AF is associated with changes in myocardial structure, including dedifferentiation, increase in cell size, perinuclear accumulation of glycogen, central loss of sarcomeres, changes in mitochondrial shape, fragmentation of the sarcoplasmic reticulum and disorganization of fiber orientation.³ These structural changes were observed in human AF as well.⁴ Importantly, structural changes are sustainable and impair electrical coupling and the functional recovery to sinus rhythm by pharmacological and electrical cardioversion. In addition, it was found that alterations of the myocardial structure underlie changes in electrophysiology as observed in AF.^{2,5} This phenomenon is commonly defined as electropathology. It should be noted that electropathology is already present when a patient enters the clinic for the first time with an AF episode. Current available pharmacological therapy is directed at alleviation of electrical changes (rhythm control) and has limited effect on patient outcome.¹ Therapeutic approaches that halt the mechanisms conveying the AF-induced structural remodelling, may offer superior therapeutic perspectives. Thus, from science to patients: reversal of electropathology of cardiomyocytes represents a key target to accomplish and maintain cardiac sinus rhythm after AF.

Paroxysmal Atrial Fibrillation



Persistent Atrial Fibrillation

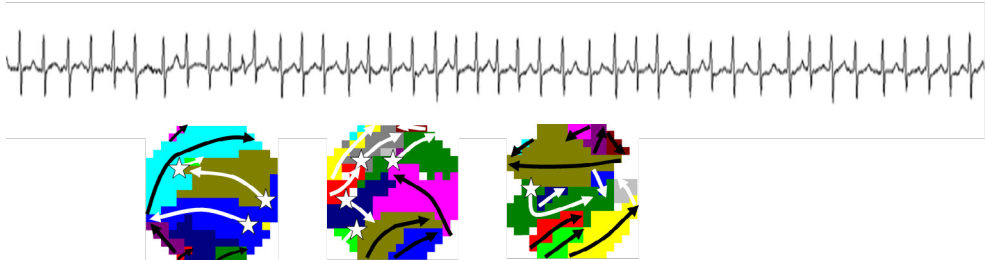


Figure 1. Persistence of atrial fibrillation. Surface electrograms of paroxysms (upper panel) and persistent (lower panel) AF. Wave-maps constructed during these different types of maps are also shown. A wave-map shows individual fibrillation waves represented by colors according to their sequence of appearance. A previously described mapping algorithm was used to classify them into peripheral waves (entering the mapping area from outside the electrode array), breakthrough waves (appearing at the epicardial surface inside the mapping area) or discontinuous conduction waves (fibrillation waves starting with a delay of 13 to 40ms from boundaries of other waves). Sites of epicardial breakthroughs are indicated by white asterisks; white arrows indicate direction(s) of expansion of epicardial breakthrough or discontinuous fibrillation waves. Peripheral fibrillation waves are indicated by black arrows.

Discontinuous Propagation in the Atria

It is generally assumed that transition of short-lasting paroxysms of AF to long-lasting episodes which do not terminate spontaneously anymore over time correspond to a progression from a trigger-driven to a substrate mediated arrhythmia due to a combination of electrical, structural and contractile atrial remodelling (Figure 1). Previous studies have demonstrated that alterations in the atrial microscopic structure impair intra-atrial conduction.⁶ Spach et al. were the first to provide evidence that '*2-dimensional propagation is discontinuous in nature at a microscopic level*' (Figure 2).^{7,8} In their experiments, variations in shape and amplitude of extracellular potential waveforms were studied when the direction of conduction was changed from longitudinal to transverse in relation to the fiber axis. They observed that in uniform anisotropic myocardium, the shape of the upstroke of the transmembrane action potential depended on the direction of propagation in relation to the fiber orientation. Fast conduction in the longitudinal direction was associated with a slow upstroke and a long τ -foot (time constant of the action potential representing voltage decay) and slow conduction in the transverse direction with a fast upstroke and a short τ -foot. Differences were explained

by the anisotropic distribution of intercellular connections (gap junctions, connexions). This was confirmed in a goat model for sustained (two months) AF, where persistence of AF was associated with a lower density and inhomogeneous distribution of gap junctions.^{9,10} Gap junctions along the fiber axis provide a low resistance to current flow which increases the space constant and hence the electrotonic current flow. Subsequently, the upstroke of the transmembrane potential in this direction decreases and the τ -foot increases. Due to the high resistance barriers in the transverse direction, the space constant is reduced and the electrotonic current is therefore smaller. This results in an increase in the upstroke of the transmembrane potential and a decrease in the τ -foot. Consequently, as the safety factor is lower during longitudinal conduction than during transverse conduction, conduction block is more likely to occur during longitudinal conduction.¹¹

Next to gap junctional remodelling, also ion channel remodelling has been demonstrated to play a role in AF progression. A marked reduction in ion (preferably L-type Ca^{2+} and transient outward K^+) channel protein expression, associated with a shortening of atrial effective refractory period, was observed in patients with AF.¹² This decrease in protein expression might be explained by increased (calcium dependent) calpain I activity, causing enhanced degradation of ion-channel proteins and contractile proteins in the myocardium.^{4,13}

Modifications of the atrial architecture affecting cardiomyocyte geometry (size and shape), gap junctions (distribution and conductivity) or the interstitial space (size and distribution) result in non-uniform anisotropic tissue. Muscle bundles become electrically dissociated due to strands of fibrotic tissue giving rise to fractionation of extracellular potentials.¹⁴ These areas of local conduction abnormalities may facilitate genesis and perpetuation of AF.

Fractionation of Extracellular Potentials

Fractionated electrograms are extracellular waveforms containing multiple, distinct deflections reflecting local asynchronous activation of myocardium surrounding the recording electrode.¹⁴ Fractionation of fibrillation potentials can be functional and/or structural in nature as local asynchronous activation can be the result of a spatial dispersion in refractory periods (functional) or non-uniform tissue anisotropy (structural, as explained above). During AF, multiple, simultaneously circulating wavelets excite the atria. A fibrillation wave may encounter atrial tissue which is partially or totally refractory due to previous excitation by another wave. This results in slowing of conduction, conduction block and turning of fibrillation waves around lines of conduction block. All these conduction abnormalities give rise to local asynchronous activation of the myocardium and thus to multiple deflections in the extracellular potentials.

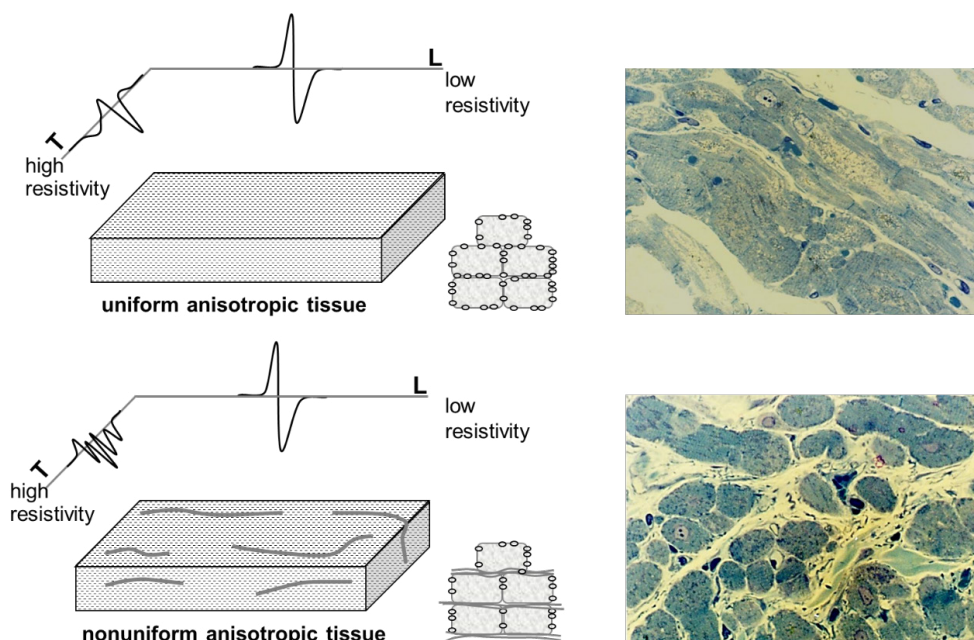


Figure 2. Discontinuous conduction. Electrograms recorded in the longitudinal and transversal conduction direction in relation to fiber orientation in uniform anisotropic and nonuniform anisotropic tissue. The electrogram in the transverse conduction direction in nonuniform anisotropic tissue consists of multiple deflections indicating discontinuous conduction. These alterations may be caused by deposition of fibrotic tissue (right panel).

High density epicardial mapping during electrically induced AF in humans without structural heart disease showed that there is a relation between the degree of fractionation in the right atrium and specific spatial patterns of activation. Double potentials were recorded along lines of conduction block (Figure 3) whereas electrograms with 3 or more deflections were recorded at pivot points or areas of slow conduction.^{15,16} In older patients with structural heart disease and longstanding persistent AF, it is likely that fractionation is more structurally determined due to dissociation of muscle bundles by fibrosis or fatty degeneration. Recent studies suggested that ablation of areas with fractionated electrograms may eliminate AF suggesting that fractionated electrograms are indeed indicative for arrhythmogenic regions perpetuating AF.¹⁷

Counteracting electropathology by heat shock proteins

Previous research has unequivocally demonstrated that the induction of the heat shock response provides protection against various cardiac diseases.¹⁸ Sensing of cellular stress activates the heat shock transcription factor-1 (HSF-1) and consequently results in the expression of heat shock proteins (HSPs). In general, HSPs function as intra-cellular chaperones for other proteins. They play an important role in protein-protein interactions such as folding and assisting in the establishment of proper protein conformation (shape) and prevention of unwanted protein aggregation, which occur during ageing of the cell and (cardiac) stress.¹⁸ Because of their essential role in protein maintenance, some members of the HSP

family are expressed at low to moderate levels in all organisms. In cardiomyocytes, HSPs bind to damaged proteins, including sarcomeric proteins, and thereby prevent cardiomyocyte toxicity and further structural remodeling and functional loss.^{19,20} HSPs consist of five HSP families, including the HSP70 and HSP27 family, which both have been suggested to convey cardioprotective effects.[19] Therefore, impairment of HSP expression, especially HSP70 and HSP27, has been related to the development of various cardiac diseases, including AF²⁰, but also metabolic diseases, such as diabetes and obesity²¹, which trigger the induction of AF.¹

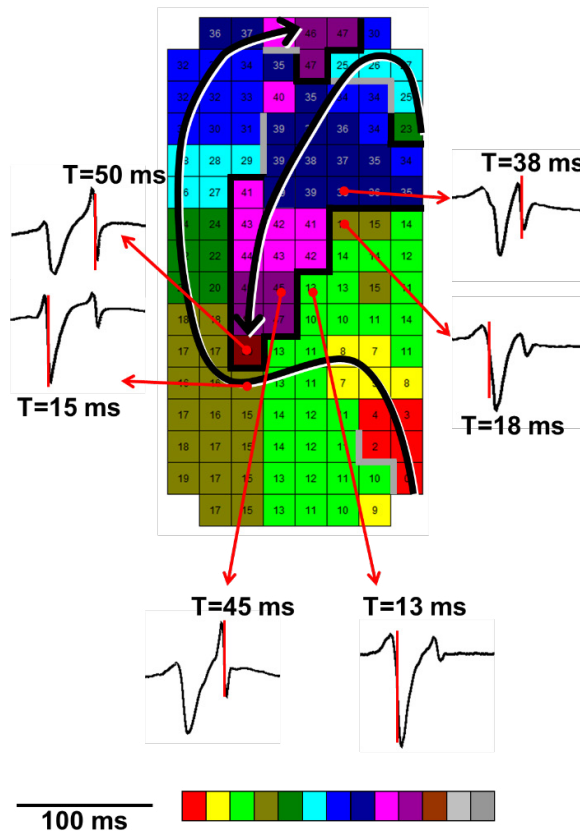


Figure 3. Double potentials recorded along lines of conduction block. The color coded activation map (interelectrode distance 2mm) shows 2 fibrillation waves (its trajectories indicated by thick black lines) separated by areas of conduction block. Electrograms consisting of 2 deflections are shown outside the activation map. They are recorded along the line of conduction block reflecting activation on either side.

These findings indicate that HSPs represent an interesting target to treat cardiac diseases such as AF. Indeed, experimental and human studies revealed that HSPs provide protection against AF initiation. In dogs, pretreatment with the HSP inducer, geranylgeranylacetone (GGA), attenuates changes in electrophysiology and conduction velocity of atrial cardiomyocytes and prevents initiation of AF in (acute) ischemia.²² Also protective effect of HSPs were observed in a rabbit model for AF induced by heart failure.²³ A further indication for the protective

effect of HSPs is obtained from 2 studies in patients undergoing cardiac surgery. In both studies an inverse correlation between higher levels of HSP70 expression in atrial tissue and lower incidence of post-operative AF was observed.^{24,25} In addition, one study described a correlation between HSP70 and HSP27 levels in tissue and improved restoration of sinus rhythm after mitral valve surgery.²⁶ In addition, high HSP27 levels in blood predict sinus rhythm maintenance after catheter ablation in patients with paroxysmal AF.²⁶ In an experimental study in mice it was observed that induction of HSP70 prevents angiotensin II-induced AF and limits atrial fibrosis formation.²⁷ Together, these results indicate that induction of HSPs, mitigates the development of the atrial substrate for the induction of AF.

In addition to the cardioprotective effect of HSPs against the induction of AF, it is expected that induced expression of HSPs also protects against AF progression. Such cardioprotective effect is supported by several studies. For example, general HSP levels were induced by a heat shock or GGA treatment in tachypaced HL-1 atrial cardiomyocytes and these cardiomyocytes were compared to normal tachypaced HL-1 cardiomyocytes.^{28,29} In these studies, tachypaced cardiomyocytes with induced HSP expression revealed improved contractile function and structural integrity. Similar protection by general HSP induction was obtained in a dog model for AF.²⁸ Dogs pretreated with GGA showed attenuation of tachypacing-induced AF promotion and limited recurrence of AF after cardioversion, most likely by limiting the electrophysiological changes including shortening of action potential duration and maintenance of L-type Ca²⁺ current.²⁸ Further studies revealed that specific members of the family of small HSPs play a key role in cardioprotection against AF. Induction of HSP27 was found sufficient to prevent tachypacing-induced structural remodelling, while overexpressing HSP70 was not protective.²⁸ Other specific small HSP family members also show protection in cellular models, including HSP20, α -HSP and HSP22, but not the other small HSP family members.²⁹ Importantly, selective knockdown of HSP27 fully attenuates the protective effect of GGA, demonstrating a main role for HSP27 in cardioprotection. A similar protective effect of the small HSP members as observed in HL-1 cardiomyocytes has been found in *Drosophila melanogaster* (fruit fly) model for tachypacing-induced contractile dysfunction. In the transparent fruit fly pupae, the heart wall can be visualized and subjected to tachypacing.³⁰ This model also allows for general induction of HSPs, either by heat shock, or by HSP-inducing compounds such as GGA, or specific induction of HSPs via genetic manipulation specifically in the heart. Indeed, induction of HSPs, especially the small HSP, by these strategies prevents tachypacing-induced contractile dysfunction and structural remodelling in *Drosophila* pupae.³⁰ Also in human AF there are indications that HSP27 may protect against cardiac remodelling and AF progression. Two independent studies report higher atrial expression levels of HSP27 to relate to a shorter duration of AF and less extensive structural damage.^{20,31} This suggests that in short duration AF the HSP response gets activated, while it exhausts in time with longer duration of AF. Since HSP27 conserves the cardiomyocyte structure, lower levels of HSP27 may trigger the progression of structural remodelling paving the way to longstanding and permanent AF. Therefore, securing HSP levels at an adequate level, e.g. by treatment with HSP inducers, may limit the expansion of the AF substrate during paroxysmal and short term AF. In agreement with this hypothesis, restoration of sinus rhythm in patients with permanent AF after mitral valve surgery is related to the HSF-1 activity and induced HSP27 levels³². Taken together, induction of HSPs attenuates electropathology of cardiomyocytes in AF. In HALT&REVERSE we will focus on the electropathological substrate of AF and dissect the mechanism of protection.

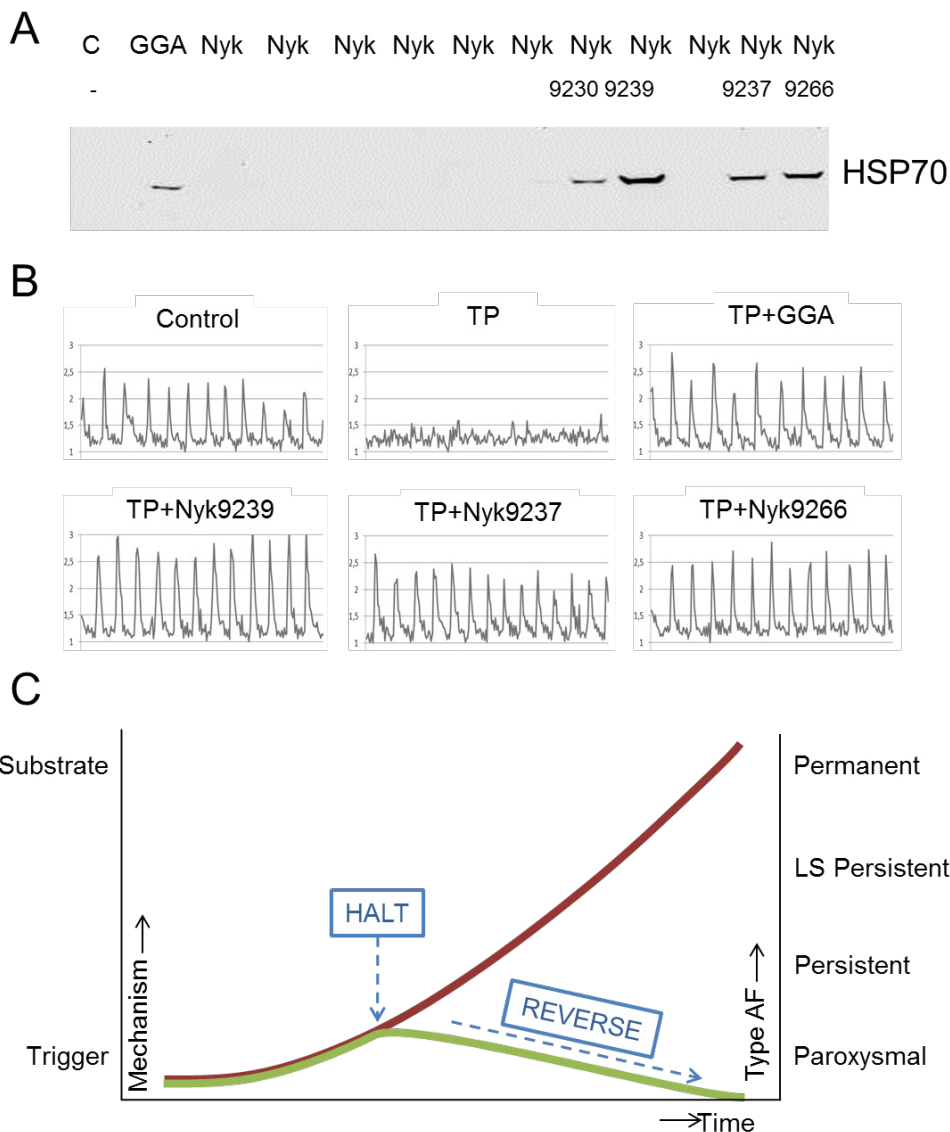


Figure 4. GGA derivatives induce HSP70 expression and reveal cardioprotective effects. A) Western Blot showing induction of HSP70 levels in HL-1 cardiomyocytes treated with GGA and some of the GGA derivatives (Nyk compounds). B) Representative calcium transient tracers of non-treated and normal paced (1Hz) HL-1 cardiomyocytes (Control) or tachypaced cardiomyocytes (TP, 5Hz) without or with treatment of 10 μ M GGA or GGA derivatives (Nyk compounds) as indicated. C) Overview of the central concept of HALT&REVERSE. AF naturally progresses in time (red line), which is rooted in the underlying electropathology. By pharmacological induction of HSP levels (blue arrow), we aim to halt or even reverse electropathology and consequently AF progression (green line).

Novel HSP-inducing agents as a therapeutic approach in AF

Pharmacological approaches to prevent mechanisms underlying atrial electropathology are being studied, with the hope that they might be useful therapeutic agents in treating AF.¹ It has been recognized that the efficacy of commonly used drugs on remodelling is limited.¹ As the protective action of HSPs depends on their temporary induction, drugs that boost the endogenous heat shock responses are of particular interest in prevention of first onset, recurrence and progression of AF. A drug often used to boost HSP expression is GGA. GGA is originally used as an anti-ulcer agent and is a nontoxic acyclic isoprenoid compound with a retinoid skeleton that induces HSP synthesis in various tissues, including gastric mucosa, intestine, liver, heart, retina, and central nervous system.^{33,34} GGA induces HSP expression through the activation of HSF-1. The protective effect of GGA-induced HSP expression on electropathology caused by tachycardia has been observed in various experimental models, including the dog model for AF.²⁸ These findings suggest that the induction of HSPs by GGA might have a potential value for clinical AF. In *in vivo* tachypaced *Drosophila*, GGA treatment protected against contractile dysfunction of the heart wall and structural remodelling.³⁰ Also in the dog model for (acute) atrial ischemia and tachypacing-induced AF promotion, an HSP-inducing GGA treatment revealed protective effects against cardiomyocyte remodelling, and consequently occurrence and recurrence of AF.²² A direct protective effect of HSP on the earlier mentioned gap junctional and ion channel remodelling has not been described (yet). However it has been shown that GGA treatment attenuates the proteolytic activity of calpain³⁰ and prevents ion channel remodelling in AF²⁸, suggesting a direct protective role of HSPs.

Although protective effects with GGA were observed, an important disadvantage of GGA is its high LogP value, which is around 9, and therefore generally high dosages are required, as found in the dog studies for AF.^{22,28} To overcome this disadvantage various derivatives of GGA have been synthesized, with improved pharmaco-chemical and HSP boosting properties (Figure 4A). Some of these derivatives also showed cardioprotective effects in tachypaced HL-1 cardiomyocytes (Figure 4B). In the HALT&REVERSE project, we will test whether these derivatives reveal improved cardioprotective effects and compared to GGA and elucidate the mode of action. In addition one of the selected GGA derivatives will be further tested in an animal model for AF. Finally, GGA has also been tested in patients undergoing cardiac surgery and atrial tissue will be used to test whether GGA induces HSP expression in patients and protects against post-surgery AF.

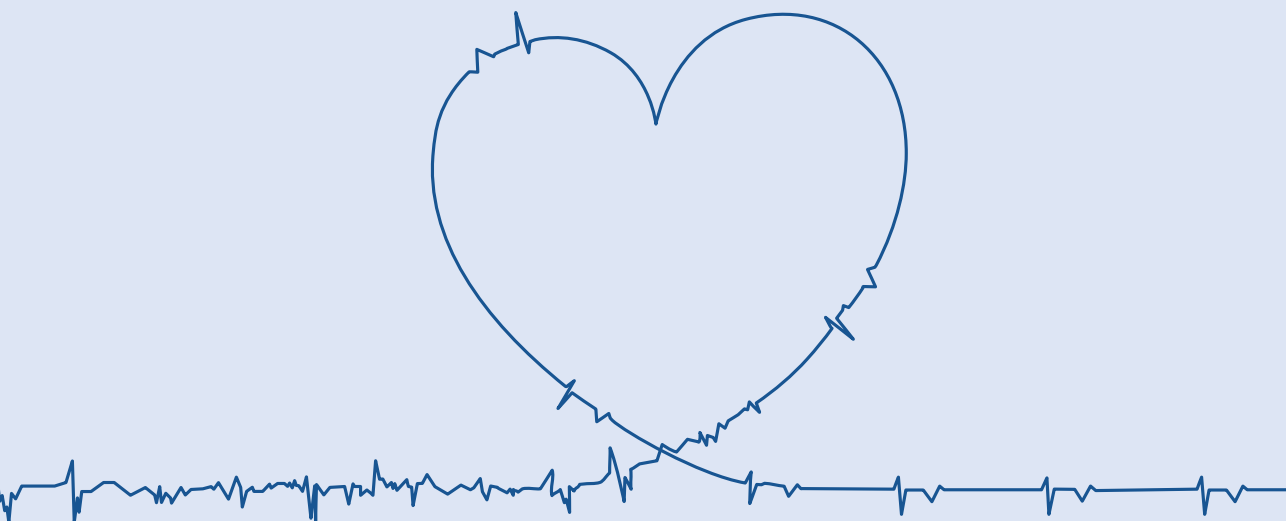
Expected findings of HALT&REVERSE

Ultimately, by inducing cardioprotective HSP expression, the HALT&REVERSE Consortium wants to halt or even reverse the structure of cardiomyocytes and therefore the electropathology in patients with AF (Figure 4C). Hereby, we expect to significantly contribute to novel rational approaches, to enhance successful recovery of heart function after ECV and/or cardiac surgery. This approach will affect the substrate underlying AF, not the trigger. For the first time, we exploit HSP levels to predict the electropathological outcome in patients, as measured by our unique mapping approaches. In addition, at the end of this project, we will know whether HSPs are suitable biomarkers for AF. Our unique approach will ultimately result in reduced hospital time, induced quality of life for the patient and lower costs for the society. The findings will be of benefit to other (cardiac, kidney) diseases, as many of those are characterized by sustainable structural remodelling. Thus the project is of major importance from a scientific, clinical and economical perspective.

REFERENCES

1. Dobrev D, Carlsson L, Nattel S. Novel molecular targets for atrial fibrillation therapy. *Nat Rev Drug Discov* 2012 Mar 30;11(4):275-291.
2. Wijffels MC, Kirchhof CJ, Dorland R, Allesie MA. Atrial fibrillation begets atrial fibrillation. A study in awake chronically instrumented goats. *Circulation* 1995;92(7):1954-1968.
3. Ausma J, Wijffels M, Thone F, Wouters L, Allesie M, Borgers M. Structural changes of atrial myocardium due to sustained atrial fibrillation in the goat. *Circulation* 1997;96(9):3157-3163.
4. Brundel BJJM, Ausma J, Van Gelder IC, et al. Activation of Proteolysis by Calpains and Structural Changes in Human Paroxysmal and Persistent Atrial Fibrillation. *Cardiovasc Res* 2002;54:380-389.
5. De Groot N, Houden R, Smeets J, et al. Electropathological substrate of longstanding persistent atrial fibrillation in patients with structural heart disease: epicardial breakthrough. *Circulation* 2010;122:1674-1682.
6. Allesie M, Ausma J, Schotten U. Electrical, contractile and structural remodeling during atrial fibrillation. *Cardiovasc Res* 2002;54:230-246.
7. Spach MS, Heidlage JF, Dolber PC, Barr RC. Electrophysiological effects of remodeling cardiac gap junctions and cell size: experimental and model studies of normal cardiac growth. *Circ Res* 2000 Feb 18;86(3):302-311.
8. Spach MS, Dolber PC. Relating extracellular potentials and their derivatives to anisotropic propagation at a microscopic level in human cardiac muscle. Evidence for electrical uncoupling of side-to-side fiber connections with increasing age. *Circ Res* 1986 Mar;58(3):356-371.
9. van der Velden HM, Ausma J, Rook MB, et al. Gap junctional remodeling in relation to stabilization of atrial fibrillation in the goat. *Cardiovasc Res* 2000 Jun;46(3):476-86.
10. Van der Velden HMW, Van Kempen MJA, Wijffels M, et al. Altered pattern of connexin40 distribution in persistent atrial fibrillation in the goat. *J Cardiovasc Electrophysiol* 1998;9:596-607.
11. Koura T, Hara M, Takeuchi S, et al. Anisotropic conduction properties in canine atria analyzed by high-resolution optical mapping: preferential direction of conduction block changes from longitudinal to transverse with increasing age. *Circulation* 2002 Apr 30;105(17):2092-2098.
12. Brundel BJJM, Van Gelder IC, Henning RH, et al. Ion channel remodeling is related to intra-operative atrial refractory periods in patients with paroxysmal and persistent atrial fibrillation. *Circulation* 2001;103:684-690.
13. Ke L, Qi XY, Dijkhuis AJ, et al. Calpain mediates cardiac troponin degradation and contractile dysfunction in atrial fibrillation. *J.Mol. Cell Cardiol.* 2008;45:685-693.
14. Spach MS. Anisotropy of cardiac tissue: a major determinant of conduction? *J Cardiovasc Electrophysiol* 1999 Jun;10(6):887-890.
15. Konings KT, Smeets JL, Penn OC, Wellens HJ, Allesie MA. Configuration of unipolar atrial electrograms during electrically induced atrial fibrillation in humans. *Circulation* 1997 Mar 4;95(5):1231-1241.
16. Yaksh A, Kik C, Knops P, et al. Atrial fibrillation: to map or not to map? *Neth Heart J* 2014 Jun;22(6):259-266.
17. Nademanee K. Trials and travails of electrogram-guided ablation of chronic atrial fibrillation. *Circulation* 2007 May 22;115(20):2592-2594.
18. Willis MS, Patterson C. Proteotoxicity and cardiac dysfunction. *N Engl J Med* 2013 May 2;368(18):1755.
19. Brundel BJJM, Ke L, Dijkhuis AJ, et al. Heat shock proteins as molecular targets for intervention in atrial fibrillation. *Cardiovasc Res* 2008;78:422-428.
20. Brundel BJJM, Henning RH, Ke L, Van Gelder IC, Crijns HJGM, Kampinga HH. Heat shock protein upregulation protects against pacing-induced myolysis in HL-1 atrial myocytes and in human atrial fibrillation. *J.Mol.Cell Cardiol.* 2006;41:555-562.

21. Chung J, Nguyen AK, Henstridge DC, et al. HSP72 protects against obesity-induced insulin resistance. *Proc Natl Acad Sci* 2008;105:1739-1744.
22. Sakabe M, Shiroshita-Takeshita A, Maguy A, et al. Effects of heat shock protein induction on Atrial Fibrillation caused by acute atrial ischemia. *Cardiovasc Res* 2008;78:63-70.
23. Chang SL, Chen YC, Hsu CP, et al. Heat shock protein inducer modifies arrhythmogenic substrate and inhibits atrial fibrillation in the failing heart. *Int J Cardiol* 2013 Oct 9;168(4):4019-4026.
24. Mandal K, Torsney E, Poloniecki J, Camm AJ, Xu Q, Jahangiri M. Association of high intracellular, but not serum, heat shock protein 70 with postoperative atrial fibrillation. *Ann Thorac Surg*. 2005;79:865-871.
25. St Rammos K, Koullias GJ, Hassan MO, et al. Low preoperative HSP70 atrial myocardial levels correlate significantly with high incidence of postoperative atrial fibrillation after cardiac surgery. *Cardiovasc Surg*. 2002;10:228-232.
26. Hu YF, Yeh HI, Tsao HM, et al. Electrophysiological correlation and prognostic impact of heat shock protein 27 in atrial fibrillation. *Circ Arrhythm Electrophysiol* 2012 Apr;5(2):334-340.
27. Wakisaka O, Takahashi N, Shinohara T, et al. Hyperthermia treatment prevents angiotensin II-mediated atrial fibrosis and fibrillation via induction of heat-shock protein 72. *J.Mol.Cell Cardiol*. 2007;436:616-626.
28. Brundel BJJM, Shiroshita-Takeshita A, Qi XY, et al. Induction of heat-shock response protects the heart against atrial fibrillation. *Circ Res* 2006;99:1394-1402.
29. Ke L, Meijering RAM, Hoogstra-Berends F, et al. HSPB1, HSPB6, HSPB7 and HSPB8 protect against RhoA GTPase-induced remodeling in tachypaced HL-1 atrial myocytes. *PlosOne* 2011;6:e20395.
30. Zhang D, Ke L, Mackovicova K, et al. Effects of different small HSPB members on contractile dysfunction and structural changes in a *Drosophila melanogaster* model for Atrial Fibrillation. *J Mol Cell Cardiol* 2011;51:381-389.
31. Yang M, Tan H, Cheng L, et al. Expression of heat shock proteins in myocardium of patients with atrial fibrillation. *Cell Stress & Chaperones* 2007;12:142-150.
32. Cao H, Xue L, Xu X, et al. Heat shock proteins in stabilization of spontaneously restored sinus rhythm in permanent atrial fibrillation patients after mitral valve surgery. *Cell Stress & Chaperones* 2011.
33. Ooie T, Takahashi N, Saikawa T, et al. Single oral dose of geranylgeranylacetone induces heat-shock protein 72 and renders protection against ischemia/reperfusion injury in rat heart. *Circulation* 2001;104:1837-1843.
34. Katsuno M, Sang C, Adachi H, et al. Pharmacological induction of heat-shock proteins alleviates polyglutamine-mediated motor neuron disease. *Proc Natl Acad Sci USA* 2005;102:16801-16806.



CHAPTER 14

A horizontal ECG line with several QRS complexes.

14

DIAGNOSIS AND THERAPY OF ATRIAL FIBRILLATION: THE PAST, THE PRESENT AND THE FUTURE

van Marion DMS, Lanthers EAH, Wiersma M, Allesie MA,
Brundel BJJM, de Groot NMS
Journal of Atrial Fibrillation (2015)

ABSTRACT

Atrial fibrillation (AF) is the most common age-related cardiac arrhythmia. It is a progressive disease, which makes treatment difficult. The progression of AF is caused by the accumulation of damage in cardiomyocytes which makes the atria more vulnerable for AF. Especially structural remodeling and electrical remodeling, together called electropathology are sustainable in the atria and impair functional recovery to sinus rhythm after cardioversion.

The exact electropathological mechanisms underlying persistence of AF are at present unknown. High resolution wavemapping studies in patients with different types of AF showed that longitudinal dissociation in conduction and epicardial breakthrough were the key elements of the substrate of longstanding persistent AF. A double layer of electrically dissociated waves propagating transmurally can explain persistence of AF (Double Layer Hypothesis) but the molecular mechanism is unknown. Derailment of proteasis –defined as the homeostasis in protein synthesis, folding, assembly, trafficking, guided by chaperones, and clearance by protein degradation systems – may play an important role in remodeling of the cardiomyocyte. As current therapies are not effective in attenuating AF progression, step-by-step analysis of this process, in order to identify potential targets for drug therapy, is essential. In addition, novel mapping approaches enabling assessment of the degree of electropathology in the individual patient are mandatory to develop patient-tailored therapies. The aims of this review are to 1) summarize current knowledge of the electrical and molecular mechanisms underlying AF, 2) discuss the shortcomings of present diagnostic instruments and therapeutic options and 3) to present potential novel diagnostic tools and therapeutic targets.

INTRODUCTION

The first electrocardiogram (ECG) of atrial fibrillation (AF) was recorded by Einthoven in 1906.¹ Nowadays, AF is one of the most common arrhythmias with a prevalence varying from <0.1% to >12% in the elderly which is expected to be doubled in patients over 55 years by 2060.^{2,3} AF is originally known as a disease of the ageing population. However, an increasing prevalence is seen in young adults, especially in endurance athletes⁴ and patients with congenital heart disease.⁵ Hence, a continuous rise in the number of AF associated hospitalizations and healthcare costs is to be expected.⁶ Several treatment modalities have been developed, but all are associated with high recurrence rates or negative side effects. The aims of this review are to 1) summarize current knowledge of the electrical and molecular mechanisms underlying AF, 2) discuss the shortcomings of present diagnostic instruments and therapeutic options and 3) to present potential novel diagnostic tools and targets for future therapy.

Deficiencies in diagnostic tools of atrial fibrillation

AF is usually diagnosed by a surface ECG or Holter recording. However, diagnosis of new onset, paroxysmal or asymptomatic AF can be challenging. An ECG only captures several seconds of the heart rhythm and episodes of AF can therefore be easily missed. The use of long-term ambulatory electrocardiography devices or implantable loop recorders increases the chance of detecting AF paroxysms. In addition, these devices also allow determination of the total duration of all AF episodes within a specific time frame, the so-called AF burden. However, electrocardiographic recordings do not provide any information on the mechanism underlying AF. Recent studies⁷⁻¹⁰ suggest that body surface mapping arrays, containing 252 electrodes, may be useful to identify driver regions in patients with AF. Yet, none of the currently available recording techniques can determine the degree and extensiveness of atrial electropathology. Hence, when a patient presents with AF, we have no diagnostic tool available for evaluating the mechanism underlying AF and determining the stage of the disease at any time in the process.

Mechanisms of atrial fibrillation: from past to the present

Experiments performed by Gordon Moe¹¹ nearly 60 years ago, provided the basis for the ongoing debate on the underlying cause for AF. In isolated canine atria, he showed that AF could be due to either *fibrillatory conduction* (AF caused by an ectopic focus with a high frequency discharge resulting in non-uniform excitation of the atria) or *true fibrillation* (AF persists independently from the site where it was initiated). In 1959, Moe¹¹ introduced the so-called Multiple Wavelet Hypothesis which further described the features of true fibrillation. In this hypothesis, Moe postulated that persistence of AF depended on the average number of wavelets. With the total number of wavelets being increased, the probability of extinguishment and thus termination of AF would become smaller. Twenty-six years later, Allesie et al.¹² performed the first experimental evaluation of Moe's multiple wavelet hypothesis. In a canine right atrium, during 0.5 second of acutely induced AF, he demonstrated in series of consecutive excitation maps that there was a continuous beat-to-beat change in activation pattern. The critical number of wavelets in both right and left atria necessary to perpetuate AF was estimated to be between three and six. Ever since, numerous experimental and clinical mapping studies^{11, 13-21}, reporting on perpetuation of AF, are supportive on either a

focal (repetitive ectopic discharges) or reentrant mechanism (mother-wave, rotor, multiple wavelets). In the past years, most clinical studies reported on the presence of rotors in patients with various types of AF²².

Electropathology associated with persistence of atrial fibrillation

High-resolution wavemapping studies²³ of AF in patients with valvular heart disease and longlasting persistent AF, demonstrated that a large proportion of fibrillation waves were so-called focal waves. These waves appeared in the middle of the mapping area and could not be explained by fibrillation waves propagating in the epicardial plane. Focal fibrillation waves appeared scattered throughout the mapping area and were not repetitive (Figure 1). The coupling interval was longer than the dominant AF cycle length, and unipolar electrograms at the epicardial origin of these waves exhibited R-waves.²³ Hence, characteristics of these focal fibrillation waves strongly suggest that they originated from endo-epicardial breakthrough. These findings were supported by a report from Lee et al.²⁴ who observed that more than one third of the fibrillation waves in patients with persistent AF were of 'focal' origin without any area sustaining focal activity. Based on our observations, we recently introduced a new mechanism explaining persistence of AF independently of the presence of foci or re-entrant circuits in our Double Layer Hypothesis^{23, 25}. The "Double Layer Hypothesis" states that the substrate of longstanding persistent AF in humans is caused by progressive endo-epicardial dissociation, transforming the atria into an electrical double layer of dissociated waves that constantly 'feed' each other (Figure 1). Whereas in patients with short-lasting episodes of AF, the endo- and epicardial layers are still activated synchronously, in patients with longstanding persistent AF, the endo- and epicardial layers of the atrial wall are activated *asynchronously*. Over time, due to electrical and structural remodeling of the atria, the atrial wall is gradually transformed into a double layer of narrow anatomically delineated pathways. The exact molecular mechanisms underlying electrical dissociation are, however, unknown.

Molecular mechanisms underlying electropathology atrial fibrillation

As mentioned above, AF is a progressive disease, which can be explained by the fact that AF itself induces alterations in both function and structure of the cardiomyocyte. These alterations induce an arrhythmogenic substrate which facilitates perpetuation of AF episodes²⁶.

During the last decennia, various researchers aimed to identify the molecular mechanisms that underlie cardiomyocyte remodeling and AF progression. Although several pathways, especially related to ion channel remodeling, have been described, the exact molecular mechanisms driving AF remodeling and progression are still unidentified. The general concept is that during AF, cardiomyocytes are subjected to rapid and irregular excitation causing calcium overload in the cells which leads to fast and reversible electrical remodeling and slower, irreversible structural remodeling (Figure 2). The cardiomyocyte responds to a calcium overload by the functional downregulation of L-type Ca^{2+} current channels, which causes the shortening of action potential duration (APD) and electrical remodeling, thereby providing a further substrate for AF.²⁷⁻³¹ Also, several other ion channel currents are affected either on the expression level or phosphorylation and redox status.³²⁻³⁴ In addition, various kinases

and phosphatases become activated and regulate the function of ion channels and other downstream target proteins, for example transcriptions factors, various calcium handling proteins (such as RyR2, Sarcoplasmic Reticulum Ca^{2+} ATPases (SERCA), or $\text{Na}^+/\text{Ca}^{2+}$ exchanger) and the actin cytoskeleton.³⁵⁻³⁹

When AF persists beyond a few days, irreversible structural remodeling occurs, especially hibernation⁴⁰ (Figure 2). Various research groups⁴⁰⁻⁴² showed that hibernation is a form of tissue adaptation. It is defined as the ability of the cardiomyocytes to turn into a non-functional phenotype featuring irreversible degradation of the myofibril structure (myolysis), which leads to loss of atrial contraction.

While the early electrical remodeling is reversible³¹ a 'second factor' underlies the persistence of AF, having a time course comparable to AF-induced structural changes (hibernation/myolysis) in the atrial cardiomyocytes.⁴³ Thus, the prevention of structural remodeling represents a key target to attenuate cardiomyocyte remodeling and dysfunction and may improve the outcome of (electrical) cardioversion to normal sinus rhythm. We have strong indications that derailment of proteostasis represents this 'second factor' that underlies AF progression.^{39, 40, 44-47}

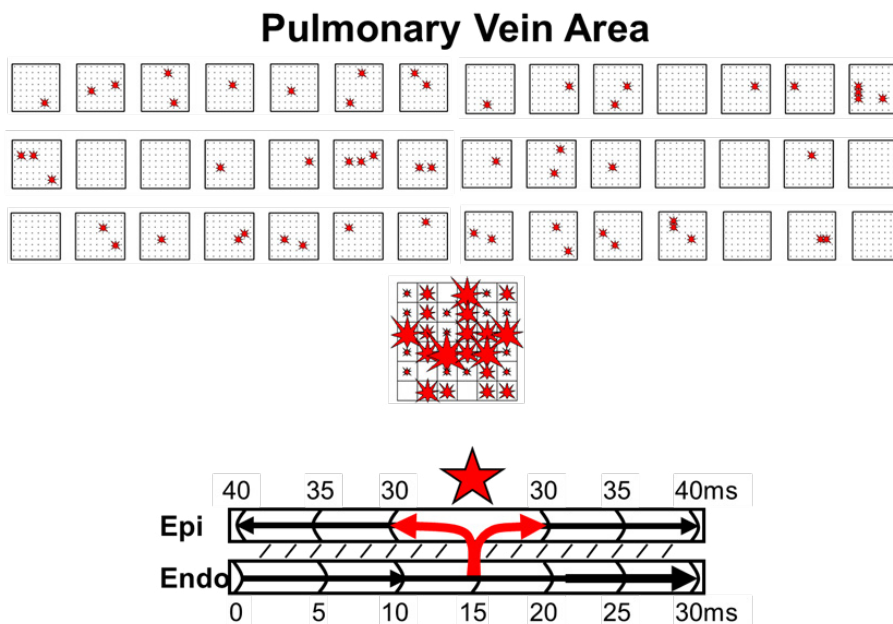


Figure 1. Epicardial breakthrough. Upper panel: beat-to-beat variation in spatiotemporal distribution of epicardial breakthrough waves ('focal waves') during 6 seconds of persistent AF in a small area of 1.25 X 1.25cm between the pulmonary veins. Each asterisk indicates a breakthrough site. The large map shows all 55 epicardial breakthrough sites. The size of the asterisk is proportional to the number of epicardial breakthroughs occurring at that site. The breakthrough map demonstrates a wide distribution of these focal waves; none of these breakthrough waves occurred, however, repetitively. Lower panel: schematic presentation of excitation of the endo- and epicardial layer explaining how transmural conduction from the endocardium to the epicardium gives rise to an epicardial breakthrough wave. Hence, the endocardial layer serves in this case as a source for 'new' fibrillation waves in the epicardial layer.

Derailed proteostasis: novel concept of cardiomyocyte remodeling

Proteostasis is defined as the homeostasis in protein synthesis, folding, assembly, trafficking, guided by chaperones, and clearance by protein degradation systems⁴⁸⁻⁵¹. Healthy proteostasis is controlled by an exquisitely regulated network of molecular components and cellular pathways, the protein quality control (PQC) system^{48, 52}. Cells, including cardiomyocytes, are very sensitive to changes in the intra- and extracellular environment, induced by stressors, including AF. Stressors can cause derailment in the proteostasis by altering the stability of proteins, leading to protein damage, unfolding and breakdown, as observed for cardiac troponins and structural proteins^{39, 44}. In the heart, various chaperones, especially Heat Shock Proteins (HSPs), are expressed to ensure a healthy cardiomyocyte proteostasis and optimal function of the heart. For example HSP27, α HSP, HSP20 and HSP22 are important members of the PQC system and attenuate derailment of proteostasis in AF by assisting in the refolding of unfolded proteins^{39, 52}, prevention of AF-induced damage to contractile proteins^{45, 53} and attenuation of protein breakdown⁴⁴. In this way, HSPs normalize the proteostasis and protect the cardiomyocyte against remodeling and AF progression.

Molecular pathways underlying derailed proteostasis

Recently, several molecular pathways were found to induce derailment of proteostasis. These pathways include the persistent activation of calpain, activation of RhoA/ROCK pathway and the activation of HDAC6. Investigators found proof for a role of persistent activation of the calcium overload-induced protease calpain to underlie impairment of proteostasis and AF progression in experimental cardiomyocyte, and *Drosophila* model systems for AF^{44, 53, 54}, but also in human permanent AF.⁴⁰ In experimental studies it was observed that calpain activation causes the degradation of contractile and structural proteins, and subsequently contributes to structural cardiomyocyte remodeling (myolysis) and dysfunction and AF progression.^{44, 54} The role of calpain was confirmed in human AF. Here, a significant induction in calpain activation was observed in patients with permanent AF, compared to patients with paroxysmal AF and controls in sinus rhythm.⁴⁰ Furthermore, patients with permanent AF revealed induced amounts of myolysis which correlated significantly with calpain activity levels, suggesting a role for calpain in derailment of cardiomyocyte proteostasis, structural remodeling and AF progression.

Also, during AF, RhoA-GTPases are activated. RhoA-GTPases represent a family of small GTP-binding proteins that are involved in cell cytoskeleton organization, migration, transcription and proliferation. They have an important role as regulators of the actin cytoskeleton in cardiomyocytes⁵⁵ and trigger the initiation of AF.^{56, 57} RhoA-GTPases activation results in conduction disturbances and cardiac dysfunction.^{58, 59} Recent studies³⁹ revealed that in AF, RhoA-GTPase become activated resulting in the activation of its downstream effector ROCK and thereby stimulate the polymerization of G-actin to filamentous F-actin stress bundles. These stress bundles impair calcium homeostasis and contribute to contractile dysfunction, cardiomyocyte remodeling and AF progression.³⁹

Furthermore, recently it was found that histone deacetylases (HDACs), such as HDAC6, are implicated in AF-induced cardiomyocyte remodeling.⁴⁴ HDACs affect cardiomyocyte proteostasis by epigenetically regulating protein expression and modulating various

cytoplasmic proteins, including α -tubulin, a structural protein from the microtubule network.⁶⁰⁻⁶² By using mutant constructs, AF-induced contractile dysfunction and structural remodeling was proven to be driven by HDAC6 via de-acetylation of α -tubulin and finally breakdown of microtubules by calpain. This effect of HDAC6 was observed in tachypaced HL-1 atrial cardiomyocytes, *Drosophila*, dogs and confirmed in patients with permanent AF.⁴⁴ HDAC6 inhibition by tubacin conserved the microtubule homeostasis and prevented depolymerized α -tubulin from calpain-mediated degradation. These results indicate a key role for HDAC6 in the derailment of cardiomyocyte proteostasis in experimental and clinical AF. So, three key pathways in AF-induced structural and functional remodeling have been identified, and all these pathways impair a healthy proteostasis of the cardiomyocyte.

Induction of HSPs normalize proteostasis

To maintain a good functioning PQC system, numerous chaperones are expressed to ensure a healthy cardiomyocyte proteostasis.³⁹ HSPs are under the control of heat shock transcription factor 1 (HSF1), and represent important chaperones in proteostatic control.^{48, 63} During excessive stress situations such as AF, HSP levels were found to become exhausted.⁴⁵ This finding suggests that upregulation of HSP levels might normalize proteostasis and improve cardiomyocyte function in AF. In clinical studies, induced HSP levels showed protection against AF initiation and progression. HSP70 atrial expression levels were found to correlate with reduced incidence of post-operative AF in patients in sinus rhythm undergoing cardiac surgery.^{64, 65} In another clinical study⁶⁶, a potent Heat Shock Response (HSR) and high HSP27 levels have been associated with restoration of normal sinus rhythm in patients with permanent AF after mitral valve surgery. Higher atrial HSP27 levels were found to be related to shorter AF duration and less myolysis when comparing paroxysmal versus persistent AF and sinus rhythm.^{45, 67} These findings suggest that HSPs become activated after AF episodes, and exhaust in time in a stress related manner.⁴⁵ Consequently, PQC is lost and incorrect/damaged proteins accumulate in cardiomyocytes, inducing or accelerating remodeling, in turn resulting in AF progression and recurrence. Next to AF, also a loss of PQC is recognized to contribute to the deterioration of heart function, reduction of stress tolerance, and the possibility of reducing the threshold for manifestation of cardiac disease.⁶⁸

Various *in vitro* and *in vivo* models for tachypacing-induced AF identified HSPs to protect against AF initiation and against the derailment of proteostasis and cardiomyocyte remodeling. HSPs increase SERCA activity and stimulate both the reuptake of Ca^{2+} into the sarcoplasmic reticulum and the removal of Ca^{2+} out of the cardiomyocyte via $\text{Na}^+/\text{Ca}^{2+}$ exchanger⁶⁹, suggesting that HSPs attenuate AF progression by protecting against (tachypacing-induced) changes in calcium handling proteins. Several HSPs (including HSP27) were shown to reduce oxidative stress, thereby potentially preventing or restoring the redox status of the ion channels⁷⁰ and preventing damage to the actin cytoskeleton. This protective effect of HSP27 was found via direct binding to actin filaments and indirectly by preserving the redox status.^{44, 45, 71-74} Reducing oxidative stress preserves proteostasis and electrophysiological and contractile function of the cardiomyocyte in AF. Moreover, HSPs prevent calpain activation^{40, 54} and thereby attenuate contractile protein degradation and contractile dysfunction.

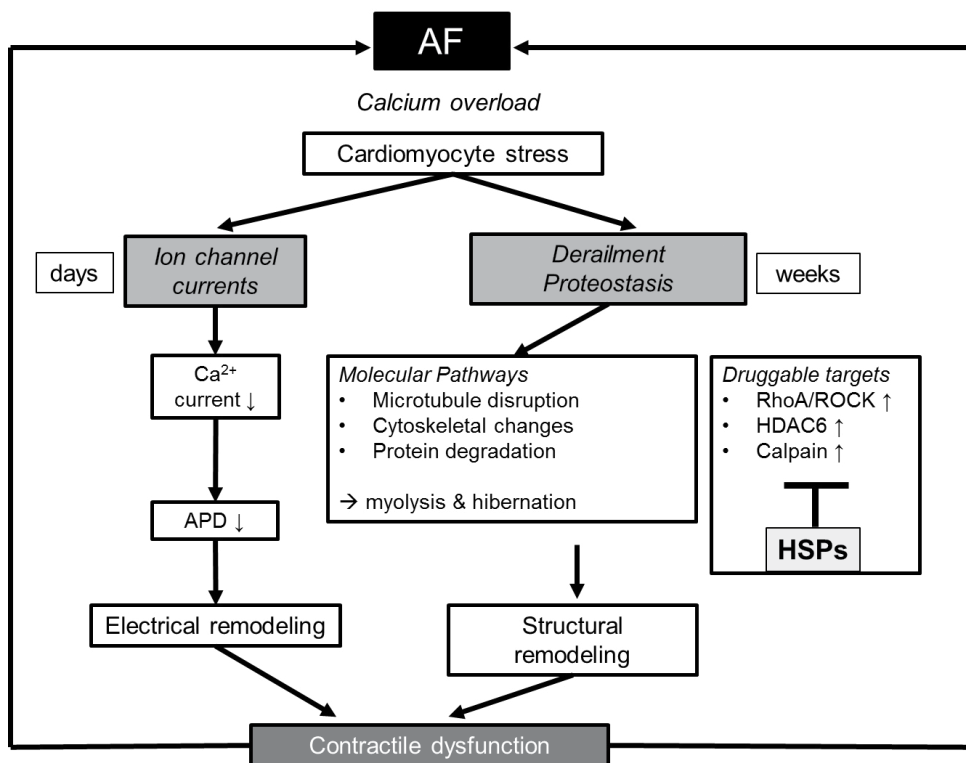


Figure 2. Overview of AF-induced cardiomyocyte remodeling. AF induces time-related progressive remodeling. First, AF causes a stressful cellular Ca^{2+} overload, which results in a direct inhibition of the L-type Ca^{2+} channel, shortening of action potential duration and contractile dysfunction. These changes have an early onset and are reversible. The early processes protect the cardiomyocyte against Ca^{2+} overload but at the expense of creating a substrate for persistent AF. When AF persists derailment of proteostasis occurs, which results in microtubule disruption, cytoskeletal changes and degradation of proteins. The targets involved in proteostasis are RhoA/ROCK, HDAC6 and calpain. In addition, HSP induction has been found to counteract these targets. Derailment of proteostasis results in structural remodeling, myolysis/hibernation, and consequently impaired contractile function and AF persistence. Thus drugs that normalize proteostasis via inhibition of RhoA/ROCK, calpain, and HDAC6, but also via induction of cardioprotective HSPs are of therapeutic interest for future treatment of clinical AF.

Deficiencies of present therapy of atrial fibrillation

Therapy of AF is aimed at either rhythm or rate control. Since AF induces electrical, structural, and contractile remodeling, therapy aimed at prevention or restoration of remodeling and consequently restoration of sinus rhythm should be the strategy of first choice.⁷⁵ The different AF treatment modalities include pharmacological therapy, electrical cardioversion (ECV), pacemaker implantation combined with His bundle ablation or surgical isolation of the pulmonary veins with or without additional linear lesions/substrate modification (endovascular or surgical). According to the Multiple Wavelet Theory, the stability of the fibrillatory process is determined by the number of simultaneously circulating wavelets. Anti-fibrillatory effects of class IA, IC and III drugs are based on widening of the excitable period (difference between

AF cycle length and refractory period). When the excitable period widens, it is less likely that a fibrillation wave encounters atrial tissue, which is still refractory. This in turn decreases the degree of fractionation of fibrillation waves and subsequently also the number of fibrillation waves. It is most likely that when patients with AF have a variable degree of remodeling due to e.g. dissimilar underlying heart diseases or AF episodes of different durations anti-arrhythmic drugs will also widen the excitable gap to a variable degree. This in turn may explain differences in inter-individual responses to anti-arrhythmic drugs. The acute success rate of intravenous chemical cardioversion (CCV) using various drugs including amiodarone and flecainide is 58-75%^{76, 77} for patients with paroxysmal or persistent AF and is highest when performed in AF <48 hours⁷⁷. Immediate (prior to discharge) AF recurrences were observed in 3% and AF relapsed in 30-40% of patients within one year with continuation of anti-arrhythmic drugs.⁷⁷ When CCV is unsuccessful, ECV is next treatment in line. Immediate restoration of sinus rhythm is achieved in 88-97%⁷⁷⁻⁷⁹. Comparable to CCV, AF recurrences are common; sinus rhythm is maintained for one year in only 40-60% of the patients.

Circumferential Pulmonary Vein Isolation (PVI), endovascular or surgical, is aimed isolating ectopic foci within the myocardial sleeves of the pulmonary veins. Endovascular PVI can be achieved with radiofrequency current, laser or cryothermal energy. Navigation of the ablation catheters can be performed either manually guided by fluoroscopy or electroanatomical mapping systems, or robotically using remote (non) magnetic navigation systems.⁸⁰⁻⁸² Despite the promising acute success rates, one year AF free survival is approximately 40-50% and redo ablations are frequently performed.⁸⁰⁻⁸³ This data is confirmed in a large meta-analysis by Ganesan et al.⁸⁴ In this study, the long-term success rate increased to 79,8%, however only after multiple ablation procedures. The overall complication rate associated with endovascular AF ablation is 5% including phrenic nerve palsy, pulmonary vein stenosis, pericardial effusion and cardiac tamponade.^{83, 85} From a theoretical point of view, PVI should be an effective treatment modality for patients with paroxysms of AF triggered by ectopic foci within the pulmonary veins. Recurrences of AF after pulmonary vein isolation can be due to incompleteness of circular lesions, conduction or an arrhythmogenic substrate located outside the pulmonary veins.⁸⁶ In addition, an arrhythmogenic substrate may also develop over time as a result of a progressive cardiomyopathy. Different ablation approaches targeting the assumed substrate of AF have therefore been developed in the past years⁸⁶ including ablation of ganglionated autonomic plexuses in epicardial fat pads or disruption of dominant rotors in the left or right atrium as recognized by high-frequency Complex Fractionated Atrial Electrograms (CFAE).⁸⁷ Wu et al.⁸⁸ concluded in a meta-analysis that CFAE ablation could reduce the recurrence of atrial tachycardia in patients with nonparoxysmal AF after a single procedure. This effect was not observed in patients with paroxysmal AF. The reported one year AF free survival after the first CFAE ablation is only 29% when performed as a standalone procedure⁸⁷ and 74% in CFAE ablation additional to PVI.^{87, 89} Endovascular ablation of the ganglionic plexi as a standalone procedure in patients with paroxysmal AF is associated with a significantly lower arrhythmia free survival when compared to the PVI.^{90, 91} When performed additionally to (repeat) PVI in patients with persistent AF, 16 months success rate rises to 59%.⁹¹ The recurrence rates of these (concomitant) substrate modifications are thus high, indicating that the arrhythmogenic substrate underlying persistence of AF was still not fully understood. Our Double Layer Hypothesis^{23, 25} provides the explanation why, in case the endo- and epicardial layers are electrically dissociated, ablative therapy is not successful anymore.

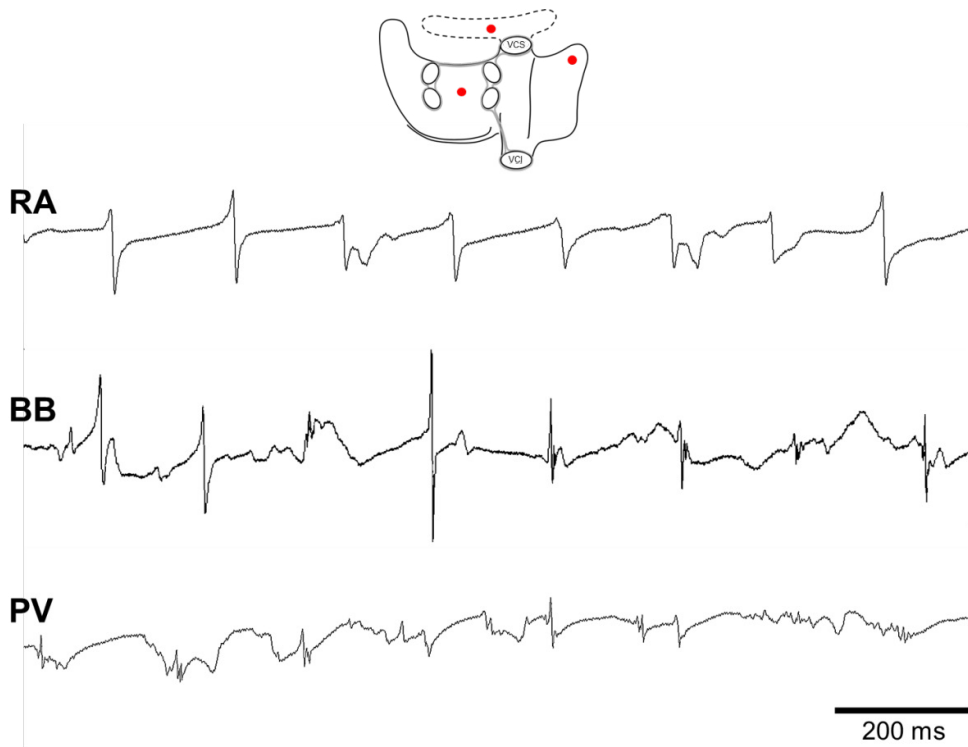


Figure 3. Intra-individual variation in electrogram morphology. Typical examples of unipolar fibrillation electrograms recorded from the middle of respectively the right atrial appendage (RA), Bachmann's Bundle (BB) and the pulmonary vein area (PV) obtained from a patient with mitral valve disease and persistent AF. In the right atrium, the fibrillation potentials contain a single deflection whereas fibrillation potentials recorded from Bachmann's Bundle and the pulmonary vein area contain multiple deflections.

Future diagnostic tools

As large numbers of disorders are associated with AF and patients with AF reveal AF episodes of variable duration, it is most likely that there is a large degree of variation in the degree of atrial remodeling. In addition to this, within a patient, it is also likely that there is intra-atrial variation in the degree of remodeling. Examples of regional differences in morphology of unipolar fibrillation potentials are shown in Figure 3. Hence, knowledge of the degree and extensiveness of the arrhythmogenic substrate in the individual patient is essential in order to evaluate a patient-tailored therapy for AF. For this purpose, we developed custom made mapping software ('wave mapping') which enabled visualization of the individual fibrillation waves and quantification of the fibrillatory process. By using this software, we compared electrophysiological properties

of fibrillation waves recorded during induced AF in patients with normal atria (physiological AF) with persistent AF in patients with valvular heart disease (pathological AF) and demonstrated that electrical dissociation of atrial muscle bundles and epicardial breakthrough of fibrillation waves play a key role in development of the substrate of persistent AF (Figure 4)²⁵. In order to

diagnose the arrhythmogenic substrate of AF in individual patients, we are currently evaluating a real-time, high resolution, multi-site epicardial mapping approach of the entire atria (Figure 5) as a novel diagnostic tool which can be applied as a routine procedure during cardiac surgery. An approach like this allows quantification of electrophysiological properties of the entire atria. In such manner, we study electropathology throughout the entire atria in patients with and without AF and with a diversity of underlying structural heart diseases. This novel mapping approach will not only be used to gain further insights into the arrhythmogenic substrate of AF, but will also be used to develop novel therapies or to improve existing treatment modalities. For example, it may guide ablative therapy when the arrhythmogenic substrate is confined to a circumscribed region. In addition, data acquired with this mapping approach will also provide the basis for development of less- or non-invasive mapping techniques.

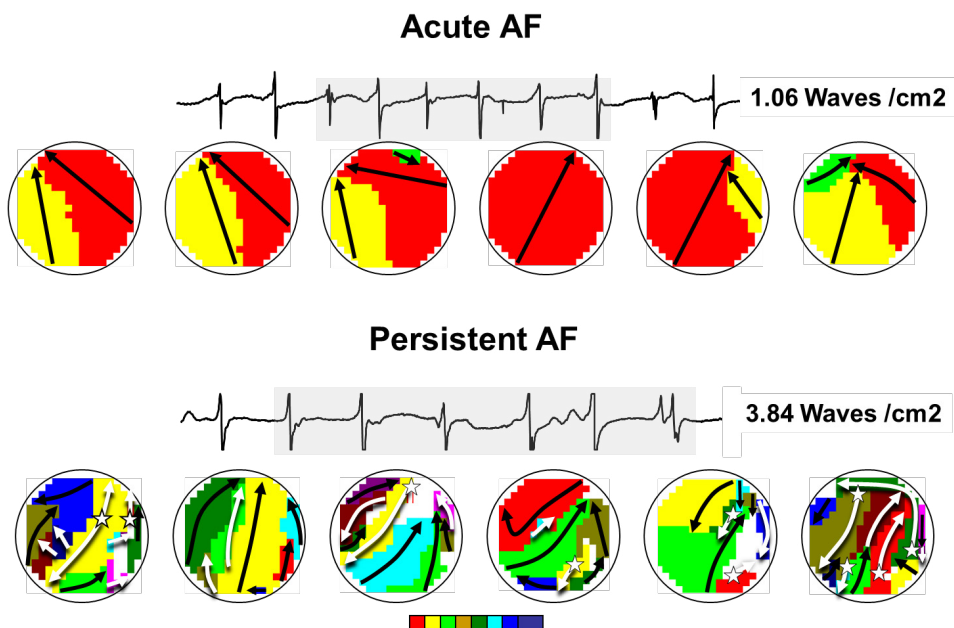


Figure 4. Inter-individual variation in characteristics of fibrillation waves. Examples of six consecutive wavemaps obtained from the right atrial free wall constructed during acute AF (upper panel) and persistent AF (lower panel); unipolar fibrillation electrograms recorded in the middle of the mapping area are shown on top. The mapping area activated by each individual fibrillation is represented by a color; every color indicates the moment of entrance in the mapping area (from red to purple); the arrows indicate the main trajectory of the fibrillation wave (black: peripheral fibrillation wave, white epicardial breakthrough wave). During acute AF, there are a fewer number of fibrillation waves and the patterns of activation are less complex, compared to persistent AF. In addition, 'focal fibrillation waves' occur more frequently during persistent AF.

The future: novel therapeutic targets

Current therapies are directed at suppression of AF symptoms, but are not effective in attenuating AF remodeling, therefore there is a high need to identify novel therapeutic targets which will improve the clinical outcome. Novel targets include RhoA, calpain and HDAC6 inhibition, but also HSP induction. Recent studies revealed the important role of the RhoA/

ROCK pathway activation in structural remodeling of cardiomyocytes during AF.³⁹ To maintain proper cardiac function, RhoA/ROCK inhibitors might be of therapeutic interest. Several RhoA and ROCK inhibitors have been developed. RhoA inhibitors CCG-1423 and Rhosin are studied in the preclinical phase.^{92, 93} Fasudil, Ezetimibe and AR-12286 are ROCK inhibitors currently studies in Phase II-IV trials for Raynaud's phenomenon, vascular function study, atherosclerosis and glaucoma (Table 1).

Calpain activation during AF causes the degradation of contractile and structural proteins, resulting in myolysis.^{39, 40, 44} *In vitro* studies showed that inhibitors of calpain conserve the cardiomyocyte structure and function and therefore might have beneficial effects in the treatment of AF.^{44, 54} Various calpain inhibitors have been developed and preclinically studied. Disadvantages of the current developed inhibitors are that they show poor selectivity for subtypes of calpain and often have a high LogP value and therefore are hard to dissolve in aqueous solutions.⁹⁴

HDAC6 inhibition, by tubacin, conserves α -tubulin proteostasis, and prevents its degradation by calpain 1 and thereby protects against loss of calcium transient and cardiac remodeling in experimental model systems for AF. As tubacin is not suitable for *in vivo* studies due to low drug-likeness⁹⁵, other promising HDAC6 inhibitors, such as tubastatin A and ACY-1215 have been recently developed⁹⁵⁻⁹⁷ (Table 1). Interestingly, tubastatin A showed to protect against tachypacing-induced cardiac remodeling in a canine model for AF⁵³, supporting the use of HDAC6 inhibitors as a novel therapeutic approach in AF.

Promoting maintenance of proteostasis by revitalization of the PQC system may prevent the derailment of proteostasis and structural and functional remodeling in AF. Interestingly, the heat shock response as part of the PQC system can be pharmacologically boosted, and consequently cardiac remodeling may be prevented, halted or even be restored. Indeed, as depicted earlier, increasing HSP expression, by either pharmacologic compounds or molecular biological means, displays cardioprotective effects in various models for AF and in patients. HSP induction provided protection against loss of actin proteostasis by reducing RhoA-GTPase-induced remodeling³⁹ and against activation of calpain.^{39, 44, 45, 47, 53, 54} Furthermore, in canine models for AF progression, treatment with geranylgeranylacetone induced HSP expression and prevented AF initiation and progression by inhibition of the prolongation of the effective refractory period (ERP), shortening of APD and reductions in L-type Ca^{2+} current and it revealed protective effects against atrial conduction abnormalities.^{45, 98}

Whether HPS induction also protects via HDAC inhibition is currently unknown. Of all HSP inducing compounds, GGA represents the most efficacious compound for the pharmacological induction of HSPs. GGA has already been applied clinically in Japan since 1984 as an antiulcer drug with no reported serious adverse reactions.⁹⁹⁻¹⁰³ Due to high LogP value for GGA, high dosages might be needed, therefore, GGA derivatives are developed with improve pharmacological properties (Table 1).¹⁰⁴ Induction of HSP is suggested to be the most promising therapeutic approach with pleiotropic protective effects.

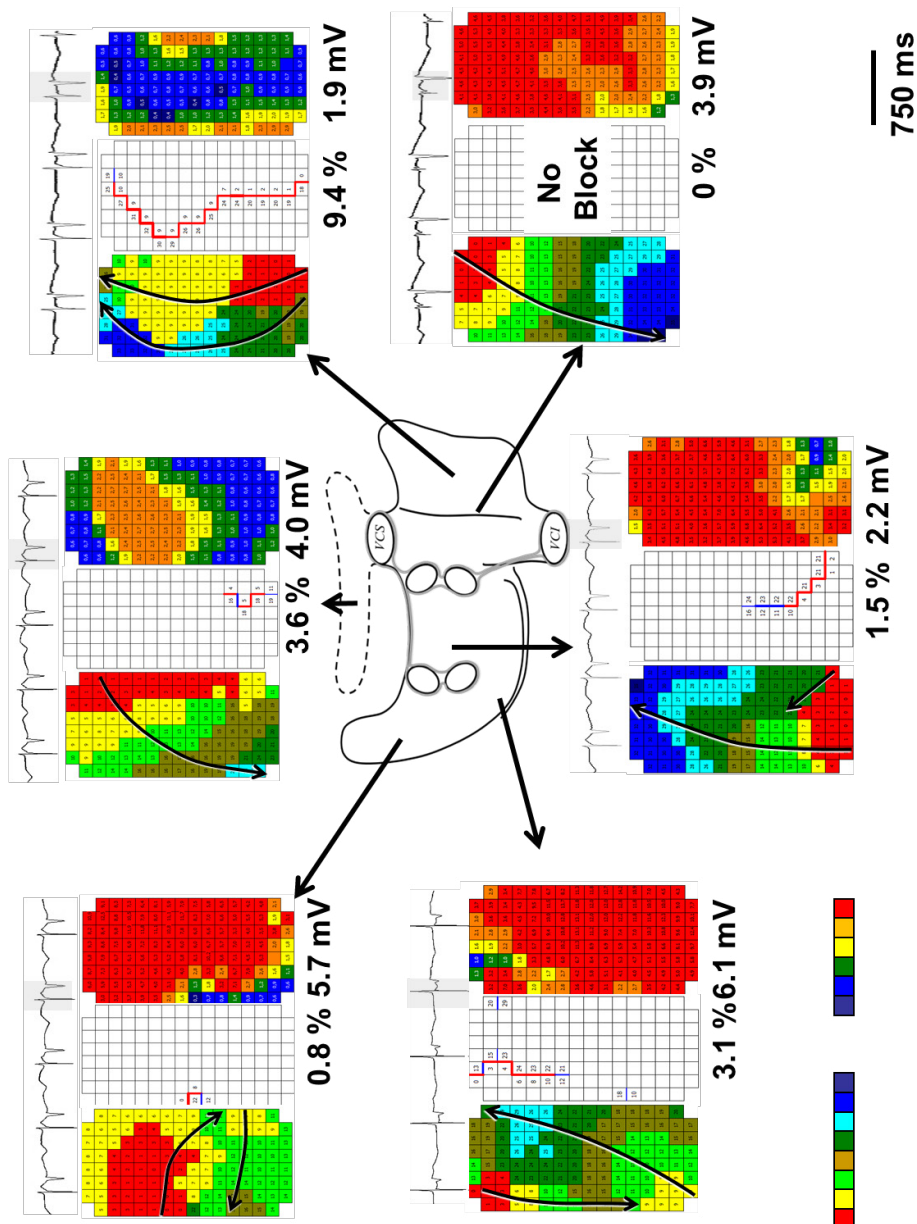


Figure 5. Atrial epicardial mapping. Activation-, conduction block- and voltage maps constructed from Bachmann's bundle, right atrium, crista terminalis, pulmonary vein area, left atrioventricular groove, left atrial appendage during sinus rhythm, obtained from a patient with coronary artery disease. Electrograms recorded from the middle of the mapping area are shown on top. Arrows in the color-coded activation maps show the main trajectory of the excitation wave. Areas of slow conduction ($<18\text{cm/s}$) and conduction block ($<30\text{cm/s}$) are represented by respectively blue and red lines. Voltage maps show the peak-to-peak amplitude of the atrial potentials.

HSPs as biomarkers

Following stress, HSPs get expressed intracellular, but can also be presented on the cell surface or released to the surroundings.¹⁰⁵ HSPs in serum may act as a biomarker to reveal the stage of AF. Elevated serum HSP60 levels were found in patients with acute myocardial infarction and seemed to be predictive for post-AMI adverse events.¹⁰⁶ Elevated serum HSP70 and HSP60 have found to correlate to the severity of metabolic syndrome-associated factors in postmenopausal women.¹⁰⁷ HSP60 and HSP70 were found to positively associate with severity of cardiovascular disease.¹⁰⁸⁻¹¹³ Patients with coronary artery disease (CAD) have revealed antibodies to HSP27 in serum¹¹⁴, but a correlation between antibody titers to HSP27 and the extent of CAD could not be found. Several studies have reported increased serum levels for HSP27 several hours after myocardial infarction^{115, 116}. In another study, anti-HSP27 levels were found to be higher in patients with more advanced cardiac artery disease, making the authors to conclude that serum anti-HSP27 titers may be associated with the presence and severity of cardiac artery disease.¹¹⁷ Anti-HSP27 titers measured in patients with stroke were found significantly elevated.¹¹⁸ These findings suggest that the measurement of HSP levels in serum, may be useful as biomarkers of disease initiation, and progression.

Table 1. Novel therapeutic targets

Drug	Target	Phase	Indication	Ref (clinical trials.gov)
GGA	HSP induction	Phase IV	Gastric ulcers Gastritis Gastric lesion	NCT01190657 NCT01547559 NCT01284647 NCT01397448
NYK9354	HSP induction	Pre-clinical	Atrial Fibrillation	(HoogstraBerends et al., 2012)
Leupeptin ALLN MDL-28170 A-705239 A-705253	Calpain induction	Pre-clinical		reviewed in Cardiovascular Research (2012) 96, 23–31
Tubastatin	HDAC6	Pre-clinical	Arthritis Anti-inflammatory	(Vishwakarma et al., 2013)
ACY-1215	HDAC6	Phase I/II	Myeloma	NCT01323751 NCT01583283
Fasudil	ROCK	Phase III Phase II Phase II	Raynaud's Phenomenon Vascular function study Atherosclerosis	NCT00498615 NCT00120718 NCT00670202 NCT00560170 NCT01936389
Ezetimibe AR-12286		Phase IV Phase II	Atherosclerosis Glaucoma	
CCG-1423 Rhosin	Rho	Pre-clinical		(Evelyn, et al., 2007) (Shang, et al., 2012)

CONCLUSION

AF naturally tends to progress from trigger dependent paroxysmal AF to a more substrate mediated (longstanding) persistent or permanent AF. Trigger focused treatments (endovascular or surgical PVI) might be successful in patients with paroxysmal AF, however this approach will not be sufficient for patients suffering from more advanced types of AF, who require substrate modification. Even treatments aimed at substrate modification, such as CFAE ablation, Cox maze III and ganglion ablation, are associated with AF recurrences. This

implies insufficient understanding of the electrophysiological and structural changes which form a substrate underlying AF. Hence, as long as the electropathological substrate remains poorly understood, and the stage of electropathology cannot be evaluated, it is challenging to define the optimal approach per individual patient. Therefore, research is focused on the dissection of molecular mechanisms underlying electropathology. New findings indicate a role for derailment of cardiomyocyte proteostasis in AF progression and identified novel innovative targets for drug therapy. These targets are directed at the attenuation of electropathology and prevention of clinical AF progression. Since various drugs are already on in clinical phase II/III for other indications, it seems worthwhile to test some in clinical AF.

REFERENCES

1. Einthoven W. Le télécardiogramme. *Arch Int Physiol* 1906;4:132-64.
2. Wilke T, Groth A, Mueller S, Pfannkuche M, Verheyen F, Linder R, et al. Incidence and prevalence of atrial fibrillation: an analysis based on 8.3 million patients. *Europace* 2013;15(4):486-93.
3. Krijthe BP, Kunst A, Benjamin EJ, Lip GYH, Franco OH, Hofman A, et al. Projections on the number of individuals with atrial fibrillation in the European Union, from 2000 to 2060. *Eur Heart J* 2013;34(35):2746-2751.
4. Aizer A, Gaziano JM, Cook NR, Manson JE, Buring JE, Albert CM. Relation of Vigorous Exercise to Risk of Atrial Fibrillation. *Am J Cardiol* 2009;103(11):1572-1577.
5. Kirsh JA, Walsh EP, Triedman JK. Prevalence of and risk factors for atrial fibrillation and intra-atrial reentrant tachycardia among patients with congenital heart disease. *Am J Cardiol* 2002;90(3):338-+.
6. Patel NJ, Deshmukh A, Pant S, Singh V, Patel N, Arora S, et al. Contemporary Trends of Hospitalization for Atrial Fibrillation in the United States, 2000 Through 2010 Implications for Healthcare Planning. *Circulation* 2014;129(23):2371-2379.
7. Haissaguerre M, Hocini M, Denis A, Shah AJ, Komatsu Y, Yamashita S, et al. Driver Domains in Persistent Atrial Fibrillation. *Circulation* 2014;130(7):530-538.
8. Konrad T, Theis C, Mollnau H, Sonnenschein S, Rostock T. Body surface potential mapping for mapping and treatment of persistent atrial fibrillation. *Herzschr Elektrophys* 2014;25:226-229.
9. Guillem MS, Climent AM, Millet J, Arenal A, Fernandez-Aviles F, Jalife J, et al. Noninvasive Localization of Maximal Frequency Sites of Atrial Fibrillation by Body Surface Potential Mapping. *Circ-Arrhythmia Elec* 2013;6(2):294-301.
10. Rodrigo M, Guillem MS, Climent AM, Pedron-Torrecilla J, Liberos A, Millet J, et al. Body surface localization of left and right atrial high-frequency rotors in atrial fibrillation patients: A clinical-computational study. *Heart Rhythm* 2014;11(9):1584-1591.
11. Moe GK. Atrial fibrillation as a self-sustaining arrhythmia independent of focal discharge. *Am Heart J* 1959;58(1):59-70.
12. Allesie MA. Experimental evaluation of Moe's multiple wavelet hypothesis of atrial fibrillation. *Cardiac Electrophysiology and Arrhythmias* 1985:265-276.
13. Allesie MA, Bonke FIM, Schopman FJG. Circus Movement in Rabbit Atrial Muscle as a Mechanism of Tachycardia .3. Leading Circle Concept - New Model of Circus Movement in Cardiac Tissue without Involvement of an Anatomical Obstacle. *Circ Res* 1977;41(1):9-18.
14. Allesie MA, Bonke FIM, Lammers WJEP, Rensma PL. The Wavelength of the Atrial Impulse and Re-Entrant Arrhythmias in the Conscious Dog. *J Physiol-London* 1985;366(Sep):P37-P37.
15. Konings KTS, Kirchhof CJHJ, Smeets JRLM, Wellens HJJ, Penn OC, Allesie MA. High-Density Mapping of Electrically-Induced Atrial-Fibrillation in Humans. *Circulation* 1994;89(4):1665-1680.
16. Mandapati R, Skanes A, Chen J, Berenfeld O, Jalife J. Stable microreentrant sources as a mechanism of atrial fibrillation in the isolated sheep heart. *Circulation* 2000;101(2):194-9.
17. Jalife J, Berenfeld O, Mansour M. Mother rotors and fibrillatory conduction: a mechanism of atrial fibrillation. *Cardiovasc Res* 2002;54(2):204-216.
18. Waldo AL. Mechanisms of atrial fibrillation. *J Cardiovasc Electr* 2003;14(12):S267-S274.
19. Moe GK. A computer model of atrial fibrillation. *Am Heart J* 1964;67(2):200-220.
20. Narayan SM, Krummen DE, Shivkumar K, Clopton P, Rappel WJ, Miller JM. Treatment of Atrial Fibrillation by the Ablation of Localized Sources CONFIRM (Conventional Ablation for Atrial Fibrillation With or Without Focal Impulse and Rotor Modulation) Trial. *J Am Coll Cardiol* 2012;60(7):628-636.

21. Lewis T. The nature of flutter and fibrillation of the auricle. *Brit Med J* 1921;1.
22. Narayan SM, Krummen DE, Shivkumar K, Clopton P, Rappel WJ, Miller JM. Treatment of atrial fibrillation by the ablation of localized sources: CONFIRM (Conventional Ablation for Atrial Fibrillation With or Without Focal Impulse and Rotor Modulation) trial. *J Am Coll Cardiol* 2012;60(7):628-36.
23. de Groot NMS, Houben RPM, Smeets JL, Boersma E, Schotten U, Schalij MJ, et al. Electropathological Substrate of Longstanding Persistent Atrial Fibrillation in Patients With Structural Heart Disease Epicardial Breakthrough. *Circulation* 2010;122(17):1674-1682.
24. Lee G, Kumar S, Teh A, Madry A, Spence S, Larobina M, et al. Epicardial wave mapping in human long-lasting persistent atrial fibrillation: transient rotational circuits, complex wavefronts, and disorganized activity. *Eur Heart J* 2014;35(2):86-97.
25. Allessie MA, de Groot NMS, Houben RPM, Schotten U, Boersma E, Smeets JL, et al. Electropathological Substrate of Long-Standing Persistent Atrial Fibrillation in Patients With Structural Heart Disease. *Circ-Arrhythmia Elec* 2010;3(6):606-615.
26. Wijffels MCEF, Kirchhof CJHJ, Dorland R, Allessie MA. Atrial-Fibrillation Begets Atrial-Fibrillation - a Study in Awake Chronically Instrumented Goats. *Circulation* 1995;92(7):1954-1968.
27. Goette A, Honeycutt C, Langberg JJ. Electrical remodeling in atrial fibrillation - Time course and mechanisms. *Circulation* 1996;94(11):2968-2974.
28. Ausma J, Dispersyn GD, Duimel H, Thone F, Donck LV, Allessie MA, et al. Changes in ultrastructural calcium distribution in goat atria during atrial fibrillation. *J Mol Cell Cardiol* 2000;32(3):355-364.
29. Brundel BJJM, Van Gelder IC, Henning RH, Tieleman RG, Tuinenburg AE, Wietes M, et al. Ion channel remodeling is related to intraoperative atrial effective refractory periods in patients with paroxysmal and persistent atrial fibrillation. *Circulation* 2001;103(5):684-690.
30. Qi XY, Yeh YH, Xiao L, Burstein B, Maguy A, Chartier D, et al. Cellular signaling underlying atrial tachycardia remodeling of L-type calcium current. *Circ Res* 2008;103(8):845-U151.
31. Schotten U, Duytschaever M, Ausma J, Eijssbouts S, Neuberger HR, Allessie M. Electrical and contractile remodeling during the first days of atrial fibrillation go hand in hand. *Circulation* 2003;107(10):1433-1439.
32. Brundel BJJM, Van Gelder IC, Henning RH, Tuinenburg AE, Deelman LE, Tieleman RG, et al. Gene expression of proteins influencing the calcium homeostasis in patients with persistent and paroxysmal atrial fibrillation. *Cardiovasc Res* 1999;42(2):443-454.
33. Wang ZG. Role of redox state in modulation of ion channel function by fatty acids and phospholipids. *Brit J Pharmacol* 2003;139(4):681-683.
34. Dobrev D, Voigt N. Ion channel remodelling in atrial fibrillation. *European Cardiology* 2011;7(2):97-103.
35. Anderson ME. Calmodulin kinase and L-type calcium channels: A recipe for arrhythmias? *Trends Cardiovasc Med* 2004;14(4):152-161.
36. Christ T, Boknik P, Wohrl S, Wettwer E, Graf EM, Bosch RF, et al. L-type Ca²⁺ current downregulation in chronic human atrial fibrillation is associated with increased activity of protein phosphatases. *Circulation* 2004;110(17):2651-2657.
37. Greiser M, Halaszovich CR, Frechen D, Boknik P, Ravens U, Dobrev D, et al. Pharmacological evidence for altered src kinase regulation of I-Ca, I-L in patients with chronic atrial fibrillation. *N-S Arch Pharmacol* 2007;375(6):383-392.
38. Dobrev D, Nattel S. Calcium Handling Abnormalities in Atrial Fibrillation as a Target for Innovative Therapeutics. *J Cardiovasc Pharm* 2008;52(4):293-299.
39. Ke L, Meijering RAM, Hoogstra-Berends F, Mackovicova K, Vos MJ, Van Gelder IC, et al. HSPB1, HSPB6, HSPB7 and HSPB8 Protect against RhoA GTPase-Induced Remodeling in Tachypaced Atrial Myocytes. *Plos One* 2011;6(6).

40. Brundel BJJM, Ausma J, van Gelder IC, Van Der Want JJJ, van Gilst WH, Crijns HJGM, et al. Activation of proteolysis by calpains and structural changes in human paroxysmal and persistent atrial fibrillation. *Cardiovasc Res* 2002;54(2):380-389.
41. Sherman AJ, Klocke FJ, Decker RS, Decker ML, Kozlowski KA, Harris KR, et al. Myofibrillar disruption in hypocontractile myocardium showing perfusion-contraction matches and mismatches. *Am J Physiol-Heart C* 2000;278(4):H1320-H1334.
42. Bito V, Heinzel FR, Weidemann F, Dommke C, van der Velden J, Verbeke E, et al. Cellular mechanisms of contractile dysfunction in hibernating myocardium. *Circ Res* 2004;94(6):794-801.
43. Todd DM, Fynn SP, Walden AP, Hobbs WJ, Arya S, Garratt CJ. Repetitive 4-week periods of atrial electrical remodeling promote stability of atrial fibrillation - Time course of a second factor involved in the self-perpetuation of atrial fibrillation. *Circulation* 2004;109(11):1434-1439.
44. Zhang DL, Wu CT, Qi XY, Meijering RAM, Hoogstra-Berends F, Tadevosyan A, et al. Activation of Histone Deacetylase-6 Induces Contractile Dysfunction Through Derailment of alpha-Tubulin Proteostasis in Experimental and Human Atrial Fibrillation. *Circulation* 2014;129(3):346-358.
45. Brundel BJJM, Henning RH, Ke L, van Gelder IC, Crijns HJGM, Kampinga HH. Heat shock protein upregulation protects against pacing-induced myolysis in HL-1 atrial myocytes and in human atrial fibrillation. *J Mol Cell Cardiol* 2006;41(3):555-562.
46. Meijering R.A.M. ZD, Hoogstra-Berends F., Henning R.H., Brundel B.J.J.M. Loss of proteostatic control as a substrate for Atrial Fibrillation; a novel target for upstream therapy by Heat Shock Proteins. *Frontiers in Cardiac Electrophysiology* 2012;3(36).
47. Brundel BJJM, Shiroshita-Takeshita A, Qi XY, Yeh YH, Chartier D, van Gelder IC, et al. Induction of heat shock response protects the heart against atrial fibrillation. *Circ Res* 2006;99(12):1394-1402.
48. Balch WE, Morimoto RI, Dillin A, Kelly JW. Adapting proteostasis for disease intervention. *Science* 2008;319(5865):916-919.
49. Powers ET, Balch WE. Diversity in the origins of proteostasis networks - a driver for protein function in evolution. *Nat Rev Mol Cell Bio* 2013;14(4):237-248.
50. Wang XJ, Robbins J. Heart failure and protein quality control. *Circ Res* 2006;99(12):1315-1328.
51. Galli A. Proteotoxicity and cardiac dysfunction. *New Engl J Med* 2013;368(18):1754-5.
52. R.A. M, Henning RH, Brundel B. Reviving the protein quality control system: Therapeutic target for cardiac disease in the elderly. *Trends Cardiovas Med* 2014;14:1050-1738.
53. Zhang DL, Ke L, Mackovicova K, Van Der Want JJJ, Sibon OCM, Tanguay RM, et al. Effects of different small HSPB members on contractile dysfunction and structural changes in a *Drosophila melanogaster* model for Atrial Fibrillation. *J Mol Cell Cardiol* 2011;51(3):381-389.
54. Ke L, Qi XY, Dijkhuis AJ, Chartier D, Nattel S, Henning RH, et al. Calpain mediates cardiac troponin degradation and contractile dysfunction in atrial fibrillation. *J Mol Cell Cardiol* 2008;45(5):685-693.
55. Brown JH, Del Re DP, Sussman MA. The Rac and Rho hall of fame - A decade of hypertrophic signaling hits. *Circ Res* 2006;98(6):730-742.
56. Sah VP, Minamisawa S, Tam SP, Wu TH, Dorn GW, Ross J, et al. Cardiac-specific overexpression of RhoA results in sinus and atrioventricular nodal dysfunction and contractile failure. *Journal of Clinical Investigation* 1999;103(12):1627-1634.
57. Adam O, Frost G, Custodis F, Sussman MA, Schafers HJ, Bohm M, et al. Role of Rac1 GTPase activation in atrial fibrillation. *J Am Coll Cardiol* 2007;50(4):359-367.
58. Reil JC, Hohl M, Oberhofer M, Kazakov A, Kaestner L, Mueller P, et al. Cardiac Rac1 overexpression in mice creates a substrate for atrial arrhythmias characterized by structural remodelling. *Cardiovasc Res* 2010;87(3):485-493.
59. Ogata T, Ueyama T, Isodono K, Tagawa M, Takehara N, Kawashima T, et al. MURC, a muscle-restricted coiled-coil protein that modulates the Rho/ROCK pathway, induces cardiac dysfunction and conduction disturbance. *Mol Cell Biol* 2008;28(10):3424-3436.

60. Hubbert C, Guardiola A, Shao R, Kawaguchi Y, Ito A, Nixon A, et al. HDAC6 is a microtubule-associated deacetylase. *Nature* 2002;417(6887):455-458.
61. Haggarty SJ, Koeller KM, Wong JC, Grozinger CM, Schreiber SL. Domain-selective small-molecule inhibitor of histone deacetylase 6 (HDAC6)-mediated tubulin deacetylation. *P Natl Acad Sci USA* 2003;100(8):4389-4394.
62. Matsuyama A, Shimazu T, Sumida Y, Saito A, Yoshimatsu Y, Seigneurin-Berny D, et al. In vivo destabilization of dynamic microtubules by HDAC6-mediated deacetylation. *Embo J* 2002;21(24):6820-6831.
63. Powers ET, Morimoto RI, Dillin A, Kelly JW, Balch WE. Biological and Chemical Approaches to Diseases of Proteostasis Deficiency. *Annu Rev Biochem* 2009;78:959-991.
64. St Rammos K, Koullias GJ, Hassan MO, Argyrakis NP, Voucharas CG, Scarupa SJ, et al. Low preoperative HSP70 atrial myocardial levels correlate significantly with high incidence of postoperative atrial fibrillation after cardiac surgery. *Cardiovasc Surg* 2002;10(3):228-232.
65. Mandal K, Torsney E, Poloniecki J, Camm AJ, Xu QB, Jahangiri M. Association of high intracellular, but not serum, heat shock protein 70 with postoperative atrial fibrillation. *Ann Thorac Surg* 2005;79(3):865-871.
66. Cao HL, Xue L, Xu XH, Wu YH, Zhu JF, Chen L, et al. Heat shock proteins in stabilization of spontaneously restored sinus rhythm in permanent atrial fibrillation patients after mitral valve surgery. *Cell Stress Chaperon* 2011;16(5):517-528.
67. Yang M, Tan H, Cheng L, He M, Wei Q, Tanguay RM, et al. Expression of heat shock proteins in myocardium of patients with atrial fibrillation. *Cell Stress Chaperon* 2007;12(2):142-150.
68. Willis MS, Patterson C. Proteotoxicity and Cardiac Dysfunction Reply. *New Engl J Med* 2013;368(18):1755-1755.
69. Liu J, Kam KWL, Borchert GH, Kravtsov GM, Ballard HJ, Wong TM. Further study on the role of HSP70 on Ca²⁺ homeostasis in rat ventricular myocytes subjected to simulated ischemia. *Am J Physiol-Cell Ph* 2006;290(2):C583-C591.
70. Kalmar B, Greensmith L. Induction of heat shock proteins for protection against oxidative stress. *Adv Drug Deliver Rev* 2009;61(4):310-318.
71. Sugiyama Y, Suzuki A, Kishikawa M, Akutsu R, Hirose T, Wayne MMY, et al. Muscle develops a specific form of small heat shock protein complex composed of MKBP/HSPB2 and HSPB3 during myogenic differentiation. *J Biol Chem* 2000;275(2):1095-1104.
72. Mounier N, Arrigo AP. Actin cytoskeleton and small heat shock proteins: how do they interact? *Cell Stress Chaperon* 2002;7(2):167-176.
73. Golenhofen N, Perng MD, Quinlan RA, Drenckhahn D. Comparison of the small heat shock proteins alpha B-crystallin, MKBP, HSP25, HSP20, and α HSP in heart and skeletal muscle. *Histochem Cell Biol* 2004;122(5):415-425.
74. Salinthon S, Tyagi M, Gerthoffer WT. Small heat shock proteins in smooth muscle. *Pharmacol Therapeut* 2008;119(1):44-54.
75. Camm AJ, Lip GYH, De Caterina R, Savelieva I, Atar D, Hohnloser SH, et al. 2012 focused update of the ESC Guidelines for the management of atrial fibrillation. *Eur Heart J* 2012;33(21):2719-2747.
76. de Paola AAV, Figueiredo E, Sesso R, Veloso HH, Nascimento LOT, Inv S. Effectiveness and costs of chemical versus electrical cardioversion of atrial fibrillation. *Int J Cardiol* 2003;88(2-3):157-166.
77. Pisters R, Nieuwlaar R, Prins MH, Le Heuzey JY, Maggioni AP, Camm AJ, et al. Clinical correlates of immediate success and outcome at 1-year follow-up of real-world cardioversion of atrial fibrillation: the Euro Heart Survey. *Europace* 2012;14(5):666-674.
78. Löwn B. New method for terminating cardiac arrhythmias. Use of synchronized capacitor discharge. *JAMA* 1962;182(5):548-555.
79. Camm AJ, Lip GYH, De Caterina R, Savelieva I, Atar D, Hohnloser SH, et al. 2012 focused update of the ESC Guidelines for the management of atrial fibrillation An update of the 2010 ESC Guidelines for the management of atrial fibrillation Developed with the special contribution of the European Heart Rhythm Association. *Europace* 2012;14(10):1385-1413.

80. Di Blase L, Fahmy TS, Patel D, Bai R, Civello K, Wazni OM, et al. Remote magnetic navigation - Human experience in pulmonary vein ablation. *J Am Coll Cardiol* 2007;50(9):868-874.
81. Luthje L, Vollmann D, Seegers J, Dorenkamp M, Sohns C, Hasenfuss G, et al. Remote magnetic versus manual catheter navigation for circumferential pulmonary vein ablation in patients with atrial fibrillation. *Clin Res Cardiol* 2011;100(11):1003-1011.
82. Saliba W, Reddy VY, Wazni O, Cummings JE, Burkhardt JD, Haissaguerre M, et al. Atrial fibrillation ablation using a robotic catheter remote control system - Initial human experience and long-term follow-up results. *J Am Coll Cardiol* 2008;51(25):2407-2411.
83. Bordignon S, Chun KRJ, Gunawardene M, Fuernkranz A, Urban V, Schulte-Hahn B, et al. Comparison of Balloon Catheter Ablation Technologies for Pulmonary Vein Isolation: The Laser Versus Cryo Study. *J Cardiovasc Electr* 2013;24(9):987-994.
84. Ganesan AN, Shipp NJ, Brooks AG, Kuklik P, Lau DH, Lim HS, et al. Long-term Outcomes of Catheter Ablation of Atrial Fibrillation: A Systematic Review and Meta-analysis. *J Am Heart Assoc* 2013;2(2).
85. Bhat T, Baydoun H, Asti D, Rijal J, Teli S, Tantray M, et al. Major complications of cryoballoon catheter ablation for atrial fibrillation and their management. *Expert Rev Anti-Infe* 2014;12(9):1111-1118.
86. Yaksh A, Kik C, Knops P, Roos-Hesselink JW, Bogers AJJC, Zijlstra F, et al. Atrial fibrillation: to map or not to map? *Netherlands Heart Journal* 2014;22(6):259-266.
87. Nademanee K, McKenzie J, Kosar E, Schwab M, Sunsaneewitayakul B, Vasavakul T, et al. A new approach for catheter ablation of atrial fibrillation: Mapping of the electrophysiologic substrate. *J Am Coll Cardiol* 2004;43(11):2044-2053.
88. Wu SH, Jiang WF, Gu J, Zhao L, Wang YL, Liu YG, et al. Benefits and risks of additional ablation of complex fractionated atrial electrograms for patients with atrial fibrillation: A systematic review and meta-analysis. *Int J Cardiol* 2013;169(1):35-43.
89. Verma A, Sanders P, Champagne J, Macle L, Nair G, Calkins H, et al. Selective Complex Fractionated Electrogram Targeting For Atrial Fibrillation Study (Select AF): A Multicenter, Randomized Trial. *Circulation* 2012;126(21).
90. Mikhaylov E, Kanidieva A, Sviridova N, Abramov M, Gureev S, Szili-Torok T, et al. Outcome of anatomic ganglionated plexi ablation to treat paroxysmal atrial fibrillation: a 3-year follow-up study. *Europace* 2011;13(3):362-70.
91. Pokushalov E, Romanov A, Artyomenko S, Turov A, Shugayev P, Shirokova N, et al. Ganglionated plexi ablation for longstanding persistent atrial fibrillation. *Europace* 2010;12(3):342-6.
92. Evelyn CR, Wade SM, Wang Q, Wu M, Iniguez-Lluhi JA, Merajver SD, et al. CCG-1423: a small-molecule inhibitor of RhoA transcriptional signaling. *Mol Cancer Ther* 2007;6(8):2249-2260.
93. Shang X, Marchioni F, Sipes N, Evelyn CR, Jerabek-Willemsen M, Duhr S, et al. Rational Design of Small Molecule Inhibitors Targeting RhoA Subfamily Rho GTPases. *Chem Biol* 2012;19(6):699-710.
94. Inserte J, Hernando V, Garcia-Dorado D. Contribution of calpains to myocardial ischaemia/reperfusion injury. *Cardiovasc Res* 2012;96(1):23-31.
95. Butler KV, Kalin J, Brochier C, Vistoli G, Langley B, Kozikowski AP. Rational Design and Simple Chemistry Yield a Superior, Neuroprotective HDAC6 Inhibitor, Tubastatin A. *J Am Chem Soc* 2010;132(31):10842-10846.
96. d'Ydewalle C, Krishnan J, Chiheb DM, Van Damme P, Irobi J, Kozikowski AP, et al. HDAC6 inhibitors reverse axonal loss in a mouse model of mutant HSPB1-induced Charcot-Marie-Tooth disease. *Nat Med* 2011;17(8):968-U86.
97. Santo L, Hideshima T, Kung AL, Tseng JC, Tamang D, Yang M, et al. Preclinical activity, pharmacodynamic, and pharmacokinetic properties of a selective HDAC6 inhibitor, ACY-1215, in combination with bortezomib in multiple myeloma. *Blood* 2012;119(11):2579-2589.
98. Sakabe M, Shiroshita-Takeshita A, Maguy A, Brundel BJJM, Fujiki A, Inoue H, et al. Effects of a

heat shock protein inducer on the atrial fibrillation substrate caused by acute atrial ischaemia. *Cardiovasc Res* 2008;78(1):63-70.

99. Murakami M, Oketani K, Fujisaki H, Wakabayashi T, Ohgo T. Anti-Ulcer Effect of Geranylgeranylacetone, a New Acyclic Polyisoprenoid on Experimentally Induced Gastric and Duodenal-Ulcers in Rats. *Arzneimittel-Forsch* 1981;31-1(5):799-804.

100. Unoshima M, Iwasaka H, Eto J, Takita-Sonoda Y, Noguchi T, Nishizono R. Antiviral effects of geranylgeranylacetone: Enhancement of MxA expression and phosphorylation of PKR during influenza virus infection. *Antimicrob Agents Ch* 2003;47(9):2914-2921.

101. Katsuno M, Sang C, Adachi H, Minamiyama M, Waza M, Tanaka F, et al. Pharmacological induction of heat-shock proteins alleviates polyglutamine-mediated motor neuron disease. *P Natl Acad Sci USA* 2005;102(46):16801-16806.

102. Yanaka A, Zhang SH, Sato D, Tauchi M, Suzuki H, Shibahara T, et al. Geranylgeranylacetone protects the human gastric mucosa from diclofenac-induced injury via induction of heat shock protein 70. *Digestion* 2007;75(2-3):148-155.

103. Fujimura N, Jitsuiki D, Maruhashi T, Mikami S, Iwamoto Y, Kajikawa M, et al. Geranylgeranylacetone, Heat Shock Protein 90/AMP-Activated Protein Kinase/Endothelial Nitric Oxide Synthase/Nitric Oxide Pathway, and Endothelial Function in Humans. *Arterioscl Throm Vas* 2012;32(1):153-U350.

104. Hoogstra-Berends F, Meijering RAM, Zhang DL, Heeres A, Loen L, Seerden JP, et al. Heat Shock Protein-Inducing Compounds as Therapeutics to Restore Proteostasis in Atrial Fibrillation. *Trends Cardiovas Med* 2012;22(3):62-68.

105. van Oosten-Hawle P, Morimoto RI. Organismal proteostasis: role of cell-nonautonomous regulation and transcellular chaperone signaling. *Gene Dev* 2014;28(14):1533-1543.

106. Novo G, Cappello F, Rizzo M, Fazio G, Zambuto S, Tortorici E, et al. Hsp60 and heme oxygenase-1 (Hsp32) in acute myocardial infarction. *Transl Res* 2011;157(5):285-292.

107. Giannessi D, Colotti C, Maltinti M, Del Ry S, Prontera C, Turchi S, et al. Circulating heat shock proteins and inflammatory markers in patients with idiopathic left ventricular dysfunction: their relationships with myocardial and microvascular impairment. *Cell Stress Chaperon* 2007;12(3):265-274.

108. Zhu JH, Quyyumi AA, Rott D, Csako G, Wu HS, Halcox J, et al. Antibodies to human heat-shock protein 60 are associated with the presence and severity of coronary artery disease - Evidence for an autoimmune component of atherogenesis. *Circulation* 2001;103(8):1071-1075.

109. Metzler B, Schett G, Kleindienst R, vanderZee R, Ottenhoff T, Hajeer A, et al. Epitope specificity of anti-heat shock protein 65/60 serum antibodies in atherosclerosis. *Arterioscl Throm Vas* 1997;17(3):536-541.

110. Burian K, Kis Z, Virok D, Endresz V, Prohaszka Z, Duba J, et al. Independent and joint effects of antibodies to human heat-shock protein 60 and Chlamydia pneumoniae infection in the development of coronary atherosclerosis. *Circulation* 2001;103(11):1503-1508.

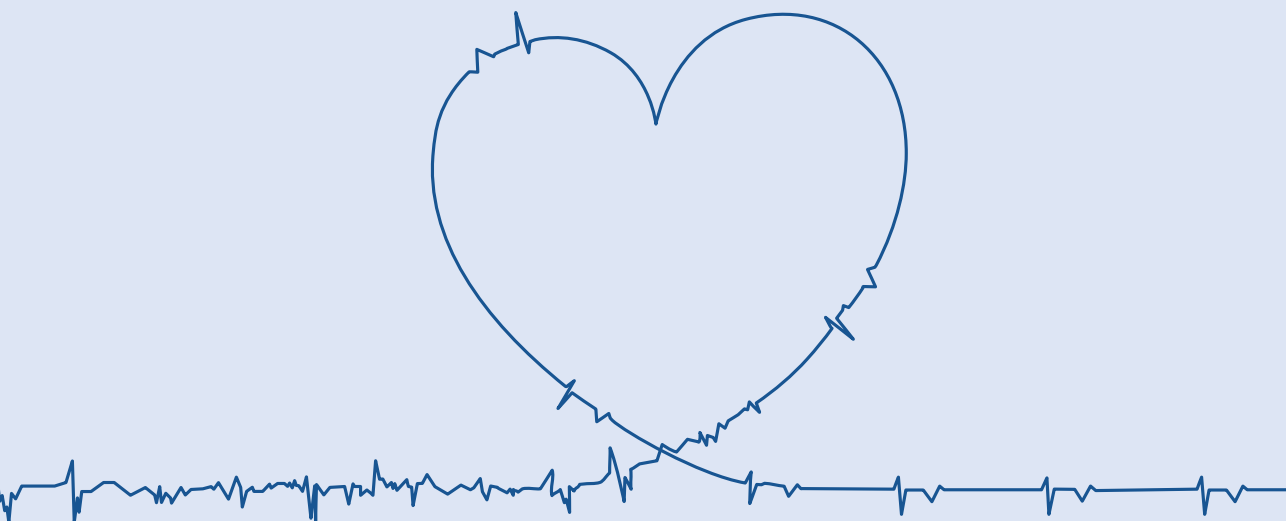
111. Xu Q, Kiechl S, Mayr M, Metzler B, Egger G, Oberhollenzer F, et al. Association of serum antibodies to heat-shock protein 65 with carotid atherosclerosis : clinical significance determined in a follow-up study. *Circulation* 1999;100(11):1169-74.

112. Hoppichler F, Lechleitner M, Traweger C, Schett G, Dzien A, Sturm W, et al. Changes of serum antibodies to heat-shock protein 65 in coronary heart disease and acute myocardial infarction. *Atherosclerosis* 1996;126(2):333-8.

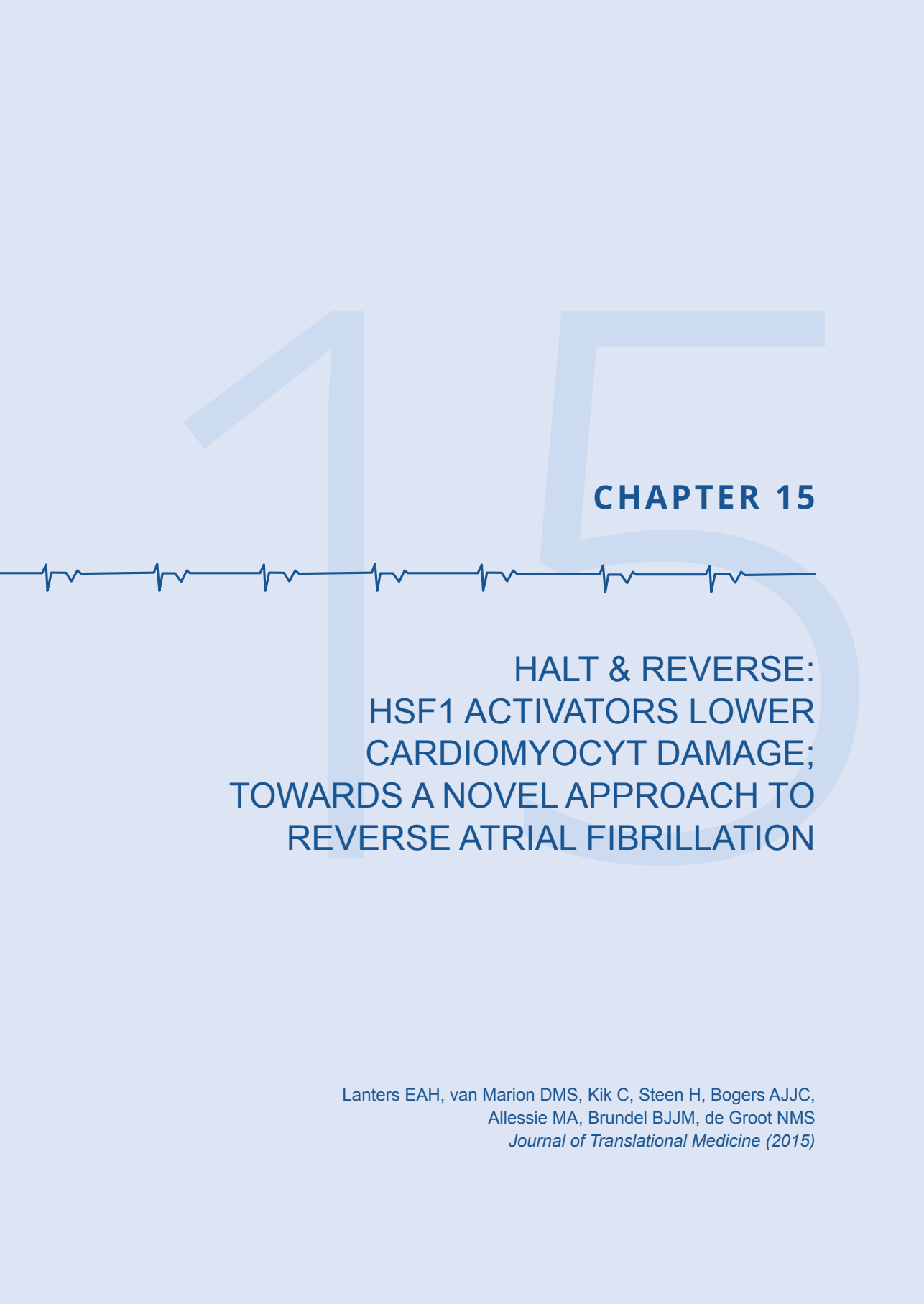
113. Birnie D, Hood S, Holmes E, Hillis WS. Anti-heat shock protein 65 titres in acute myocardial infarction. *Lancet* 1994;344(8934):1443.

114. Lavoie JN, Lambert H, Hickey E, Weber LA, Landry J. Modulation of cellular thermoresistance and actin filament stability accompanies phosphorylation-induced changes in the oligomeric structure of heat shock protein 27. *Mol Cell Biol* 1995;15(1):505-16.

115. Vander Heide RS. Increased expression of HSP27 protects canine myocytes from simulated ischemia-reperfusion injury. *Am J Physiol-Heart C* 2002;282(3):H935-H941.
116. Knowlton AA. The Role of Heat-Shock Proteins in the Heart. *J Mol Cell Cardiol* 1995;27(1):121-131.
117. Pourghadamyari H, Moohebbati M, Parizadeh SM, Falsoleiman H, Dehghani M, Fazlinezhad A, et al. Serum antibody titers against heat shock protein 27 are associated with the severity of coronary artery disease. *Cell Stress Chaperon* 2011;16(3):309-16.
118. Azarpazhooh MR, Mobarra N, Parizadeh SM, Tavallaie S, Bhageri M, Rahsepar AA, et al. Serum high-sensitivity C-reactive protein and heat shock protein 27 antibody titers in patients with stroke and 6-month prognosis. *Angiology* 2010;61(6):607-12.



CHAPTER 15



HALT & REVERSE: HSF1 ACTIVATORS LOWER CARDIOMYOCYTE DAMAGE; TOWARDS A NOVEL APPROACH TO REVERSE ATRIAL FIBRILLATION

Lanters EAH, van Marion DMS, Kik C, Steen H, Bogers AJJC,
Allessie MA, Brundel BJJM, de Groot NMS
Journal of Translational Medicine (2015)

ABSTRACT

Background Atrial Fibrillation is a progressive arrhythmia, the exact mechanism underlying the progressive nature of recurrent AF episodes is still unknown. Recently, it was found that key players of the protein quality control system of the cardiomyocyte, i.e. Heat Shock Proteins, protect against atrial fibrillation progression by attenuating atrial electrical and structural remodeling (electropathology). HALT & REVERSE aims to investigate the correlation between electropathology, as defined by endo- or epicardial mapping, Heat Shock Protein levels and development or recurrence of atrial fibrillation following pulmonary vein isolation, or electrical cardioversion or cardiothoracic surgery.

Study design This study is a prospective observational study. Three separate study groups are defined: 1) cardiothoracic surgery, 2) pulmonary vein isolation and 3) electrical cardioversion. An intraoperative high-resolution epicardial (group 1) or endocardial (group 2) mapping procedure of the atria is performed to study atrial electropathology. Blood samples for Heat Shock Protein determination are obtained at baseline and during the follow-up period at 3 months (group 2), 6 months (groups 1 and 2) and one year (group 1 and 2). Tissue samples of the right and left atrial appendages in patients in group 1 are analysed for Heat Shock Protein levels and for tissue characteristics. Early post procedural atrial fibrillation is detected by continuous rhythm monitoring, whereas late post procedural atrial fibrillation is documented by either electrocardiogram or 24-hour Holter registration.

Conclusions HALT & REVERSE aims to identify the correlation between Heat Shock Protein levels and degree of electropathology. The study outcome will contribute to novel diagnostic tools for the early recognition of clinical atrial fibrillation.

INTRODUCTION

Atrial Fibrillation (AF) initially presents with short, self-terminating episodes and progresses into long-lasting episodes which are unlikely to convert spontaneously to sinus rhythm.¹ The exact mechanism underlying this progression is unknown. At present, there are no diagnostic tests or biomarkers available predicting recurrences of progressive AF episodes. In daily clinical practice, we can for example, not predict which patients develop AF following cardiac surgery or AF recurrences after pulmonary vein isolation (PVI) or electrical cardioversion (ECV).

AF persistence induces atrial remodeling on an electrical, structural and contractile level, also referred to as electropathology.² Electrical changes such as shortening of AF cycle length and contractile dysfunction occur within days after AF onset.^{3, 4} After weeks of AF persistence, structural alterations become manifest in the extracellular matrix and in cardiomyocytes.^{1, 5-7} Electrical and contractile abnormalities are completely reversible within weeks or days after restoration of sinus rhythm^{3, 7-10}, whereas recovery from structural remodeling is slow and takes up to months.¹¹ This finding indicates that structural remodeling underlies AF progression and recurrences. Therefore, research is directed at identifying key pathways involved in structural remodeling. Recently it was demonstrated that derailment of cardiomyocyte proteostasis, underlies AF progression and recurrences.¹²⁻¹⁵ Cells, including cardiomyocytes, depend for proper functioning on the maintenance of proteostasis: the balance in protein synthesis, folding, assembling, trafficking, and clearance (Figure 1).^{16, 17} Chaperones, mainly consisting of Heat Shock Proteins (HSPs), assist in the maintenance of proteostasis.¹⁷⁻¹⁹ Upon acute stress e.g. in paroxysmal AF, HSPs are upregulated.²⁰ The progressive nature of AF lies in the gradual, often age-related, exhaustion of the HSP levels and subsequent derailment of proteostasis, resulting in structural remodeling and contractile dysfunction of cardiomyocytes (Figure 2). Therefore, compounds that boost HSP expression, such as geranylgeranylacetone (GGA) and GGA derivatives^{21, 22}, are of clinical interest. Indeed, HSPs boosting, via Heat Shock Factor-1 activation, protected against derailment of proteostasis and AF progression and recurrences in several experimental AF models, including tachypaced cardiomyocytes²³, *Drosophila*¹⁵ and canine models²⁴.

The HALT & REVERSE (*Hsf1* Activators Lower Cardiomyocyt damage: Towards a novel approach to REVERSE atrial fibrillation, MEC 2014-393, NTR 4658) project focusses on the correlation between HSPs and progression of electropathology.² Hereto, the HSP levels in blood and atrial samples are determined and related to electrophysiological characteristics of the atria obtained from epicardial mapping during cardiothoracic surgery and endovascular mapping during PVI. The findings will elucidate whether HSP levels and electrophysiological characteristics represent a novel diagnostic tool (a so-called “bio-electrical fingerprint”) to predict the clinical outcome for AF patients and/or cardiac surgery.

Study population

For the HALT & REVERSE project, three separate study groups are defined, consisting of patients scheduled for 1) cardiothoracic surgery, 2) PVI and 3) ECV for symptomatic AF. Each group contains 100 consecutive patients. Patients are recruited at the Department of Cardiothoracic Surgery or at the Department of Cardiology at the Erasmus Medical Center, Rotterdam, The Netherlands. Prior to enrolling in the study, each patient is provided an oral and a written explanation of the study procedure. Written informed consent is obtained from all patients. Blood samples for baseline HSP level determination taken from all patients prior to the scheduled intervention (surgery, PVI or ECV) (Figure 3). Patient characteristics (e.g. age, medical history, cardiovascular risk factors) are obtained from the patient's file.

Inclusion criteria

In order to be eligible to participate in this study, all subjects must be > 18 years old. In the cardiothoracic surgery group, only patients scheduled for elective cardiothoracic surgery for structural heart disease with or without a history of AF are included. The PVI group will enrol patients with paroxysmal or (long-standing) persistent AF. The ECV group will consist of patients with symptomatic, AF presenting for electrical cardioversion.

Exclusion criteria

A potential subject who meets any of the following criteria in all four study groups are excluded from participation in this study: paced atrial rhythm, haemodynamic instability, presence of cardiac assist devices, usage of inotropic agents prior to intervention or patients undergoing emergency or redo cardiac surgery.

Sample size calculation

Approximately 25% of patients undergoing cardiothoracic surgery develop early postoperative AF.²⁵ Estimated AF recurrence rate one year after PVI is 45% as has been shown in previous studies²⁶⁻²⁸, whereas the arrhythmia tends to recur within one year in 25% to 40%²⁹⁻³¹ after ECV. For none of our study groups, data testing the correlation between HSP and AF development or recurrence (in humans) is available. Therefore, a reliable parameter for sample size calculation is not available. Based upon the data mentioned above, we expect a pilot study with 100 patients in each group to be suitable for further determination of the exact number of patients needed to generate a power of 0,95 with a significance of 0,05.

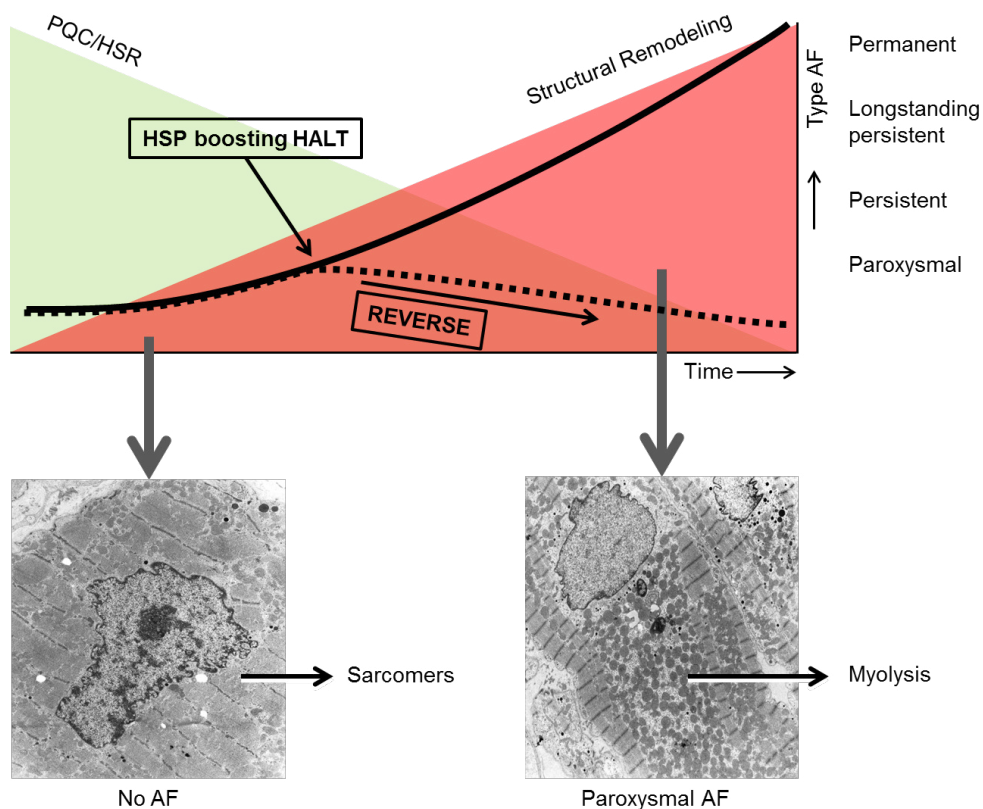


Figure 2. Concept of the HALT & REVERSE project. In the normal heart Protein Quality Control (PQC) and the Heat Shock Response (HSR, upper panel: green area) maintain proteostasis in times of stress. However, with the duration of AF and with increasing age, the heat shock protein (HSP) levels get exhausted. This leads to a derailment of proteostasis (upper panel: red area), resulting in structural remodeling and contractile dysfunction of cardiomyocytes, because of, amongst others, degradation of sarcomers (myolysis, left and right lower panel). AF progresses in time (upper panel: solid line), which is rooted in the underlying electropathology. By pharmacological boosting of HSPs, we aim to HALT or even REVERSE atrial electropathology and consequently AF progression (upper panel: dashed line).

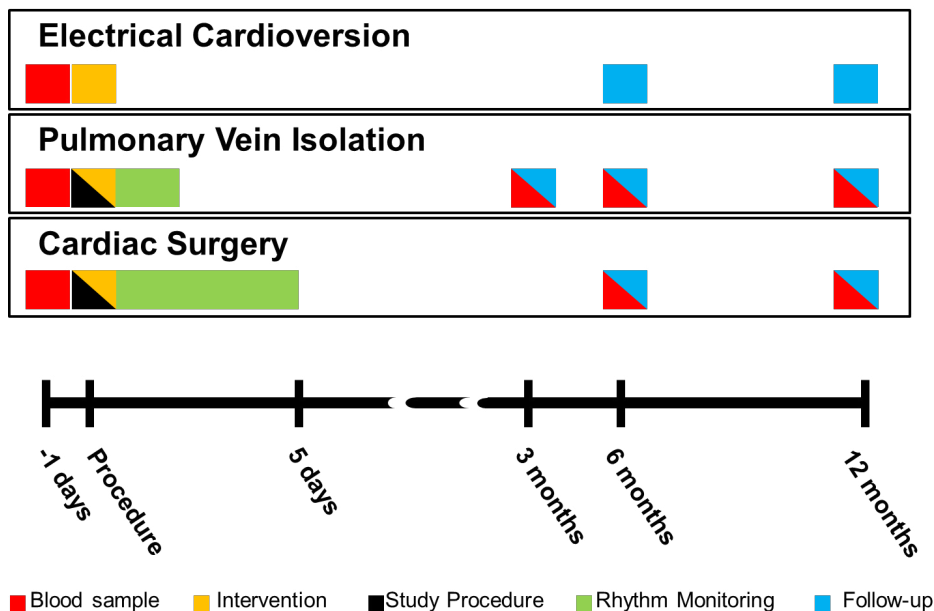


Figure 3. Time course of the HALT & REVERSE project. A baseline blood sample (red bar) is obtained from all patients one day prior to the procedure. In the pulmonary vein isolation – and cardiac surgery group, the study procedure (black bar, epicardial or endocardial mapping procedure) is performed during the elective therapeutic intervention (yellow bar) and post-procedural continuous rhythm monitoring afterwards (green bars). The blue bars indicate long term follow-up (>3 months) including a visit to the outpatient clinic with electrocardiography, blood samples and 24-hour Holter recordings when indicated.

Intra-operative mapping procedure

High resolution epicardial mapping of the entire atria according to a previously described mapping scheme is performed during open chest cardiac surgery³². A reference electrode is temporarily attached to the right atrial appendage. An indifferent electrode consists of a steel wire, placed in subcutaneous tissue. The mapping procedure will be performed using a custom made 192-site electrode array³² with a two millimeter inter-electrode distance. Recordings are made at nine consecutive sites following a predefined mapping scheme (Figure 4) during sinus rhythm (5 seconds/site), during pacing maneuvers for inducing AF (1 site, Bachman's Bundle), and during AF (10 seconds/site). Pacing maneuvers will be performed with epicardial atrial fixed rate pacing at 250-300-350 beats per minute successively, using a standard temporary pacemaker device. If AF sustains until the end of the mapping procedure, sinus rhythm will be restored with 5-10 Joule synchronous electric cardioversion. After introduction cannulas of the cardiopulmonary bypass into the right atrium via the right atrial appendage (RAA) a tissue sample is obtained from the incision site in all patients. A tissue sample of the left atrial appendage (LAA) is obtained if the LAA is incised or amputated during surgery. All collected tissue samples are immediately snap-frozen in liquid nitrogen and stored at -80°C . After the surgical procedure, heart rhythm is continuously monitored until hospital discharge in order to detect early post-operative AF (PoAF). PoAF is defined as a complete irregular heartbeat without consistent P waves, sustaining for at least 30 seconds. At six months and one year

after the procedure, patients visit the outpatient clinic for detection of late post-operative AF. A 12-lead electrocardiogram and a blood sample for HSP analysis are obtained. A 24-hour Holter registration is performed when AF is suspected.

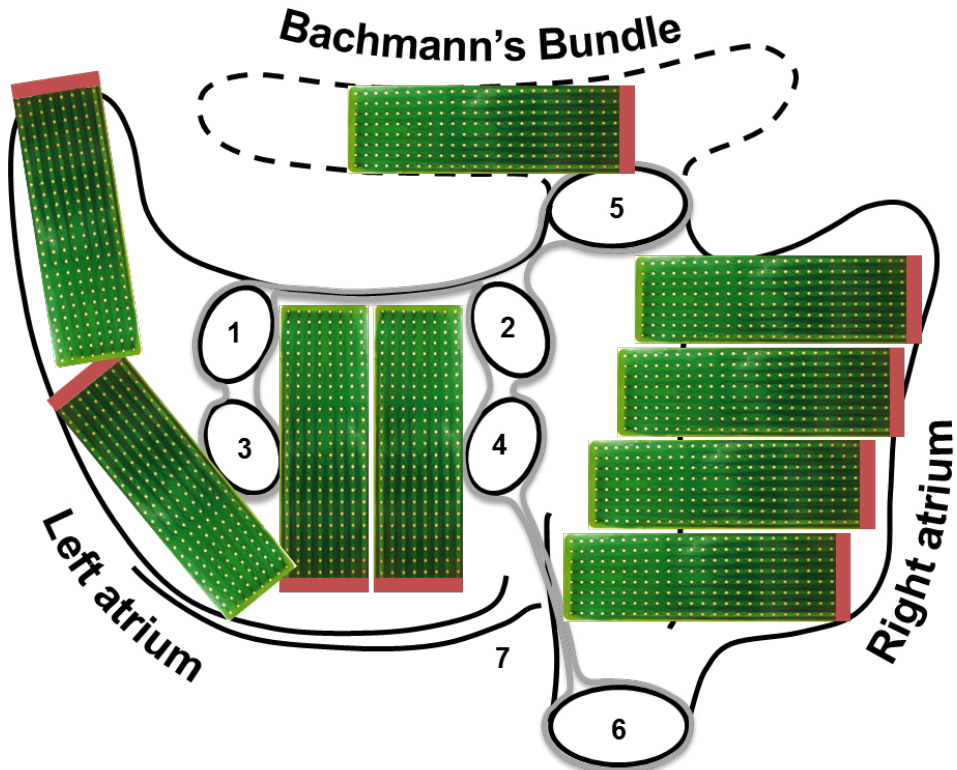


Figure 4. Epicardial mapping scheme. The left and right atrium and Bachmann's Bundle are mapped following a predefined epicardial mapping scheme along anatomical structures, by the use of an 192 polar electrode array (green). 1: Left Superior Pulmonary Vein; 2: Right Superior Pulmonary Vein; 3: Left Inferior Pulmonary vein; 4: Right Inferior Pulmonary Vein; 5: Inferior Caval Vein; 6: Superior Caval Vein; 7: Coronary Sinus.

Pulmonary vein isolation

An endovascular mapping procedure is performed prior to isolation of the pulmonary veins. Atrial electropathology is studied by means of programmed electrical stimulation in the right and the left atrium, including fixed rate atrial pacing, delivery of atrial extra systoles and decremental pacing maneuvers. Recordings of the right atrium are made by a decapolar catheter at the right atrial free wall and pacing is performed from the ablation catheter, which is positioned in the RAA. Mapping in the left atrium is performed by placing a Lasso catheter at the posterior wall and a decapolar catheter in the coronary sinus, while pacing from the left atrial roofline. Subsequently, the PVI is performed according to the electrophysiologist's choice by either radiofrequency ablation or cryoballoon ablation. According to standard care, heart rhythm is monitored continuously until discharge. Recordings are analyzed to detect

early AF episodes, sustained for at least 30 seconds. At three, six months and one year after the procedure, patients visit the outpatient clinic. During these visits, 12-lead ECGs and 24-hour Holter registrations are performed to detect late post procedural AF recurrences and an additional blood sample is obtained for HSP level determination.

Electrical cardioversion

Patients will be interviewed by telephone at 6 and 12 months to detect AF recurrences.

Tissue analysis

All obtained blood samples and atrial tissue samples are stored at -80°C until analysis. All samples are tested for HSP biomarkers, including HSP70 and HSP27. Biomarker levels are determined by commercially available ELISA's and Western blot analysis.

MAIN STUDY PARAMETERS

Intra-operative mapping

Custom-made software used for off-line analysis of the recordings have previously been described in detail³²⁻³⁴. Local activation times of the unipolar atrial potentials are automatically detected in order to reconstruct color-coded activation -, conduction block -, breakthrough -, voltage- and wavemaps during sinus rhythm and AF.³²⁻³⁴ An example of an activation and wavemap constructed during AF is given in Figure 5. The maps are used to quantify electrophysiological variables. These variables are correlated with the pre-operative HSP level and development of post-operative AF.

Pulmonary vein isolation

The degree of fractionated electrograms obtained from multiple sites in the right and left atrium are studied for fractionation and cycle length variation. HSP levels prior to PVI are correlated with the development of AF recurrence.

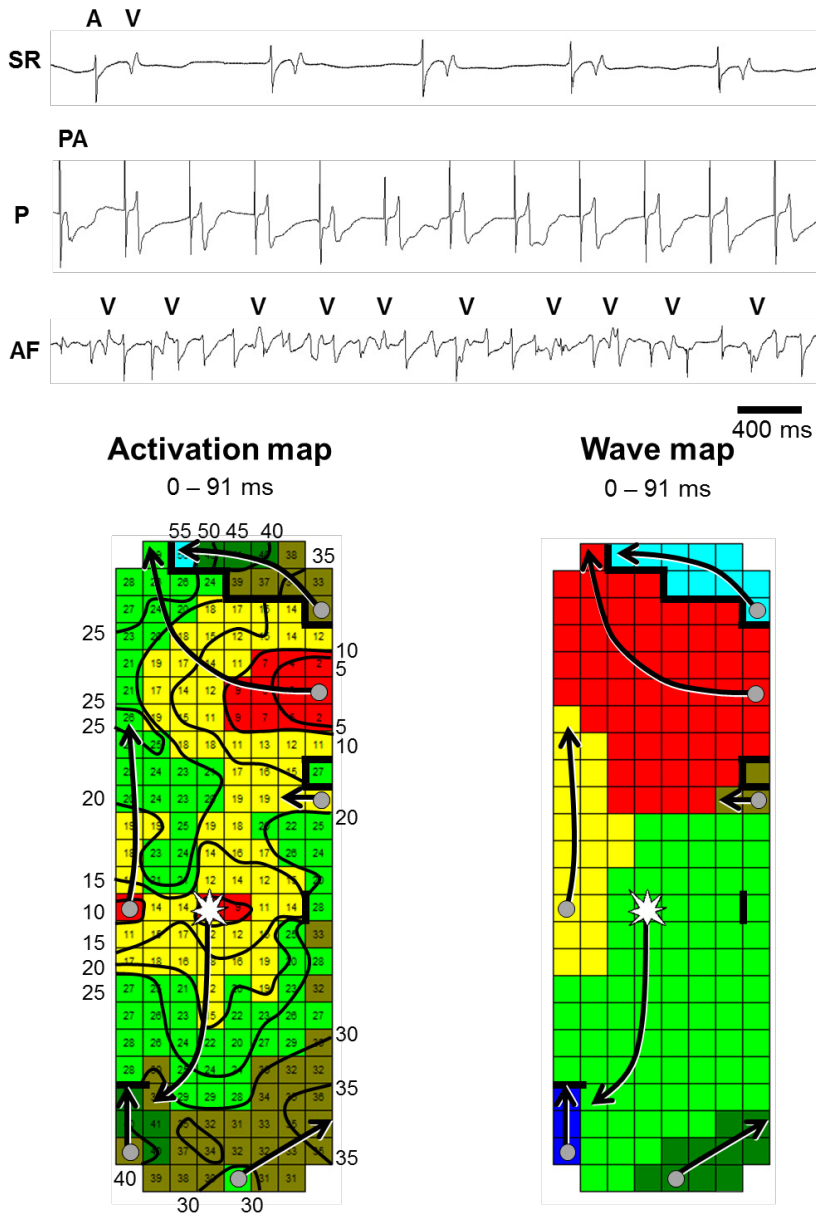


Figure 5. Epicardial high resolution mapping of the atria. Atrial electrograms recorded during sinus rhythm (SR), atrial pacing (P) and (electrically induced) atrial fibrillation (AF) obtained during the epicardial mapping procedure are shown in the upper panel. The left lower panel shows an example of an activation map during electrically induced AF of the right atrium in a patient undergoing coronary artery bypass grafting without a history of AF. Isochrones are drawn at 5ms, areas of conduction block are indicated by black bars, the origin of peripheral and epicardial breakthrough waves by respectively grey dots and white asterisks. The arrows indicate main activation direction. Corresponding wavemap is displayed in the right lower panel. The wavemap shows the different types of fibrillation waves entering the mapping area from various directions. These maps are used to determine the incidence of e.g. conduction block and epicardial breakthrough.

Electrical cardioversion

Correlation between HSP levels prior to cardioversion and successful restoration of sinus rhythm and AF recurrences is determined.

Study endpoints

For all groups, endpoint of the study is reached when AF develops after cardiac surgery or recurs after ECV or PVI. The correlation between several biomarkers (HSP70, HSP27) and development or recurrences of AF is determined, but also the correlation between degree of electropathology and development or recurrences of AF. The relationship between atrial electrophysiological variables, as visualised by epicardial mapping, and structural tissue characteristics are tested. The findings will indicate whether HSP levels and/or the degree of electropathology represent a novel diagnostic tool to predict the clinical outcome of AF progression and/or recurrences.

STATISTICAL ANALYSIS

The association between biomarker levels and development or recurrence of atrial fibrillation is calculated using multivariate logistic regression (for short term outcome) and cox regression models (for long-term outcome). Furthermore, Kaplan Meier lifetables are created for the three groups (cardiac surgery, PVI and ECV) and Log rank tests are used to compare the different groups. ANOVA is utilized to compare various electrophysiological continuous parameters, for categorical parameters the chi-square test will be used. Repeated HSP measurements are conducted by Joint modeling and mixed modeling analysis. Multiple biomarkers levels are corrected by ANOVA with Bonferoni adjustments.

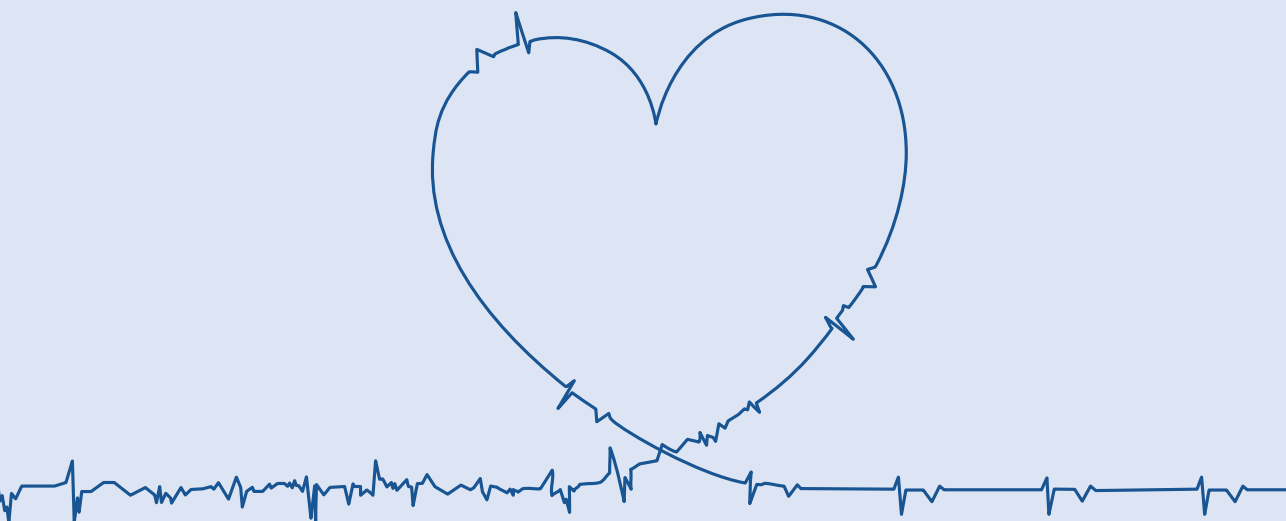
CONCLUSION

HALT & REVERSE aims to examine the interplay between electropathological substrate underlying AF, and HSP levels in the blood and atrial tissue, in order to predict development, recurrence or progression of AF. The results will elucidate whether HSP levels and electrophysiological characteristics can be used as a future diagnostic tool in the clinical setting.

REFERENCES

1. Camm AJ, Kirchhof P, Lip GYH, Schotten U, Savelieva I, Ernst S, et al. Guidelines for the management of atrial fibrillation The Task Force for the Management of Atrial Fibrillation of the European Society of Cardiology (ESC). *Eur Heart J* 2010;31(19):2369-2429.
2. Lanters EAH, van Marion DMS, Steen H, de Groot NMS, Brundel BJJM. The future of atrial fibrillation therapy: intervention on heat shock proteins influencing electropathology is the next in line. *Netherlands Heart Journal* 2015;23(6):327-333.
3. Allesie M, Ausma J, Schotten U. Electrical, contractile and structural remodeling during atrial fibrillation. *Cardiovasc Res* 2002;54(2):230-246.
4. Schotten U, Duytschaever M, Ausma J, Eijssbouts S, Neuberger HR, Allesie M. Electrical and contractile remodeling during the first days of atrial fibrillation go hand in hand. *Circulation* 2003;107(10):1433-1439.
5. Ausma J, Litjens N, Lenders MH, Duimel H, Mast F, Wouters L, et al. Time course of atrial fibrillation-induced cellular structural remodeling in atria of the goat. *J Mol Cell Cardiol* 2001;33(12):2083-2094.
6. Neuberger HR, Schotten U, Blaauw Y, Vollmann D, Eijssbouts S, van Hunnik A, et al. Chronic atrial dilation, electrical remodeling, and atrial fibrillation in the goat. *J Am Coll Cardiol* 2006;47(3):644-653.
7. Wijffels MCEF, Kirchhof CJHJ, Dorland R, Allesie MA. Atrial-Fibrillation Begets Atrial-Fibrillation - a Study in Awake Chronically Instrumented Goats. *Circulation* 1995;92(7):1954-1968.
8. Yu WC, Lee SH, Tai CT, Tsai CF, Hsieh MH, Chen CC, et al. Reversal of atrial electrical remodeling following cardioversion of long-standing atrial fibrillation in man. *Cardiovasc Res* 1999;42(2):470-476.
9. Ausma J, Duimel H, Borgers M, Allesie MA. Recovery of structural remodeling after cardioversion of chronic atrial fibrillation. *Circulation* 2000;102(18):153-153.
10. Ausma J, Duimel H, Lenders MH, Allesie M, Ramaekers F, Borgers M. Altered expression patterns of structural proteins induced by 16 weeks of atrial fibrillation are partially restored 8 weeks after cardioversion. *Eur Heart J* 2000;21:241-241.
11. Ausma J, van der Velden HMW, Lenders MH, van Ankeren EP, Jongsma HJ, Ramaekers FCS, et al. Reverse structural and gap-junctional remodeling after prolonged atrial fibrillation in the goat. *Circulation* 2003;107(15):2051-2058.
12. Meijering RAM, Henning RH, Brundel BJJM. Reviving the protein quality control system: Therapeutic target for cardiac disease in the elderly. *Trends Cardiovasc Med* 2015;25(3):243-247.
13. Meijering RAM, Zhang DL, Hoogstra-Berends F, Henning RH, Brundel BJJM. Loss of proteostatic control as a substrate for atrial fibrillation: a novel target for upstream therapy by heat shock proteins. *Front Physiol* 2012;3.
14. Zhang DL, Wu CT, Qi XY, Meijering RAM, Hoogstra-Berends F, Tadevosyan A, et al. Activation of Histone Deacetylase-6 Induces Contractile Dysfunction Through Derailment of alpha-Tubulin Proteostasis in Experimental and Human Atrial Fibrillation. *Circulation* 2014;129(3):346-358.
15. Zhang DL, Ke L, Mackovicova K, Van Der Want JJL, Sibon OCM, Tanguay RM, et al. Effects of different small HSPB members on contractile dysfunction and structural changes in a *Drosophila melanogaster* model for Atrial Fibrillation. *J Mol Cell Cardiol* 2011;51(3):381-389.
16. Balch WE, Morimoto RI, Dillin A, Kelly JW. Adapting proteostasis for disease intervention. *Science* 2008;319(5865):916-919.
17. Willis MS, Patterson C. Proteotoxicity and Cardiac Dysfunction Reply. *New Engl J Med* 2013;368(18):1755-1755.
18. Powers ET, Balch WE. Diversity in the origins of proteostasis networks - a driver for protein function in evolution. *Nat Rev Mol Cell Bio* 2013;14(4):237-248.
19. Wang XJ, Robbins J. Heart failure and protein quality control. *Circ Res* 2006;99(12):1315-1328.

20. Brundel BJJM, Henning RH, Ke L, van Gelder IC, Crijns HJGM, Kampinga HH. Heat shock protein upregulation protects against pacing-induced myolysis in HL-1 atrial myocytes and in human atrial fibrillation. *J Mol Cell Cardiol* 2006;41(3):555-562.
21. Brundel BJ, Oi XY, Yeh YH, Shiroshita-Takeshita A, Chartier D, Henning RH, et al. HSP27 is sufficient and required for prevention of tachycardia induced remodeling in a cell model for tachypacing. *Circulation* 2006;114(18):9-9.
22. Hoogstra-Berends F, Meijering RAM, Zhang DL, Heeres A, Loen L, Seerden JP, et al. Heat Shock Protein-Inducing Compounds as Therapeutics to Restore Proteostasis in Atrial Fibrillation. *Trends Cardiovas Med* 2012;22(3):62-68.
23. Brundel BJJM, Kampinga HH, Henning RH. Calpain inhibition prevents pacing-induced cellular remodeling in a HL-1 myocyte model for atrial fibrillation. *Cardiovasc Res* 2004;62(3):521-528.
24. Sakabe M, Shiroshita-Takeshita A, Brundel B, Nattel S. Effects of heat shock protein induction on atrial fibrillation caused by acute atrial ischemia. *Circulation* 2006;114(18):200-200.
25. Pillarisetti J, Patel A, Bommana S, Guda R, Falbe J, Zorn GT, et al. Atrial fibrillation following open heart surgery: long-term incidence and prognosis. *J Interv Card Electr* 2014;39(1):69-75.
26. Kuhne M, Schaer B, Ammann P, Suter Y, Osswald S, Sticherling C. Cryoballoon ablation for pulmonary vein isolation in patients with paroxysmal atrial fibrillation. *Swiss Med Wkly* 2010;140(15-16):214-221.
27. Steinberg JS, Palekar R, Sichrovsky T, Arshad A, Preminger M, Musat D, et al. Very long-term outcome after initially successful catheter ablation of atrial fibrillation. *Heart Rhythm* 2014;11(5):771-776.
28. Van Belle Y, Janse P, Theuns D, Szili-Torok T, Jordaens L. One year follow-up after cryoballoon isolation of the pulmonary veins in patients with paroxysmal atrial fibrillation. *Europace* 2008;10(11):1271-1276.
29. Gitt AK, Smolka W, Michailov G, Bernhardt A, Pittrow D, Lewalter T. Types and outcomes of cardioversion in patients admitted to hospital for atrial fibrillation: results of the German RHYTHM-AF Study. *Clin Res Cardiol* 2013;102(10):713-723.
30. Blich M, Edoute Y. Electrical cardioversion for persistent or chronic atrial fibrillation: Outcome and clinical factors predicting short and long term success rate. *Int J Cardiol* 2006;107(3):389-394.
31. Pistors R, Nieuwlaat R, Prins MH, Le Heuzey JY, Maggioni AP, Camm AJ, et al. Clinical correlates of immediate success and outcome at 1-year follow-up of real-world cardioversion of atrial fibrillation: the Euro Heart Survey. *Europace* 2012;14(5):666-674.
32. Yaksh A, Kik C, Knops P, Roos-Hesselink JW, Bogers AJJC, Zijlstra F, et al. Atrial fibrillation: to map or not to map? *Netherlands Heart Journal* 2014;22(6):259-266.
33. de Groot NMS, Houben RPM, Smeets JL, Boersma E, Schotten U, Schalij MJ, et al. Electropathological Substrate of Longstanding Persistent Atrial Fibrillation in Patients With Structural Heart Disease Epicardial Breakthrough. *Circulation* 2010;122(17):1674-1682.
34. Allesie MA, de Groot NMS, Houben RPM, Schotten U, Boersma E, Smeets JL, et al. Electropathological Substrate of Long-Standing Persistent Atrial Fibrillation in Patients With Structural Heart Disease. *Circ-Arrhythmia Elec* 2010;3(6):606-615.



CHAPTER 16



EVALUATING SERUM HEAT SHOCK PROTEIN LEVELS AS NOVEL BIOMARKERS FOR ATRIAL FIBRILLATION

van Marion DMS*, Lanthers EAH*, Ramos KS, Li J, Wiersma M, Baks-te Bulte L,
Muskens A, Boersma E, de Groot NMS, Brundel BJJM

** both authors contributed equally*

Cells (2020)

ABSTRACT

Background Staging of atrial fibrillation (AF) is essential to understand disease progression and the accompanied increase in therapy failure. Blood-based heat shock protein (HSP) levels may enable staging of AF and identification of patients with higher risk for AF recurrence after treatment. This study evaluates the relation between serum HSP levels, presence of AF, AF stage and AF recurrence following electrocardioversion (ECV) or pulmonary vein isolation (PVI).

Methods To determine HSP27, HSP70, cardiovascular (cv)HSP and HSP60 levels, serum samples were collected from control patients without AF and patients with paroxysmal (PAF), persistent (PeAF) and longstanding persistent (LSPeAF) AF presenting for ECV or PVI, prior to intervention and at 3-, 6- and 12-months post-PVI.

Results The study population (N=297) consisted of 98 control and 199 AF patients admitted for ECV (N=98) or PVI (N=101). HSP27, HSP70, cvHSP and HSP60 serum levels did not differ between patients without or with PAF, PeAF or LSPeAF. Also, baseline HSP levels did not correlate with AF recurrence after ECV or PVI. However, in AF patients with AF recurrence, HSP27 levels were significantly elevated post-PVI relative to baseline, compared to patients without recurrence.

Conclusions No association was observed between baseline HSP levels and the presence of AF, AF stage or AF recurrence. However, HSP27 levels were increased in serum samples of patients with AF recurrence within one year after PVI, suggesting that HSP27 levels may predict recurrence of AF after ablative therapy.

INTRODUCTION

Atrial fibrillation (AF) is the most common cardiac arrhythmia with a rising prevalence due to the aging population.¹ Proper staging of AF is essential to select the optimal treatment strategies to prevent AF progression, and the accompanied risk to develop severe complications such as thromboembolic events, heart failure, cognitive impairment and increased mortality.^{2,3} At present, AF can only be diagnosed with a surface electrocardiogram when a patient already suffers from AF, presenting with palpitations or thromboembolic complications. However, diagnosis of AF may be challenging in patients with asymptomatic or very short-lasting episodes of AF.⁴ In addition, treatment aimed at rhythm control, such as ablative therapy, is less successful in patients with persistent AF compared to paroxysmal AF.³ Hence, proper staging of AF and start of effective treatment of AF is of utmost importance. Therefore, there is an urgent need to identify diagnostic biomarkers to stage AF and guide patient tailored therapy.⁵

Biomarkers are widely accepted as a diagnostic tool to screen or monitor patients for a variety of cardiovascular diseases. At present, there are no recommendations on the use of AF-specific biomarkers in the most recent guidelines^{3,6} despite that several blood-based biomarkers related to AF pathology have been identified. These biomarkers include brain natriuretic peptides, cancer-antigen-125, fibroblast growth factor-23^{7,8} and -21⁹, high-sensitive cardiac troponin I¹⁰, homocysteine¹¹, (a)symmetric dimethylarginine¹², interleukine-6 and matrix metalloproteinase-9/tissue inhibitor of metalloproteinase-1 ratio¹³. Although potential AF-related biomarkers are available, the role of these biomarkers to stage of AF (paroxysmal or (longstanding) persistent AF) or predict AF recurrence after AF therapy has only been moderately studied.

Emerging evidence indicates that heat shock proteins (HSPs) may represent a suitable biomarker to predict AF recurrence after treatment. HSPs are chaperones with an important role in safeguarding proteostasis, the homeostasis of protein expression, function and degradation in cells.¹⁴ Derailment of proteostasis has been identified as a key factor underlying electropathology and AF progression.¹⁴⁻¹⁶ During stress or disease, such as AF, especially activation of the heat shock transcription factor 1 regulates HSP transcription.¹⁷ Within the HSP family, small HSPs, including HSP27, are probably the most important in maintaining proteostasis in cardiomyocytes by stabilizing the contractile proteins.¹⁸⁻²¹ Previously, atrial HSP27 levels were found to be induced in atrial tissue samples of patient with paroxysmal AF, while tissue HSP27 levels get exhausted in patients with (longstanding) persistent AF¹⁸, indicating that low tissue HSP levels are associated with AF progression. The study of Hu, et al. described that low baseline serum HSP27 levels of patients who received ablative therapy predict AF recurrence and patients with high baseline serum levels of HSP27 showed an improved maintenance rate of sinus rhythm.²² So far, it is unknown which HSP family member(s) represent biomarkers to identify the stage of AF and recurrence after therapy. In the current study, various members of the HSP family, including HSP27, HSP70, cardiovascular (cv)HSP and HSP60, were measured in serum samples of control and patients with paroxysmal (PAF), persistent (PeAF) and longstanding persistent (LSPeAF) AF, undergoing elective electrical cardioversion (ECV) or pulmonary vein isolation (PVI), to identify whether HSPs associate with the stage of AF and recurrences after either PVI or ECV. Herein, we report that baseline HSP levels between control and AF patients are comparable. However, HSP27 levels were increased in follow-up samples of patients with AF recurrence after PVI, suggesting that increased HSP27 levels may predict recurrence of AF after ablative therapy.

METHODS

Study population

From December 2014 till November 2016, 297 subjects >18 years with or without a history of AF were prospectively enrolled for the HALT & REVERSE study²³ at the department of cardiology in the Erasmus MC, Rotterdam, the Netherlands. The study population consists of a control group of patients without a history of AF and a study group of patients with symptomatic AF who were scheduled for electrical cardioversion (ECV) or pulmonary vein isolation (PVI).

The control group consisted of patients (N=98), who were scheduled for elective ablation of premature ventricular contractions (PVC), Wolff-Parkinson-White syndrome (WPW) or Ajmaline testing. These patients were eligible for inclusion in case of absence of structural heart disease and any atrial tachyarrhythmia. Blood serum samples were obtained 1 day prior to the scheduled intervention. Follow-up was not performed.

The study group included patients presenting for ECV (N=98) or PVI (N=101) for either symptomatic PAF (less than 7 days of AF), PeAF (having AF between 7 days and 1 year) or LSPeAF (more than 1 year of AF). Exclusion criteria included paced atrial rhythms, cancer, inflammation and rheumatic diseases. Blood samples were obtained 1 day prior to the scheduled intervention. PVI was unsuccessful in two patients.

Patients who underwent PVI visited the outpatient clinic at 3-, 6- and 12-months after the procedure to provide follow up serum samples and to screen for AF recurrences. Due to rescheduling of patients to different hospitals, follow up serum samples were not available for some patients in both the AF recurrence and no recurrence group. In addition, AF recurrence data is available via recordings during in between visits due to AF complaints of the patients. AF recurrence was defined as an AF episode documented on either a 12-lead surface ECG or Holter monitor recordings. In patients undergoing ECV, for each individual patient only a 3-, 6- and 12-months post-procedural follow up telephone consultation was scheduled. Study endpoint was the completion of the 12- months follow up period or earlier due to withdrawn informed consent, pacemaker implant or AF recurrence. Clinical characteristics were obtained from the electronic patients' files.

All patients signed written informed consent prior to inclusion. This sub-study is part of the HALT & REVERSE trial (MEC-2014-393)²² and is approved by the institutional medical ethical committee. The study is carried out according to the principals of the Declaration of Helsinki in accordance with the Medical Research Committee involving the Human Subjects Act.

HSP measurement in serum samples

Immediately after blood sample collection, serum was harvested from blood in BD Vacutainer™ SST™ II Advance Tubes (Fisher Scientific) by centrifugation at 2000 x g for 10 min at 4°C and frozen in -80°C until analysis of HSP27, HSP70, cvHSP and HSP60 levels. For measurement of serum HSP27 levels, samples were diluted six times and for HSP70 levels samples were diluted twice in 1% BSA in PBS. The amount of HSP27 and HSP70 protein was detected in triplicates using human HSP27 or HSP70 DuoSet® ELISA kits from R&D

(Cat. no. DY1580 and DY1663, respectively) according to the manufacturer's instructions with minor adjustments (serum was incubated at 4°C overnight, instead of 2 hours at room temperature). Undiluted serum was used to measure cvHSP protein (singular) with ELISA kits from Cusabio (CSB-EL010838HU) according to manufacturer's instructions with minor adjustments (kept incubation temperature at 20°C). Undiluted serum was used to measure HSP60 protein in duplicate with the HSP60 DuoSet® ELISA kit from R&D (DYC1800) according to manufacturer's instructions.

Statistical Analysis

Data were analyzed with SPSS Statistics version 26.0 for Windows (SPSS, Inc.) and GraphPad Prism version 8.0 (Graphpad Software Inc., San Diego, CA). All data were tested for Gaussian distribution. Continuous and normally distributed data are presented as mean \pm standard deviation (SD), non-normally distributed data as median [interquartile range (IQR)], and categorical data as number (percentage). Differences in clinical characteristics and HSP levels between patients with and without AF were tested with independent-samples t-test,

Table 1. Clinical characteristics of the study population

	Control	PAF	PeAF	LSPeAF	All AF patients
N (%)	98 (33)	86 (29)	108 (36.4)	5 (1.7)	199 (67)
Group, N (%)					
Control	98 (100)	-	-	-	-
Electro cardioversion	-	12 (14)	83 (76.9)	3 (60)	98 (49)
Pulmonary vein isolation	-	74 (86)	25 (23.1)	2 (40)	101 (51)
Age (years), mean \pm SD	48.2 \pm 15.3	61.3 \pm 9.5***	60.8 \pm 10.6***	57.5 \pm 9	60.9 \pm 10.1***
Gender, male, N (%)	51 (52)	64 (74.4)**	81 (75)**	4 (80)	149 (74.9)***
BMI (kg/m²), mean \pm SD	25.1 \pm 3.7	27.2 \pm 3.8*	28.8 \pm 5.4***	30.4 \pm 7.4	28.2 \pm 4.9***
Hypertension, yes, N (%)	23 (23.5)	43 (50)***	51 (47.2)**	3 (60)	97 (48.7)***
Diabetes mellitus, yes, N (%)	5 (5.1)	10 (11.6)	15 (13.9)	1 (20)	26 (13.1)*
Dyslipidemia, yes, N (%)	16 (16.3)	25 (29.1)	33 (30.6)	3 (60)	61 (30.7)**
Thyroid disease, yes, N (%)	2 (2)	4 (4.7)	8 (7.4)	1 (20)	13 (6.5)
Left ventricular function, N (%)			*/###		
Normal	61 (79.2)	73 (84.9)	60 (58.3)	3 (60)	136 (70.1)
Mild impairment	10 (13)	9 (10.5)	29 (28.2)	2 (40)	40 (20.6)
Moderate impairment	3 (3.9)	3 (3.5)	10 (9.7)	0 (0)	13 (6.7)
Severe impairment	3 (3.9)	1 (1.2)	4 (3.9)	0 (0)	5 (2.9)
Missing^f	21	0	5	0	5
Left atrial volume index (ml/m2), median [IQR]	27.9 [21.2-39.7]	38.6 [29.3-48.4]*	47 [35.7-60.5]**/###	43.1 [25.9-73.6]	41.1 [31.8 – 54]**
Drugs, yes, N (%)					
Drugs total	52 (53.6)	84 (97.7)***	104 (96.3)***	5 (100)	193 (97)***
ACE. ARB. AT2 antagonist	26 (26.8)	40 (46.5)*	48 (44.9)*	3 (60)	91 (46)**

	Control	PAF	PeAF	LSPeAF	All AF patients
Statin	17 (17.5)	32 (37.2)*	37 (34.3)*	4 (80)*	73 (36.7)***
Antiarrhythmic drugs (AAD) total‡	43 (44.3)	79 (91.9)***	103 (95.4)***	5 (100)	187 (94)***
Class I AAD	5 (5.2)	31 (36.0)***	14 (13)###	1 (20)	46 (23.1)***
Class II AAD	31 (32)	36 (41.9)	55 (50.9)*	1 (20)	92 (46.2)*
Class III AAD	6 (6.2)	42 (48.8)	55 (50.9)	2 (40)	99 (49.7)***
Class IV AAD	3 (3.1)	4 (4.7)	7 (6.5)	5 (100)	11 (5.5)
Digoxin	0 (0)	6 (7)*	18 (16.7)***	1 (20)	25 (12.6)***

[†] The percentages of LVF are the valid percentage, thus corrected for the missing values

[‡] Patients could use more than one type of AAD; therefore, the sum of all classes is not equal to total. * $P<0.05$;

** $P<0.01$ and *** $P<0.001$ compared to control. ## $P<0.01$ and ### $P<0.001$ comparing paroxysmal AF with persistent AF

Mann-Whitney and Chi-square test. Differences in clinical characteristics and HSP levels between patients without a history of AF, PAF, PeAF and LSPeAF were tested with one-way analysis of variance (ANOVA), Kruskal-Wallis test, Chi-square test and Fisher's Exact test. When serum HSP levels were below detection limit of the ELISA (only for N=7 cvHSP and N=41 HSP60 samples), values at the lower limit of detection were used for statistical analysis. HSP levels are not normally distributed and are Log transformed for statistical analysis (original HSP values are presented in Tables and Figures). Uni- and multivariate linear regression was used to correlate baseline serum HSP levels with clinical parameters and bivariate spearman correlation was used to correlate AF recurrence with clinical parameters. The difference between baseline and follow up serum HSP levels was calculated with a repeated measures model. To relate HSP levels over time with AF recurrence and to analyze the sensitivity of the results, sensitivity analysis was performed using joint modeling. Hereto, the occurrence of the first AF recurrence (endpoint) in relation to the standardized ('Z') value of $\log_2(\text{HSP})$ was modeled, while using all measurements up to and including the moment of the first AF recurrence in endpoint event cases, and all measurements in those who remained event-free. A two-sided P value of <0.05 indicates statistical significance.

RESULTS

Study population

The entire study population consisted of 297 patients (67% males, age 56.7 ± 13.4 years), including a control group of 98 patients without AF and a study group of 199 patients with either PAF (N=86, 29%), PeAF (N=108, 36.4%), or LSPeAF (N=5, 1.7%) AF. Table 1 outlines baseline characteristics of the entire study population. Patients with AF were older ($P<0.001$), more often male ($P<0.001$), had a higher BMI ($P<0.001$), had more often hypertension ($P<0.001$), diabetes mellitus ($P<0.01$) and dyslipidemia ($P<0.05$) compared to patients without AF (Table 1). Clinical parameters did not differ between patients with paroxysmal and persistent AF except for an impaired LVF ($P<0.001$) and larger left atrial volume ($P<0.01$) in the persistent AF patients.

Baseline HSP levels related to clinical stage of AF

To study the relation between baseline HSP levels and the stage of AF, HSP27, HSP70, cvHSP and HSP60 levels were determined in serum samples of PAF, PeAF and LSPeAF patients and compared to controls. Figure 1 shows baseline concentrations of serum HSP27, HSP70, cvHSP and HSP60 of both control and AF patients; corresponding values are depicted in Supplemental Table 1. These findings and the absence of a correlation between AF stage and HSP levels after correction for potential confounders in a multivariate model (Supplemental Table 2 and 3), indicate that there are no differences in serum HSP values between the control patients and AF patients with PAF, PeAF and LSPeAF.

Relation between baseline HSP levels and AF recurrence

In the total AF population, AF recurrence was significantly correlated to AF stage, age, dyslipidemia and LVF, but not related to medication usage (Supplemental Table 4).

After ECV, AF recurrence was determined within 3 months (N=52, 53.1%), 6 months (N=55, 56.1%) and one year (N=64, 65.3%) (Supplemental Table 5). Figure 2 shows the distribution of the various HSP levels in patients with AF recurrence (red) compared to the remainder of the ECV population (green). Baseline HSP27, HSP70, cvHSP and HSP60 levels did not differ between patients with or without AF recurrences within the first year after ECV (Figure 2, Supplemental Table 5 and 6).

AF recurrences after PVI occurred within 3 months (N=34, 34%), 6 months (N=47, 47%) and within 1 year (N= 59, 58%) (Supplemental Table 7). For all time points, AF episodes were more often observed in patients with PeAF or LSPeAF compared to patients with PAF ($P<0.01$). Baseline serum HSP levels did not discriminate between patients with and without

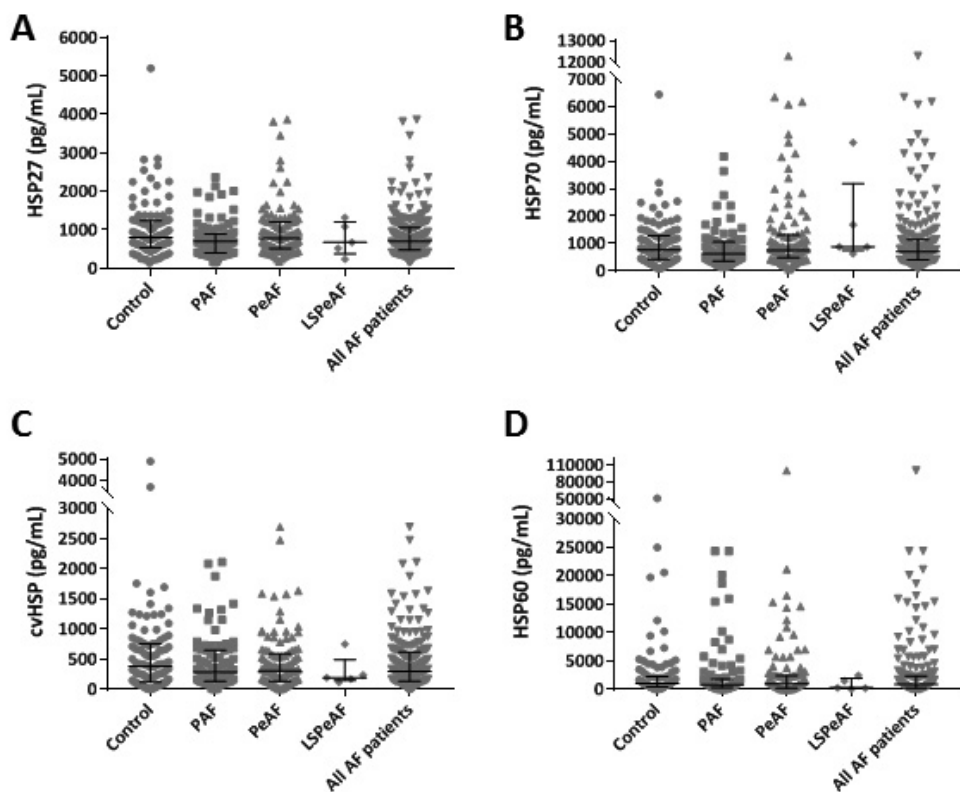


Figure 1. Baseline HSP serum levels in patients without and with (paroxysmal, persistent and longstanding persistent) AF. HSP27 (A), HSP70 (B), cvHSP (C) and HSP60 (D) expression levels (pg/mL) in baseline serum of control, PAF, PeAF, LSPeAF and all AF patients.

AF recurrence, as demonstrated in Figure 3, and Supplemental Table 6. However, HSP27 and HSP70 levels were significantly increased at 3-, 6- and 12-months post-PVI treatment in patients with an AF recurrence within one year compared to baseline levels (Figure 4 and Supplemental Table 6). The increase in serum HSP27 levels, and not HSP70 levels, corrected for repeated measures, is significantly associated with AF recurrence ($P < 0.013$), substantiating the role of HSP27 in the prediction of AF recurrence after PVI.

To relate HSP levels over time with AF recurrence as an endpoint, joint modeling was utilized. Therefore, the occurrence of first AF recurrence (endpoint) in relation to the standardized ('Z') value of $\log_2(\text{HSP})$ was modeled, while using all measurements up to and including the moment of the first AF recurrence in endpoint event cases, and all measurements in those who remained event-free. The results are depicted in the Table 2 (row 'all events'). One standard deviation (SD) difference in \log_2 HSP27 level was associated with a hazard ratio (HR) of 1.32 for having an AF recurrence, supporting the outcomes from the repeated measure model. Unfortunately, the joint modeling for HSP70 did not converge, and therefore no reliable HR estimate could be obtained.

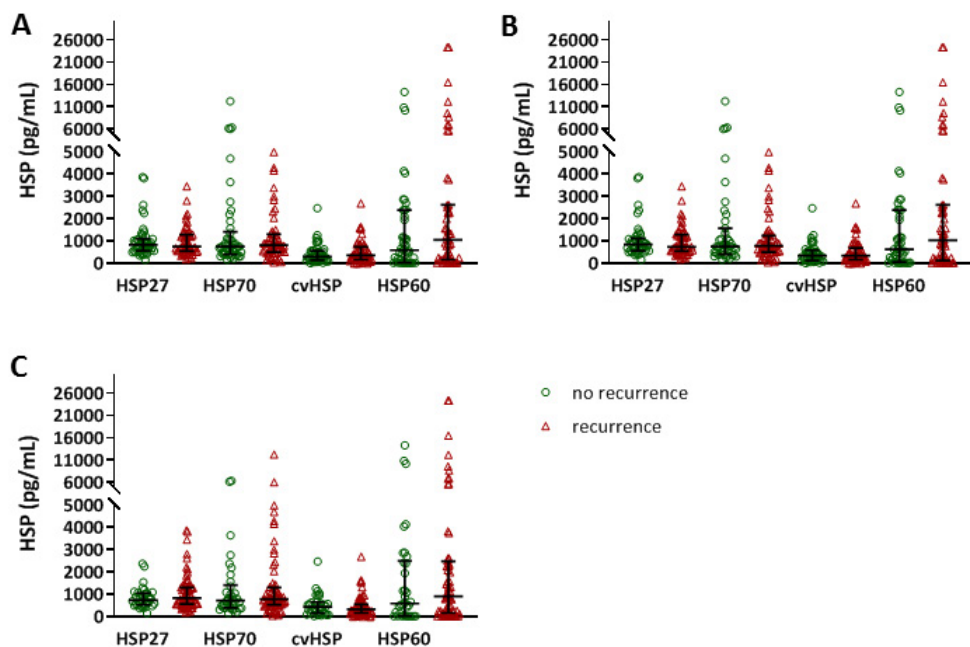


Figure 2. No differences in baseline HSP27, HSP70, cvHSP or HSP60 serum levels between patients with and without AF recurrence after ECV. HSP27, HSP70, cvHSP and HSP60 serum levels (pg/mL) at baseline comparing patients with and without AF recurrence within 3 months (A), 6 months (B) and 1 year (C) after ECV treatment.

Sensitivity analysis non-random dropout

Although an association between HSP27 levels and the recurrence of AF after PVI was observed, sensitivity analyses were conducted to evaluate the robustness of our findings in relation to possible non-random drop out. Therefore, joint models based on the following sensitivity datasets were run: all available data (all events); patients with an AF recurrence at 3 months who also had an HSP measurement at 3 months (21 cases), in combination with patients who were free of AF recurrence at 3 months and with an HSP measurement ≥ 3 months (54 patients) (complete until 3m); patients with an AF recurrence at 3 or 6 months who also had an HSP measurement at the moment of the AF recurrence (29 cases), in combination with patients who were free of AF recurrence at 6 months and with an HSP measurement ≥ 6 months (36 patients) (complete until 6m); and patients with an AF recurrence at 3-, 6- or 12-months who also had an HSP measurement at the moment of the AF recurrence (31 cases), in combination with patients who were free of AF recurrence at 12 months and with an HSP measurement at 12 months (13 patients) (complete until 12m). The findings of the sensitivity analyses are provided in Table 2. HSP27 levels were associated with a HR of 2.03 for having an AF recurrence within 6 months post PVI treatment. The results confirm that HSP27 is associated with AF recurrence, and may be used as a predictor. However, HSP70 does not seem to be associated with AF recurrence.

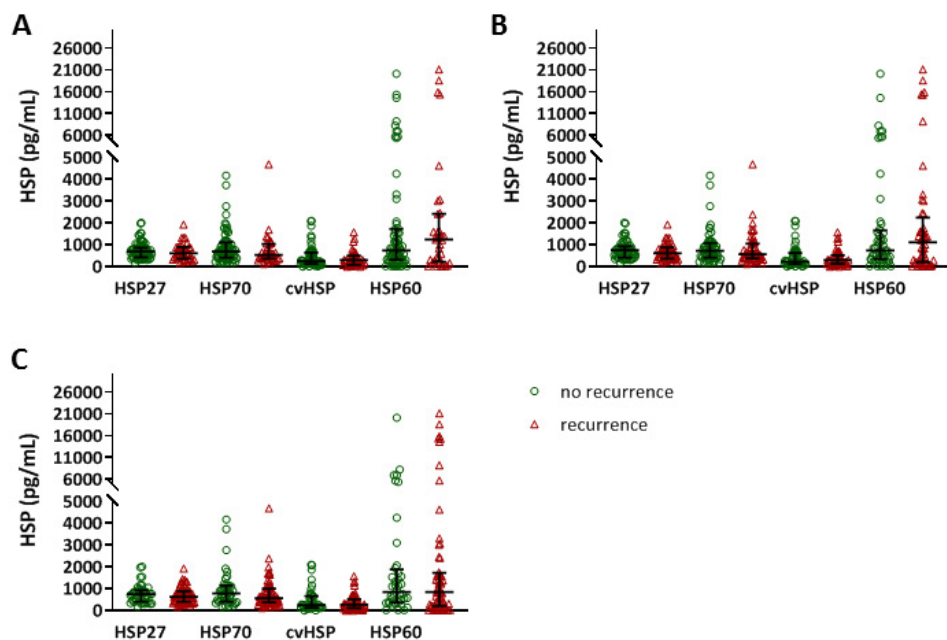


Figure 3. No differences in baseline HSP27, HSP70, cvHSP or HSP60 serum levels between patients with and without AF recurrence after PVI. HSP27, HSP70, cvHSP and HSP60 serum levels (pg/mL) at baseline comparing patients with and without AF recurrence within 3 months (A), 6 months (B) and 1 year (C) after PVI treatment.

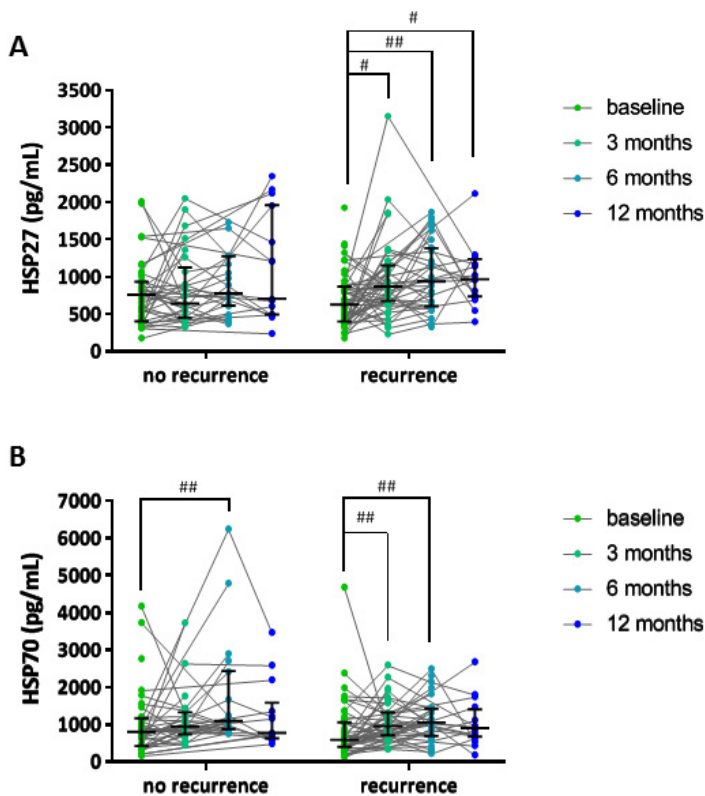


Figure 4. HSP27 and HSP70 levels in follow up serum were higher compared to baseline in patients having AF recurrence. HSP27 serum levels (pg/mL) at baseline and at 3-, 6- and 12-months follow up in patients having AF recurrence within one year compared to patients not having AF recurrence (A). HSP70 serum levels (pg/mL) at baseline and at 3-, 6- and 12-months follow up in patients having AF recurrence within one year compared to patients not having AF recurrence (B). # $P<0.05$ and ## $P<0.01$ compared to baseline serum HSP levels.

DISCUSSION

In this study, we observed that serum HSP27, HSP70, cvHSP and HSP60 levels in control patients and patients with paroxysmal and (longstanding) persistent AF were comparable between the groups. Thus, HSP27, HSP70, cvHSP or HSP60 levels could not discriminate between the different AF stages in the total AF population. Additionally, at baseline, HSP27 and HSP70 serum levels were similar in patients without and with AF recurrence within one year after treatment. However, both HSP27 and HSP70 levels were higher at 3-, 6- and 12-months post-PVI compared to baseline levels in patients with AF recurrence within one year. After joint modeling and sensitivity analyses, only increased HSP27 levels post-PVI remained as a predictor of AF recurrence.

Heat Shock Proteins are not biomarkers to differentiate the stage of Atrial Fibrillation

There is a great need for biomarkers to stage AF and to improve the selection of the proper treatment for patients. Several (AF-related) serum biomarkers are routinely measured in

clinical practice, such as natriuretic peptide, troponin I, troponin T, creatinine and C-reactive protein²⁴⁻²⁶, but lack specificity for AF. Our findings indicate no role for HSP27, HSP70, cvHSP or HSP60 as a biomarker for the presence or staging of AF. Our findings are in contrast to findings observed in other studies, as reports revealed a correlation between serum HSP levels and AF. Hu, et al. revealed an association between baseline serum HSP27 levels and AF. In this study, serum HSP27 levels were reduced in paroxysmal AF and (longstanding) persistent AF patients compared to controls in normal sinus rhythm.²² Also, low serum HSP27 associated with larger left atrial diameter, low atrial voltage (indication of fibrosis²⁷), and non-pulmonary ectopies. In addition, serum HSP27 could predict sinus rhythm maintenance and low serum HSP27 correlated with a higher AF recurrence rate.²² Our study could not confirm these findings. On the contrary, we did observe an increase in follow-up serum HSP27 and HSP70 levels in patients who developed AF recurrence post-PVI. In addition, the increased HSP27 levels significantly correlate with AF recurrence. Despite this interesting observation, due to the current study design we cannot determine whether the increase in serum HSP levels is correlated to the duration of the AF episodes and whether this increase started prior or post AF recurrence.

Serum HSP70 levels were similar in control and AF patients in our study and that of others.^{22,28} In line with our study, no correlation between clinical or echocardiographic variables and serum HSP70 levels was found and increased serum HSP70 levels at 6 months post-PVI correlated with AF recurrence, substantiating our findings.²⁸

In patients who underwent CABG, baseline serum HSP70 levels were not predictive for post-operative AF.^{29,3} While no association between serum HSP60 level and occurrence of AF was found by Maan, et al.³¹, Cao, et al.³² described that patients undergoing mitral valve replacement with AF had higher plasma HSP60 levels compared to patients in sinus rhythm. Higher plasma HSP60 levels were also predictive for early (<7days) post-operative AF.³² Although not the protein itself, pre- and post- operative circulating anti-HSP60 antibodies are associated with post-operative AF in patients undergoing CABG.³³ In our study, serum HSP60, as well as cvHSP, did not discriminate between the stage of AF or AF recurrence. The findings indicate that for baseline serum HSP27, HSP70, cvHSP and HSP60 levels, no clear consensus exists for their use as a biomarker in AF.

Table 2. Outcomes joint modeling of AF recurrence in relation to HSP levels, and sensitivity analyses

	Patients		Samples		HR	HSP27		P-value	HR	HSP70		
	AF	AF-free	AF	AF-free		95%CI LL	95%CI UL			95%CI LL	95%CI UL	P-value
All events	59	41	114	99	1.32	1.71	1.54	<0.001	model does not converge			
Complete until 3m	21	54	42	129	1.31	0.84	2.89	0.258	0.97	0.56	1.5	0.969
Complete until 6m	29	36	63	99	2.03	1.17	3.7	<0.001	1.03	0.54	1.97	0.926
Complete until 12m	31	13	70	34	model does not converge				model does not converge			

Limitations and future directions: HSP in relation to degree of electropathology

The current cross-sectional analysis provides information whether HSP levels in serum samples of AF patients differ from controls in sinus rhythm. To elucidate whether HSP levels predict AF onset, detect early AF or progression of AF, a longitudinal study with repeated blood sampling for HSP measurements and AF testing in subjects with normal sinus rhythm is required. Our control serum HSP27 and HSP70 range is lower compared to the ranges described in other reports, which can be explained by differences in the analytic assays used^{22,29,30} and due to differences in disease status of the various patient groups. The absence of difference in serum HSP levels between control and AF patients may be attributed to the clinical nature of the control group.

It is generally accepted that AF is a multifactorial disease and predisposing conditions such as e.g. diabetes mellitus, hypertension and higher age were omnipresent in all our study groups, including the control group. It might be possible that the clinical variables we studied were too common and we might need to search for more AF specific parameters, such as markers of structural damage which are found to underlie atrial electrical conduction disorders, i.e. electropathology.³⁵ It has been suggested that the clinical classification of AF, based on ECG measurements, as presented in the guidelines, is inaccurate for AF staging because it is not related to the degree of atrial electropathology as measured by high-resolution epicardial mapping [36]. Also, undiagnosed, silent and/or very short-lasting AF episodes might have been overlooked in control patients and during follow up of ECV or PVI patients by using ECG measurements. As previous studies revealed exhaustion of HSP levels in atrial tissue of persistent AF patients¹⁸, in future research projects it is recommended to investigate human HSP levels in both serum and atrial tissue and their relation to parameters related to AF-induced electrical and/or structural remodeling and also structural remodeling-induced (post-operative) AF.³⁷ Thus, a lack of correlation between HSPs and AF stage in the current study does not negate a role for HSPs as potential biomarker in AF. It is conceivable that serum HSP levels do correlate with the degree of electropathology. Future studies with continuous monitoring of electrical parameters and HSP levels should elucidate such an association.

CONCLUSIONS

Serum HSP27, HSP70, cvHSP and HSP60 levels did not differentiate between AF stages and controls in sinus rhythm. Moreover, AF recurrence after ECV or PVI was not associated with baseline HSP levels. However, both HSP27 levels were increased during follow up in patients with AF recurrence after ablative therapy and may be used as a predictor. Future research directed at elucidation of an association between HSP levels and the degree of electropathology is recommended.

REFERENCES

1. Mozaffarian D, Benjamin EJ, Go AS, et al. Heart disease and stroke statistics--2015 update: a report from the American Heart Association. *Circulation* 2015;131:e29-322.
2. Heijman J, Guichard JB, Dobrev D, Nattel S. Translational Challenges in Atrial Fibrillation. *Circ Res* 2018;122:752-773.
3. Kirchhof P, Benussi S, Kotecha D, et al. 2016 ESC Guidelines for the management of atrial fibrillation developed in collaboration with EACTS. *Europace* 2016;18:1609-1678.
4. Turakhia MP, Ullal AJ, Hoang DD, et al. Feasibility of extended ambulatory electrocardiogram monitoring to identify silent atrial fibrillation in high-risk patients: the Screening Study for Undiagnosed Atrial Fibrillation (STUDY-AF). *Clin Cardiol* 2015;38:285-292.
5. Andrade JG, Deyell MW, Verma A, et al. Association of Atrial Fibrillation Episode Duration With Arrhythmia Recurrence Following Ablation: A Secondary Analysis of a Randomized Clinical Trial. *JAMA Netw Open* 2020;3:e208748.
6. January CT, Wann LS, Alpert JS, et al. 2014 AHA/ACC/HRS guideline for the management of patients with atrial fibrillation: a report of the American College of Cardiology/American Heart Association Task Force on Practice Guidelines and the Heart Rhythm Society. *J Am Coll Cardiol* 2014;64:e1-76.
7. Dudink EA, Weijs B, Tull S, et al. The Biomarkers NT-proBNP and CA-125 are Elevated in Patients with Idiopathic Atrial Fibrillation. *J Atr Fibrillation* 2018;11:2058.
8. Chua W, Purmah Y, Cardoso VR, et al. Data-driven discovery and validation of circulating blood-based biomarkers associated with prevalent atrial fibrillation. *Eur Heart J* 2019;40:1268-1276.
9. Hui TH, McClelland RL, Allison MA, et al. The relationship of circulating fibroblast growth factor 21 levels with incident atrial fibrillation: The Multi-Ethnic Study of Atherosclerosis. *Atherosclerosis* 2018;269:86-91.
10. Zhu K, Hung J, Divitini M, et al. High-sensitivity cardiac troponin I and risk of incident atrial fibrillation hospitalisation in an Australian community-based cohort: The Busselton health study. *Clin Biochem* 2018;58:20-25.
11. Kubota Y, Alonso A, Heckbert SR, Norby FL, Folsom AR. Homocysteine and Incident Atrial Fibrillation: The Atherosclerosis Risk in Communities Study and the Multi-Ethnic Study of Atherosclerosis. *Heart Lung Circ* 2019;28:615-622.
12. Csecsei P, Varnai R, Nagy L, et al. L-Arginine Pathway Metabolites Can Discriminate Paroxysmal from Permanent Atrial Fibrillation in Acute Ischemic Stroke. *Ideggyogy Szemle* 2019;72:79-88.
13. Stanciu AE, Vatasescu RG, Stanciu MM, Serdarevic N, Dorobantu M. The role of pro-fibrotic biomarkers in paroxysmal and persistent atrial fibrillation. *Cytokine* 2018;103:63-68.
14. Henning RH, Brundel B. Proteostasis in cardiac health and disease. *Nat Rev Cardiol* 2017;14:637-653.
15. Brundel BJ, Shiroshita-Takeshita A, Qi X, et al. Induction of heat shock response protects the heart against atrial fibrillation. *Circ Res* 2006;99:1394-1402.
16. Wiersma M, Meijering RAM, Qi XY, et al. Endoplasmic Reticulum Stress Is Associated With Autophagy and Cardiomyocyte Remodeling in Experimental and Human Atrial Fibrillation. *J Am Heart Assoc* 2017;6.
17. Baler R, Dahl G, Voellmy R. Activation of human heat shock genes is accompanied by oligomerization, modification, and rapid translocation of heat shock transcription factor HSF1. *Mol Cell Biol* 1993;13:2486-2496.
18. Brundel BJ, Henning RH, Ke L, et al. Heat shock protein upregulation protects against pacing-induced myolysis in HL-1 atrial myocytes and in human atrial fibrillation. *J Mol Cell Cardiol* 2006;41:555-562.
19. Kotter S, Unger A, Hamdani N, et al. Human myocytes are protected from titin aggregation-induced stiffening by small heat shock proteins. *J Cell Biol* 2014;204:187-202.

20. Ghosh JG, Houck SA, Clark JI. Interactive domains in the molecular chaperone human alphaB crystallin modulate microtubule assembly and disassembly. *PLoS One* 2007;2:e498.
21. Hu X, Li J, van Marion DMS, Zhang D, Brundel B. Heat shock protein inducer GGA*-59 reverses contractile and structural remodeling via restoration of the microtubule network in experimental Atrial Fibrillation. *J Mol Cell Cardiol* 2019;134:86-97.
22. Hu YF, Yeh HI, Tsao HM, et al. Electrophysiological correlation and prognostic impact of heat shock protein 27 in atrial fibrillation. *Circ Arrhythm Electrophysiol* 2012;5:334-340.
23. Lanters EA, van Marion DM, Kik C, et al. HALT & REVERSE: Hsf1 activators lower cardiomyocyte damage; towards a novel approach to REVERSE atrial fibrillation. *J Transl Med* 2015;13:347.
24. Hijazi Z, Aulin J, Andersson U, et al. Biomarkers of inflammation and risk of cardiovascular events in anticoagulated patients with atrial fibrillation. *Heart* 2016;102:508-517.
25. Ellinor PT, Low AF, Patton KK, Shea MA, Macrae CA. Discordant atrial natriuretic peptide and brain natriuretic peptide levels in lone atrial fibrillation. *J Am Coll Cardiol* 2005;45:82-86.
26. Patton KK, Ellinor PT, Heckbert SR, et al. N-terminal pro-B-type natriuretic peptide is a major predictor of the development of atrial fibrillation: the Cardiovascular Health Study. *Circulation* 2009;120:1768-1774.
27. Yamaguchi T, Fukui A, Node K. Bipolar Voltage Mapping for the Evaluation of Atrial Substrate: Can We Overcome the Challenge of Directionality? *J Atr Fibrillation* 2019;11:2116.
28. Kornej J, Reinhardt C, Kosiuk J, et al. Response of circulating heat shock protein 70 and anti-heat shock protein 70 antibodies to catheter ablation of atrial fibrillation. *J Transl Med* 2013;11:49.
29. Mandal K, Torsney E, Poloniecki J, et al. Association of high intracellular, but not serum, heat shock protein 70 with postoperative atrial fibrillation. *Ann Thorac Surg* 2005;79:865-871; discussion 871.
30. Afzal AR, Mandal K, Nyamweya S, et al. Association of Met439Thr substitution in heat shock protein 70 gene with postoperative atrial fibrillation and serum HSP70 protein levels. *Cardiology* 2008;110:45-52.
31. Maan A, Jorgensen NW, Mansour M, et al. Association between Heat Shock Protein-60 and Development of Atrial Fibrillation: Results from the Multi-Ethnic Study of Atherosclerosis (MESA). *Pace* 2016;39:1373-1378.
32. Cao H, Xue L, Xu X, et al. Heat shock proteins in stabilization of spontaneously restored sinus rhythm in permanent atrial fibrillation patients after mitral valve surgery. *Cell Stress Chaperones* 2011;16:517-528.
33. Oc M, Ucar HI, Pinar A, et al. Heat shock protein 60 antibody. A new marker for subsequent atrial fibrillation development. *Saudi Med J* 2007;28:844-847.
34. Kardys I, Rifai N, Meilhac O, et al. Plasma concentration of heat shock protein 27 and risk of cardiovascular disease: a prospective, nested case-control study. *Clin Chem* 2008;54:139-146.
35. de Groot NM, Houben RP, Smeets JL, et al. Electropathological substrate of longstanding persistent atrial fibrillation in patients with structural heart disease: epicardial breakthrough. *Circulation* 2010;122:1674-1682.
36. Mouws EMJP, van der Does LJME, Kik C, et al. Impact of the arrhythmogenic potential of long lines of conduction slowing at the pulmonary vein area. *Heart Rhythm* 2019;16:511-519.
37. Fakuade FE, Steckmeister V, Seibert F, et al. Altered atrial cytosolic calcium handling contributes to the development of postoperative atrial fibrillation. *Cardiovascular Research* 2020;cvaa162

SUPPLEMENTARY MATERIALS

The following are available online at www.mdpi.com/xxx/s1.

Table S1. Concentration of HSPs in serum at baseline of patients without AF and with (paroxysmal, persistent or longstanding persistent) AF

	Control	PAF	PeAF	LSPeAF	All AF patients
N	98	86	108	5	199
HSPB1, median [IQR]	807.9 [538.5-1240]	705.5 [406.5-898]	783.5 [519.8-1203]	679 [382-1206]	708 [479-1056]
HSPA1, median [IQR]	758.7 [420.6-1287]	624.5 [359.8-1058]	750.5 [472.5-1306]	876 [751-3186]	701 [406-1144]
HSPB7, median [IQR]	381 [120.8-752.8]	286 [131-646]	301 [135-585]	189 [144-490]	293 [131-615]
HSPD1, median [IQR]	1020 [438.5-2236]	775 [271.3-1804]	927 [165-2423]	246 [107.5-1941]	851 [219.7-2358]

Table S2. Univariate linear regression associations between clinical parameters and HSP levels in baseline serum

	HSPB1 St β	HSPA1 St β	HSPB7 St β	HSPD1 St β
AF	-0.087	0.016	-0.029	-0.079
Stage of AF	-0.048	0.066	-0.030	-0.084
Age (years)	-0.058	-0.028	0.080	-0.117*
Gender	0.077	0.012	0.089	0.130*
BMI (kg/m ²)	0.073	0.057	0.039	-0.098
Hypertension	-0.033	-0.053	0.027	-0.107
Diabetes mellitus	-0.009	0.022	0.167**	-0.098
Dyslipidemia	-0.043	0.042	0.076	-0.047
Thyroid disease	0.025	0.046	0.039	-0.007
Left ventricular function	0.061	0.072	0.116	0.059
ACE. ARB. AT2 antagonist	-0.061	-0.058	0.060	-0.146*
Statin	-0.030	0.076	0.053	-0.108
Class I AAD	-0.14*	-0.097	0.042	0.058
Class II AAD	0.031	-0.005	0.127*	0.002
Class III AAD	0.023	0.027	-0.110	-0.078
Class IV AAD	-0.080	-0.025	0.023	0.068
Digoxin	0.003	0.017	-0.013	-0.016
Recurrence within one year	0.046	-0.051	-0.102	0.003

Table S3. Multivariate linear regression associations between AF, AF stage and recurrence within one year and HSP levels in baseline serum, corrected for potential confounders

	HSPB1 St β corrected for age, gender, diabetes mellitus and Class I AAD	HSPA1 St β corrected for age, gender and diabetes mellitus	HSPB7 St β corrected for age, gender, diabetes mellitus and Class II AAD	HSPD1 St β corrected for age, gender, diabetes mellitus and ACE. ARB. AT2 antagonist
AF	-0.043	0.038	-0.108	0.024
Stage of AF	-0.009	0.097	-0.104	0.013
Recurrence within one year	0.035	-0.063	-0.151*	0.031

Table S4. Bivariate spearman correlation between clinical parameters and recurrence within 3 months, 6 months and 12 months

	Recurrence within 3M	Recurrence within 6M	Recurrence within 1Y
Stage of AF	0.212**	0.276**	0.190**
Age (years)	0.199**	0.144*	0.164*
Gender	0.086	0.088	0.065
BMI (kg/m ²)	0.050	0.086	0.022
Hypertension	0.174*	0.067	0.092
Diabetes mellitus	0.057	-0.009	0.048
Dyslipidemia	0.152*	0.087	0.156*
Thyroid disease	0.081	-0.068	-0.069
Left ventricular function	0.123	0.214**	0.173*
ACE. ARB. AT2 antagonist	0.097	0.077	0.048
Statin	0.136	0.079	0.103
Class I AAD	-0.024	-0.111	-0.077
Class II AAD	0.072	-0.011	0.023
Class III AAD	-0.031	-0.041	-0.040
Class IV AAD	0.008	0.099	0.059
Digoxin	-0.029	-0.044	-0.042

Table S5. Clinical characteristics and serum HSP levels for subjects without AF and with (paroxysmal, persistent and longstanding persistent) AF in the ECV group

	Control	PAF	PeAF	LSPeAF	All AF patients
N	98	12	83	3	98
Age (years), mean \pm SD	48.2 \pm 15.3	62.2 \pm 10.8	60.9 \pm 11.2	60.3 \pm 8.2	61 \pm 11
Gender, male, N (%)	51 (52)	10 (83.3)	63 (75.9)	3 (100)	76 (77.6)
BMI (kg/m²), mean \pm SD	25.1 \pm 3.7	28.7 \pm 3.0	29 \pm 5.8	25.8 \pm 1.6	28.9 \pm 5.4
Hypertension, yes, N (%)	23 (23.5)	9 (75)	37 (44.6)	1 (33.3)	47 (48)
Diabetes mellitus, yes, N (%)	5 (5.1)	1 (8.3)	12 (14.5)	0 (0)	13 (13.3)
Dyslipidemia, yes, N (%)	16 (16.3)	5 (41.7)	23 (27.7)	1 (33.3)	29 (29.6)
Thyroid disease, yes, N (%)	2 (2)	0 (0)	7 (8.4)	1 (33.3)	8 (8.2)
Left ventricular function, N (%)					
Normal	61 (79.2)	10 (83.3)	40 (51.3)	2 (66.7)	52 (55.9)
Mild impairment	10 (13)	0 (0)	25 (32.1)	1 (33.3)	26 (28)
Moderate impairment	3 (3.9)	1 (8.3)	9 (11.5)	0 (0)	10 (10.8)
Severe impairment	3 (3.9)	1 (8.3)	4 (5.1)	0 (0)	5 (5.4)
Missing[†]	21	0	5	0	5
Left atrial volume index (ml/m²), median [IQR]	27.9 [21.2-39.7]	46 [29.5-54]	47.5 [37.5-60.8]	52 [N/A]	47 [35-60]
Cumulative recurrence, yes, N (%)					
Within 3 months	-	6 (50)	43 (51.8)	3 (100)	52 (53.1)
Within 6 months	-	7 (58.3)	45 (54.2)	3 (100)	55 (56.1)
Within 1 year	-	7 (58.3)	54 (65.1)	3 (100)	64 (65.3)
Baseline HSP serum levels, N	98	12	83	3	98
HSPB1, median [IQR]	807.9 [538.5-1240]	766 [609.5-1655]	843 [561-1236]	522 [N/A]	795.5 [560-1235]
HSPA1, median [IQR]	758.7 [420.6-1287]	317 [229-1127]	787 [510-1366]	873 [N/A]	774 [490-1333]
HSPB7, median [IQR]	381 [120.8-752.8]	388 [196.5-1178]	335 [150-615]	171 [N/A]	345 [164-635.8]
HSPD1, median [IQR]	1020 [438.5-2236]	1713 [55.3-9843]	882 [132-2382]	246 [N/A]	849 [124-2445]

[†]The percentages of LVF are the valid percentage, thus corrected for the missing values.

Statistical testing performed on cumulative recurrence and baseline HSP serum levels: Students T test on log transformed values (No AF vs All AF patients), Anova with Bonferroni corrections on the log transformed values (No AF vs PAF or No AF vs PeAF or No AF vs LSPeAF)

Table S6. Serum HSP concentrations after one year follow up

	No recurrence	Recurrence
ECV patients		
Baseline, N	34	64
HSPB1, median [IQR]	737 [523.8-1059]	832.5 [569.5-1314]
HSPA1, median [IQR]	727.5 [391-1409]	787 [533.8-1306]
HSPB7, median [IQR]	441.5 [153.5-648.8]	330.5 [164-553.3]
HSPD1, median [IQR]	587 [32-2491]	907.5 [167-2482]
PVI patients		
Baseline, N	41	59
HSPB1, median [IQR]	753 [398.5-925]	620 [394-862]
HSPA1, median [IQR]	787 [406-1150]	566 [384-1040]
HSPB7, median [IQR]	247 [131-663]	280 [112-522]
HSPD1, median [IQR]	854.5 [357-1888]	850 [206-1756]
3 months follow up, N	26	40
HSPB1, median [IQR]	633 [445.5-1119]	862.5 [668-1147] [#]
HSPA1, median [IQR]	922 [721.8-1312]	939 [693-1302] ^{##}
6 months follow up, N	19	32
HSPB1, median [IQR]	771 [607-1270]	930 [598.5-1378] ^{##}
HSPA1, median [IQR]	1079 [858-2415] ^{###}	1034 [675.3-1410] ^{*,##}
12 months follow up, N	15	16
HSPB1, median [IQR]	700 [489-1957]	961.5 [730-1232] [#]
HSPA1, median [IQR]	756.5 [489-1957]	883.5 [656.8-1385]

** P<0.05 compared to no recurrence, # P<0.05 and ### P<0.01 compared to baseline serum Statistical testing performed: Students T test on log transformed values (No recurrence vs Recurrence), Anova with Bonferroni corrections on the log transformed values (baseline vs follow up serum samples for HSPB1 and HSPA1 within the group of patients with or without recurrence)*

Table S7. Clinical characteristics and serum HSP levels for subjects without AF and with (paroxysmal, persistent and longstanding persistent) AF in the PVI group

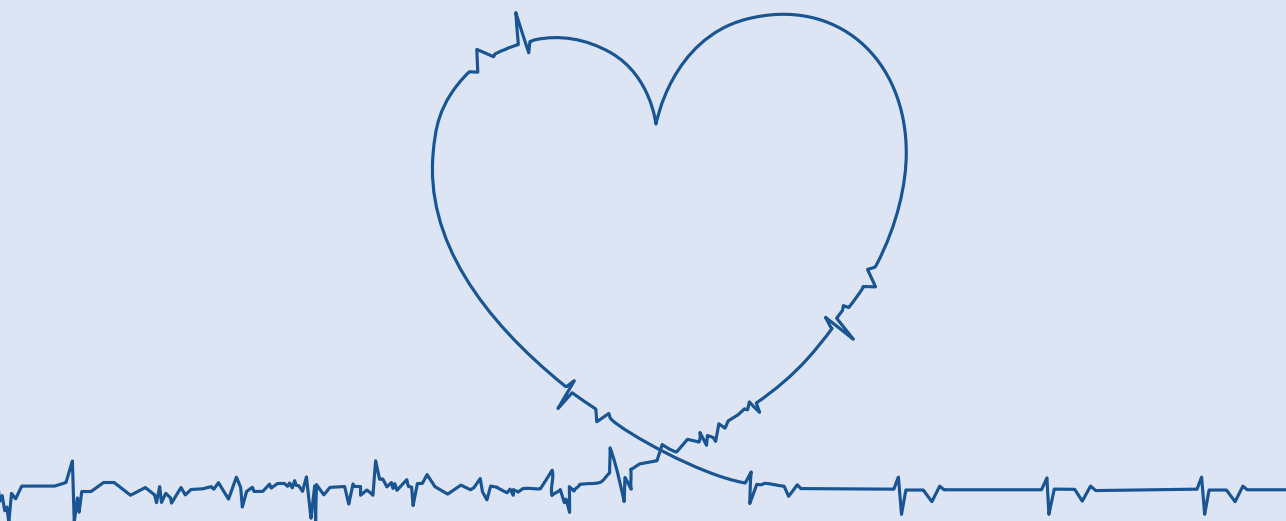
	Control	PAF	PeAF	LSPeAF	All AF patients
N	98	74	25	3	102
Age (years), mean \pm SD	48.2 \pm 15.3	61.2 \pm 9.4	60.5 \pm 8.3	53.3 \pm 11.3	60.8 \pm 9.1
Gender, male, N (%)	51 (52)	54 (73)	18 (72)	1 (50)	73 (72.3)
BMI (kg/m²), mean \pm SD	25.1 \pm 3.7	27 \pm 3.9	28.1 \pm 3.9	37.3 \pm 7.5	27.4 \pm 4.2
Hypertension, yes, N (%)	23 (23.5)	34 (45.9)	14 (56)	2 (100)	50 (49.5)
Diabetes mellitus, yes, N (%)	5 (5.1)	9 (12.2)	3 (12)	1 (50)	13 (12.9)
Dyslipidemia, yes, N (%)	16 (16.3)	20 (27)	10 (40)	2 (100)	32 (31.7)
Thyroid disease, yes, N (%)	2 (2)	4 (5.4)	1 (4)	0 (0)	5 (5)
Left ventricular function, N (%)					
Normal	61 (79.2)	63 (85.1)	20 (80)	1 (50)	84 (83.2)
Mild impairment	10 (13)	9 (12.2)	4 (16)	1 (50)	14 (13.9)
Moderate impairment	3 (3.9)	2 (2.7)	1 (4)	0 (0)	3 (3)
Severe impairment	3 (3.9)	0 (0)	0 (0)	0 (0)	0 (0)
Missing^t	21	0	0	0	0
Left atrial volume index (ml/m²), median [IQR]	27.9 [21.2-39.7]	38.5 [29.1-47.6]	39.5 [29.3-60]	43.1 [N/A]	38.7 [29.8-49.5]
Cumulative recurrence, yes, N (%)					
Within 3 months	-	19 (25.7)	13 (54.2) ^{**}	2 (100) ^{**}	34 (34)
Within 6 months	-	29 (39.2)	16 (66.7) ^{**}	2 (100) ^{**}	47 (47)
Within 1 year	-	37 (50)	20 (83.3) ^{**}	2 (100) ^{**}	59 (58)
Baseline HSP serum levels, N	98	74	25	2	101
HSPB1, median [IQR]	807.9 [538.5-1240]	678.5* [393-869]	610 [405-877]	1205 [N/A]	659** [400.5-891.5]
HSPA1, median [IQR]	758.7 [420.6-1287]	641 [396-1043]	529 [347-951]	3186 [N/A]	636 [385.5-1058]
HSPB7, median [IQR]	381 [120.8-752.8]	276 [122.5-645]	224 [122-564.5]	211 [N/A]	248 [126-573]
HSPD1, median [IQR]	1020 [438.5-2236]	739.5 [293.3-645]	1394 [483.3-5066]	1305 [N/A]	851 [297.3-1744]
3 months FU, N		50	15	2	67
HSPB1, median [IQR]	-	823 [#] [563.8-1194]	784 [627-1115]	617.5 [N/A]	811 [#] [569-1157]
HSPA1, median [IQR]	-	939 ^{###} [721-1323]	755 [541-1229]	1091 [N/A]	930.5 ^{###} [711-1308]
6 months FU, N		37	14	1	52
HSPB1, median [IQR]	-	806 [#] [601.5-1271]	1138 [#] [810.8-1659]	440 [N/A]	907 ^{###} [606.3-1282]
HSPA1, median [IQR]	-	1065 ^{###} [822.5-1427]	923 [660.8-1593]	1052 [N/A]	1059 ^{###} [791.5-1434]

	Control	PAF	PeAF	LSPeAF	All AF patients
12 months FU, N		22	8	1	31
HSPB1, median [IQR]	-	961.5 ^{##} [590.3-1339]	841 [470-1240]	1021 [N/A]	959 ^{##} [605-1261]
HSPA1, median [IQR]	-	924 [615.5-1415]	739 [637.3-916.5]	1748 [N/A]	804 [#] [634.5-1385]


[†] The percentages of LVF are the valid percentage, thus corrected for the missing values.

* $P < 0.05$ and ** $P < 0.01$ compared to control, ^{##} $P < 0.01$ PeAF and LSPeAF compared to PAF, [#] $P < 0.05$, ^{##} $P < 0.01$ and ^{###} $P < 0.001$ compared to baseline.

Statistical testing performed on cumulative recurrence and baseline HSP serum levels: Students T test on log transformed values (No AF vs All AF patients), Anova with Bonferroni corrections on the log transformed values (No AF vs PAF or No AF vs PeAF or No AF vs LSPeAF or baseline vs follow up (FU) serum samples for HSPB1 and HSPA1 within the group of patients with PAF, PeAF and All AF patients).



CHAPTER 17



BIOMARKING THE ELECTROPATHOLOGICAL SUBSTRATE: TISSUE AND SERUM HEAT SHOCK PROTEIN LEVELS AND THEIR RELATION TO ATRIAL CONDUCTION PROPERTIES

Lanters EAH, van Marion DMS, Silva Ramos K, van der Does WFD,
Bogers AJJC, Brundel BJJM, de Groot NMS
Manuscript in preparation

ABSTRACT

Background Electrical alterations caused by structural remodeling are associated with development of atrial fibrillation (AF). However, non-invasive biomarkers of remodeling are lacking. The goal of this study was to investigate the relation between electrical alterations, clinical profiles and Heat Shock Proteins as biomarkers of local conduction abnormalities.

Methods High-resolution epicardial mapping was performed during sinus rhythm in patients undergoing cardiothoracic surgery and studied for the presence and severity of conduction block (CB). HSP levels were determined in serum samples (HSP27, HSP70, HP60 and HSPB7.) and right atrial appendage (RAA) tissue samples (HSP27, HSP70 HSPA5, HSP60, HSPB5 and HSF1).

Results 122 patients (75% male, 70[63-76] years) were enrolled, including 62 AF and 60 No AF patients. CB was more pronounced in AF patients: 2.9[2.0-3.9]% vs 1.8[1.1-2.8]%, $P = 0.006$, due to an increment in maximal length of CB lines (42.0[32.0-56.0]mm vs 28.0[18.0-37.0], $P = 0.002$). Serum and RAA HSP levels did not differentiate between AF and No AF, or between different stages of AF ($P > 0.05$). In addition, there were no relevant correlations between serum and RAA HSP levels, nor between HSP levels and local conduction abnormalities.

Conclusion HSP levels in either serum or RAA samples are not correlated to conduction abnormalities or voltages, as investigated by high resolution epicardial mapping. Furthermore, HSPs do not differentiate between AF and No AF patients. Hence, HSPs are not suitable as an AF-specific biomarker.

INTRODUCTION

High-resolution epicardial mapping of the atrium during sinus rhythm (SR) revealed the presence of conduction abnormalities related to the presence of atrial fibrillation (AF) episodes¹⁻³. Conduction abnormalities are caused by structural remodeling of atrial tissue, including e.g. gap-junction - and ion channel remodeling, dedifferentiation and fibrosis. However, biomarkers indicative of conduction abnormalities associated with AF are not included in guidelines^{4, 5} although various biomarkers including brain natriuretic peptides, cancer-antigen-125 and fibroblast growth factors 21 and 23 and high-sensitive cardiac troponin I⁶⁻⁹ have been proposed.

Prior studies have demonstrated that exhaustion of atrial tissue Heat Shock Protein (HSP) levels correlates with AF progression and pharmacological induction of HSPs to protect against AF onset¹⁰⁻¹⁴. Furthermore, HSPs correlate to AF presence^{15, 16}, duration¹⁰ and AF recurrence¹⁷. At present, HSP levels in serum and atrial tissue have never been correlated to atrial electropathology. We therefore aim to investigate the correlation between HSP levels in atrial tissue and serum samples, clinical profiles and electrophysiological parameters.

METHODS

Study Population

For the current study, patients were included in the HALT&REVERSE protocol¹⁵. Patients were eligible for inclusion when scheduled for elective cardiothoracic surgery; either coronary artery bypass grafting and/or mitral valve surgery and/or aortic valve surgery and/or first correction of a congenital heart defect (mostly atrial septal defects). Patients were over 18 years of age. Exclusion criteria are manifest heart failure, need for inotropic or mechanical support, prior heart surgery or atrial ablative therapy, pericarditis or the presence of an atrial pacing device. Patients were allocated to subgroups "AF" or "No AF", dependent on the presence of AF prior to surgery.

All patients provided written informed consent prior to inclusion. Clinical information was obtained from the digital patient file. This study was carried out in adherence to the declaration of Helsinki and was approved by our local medical ethical committee (MEC 2014-393).

High Resolution Sinus Rhythm Mapping

Epicardial mapping was performed during SR, prior to insertion of the extracorporeal circulation. In patients with spontaneous AF, electrical cardioversion was executed to restore sinus rhythm. An indifferent electrode was attached to a steel wire and stitched to the patients thoracic cavity. An unipolar electrode, stitched to the right atrial appendage served as a reference electrode. Our mapping approach has been described extensively in previous manuscripts^{1, 2, 18-21}. Unipolar atrial electrograms were recorded from the entire left and right atrial epicardial surface, including Bachmann's Bundle. For this purpose we used a flexible 192-polar electrode array with inter-electrode distances of 2mm. The array was moved across the epicardial surface following a predefined mapping scheme. At each mapping site, 5 seconds of sinus rhythm were recorded, including a simultaneously recorded surface ECG, a bipolar temporal reference electrogram, a calibration signal (2mV, 1000ms) and unipolar epicardial electrograms.

Analysis of Electrical parameters

Analysis of the mapping data was performed using dedicated mapping software. For voltages, unipolar peak-to-peak amplitudes were determined by annotation of all intrinsic deflections (the steepest negative deflection) with a minimum negative slope of -0.05 V/s.

Analysis of conduction properties was executed in adherence to previous studies: ^{1, 2, 21 22, 23}. For each pair of neighboring electrodes, the conduction time (CT) was calculated as the difference in local activation time (ms). Conduction block (CB, $CT \geq 12$ ms) and combined conduction delay and block (CDCB, $CT \geq 7$ ms) were quantified as the percentage of the total mapped area. In addition, the number of CB lines were analyzed, as well as the number of consecutive CDCB lines. Finally, the length of these CB and CDCB lines was also determined. The severity of CTs was defined as the size of inter-electrode differences in ms.

Analysis of Blood Serum Samples

To determine the levels of HSP27, HSP70, HSPB7 and HSP60, blood samples were obtained 12-24 hours prior to surgery in BDTM Vacutainer™ SST™ II Advance Tubes (Thermo Fisher Scientific, The Netherlands). Serum was separated from blood by centrifugation at 2000 x g for 10 min at 4°C and subsequently frozen at -80°C until analysis. HSP27 (serum 6x diluted in 1% BSA in PBS) and HSP70 protein (serum 2x diluted in 1% BSA in PBS) levels were measured in triplicates using human HSP27 or HSP70 DuoSet® ELISA kits from R&D (Cat. no. DY1580 and DY1663, respectively) according to the manufacturer's instructions with minor adjustments (serum was incubated at 4°C overnight, instead of 2 hours at room temperature (RT)). HSP60 protein levels (undiluted serum) were measured in duplicates with the HSP60 DuoSet® ELISA kit from R&D (DYC1800) according to manufacturer's instructions. cvHSP protein (undiluted serum measured singular) were determined with ELISA kits from Cusabio (CSB-EL010838HU) according to manufacturer's instructions with minor adjustments (kept incubation temperature at 20°C).

Table 1. Baseline characteristics of the study population

	Total population (N=122)	No AF (N=62)	AF (N=60)	P
Age (years), median [P25-P75]	70 [63-76]	69 [60-72]	70 [65-77]	0.320
Male gender, N (%)	91 (75)	48 (77)	43 (72)	0.466
BMI, median [P25-P75]	27 [24-30]	28 [25-31]	26 [24-30]	0.177
Hypertension, N (%)	78 (64)	40 (65)	38 (63)	0.982
Hyperlipidemia, N (%)	44 (36)	25 (40)	19 (32)	0.320
Diabetes Mellitus, N (%)	30 (25)	19 (29)	12 (20)	0.247
Thyroid Disease, N (%)	9 (7)	3 (5)	6 (10)	0.276
Left Ventricular Function, N (%)				0.062
Normal	87 (71)	47 (76)	40 (67)	
Mild impairment	25 (21)	14 (23)	11 (18)	
Moderate impairment	9 (7)	1 (1)	8 (13)	
Severe impairment	1 (1)	-	1 (2)	
LAVI (ml/m ²)				<0.001
N	40	29	11	
median [P25-P75]	31 [27-46]	28 [23-32]	48 [41-73]	
Type AF, N (%)				
No AF	62 (51)	62 (100)	-	
Paroxysmal AF	18 (15)	-	18 (30)	
Persistent AF	25 (20)	-	25 (42)	
LS Persistent AF	17 (14)	-	17 (28)	
Type of Surgery, N (%)				<0.001
CABG	45 (37)	36 (58)	9 (15)	
AVS	18 (15)	6 (10)	12 (20)	
MVS	23 (19)	5 (8)	18 (30)	
CABG + AVS	16 (13)	8 (13)	8 (13)	
CABG + MVS	7 (6)	3 (5)	4 (7)	
CHD	10 (8)	4 (6)	6 (10)	
Other	3 (2)	-	3 (5)	

AF: atrial fibrillation; BMI: body mass index; LAVI: left atrium volume index; LS Persistent: longstanding persistent; CABG: coronary artery bypass grafting; AVS: aortic valve surgery; MVS: mitral valve surgery; CHD: congenital heart defect

Analysis of Right Atrial Appendages

Right atrial appendages (RAA) were obtained from all patients with and without AF after mapping and during cannulation for extracorporeal circulation. RAA's were immediately snap frozen in liquid nitrogen and stored at -80°C until further use.

Frozen RAA's were cut in small fragments on dry ice and added to ice cold sample buffer (15% glycerol; 1% SDS; 12.5% 0.5 M Tris, pH 6.8; 2% bromophenol-blue solution and protease and phosphatase inhibitors). The tissue was homogenized using metal beads in the Qiagen TissueLyser II for 3 min at 30 Hz, left on ice for 30 min for subsequent cell lysis and homogenized again for 3 min at 30 Hz. The lysates were centrifuged (20 min, 14,000 rpm at 4°C), supernatant was collected, passed through an insulin syringe, boiled for 5 min at 95°C and samples were stored at -20°C until analysis.

For Western blot analysis, equal amounts (10 µg) of protein were separated on 4–20% Criterion TGX precast gels (Bio-Rad, Lunteren, The Netherlands) and transferred to nitrocellulose membranes (Bio-Rad). Membranes were blocked in 5% skim milk in TBST for 1 hour at room temperature. Overnight incubation at 4°C with primary antibody (in 3% BSA in TBST, Table S1) was followed by secondary antibody (in 3% BSA in TBST) incubation for 1 hour at room temperature with horseradish peroxidase-conjugated goat-anti-rabbit or goat-anti-mouse antibodies (Dako Cytomation, Denmark), depending on the species origin of the primary antibody. Signals were detected by the Amersham ECL prime Western blotting detection reagent (GE Healthcare Life Sciences, Hoevelaken, The Netherlands) utilizing the Amersham Imager 600 (GE Healthcare Life Sciences) and quantified by densitometry (ImageQuantTL, GE Healthcare Life Sciences). Protein amounts were expressed relative to GAPDH for whole protein lysates.

Statistical Analysis

Analysis was performed using SPSS software (Version 25. Armonk, NY: IBM Corp.). All data were tested for normality. Normally distributed data are displayed as mean±standard deviation, whereas skewed data are presented as median [P25-P75]. Numerical samples were compared using unpaired T-test or non-parametrical tests including Kruskal-Wallis (independent samples) and Wilcoxon Signed Rank tests (for related samples) where appropriate. Categorical data was compared using Chi-squared tests. Correlations were investigated using Spearmans test for skewed datasets.

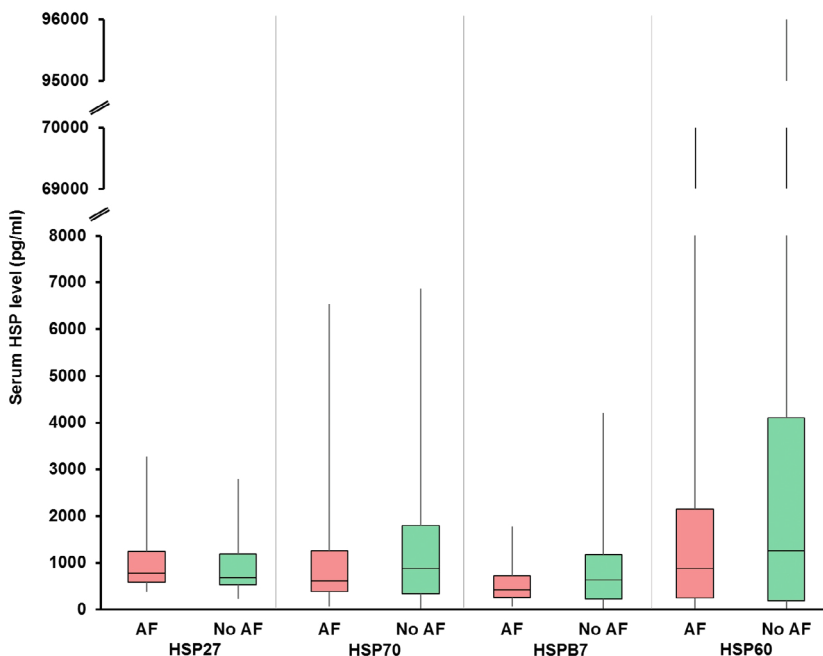


Figure 1. Baseline serum HSP levels. Levels of serum HSP levels prior to surgery, in AF (red bars) and No AF (green bars) patients. HSP: heat shock protein; AF: atrial fibrillation.

RESULTS

Study Population

The study population consisted of 122 patients (male: 91 (75%), median age: 70 years) including 62 (51%) No AF patients and 60 (49%) with AF; baseline characteristics are displayed in Table 1. Systolic left ventricular function was normal in majority of patients. Baseline characteristics did not differ between AF and No AF patients except for the left atrial volume index, which was 48 ml/m² in AF patients, versus 28 ml/m² in No AF patients ($P < 0.001$).

Patient Characteristics and Heat Shock Protein Levels in Serum Samples

Figure 1 shows baseline concentrations of serum levels of HSP27, HSP70, HSPB7 and HSP60 of both AF and No AF patients; corresponding values are depicted in Table 2. As can be seen, there are no differences in serum HSP27, HSP70, cvHSP and HSP60 values between AF and No AF patients, but also not between patients with PAF, PeAF or LSPeAF (all $P > 0.05$). HSPB7 levels correlated with gender ($\rho = 0.313$, $P = 0.001$) and were higher in females (629 [392-1082] pg/ml) than in males (374 [197-601] pg/mL).

Heat Shock Proteins in Right Atrial Tissue Samples

HSP tissue levels were quantified in RAA tissue obtained from 85 patients. Tissue levels of HSP27, HSP70, HSPA5, HSP60, HSPB5 and HSF1 are shown in Figure 2 and summarized in Table 2 for AF and No AF patients separately. There were no differences in levels of HSP27, HSP70, HSPB5 and HSF1 between the subgroups. However, HSPA5 was higher in No AF patients ($P = 0.011$) whereas HSP60 was higher in AF patients ($P = 0.015$).

Correlation Between Serum and Tissue Heat Shock Protein Levels

Correlation coefficients and P-values for the correlations between tissue and serum HSP levels are depicted in Table S2. There were no correlations between all serum HSP levels and corresponding RAA HSP levels (all $P > 0.05$).

Quantification of Electrophysiological Parameters

Epicardial mapping of the atrial surface during sinus rhythm was performed in 72 patients; results of quantification of various electrophysiological parameters are summarized in Table 3. Mean atrial voltage was 5.3 ± 1.6 mV and ranged from 1.4 mV to 9.3 mV and did not differ between AF and No AF patients. Conduction block was present in 96% of the patients. AF patients had a higher percentage of CB compared to No AF patients $1.8 [1.1-2.8]\%$ versus $2.9 [2.0-3.9]\%$ ($P = 0.006$). This difference was caused by an increase in number CB ($P = 0.034$) lines in AF patients and not by an increment in their lengths (all $P > 0.05$, Table 3).

Furthermore, electrical parameters were also quantified for the different atrial regions, as displayed in Table S3. Conduction abnormalities, particularly the number of CB ($P = 0.015$) and CDCB ($P = 0.003$) lines, were more pronounced at BB in AF patients than in No AF patients. At the RA however, maximal length of CB ($P = 0.006$) and CDCB ($P = 0.024$) lines were remarkably longer in AF patients.

Table 2. Baseline HSP levels

	No AF	AF	P	PAF	PeAF	LSPeAF	P
Serum							
HSP27	691 [532-1222]	783 [579-1262]	0.385	612 [507-1353]	939 [617-1384]	760 [568-1057]	0.199
HSP70	545 [300-940]	616 [386-1289]	0.224	931 [354-1629]	711 [436-1311]	446 [370-616]	0.147
HSPB7	405 [202-571]	421 [255-729]	0.367	556 [301-810]	420 [246-690]	371 [195-948]	0.584
HSP60	1067 [183-2953]	883 [238 – 2188]	0.555	678 [162-4995]	1184 [552-2068]	530 [20-1253]	0.154
RAA							
HSP27	0.57 [0.37-0.78]	0.48 [0.33-0.60]	0.072	0.55 [0.47-0.71]	0.44 [0.32-0.67]	0.37 [0.29-0.55]	0.138
HSP70	0.63 [0.44-0.80]	0.54 [0.42-0.79]	0.499	0.52 [0.29-0.75]	0.62 [0.43-1.25]	0.56 [0.43-0.81]	0.338
HSPA5	0.65 [0.47-0.87]	0.48 [0.33-0.68]	0.011	0.45 [0.32-0.65]	0.57 [0.38-0.95]	0.33 [0.30-0.57]	0.084
HSP60	0.49 [0.38-0.83]	0.64 [0.50-0.96]	0.015	0.58 [0.45-0.78]	0.79 [0.63-1.03]	0.63 [0.46-0.96]	0.160
HSPB5	0.63 [0.42-0.77]	0.73 [0.56-0.87]	0.103	0.76 [0.56-0.90]	0.68 [0.56-0.96]	0.72 [0.48-0.85]	0.666
HSP1	0.93 [0.80-1.24]	1.02 [0.81-1.33]	0.539	1.04 [0.93-1.67]	0.94 [0.63-1.13]	1.12 [0.88-1.37]	0.186

AF: atrial fibrillation; HSP: heat shock protein; HSF: heat shock factor; RAA: right atrial appendage

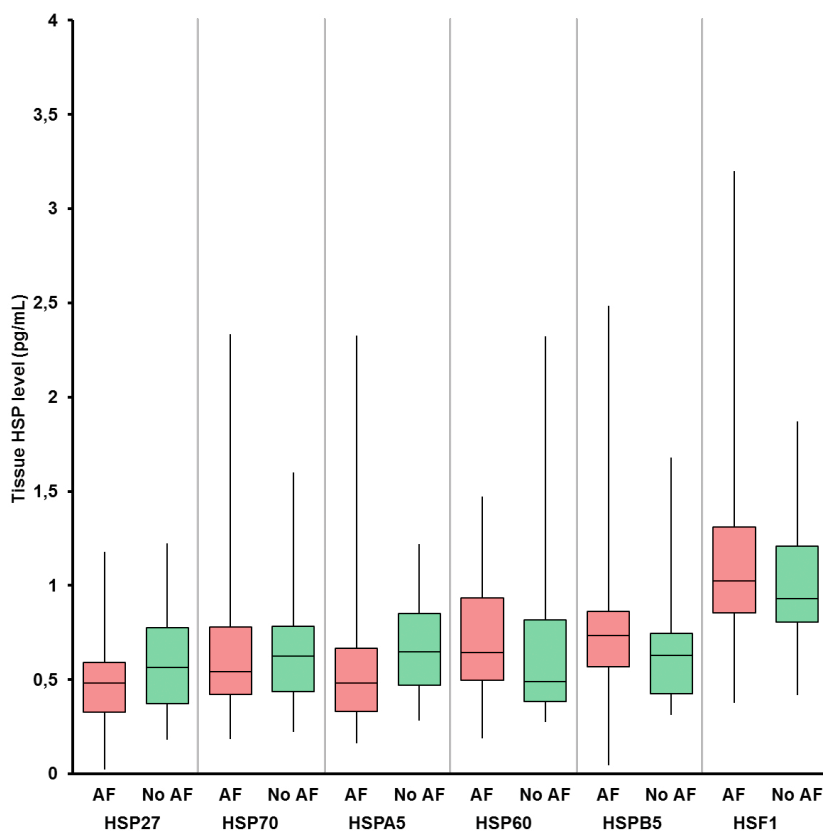


Figure 2. Baseline tissue HSP levels. Levels of tissue HSP levels prior to surgery, in AF (red bars) and No AF (green bars) patients. HSP: heat shock protein; HSF: heat shock factor; AF: atrial fibrillation.

Table 3. Electrophysiological parameters of the entire atrial surface

	All patients	No AF	AF	P-value
Mean Voltage, mV	5.3±1.6	5.4±1.7	4.9±1.6	0.296
Percentage CB, %	2.0[1.1-3.2]	1.8[1.1-2.8]	2.9[2.0-3.9]	0.006
Number CB lines, n	15.5[10.0-21.6]	13.5[9.5-19.0]	20.0[11.5-25.0]	0.034
Med Length CB lines, mm	4.9[4.0-6.0]	4.6[3.9-6.0]	5.5[4.5-7.0]	0.148
Max Length CB lines, mm	32.0[20.5-43.5]	28.0[18.0-37.0]	42.0[32.0-56.0]	0.002
Percentage CDCB, %	5.1[3.4-6.8]	4.3[3.2-6.3]	6.3[5.3-8.6]	0.001
Number CDCB lines, n	7.5[6.0-12.0]	7.0[5.3-11.0]	11.5[7.0-13.5]	0.035
Med Length CDCB lines, mm	13.8[11.4-17.4]	13.3[10.0-16.6]	15.8[11.8-22.0]	0.056
Max Length CDCB lines, mm	48.0[34.0-67.5]	42.0[29.0-57.0]	60.0[42.0-98.0]	0.004
CT severity, ms	47.0[32.3-61.8]	44.0[31.5-56.5]	56.0[47.0-70.0]	0.011

CB: conduction block; Med: median; Max: maximal, CDCB: combined conduction delay + conduction block; CT: conduction time

Correlation between Serum HSP levels and Electrophysiological Parameters

Correlations between serum HSP levels and electrophysiological parameters were evaluated for both the entire atrial surface and the different atrial regions. Correlations between serum HSP levels and atrial electrical parameters were all lacking ($P > 0.05$). For the separate atrial regions, several significant correlations were present as shown by the asterisks in Supplemental Table 4, although the correlation coefficient did not exceed $\rho = -0.335$ (maximal length of CB lines and HSP70 serum levels).

Correlation between RAA Tissue HSP levels and Electrophysiological Parameters

RAA HSP tissue levels were determined in 53 patients in whom SR mapping was performed. Correlation coefficients for HSP levels and electrical parameters at the RAA are depicted in Table S5. Though there are some significant correlations, correlation coefficients never exceeded $\rho = 0.343$.

DISCUSSION

Key Findings

Conduction abnormalities were present in all patients but there were no correlations with serum and tissue HSP levels. In addition, both serum and tissue HSP levels did not differentiate between AF and No AF patients, or between the various stages of AF. However, HSPB7 levels were associated with female gender.

Electrical Parameters

Previous epicardial mapping studies demonstrated the important role of heterogeneity in conduction for the electrophysiological substrate underlying AF²⁴. In addition, large-scale high-resolution epicardial mapping studies during SR in patients with and without AF showed that conduction abnormalities (prevalence, length and number of lines of conduction block) are present in all patients with various underlying heart diseases^{1, 2}. Comparable to the findings in the present study, extensiveness of conduction abnormalities at BB²¹ and the RA²⁵ was associated with AF.

In our study population, unipolar voltages did not differ between AF and no AF patients. Unipolar voltages are influenced by many physiological and technical variables including e.g. volume of the myocardium surrounding the electrodes, area of the dipole layer, distances between dipoles and recording electrodes, intra- and extracellular resistances and electrode-wall contact. Consequently, the amplitude of unipolar potentials are most likely not suitable for differentiation between various patient groups.

Heat Shock Proteins

HSPs have an important chaperone function in cardiomyocyte proteolysis and play a key role in AF induced remodeling. They assist by refolding of unfolded proteins, debilitate protein breakdown and prevent damage to contractile proteins.^{10, 13, 26-28} Atrial stress (such as AF) results in an initial increase in (intracellular) HSP levels, induced by Heat Shock transcription

factor 1.^{29, 30} However, HSP levels become exhausted if stress persists over time, hereby also losing the HSP related cardioprotective effects.¹⁰ Consequently, remodeling of the myocardium occurs, leading to AF progression. Various *in vivo* and *in vitro* models demonstrated that upregulation of HSPs indeed protects against AF induced remodeling.³¹⁻³² Previous studies also showed that e.g. HSP60 levels differed significantly between patients in “chronic AF” or in SR¹⁶, although we could not confirm these findings. This might be caused by a difference in patient population; whereas Schäfler et al.¹⁶ only included patient with “chronic AF”, we included patients with all different types of AF. In a recent study by Van Marion et al. we present an in-depth analysis of the serum HSP levels in AF and No AF patients in a larger cohort of 297 patients. Serum HSP27, HSP70, HSPB7 and HSP60 levels did not differentiate between AF stages, nor were they correlated to AF recurrence after pulmonary vein isolation or electrical cardioversion.³³

Correlation between Electrical Parameters and Heat Shock Proteins

This study is the first to investigate whether HSPs are suitable biomarkers for the degree of atrial conduction abnormalities (as identified by epicardial mapping). As mentioned previously, conduction abnormalities during SR are associated with AF. The same is true for HSPs. However, correlations between the electrophysiological parameters and HSPs are lacking. Potential explanations include e.g. large intra- and inter-individual differences in degree and location of CB¹⁻³ and the multifactorial nature of both CB and HSP release. CB is for example influenced by hypertension, diabetes, obesity and aging. In addition, HSP upregulation is not solely influenced by AF, but also by other (cardiac) conditions such as ischemia^{34,35}, kidney disease³⁶, hypertension³⁷, atherosclerotic vascular diseases³⁸, chronic obstructive pulmonary disease and smoking status^{39,40}. Thus, HSPs alone are not indicative of conduction abnormalities.

Study Limitations

Serum and tissue samples for HSP levels were not obtained at the same moment, however the time interval was usually less than 18-24 hours during which the patients were admitted to the hospital in a clinically stable condition. HSP tissue levels were only determined in RAA samples, not at other atrial sites. As electrical changes in RAA do not represent changes in the rest of the atria, RAA HSP levels may not be representable for the rest of the atria. It would have been of interest to study HSP levels at various atrial sites, but ethical reasons impede such a study.

Conclusion

HSP levels in either serum or tissue samples are not correlated to conduction abnormalities or voltages, as investigated by high resolution epicardial mapping. Furthermore, HSPs do not differentiate between AF and No AF patients. Hence, HSPs are not suitable as a AF-specific biomarker.

REFERENCES

1. Lanters EAH, Yaksh A, Teuwen CP, van der Does L, Kik C, Knops P, van Marion DMS, Brundel B, Bogers A, Allessie MA and de Groot NMS. Spatial distribution of conduction disorders during sinus rhythm. *Int J Cardiol.* 2017;249:220-225.
2. van der Does L, Lanters EAH, Teuwen CP, Mouws E, Yaksh A, Knops P, Kik C, Bogers A and de Groot NMS. The Effects of Valvular Heart Disease on Atrial Conduction During Sinus Rhythm. *J Cardiovasc Transl Res.* 2019.
3. Heida A, van der does WFB, van Staveren LN, Taverne YJHJ, Roos-Serote MC, Bogers AJJC and de Groot NMS. Conduction heterogeneity; impact of underlying heart disease and atrial fibrillation. *JACC Clin Electrophysiol.* 2020.
4. January CT, Wann LS, Alpert JS, Calkins H, Cigarroa JE, Cleveland JC, Jr., Conti JB, Ellinor PT, Ezekowitz MD, Field ME, Murray KT, Sacco RL, Stevenson WG, Tchou PJ, Tracy CM, Yancy CW and American College of Cardiology/American Heart Association Task Force on Practice G. 2014 AHA/ACC/HRS guideline for the management of patients with atrial fibrillation: a report of the American College of Cardiology/American Heart Association Task Force on Practice Guidelines and the Heart Rhythm Society. *J Am Coll Cardiol.* 2014;64:e1-76.
5. Kirchhof P, Benussi S, Kotecha D, Ahlsson A, Atar D, Casadei B, Castella M, Diener HC, Heidbuchel H, Hendriks J, Hindricks G, Manolis AS, Oldgren J, Popescu BA, Schotten U, Van Putte B, Vardas P and Group ESCSD. 2016 ESC Guidelines for the management of atrial fibrillation developed in collaboration with EACTS. *Eur Heart J.* 2016;37:2893-2962.
6. Dudink EA, Weijs B, Tull S, Luermans JG, Fabritz L, Chua W, Rienstra M, Gelder ICV, Schotten U, Kirchhof P and Crijns HJ. The Biomarkers NT-proBNP and CA-125 are Elevated in Patients with Idiopathic Atrial Fibrillation. *J Atr Fibrillation.* 2018;11:2058.
7. Chua W, Purmah Y, Cardoso VR, Gkoutos GV, Tull SP, Neculau G, Thomas MR, Kotecha D, Lip GYH, Kirchhof P and Fabritz L. Data-driven discovery and validation of circulating blood-based biomarkers associated with prevalent atrial fibrillation. *Eur Heart J.* 2019;40:1268-1276.
8. Zhu K, Hung J, Divitini M, Murray K, Lim EM, St John A, Walsh JP and Knuiman M. High-sensitivity cardiac troponin I and risk of incident atrial fibrillation hospitalisation in an Australian community-based cohort: The Busselton health study. *Clin Biochem.* 2018;58:20-25.
9. Hui TH, McClelland RL, Allison MA, Rodriguez CJ, Kronmal RA, Heckbert SR, Michos ED, Barter PJ, Rye KA and Ong KL. The relationship of circulating fibroblast growth factor 21 levels with incident atrial fibrillation: The Multi-Ethnic Study of Atherosclerosis. *Atherosclerosis.* 2018;269:86-91.
10. Brundel BJ, Henning RH, Ke L, van Gelder IC, Crijns HJ and Kampinga HH. Heat shock protein upregulation protects against pacing-induced myolysis in HL-1 atrial myocytes and in human atrial fibrillation. *J Mol Cell Cardiol.* 2006;41:555-62.
11. Brundel BJ, Shiroshita-Takeshita A, Qi X, Yeh YH, Chartier D, van Gelder IC, Henning RH, Kampinga HH and Nattel S. Induction of heat shock response protects the heart against atrial fibrillation. *Circ Res.* 2006;99:1394-402.
12. Brundel BJ, Ke L, Dijkhuis AJ, Qi X, Shiroshita-Takeshita A, Nattel S, Henning RH and Kampinga HH. Heat shock proteins as molecular targets for intervention in atrial fibrillation. *Cardiovasc Res.* 2008;78:422-8.
13. Zhang D, Ke L, Mackovicova K, Van Der Want JJ, Sibon OC, Tanguay RM, Morrow G, Henning RH, Kampinga HH and Brundel BJ. Effects of different small HSPB members on contractile dysfunction and structural changes in a *Drosophila melanogaster* model for Atrial Fibrillation. *J Mol Cell Cardiol.* 2011;51:381-9.
14. Sakabe M, Shiroshita-Takeshita A, Maguy A, Brundel BJ, Fujiki A, Inoue H and Nattel S. Effects of a heat shock protein inducer on the atrial fibrillation substrate caused by acute atrial ischaemia. *Cardiovasc Res.* 2008;78:63-70.

15. Kirmanoglou K, Hannekum A and Schafier AE. Expression of mortalin in patients with chronic atrial fibrillation. *Basic Res Cardiol.* 2004;99:404-8.
16. Schafier AE, Kirmanoglou K, Balbach J, Pecher P, Hannekum A and Schumacher B. The expression of heat shock protein 60 in myocardium of patients with chronic atrial fibrillation. *Basic Res Cardiol.* 2002;97:258-61.
17. Hu YF, Yeh HI, Tsao HM, Tai CT, Lin YJ, Chang SL, Lo LW, Tuan TC, Suenari K, Li CH, Chao TF and Chen SA. Electrophysiological correlation and prognostic impact of heat shock protein 27 in atrial fibrillation. *Circ Arrhythm Electrophysiol.* 2012;5:334-40.
18. Lanter EA, van Marion DM, Kik C, Steen H, Bogers AJ, Alessie MA, Brundel BJ and de Groot NM. HALT & REVERSE: Hsf1 activators lower cardiomyocyte damage; towards a novel approach to REVERSE atrial fibrillation. *J Transl Med.* 2015;13:347.
19. van der Does LJ, Yaksh A, Kik C, Knops P, Lanter EA, Teuwen CP, Oei FB, van de Woestijne PC, Bekkers JA, Bogers AJ, Alessie MA and de Groot NM. QUES for the Arrhythmogenic Substrate of Atrial fibrillation in Patients Undergoing Cardiac Surgery (QUASAR Study): Rationale and Design. *J Cardiovasc Transl Res.* 2016;9:194-201.
20. Mouws E, Lanter EAH, Teuwen CP, van der Does L, Kik C, Knops P, Bekkers JA, Bogers A and de Groot NMS. Epicardial Breakthrough Waves During Sinus Rhythm: Depiction of the Arrhythmogenic Substrate? *Circ Arrhythm Electrophysiol.* 2017;10.
21. Teuwen CP, Yaksh A, Lanter EA, Kik C, van der Does LJ, Knops P, Taverne YJ, van de Woestijne PC, Oei FB, Bekkers JA, Bogers AJ, Alessie MA and de Groot NM. Relevance of Conduction Disorders in Bachmann's Bundle During Sinus Rhythm in Humans. *Circ Arrhythm Electrophysiol.* 2016;9:e003972.
22. Mouws E, van der Does L, Kik C, Lanter EAH, Teuwen CP, Knops P, Bogers A and de Groot NMS. Impact of the arrhythmogenic potential of long lines of conduction slowing at the pulmonary vein area. *Heart Rhythm.* 2019;16:511-519.
23. Houck CA, Lanter EAH, Heida A, Taverne Y, van de Woestijne PC, Knops P, Roos-Serote MC, Roos-Hesselink JW, Bogers A and de Groot NMS. Distribution of Conduction Disorders in Patients With Congenital Heart Disease and Right Atrial Volume Overload. *JACC Clin Electrophysiol.* 2020;6:537-548.
24. Alessie MA, de Groot NM, Houben RP, Schotten U, Boersma E, Smeets JL and Crijns HJ. Electropathological substrate of long-standing persistent atrial fibrillation in patients with structural heart disease: longitudinal dissociation. *Circ Arrhythm Electrophysiol.* 2010;3:606-15.
25. Zaman JA, Harling L, Ashrafian H, Darzi A, Gooderham N, Athanasiou T and Peters NS. Post-operative atrial fibrillation is associated with a pre-existing structural and electrical substrate in human right atrial myocardium. *Int J Cardiol.* 2016;220:580-8.
26. Ke L, Meijering RA, Hoogstra-Berends F, Mackovicova K, Vos MJ, Van Gelder IC, Henning RH, Kampinga HH and Brundel BJ. HSPB1, HSPB6, HSPB7 and HSPB8 protect against RhoA GTPase-induced remodeling in tachypaced atrial myocytes. *PLoS One.* 2011;6:e20395.
27. Meijering RA, Henning RH and Brundel BJ. Reviving the protein quality control system: therapeutic target for cardiac disease in the elderly. *Trends Cardiovasc Med.* 2015;25:243-7.
28. Zhang D, Wu CT, Qi X, Meijering RA, Hoogstra-Berends F, Tadevosyan A, Cubukcuoglu Deniz G, Durdu S, Akar AR, Sibon OC, Nattel S, Henning RH and Brundel BJ. Activation of histone deacetylase-6 induces contractile dysfunction through derailment of alpha-tubulin proteostasis in experimental and human atrial fibrillation. *Circulation.* 2014;129:346-58.
29. Balch WE, Morimoto RI, Dillin A and Kelly JW. Adapting proteostasis for disease intervention. *Science.* 2008;319:916-9.
30. Powers ET, Morimoto RI, Dillin A, Kelly JW and Balch WE. Biological and chemical approaches to diseases of proteostasis deficiency. *Annu Rev Biochem.* 2009;78:959-91.

31. Hu X, Li J, van Marion DMS, Zhang D and Brundel B. Heat shock protein inducer GGA*-59 reverses contractile and structural remodeling via restoration of the microtubule network in experimental Atrial Fibrillation. *J Mol Cell Cardiol.* 2019;134:86-97.
32. van Marion DM, Hu X, Zhang D, Hoogstra-Berends F, Seerden JG, Loen L, Heeres A, Steen H, Henning RH and Brundel BJ. Screening of novel HSP-inducing compounds to conserve cardiomyocyte function in experimental atrial fibrillation. *Drug Des Devel Ther.* 2019;13:345-364.
33. Marion D, Lanters EAH, Ramos KS, Li J, Wiersma M, Baks-Te Bulte L, A JQMM, Boersma E, de Groot NMS and Brundel B. Evaluating Serum Heat Shock Protein Levels as Novel Biomarkers for Atrial Fibrillation. *Cells.* 2020;9.
34. Kraemer BF, Mannell H, Lamkemeyer T, Franz-Wachtel M and Lindemann S. Heat-Shock Protein 27 (HSPB1) Is Upregulated and Phosphorylated in Human Platelets during ST-Elevation Myocardial Infarction. *Int J Mol Sci.* 2019;20.
35. Kim N, Ullah I, Chung K, Lee D, Cha MJ, Ban H, Choi CS, Kim S, Hwang KC, Kumar P and Lee SK. Targeted Delivery of Recombinant Heat Shock Protein 27 to Cardiomyocytes Promotes Recovery from Myocardial Infarction. *Mol Pharm.* 2020;17:2034-2043.
36. Chebotareva N, Bobkova I and Shilov E. Heat shock proteins and kidney disease: perspectives of HSP therapy. *Cell Stress Chaperones.* 2017;22:319-343.
37. Pockley AG, De Faire U, Kiessling R, Lemne C, Thulin T and Frostegard J. Circulating heat shock protein and heat shock protein antibody levels in established hypertension. *J Hypertens.* 2002;20:1815-20.
38. Mehta TA, Greenman J, Ettelaie C, Venkatasubramanian A, Chetter IC and McCollum PT. Heat shock proteins in vascular disease--a review. *Eur J Vasc Endovasc Surg.* 2005;29:395-402.
39. Dong J, Guo L, Liao Z, Zhang M, Zhang M, Wang T, Chen L, Xu D, Feng Y and Wen F. Increased expression of heat shock protein 70 in chronic obstructive pulmonary disease. *Int Immunopharmacol.* 2013;17:885-93.
40. Somborac-Bacura A, Rumora L, Novak R, Rasic D, Dumic J, Cepelak I and Zanic-Grubisic T. Differential expression of heat shock proteins and activation of mitogen-activated protein kinases in A549 alveolar epithelial cells exposed to cigarette smoke extract. *Exp Physiol.* 2018;103:1666-1678.

SUPPLEMENTAL TABLES

Supplemental Table 1. Primary antibodies

Primary antibody	Cat. no	Company
Mouse anti-HSP27	ADI-SPA-800	Enzo-Lifesciences, USA
Mouse anti-HSP70	ADI-SPA-810	Enzo-Lifesciences, USA
Rabbit anti-HSP60	ADI-SPA-805	Enzo Life Sciences, Farmingdale, NY, USA
Rabbit anti-HSPA5	ab21685	Abcam, UK
Rabbit anti-HSF1	4356	Cell Signaling Technology, USA
Rabbit anti-pHSF1	sc-30443-R	Santa-Cruz Biotechnology, USA
Mouse anti-GAPDH	10R-G109a	Fitzgerald Industries International, Acton, MA, USA

Supplemental Table 2. Correlation between tissue and serum Heat Shock Proteins

		Serum HSP27	Serum HSP70	Serum HSPB7	Serum HSP60
RAA HSP27	ρ	0,120	-0,081	0,023	0,085
	P	0,279	0,472	0,840	0,443
RAA HSP70	ρ	0,088	-0,155	0,078	0,046
	P	0,427	0,163	0,484	0,681
RAA HSPA5	ρ	0,012	-0,055	-0,071	0,024
	P	0,913	0,618	0,526	0,825
RAA HSP60	ρ	-0,009	-0,110	-0,014	-0,178
	P	0,938	0,324	0,899	0,109
RAA HSPB5	ρ	0,049	0,024	0,143	-0,198
	P	0,659	0,831	0,198	0,069
RAA HSF1	ρ	-0,189	0,167	-0,039	-0,121
	P	0,089	0,137	0,729	0,278

RAA: right atrial appendage; HSP: heat shock protein; ρ : correlation coefficient (rho).

Supplemental Table 3. Electrophysiological parameters per atrial region

	RA	BB	LA	PV
Median voltage, mV	4.6[3.2-6.0]	3.5[2.2-6.0]	6.2[4.0-7.9]	6.1[2.9-9.3]
AF	4.2[3.3-5.5]	2.9[1.4-4.5]	5.9[2.6-8.1]	3.0[2.4-6.8]
No AF	4.6[3.0-6.1]	3.9[2.6-6.2]	6.2[4.1-7.8]	7.0[3.7-9.7]
P-value	0.873	0.162	0.759	0.043
Percentage CB, %	2.2[1.2-4.3]	3.0[1.3-5.9]	0.8[0.2-1.7]	0.5[0.2-1.3]
AF	2.5[1.3-5.3]	5.0[2.2-8.8]	0.8[0.0-3.7]	1.0[0.3-2.1]
No AF	1.9[1.1-4.2]	2.5[1.0-5.5]	0.8[0.2-1.6]	0.5[0.1-1.1]
P	0.112	0.054	0.596	0.112
Number of CB lines, N	8.25[4.5-13.4]	2.75[1.0-4.0]	2.0[0.5-3.0]	1.5[0.0-3.0]
AF	9.5[5.5-17.0]	3.8[2.8-5.0]	1.0[0.0-3.0]	2.0[0.5-3.5]
No AF	7.5[3.5-13.0]	2.0[1.0-3.0]	2.0[0.6-3.0]	1.0[0.0-2.4]
P	0.056	0.015	0.512	0.149
Median length CB lines, mm	5.1[3.7-6.8]	5.0[4.0-8.0]	5.0[3.7-8.0]	4.0[2.4-6.0]
AF	5.0[3.8-6.7]	5.0[2.5-7.0]	6.0[4.5-12.3]	6.0[2.5-10.0]
No AF	5.3[3.6-7.3]	5.0[4.0-8.0]	4.8[3.1-7.8]	4.0[2.0-5.0]
P	0.947	0.623	0.079	0.161
Maximal length CB lines, mm	25.0[14.0-36.5]	16.0[8.0-32.0]	12.0[8.0-16.0]	9.0[6.0-18.0]
AF	36.0[20.-54.0]	26.0[17.0-36.0]	14.0[8.0-25.0]	10.0[8.0-20.0]
No AF	22.0[14.0-32.0]	12.0[8.0-31.5]	11.0[8.0-19.5]	8.0[6.0-18.0]
P	0.006	0.076	0.284	0.183
Percentage CDCB, %	5.7[3.4-9.0]	7.1[4.3-11.4]	2.9[1.5-4.2]	3.3[1.4-4.9]
AF	6.8[4.7-9.5]	11.8[6.6-15.3]	3.2[1.9-.2]	4.3[2.4-7.4]
No AF	4.8[3.1-8.2]	6.5[3.9-10.0]	2.8[1.3-4.0]	3.0[1.2-4.5]
P	0.071	0.008	0.319	0.042
Number of CDCB lines, N	4.5[2.5-6.9]	1.0[1.0-2.0]	1.0[0.0-2.0]	1.0[0.0-2.0]
AF	6.0[4.0-8.0]	2.0-1.0-3.0]	1.0[0.0-2.3]	2.0-2.3]
No AF	4.0[2.0-6.0]	1.0[1.0-1.5]	1.0[0.5-2.0]	1.0[0.0-1.0]
P	0.071	0.003	0.302	0.143
Median length CDCB lines, mm	13.6[10.4-17.0]	16.0[10.0-24.0]	13.3[10.5-17.8]	11.5[8.0-16.5]
AF	14.8[12.5-17.0]	19.5[11.0-26.0]	17.0[12.0-22]	10.0[8.0-16.5]
No AF	13.3[10.0-16.7]	15.0[9.0-24.0]	13.0[12.3-15.8]	13.0[9.0-24.3]
P	0.212	0.323	0.092	0.102
Maximal length CDCB lines, mm	34.0[24.0-56.0]	30.0[16.0-48.0]	22.0[14.0-29.5]	21.0[12.0-30.0]
AF	48.0[28.0-84.0]	40.0[28.0-56.0]	26.0[18.0-30.0]	28.0[18.0-54.0]
No AF	34.0[20.0-50.0]	28.0[14.0-44.0]	20.0[14.0-28.0]	20.0[12.0-28.0]
P	0.024	0.014	0.147	0.129
CT severity, ms	43.5[29.0-56.0]	25.0[19.0-43.0]	20.0[14.5-26.0]	18.0[13.0-25.0]
AF	27.0[28.5-49.5]	34.0[20.0-50.3]	21.0[11.5-28.0]	20.0[15.5-28.5]
No AF	50.0[32.0-67.0]	23.0[18.3-40.3]	20.0[15.0-25.0]	16.5[13.0-22.0]
P	0.029	0.226	0.933	0.080

Data is presented as median[P25-P75]. RA: right atrium; BB: Bachmann's bundle; LA: left atrium; PV: pulmonary veins; CB: conduction block; CDCB: combined conduction delay + conduction block; CT: conduction times.

Supplemental Table 4. Correlation between serum HSP levels and electrophysiological parameters

		HSP27	HSP70	HSPB7	HSP60
Atrium					
Mean voltage	ρ	0,131	0,017	0,158	-0,032
	P	0,288	0,893	0,199	0,795
Percentage CB	ρ	-0,114	0,147	0,053	-0,009
	P	0,349	0,227	0,663	0,941
Number CB lines	P	-0,133	0,113	-0,005	-0,044
	ρ	0,274	0,355	0,967	0,714
Median length CB lines	ρ	0,007	0,116	0,075	0,103
	P	0,957	0,342	0,537	0,391
Maximal length CB lines	ρ	-0,053	0,155	0,185	-0,032
	P	0,665	0,204	0,125	0,789
Percentage CDCB	ρ	-0,104	0,120	0,044	-0,038
	P	0,393	0,328	0,719	0,754
Number CDCB lines	P	-0,082	0,097	-0,025	-0,035
	ρ	0,497	0,430	0,836	0,775
Median length CDCB lines	ρ	-0,011	-0,014	-0,111	-0,085
	P	0,927	0,907	0,362	0,483
Maximal length CDCB lines	ρ	-0,101	0,064	0,090	-0,057
	P	0,407	0,600	0,458	0,636
CT severity	ρ	-0,011	0,211	0,126	-0,021
	P	0,927	0,082	0,299	0,861
Right Atrium					
Median voltage	ρ	0,199	-0,061	-0,007	0,083
	P	0,098	0,616	0,952	0,491
Percentage CB	ρ	-0,051	0,231	0,122	-0,036
	P	0,673	0,056	0,314	0,766
Number CB lines	ρ	-0,057	0,181	0,086	-0,064
	P	0,640	0,136	0,481	0,597
Median length CB lines	ρ	0,104	0,001	0,045	0,104
	P	0,397	0,991	0,716	0,395
Maximal length CB lines	ρ	-0,054	0,184	0,171	-0,012
	P	0,659	0,135	0,163	0,921
Percentage CDCB	ρ	-0,081	0,211	0,079	-0,003
	P	0,505	0,082	0,515	0,978

		HSP27	HSP70	HSPB7	HSP60
Number CDCB lines	ρ	-0,034	0,188	0,112	-0,039
	P	0,777	0,123	0,358	0,746
Median length CDCB lines	ρ	-0,034	-0,110	0,045	0,031
	P	0,786	0,374	0,716	0,799
Maximal length CDCB lines	ρ	-0,088	0,086	0,097	0,084
	P	0,477	0,489	0,430	0,492
CT severity	ρ	0,009	0,234	0,267*	-0,030
	P	0,940	0,053	0,026	0,802
Bachmann's Bundle		HSP27	HSP70	cvHSP	HSP60
Median voltage	ρ	0,059	-0,030	0,129	-0,078
	P	0,632	0,807	0,294	0,525
Percentage CB	ρ	-0,023	0,051	-0,032	0,057
	P	0,850	0,683	0,797	0,644
Number CB lines	ρ	-0,109	-0,004	-0,098	-0,053
	P	0,374	0,974	0,426	0,667
Median length CB lines	ρ	0,083	0,099	0,170	0,159
	P	0,518	0,442	0,183	0,210
Maximal length CB lines	ρ	0,008	0,141	0,056	-0,028
	P	0,949	0,275	0,661	0,827
Percentage CDCB	ρ	-0,055	0,033	-0,017	-0,075
	P	0,657	0,788	0,894	0,538
Number CDCB lines	ρ	-0,031	0,018	-0,047	-0,097
	P	0,801	0,885	0,703	0,427
Median length CDCB lines	ρ	0,097	0,165	0,013	-0,037
	P	0,452	0,203	0,918	0,776
Maximal length CDCB lines	ρ	-0,009	0,063	0,019	-0,145
	P	0,943	0,627	0,884	0,258
CT severity	ρ	-0,008	0,075	0,000	-0,031
	P	0,947	0,547	0,997	0,802
Pulmonary Veins		HSP27	HSP70	cvHSP	HSP60
Median voltage	ρ	0,105	0,165	0,053	-0,012
	P	0,397	0,181	0,667	0,923
Percentage CB	ρ	-0,131	-0,247*	0,070	-0,051
	P	0,292	0,044	0,575	0,682

		HSP27	HSP70	HSPB7	HSP60
Number CB lines	ρ	-0,071	-0,129	-0,028	-0,097
	P	0,571	0,299	0,824	0,431
Median length CB lines	ρ	-0,183	-0,245	0,042	-0,045
	P	0,178	0,068	0,758	0,742
Maximal length CB lines	ρ	-0,275*	-0,335*	0,006	-0,065
	P	0,040	0,012	0,963	0,632
Percentage CDCB	ρ	-0,086	-0,114	0,002	-0,044
	P	0,487	0,357	0,985	0,723
Number CDCB lines	ρ	0,014	-0,154	-0,106	-0,087
	P	0,910	0,213	0,394	0,480
Median length CDCB lines	ρ	-0,093	-0,185	-0,215	-0,142
	P	0,502	0,181	0,119	0,302
Maximal length CDCB lines	ρ	-0,211	-0,242	-0,128	-0,229
	P	0,125	0,078	0,358	0,092
CT severity	ρ	-0,104	-0,309*	0,095	-0,154
	P	0,402	0,011	0,443	0,211
Left Atrium		HSP27	HSP70	cvHSP	HSP60
Median voltage	ρ	0,044	0,014	0,274*	-0,021
	P	0,722	0,909	0,025	0,867
Percentage CB	ρ	-0,128	0,071	-0,095	-0,003
	P	0,300	0,573	0,447	0,979
Number CB lines	ρ	-0,198	-0,034	-0,065	0,025
	P	0,105	0,789	0,599	0,841
Median length CB lines	ρ	-0,009	0,151	-0,071	-0,047
	P	0,949	0,271	0,602	0,731
Maximal length CB lines	ρ	0,012	0,108	-0,188	0,054
	P	0,931	0,434	0,165	0,695
Percentage CDCB	ρ	-0,128	-0,151	-0,110	0,007
	P	0,297	0,226	0,376	0,954
Number CDCB lines	ρ	-0,161	-0,085	-0,084	0,041
	P	0,189	0,497	0,498	0,737
Median length CDCB lines	ρ	-0,013	0,165	-0,094	-0,203
	P	0,929	0,251	0,510	0,153

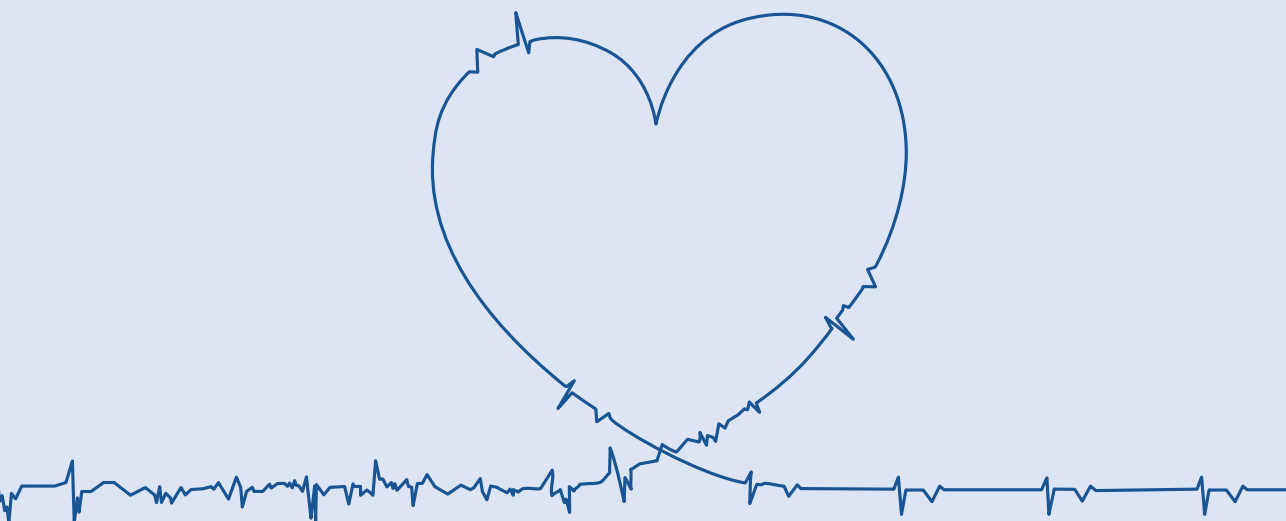
		HSP27	HSP70	HSPB7	HSP60
Maximal length CDCB lines	ρ	-0,069	0,103	-0,162	-0,060
	P	0,631	0,478	0,257	0,676
CT severity	ρ	-0,034	0,277*	-0,019	-0,054
	P	0,785	0,024	0,876	0,659

HSP: heat shock protein; CB: conduction block; CDCB: combined conduction delay + conduction block; CT: conduction times; ρ : correlation coefficient (rho).

Supplemental Table 5. Correlation between RAA tissue HSP levels and RAA electrical parameters

		HSP27	HSP70	HSPA5	HSP60	HSPB5	HSF1
Mean voltage	ρ	-0.086	-0.041	-0.061	0.019	-0.200	-0.231
	P	0.551	0.770	0.666	0.897	0.151	0.102
Percentage CB	ρ	0.035	-0.110	0.026	-0.030	0.284*	0.227
	P	0.810	0.437	0.857	0.839	0.039	0.110
Number of CB lines	ρ	-0.018	-0.027	-0.111	-0.133	0.343*	0.300*
	P	0.900	0.852	0.433	0.356	0.012	0.033
Median length CB lines	ρ	0.062	-0.206	0.160	0.223	0.252	0.056
	P	0.688	0.169	0.289	0.145	0.087	0.710
Maximal length CB lines	ρ	0.107	0.137	-0.168	0.232	0.204	0.148
	P	0.456	0.332	0.235	0.105	0.143	0.299
Percentage CDCB	ρ	0.067	-0.022	-0.043	-0.089	0.328*	0.144
	P	0.642	0.877	0.764	0.537	0.016	0.313
Number of CDCB lines.	ρ	0.031	0.092	-0.118	-0.156	0.325*	0.179
	P	0.828	0.518	0.406	0.278	0.018	0.208
Median length CDCB lines	ρ	0.214	-0.161	0.137	0.212	0.234	0.160
	P	0.154	0.281	0.358	0.162	0.109	0.283
Maximal length CDCB lines	ρ	0.217	-0.094	0.099	0.133	0.332*	0.107
	P	0.152	0.535	0.513	0.389	0.022	0.479
Maximum CT	ρ	0.088	-0.093	0.054	0.026	0.328*	0.181
	P	0.539	0.513	0.705	0.855	0.016	0.204

HSP: heat shock protein; CB: conduction block; CDCB: combined conduction delay + conduction block; CT: conduction times; ρ : correlation coefficient (rho).



18

CHAPTER 18

GENERAL DISCUSSION



Lanters EAH

The mechanisms and substrate of atrial fibrillation; novel findings during AF mapping

As described in Chapter 1, the two main potential mechanisms underlying AF include either true fibrillation or fibrillatory conduction.¹ At present, it is unknown whether these mechanisms play a role in different stages of AF or whether they can occur within the same individual. The same is true for the AF-related electropathological substrate. Although it is generally accepted that the substrate is more advanced in patients with (long-standing) persistent AF than in paroxysmal AF patients, the exact components of the substrate remain a matter of debate.

In this thesis, conduction block and focal waves have been identified as cornerstones of the electropathological substrate.^{2,3} These focal waves can only arise when there is electrical asynchrony between the endo- and epicardial layer.⁴ Indeed, de Groot et al reported on increasing endo-epicardial asynchrony with AF persistence.² Electrical asynchrony between the endo- and epicardium allows propagation of numerous fibrillation waves between these layers, ultimately leading to stabilization and thus persistence of AF. Thus, endo-epicardial asynchrony might be an indicator of the extensiveness of the electropathological substrate underlying AF. In this extend, we also showed that the number of focal waves is associated with a higher complexity of patterns of activation during AF. Although these findings are promising, (endo-) epicardial mapping approach can only be performed during open chest cardiac surgery. Identification of a surrogate marker that can be obtained by less - or even non-invasive studies, is therefore of utmost importance and should be the goal of future studies.

The mechanisms and substrate of atrial fibrillation; novel findings during SR mapping

In the current thesis, we also investigated the electropathological substrate during sinus rhythm, in patients with various underlying heart diseases. Patients with isolated coronary artery disease (Chapters 3, 5 and 6), isolated valvular heart disease (Chapters 4, 5 and 6), a combination of coronary artery disease and valvular heart disease (Chapter 4, 5 and 6) and in patients with a congenital heart disease (Chapter 8), all both with and without AF, were included. We demonstrated a wide variance in incidence and extensiveness of conduction block.^{6,7} These differences were not only present between various patients, but also between the various atrial regions within a single patient. A predilection site for atrial conduction abnormalities was identified at the high right atrium near the superior caval vein.^{6,7}

In patients with AF, lines of conduction block during sinus rhythm at Bachmann's bundle were longer than in patients without AF.⁸ However, Bachmann's bundle was not an indicator of electropathology elsewhere in the atria.⁷ There was no correlation between incidence or extensiveness of conduction block and development of early post-operative AF.⁷ Altogether these findings are consistent with the hypothesis that AF might be more than "just" a left atrial disease. To understand the role of these conduction abnormalities during SR for initiation and perpetuation of AF, activation patterns are currently being studied during AF. Recordings are repeated at the exact same mapping sites, but during (acutely induced) AF and investigated for the presence of conduction abnormalities as observed during sinus rhythm. Furthermore, the impact of conduction block during SR on the patterns of activation during AF is studied to confirm the hypothesis that conduction block during SR causes local micro-reentry or endo-epicardial dissociation.

Correlation between electrical and structural alterations

Until now, studies mainly report on either electrical or on structural remodeling. Experimental studies investigating electrical conduction in *in vitro* preparations of canine atria showed that conduction abnormalities result from non-uniform tissue anisotropy, which is most likely caused by interstitial fibrosis.^{9,10} Furthermore, conduction abnormalities may also result from interruption of the atrial myocardium by arteries, pericardial folds or extensions of sinus venosus myocardium.^{11,12} In addition, the right atrial terminal crest area in particular is known for its lower density of transversal intercellular connections.¹³

Data relating atrial conduction abnormalities to underlying structural changes are scarce. In the goat model of AF, atrial conduction abnormalities were correlated to alterations of the myocardial structure.¹⁴ After three months of (induced) AF, conduction block and fractionation of atrial potentials were accompanied by an inhomogeneous redistribution (Cx40) and lateralization (Cx43) in RAA myocytes. However, there was no increase in fibrosis.¹⁴ Markides et al.¹⁵ performed an endocardial mapping study of the left atrium in 19 paroxysmal AF patients and found a line of CB (difference in local activation time >30ms) at the LA posterior wall in all patients. In 10 postmortem hearts from other patients they identified an abrupt change in subendocardial fiber orientation at the same location as the line of CB.¹⁵ Future research studies should further investigate the correlation between atrial microstructure and conduction properties.

Bloodbased AF biomarkers

The emerging need for non-invasive AF biomarkers was emphasized in Chapters 13 and 14 of this thesis. There is a variety of bloodbased biomarkers that correlates to AF, including brain natriuretic peptides, cancer-antigen-125, fibroblast growth factor-23^{16,17} and -21¹⁸, high-sensitive cardiac troponin I¹⁹, homocysteine²⁰, (a)symmetric dimethylarginine²¹, interleukine-6 and matrix metalloproteinase-9/tissue inhibitor of metalloproteinase-1 ratio²². However, majority of these parameters are not AF specific, do not relate to the type of AF and/or rhythm outcome after electrocardioversion or catheter ablation. Heat shock proteins were introduced as novel, potential bloodbased biomarkers after various experimental studies showed a key role as a chaperone in the protein folding system.

Studies in this thesis demonstrated a wide distribution in HSP levels in the various patients groups including patients in sinus rhythm (without AF), paroxysmal AF and (longstanding) persistent AF undergoing either standard electrophysiology studies, electrocardioversion, pulmonary vein isolation or cardiothoracic surgery for coronary, valvular and/or congenital heart disease. Baseline levels of HSP27, HSP70, cvHSP and HSP60 did not differentiate between various types of AF and did not predict AF recurrence. During follow-up, HSP27 and HSP70 levels were increased in patients with AF recurrences within one year after pulmonary vein isolation. In patients undergoing cardiothoracic surgery, there were no clinically relevant correlations between baseline HSP levels in serum and electrical markers for impaired conduction such as the presence and severity of conduction delay/block, local conduction times and low voltage areas in any of the atrial mapping region including the right atrium, Bachmanns bundle, pulmonary vein area and left atrium. Based on these results, HSPs are not suitable as biomarkers to distinguish between AF or SR, to discriminate between different stages of AF or to predict AF recurrences.

Upregulation by HSP inducing compounds resulted in an improved recovery of structural and contractile remodeling, induced by prolonged tachypacing of a cell-model.²³ Furthermore, HSP boosting by oral geranylgeranylacetone treatment resulted in an increase in HSPB1 and HSPA1 levels in RAA and LAA of patients (N = 13) undergoing coronary artery bypass grafting.²⁴ Upregulation of HSPs can also be accomplished by glutamin, a semi-essential amino-acid present in the food supplement L-glutamine (availability: over the counter). Research is currently being conducted to verify if this approach indeed increases serum HSP levels in AF patients. Thereafter, effects on AF symptoms and burden are to be evaluated.

In the protein quality control system, an essential role is reserved for histone deacetylases (HDACs). Whereas HSPs are chaperones in this process, HDACs serve more as modulators/regulators of proteostasis by their ability to change protein function, eventually resulting in changes in gene expression and cell function.^{25,26} Upregulation of HDACs due to AF-related atrial stress induces both structural (e.g. hypertrophy, remodeling of the ion channels or fibrosis) and contractile remodeling of cardiomyocytes.²⁷ Pharmacological inhibition of HDACs showed protection for contractile remodeling in tachypaced cells and *Drosophila* hearts, whereas electric and contractile remodeling were suppressed in tachypaced dogs.²⁸

Recently, biomarkers related to DNA damage were identified as alternative AF sensitive biomarkers. Atrial tachycardia leads to oxidative DNA damage including DNA breaks, which in turn activates the poly(ADP)-ribose polymerase 1 (PARP1). Thereafter, synthesis of ADP-ribose chains causes depletion of nicotinamide adenine dinucleotide (NAD⁺), resulting in even more DNA damage and contractile dysfunction of the atrial myocytes. This hypothesis was confirmed in tachypaced myocardial cell models and in a *drosophila* model.²⁹ In the same manuscript, this was validated in tissue samples of the right or left atrial appendages of patients with SR or AF. Similarly, to the cell-lines and *drosophila*'s, markers for oxidative DNA-damage were increased in patients with (longstanding) persistent AF, indicating a potential role as AF related biomarker for PARP1. Furthermore, PARP1 inhibition as well as NAD⁺ replenishment prevented tachypacing induced remodeling in cardiomyocytes and *drosophila* models.²⁹

AF-induced intracellular calcium overload triggers stress of the endoplasmatic reticulum which promotes autophagy, leading to further structural remodeling of the atrium.³⁰ As demonstrated by Wiersma et al, *pharmacological blocking* of this endoplasmatic reticulum stress by various compounds represses autophagy.³¹ Subsequently, AF induced structural cardiomyocyte remodeling was suppressed in various models, including tachypaced (mice) cardiomyocytes, *Drosophila*, dogs and atrial appendages of AF patients. Due to the close interrelationship between the endoplasmatic reticulum and the mitochondria, ER stress provokes mitochondrial stress.³² Mitochondrial function depends on NAD⁺ levels, which are decreased in AF.³³ Furthermore, mitochondria buffer cytosolic calcium and a calcium overload may thus further comprise mitochondrial function.³⁴ Via tachypacing of cardiomyocytes it was proven that the mitochondrial function indeed was affected, showing for example impairment of mitochondrial calcium handling, an increase in biomarkers/chaperones for mitochondrial stress and structural damage of the mitochondria.³⁵ Inhibition of the mitochondrial calcium channels by pharmacological agents resulted in less tachycardia-induced mitochondrial damage in the cardiomyocyte line. In *Drosophila*, it protected against contractile dysfunction.³⁵ From the abovementioned studies, it can be postulated that markers for stress of the

endoplasmatic reticulum or mitochondria may serve as novel AF related biomarkers. Furthermore, we can conclude that druggable targets include PARP1 inhibition, NAD⁺ replenishment, blocking of endoplasmatic reticulum and/or mitochondrial stress. Future studies have to elucidate on the value of these observations in human hearts.

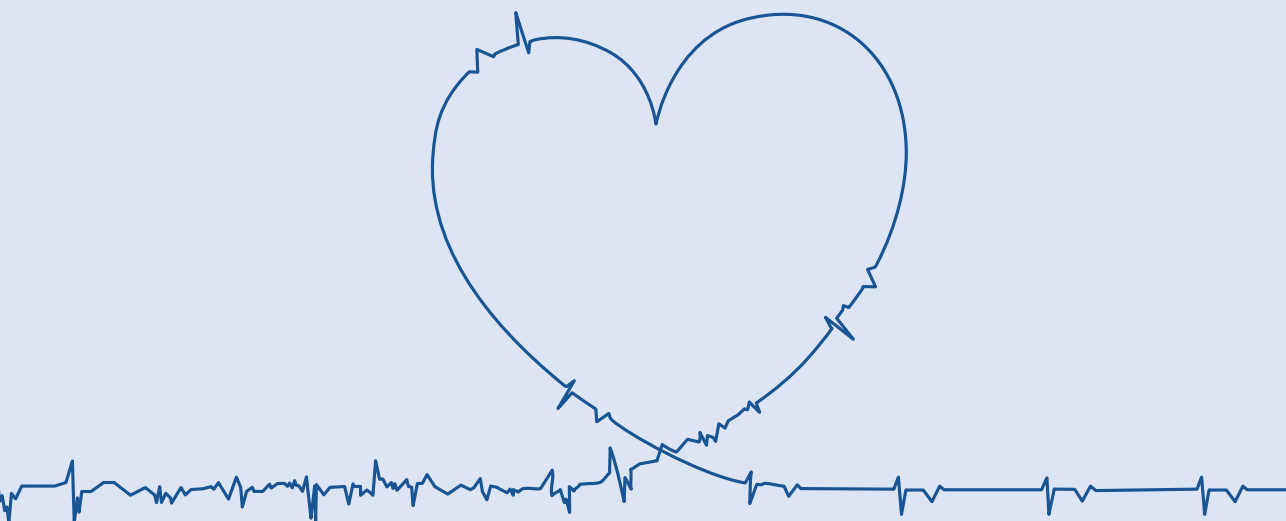
Integration in Daily Clinical Practice: Future Perspectives

Altogether, a set of non-invasive electrical, chemical (blood-based) and clinical biomarkers that all contribute to a scoring system for staging AF that is applicable at the majority of patients presenting with AF is required. Given the multifactorial nature of AF and the co-existence of comorbidities in AF patients, it is utopic to assume that the electropathological substrate underlying AF can be captured with just one biomarker. The ultimate goal of AF research studies remains to identify in a non-invasive manner the degree of electropathology and determine what therapy is most likely to succeed in each patient individually.

REFERENCES

1. Moe GK, Abildskov JA. Atrial fibrillation as a self-sustaining arrhythmia independent of focal discharge. *Am Heart J*. 1959;58(1):59-70.
2. de Groot NM, Houben RP, Smeets JL, Boersma E, Schotten U, Schalij MJ, et al. Electropathological substrate of longstanding persistent atrial fibrillation in patients with structural heart disease: epicardial breakthrough. *Circulation*. 2010;122(17):1674-82.
3. Allessie MA, de Groot NM, Houben RP, Schotten U, Boersma E, Smeets JL, et al. Electropathological substrate of long-standing persistent atrial fibrillation in patients with structural heart disease: longitudinal dissociation. *Circ Arrhythm Electrophysiol*. 2010;3(6):606-15.
4. de Groot N, van der Does L, Yaksh A, Lanfers E, Teuwen C, Knops P, et al. Direct Proof of Endo-Epicardial Asynchrony of the Atrial Wall During Atrial Fibrillation in Humans. *Circ Arrhythm Electrophysiol*. 2016;9(5).
5. van der Graaf AW, Bhagirath P, Ramanna H, van Driel VJ, de Hooze J, de Groot NM, et al. Noninvasive imaging of cardiac excitation: current status and future perspective. *Ann Noninvasive Electrocardiol*. 2014;19(2):105-13.
6. van der Does L, Lanfers EAH, Teuwen CP, Mouws E, Yaksh A, Knops P, et al. The Effects of Valvular Heart Disease on Atrial Conduction During Sinus Rhythm. *J Cardiovasc Transl Res*. 2019.
7. Lanfers EAH, Yaksh A, Teuwen CP, van der Does L, Kik C, Knops P, et al. Spatial distribution of conduction disorders during sinus rhythm. *Int J Cardiol*. 2017;249:220-5.
8. Teuwen CP, Yaksh A, Lanfers EA, Kik C, van der Does LJ, Knops P, et al. Relevance of Conduction Disorders in Bachmann's Bundle During Sinus Rhythm in Humans. *Circ Arrhythm Electrophysiol*. 2016;9(5):e003972.
9. Spach MS, Boineau JP. Microfibrosis produces electrical load variations due to loss of side-to-side cell connections: a major mechanism of structural heart disease arrhythmias. *Pacing Clin Electrophysiol*. 1997;20(2 Pt 2):397-413.
10. Spach MS, Miller WT, 3rd, Dolber PC, Kootsey JM, Sommer JR, Mosher CE, Jr. The functional role of structural complexities in the propagation of depolarization in the atrium of the dog. Cardiac conduction disturbances due to discontinuities of effective axial resistivity. *Circ Res*. 1982;50(2):175-91.
11. Sanchez-Quintana D, Cabrera JA, Farre J, Climent V, Anderson RH, Ho SY. Sinus node revisited in the era of electroanatomical mapping and catheter ablation. *Heart*. 2005;91(2):189-94.
12. Jongbloed MR, Vicente Steijn R, Hahurij ND, Kelder TP, Schalij MJ, Gittenberger-de Groot AC, et al. Normal and abnormal development of the cardiac conduction system; implications for conduction and rhythm disorders in the child and adult. *Differentiation*. 2012;84(1):131-48.
13. Spach MS, Heidlage JF, Barr RC, Dolber PC. Cell size and communication: role in structural and electrical development and remodeling of the heart. *Heart Rhythm*. 2004;1(4):500-15.
14. Kirubakaran S, Chowdhury RA, Hall MC, Patel PM, Garratt CJ, Peters NS. Fractionation of electrograms is caused by colocalized conduction block and connexin disorganization in the absence of fibrosis as AF becomes persistent in the goat model. *Heart Rhythm*. 2015;12(2):397-408.
15. Markides V, Schilling RJ, Ho SY, Chow AW, Davies DW, Peters NS. Characterization of left atrial activation in the intact human heart. *Circulation*. 2003;107(5):733-9.
16. Dudink EA, Weijs B, Tull S, Luermans JG, Fabritz L, Chua W, et al. The Biomarkers NT-proBNP and CA-125 are Elevated in Patients with Idiopathic Atrial Fibrillation. *J Atr Fibrillation*. 2018;11(4):2058.
17. Chua W, Purmah Y, Cardoso VR, Gkoutos GV, Tull SP, Neculau G, et al. Data-driven discovery and validation of circulating blood-based biomarkers associated with prevalent atrial fibrillation. *Eur Heart J*. 2019;40(16):1268-76.
18. Hui TH, McClelland RL, Allison MA, Rodriguez CJ, Kronmal RA, Heckbert SR, et al. The relationship of circulating fibroblast growth

- factor 21 levels with incident atrial fibrillation: The Multi-Ethnic Study of Atherosclerosis. *Atherosclerosis*. 2018;269:86-91.
19. Zhu K, Hung J, Divitini M, Murray K, Lim EM, St John A, et al. High-sensitivity cardiac troponin I and risk of incident atrial fibrillation hospitalisation in an Australian community-based cohort: The Busselton health study. *Clin Biochem*. 2018;58:20-5.
 20. Kubota Y, Alonso A, Heckbert SR, Norby FL, Folsom AR. Homocysteine and Incident Atrial Fibrillation: The Atherosclerosis Risk in Communities Study and the Multi-Ethnic Study of Atherosclerosis. *Heart Lung Circ*. 2019;28(4):615-22.
 21. Csecsei P, Varnai R, Nagy L, Keki S, Molnar T, Illes Z, et al. L-Arginine Pathway Metabolites Can Discriminate Paroxysmal from Permanent Atrial Fibrillation in Acute Ischemic Stroke. *Ideggyogy Szemle*. 2019;72(3-4):79-88.
 22. Stanciu AE, Vatasescu RG, Stanciu MM, Serdarevic N, Dorobantu M. The role of pro-fibrotic biomarkers in paroxysmal and persistent atrial fibrillation. *Cytokine*. 2018;103:63-8.
 23. Hu X, Li J, van Marion DMS, Zhang D, Brundel B. Heat shock protein inducer GGA*-59 reverses contractile and structural remodeling via restoration of the microtubule network in experimental Atrial Fibrillation. *J Mol Cell Cardiol*. 2019;134:86-97.
 24. van Marion DMS, Dorsch L, Hoogstra-Berends F, Kakuchaya T, Bockeria L, de Groot NMS, et al. Oral geranylgeranylacetone treatment increases heat shock protein expression in human atrial tissue. *Heart Rhythm*. 2020;17(1):115-22.
 25. McKinsey TA. Therapeutic potential for HDAC inhibitors in the heart. *Annu Rev Pharmacol Toxicol*. 2012;52:303-19.
 26. Haberland M, Montgomery RL, Olson EN. The many roles of histone deacetylases in development and physiology: implications for disease and therapy. *Nat Rev Genet*. 2009;10(1):32-42.
 27. Zhang D, Hu X, Henning RH, Brundel BJ. Keeping up the balance: role of HDACs in cardiac proteostasis and therapeutic implications for atrial fibrillation. *Cardiovasc Res*. 2016;109(4):519-26.
 28. Zhang D, Wu CT, Qi X, Meijering RA, Hoogstra-Berends F, Tadevosyan A, et al. Activation of histone deacetylase-6 induces contractile dysfunction through derailment of alpha-tubulin proteostasis in experimental and human atrial fibrillation. *Circulation*. 2014;129(3):346-58.
 29. Zhang D, Hu X, Li J, Liu J, Baks-Te Bulte L, Wiersma M, et al. DNA damage-induced PARP1 activation confers cardiomyocyte dysfunction through NAD(+) depletion in experimental atrial fibrillation. *Nat Commun*. 2019;10(1):1307.
 30. Nakai A, Yamaguchi O, Takeda T, Higuchi Y, Hikoso S, Taniike M, et al. The role of autophagy in cardiomyocytes in the basal state and in response to hemodynamic stress. *Nat Med*. 2007;13(5):619-24.
 31. Wiersma M, Meijering RAM, Qi XY, Zhang D, Liu T, Hoogstra-Berends F, et al. Endoplasmic Reticulum Stress Is Associated With Autophagy and Cardiomyocyte Remodeling in Experimental and Human Atrial Fibrillation. *J Am Heart Assoc*. 2017;6(10).
 32. Rainbolt TK, Saunders JM, Wiseman RL. Stress-responsive regulation of mitochondria through the ER unfolded protein response. *Trends Endocrinol Metab*. 2014;25(10):528-37.
 33. Mericskay M. Nicotinamide adenine dinucleotide homeostasis and signalling in heart disease: Pathophysiological implications and therapeutic potential. *Arch Cardiovasc Dis*. 2016;109(3):207-15.
 34. Babcock DF, Herrington J, Goodwin PC, Park YB, Hille B. Mitochondrial participation in the intracellular Ca²⁺ network. *J Cell Biol*. 1997;136(4):833-44.
 35. Wiersma M, van Marion DMS, Wust RCI, Houtkooper RH, Zhang D, Groot NMS, et al. Mitochondrial Dysfunction Underlies Cardiomyocyte Remodeling in Experimental and Clinical Atrial Fibrillation. *Cells*. 2019;8(10).



19

CHAPTER 19



ENGLISH SUMMARY

Lanters EAH

Chapter 1 outlines the current knowledge on the arrhythmogenic substrate and mechanisms underlying atrial fibrillation (AF). In addition, it also shows the lack of a complete understanding of the arrhythmia. The clinical case report in **Chapter 2** illustrates from a clinical point of view how both patient and cardiologist challenge (treatment of) AF. Despite the variety in potential therapeutic modalities, AF tends to recur frequently. The case report emphasizes the need for more insight into the arrhythmogenic substrate and mechanisms underlying both initiation and perpetuation of AF. It also shows that lack of knowledge of the arrhythmogenic substrate causes repetitive therapy failure. For optimal understanding and recognition of electropathological changes at an atrial level during (or introduced by) AF knowledge of the more or less physiological electrophysiological characteristics during sinus rhythm (SR) is of utmost importance. For this purpose, the first part of this thesis describes conduction properties of the entire atria during SR.

We investigated in **Chapter 3** the spatial distribution and extensiveness of conduction delay (CD, Δ local activation time ≥ 7 ms) and conduction block (CB, Δ local activation time ≥ 12 ms) during SR. For this purpose, high-resolution epicardial mapping studies (192 unipolar electrodes, inter-electrode distances: 2 mm) of the right atrium (RA), pulmonary vein area (PVA), left atrioventricular groove (LAVG) and Bachmann's Bundle (BB) were performed in 209 patients undergoing coronary artery bypass grafting (CABG). Areas with CD or CB were present in all patients, overall prevalence at the entire atrial surface was respectively 1.4(0.2-4.0)% and 1.3(0.1-4.3)%. Extensiveness and spatial distribution of CD/CB showed considerable intra-atrial but also inter-individual variation. Despite these differences, a predilection site is present at the superior intercaval RA. Extensiveness of CB at the superior intercaval RA or BB does not reflect CB elsewhere in the atria.

A similar mapping study was performed in **Chapter 4** in patients with aortic valve (N=85) or mitral valve (N=54) disease and included 38 patients with AF. Nearly all patients demonstrated CD and CB with, comparable to the CABG patients, a predilection site at the superior intercaval RA. Patients with mitral valve disease had a higher maximal degree of CD at the LAVG than patients with aortic valve disease. A history of AF was correlated with CD and/or CB at BB. Total atrial activation patterns during SR in patients with ischemic (N=132) and/or valvular (N=121) heart disease were evaluated in **Chapter 5**. SR origin was located at the superior intercaval RA in 92% of patients. BB activation occurred via one wavefront from right-to-left (64%), from the central part (7%) or via multiple wavefronts (28%). LAVG activation occurred via BB (43%), PVA (3%) or BB and PVA (54%); depending on which route had the shortest interatrial conduction time ($p < 0.001$). Total activation times were longer in patients with AF, due to prolongation of RA and BB conduction times.

In addition to atrial activation patterns, the incidence and spatial distribution of epicardial breakthrough waves (EBW) and sinus node breakthrough waves (SNBW) were demonstrated in **Chapter 6**. Epicardial mapping during SR was performed in 381 patients with ischemic and/or valvular heart disease. A total of 218 EBWs and 57 SNBW were observed in 44% of patients and occurred mainly at RA (48%) and LAVG (31%). EBWs occurred more frequently in patients with ischemic heart disease than with valvular heart disease. Electrograms of EBW origins most often consisted of double and fractionated potentials. In case of single potentials, an R-wave was observed in 88% of EBWs, as opposed to 21% of SNBW. Fractionation of

EBW potentials was more often observed at RA and BB. These findings indicate that muscular connections between endo and epicardium underlie EBWs and that a slight degree of endo-epicardial asynchrony required for EBWs to occur is already present in some areas during SR. Spatial distribution of EBW was not related to underlying heart disease or presence of AF.

In **Chapter 7** the relevance of conduction abnormalities during SR at Bachmann's Bundle is evaluated. High-resolution epicardial mapping of BB was performed in 185 patients undergoing CABG, 13 of them had a medical history of paroxysmal AF. In the majority of patients, BB was activated in a right-to-left manner. However, wavefronts traveling from right and central, right, central and left or from central entry sites were also observed. Mean effective conduction velocity was 89 cm/s. CB in transversal and longitudinal direction was present in 75% of patients and was more pronounced in patients with paroxysmal AF. More than 4% CB and length of longitudinal CB lines >10mm were both associated with the presence of pre- and post-operative AF episodes.

Patients with congenital heart disease (CHD) frequently present with right sided atrial tachyarrhythmia. In **Chapter 8** we examine the characteristics of CD and CB in CHD patients with RA volume overload. We therefore performed the same epicardial SR mapping approach as presented in the previous chapters in 31 patients undergoing first-time open chest cardiac surgery for an interatrial shunt. CD and CB were present in all patients, showing considerable variation in prevalence and lengths of lines of CD/CB. Prevalence of CD and CB was higher in the RA and BB than in the LA ($p<0.0083$). In 52% of patients, the longest line of CD/CB was located at the RA. Within the RA, conduction disorders were more prevalent and more severe in the intercaval region than in the RA free wall ($p<0.05$).

The chaotic nature of AF is illustrated in **Chapter 9**. Epicardial mapping was performed during persistent AF in a 71-year old patient. EBWs were omnipresent throughout the entire atria. The frequent, non-repetitive, widespread and capricious distribution of focal waves suggest that transmural conduction of fibrillation waves is most likely the mechanism underlying focal fibrillation waves. The presence of transmural conduction suggests asynchronous activation of the endo- and epicardial layer of the atrial wall. Simultaneous endo-epicardial mapping of the right atrium was performed to investigate this hypothesis, as presented in **Chapter 10**. Asynchronous endo-epicardial activation ranged between 0.9-55.9% without preference for either side. Focal waves appeared equally frequent at endocardium and epicardium (11% vs 13%, $p=0.18$). Using strict criteria for breakthrough (presence of an opposite wave within 4mm and ≤ 14 ms before the origin of the focal wave), the majority (65%) of all focal fibrillation waves could be attributed to endo-epicardial excitation.

The predictive value of intra-operative AF-inducibility for development of post-operative AF (PoAF) was investigated in **Chapter 11**. In a population of 496 patients undergoing coronary artery bypass grafting and/or valvular repair, sustained AF was inducible in 56%. In patients without AF prior to surgery, the incidence of (de novo) early and late post-operative AF (EPoAF and LPoAF) was 37% and 2%. AF recurrences however were observed in majority of patients with a history of pre-operative AF; both early 58% and late 53%. There were no correlations between intra-operative inducibility and EPoAF or LPoAF ($P>0.05$). EPoAF was not correlated with LPoAF in patients without a history of AF ($P=0.116$), in contrast to patients with AF prior

to surgery ($P < 0.001$). Hence, intra-operative AF inducibility does not predict development of de novo post-operative AF. In patients with AF prior to surgery, early post-operative AF is correlated with late AF recurrences.

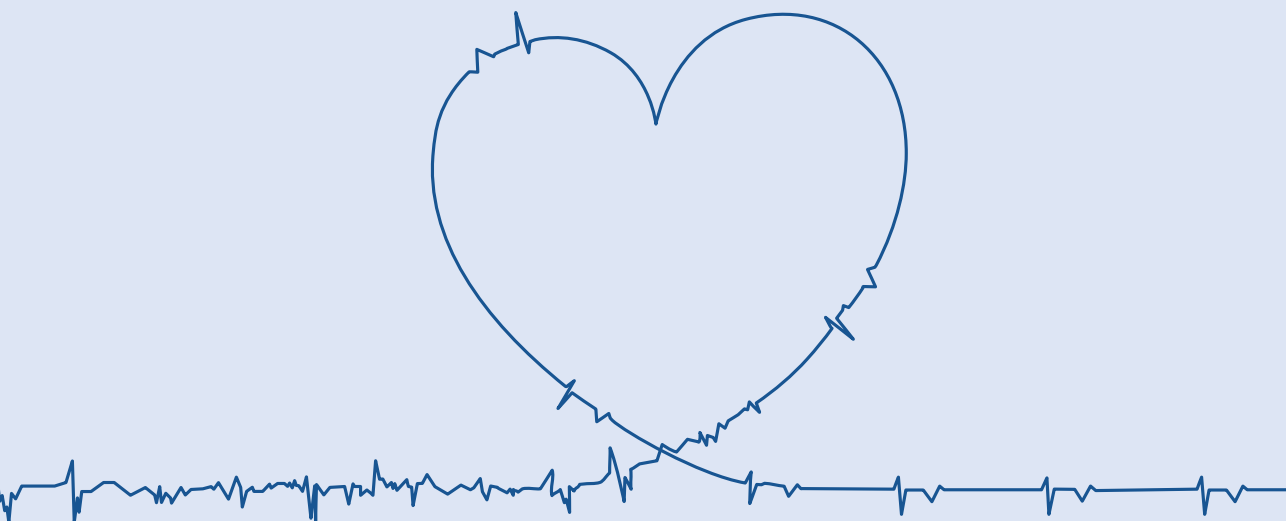
Post procedural atrial extrasystole (AES) frequency predicts AF recurrence after pulmonary vein isolation (PVI) in patients with paroxysmal AF. However, the predictive value of pre-procedural AES frequency for AF recurrence after PVI is unknown. In **Chapter 12** we investigate whether pre-procedural AES frequency is a feasible marker to predict (timing of) AF recurrence after PVI. Hereto, we evaluated the total amount of AES per day on Holter recordings prior to PVI in 684 patients with paroxysmal or persistent AF. Pre-procedural AES/day was similar in patients with paroxysmal (66(20-295)AES/day) and persistent AF (115(12-248)AES/day, $P = 0.915$). AF recurred in 379(55.4%) patients at 203(105-400) days after PVI. There was no correlation with development ($P = 0.203$) or timing ($P = 0.478$) of AF recurrences and therefore AES frequency prior to PVI is not a feasible marker for AF recurrence after PVI. During the blanking period, 302(44.2%) patients showed AF episodes. AF recurrences occurred both more frequently ($P < 0.001$) and earlier ($P < 0.000$) in patients with AF during the blanking period.

AF induces structural, electrical and contractile remodeling of the atria, hereby making the atria more prone to develop new AF episodes with a longer duration. Sensing of cellular stress (as present during AF) activates the heat shock transcription factor-1 (HSF-1) and consequently results in the expression of heat shock proteins (HSPs). HSPs play an important role in protein-protein interactions such as folding and assisting in the establishment of proper protein conformation (shape) and prevention of unwanted protein aggregation, which occur during ageing of the cell and (cardiac) stress. Previously, it was observed that exhaustion of cardio-protective heat shock proteins (HSPs) contributes to structural damage in AF patients. Also, boosting of HSPs, by the heat shock factor-1 activator geranylgeranylacetone, halted AF initiation and progression in experimental cardiomyocyte and dog models for AF. In **Chapter 13**, we discuss the role of HSPs in the pathophysiology of AF. **Chapter 14** further elaborates on the potential role of HSPs as a druggable target to reverse atrial remodelling. Based on the previous findings, we postulated that HSPs may be novel biomarkers associated with AF severity, outcome of AF conversion and/or occurrence of post-operative AF. In **Chapter 15** we outline the design of the HALT&REVERSE project; that aims to investigate the correlation between electropathology, as defined by endo- or epicardial mapping, HSP levels and development or recurrence of AF following pulmonary vein isolation, electrical cardioversion or cardiothoracic surgery.

The first results of the HALT & REVERSE project are presented in **Chapter 16**. In this chapter we evaluate the relation between serum HSP levels, presence of AF, type of AF and AF recurrence in patients undergoing electrical cardioversion ($N = 98$) or PVI ($N = 101$) for AF. In addition, we included 98 control patients without a history of persistent tachyarrhythmias. HSP27, HSP70, cvHSP and HSP60 serum levels did not differ between patients without or with PAF, PeAF or LSPeAF. Also, baseline HSP levels did not correlate with AF recurrence after ECV or PVI. However, in AF patients with AF recurrence within one year, HSP27 levels were significantly elevated post-PVI relative to baseline, compared to patients without recurrence. This suggests that HSP27 levels may predict AF recurrence after PVI.

The correlation between HSPs as non-invasive biomarkers and invasive electrical markers is investigated in **Chapter 17**. For this purpose included 122 patients with and without AF and quantified HSP levels in serum and tissue samples from the right atrial appendage. High-resolution epicardial mapping of the atria was performed for identification of the presence and severity of conduction block. Serum and tissue HSP levels did not differentiate between patients with and without AF, or between the different stages of AF. In addition, there were no relevant correlations between serum and tissue HSP levels, nor between HSP levels and local conduction abnormalities. Hence, HSPs are not suitable as an AF-specific biomarker.

Finally, **Chapter 18** provides an overview and clinical interpretation of all studies incorporated in this thesis. In addition, recommendations for future research projects are made.



20

CHAPTER 20



NEDERLANDSE SAMENVATTING

Lanters EAH

Hoofdstuk 1 is een uiteenzetting van de huidige kennis over het arritmogeen substraat en de mechanismes die aan atriumfibrilleren (AF) ten grondslag liggen. Ook toont het aan dat de ritmestoornis nog niet volledig wordt begrepen. De casus in **Hoofdstuk 2** illustreert vanuit een klinisch oogpunt hoe zowel de patiënt als de cardioloog met (de behandeling van) AF worstelen. Ondanks de grote variëteit in de mogelijke behandelingen recidiveert AF frequent. De casus benadrukt de behoefte aan meer inzicht in het arritmogeen substraat en de mechanismes van zowel de initiatie als de perpetuatie van AF. Het toont ook dat het gebrek aan goed begrip van dit arritmogeen substraat leidt tot herhaaldelijk falen van de therapie. Voor optimaal begrip en ook voor de herkenning van electropathologische veranderingen in het atrium tijdens (of veroorzaakt door) AF, is kennis van de fysiologische electrofysiologische eigenschappen tijdens sinus ritme (SR) van het grootste belang. Het eerste deel van deze thesis beschrijft daarom de geleidingseigenschappen van de gehele atria tijdens SR.

Wij onderzochten in **Hoofdstuk 3** de spatiële distributie en de uitgebreidheid van geleidingsvertraging (CD, Δ lokale activatietijd ≥ 7 ms) en geleidingsblok (CB, Δ lokale activatietijd ≥ 12 ms) tijdens SR. Hiervoor werden hoge resolutie epicardiale mapping studies (192 unipolaire elektrodes, inter-elektrode afstand: 2 mm) van het rechter atrium (RA), pulmonaalvene gebied (PV), linker atrioventriculaire groeve (LAVG) en de Bundel van Bachmann (BB) verricht in 209 patiënten die een coronaire bypass operatie ondergingen. Gebieden met CD en CB waren aanwezig in alle patiënten, de totale prevalentie op het gehele atriale oppervlak was respectievelijk 1.4(0.2-4.0)% en 1.3(0.1-4.3)%. De uitgebreidheid en spatiële distributie van CD/CB toonden aanzienlijke intra-atriale maar ook inter-individuele variatie. Ondanks deze verschillen bestaat er een predilectieplaats op het superiore, intercavale deel van het RA. De uitgebreidheid van CB op het superior intercavaal RA of BB is geen reflectie van CB elders in de atria.

Een vergelijkbare mappingstudie werd uitgevoerd in **Hoofdstuk 4** bij patiënten met aortaklep (N=85) of mitraalklep (N=54) afwijkingen en bevatte 38 patiënten met AF. Bijna alle patiënten hadden zowel CD als CB en (vergelijkbaar aan de patiënten die een coronaire bypass kregen) er was een predilectieplaats op het superior intercavaal RA. Patiënten met mitraalklepafwijkingen hadden een hoger maximaal percentage CD op het LAVG dan patiënten met aortaklepafwijkingen. Een voorgeschiedenis van AF was gecorreleerd met CD en/of CB op BB.

Totale activatiepatronen tijdens SR in patiënten met ischemische (N=132) en/of valvulaire (N=121) hartziekte werd geëvalueerd in **Hoofdstuk 5**. De origo van SR was gelokaliseerd op het superior intercavaal RA in 92% van de patiënten. BB activatie vond plaats via één golf front van rechts naar links (64%0, via het centrum (7%) of via multiële golf fronten (28%). LAVG activatie vond plaats via BB (43%), PVA (3%) of BB én PVA (54%); afhankelijk van welke route de kortste interatriale geleidingstijd had ($P < 0.001$). Totale activatietijden waren langer in patiënten met AF, als gevolg van verlenging van geleidingstijden op RA en BB.

In aanvulling op de atriale activatiepatronen werden de incidentie en spatiële distributie van epicardiale breakthrough golven (EBW) en sinusknoop breakthrough golven (SNBW) onderzocht in **Hoofdstuk 6**. Epicardiale mapping tijdens SR werd uitgevoerd bij 381 patiënten met ischemische en/of valvulaire hartziekte. In totaal werden 218 EBW en 57 SNBW geobserveerd in 44% van de patiënten. Deze golven kwamen voornamelijk voor op

het RA (48%) en LAVG (31%). EBW kwam vaker voor in patiënten met ischemische hartziekte dan in patiënten met valvulaire hartziekte. Electrogrammen van EBW bestonden meestal uit dubbele en gefractioneerde potentialen. In het geval van enkele potentialen werd een R-golf in 88% van de EBW gezien, in contrast tot slechts 21% van de SNWB. Fractionatie van de EBW potentialen werd voornamelijk gezien op RA en BB. Deze bevindingen indiceren dat musculaire verbindingen tussen het endo- en epicard ten grondslag liggen aan EBW en dat een bepaalde mate van endo-epicardiale asynchronie die vereist is voor EBW in sommige gebieden al aanwezig zijn tijdens SR. De spatiële distributie van EBW was niet gerelateerd aan onderliggende hartziekte of aan aanwezigheid van AF.

In **Hoofdstuk 7** wordt de relevantie van geleidingsstoornissen tijdens SR op BB geëvalueerd. Hoge resolutie epicardiale mapping van BB werd verricht bij 185 patiënten die coronaire bypass chirurgie ondergingen, 13 van hen hadden een voorgeschiedenis van paroxysmaal AF. In de meerderheid van de patiënten werd BB geactiveerd van rechts naar links. Echter, golffronten die bewogen vanaf de rechterzijde en het centrum, rechts, centrum en linkerzijde, of van centrale punten werden ook gezien. De gemiddelde effectieve geleidingssnelheid van 89 cm/s. CB in de transversale en longitudinale richting was aanwezig in 75% van de patiënten en was meer uitgesproken bij patiënten met paroxysmaal AF. Meer dan 4% CB en een lengte van longitudinale CB lijnen langer dan 10mm waren geassocieerd met de aanwezigheid van pre- en postoperatieve AF episodes.

Patiënten met congenitale hartziekte (CHD) presenteren zich frequent met rechtszijdige tachyarritmieën. In **Hoofdstuk 8** onderzochten we de karakteristieken van CD en CB in CHD patiënten met een volume overbelasting van het RA. Hiervoor pasten we de zelfde epicardiale SR mapping methode als in de voorgaande hoofdstukken toe bij 31 patiënten die voor de eerste keer open hart chirurgie ondergingen voor een interatriale verbinding. CD en CB waren aanwezig in alle patiënten en toonden een aanzienlijke variatie in prevalentie en lengte van CD / CB lijnen. De prevalentie van CD en CB was hoger op het RA en BB dan op het LA ($P < 0.0083$). In 52% van de patiënten was de langste CD / CB lijn gelokaliseerd op het RA. Binnen het RA waren geleidingsstoornissen meer prevalent en ernstiger in het intercavaal gebied dan op de vrije wand van het RA ($P < 0.05$).

De chaotische eigenschappen van AF worden geïllustreerd in **Hoofdstuk 9**. Epicardiale mapping werd verricht tijdens persistent AF bij een 71-jarige patiënt. EBWs waren alom aanwezig, verspreid door de gehele atria. De frequente, non-repetitieve, wijdverspreide en willekeurige distributie van deze focale golven suggereert dat transmurale geleiding van fibrillatiegolven het meest waarschijnlijke mechanisme is dat aan deze focale golven ten grondslag ligt. De aanwezigheid van transmurale geleiding suggereert asynchrone activatie van de endo- en epicardiale laag van de wand van het atrium. Simultane endo-epicardiale mapping van het RA werd verricht om deze hypothese te onderzoeken, zoals beschreven wordt in **Hoofdstuk 10**. Asynchrone endo-epicardiale activatie varieerde tussen de 0.9-55.9% zonder voorkeur van een van beide zijdes. Focale golven verschenen even vaak aan endocardiale als aan epicardiale zijde (11% vs 13%, $P = 0.18$). Na het toepassen van strenge criteria voor breakthrough (aanwezigheid van een tegenoverliggende golf binnen 4mm en ≤ 14 ms voor de origo van de focale golf), kon de meerderheid (65%) van alle fibrillatiegolven worden toegewezen aan endo-epicardiale excitatie.

De voorspellende waarde van intra-operatieve induceerbaarheid van AF voor de ontwikkeling van post-operatief AF (PoAF) werd onderzocht in **Hoofdstuk 11**. AF was induceerbaar in 56% van een populatie van 496 patiënten die coronaire bypasschirurgie en/of klepchirurgie ondergingen. In patiënten zonder AF voor chirurgie was de incidentie van (de novo) vroeg en laat post-operatief AF respectievelijk 37% en 2%. AF recidieven werden geobserveerd in de meerderheid van de patiënten met een voorgeschiedenis van pre-operatief AF: zowel vroeg (58%) als laat (53%). Er waren geen correlaties tussen intra-operatieve induceerbaarheid en vroeg (EPoAF)- of laat PoAF (LPoAF) ($P > 0.05$). EPoAF was niet gecorreleerd met LPoAF in patiënten zonder pre-operatief AF ($P = 0.116$), in tegenstelling tot patiënten die wel AF voor chirurgie hadden ($P < 0.001$). Dus, intra-operatieve induceerbaarheid van AF voorspelt niet het optreden van de novo PoAF. In patiënten met AF voor chirurgie, EPoAF is gecorreleerd met late AF recidieven.

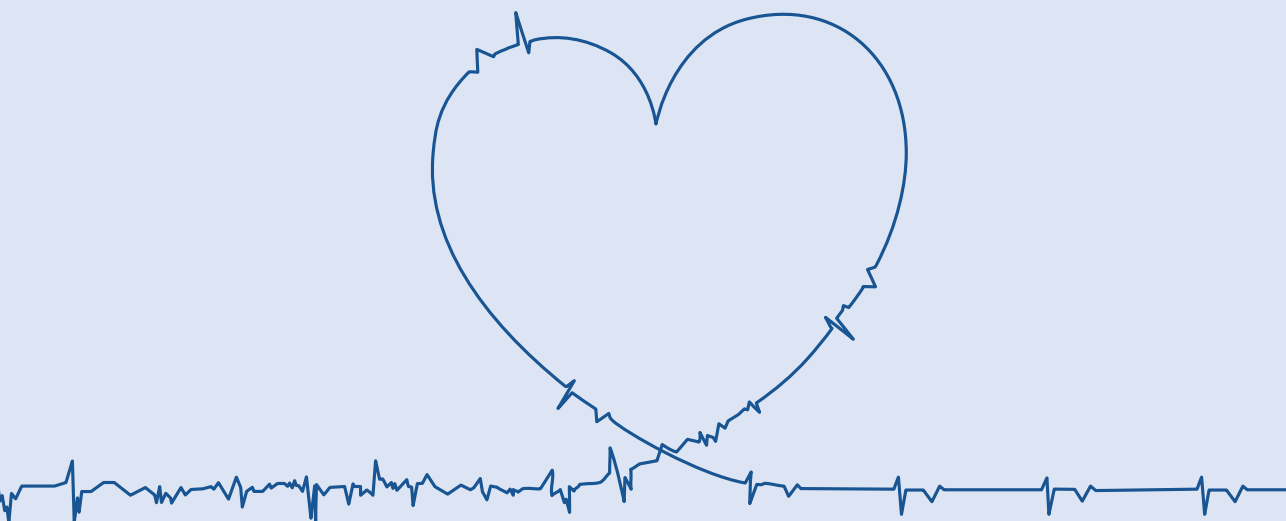
De frequentie van postprocedurele atriale extrasystolen (AES) voorspelt AF recidieven na pulmonaalvenen isolatie (PVI) bij patiënten met paroxysmaal AF. Echter, de voorspellende waarde van de pre-procedurele AES frequentie voor AF recidief na PVI is nog onbekend. In **Hoofdstuk 12** onderzochten we of de pre-procedurele AES frequentie een geschikte marker is om (timing van) AF recidieven na PVI te voorspellen. Hiervoor evalueerden we het totale aantal AES per dag op Holter registraties voorafgaand aan PVI in 684 patiënten met paroxysmaal of persistent AF. Pre-procedurele aantal AES-dag was vergelijkbaar in patiënten met paroxysmaal 66(20-295)AES/dag en persistent AF (115(12-248)AES/day, $P = 0.915$). AF recidiveerde in 379 (55.4%) patiënten op 203 (105-400) dagen na PVI. Er was geen correlatie met ontwikkeling ($P = 0.203$) of timing ($P = 0.478$) van AF recidieven. De AES frequentie vóór PVI is daarom geen geschikte marker voor AF recidieven na PVI. Tijdens de blanking periode toonden 302 (44.2%) van de patiënten AF episodes. AF recidieven traden zowel vaker ($P < 0.001$) als vroeger ($P < 0.001$) op in patiënten met AF tijdens de blanking periode.

AF induceert structurele, elektrische en contractiele remodelering van de atria, waarmee de atria gevoeliger worden om nieuwe AF episodes met een langere duur te ontwikkelen. Het registreren van cellulaire stress (zoals tijdens AF) activeert heat shock transcriptie factor-1 (HSF-1) hetgeen resulteert in de expressie van heat shock proteïnes (HSPs). HSPs spelen een belangrijke rol in de communicatie tussen proteïnes, zoals bijvoorbeeld het vouwen en assisteren bij het verkrijgen van een goede proteïne conformatie (vorm) en het voorkomen van ongewenste proteïne aggregatie hetgeen op kan treden door veroudering van de cellen en (cardiale) stress. Eerder werd al geobserveerd dat uitputting van de cardioprotectieve HSPs bijdraagt aan de structurele schade bij AF patiënten. Stimulatie van HSPs via de HSF-1 activator geranylgeranylacetone remde AF initiatie en progressie in experimentele cardiomyocytymodellen en hondenmodellen voor AF. In **Hoofdstuk 13** bespraken we deze rol van HSPs in de pathofysiologie van AF. **Hoofdstuk 14** ging verder in op de potentiële rol van HSPs als doelwit voor medicatie om atriale remodelering om te keren. Gebaseerd op deze bevindingen veronderstelden we dat HSPs potentiële nieuwe biomarkers zijn die geassocieerd zijn met de ernst van AF, de uitkomst na conversie en/of optreden van postoperatief AF. In **Hoofdstuk 15** presenteerden we het HALT&REVERSE project, dat als doel stelt om de correlaties te onderzoeken tussen electropathologie zoals aangetoond met endo- of epicardiale mapping, HSP niveaus en ontwikkeling of recidief van AF na PVI, elektrische cardioversie of open hartchirurgie.

De eerste resultaten van het HALT&REVERSE project zijn gepresenteerd in **Hoofdstuk 16**. In dit hoofdstuk onderzochten we de relatie tussen serum HSP niveaus, de aanwezigheid van AF, het type AF en AF recidieven in patiënten die een elektrische cardioversie (N = 98) of PVI (N = 101) voor AF ondergingen. We includeerden ook 98 controle patiënten zonder AF of persisterende ritmestoornissen. HSP27, HSP70, cvHSP en HSP60 serum levels varieerden niet tussen patiënten met of zonder paroxysmaal AF, persistent AF of longstanding persistent AF. HSP levels voorafgaand aan de interventie correleerden niet met AF recidieven na ECV of PVI. Echter, in AF patiënten met recidieven binnen één jaar waren HSP niveaus significant verhoogd na PVI in verhouding tot de baseline, vergeleken met patiënten zonder recidieven. Dit suggereert dat HSP27 levels mogelijk AF recidief na PVI kunnen voorspellen.

De correlatie tussen HSPs als non-invasieve biomarkers en invasieve elektrische markers werd onderzocht in **Hoofdstuk 17**. Hiervoor werden 122 patiënten met én zonder AF geïncubeerd en HSPs levels werden gequantificeerd in serum en weefsel van het rechter hartoor. Hoge resolutie epicardiale mapping van de atria werd verricht om de aanwezigheid en ernst van geleidingsstoornissen te onderzoeken. Serum en weefsel HSP levels differentieerden niet tussen patiënten met en zonder AF, of tussen de verschillende stadia van AF. Er waren ook geen relevante correlaties tussen serum en weefsel HSP niveaus, of tussen HSP niveaus en lokale geleidingsstoornissen. HSPs zijn dus niet geschikt als AF-specifieke biomarker.

Uiteindelijk gaf **Hoofdstuk 18** een overzicht en klinische interpretatie van alle studies die in deze thesis zijn opgenomen. Tevens werden aanbevelingen gedaan voor toekomstige onderzoeksprojecten.



21

CHAPTER 21

APPENDICES



PHD PORTFOLIO
LIST OF PUBLICATIONS
ABOUT THE AUTHOR
DANKWOORD

PHD PORTFOLIO

Name PhD student: Eva A.H. Blankman - Lanthers
Erasmus MC department: Cardiology
Research School: COEUR
Title thesis: Atrial fibrillation from a sinus rhythm point of view
Promotors: prof. dr. N.M.S. de Groot, prof. dr. B.J.J.M. Brundel

1. PhD training

	Year	ECTS
General Academic skills		
BROK course	09-2015	1.5
Research Integrity	08-2015	0.3
In-depth courses		
Construction of the vertebrate heart, its chambers and its conduction system	09-2014	0.1
Imaging of cardiac arrhythmias	11-2014	0.2
CMR for the modern cardiologist	11-2014	0.4
Costs, Quality and Value in Cardiovascular Interventions	02-2015	0.1
Secondary prevention with anti-thrombotics: unrevealing the cocundrum of bleeding vs. efficacy.	03-2015	0.2
The role of biomarkers in the pathophysiology of atrial fibrillation	12-2015	0.2
Arrhythmia research methodology	01-2016	1.5
Biotronik SVT course (2 days)	03-2016	0.8
Symposia and conferences		
NVVC najaarscongres, Papendal	10-2011	0.6
ESC congress, Barcelona	09-2014	1.5
NVVC najaarscongres, Papendal	10-2014	0.6
COEUR PhD Dag	2015	0.3
Promeras PhD Dag	2015	0.3
NVVC voorjaarscongres, Noordwijkerhout	04-2015	0.6

	Year	ECTS
Molecular footprints and novel therapeutic strategies in Atrial Fibrillation, Groningen	10-2015	0.3
NVVC najaarscongres, Papendal	11-2015	0.3
AHA congress, Orlando	11-2015	1.5
NVVC voorjaarscongres, Noordwijkerhout	03-2016	0.3
ECAS congress, Parijs	04-2016	1.2
HRS congress, San Francisco	05-2016	1.5
Cardiostim, Nice	06-2016	0.6
Restart your heart symposium, Amsterdam	05-2016	0.3
Dutch-German joint meeting, Amsterdam	03-2018	0.3
Nederlandse Internistendagen, Maastricht	04-2019	0.6

Presentations

First application of a remote, robotic, non-magnetic navigation system for catheter ablation of atrial flutter in The Netherlands <i>NVVC voorjaarscongres 2011, oral presentation</i>	10-2011	0.6
Tachyarrhythmias in a congenital patient. <i>Staflunch, oral presentation</i>	01-2014	0.6
Ritmevertraging in de behandeling van hartfalen <i>Assistentenonderwijs, oral presentation</i>	02-2014	0.6
Hypothermia after out of hospital cardiac arrest <i>Journal club, oral presentation</i>	12-2013	0.6
Intra-Operative Mapping Procedure for Diagnosis of the Substrate of Atrial Fibrillation. <i>ESC congress 2014, poster presentation</i>	09-2014	0.3
Intra-Operative Mapping Procedure for Diagnosis of the Substrate of Atrial Fibrillation. <i>COEUR symposium 2014, poster presentation</i>	10-2014	0.3
Perioperative Inducibility of AF: Predictor for Development of Early Postoperative AF? <i>European Cardiac Arrhythmia Society, poster presentation</i>	04-2015	0.3
A(F) never ending story <i>Staflunch oral presentation</i>	03-2015	0.6

	Year	ECTS
Heterogeneity in Conduction during Sinus Rhythm in Electrically Non-Remodeled Atria. <i>NVVC najaarscongres 2015, oral presentation</i>	11-2015	0.6
Feasibility and Safety of Intra-operative Mapping for Diagnosis of the Substrate of Atrial Fibrillation. <i>AHA congress 2015, poster presentation</i>	11-2015	0.3
Bio(logical) markers of atrial fibrillation. <i>COEUR symposium, oral presentation</i>	12-2015	0.6
Predilection Sites for Electropathology during Sinus Rhythm in Patients with Congenital Heart Diseases <i>NVVC voorjaarscongres, oral presentation</i>	03-2016	0.6
Is Conduction Block during Sinus Rhythm associated with Development of Postoperative Atrial Fibrillation? <i>European Cardiac Arrhythmia Society, moderated poster presentation</i>	04-2016	0.3
Is Conduction Block during Sinus Rhythm associated with Development of Postoperative Atrial Fibrillation? <i>Heart Rhythm Society annual conference, poster presentation</i>	05-2016	0.3
High-resolution Voltage Mapping during Sinus Rhythm in Electrically Non-remodeled Atria <i>Cardiostim, poster presentation</i>	06-2016	0.3
H&R from 2014 to 2016 <i>Nederlandse Hartstichting, oral presentation</i>	01-2016	0.6
Is Conduction Block during Sinus Rhythm associated with Development of Postoperative Atrial Fibrillation? <i>Cardiostim, moderated poster presentation</i>	06-2016	0.3
H&R Update September 2016 <i>HALT & REVERSE meeting Amsterdam, oral presentation</i>	09-2016	0.6
Introducing: the Biobank <i>HALT & REVERSE meeting Rotterdam, oral presentation</i>	12-2016	0.6
A leadless intracardiac transcatheter pacing system. <i>Journal club EMC, oral presentation</i>	12-2016	0.6
What did we learn from Sinus Rhythm Mapping <i>COEUR symposium, oral presentation</i>	01-2017	0.6

	Year	ECTS
Elektrische Geleiding <i>HALT & REVERSE patiëntendag, oral presentation</i>	04-2017	0.6
Spatial Distribution of Conduction Disorders during Sinus Rhythm <i>Dutch German Joint Meeting Amsterdam, poster presentation</i>	03-2018	0.3
Other courses		
Fundamental Critical Care Support	2017	1
CVOI Anamnese en Lichamelijk Onderzoek	2018	1
DOO Teach the teacher	2018	1
Basiscursus nierziekten	2018	1
Cursus stralingshygiëne	2019	1
BOC Hartfalen	2019	1
Basiscursus echocardiografie	2019	1
BOC Pijn op de borst	2020	1
BOC Acute cardiologie	2020	1

Teaching activities

Lecturing

HALT & REVERSE meetings	0.6
Translational electrophysiology meetings	0.6

Supervision of students

J van der Ven, master student (17 weeks)	0.6
J van der Spek, master student (21 weeks)	0.8
K Zwiers, minor student (31 weeks)	1.1
R Jansen, minor student (35 weeks)	1.3
R Coolen, minor student (10 weeks)	0.4
Z Gocmen, researcher (43 weeks)	1.5
TU Delft, 4 minor students (3 weeks)	0.1
N van Groningen, master student (22 weeks)	0.8
A van Zadelhoff, minor student (30 weeks)	1.1
S Rohde, minor student (21 weeks)	0.8
T Hokken, master student (21 weeks)	0.8
R Jansen, master student (21 weeks)	0.8
J Hermans, master student (21 weeks)	0.8
B Metselaar, master student (21 weeks)	0.8
TU Twente, 4 bachelor students (10 weeks)	0.4

TOTAL	49.5
--------------	-------------

LIST OF PUBLICATIONS

PUBLISHED

1. **The future of atrial fibrillation therapy: intervention on heat shock proteins influencing electropathology is the next in line.**
Lanterns EA, van Marion DM, Steen H, de Groot NM, Brundel BJ.
Neth Heart J. 2015 Jun;23(6):327-33. doi: 10.1007/s12471-015-0699-0.
PMID: 25947079
2. **Diagnosis and Therapy of Atrial Fibrillation: The Past, The Present and The Future.**
van Marion DM, Lanterns EA, Wiersma M, Allessie MA, Brundel BB, de Groot NM.
J Atr Fibrillation. 2015 Aug 31;8(2):1216. doi: 10.4022/jafib.1216. eCollection 2015 Aug-Sep.
PMID: 27957185
3. **HALT & REVERSE: Hsf1 activators lower cardiomyocyte damage; towards a novel approach to REVERSE atrial fibrillation.**
Lanterns EA, van Marion DM, Kik C, Steen H, Bogers AJ, Allessie MA, Brundel BJ, de Groot NM.
J Transl Med. 2015 Nov 5;13:347. doi: 10.1186/s12967-015-0714-7.
PMID: 26541406
4. **Dynamics of Focal Fibrillation Waves during Persistent Atrial Fibrillation.**
Lanterns EA, Allessie MA, DE Groot NM.
Pacing Clin Electrophysiol. 2016 Apr;39(4):403-4. doi: 10.1111/pace.12807. Epub 2016 Feb 4.
PMID: 26711082
5. **QuesT for the Arrhythmogenic Substrate of Atrial fibrillation in Patients Undergoing Cardiac Surgery (QUASAR Study): Rationale and Design.**
van der Does LJME, Yaksh A, Kik C, Knops P, Lanterns EAH, Teuwen CP, Oei FBS, van de Woestijne PC, Bekkers JA, Bogers AJJC, Allessie MA, de Groot NMS.
J Cardiovasc Transl Res. 2016 Jun;9(3):194-201. doi: 10.1007/s12265-016-9685-1. Epub 2016 Mar 2.
PMID: 26935733
6. **Direct Proof of Endo-Epicardial Asynchrony of the Atrial Wall During Atrial Fibrillation in Humans.**
de Groot N, van der Does L, Yaksh A, Lanterns E, Teuwen C, Knops P, van de Woestijne P, Bekkers J, Kik C, Bogers A, Allessie M.
Circ Arrhythm Electrophysiol. 2016 May;9(5):e003648. doi: 10.1161/CIRCEP.115.003648.
PMID: 27103089

7. **Relevance of Conduction Disorders in Bachmann's Bundle During Sinus Rhythm in Humans.**
 Teuwen CP, Yaksh A, Lanterns EA, Kik C, van der Does LJ, Knops P, Taverne YJ, van de Woestijne PC, Oei FB, Bekkers JA, Bogers AJ, Allessie MA, de Groot NM.
Circ Arrhythm Electrophysiol. 2016 May;9(5):e003972. doi: 10.1161/CIRCEP.115.003972.
 PMID: 27153879
8. **Pharmacological Therapy of Tachyarrhythmias During Pregnancy.**
 Yaksh A, van der Does LJ, Lanterns EA, de Groot NM.
Arrhythm Electrophysiol Rev. 2016 May;5(1):41-4. doi: 10.15420/AER.2016.1.2.
 PMID: 27408722
9. **Usefulness of the R-Wave Sign as a Predictor for Ventricular Tachyarrhythmia in Patients With Brugada Syndrome.**
 Ragab AAY, Houck CA, van der Does LJME, Lanterns EAH, Burghouwt DE, Muskens AJQM, de Groot NMS.
Am J Cardiol. 2017 Aug 1;120(3):428-434. doi: 10.1016/j.amjcard.2017.04.044. Epub 2017 May 11.
 PMID: 28583685
10. **Aberrant coronary artery spasms cause ST-T segment depression during endovascular ablation of atrial flutter.**
Lanterns EAH, Coenen A, Lubbers MM, Nieman K, de Groot NMS.
Clin Case Rep. 2017 Jun 21;5(8):1252-1254. doi: 10.1002/ccr3.1023. eCollection 2017 Aug.
 PMID: 28781835
11. **Impact of Supraventricular Tachyarrhythmia in Patients With Inherited Cardiac Arrhythmia.**
 Ragab AAY, Houck CA, van der Does LJME, Lanterns EAH, Muskens AJQM, de Groot NMS.
Am J Cardiol. 2017 Dec 1;120(11):1985-1989. doi: 10.1016/j.amjcard.2017.08.016. Epub 2017 Aug 30.
 PMID: 28951021
12. **Epicardial Breakthrough Waves During Sinus Rhythm: Depiction of the Arrhythmogenic Substrate?**
 Mouws EMJP, Lanterns EAH, Teuwen CP, van der Does LJME, Kik C, Knops P, Bekkers JA, Bogers AJJC, de Groot NMS.
Circ Arrhythm Electrophysiol. 2017 Sep;10(9):e005145. doi: 10.1161/CIRCEP.117.005145.
 PMID: 28912205
13. **Spatial distribution of conduction disorders during sinus rhythm.**
Lanterns EAH, Yaksh A, Teuwen CP, van der Does LJME, Kik C, Knops P, van Marion DMS, Brundel BJJM, Bogers AJJC, Allessie MA, de Groot NMS.
Int J Cardiol. 2017 Dec 15;249:220-225. doi: 10.1016/j.ijcard.2017.08.067. Epub 2017 Sep 2.
 PMID: 28888481

14. **Quantification of the Arrhythmogenic Effects of Spontaneous Atrial Extrasystole Using High-Resolution Epicardial Mapping.**
 Teuwen CP, Kik C, van der Does LJME, [Lanters EAH](#), Knops P, Mouws EMJP, Bogers AJJC, de Groot NMS.
Circ Arrhythm Electrophysiol. 2018 Jan;11(1):e005745. doi: 10.1161/CIRCEP.117.005745.
 PMID: 29269560
15. **Unipolar atrial electrogram morphology from an epicardial and endocardial perspective.**
 van der Does LJME, Knops P, Teuwen CP, Serban C, Starreveld R, [Lanters EAH](#), Mouws EMJP, Kik C, Bogers AJJC, de Groot NMS.
Heart Rhythm. 2018 Jun;15(6):879-887. doi: 10.1016/j.hrthm.2018.02.020. Epub 2018 Feb 22.
 PMID: 29476825
16. **Impact of Ischemic and Valvular Heart Disease on Atrial Excitation: A High-Resolution Epicardial Mapping Study.**
 Mouws EMJP, [Lanters EAH](#), Teuwen CP, van der Does LJME, Kik C, Knops P, Yaksh A, Bekkers JA, Bogers AJJC, de Groot NMS.
J Am Heart Assoc. 2018 Mar 8;7(6):e008331. doi: 10.1161/JAHA.117.008331.
 PMID: 29519812
17. **Intraoperative Inducibility of Atrial Fibrillation Does Not Predict Early Postoperative Atrial Fibrillation.**
[Lanters EAH](#), Teuwen CP, Yaksh A, Kik C, van der Does LJME, Mouws EMJP, Knops P, van Groningen NJ, Hokken T, Bogers AJJC, de Groot NMS.
J Am Heart Assoc. 2018 Mar 10;7(6):e007879. doi: 10.1161/JAHA.117.007879.
 PMID: 29525787
18. **Prediction of ventricular tachyarrhythmia in Brugada syndrome by right ventricular outflow tract conduction delay signs.**
 Ragab AAY, Houck CA, van der Does LJME, [Lanters EAH](#), Muskens AJQM, de Groot NMS.
J Cardiovasc Electrophysiol. 2018 Jul;29(7):998-1003. doi: 10.1111/jce.13496. Epub 2018 Apr 20.
 PMID: 29608225
19. **Application of kinomic array analysis to screen for altered kinases in atrial fibrillation remodeling.**
 Meijering RAM, Wiersma M, Zhang D, [Lanters EAH](#), Hoogstra-Berends F, Scholma J, Diks S, Qi X, de Groot NMS, Nattel S, Henning RH, Brundel BJJM.
Heart Rhythm. 2018 Nov;15(11):1708-1716. doi: 10.1016/j.hrthm.2018.06.014. Epub 2018 Jun 11.
 PMID: 29902583

20. **Intraoperative arrhythmias in children with congenital heart disease: transient, innocent events?**
 Houck CA, Ramdjan TTTK, Yaksh A, Teuwen CP, [Lanters EAH](#), Bogers AJJC, de Groot NMS.
Europace. 2018 Jul 1;20(7):e115-e123. doi: 10.1093/europace/eux072.
 PMID: 28666343

21. **Impact of the arrhythmogenic potential of long lines of conduction slowing at the pulmonary vein area.**
 Mouws EMJP, van der Does LJME, Kik C, [Lanters EAH](#), Teuwen CP, Knops P, Bogers AJJC, de Groot NMS.
Heart Rhythm. 2019 Apr;16(4):511-519. doi: 10.1016/j.hrthm.2018.10.027. Epub 2018 Oct 26.
 PMID: 30744910

22. **Novel Insights in the Activation Patterns at the Pulmonary Vein Area.**
 Mouws EMJP, Kik C, van der Does LJME, [Lanters EAH](#), Teuwen CP, Knops P, Bogers AJJC, de Groot NMS.
Circ Arrhythm Electrophysiol. 2018 Nov;11(11):e006720. doi: 10.1161/CIRCEP.118.006720.
 PMID: 30520348

23. **QRS Vector Magnitude as Predictor of Ventricular Arrhythmia in Patients With Brugada Syndrome.**
 Ragab AAY, Houck CA, van der Does LJME, [Lanters EAH](#), Muskens AJQM, de Groot NMS.
Am J Cardiol. 2019 Jun 15;123(12):1962-1966. doi: 10.1016/j.amjcard.2019.03.018. Epub 2019 Mar 16.
 PMID: 30955864

24. **DNA damage-induced PARP1 activation confers cardiomyocyte dysfunction through NAD⁺ depletion in experimental atrial fibrillation.**
 Zhang D, Hu X, Li J, Liu J, Baks-Te Bulte L, Wiersma M, Malik NU, van Marion DMS, Tolouee M, Hoogstra-Berends F, [Lanters EAH](#), van Roon AM, de Vries AAF, Pijnappels DA, de Groot NMS, Henning RH, Brundel BJJM.
Nat Commun. 2019 Mar 21;10(1):1307. doi: 10.1038/s41467-019-09014-2.
 PMID: 30898999

25. **The impact of obesity on early postoperative atrial fibrillation burden.**
 Serban C, Arinze JT, Starreveld R, [Lanters EAH](#), Yaksh A, Kik C, Acardag Y, Knops P, Bogers AJJC, de Groot NMS.
J Thorac Cardiovasc Surg. 2020 Mar;159(3):930-938.e2. doi: 10.1016/j.jtcvs.2019.03.073. Epub 2019 Apr 4.
 PMID: 31043315

26. **Ventricular Dysrhythmias During Long-Term Follow-Up in Patients With Inherited Cardiac Arrhythmia.**
Sitorus GDS, Ragab AAY, Houck CA, Lanters EAH, Heida A, van Gastel VE, Muskens AJQM, de Groot NMS.
Am J Cardiol. 2019 Nov 1;124(9):1436-1441. doi: 10.1016/j.amjcard.2019.07.050.
Epub 2019 Aug 8.
PMID: 31481179
27. **Atrial fibrillation: A never ending story?**
Lanters EAH, Knops P, Kik C, de Groot NMS.
Clin Case Rep. 2019 Oct 24;7(12):2368-2370. doi: 10.1002/ccr3.2415. eCollection 2019 Dec.
PMID: 31893060
28. **The Effects of Valvular Heart Disease on Atrial Conduction During Sinus Rhythm.**
van der Does LJME, Lanters EAH, Teuwen CP, Mouws EMJP, Yaksh A, Knops P, Kik C, Bogers AJJC, de Groot NMS.
J Cardiovasc Transl Res. 2020 Aug;13(4):632-639. doi: 10.1007/s12265-019-09936-8. Epub 2019 Nov 26.
PMID: 31773460
29. **Early markers of atrial fibrillation recurrence after pulmonary vein isolation.**
Lanters EAH, Teuwen CP, Hokken T, Rohde S, Haitsma DB, Zijlstra F, Jordaens LJLM, de Groot NMS.
J Arrhythm. 2020 Feb 7;36(2):304-310. doi: 10.1002/joa3.12307. eCollection 2020 Apr.
PMID: 32256879
30. **Distribution of Conduction Disorders in Patients With Congenital Heart Disease and Right Atrial Volume Overload.**
Houck CA, Lanters EAH, Heida A, Taverne YJHJ, van de Woestijne PC, Knops P, Roos-Serote MC, Roos-Hesselink JW, Bogers AJJC, de Groot NMS.
JACC Clin Electrophysiol. 2020 May;6(5):537-548. doi: 10.1016/j.jacep.2019.12.009.
Epub 2020 Feb 26.
PMID: 32439038
31. **Cell-Free Circulating Mitochondrial DNA: A Potential Blood-Based Marker for Atrial Fibrillation.**
Wiersma M, van Marion DMS, Bouman EJ, Li J, Zhang D, Ramos KS, Lanters EAH, de Groot NMS, Brundel BJJM.
Cells. 2020 May 8;9(5):1159. doi: 10.3390/cells9051159.
PMID: 32397106
32. **Sinus Rhythm Conduction Properties across Bachmann's Bundle: Impact of Underlying Heart Disease and Atrial Fibrillation.**
Tewen CP, Does LJMEV, Kik C, Mouws EMJP, Lanters EAH, Knops P, Taverne YJHJ, Bogers AJJC, de Groot NMS.
J Clin Med. 2020 Jun 16;9(6):1875. doi: 10.3390/jcm9061875.
PMID: 32560096

33. **Evaluating Serum Heat Shock Protein Levels as Novel Biomarkers for Atrial Fibrillation.**
Marion DMSV, [Lanters EAH](#), Ramos KS, Li J, Wiersma M, Baks-Te Bulte L, J Q M Muskens A, Boersma E, de Groot NMS, Brundel BJJM.
Cells. 2020 Sep 16;9(9):2105. doi: 10.3390/cells9092105.
PMID: 32947824
34. **Blood-based 8-hydroxy-2'-deoxyguanosine level: A potential diagnostic biomarker for atrial fibrillation.**
Li J, Zhang D, Ramos KS, Baks L, Wiersma M, [Lanters EAH](#), Bogers AJJC, de Groot NMS, Brundel BJJM.
Heart Rhythm. 2020 Oct 5:S1547-5271(20)30934-6. doi: 10.1016/j.hrthm.2020.09.017. Online ahead of print.
PMID: 33031960

IN PREPARATION

35. **Beat-to-Beat Irregularity of Fibrillation Intervals as Novel Electrical Biomarker of Atrial Fibrillation Persistence.**
de Groot NMS, [Lanters EAH](#), van Staveren LN, Zijlstra F.
36. **Exploring Spatial Cycle Length Irregularity to Identify the Arrhythmogenic Substrate of Atrial Fibrillation.**
van Staveren LN, [Lanters EAH](#), de Groot NMS.
37. **Biomarking the Electropathological Substrate: Tissue and Serum Heat Shock Protein levels and their Relation to Atrial Conduction Properties.**
[Lanters EAH](#), van Marion DMS, Ramos KS, van der Does WFD, Bogers AJJC, Brundel BJJM*, de Groot NMS*
* both authors contributed equally
38. **Preservation of the Microtubule Network to Beat Atrial Fibrillation: a Key Role of SR-Mitochondrial Contacts.**
Li J, Ramos KS, Wiersma M, [Lanters E](#), de Groot N, Brundel BJJM*, Zhang D*.
* both authors contributed equally
39. **Heat Shock Protein Levels are associated with AF Persistence and AF Recurrence**
van Marion DMS, Ramos KS, [Lanters EAH](#), Baks-te Bulte L, de Groot NMS, Brundel BJJM

ABOUT THE AUTHOR

Eva A.H. Blankman-Lanters was born on June 5th, 1989 in Breda, the Netherlands. In 2007 she graduated from secondary school (gymnasium) at Onze Lieve Vrouweylyceum, Breda. In the same year she entered medical school at the Erasmus Universiteit Rotterdam. In 2010 she started as a student investigator in the researchgroup of the translational electrophysiology at the Erasmus Medical Center (Rotterdam), guided by professor N.M.S. de Groot and continued to work in this department for her Master thesis, which was finished in 2011. In 2013 she obtained her Medical Doctor's degree. Eva started working as a resident at the department of Cardiology of the Erasmus Medical Center. Subsequently she started her PhD-project "Atrial fibrillation from a sinus rhythm point of view", which is represented in this thesis and supervised by professor N.M.S. de Groot (Erasmus MC) and professor B.J.J.M. Brundel (Amsterdam UMC, VU).

In 2017 she concomitantly started on her specialty training at the department of Cardiology at the Erasmus Medical Center, supervised by dr. T. Galema and E. Dubois. For this purpose she worked as a resident at the department of Internal Medicine at the Franciscus Gasthuis/Vlietland, Rotterdam (supervision by dr. Y. Schrama and dr. A. Rietveld). She is currently working at the department of Cardiology at the Amphia hospital, Breda (supervision by dr. B. van den Branden). In 2022 she will return to the department of Cardiology of the Erasmus Medical Center to complete her specialty training.

In 2018 she married Paul Blankman, whom she has known since 2007. Together, they welcomed their beloved sons Victor (2018) and Oscar (2020).

DANKWOORD

Het is zo ver, na jaren werk ben ik eindelijk toegekomen aan het meest gelezen hoofdstuk van elke thesis. Hoewel hier gelukkig geen honderden electrogrammen, statistische hocuspocus of word count meer aan te pas komen, vind ik het toch het moeilijkste om te schrijven. Ik ben aan zóveel mensen dank verschuldigd de afgelopen jaren en de uitdaging is dan ook om zo compleet mogelijk te zijn, zonder dat je werkelijk iedereen persoonlijk kan benoemen. Hier gaan we dan...

Dit proefschrift zou nooit voor mij liggen zonder de (op moment van schrijven) 1,167 verschillende **patiënten** die actief hebben deelgenomen aan de QUASAR en HALT & REVERSE studies. De vraag om deel te nemen aan onze studie stellen wij u vaak tijdens de meest spannende dagen/uren voorafgaand aan de geplande electrofysiologische onderzoeken of open hart operatie. Uw bereidwilligheid om hier op zo'n moment over mee te denken én te besluiten daadwerkelijk mee te willen doen is van onschatbare waarde voor medisch wetenschappelijk onderzoek. Mijn dank en bewondering hiervoor is groot!

Mijn eerste promotor, **prof. dr. N.M.S. de Groot**, Natasja, in 2010 leerden wij elkaar kennen tijdens mijn zoektocht naar een interessant onderzoek voor mijn masterscriptie. Deze periode blijkt achteraf tekenend geweest te zijn voor de jaren die volgden: maandenlange analyse van home-monitoring data (later electrogrammen), dan op het matje komen bij een hoge baas (in Berlijn in dit geval, daar zat ik dan als groentje) om de technische tekortkomingen aan de kaak te stellen en vervolgens in noodvaart alsnog zorgen dat er niet ál te lang na de deadline toch een mooi artikel lag. Gelukkig heb ik me hierdoor nooit laten ontmoedigen. Ik kijk met plezier terug op mijn tijd bij jouw groep. De beste ideeën en mooiste creaties ontstonden vaak boven de sushi, gevulde koeken, witte oreo's, en sloten thee. Het schoonmaakpersoneel heeft ons meer dan eens na vijven op de vloer van een verlaten stafgang aangetroffen. Tijdens de verschillende trips in binnen- en buitenland was er altijd ruimte voor ontspanning en het verkennen van de omgeving. Niemand kon echter vermoeden dat juist een banaal autorijtje over de A6 bij Lelystad bijna in de koninklijke kerkers zou eindigen. Dank voor de kansen en het vertrouwen dat je me vanaf het allereerste begin hebt gegeven.

Prof. dr. B.J.J.M. Brundel, beste Bianca, dank voor het hartelijk verwelkomen van de klinici zonder enige notie wat er allemaal op jouw laboratorium gebeurde. In zowel Groningen als Amsterdam heb je me trots de ins- en outs van jullie experimenten laten zien. Nooit geweten dat fruitvliegen zowel doorzichtig als interessant voor de cardiologie zijn! Tijdens de opstartfase van het HALT & REVERSE traject, maar ook tot ver in mijn promotietijd mocht ik jou (en je promovendi) altijd laagdrempelig benaderen voor vragen die in de ogen van biologen vast erg vanzelfsprekend geweest moeten zijn, maar dat waren ze voor mij vaak niet! Dank voor de goede samenwerking de afgelopen periode, ik vind het leuk om te zien dat deze constructie tussen de 010 en de 020 inmiddels al een mooi vervolg heeft gekregen in de vorm van nog veel meer promovendi.

Prof. dr. A.J.J.C. Bogers, **prof. dr. F. Zijlstra**, **prof. dr. D. Von Wagoner**, **prof. dr. K. Vernooy**, **dr. A.R. Ramdat Misier** en **dr. S.G. Molhoek**, dank voor het zitting nemen in de kleine en grote leescommissie en het beoordelen van mijn proefschrift.

De afgelopen jaren hebben wij voor het uitvoeren van de mapping een beroep moeten doen op de thoraxchirurgen van het Erasmus MC. **Dr. Oei, dr. Van de Woestijne, dr. Bekkers, dr. Van Leeuwen, dr. Van der Pijl en dr. De Lind van Wijngaarden** dank voor jullie hulp en bereidwilligheid om ons hierbij te helpen, gelukkig is het over de jaren heen steeds sneller en gemakkelijker geworden. **Dr. Kik**, uw betrokkenheid ging verder dan mappen alleen en u dacht mee over de ontwikkeling van nieuwe apparatuur, het opstellen van een protocol en de visualisatie hiervan in het inmiddels beruchte mappingschema. Uiteraard wil ik ook al het **OK-personeel, verpleging, perfusionisten, anesthesisten en anesthesiemedewerkers** bedanken voor hun bijdrage, het soms ad hoc op tafel toveren van alle materialen als we de mapping weer eens te laat hadden aangekondigd en het geduld tijdens het uitvoeren van de mappings.

Electrofysiologen van het Erasmus MC, beste **Sip, Sing, Tamas en Rohit**, bedankt voor jullie participatie aan de cathlab metingen bij onze HALT & REVERSE patiënten, ook toen het protocol nog in de kinderschoenen stond. Sorry dat jullie meer dan eens van je eigen werkplek zijn verdreven door mij met mijn laptop, of door ladingen uitgeprinte blockmaps, activatiemaps of mappingverslagen.

Verpleegkundigen van de afdelingen cardiologie, dagbehandeling cardiologie, thoraxchirurgie en polikliniek cardiologie, dank voor het afnemen van inmiddels een immense hoeveelheid bloedsamples bij al onze studiepatiënten. Medewerkers van het **triallab** en in het bijzonder **Monique de Waart**, dank voor het verwerken en opslaan van onze serum samples en hartoren.

Cardiologen en medewerkers polikliniek Cardiologie van het voormalig Havenziekenhuis, dank voor de mogelijkheid om ook bij onze post-ablatie patiënten op de buitenpoli de follow-up zoals gepland voort te kunnen zetten.

De unit translationele elektrofysiologie heeft de voorbije jaren een ware transformatie ondergaan. Waar we ooit met drie studenten zonder eigen werkplek begonnen aan het bureau van een ander, gingen we naar een opslaghok in het Bd-gebouw (geen ramen, meestal licht, soms hemelwater), om vervolgens jaren te resideren in een ontmanteld laboratorium waar eenieder ons bestaan vergeten was en we moesten strijden voor het behoud van een toilet in het gebouw. Inmiddels beslaat de onderzoeksgroep een hele gang in de onderzoekstoren, en toen ik enigszins spottend vroeg of ik mijn vuile vaat tegenwoordig ook in een vaatwasser mocht zetten, werd mij die warempel direct aangewezen.

Beste **Ameeta en Tanwier**, samen waren we de onderzoekers van het eerste uur. Het monnikenwerk van toen doet inmiddels middeleeuws aan, maar wat hebben we gelachen toen we zelf de mappingelektrode in elkaar aan het solderen waren in de kleedkamer van de thoraxOK. Dat lachen verging ons wel tijdens het manueel annoteren van alle elektrogrammen, het opslaan van de telemetrie, maar vooral tijdens het uitwerken hiervan, hetgeen (uiteraard) ook volledig handmatig ging. Inmiddels alle drie op een andere plek in opleiding tot cardioloog, we komen elkaar zeker weer tegen!

Christophe, tegelijkertijd startten wij na onze periode als onderzoeksstudent dan eindelijk als PhD-studenten en ik kon eigenlijk altijd op je rekenen. Aan de stand van mijn kop kon jij vaak wel zien hoe laat het was, en we hebben dan ook menig rondje gelopen of koffietje gedronken als de telemetrie of mapping ons weer tot het uiterste had gedreven. Een prachtig appartement en tafels vol tapas naast de Sagrada Familia, de downward facing dog in Parijs en die kleine groene paprika die toch een echte Jalapeño bleek in San Francisco: ik heb een toptijd gehad!

Beste **Lisette**, met jouw komst vond ik eindelijk een medestander die de top-500 van het foute uur woord voor woord mee kan zingen (kwantiteit boven kwaliteit)! Achter je rustige en bedachtzame houding bleek een hele harde werker schuil te gaan, handig met de cijfertjes en met computer. Het klikte en we besloten een samen roadtrip door Florida te maken na ons congres in Orlando. Hoewel we onszelf best technisch vonden leek het nachtelijk oppompen van de autobanden langs de snelweg een vrij kansloze missie. Onze ervaring binnen het onderzoek (trial and error, geef nooit op en eindig altijd met de eerste versie) heeft ons uiteindelijk weer op weg geholpen. Dat je vervolgens hebt geprobeerd me te vermoorden in de Tower of Terror heb ik je inmiddels vergeven. Ik vind het fijn dat we elkaar ook na de onderzoeksperiode nog regelmatig weten te vinden, 29 juni sta je dan ook naast me als mijn paranimf!

Beste **Ilse**, met vliegende vaart kwam jij de groep binnen, produceerde papers en de meest ingewikkelde analyses alsof het niets was en eenieder die jouw brainwaves niet begreep kon rekenen op een vurig betoog. De eigenwijzen uit alle lagen van de hiërarchie legde je zonder twijfel het vuur aan de schenen, super efficiënt en doeltreffend (en je had stiekem ook altijd wel gelijk).

Charlotte, “Eva mag ik je eventjes wat vragen” was een jaar lang de standaard. Je was opgezadeld met een lastig telemetrie-project en bleek al snel net zo’n OCD-er als ik te zijn, elke beat moest en zou dus goed geannoteerd worden, en alle figuren perfect uitgelijnd. Onder andere de mapping-paper over de congenitale mapping heb je een prachtige draai gegeven. Na al die jaren begrijp ik alleen nog steeds niet waar je al dat lekkere eten toch laat...

Ahmed, I respect your commitment to your work and studies, it must be hard being away from your family for such a long time. I enjoyed the little non-work oriented discussions we had, hopefully you’ll find the often talked about white, pearl-like objects! **Eliene en Corina**, bedankt voor jullie frisse en nieuwe blik op onze onderzoeken! Niet eerder hadden we een technisch geneeskundige of dierenarts die ons kwamen vergezellen. **Gustav**, I would have liked for you to come back to The Netherlands and do some more research together, but due to current restrictions you are still in Indonesia. We’ll meet again! **Danny**, tijdens de (robot)ablaties had ik al de grootste pret met jou achter de knoppen. Ik vind het knap dat je je dromen nastreeft en nu keihard werkt om ook je promotie waar te maken.

Beste **Denise**, gelukkig werd er ook een promovendus aangesteld op de biologische tak van de HALT & REVERSE. Waar ik een complete nul was op het gebied van fruitvliegen en Western Blotjes, zo was het andersom ook de uitdaging om de “echte patiënt” bij de biologen te introduceren. Ik vind het leuk dat we elkaar een uniek inkijkje hebben kunnen geven in zulke verschillende (en toch wel bijzondere) wereldjes.

Paul Knops, een stille kracht met gouden handjes. Van quick-fixes tot volledig nieuwe mappingkasten, je draait er je hand niet voor om. Samen “shopten” we een deel van het interieur van het oude lab bij elkaar. Dank voor je vermogen om in sommige gevallen ook eens niets te zeggen, maar me vervolgens wel een mascaraatje aan te reiken om mijn onbedoelde blotebillofhoofd op te kalefateren.

Een team functioneert niet zonder een **Agnes** of **Thea**. Agnes, je bracht de patiënten terug in de beeld als ik er weer eens een kwijt was geraakt en wat een opluchting was het toen jij het beheer over de agenda van de follow-up overnam. Thea, jij wist feilloos je weg te vinden binnen de bureaucratie die ons soms parten speelde en je interesse in wat er allemaal op het lab gebeurde was oprecht.

Beste **Ba-308tjes**, dank dat ik als niet-congenitaaltje tóch vanaf het begin bij jullie mocht aanschuiven! Ik denk met veel plezier terug aan de vele lunches, congressen (inclusief challenges en kostuums) en feestjes die ik mocht meemaken.

Iris, het is fijn om sindsdien gelijk op te gaan met de opleiding, maar ook op privé gebied met onze jongens. Dank voor het regelmatig inchecken het afgelopen jaar, dat heeft me goed gedaan!

Beste **Lennart**, de Doppio zou zonder ons geen bestaansrecht hebben. Het deed me altijd goed om even het lab te verlaten en te kleppen met iemand over iets anders dan electrogrammen. Je bent naast een prettige collega inmiddels ook een goede vriend gebleken.

De voorbije jaren in de kliniek als arts-assistent zijn voorbij gevlogen dankzij alle collega-assistenten van de **Interne Geneeskunde van het Franciscus Gasthuis & Vlietland, cardiologie van het Erasmus MC**, en de huidige collega's van de **cardiologie van het Amphia**.

Mijn dank aan de **vakgroep Cardiologie van het Amphia** is groot, jullie hebben heel erg veel geduld met mij het afgelopen jaar. Het is voor mij van grote waarde gebleken om op zo'n leuke stek zonder druk “van bovenaf” weer terug te mogen werken naar het gewenste niveau.

De allerleukste meisjes, **Anne, Angelique** en **Esther**, wat gaan we al ver terug! Hoewel we inmiddels allemaal zijn uitgevlogen proberen we toch regelmatig met zijn allen te daten. Dit voorjaar gaat er een heleboel veranderen en ik kijk dan ook reikhalzend uit naar de eerstvolgende kans dat wij elkaar in het echt weer kunnen zien! Hoe vreemd zal het zijn om van een tafeltje voor 4 in 't Hart van Breda ineens te moeten upgraden naar een speeltuin om onze inmiddels 6 kinders te kunnen huisvesten!

Beste **Vincent** en **Kim**, dank voor de dagelijkse dosis zwartgallige humor en pasklare oplossing voor elk probleem. Vin, de file op de A27 (HM 13,6Re) voelt iets korter als we samen op afstand zoeken. Kim, een baktalent zal ik nooit worden, maar die worstenbroodjes waren echt de bom. Ik eet wel gewoon wat jij maakt.

Lieve **Marloes en Erik**, Lulu al vrij snel na de eerste week van de opleiding geneeskunde trokken we naar elkaar toe. Groot was later ook het plezier toen onze mannen ook wel erg goed door een deur bleken te kunnen. Bedankt dat je er altijd voor me bent, voor de liters thee en kilo's chocolade, voor het plezier maar ook voor de geplengde tranen. Het is dan ook niet meer dan logisch dat jij mijn paranimf bent.

Simon en Joyce, wij vertrouwen jullie met de ogen dicht onze grootste trots toe. Dank voor de vele gezellige uurtjes, wijntjes en zelfs een mini-vakantie in eigen land. Het is fijn om te merken dat we elkaar weten te vinden wanneer hieraan behoefte is, ook al is er niets wat je soms voor elkaar kan doen. Juist een luisterend oor of een informerend appje is dan al genoeg.

Jan en Everdien, dank voor een warm tweede thuis vanaf het allereerste begin. **Frank**, door de afstand is het contact spaarzaam, maar zijn de momenten wel intensiever. Dank voor je eindeloze gastvrijheid. **Anna**, välkommen till familjen. Jag ser fram emot att lära känna dig bättre.

Lieve **papa en mama**, jullie leerden mij altijd maximaal te genieten. Nu dit boekje eindelijk klaar is, wordt het tijd om eens wat harder op die les te gaan oefenen. Hoewel de medische wereld voor jullie soms een vraagstuk blijft, hebben jullie je er altijd voor in gezet om mij op de gewenste plekken te helpen komen. Zelfs het redigeren van een proefschrift dat soms Chinees lijkt hoorde hierbij, dank! **Maarten**, het is hoog tijd dat we binnenkort die beloftes over en weer van de duikcursus, bierbrouwerij en de hapjes-met-wijn-bar nu eens in te gaan lossen. Je bent erg bescheiden, maar wat mag je trots zijn op waar je nu staat! Mijn **Omaatje**, jij bent het voorbeeld dat je met een fikse dosis nieuwsgierigheid, leergierigheid en een voorliefde voor ijs, kroketten en chocolade misschien wel 100 kan worden!

Mijn kleine Blankmannen, **Victor en Oscar**, ik houd onvoorwaardelijk van jullie. Wees kind, speel zoveel je kan en streef altijd je dromen na. Papa en ik zullen er altijd voor jullie zijn.

Allerliefste **Paul**, woorden kunnen niet omschrijven hoeveel ik van je houd. Dankjewel dat je er voor me bent, niet alleen op de talloze leuke momenten maar ook op mijn allerlelijkste rotmomenten was je daar. Je kent mij beter dan dat ik mijzelf ken (ik ben soms alleen te eigenwijs om dat toe te geven). Je bent de allerbeste papa voor onze jongens. Ik weet je altijd naast me te vinden en ben verschrikkelijk trots op jou en alles wat je weet te bereiken.

Financial support for printing of this thesis was kindly provided by:

Erasmus Universiteit Rotterdam
Erasmus MC, afdeling cardiologie
Hartstichting
Chipsoft

